and

$$Nu_D = \frac{hD}{k} = \frac{(4k/r_o) \times 2r_o}{k} = 8 \quad \triangleleft$$

8.3 The Energy Balance

8.3.1 General Considerations

Because the flow in a tube is completely enclosed, an energy balance may be applied to determine how the mean temperature $T_m(x)$ varies with position along the tube and how the total convection heat transfer q_{conv} is related to the difference in temperatures at the tube inlet and outlet. Consider the tube flow of Figure 8.6. Fluid moves at a constant flow rate $\dot{m}$, and convection heat transfer occurs at the inner surface. Typically, it will be reasonable to make one of the four assumptions in Section 1.3 that leads to the simplified steady-flow thermal energy equation, Equation 1.11e. For example, it is often the case that viscous dissipation is negligible (see Problem 8.10) and that the fluid can be modeled as either an incompressible liquid or an ideal gas with negligible pressure variation. In addition, it is usually reasonable to neglect heat transfer by conduction in the axial direction, so the heat transfer term in Equation 1.11e includes only q_{conv}. Therefore, Equation 1.11e may be written in the form

$$q_{\text{conv}} = \dot{m}c_p(T_{m,o} - T_{m,i}) \tag{8.34}$$

for a tube of finite length. This simple overall energy balance relates three important thermal variables (q_{conv}, $T_{m,o}$, $T_{m,i}$). *It is a general expression that applies irrespective of the nature of the surface thermal or tube flow conditions.*

Applying Equation 1.11e to the differential control volume of Figure 8.6 and recalling that the mean temperature is defined such that $\dot{m}c_pT_m$ represents the true rate of thermal energy (or enthalpy) advection integrated over the cross-section, we obtain

$$dq_{\text{conv}} = \dot{m}c_p[(T_m + dT_m) - T_m] \tag{8.35}$$

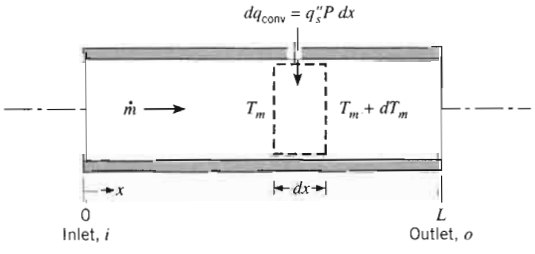


FIGURE 8.6 Control volume for internal flow in a tube.

Patent Owner Manufacturing Resources International, Inc.
Exhibit 2017 - Page 504 of 999

or

$$dq_{conv} = \dot{m}c_p dT_m \tag{8.36}$$

Equation 8.36 may be cast in a convenient form by expressing the rate of convection heat transfer to the differential element as $dq_{conv} = q_s'' P\,dx$, where P is the surface perimeter ($P = \pi D$ for a circular tube). Substituting from Equation 8.27, it follows that

$$\frac{dT_m}{dx} = \frac{q_s'' P}{\dot{m}c_p} = \frac{P}{\dot{m}c_p} h(T_s - T_m) \tag{8.37}$$

This expression is an extremely useful result, from which the axial variation of T_m may be determined. If $T_s > T_m$, heat is transferred to the fluid and T_m increases with x; if $T_s < T_m$, the opposite is true.

The manner in which quantities on the right-hand side of Equation 8.37 vary with x should be noted. Although P may vary with x, most commonly it is a constant (a tube of constant cross-sectional area). Hence the quantity $(P/\dot{m}c_p)$ is a constant. In the fully developed region, the convection coefficient h is also constant, although it varies with x in the entrance region (Figure 8.5). Finally, although T_s may be constant, T_m must always vary with x (except for the trivial case of no heat transfer, $T_s = T_m$).

The solution to Equation 8.37 for $T_m(x)$ depends on the surface thermal condition. Recall that the two special cases of interest are *constant surface heat flux* and *constant surface temperature*. It is common to find one of these conditions existing to a reasonable approximation.

8.3.2 Constant Surface Heat Flux

For constant surface heat flux we first note that it is a simple matter to determine the total heat transfer rate q_{conv}. Since q_s'' is independent of x, it follows that

$$q_{conv} = q_s''(P \cdot L) \tag{8.38}$$

This expression could be used with Equation 8.34 to determine the fluid temperature change, $T_{m,o} - T_{m,i}$.

For constant q_s'' it also follows that the middle expression in Equation 8.37 is a constant independent of x. Hence

$$\frac{dT_m}{dx} = \frac{q_s'' P}{\dot{m}c_p} \neq f(x) \tag{8.39}$$

Integrating from $x = 0$, it follows that

$$T_m(x) = T_{m,i} + \frac{q_s'' P}{\dot{m}c_p} x \qquad q_s'' = \text{constant} \tag{8.40}$$

Accordingly, the mean temperature varies *linearly* with x along the tube (Figure 8.7*a*). Moreover, from Equation 8.27 and Figure 8.5 we also expect the temperature difference $(T_s - T_m)$ to vary with x, as shown in Figure 8.7*a*. This difference is initially

Patent Owner Manufacturing Resources International, Inc.
Exhibit 2017 - Page 505 of 999

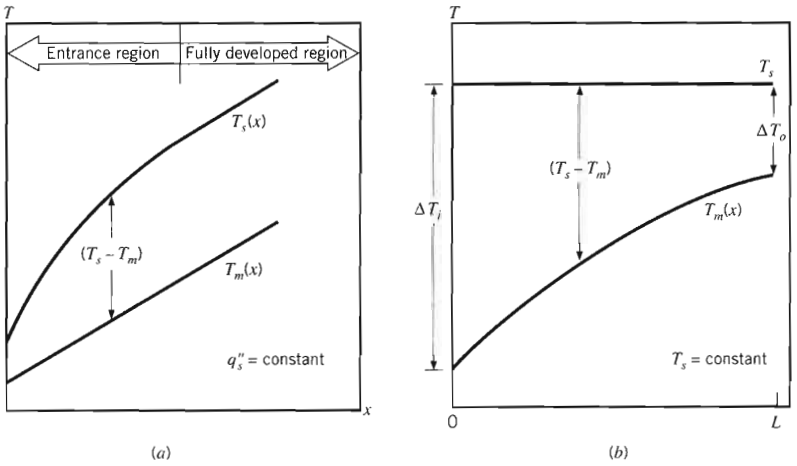


FIGURE 8.7 Axial temperature variations for heat transfer in a tube. (*a*) Constant surface heat flux. (*b*) Constant surface temperature.

small (due to the large value of h near the entrance) but increases with increasing x due to the decrease in h that occurs as the boundary layer develops. However, in the fully developed region we know that h is independent of x. Hence from Equation 8.27 it follows that $(T_s - T_m)$ must also be independent of x in this region.

It should be noted that, if the heat flux is not constant but is, instead, a known function of x, Equation 8.37 may still be integrated to obtain the variation of the mean temperature with x. Similarly, the total heat rate may be obtained from the requirement that $q_{conv} = \int_0^L q_s''(x) P\, dx$.

EXAMPLE 8.2

A system for heating water from an inlet temperature of $T_{m,i} = 20°C$ to an outlet temperature of $T_{m,o} = 60°C$ involves passing the water through a thick-walled tube having inner and outer diameters of 20 and 40 mm. The outer surface of the tube is well insulated, and electrical heating within the wall provides for a uniform generation rate of $\dot{q} = 10^6\ W/m^3$.

1. For a water mass flow rate of $\dot{m} = 0.1$ kg/s, how long must the tube be to achieve the desired outlet temperature?
2. If the inner surface temperature of the tube is $T_s = 70°C$ at the outlet, what is the local convection heat transfer coefficient at the outlet?

SOLUTION

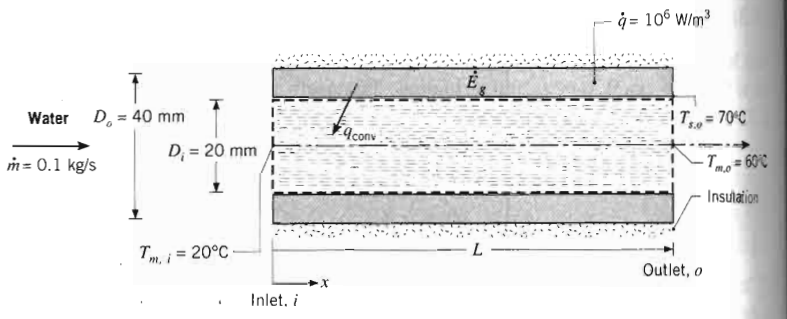
Known: Internal flow through thick-walled tube having uniform heat generation.

Find:

1. Length of tube needed to achieve the desired outlet temperature.
2. Local convection coefficient at the outlet.

Patent Owner Manufacturing Resources International, Inc.
Exhibit 2017 - Page 506 of 999

Schematic:



Assumptions:

1. Steady-state conditions.
2. Uniform heat flux.
3. Incompressible liquid and negligible viscous dissipation.
4. Constant properties.
5. Adiabatic outer tube surface.

Properties: Table A.6, water ($\bar{T}_m = 313$ K): $c_p = 4179$ J/kg · K.

Analysis:

1. Since the outer surface of the tube is adiabatic, the rate at which energy is generated within the tube wall must equal the rate at which it is convected to the water.

$$\dot{E}_g = q_{conv}$$

With

$$\dot{E}_g = \dot{q}\frac{\pi}{4}(D_o^2 - D_i^2)L$$

it follows from Equation 8.34 that

$$\dot{q}\frac{\pi}{4}(D_o^2 - D_i^2)L = \dot{m}c_p(T_{m,o} - T_{m,i})$$

or

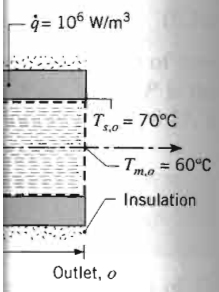
$$L = \frac{4\dot{m}c_p}{\pi(D_o^2 - D_i^2)\dot{q}}(T_{m,o} - T_{m,i})$$

$$L = \frac{4 \times 0.1 \text{ kg/s} \times 4179 \text{ J/kg} \cdot \text{K}}{\pi(0.04^2 - 0.02^2)\text{ m}^2 \times 10^6 \text{ W/m}^3}(60 - 20)°\text{C} = 17.7 \text{ m}$$ ◁

2. From Newton's law of cooling, Equation 8.27, the local convection coefficient at the tube exit is

$$h_o = \frac{q_s''}{T_{s,o} - T_{m,o}}$$

Patent Owner Manufacturing Resources International, Inc.
Exhibit 2017 - Page 507 of 999



Assuming that uniform heat generation in the wall provides a constant surface heat flux, with

$$q_s'' = \frac{\dot{E}_g}{\pi D_i L} = \frac{\dot{q}}{4}\frac{D_o^2 - D_i^2}{D_i}$$

$$q_s'' = \frac{10^6\ \text{W/m}^3}{4}\ \frac{(0.04^2 - 0.02^2)\ \text{m}^2}{0.02\ \text{m}} = 1.5 \times 10^4\ \text{W/m}^2$$

it follows that

$$h_o = \frac{1.5 \times 10^4\ \text{W/m}^2}{(70 - 60)°\text{C}} = 1500\ \text{W/m}^2 \cdot \text{K} \qquad \triangleleft$$

Comments:

1. If conditions are fully developed over the entire tube, the local convection coefficient and the temperature difference $(T_s - T_m)$ are independent of x. Hence $h = 1500\ \text{W/m}^2 \cdot \text{K}$ and $(T_s - T_m) = 10°\text{C}$ over the entire tube. The inner surface temperature at the tube inlet is then $T_{s,i} = 30°\text{C}$.
2. The required tube length L could have been computed by applying the expression for $T_m(x)$, Equation 8.40, at $x = L$.

8.3.3 Constant Surface Temperature

Results for the total heat transfer rate and the axial distribution of the mean temperature are entirely different for the *constant surface temperature* condition. Defining ΔT as $T_s - T_m$, Equation 8.37 may be expressed as

$$\frac{dT_m}{dx} = -\frac{d(\Delta T)}{dx} = \frac{P}{\dot{m}c_p} h\,\Delta T$$

Separating variables and integrating from the tube inlet to the outlet,

$$\int_{\Delta T_i}^{\Delta T_o} \frac{d(\Delta T)}{\Delta T} = -\frac{P}{\dot{m}c_p}\int_0^L h\,dx$$

or

$$\ln\frac{\Delta T_o}{\Delta T_i} = -\frac{PL}{\dot{m}c_p}\left(\frac{1}{L}\int_0^L h\,dx\right)$$

From the definition of the average convection heat transfer coefficient, Equation 6.13, it follows that

$$\ln\frac{\Delta T_o}{\Delta T_i} = -\frac{PL}{\dot{m}c_p}\bar{h}_L \qquad T_s = \text{constant} \qquad (8.41a)$$

Patent Owner Manufacturing Resources International, Inc.
Exhibit 2017 - Page 508 of 999

where $\overline{h}_L$, or simply $\overline{h}$, is the average value of h for the entire tube. Rearranging,

$$\frac{\Delta T_o}{\Delta T_i} = \frac{T_s - T_{m,o}}{T_s - T_{m,i}} = \exp\left(-\frac{PL}{\dot{m}c_p}\overline{h}\right) \qquad T_s = \text{constant} \tag{8.41b}$$

Had we integrated from the tube inlet to some axial position x within the tube, we would have obtained the similar, but more general, result that

$$\frac{T_s - T_m(x)}{T_s - T_{m,i}} = \exp\left(-\frac{Px}{\dot{m}c_p}\overline{h}\right) \qquad T_s = \text{constant} \tag{8.42}$$

where $\overline{h}$ is now the average value of h from the tube inlet to x. This result tells us that the temperature difference $(T_s - T_m)$ *decays exponentially* with distance along the tube axis. The axial surface and mean temperature distributions are therefore as shown in Figure 8.7*b*.

Determination of an expression for the total heat transfer rate q_{conv} is complicated by the exponential nature of the temperature decay. Expressing Equation 8.34 in the form

$$q_{\text{conv}} = \dot{m}c_p[(T_s - T_{m,i}) - (T_s - T_{m,o})] = \dot{m}c_p(\Delta T_i - \Delta T_o)$$

and substituting for $\dot{m}c_p$ from Equation 8.41a, we obtain

$$q_{\text{conv}} = \overline{h}A_s\Delta T_{\text{lm}} \qquad T_s = \text{constant} \tag{8.43}$$

where A_s is the tube surface area ($A_s = P \cdot L$) and ΔT_{lm} is the *log mean temperature difference,*

$$\Delta T_{\text{lm}} \equiv \frac{\Delta T_o - \Delta T_i}{\ln(\Delta T_o/\Delta T_i)} \tag{8.44}$$

Equation 8.43 is a form of Newton's law of cooling for the entire tube, and ΔT_{lm} is the appropriate *average* of the temperature difference over the tube length. The logarithmic nature of this average temperature difference [in contrast, e.g., to an *arithmetic mean temperature* difference of the form $\Delta T_{\text{am}} = (\Delta T_i + \Delta T_o)/2$] is due to the exponential nature of the temperature decay.

Before concluding this section, it is important to note that, in many applications, it is the temperature of an *external* fluid, rather than the tube surface temperature, that is fixed (Figure 8.8). In such cases, it is readily shown that the results of this section may still be used if T_s is replaced by T_∞ (the free stream temperature of the external fluid) and $\overline{h}$ is replaced by $\overline{U}$ (the average overall heat transfer coefficient). For such cases, it follows that

$$\frac{\Delta T_o}{\Delta T_i} = \frac{T_\infty - T_{m,o}}{T_\infty - T_{m,i}} = \exp\left(-\frac{\overline{U}A_s}{\dot{m}c_p}\right) \tag{8.45a}$$

and

$$q = \overline{U}A_s\Delta T_{\text{lm}} \tag{8.46a}$$

Patent Owner Manufacturing Resources International, Inc.
Exhibit 2017 - Page 509 of 999

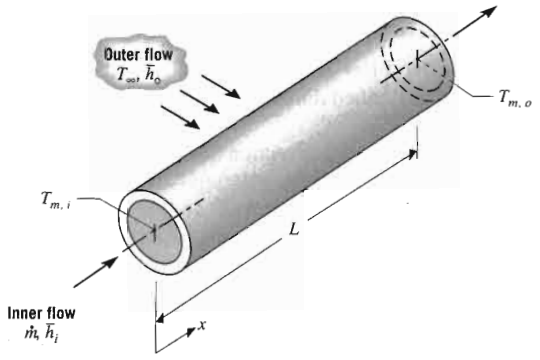


FIGURE 8.8 Heat transfer between fluid flowing over a tube and fluid passing through the tube.

The overall heat transfer coefficient is defined in Section 3.3.1, and for this application it would include contributions due to convection at the tube inner and outer surfaces. For a thick-walled tube of small thermal conductivity, it would also include the effect of conduction across the tube wall. Note that the product $\overline{U}A_s$ yields the same result, irrespective of whether it is defined in terms of the inner ($\overline{U}_i A_{s,i}$) or outer ($\overline{U}_o A_{s,o}$) surface areas of the tube (see Equation 3.32). Also note that $(\overline{U}A_s)^{-1}$ is equivalent to the total thermal resistance between the two fluids, in which case Equations 8.45a and 8.46a may be expressed as

$$\frac{\Delta T_o}{\Delta T_i} = \frac{T_\infty - T_{m,o}}{T_\infty - T_{m,i}} = \exp\left(-\frac{1}{\dot{m}c_p R_{tot}}\right) \tag{8.45b}$$

and

$$q = \frac{\Delta T_{lm}}{R_{tot}} \tag{8.46b}$$

A common variation of the foregoing conditions is one for which the uniform temperature of an *outer* surface, $T_{s,o}$, rather than the free stream temperature of an external fluid, T_∞, is known. In the foregoing equations, T_∞ is then replaced by $T_{s,o}$, and the total resistance embodies the convection resistance associated with the internal flow, as well as the total resistance due to conduction between the inner surface of the tube and the surface corresponding to $T_{s,o}$.

EXAMPLE 8.3

Steam condensing on the outer surface of a thin-walled circular tube of diameter $D = 50$ mm and length $L = 6$ m maintains a uniform outer surface temperature of 100°C. Water flows through the tube at a rate of $\dot{m} = 0.25$ kg/s, and its inlet and outlet temperatures are $T_{m,i} = 15$°C and $T_{m,o} = 57$°C. What is the average convection coefficient associated with the water flow?

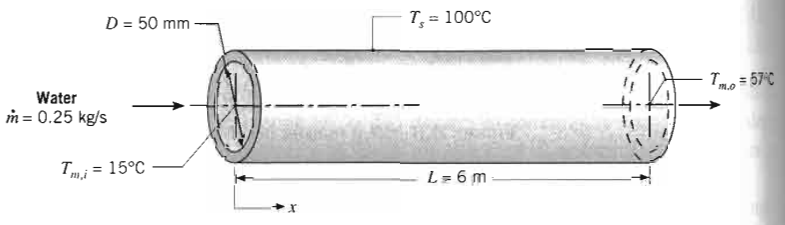
Patent Owner Manufacturing Resources International, Inc.
Exhibit 2017 - Page 510 of 999

SOLUTION

Known: Flow rate and inlet and outlet temperatures of water flowing through a tube of prescribed dimensions and surface temperature.

Find: Average convection heat transfer coefficient.

Schematic:



Assumptions:

1. Negligible tube wall conduction resistance.
2. Incompressible liquid and negligible viscous dissipation.
3. Constant properties.

Properties: Table A.6, water (36°C): $c_p = 4178$ J/kg · K.

Analysis: Combining the energy balance, Equation 8.34, with the rate equation, Equation 8.43, the average convection coefficient is given by

$$\bar{h} = \frac{\dot{m}c_p}{\pi DL}\frac{(T_{m,o} - T_{m,i})}{\Delta T_{lm}}$$

From Equation 8.44

$$\Delta T_{lm} = \frac{(T_s - T_{m,o}) - (T_s - T_{m,i})}{\ln[(T_s - T_{m,o})/(T_s - T_{m,i})]}$$

$$\Delta T_{lm} = \frac{(100 - 57) - (100 - 15)}{\ln[(100 - 57)/(100 - 15)]} = 61.6°C$$

Hence

$$\bar{h} = \frac{0.25\ \text{kg/s} \times 4178\ \text{J/kg} \cdot \text{K}}{\pi \times 0.05\ \text{m} \times 6\ \text{m}}\frac{(57 - 15)°C}{61.6°C}$$

or

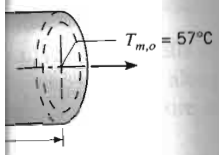
$$\bar{h} = 755\ \text{W/m}^2 \cdot \text{K}$$

Comments: If conditions were fully developed over the entire tube, the local convection coefficient would be everywhere equal to 755 W/m^2 · K.

8.4 *Laminar Flow Analysis and* (

Patent Owner Manufacturing Resources International, Inc.
Exhibit 2017 - Page 511 of 999

ater flowing through a



with the rate equation,
y

,6°C

)°C
C

◁

he entire tube, the local
W/m² · K.

8.4 *Laminar Flow in Circular Tubes: Thermal Analysis and Convection Correlations*

To use many of the foregoing results, the convection coefficients must be known. In this section we outline the manner in which such coefficients may be obtained theoretically for laminar flow in a circular tube. In subsequent sections we consider empirical correlations pertinent to turbulent flow in a circular tube, as well as to flows in tubes of noncircular cross section.

8.4.1 The Fully Developed Region

Here, the problem of heat transfer in *laminar flow* of an *incompressible, constant property fluid* in the *fully developed region* of a *circular tube* is treated theoretically. The resulting temperature distribution is used to determine the convection coefficient.

A differential equation governing the temperature distribution is determined by applying the simplified, steady-flow, thermal energy equation, Equation 1.11e [$q = \dot{m}c_p\,(T_{out} - T_{in})$], to the annular differential element of Figure 8.9. If we neglect the effects of net axial conduction, the heat input, q, is due only to conduction through the radial surfaces. Since the radial velocity is zero in the fully developed region, there is no advection of thermal energy through the radial control surfaces, and the only advection is in the axial direction. Thus, Equation 1.11e leads to Equation 8.47, which expresses a balance between radial conduction and axial advection:

$$q_r - q_{r+dr} = (d\dot{m})c_p\left[\left(T + \frac{\partial T}{\partial x}dx\right) - T\right] \tag{8.47a}$$

or

$$(d\dot{m})c_p\frac{\partial T}{\partial x}dx = q_r - \left(q_r + \frac{\partial q_r}{\partial r}dr\right) = -\frac{\partial q_r}{\partial r}dr \tag{8.47b}$$

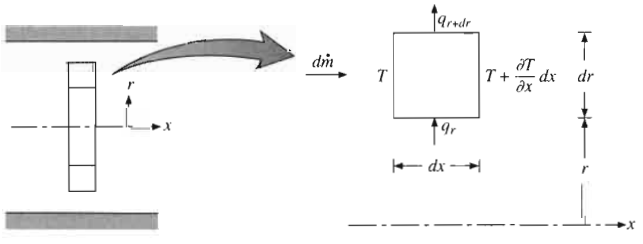


FIGURE 8.9 Thermal energy balance on a differential element for laminar, fully developed flow in a circular tube.

Patent Owner Manufacturing Resources International, Inc.
Exhibit 2017 - Page 512 of 999

The differential mass flow rate in the axial direction is $d\dot{m} = \rho u 2\pi r dr$, and the radial heat transfer rate is $q_r = -k(\partial T/\partial r)2\pi r dx$. If we assume constant properties, Equation 8.47b becomes

$$u\frac{\partial T}{\partial x} = \frac{\alpha}{r}\frac{\partial}{\partial r}\left(r\frac{\partial T}{\partial r}\right) \tag{8.48}$$

We will now proceed to solve for the temperature distribution for the case of *constant surface heat flux*. In this case, the assumption of negligible net axial conduction is exactly satisfied, that is, $(\partial^2 T/\partial x^2) = 0$. Substituting for the axial temperature gradient from Equation 8.32 and for the axial velocity component, u, from Equation 8.15, the energy equation, Equation 8.48, reduces to

$$\frac{1}{r}\frac{\partial}{\partial r}\left(r\frac{\partial T}{\partial r}\right) = \frac{2u_m}{\alpha}\left(\frac{dT_m}{dx}\right)\left[1 - \left(\frac{r}{r_o}\right)^2\right] \qquad q_s'' = \text{constant} \tag{8.49}$$

where $T_m(x)$ varies linearly with x and $(2u_m/\alpha)(dT_m/dx)$ is a constant. Separating variables and integrating twice, we obtain an expression for the radial temperature distribution:

$$T(r, x) = \frac{2u_m}{\alpha}\left(\frac{dT_m}{dx}\right)\left[\frac{r^2}{4} - \frac{r^4}{16r_o^2}\right] + C_1 \ln r + C_2$$

The constants of integration may be evaluated by applying appropriate boundary conditions. From the requirement that the temperature remain finite at $r = 0$, it follows that $C_1 = 0$. From the requirement that $T(r_o) = T_s$, where T_s varies with x, it also follows that

$$C_2 = T_s(x) - \frac{2u_m}{\alpha}\left(\frac{dT_m}{dx}\right)\left(\frac{3r_o^2}{16}\right)$$

Accordingly, for the fully developed region with constant surface heat flux, the temperature profile is of the form

$$T(r, x) = T_s(x) - \frac{2u_m r_o^2}{\alpha}\left(\frac{dT_m}{dx}\right)\left[\frac{3}{16} + \frac{1}{16}\left(\frac{r}{r_o}\right)^4 - \frac{1}{4}\left(\frac{r}{r_o}\right)^2\right] \tag{8.50}$$

From knowledge of the temperature profile, all other thermal parameters may be determined. For example, if the velocity and temperature profiles, Equations 8.15 and 8.50, respectively, are substituted into Equation 8.26 and the integration over r is performed, the mean temperature is found to be

$$T_m(x) = T_s(x) - \frac{11}{48}\left(\frac{u_m r_o^2}{\alpha}\right)\left(\frac{dT_m}{dx}\right) \tag{8.51}$$

From Equation 8.39, where $P = \pi D$ and $\dot{m} = \rho u_m(\pi D^2/4)$, we then obtain

$$T_m(x) - T_s(x) = -\frac{11}{48}\frac{q_s'' D}{k} \tag{8.52}$$

Combining Newton's law of cooling, Equation 8.27, and Equation 8.52, it follows that

$$h = \frac{48}{11}\left(\frac{k}{D}\right)$$

Patent Owner Manufacturing Resources International, Inc.
Exhibit 2017 - Page 513 of 999

or

$$Nu_D \equiv \frac{hD}{k} = 4.36 \qquad q_s'' = \text{constant} \tag{8.53}$$

Hence in a *circular tube* characterized by *uniform surface heat flux* and *laminar, fully developed conditions,* the *Nusselt number is a constant,* independent of Re_D, Pr, and axial location.

For *laminar, fully developed conditions* with a *constant surface temperature,* the assumption of negligible axial conduction is often reasonable. Substituting for the velocity profile from Equation 8.15 and for the axial temperature gradient from Equation 8.33, the energy equation becomes

$$\frac{1}{r}\frac{\partial}{\partial r}\left(r\frac{\partial T}{\partial r}\right) = \frac{2u_m}{\alpha}\left(\frac{dT_m}{dx}\right)\left[1 - \left(\frac{r}{r_o}\right)^2\right]\frac{T_s - T}{T_s - T_m} \qquad T_s = \text{constant} \tag{8.54}$$

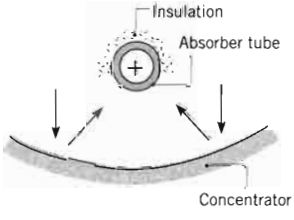
A solution to this equation may be obtained by an iterative procedure, which involves making successive approximations to the temperature profile. The resulting profile is not described by a simple algebraic expression, but the resulting Nusselt number may be shown to be [2]

$$Nu_D = 3.66 \qquad T_s = \text{constant} \tag{8.55}$$

Note that in using Equation 8.53 or 8.55 to determine h, the thermal conductivity should be evaluated at T_m.

EXAMPLE 8.4

One concept used for solar energy collection involves placing a tube at the focal point of a parabolic reflector and passing a fluid through the tube.



The net effect of this arrangement *may be approximated* as one of creating a condition of uniform heating at the surface of the tube. That is, the resulting heat flux to the fluid q_s'' may be assumed to be a constant along the circumference and axis of the tube. Consider operation with a tube of diameter $D = 60$ mm on a sunny day for which $q_s'' = 2000$ W/m^2.

1. If pressurized water enters the tube at $\dot{m} = 0.01$ kg/s and $T_{m,i} = 20$°C, what tube length L is required to obtain an exit temperature of 80°C?
2. What is the surface temperature at the outlet of the tube, where fully developed conditions may be assumed to exist?

Patent Owner Manufacturing Resources International, Inc.
Exhibit 2017 - Page 514 of 999

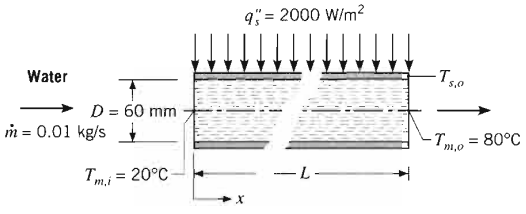
SOLUTION

Known: Internal flow with uniform surface heat flux.

Find:

1. Length of tube L to achieve required heating.
2. Surface temperature $T_s(L)$ at the outlet section, $x = L$.

Schematic:



Assumptions:

1. Steady-state conditions.
2. Incompressible liquid and negligible viscous dissipation.
3. Constant properties.
4. Fully developed conditions at tube outlet.

Properties: Table A.6, water ($\bar{T}_m = 323$ K): $c_p = 4181$ J/kg · K. Table A.6, water ($T_{m,o} = 353$ K): $k = 0.670$ W/m · K, $\mu = 352 \times 10^{-6}$ N · s/m^2, $Pr = 2.2$.

Analysis:

1. For constant surface heat flux, Equation 8.38 may be used with the energy balance, Equation 8.34, to obtain

$$A_s = \pi DL = \frac{\dot{m}c_p(T_{m,o} - T_{m,i})}{q_s''}$$

$$L = \frac{\dot{m}c_p}{\pi D q_s''}(T_{m,o} - T_{m,i})$$

Hence

$$L = \frac{0.01 \text{ kg/s} \times 4181 \text{ J/kg} \cdot \text{K}}{\pi \times 0.060 \text{ m} \times 2000 \text{ W/m}^2}(80 - 20)\text{°C} = 6.65 \text{ m} \quad \triangleleft$$

2. The surface temperature at the outlet may be obtained from Newton's law of cooling, Equation 8.27, where

$$T_{s,o} = \frac{q_s''}{h} + T_{m,o}$$

Patent Owner Manufacturing Resources International, Inc.
Exhibit 2017 - Page 515 of 999

To find the local convection coefficient at the tube outlet, the nature of the flow condition must first be established. From Equation 8.6,

$$Re_D = \frac{4\dot{m}}{\pi D\mu} = \frac{4 \times 0.01 \text{ kg/s}}{\pi \times 0.060 \text{ m} \times 352 \times 10^{-6} \text{ N} \cdot \text{s/m}^2} = 603$$

Hence the flow is laminar. With the assumption of fully developed conditions, the appropriate heat transfer correlation is then

$$Nu_D = \frac{hD}{k} = 4.36$$

and

$$h = 4.36 \frac{k}{D} = 4.36 \frac{0.670 \text{ W/m} \cdot \text{K}}{0.06 \text{ m}} = 48.7 \text{ W/m}^2 \cdot \text{K}$$

The surface temperature at the tube outlet is then

$$T_{s,o} = \frac{2000 \text{ W/m}^2}{48.7 \text{ W/m}^2 \cdot \text{K}} + 80°\text{C} = 121°\text{C} \quad \triangleleft$$

Comments: For the conditions given, $(x_{fd}/D) = 0.05 Re_D Pr = 66.3$, while $L/D = 110$. Hence the assumption of fully developed conditions is justified. Note, however, that with $T_{s,o} > 100°\text{C}$, boiling may occur at the tube surface.

EXAMPLE 8.5

In the human body, blood flows from the heart in a series of branching blood vessels having successively smaller diameters. The capillaries are the smallest blood vessels. In developing the bioheat equation (Section 3.7), Pennes assumed that blood enters the capillaries at the arterial temperature and exits at the temperature of the surrounding tissue. This problem tests that assumption [5,6]. The diameters and average blood velocities for three different types of blood vessels are given in the table below. For each of these blood vessels, estimate the length required for the mean blood temperature to closely approach the tissue temperature, specifically, to satisfy $(T_t - T_{m,o})/(T_t - T_{m,i}) = 0.05$. The heat transfer between the vessel wall and surrounding tissue can be approximated by an effective heat transfer coefficient, $h_t = k_t/D$, where $k_t = 0.5$ W/m · K.

Vessel	Diameter, D (mm)	Blood Velocity, u_m (mm/s)
Large artery	3	130
Arteriole	0.02	3
Capillary	0.008	0.7

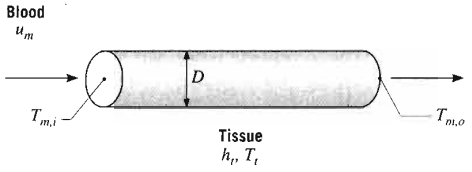
SOLUTION

Known: Blood vessel diameter and average blood velocity. Tissue thermal conductivity and effective heat transfer coefficient.

Patent Owner Manufacturing Resources International, Inc.
Exhibit 2017 - Page 516 of 999

Find: Length of blood vessel needed to satisfy $(T_t - T_{m,o})/(T_t - T_{m,i}) = 0.05$.

Schematic:



Assumptions:

1. Steady-state conditions.
2. Constant properties.
3. Negligible blood vessel wall thermal resistance.
4. Thermal properties of blood can be approximated by those of water.
5. Blood is incompressible liquid with negligible viscous dissipation.
6. Tissue temperature is fixed.
7. Effects of pulsation of flow are negligible.

Properties: Table A.6, water ($\overline{T}_m = 310$ K) $\rho = \upsilon_f^{-1} = 993$ kg/m^3, $c_p = 4178$ J/kg · K, $\mu = 695 \times 10^{-6}$ N · s/m^2, $k = 0.628$ W/m · K, $Pr = 4.62$.

Analysis: Since the tissue temperature is fixed and heat transfer between the blood vessel wall and the tissue can be represented by an effective heat transfer coefficient, Equation 8.45a is applicable, with the "free stream" temperature equal to the tissue temperature, T_t. This equation can be used to find the required length L, since $A_s = \pi DL$. However, we must first find $\overline{U}$, which requires knowledge of the heat transfer coefficient for the blood flow, h_b. Taking the large artery as an example, the Reynolds number is given by

$$Re_D = \frac{\rho u_m D}{\mu} = \frac{993 \text{ kg/m}^3 \times 130 \times 10^{-3} \text{ m/s} \times 3 \times 10^{-3} \text{ m}}{695 \times 10^{-6} \text{ N} \cdot \text{s/m}^2} = 557$$

so the flow is laminar. Since the other blood vessels have smaller diameters and velocities, their flows will also be laminar. Because we don't yet know the length of the vessel, we don't know whether the flow becomes fully developed. However, we will begin by assuming fully developed conditions. Moreover, because the situation is neither one of constant surface temperature nor constant surface heat flux, we will estimate the required length by approximating the Nusselt number as $Nu \approx 4$, in which case $h_b = 4k_b/D$. Neglecting the thermal resistance of the vessel wall, for the large artery

$$\frac{1}{\overline{U}} = \frac{1}{h_b} + \frac{1}{h_t} = \frac{D}{4k_b} + \frac{D}{k_t} = \frac{3 \times 10^{-3} \text{ m}}{4 \times 0.628 \text{ W/m} \cdot \text{K}} + \frac{3 \times 10^{-3} \text{ m}}{0.5 \text{ W/m} \cdot \text{K}}$$

$$= 7.2 \times 10^{-3} \text{ m}^2 \cdot \text{K/W}$$

Patent Owner Manufacturing Resources International, Inc.
Exhibit 2017 - Page 517 of 999

or

$$\overline{U} = 140 \text{ W/m}^2 \cdot \text{K}$$

The length can then be found by solving Equation 8.45a, with $\dot{m} = \rho u_m \pi D^2/4$:

$$L = -\frac{\rho u_m D c_p}{4\overline{U}} \ln\left(\frac{T_t - T_{m,o}}{T_t - T_{m,i}}\right)$$

$$= -\frac{993 \text{ kg/m}^3 \times 130 \times 10^{-3} \text{ m/s} \times 3 \times 10^{-3} \text{ m} \times 4178 \text{ J/kg} \cdot \text{K}}{4 \times 140 \text{ W/m}^2 \cdot \text{K}} \ln(0.05)$$

$$= 8.7 \text{ m}$$

We can now test the assumption that the flow is hydrodynamically and thermally fully developed, using Equations 8.3 and 8.23:

$$x_{\text{fd},h} = 0.05 Re_D D = 0.05 \times 557 \times 3 \times 10^{-3} \text{ m} = 0.08 \text{ m}$$

$$x_{\text{fd},t} = x_{\text{fd},h} Pr = 0.08 \text{ m} \times 4.62 = 0.4 \text{ m}$$

The flow would indeed be fully developed well within the length of 8.7 m. The calculations can be repeated for the other two cases and are tabulated below.

Vessel	Re_D	$\overline{U}$ (W/m² · K)	L (m)	$x_{\text{fd},h}$ (m)	$x_{\text{fd},t}$ (m)
Large artery	557	140	8.7	0.08	0.4
Arteriole	0.086	21,000	8.9×10^{-6}	9×10^{-8}	4×10^{-7}
Capillary	0.0080	52,000	3.3×10^{-7}	3×10^{-9}	1×10^{-8}

Comments:

1. The blood temperature in the large artery approaches the tissue temperature very slowly. This is due to its relatively large diameter, which leads to a small overall heat transfer coefficient. Thus, the temperature in large arteries remains close to the inlet arterial blood temperature.
2. In arterioles, the blood temperature comes close to the tissue temperature within a length on the order of 10 μm. Since arterioles are on the order of millimeters in length, the blood temperature exiting them would be essentially the same as the tissue temperature. There would then be no further temperature drop in the capillaries, which are the next smallest vessel. Thus, it is in the arterioles and slightly larger vessels in which the blood temperature equilibrates to the tissue temperature, not in the capillaries as Pennes described. Despite this flaw, the bioheat equation has proved a useful tool in analyzing heat transfer in the human body.
3. The properties of blood are moderately close to those of water. The property which differs most is the viscosity, as blood is more viscous than water. However, that change would have no effect on the foregoing calculations. Since the Reynolds number would be even smaller, the flow would still be laminar and the heat transfer would be unaffected.
4. Individual blood cells have dimensions on the order of the capillary diameter. Thus, for the capillaries, an accurate model of blood flow would account for the individual cells surrounded by plasma.

Patent Owner Manufacturing Resources International, Inc.
Exhibit 2017 - Page 518 of 999

8.4.2 The Entry Region

The energy equation for the entry region is more complicated than Equation 8.48 because there would be a radial advection term (since $v \neq 0$ in the entry region). In addition, both velocity and temperature now depend on x, as well as r, and the axial temperature gradient $\partial T/\partial x$ may no longer be simplified through Equation 8.32 or 8.33. However, two different entry length solutions have been obtained. The simplest solution is for the *thermal entry length problem*, and it is based on assuming that thermal conditions develop in the presence of a *fully developed velocity profile*. Such a situation would exist if the location at which heat transfer begins were preceded by an *unheated starting length*. It could also be assumed to a reasonable approximation for large Prandtl number fluids, such as oils. Even in the absence of an unheated starting length, velocity boundary layer development would occur far more rapidly than thermal boundary layer development for large Prandtl number fluids, and a thermal entry length approximation could be made. In contrast, the *combined* (thermal and velocity) *entry length problem* corresponds to the case for which the temperature and velocity profiles develop simultaneously.

Solutions have been obtained for both entry length conditions [2], and selected results are shown in Figure 8.10. As evident in Figure 8.10*a*, local Nusselt numbers, Nu_D, are, in principle, infinite at $x = 0$ and decay to their asymptotic (fully developed) values with increasing x. When plotted against the dimensionless parameter

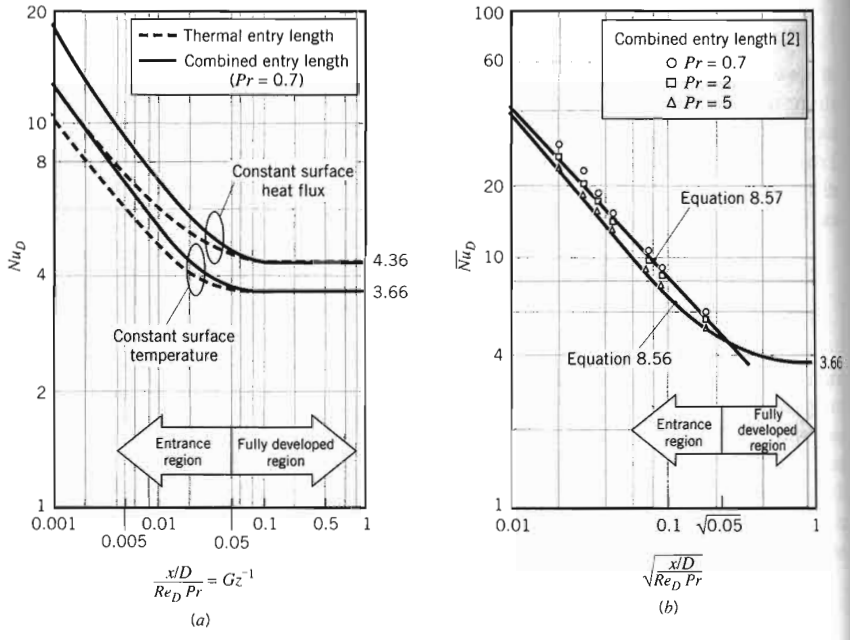


FIGURE 8.10 Results obtained from entry length solutions for laminar flow in a circular tube: (*a*) local Nusselt numbers and (*b*) average Nusselt numbers [2].

Patent Owner Manufacturing Resources International, Inc.
Exhibit 2017 - Page 519 of 999

$x\alpha/(u_m D^2) = x/(DRe_D Pr)$, which is the reciprocal of the *Graetz* number, $Gz_D \equiv (D/x)Re_D Pr$, the manner in which Nu_D varies with Gz_D^{-1} is independent of Pr for the thermal entry problem, since the fully developed velocity profile, given by Equation 8.13, is independent of the fluid viscosity. In contrast, for the combined entry length problem, results depend on the manner in which the velocity distribution develops, which is highly sensitive to the fluid viscosity. Hence, heat transfer results depend on the Prandtl number for the combined entry length case and are presented in Figure 8.10*a* for $Pr = 0.7$, which is representative of most gases. At any location within the entry region, Nu_D decreases with increasing Pr and approaches the thermal entry length condition as $Pr \to \infty$. Note that fully developed conditions are reached for $[(x/D)/Re_D Pr] \approx 0.05$.

For the *constant surface temperature* condition, it is desirable to know the *average* convection coefficient for use with Equation 8.43. Kays [7] presents a correlation attributed to Hausen [8], which is of the form

$$\overline{Nu}_D = 3.66 + \frac{0.0668(D/L)Re_D Pr}{1 + 0.04[(D/L)Re_D Pr]^{2/3}} \tag{8.56}$$

$$\left[\begin{array}{l}\text{thermal entrance length}\\ \textit{or}\\ \text{combined entrance length with } Pr \gtrsim 5\end{array}\right]$$

where $\overline{Nu}_D \equiv \overline{h}D/k$. Because this result is for the thermal entry length problem, it is applicable to all situations where the velocity profile is already fully developed. For the combined entry length, a suitable correlation for use at moderate Prandtl numbers, due to Sieder and Tate [9], is of the form

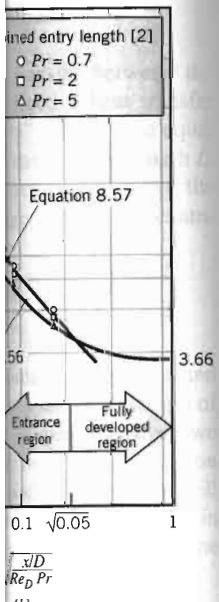
$$\overline{Nu}_D = 1.86\left(\frac{Re_D Pr}{L/D}\right)^{1/3}\left(\frac{\mu}{\mu_s}\right)^{0.14} \tag{8.57}$$

$$0.60 \lesssim Pr \lesssim 5$$

$$0.0044 \lesssim \left(\frac{\mu}{\mu_s}\right) \lesssim 9.75$$

Equation 8.57 is recommended for use when $0.60 \lesssim Pr \lesssim 5$, provided $\overline{Nu}_D \gtrsim 3.66$ [2, 10]. If $\overline{Nu}_D$ falls below this value, it is reasonable to use $\overline{Nu}_D = 3.66$, since fully developed conditions then encompass much of the tube. For larger Prandtl numbers ($Pr \gtrsim 5$), hydrodynamic conditions develop much faster than thermal conditions, and Equation 8.56 is recommended instead of Equation 8.57 [2]. Equations 8.56 and 8.57, along with numerical predictions of $\overline{Nu}_D$ versus $\sqrt{x/(D\,Re_D\,Pr)}$ and Pr, are shown in Figure 8.10*b*. All properties appearing in Equations 8.56 and 8.57, except μ_s, should be evaluated at the average value of the mean temperature, $\overline{T}_m = (T_{m,i} + T_{m,o})/2$.

The subject of laminar flow in ducts has been studied extensively, and numerous results are available for a variety of duct cross sections and surface conditions. These results have been compiled in a monograph by Shah and London [11] and in an updated review by Shah and Bhatti [12].



(*b*)

Patent Owner Manufacturing Resources International, Inc.
Exhibit 2017 - Page 520 of 999

8.5 *Convection Correlations: Turbulent Flow in Circular Tubes*

Since the analysis of turbulent flow conditions is a good deal more involved, greater emphasis is placed on determining empirical correlations. A classical expression for computing the *local* Nusselt number for *fully developed* (*hydrodynamically* and *thermally*) *turbulent flow* in a *smooth circular tube* is due to Colburn [13] and may be obtained from the Chilton–Colburn analogy. Substituting Equation 6.70 into Equation 8.18, the analogy is of the form

$$\frac{C_f}{2} = \frac{f}{8} = St\,Pr^{2/3} = \frac{Nu_D}{Re_D\,Pr}\,Pr^{2/3} \tag{8.58}$$

Substituting for the friction factor from Equation 8.21, the *Colburn equation* is then

$$Nu_D = 0.023 Re_D^{4/5}\,Pr^{1/3} \tag{8.59}$$

The *Dittus–Boelter equation* [14] is a slightly different and preferred version of the above result and is of the form[1]

$$Nu_D = 0.023 Re_D^{4/5}\,Pr^{n} \tag{8.60}$$

where $n = 0.4$ for heating ($T_s > T_m$) and 0.3 for cooling ($T_s < T_m$). These equations have been confirmed experimentally for the range of conditions

$$\begin{bmatrix} 0.6 \leq Pr \leq 160 \\ Re_D \geq 10{,}000 \\ \dfrac{L}{D} \geq 10 \end{bmatrix}$$

The equations may be used for small to moderate temperature differences, $T_s - T_m$, with all properties evaluated at T_m. For flows characterized by large property variations, the following equation, due to Sieder and Tate [9], is recommended:

$$Nu_D = 0.027 Re_D^{4/5}\,Pr^{1/3}\left(\frac{\mu}{\mu_s}\right)^{0.14} \tag{8.61}$$

$$\begin{bmatrix} 0.7 \leq Pr \leq 16{,}700 \\ Re_D \geq 10{,}000 \\ \dfrac{L}{D} \geq 10 \end{bmatrix}$$

[1] Although it has become common practice to refer to Equation 8.60 as the *Dittus–Boelter equation*, the original Dittus–Boelter equations are actually of the form

$Nu_D = 0.0243\,Re_D^{4/5}\,Pr^{0.4}$ (Heating)

$Nu_D = 0.0265\,Re_D^{4/5}\,Pr^{0.3}$ (Cooling)

The historical origins of Equation 8.60 are discussed by Winterton [14].

Patent Owner Manufacturing Resources International, Inc.
Exhibit 2017 - Page 521 of 999

where all properties except μ_s are evaluated at T_m. *To a good approximation, the foregoing correlations may be applied for both the uniform surface temperature and heat flux conditions.*

Although Equations 8.60 and 8.61 are easily applied and are certainly satisfactory for the purposes of this text, errors as large as 25% may result from their use. Such errors may be reduced to less than 10% through the use of more recent, but generally more complex, correlations [4, 15]. One correlation, valid over a large Reynolds number range including the transition region, is provided by Gnielinski [16]:

$$Nu_D = \frac{(f/8)(Re_D - 1000)Pr}{1 + 12.7(f/8)^{1/2}(Pr^{2/3} - 1)} \tag{8.62}$$

where the friction factor may be obtained from the Moody diagram, or, for smooth tubes, from Equation 8.21. The correlation is valid for $0.5 \leq Pr \leq 2000$ and $3000 \leq Re_D \leq 5 \times 10^6$. In using Equation 8.62, which applies for both uniform surface heat flux and temperature, properties should be evaluated at T_m. If temperature differences are large, additional consideration must be given to variable-property effects and available options are reviewed by Kakac [17].

We note that, unless specifically developed for the transition region ($2300 < Re_D < 10^4$), caution should be exercised when applying a turbulent flow correlation for $Re_D < 10^4$. If the correlation was developed for fully turbulent conditions ($Re_D > 10^4$), it may be used as a first approximation at smaller Reynolds numbers, with the understanding that the convection coefficient will be overpredicted. If a higher level of accuracy is desired, the Gnielinski correlation, Equation 8.62, may be used. A comprehensive discussion of heat transfer in the transition region is provided by Ghajar and Tam [18].

We also note that Equations 8.59 through 8.62 pertain to smooth tubes. For turbulent flow, the heat transfer coefficient increases with wall roughness, and, as a first approximation, it may be computed by using Equation 8.62 with friction factors obtained from the Moody diagram, Figure 8.3. However, although the general trend is one of increasing h with increasing f, the increase in f is proportionately larger, and when f is approximately four times larger than the corresponding value for a smooth surface, h no longer changes with additional increases in f [19]. Procedures for estimating the effect of wall roughness on convection heat transfer in fully developed turbulent flow are discussed by Bhatti and Shah [15].

Since entry lengths for turbulent flow are typically short, $10 \leq (x_{fd}/D) \leq 60$, it is often reasonable to assume that the average Nusselt number for the entire tube is equal to the value associated with the fully developed region, $\overline{Nu}_D \approx Nu_{D,fd}$. However, for short tubes $\overline{Nu}_D$ will exceed $Nu_{D,fd}$ and may be calculated from an expression of the form

$$\frac{\overline{Nu}_D}{Nu_{D,fd}} = 1 + \frac{C}{(x/D)^m} \tag{8.63}$$

where C and m depend on the nature of the inlet (e.g., sharp-edged or nozzle) and entry region (thermal or combined), as well as on the Prandtl and Reynolds numbers [2, 15, 20]. Typically, errors of less than 15% are associated with assuming

Patent Owner Manufacturing Resources International, Inc.
Exhibit 2017 - Page 522 of 999

$\overline{Nu}_D = Nu_{D,fd}$ for $(L/D) > 60$. When determining $\overline{Nu}_D$, all fluid properties should be evaluated at the arithmetic average of the mean temperature, $\overline{T}_m \equiv (T_{m,i} + T_{m,o})/2$.

Finally, we note that the foregoing correlations do not apply to liquid metals ($3 \times 10^{-3} \lesssim Pr \lesssim 5 \times 10^{-2}$). For fully developed turbulent flow in smooth circular tubes with constant surface heat flux, Skupinski et al. [21] recommend a correlation of the form

$$Nu_D = 4.82 + 0.0185 Pe_D^{0.827} \qquad q_s'' = \text{constant} \tag{8.64}$$

$$\begin{bmatrix} 3.6 \times 10^3 \lesssim Re_D \lesssim 9.05 \times 10^5 \\ 10^2 \lesssim Pe_D \lesssim 10^4 \end{bmatrix}$$

Similarly, for constant surface temperature Seban and Shimazaki [22] recommend the following correlation for $Pe_D \gtrsim 100$:

$$Nu_D = 5.0 + 0.025\, Pe_D^{0.8} \qquad T_s = \text{constant} \tag{8.65}$$

Extensive data and additional correlations are available in the literature [23].

EXAMPLE 8.6

Hot air flows with a mass rate of $\dot{m} = 0.050$ kg/s through an uninsulated sheet metal duct of diameter $D = 0.15$ m, which is in the crawlspace of a house. The hot air enters at 103°C and, after a distance of $L = 5$ m, cools to 77°C. The heat transfer coefficient between the duct outer surface and the ambient air at $T_\infty = 0$°C is known to be $h_o = 6$ W/m$^2 \cdot$ K.

1. Calculate the heat loss (W) from the duct over the length L.
2. Determine the heat flux and the duct surface temperature at $x = L$.

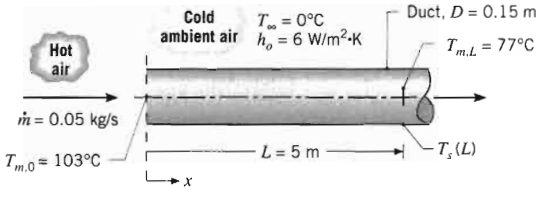
SOLUTION

Known: Hot air flowing in a duct.

Find:

1. Heat loss from the duct over the length L, q (W).
2. Heat flux and surface temperature at $x = L$.

Schematic:



Assumptions:

1. Steady-state conditions.
2. Constant properties.

Patent Owner Manufacturing Resources International, Inc.
Exhibit 2017 - Page 523 of 999

3. Ideal gas behavior.
4. Negligible viscous dissipation and negligible pressure variations.
5. Negligible duct wall thermal resistance.
6. Uniform convection coefficient at outer surface of duct.

Properties: Table A.4, air ($\bar{T}_m = 363$ K): $c_p = 1010$ J/kg · K. Table A.4, air ($T_{m,L} = 350$ K): $k = 0.030$ W/m · K, $\mu = 208.2 \times 10^{-7}$ N · s/m^2, $Pr = 0.70$.

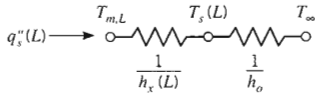
Analysis:

1. From the energy balance for the entire tube, Equation 8.34,

$$q = \dot{m} c_p (T_{m,L} - T_{m,0})$$

$$q = 0.05 \text{ kg/s} \times 1010 \text{ J/kg} \cdot \text{K} \, (77 - 103)^\circ\text{C} = -1313 \text{ W} \quad \triangleleft$$

2. An expression for the heat flux at $x = L$ may be inferred from the resistance network



where $h_x(L)$ is the inside convection heat transfer coefficient at $x = L$. Hence

$$q_s''(L) = \frac{T_{m,L} - T_\infty}{[1/h_x(L)] + (1/h_o)}$$

The inside convection coefficient may be obtained from knowledge of the Reynolds number. From Equation 8.6

$$Re_D = \frac{4\dot{m}}{\pi D \mu} = \frac{4 \times 0.05 \text{ kg/s}}{\pi \times 0.15 \text{ m} \times 208.2 \times 10^{-7} \text{ N} \cdot \text{s/m}^2} = 20{,}384$$

Hence the flow is turbulent. Moreover, with $(L/D) = (5/0.15) = 33.3$, it is reasonable to assume fully developed conditions at $x = L$. Hence from Equation 8.60, with $n = 0.3$,

$$Nu_D = \frac{h_x(L) D}{k} = 0.023 \, Re_D^{4/5} \, Pr^{0.3} = 0.023(20{,}384)^{4/5} \, (0.70)^{0.3} = 57.9$$

$$h_x(L) = Nu_D \frac{k}{D} = 57.9 \frac{0.030 \text{ W/m} \cdot \text{K}}{0.15 \text{ m}} = 11.6 \text{ W/m}^2 \cdot \text{K}$$

Hence

$$q_s''(L) = \frac{(77 - 0)^\circ \text{C}}{[(1/11.6) + (1/6.0)] \text{ m}^2 \cdot \text{K/W}} = 304.5 \text{ W/m}^2$$

Referring back to the network, it also follows that

$$q_s''(L) = \frac{T_{m,L} - T_{s,L}}{1/h_x(L)}$$

in which case

$$T_{s,L} = T_{m,L} - \frac{q_s''(L)}{h_x(L)} = 77^\circ\text{C} - \frac{304.5 \text{ W/m}^2}{11.6 \text{ W/m}^2 \cdot \text{K}} = 50.7^\circ\text{C} \quad \triangleleft$$

Patent Owner Manufacturing Resources International, Inc.
Exhibit 2017 - Page 524 of 999

Comments:

1. In using the energy balance of part 1 for the entire tube, properties (in this case, only c_p) are evaluated at $\overline{T}_m = (T_{m,0} + T_{m,L})/2$. However, in using the correlation for a local heat transfer coefficient, Equation 8.60, properties are evaluated at the local mean temperature, $T_{m,L} = 77°C$.
2. This problem is characterized neither by constant surface temperature nor by constant surface heat flux. It would therefore be erroneous to presume that the total heat loss from the tube is given by $q_s''(L)\pi DL = 717$ W. This result is substantially less than the actual heat loss of 1313 W because $q_s''(x)$ decreases with increasing x. This decrease in $q_s''(x)$ is due to reductions in both $h_x(x)$ and $[T_m(x) - T_\infty]$ with increasing x.

8.6 *Convection Correlations: Noncircular Tubes and the Concentric Tube Annulus*

Although we have thus far restricted our consideration to internal flows of circular cross section, many engineering applications involve convection transport in *noncircular tubes.* At least to a first approximation, however, many of the circular tube results may be applied by using *an effective diameter* as the characteristic length. It is termed the *hydraulic diameter* and is defined as

$$D_h \equiv \frac{4A_c}{P} \tag{8.66}$$

where A_c and P are the *flow* cross-sectional area and the *wetted perimeter,* respectively. It is this diameter that should be used in calculating parameters such as Re_D and Nu_D.

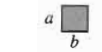
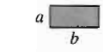
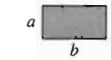
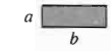
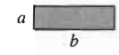
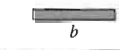
For turbulent flow, which still occurs if $Re_D \gtrsim 2300$, it is reasonable to use the correlations of Section 8.5 for $Pr \gtrsim 0.7$. However, in a noncircular tube the convection coefficients vary around the periphery, approaching zero in the corners. Hence in using a circular tube correlation, the coefficient is presumed to be an average over the perimeter.

For laminar flow, the use of circular tube correlations is less accurate, particularly with cross sections characterized by sharp corners. For such cases the Nusselt number corresponding to fully developed conditions may be obtained from Table 8.1, which is based on solutions of the differential momentum and energy equations for flow through the different duct cross sections. As for the circular tube, results differ according to the surface thermal condition. Nusselt numbers tabulated for a uniform surface heat flux presume a constant flux in the axial (flow) direction, but a constant temperature around the perimeter at any cross section. This condition is typical of highly conductive tube wall materials. Results tabulated for a uniform surface temperature apply when the temperature is constant in both the axial and peripheral directions.

Although the foregoing procedures are generally satisfactory, exceptions do exist. Detailed discussions of heat transfer in noncircular tubes are provided in several sources [11, 12, 24].

Patent Owner Manufacturing Resources International, Inc.
Exhibit 2017 - Page 525 of 999

TABLE 8.1 Nusselt numbers and friction factors for fully developed laminar flow in tubes of differing cross section

Cross Section	$\frac{b}{a}$	$Nu_D \equiv \frac{hD_h}{k}$ (Uniform q_s'')	$Nu_D \equiv \frac{hD_h}{k}$ (Uniform T_s)	$f\,Re_{D_h}$
	—	4.36	3.66	64
	1.0	3.61	2.98	57
	1.43	3.73	3.08	59
	2.0	4.12	3.39	62
	3.0	4.79	3.96	69
	4.0	5.33	4.44	73
	8.0	6.49	5.60	82
	∞	8.23	7.54	96
 Heated Insulated	∞	5.39	4.86	96
	—	3.11	2.49	53

Used with permission from W. M. Kays and M. E. Crawford, *Convection Heat and Mass Transfer*, 3rd ed. McGraw-Hill, New York, 1993.

Many internal flow problems involve heat transfer in a *concentric tube annulus* (Figure 8.11). Fluid passes through the space (annulus) formed by the concentric tubes, and convection heat transfer may occur to or from both the inner and outer tube surfaces. It is possible to independently specify the heat flux or temperature,

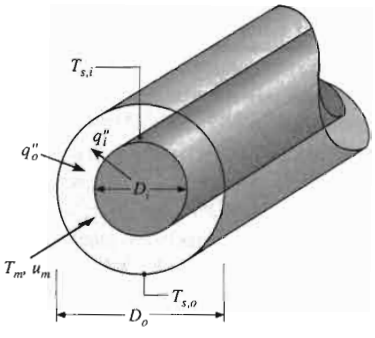


FIGURE 8.11
The concentric tube annulus.

Patent Owner Manufacturing Resources International, Inc.
Exhibit 2017 - Page 526 of 999

that is, the thermal condition, at each of these surfaces. In any case the heat flux from each surface may be computed with expressions of the form

$$q_i'' = h_i(T_{s,i} - T_m) \tag{8.67}$$

$$q_o'' = h_o(T_{s,o} - T_m) \tag{8.68}$$

Note that separate convection coefficients are associated with the inner and outer surfaces. The corresponding Nusselt numbers are of the form

$$Nu_i \equiv \frac{h_i D_h}{k} \tag{8.69}$$

$$Nu_o \equiv \frac{h_o D_h}{k} \tag{8.70}$$

where, from Equation 8.66, the hydraulic diameter D_h is

$$D_h = \frac{4(\pi/4)(D_o^2 - D_i^2)}{\pi D_o + \pi D_i} = D_o - D_i \tag{8.71}$$

For the case of fully developed laminar flow with one surface insulated and the other surface at a constant temperature, Nu_i or Nu_o may be obtained from Table 8.2. Note that in such cases we would be interested only in the convection coefficient associated with the isothermal (nonadiabatic) surface.

If uniform heat flux conditions exist at both surfaces, the Nusselt numbers may be computed from expressions of the form

$$Nu_i = \frac{Nu_{ii}}{1 - (q_o''/q_i'')\theta_i^*} \tag{8.72}$$

$$Nu_o = \frac{Nu_{oo}}{1 - (q_i''/q_o'')\theta_o^*} \tag{8.73}$$

The influence coefficients (Nu_{ii}, Nu_{oo}, θ_i^*, and θ_o^*) appearing in these equations may be obtained from Table 8.3. Note that q_i'' and q_o'' may be positive or negative, depending on whether heat transfer is to or from the fluid, respectively. Moreover, situations may arise for which the values of h_i and h_o are negative. Such results,

TABLE 8.2 Nusselt number for fully developed laminar flow in a circular tube annulus with one surface insulated and the other at constant temperature

D_i/D_o	Nu_i	Nu_o	*Comments*
0	—	3.66	See Equation 8.55
0.05	17.46	4.06	
0.10	11.56	4.11	
0.25	7.37	4.23	
0.50	5.74	4.43	
≈1.00	4.86	4.86	See Table 8.1, $b/a \rightarrow \infty$

Used with permission from W. M. Kays and H. C. Perkins, in W. M. Rohsenow and J. P. Hartnett, Eds., *Handbook of Heat Transfer,* Chap. 7, McGraw-Hill, New York, 1972.

8.7 Heat Transfe

Patent Owner Manufacturing Resources International, Inc.
Exhibit 2017 - Page 527 of 999

TABLE 8.3 Influence coefficients for fully developed laminar flow in a circular tube annulus with uniform heat flux maintained at both surfaces

D_i/D_o	Nu_{ii}	Nu_{oo}	θ_i^*	θ_o^*
0	—	4.364	∞	0
0.05	17.81	4.792	2.18	0.0294
0.10	11.91	4.834	1.383	0.0562
0.20	8.499	4.833	0.905	0.1041
0.40	6.583	4.979	0.603	0.1823
0.60	5.912	5.099	0.473	0.2455
0.80	5.58	5.24	0.401	0.299
1.00	5.385	5.385	0.346	0.346

Used with permission from W. M. Kays and H. C. Perkins, in W. M. Rohsenow and J. P. Hartnett, Eds., *Handbook of Heat Transfer*, Chap. 7, McGraw-Hill, New York, 1972.

when used with the sign convention implicit in Equations 8.67 and 8.68, reveal the relative magnitudes of T_s and T_m.

For fully developed turbulent flow, the influence coefficients are a function of the Reynolds and Prandtl numbers [24]. However, to a first approximation the inner and outer convection coefficients may be assumed to be equal, and they may be evaluated by using the hydraulic diameter, Equation 8.71, with the Dittus–Boelter equation, Equation 8.60.

8.7 *Heat Transfer Enhancement*

Several options are available for enhancing heat transfer associated with internal flows. Enhancement may be achieved by increasing the convection coefficient and/or by increasing the convection surface area. For example, h may be increased by introducing surface roughness to enhance turbulence, as, for example, through machining or insertion of a coil-spring wire. The wire insert (Figure 8.12*a*) provides a helical roughness element in contact with the tube inner surface. Alternatively, the convection coefficient may be increased by inducing swirl through insertion of a twisted tape (Figure 8.12*b*). The insert consists of a thin strip that is periodically twisted through 360°. Introduction of a tangential velocity component increases the speed of the flow, particularly near the tube wall. The heat transfer area may be increased by manufacturing a tube with a grooved inner surface (Figure 8.12*c*), while both the convection coefficient and area may be increased by using spiral fins or ribs (Figure 8.12*d*). In evaluating any heat transfer enhancement scheme, attention must also be given to the attendant increase in pressure drop and hence fan or pump power requirements. Comprehensive assessments of enhancement options have been published [25–28], and the *Journal of Enhanced Heat Transfer* provides access to recent developments in the field.

By coiling a tube (Figure 8.13), heat transfer may be enhanced without turbulence or additional heat transfer surface area. In this case, centrifugal forces within

Patent Owner Manufacturing Resources International, Inc.
Exhibit 2017 - Page 528 of 999

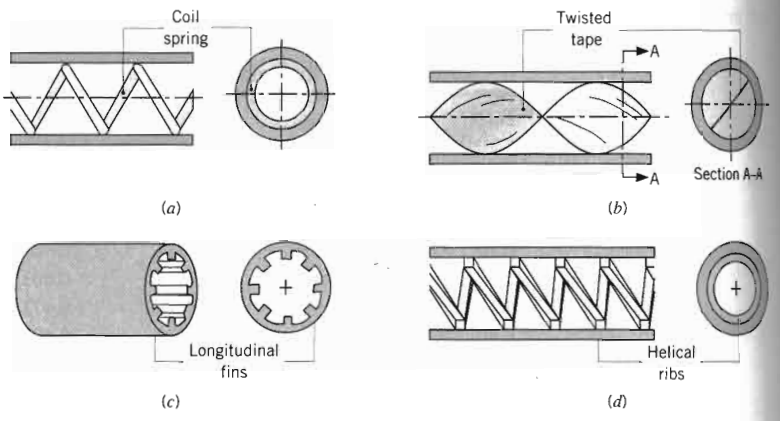


FIGURE 8.12 Internal flow heat transfer enhancement schemes: (*a*) longitudinal section and end view of coil-spring wire insert, (*b*) longitudinal section and cross-sectional view of twisted tape insert, (*c*) cut-away section and end view of longitudinal fins, and (*d*) longitudinal section and end view of helical ribs.

the fluid induce a *secondary flow* consisting of a pair of longitudinal vortices that, in contrast to conditions in a straight tube, can result in highly nonuniform local heat transfer coefficients around the periphery of the tube. Hence, local heat transfer coefficients vary with θ as well as x. If constant heat flux conditions are applied, the mean fluid temperature, $T_m(x)$, may be calculated using the conservation of energy principle, Equation 8.40. For situations where the fluid is heated, maximum fluid temperatures occur at the tube wall, but calculation of the maximum local temperature is not straightforward because of the θ-dependence of the heat transfer coefficient. Therefore, correlations for the *peripherally averaged* Nusselt number are of little use if constant heat flux conditions are applied. In contrast, correlations for the peripherally averaged Nusselt number for constant wall temperature boundary conditions are useful, and the relationships recommended by Shah and Joshi [29] are provided in the next paragraphs.

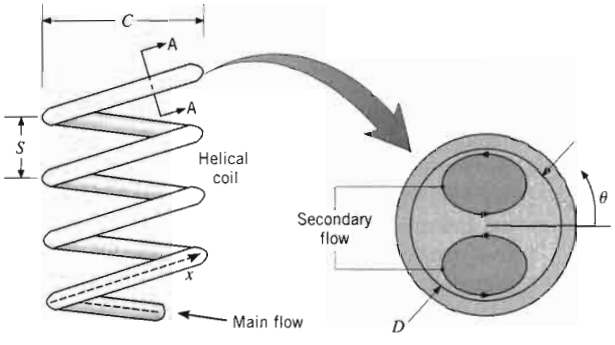
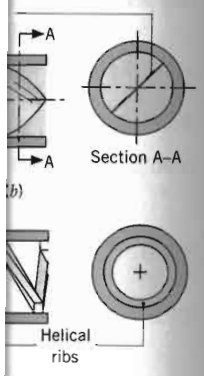


FIGURE 8.13 Schematic of helically coiled tube and secondary flow in enlarged cross-sectional view.

Patent Owner Manufacturing Resources International, Inc.
Exhibit 2017 - Page 529 of 999



(b)

(d)

ngitudinal section and
tional view of twisted
) longitudinal section

linal vortices that, in
nuniform local heat
local heat transfer
ions are applied, the
nservation of energy
ted, maximum fluid
mum local tempera-
heat transfer coeffi-
sselt number are of
correlations for the
ature boundary con-
and Joshi [29] are

The secondary flow increases friction losses and heat transfer rates. In addition, the secondary flow decreases entrance lengths and reduces the difference between laminar and turbulent heat transfer rates, relative to the straight tube cases considered previously in this chapter. Pressure drops and heat transfer rates exhibit little dependence on the coil pitch, S. The critical Reynolds number corresponding to the onset of turbulence for the helical tube, $Re_{D,c,h}$, is

$$Re_{D,c,h} = Re_{D,c}[1 + 12(D/C)^{0.5}] \tag{8.74}$$

where $Re_{D,c}$ is given in Equation 8.2 and C is defined in Figure 8.13. Strong secondary flow associated with tightly wound helically coiled tubes delays the transition to turbulence.

For fully developed laminar flow with $C/D \gtrsim 3$, the friction factor is

$$f = \frac{64}{Re_D} \qquad Re_D(D/C)^{1/2} \lesssim 30 \tag{8.19}$$

$$f = \frac{27}{Re_D^{0.725}}(D/C)^{0.1375} \qquad 30 \lesssim Re_D(D/C)^{1/2} \lesssim 300 \tag{8.75a}$$

$$f = \frac{7.2}{Re_D^{0.5}}(D/C)^{0.25} \qquad 300 \lesssim Re_D(D/C)^{1/2} \tag{8.75b}$$

For cases where $C/D \lesssim 3$, recommendations provided in [29] should be followed. The heat transfer coefficient for use in Equation 8.27 may be evaluated from a correlation of the form

$$Nu_D = \left[\left(3.66 + \frac{4.343}{a}\right)^3 + 1.158\left(\frac{Re_D(D/C)^{1/2}}{b}\right)^{3/2}\right]^{1/3}\left(\frac{\mu}{\mu_s}\right)^{0.14} \tag{8.76}$$

where

$$a = \left(1 + \frac{927(C/D)}{Re_D^2 Pr}\right) \qquad \text{and} \qquad b = 1 + \frac{0.477}{Pr} \tag{8.77a,b}$$

$$\begin{bmatrix} 0.005 \lesssim Pr \lesssim 1600 \\ 1 \lesssim Re_D(D/C)^{1/2} \lesssim 1000 \end{bmatrix}$$

Friction factor correlations for turbulent flow are based on limited data. Furthermore, heat transfer augmentation due to the secondary flow is minor when the flow is turbulent and is less than 10% for $C/D \gtrsim 20$. As such, augmentation by using helically coiled tubes is typically employed only for laminar flow situations. In laminar flow, the entrance length is 20% to 50% shorter than that of a straight tube, while the flow becomes fully developed within the first half-turn of the helically coiled tube under turbulent conditions. Therefore, the entrance region may be neglected in most engineering calculations.

When a gas or liquid is heated in a straight tube, a fluid parcel that enters near the centerline of the tube will exit the tube faster, and always be cooler than, a fluid parcel

Patent Owner Manufacturing Resources International, Inc.
Exhibit 2017 - Page 530 of 999

that enters near the tube wall. Hence, the *time-temperature histories* of individual fluid parcels, processed in the same heating tube, can be dramatically different. In addition to augmenting heat transfer, the secondary flow associated with the helically coiled tube serves to *mix* the fluid relative to laminar flow in a straight tube, resulting in similar time-temperature histories for all the fluid parcels. It is for this reason that coiled tubes are routinely used to process and manufacture highly viscous, high value-added fluids, such as pharmaceuticals, cosmetics, and personal care products.

8.8 *Microscale Internal Flow*

The tubes and channels considered so far have been characterized by hydraulic diameters of conventional size. Many new technologies involve microscale internal flows where the hydraulic diameters are in the range $D_h \lesssim 100\ \mu$m. An important motivation for developing various *microfluidic devices* is readily evident by inspecting the correlations for the Nusselt numbers associated with laminar, fully developed flow. Specifically, heat transfer coefficients are inversely proportional to the hydraulic diameter. Therefore, as the size of the flow channel is decreased significantly, a dramatic increase in heat transfer coefficients will occur [30].

8.8.1 Flow Conditions in Microscale Internal Flow

In Section 2.2.1, we saw that heat transfer in gases can be affected significantly as the characteristic length scale of the material volume, L, is reduced to the same order of magnitude as the mean free path of the gas, λ_{mfp}. At very small values of the hydraulic diameter D_h, therefore, the gas will no longer behave as a continuum. Because the continuum assumption has been made throughout our discussion of convection so far, the results of Chapters 6 through 8 are not expected to apply for gases when $D_h/\lambda_{mfp} \lesssim 10$, and recourse must be made to advanced methods to estimate the velocity distribution and pressure drops associated with internal flow [31].

For liquids, experiments have shown that, for laminar flow in circular tubes with diameters as small as 50 μm, Equations 8.19 and 8.22a successfully predict the pressure drop over the tube length [32]. These equations are expected to be valid for most liquids for hydraulic diameters as small as 1 μm [32, 33].

From the discussion in Section 6.3.1 one might anticipate that, since turbulence is characterized by the motion of relatively large parcels of fluid in conventional-sized devices, Equations 8.20 and 8.21 will not be applicable for flow in microfluidic devices because the volume of the fluid parcel is restricted by the hydraulic diameter of the channel. One may similarly anticipate that the criterion for the onset of turbulence, Equation 8.2, will be different for microscale internal flows. Careful measurements using various liquids have shown that the critical Reynolds number corresponding to the onset of turbulence is, in fact, well described by Equation 8.2 for liquid flow in tubes with diameters as small as 50 μm [32]. Since extremely high mean velocities are necessary to achieve $Re_D = 2300$, one is seldom concerned about turbulent microscale convection.

Patent Owner Manufacturing Resources International, Inc.
Exhibit 2017 - Page 531 of 999

8.8.2 Thermal Considerations in Microscale Internal Flow

Convective heat transfer in microscale internal flows continues to be the subject of ongoing research. The analytical results and convection correlations of Chapters 6 and 8 should not be used for gases when $D_h/\lambda_{mfp} \lesssim 10$ and should be used with caution for liquids when $D_h \lesssim 1$ μm.

EXAMPLE 8.7

Combinatorial chemistry and biology are used in the pharmaceutical and biotechnology industries to reduce the time and cost associated with producing new drugs. Scientists desire to create large populations of molecules, or *libraries*, that can be subsequently screened en masse. Producing vast libraries increases the probability that novel compounds of significant therapeutic value will be discovered. A crucial variable in producing new compounds is the temperature at which the reactants are processed.

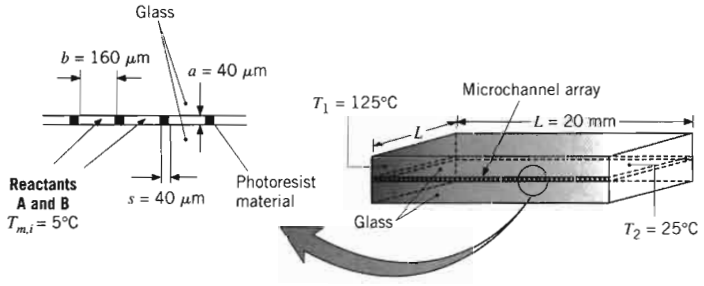
A *microreactor chip* is fabricated by first coating a 1-mm-thick glass microscope slide with a photoresist material. Lines are subsequently etched into the photoresist and a second glass plate is attached to the top of the structure, resulting in multiple parallel channels of rectangular cross section that are $a = 40$ μm deep, $b = 160$ μm wide, and $L = 20$ mm long. The spacing between channels is $s = 40$ μm, so that $N = L/(w + s) = 100$ channels are present within the 20 mm $\times$ 20 mm microreactor. A mixture of two reactants, both initially at $T_{m,i} = 5$°C, is introduced into each channel, and the edges of the chip are maintained at temperatures $T_1 = 125$°C and $T_2 = 25$°C so that the reactants in each channel are subject to a unique processing temperature. Flow is induced through the structure by applying an overall pressure difference of $\Delta P = 500$ kPa. The reactants and the product of reaction have thermophysical properties similar to ethylene glycol. Estimate the time that elapses for the entering reactants to come within 1°C of the desired processing temperature.

SOLUTION

Known: Dimensions and operating conditions for flow of reactants and product of reaction in a microreactor.

Find: Time needed to bring the reactants to within 1°C of the processing temperature.

Schematic:



Patent Owner Manufacturing Resources International, Inc.
Exhibit 2017 - Page 532 of 999

Assumptions:

1. Laminar flow.
2. Linear temperature distribution across the width of the microreactor.
3. Steady-state conditions.
4. Incompressible liquid with constant properties.
5. Negligible viscous dissipation.

Properties: Table A.5, ethylene glycol ($\overline{T}_m = 288$ K): $\rho = 1120.2$ kg/m^3, $c_p = 2359$ J/kg · K, $\mu = 2.82 \times 10^{-2}$ N · s/m^2, $k = 247 \times 10^{-3}$ W/m · K, $Pr = 269$. ($\overline{T}_m = 338$ K): $\rho = 1085$ kg/m^3, $c_p = 2583$ J/kg · K, $\mu = 0.427 \times 10^{-2}$, N · s/m^2, $k = 261 \times 10^{-3}$ W/m · K, $Pr = 45.2$.

Analysis: We will bracket the heat transfer and fluid flow behavior by evaluating the performance at the extreme processing temperatures.

The flow of reactants is induced by the applied pressure difference between the inlet and outlet of the microreactor. Because of the large variation of the viscosity with temperature, we expect the flow rate that is associated with the highest processing temperature to be the largest.

The perimeter of each microchannel is

$$P = 2a + 2b = 2 \times 40 \times 10^{-6}\ \text{m} + 2 \times 160 \times 10^{-6}\ \text{m} = 0.4 \times 10^{-3}\ \text{m}$$

and the hydraulic diameter of each microchannel is found from Equation 8.66 as

$$D_h = \frac{4A_c}{P} = \frac{4ab}{P} = \frac{4 \times 40 \times 10^{-6}\ \text{m} \times 160 \times 10^{-6}\ \text{m}}{0.4 \times 10^{-3}\ \text{m}} = 64 \times 10^{-6}\ \text{m}$$

We begin by assuming a relatively short entrance length, to be verified later, so the flow rate may be estimated by using the friction factor for fully developed conditions. From Table 8.1 for $b/a = 4$, $f = 73/Re_{D_h}$. Substituting this expression into Equation 8.22a, rearranging terms, and using properties at $T = 125$°C (in this equation and those following) results in

$$u_m = \frac{2}{73}\frac{D_h^2 \Delta p}{\mu L} = \frac{2}{73} \times \frac{(64 \times 10^{-6}\ \text{m})^2 \times 500 \times 10^3\ \text{N/m}^2}{0.427 \times 10^{-2}\ \text{N} \cdot \text{s/m}^2 \times 20 \times 10^{-3}\ \text{m}} = 0.657\ \text{m/s}$$

Hence, the Reynolds number is

$$Re_{D_h} = \frac{u_m D_h \rho}{\mu} = \frac{0.657\ \text{m/s} \times 64 \times 10^{-6}\ \text{m} \times 1085\ \text{kg/m}^3}{0.427 \times 10^{-2}\ \text{N} \cdot \text{s/m}^2} = 10.7$$

and the flow is deep in the laminar regime. Equation 8.3 may be used to determine the hydrodynamic entrance length, which is

$$x_{\text{fd},h} \approx 0.05 D_h Re_D = 0.05 \times 64 \times 10^{-6}\ \text{m} \times 10.7 = 34.2 \times 10^{-6}\ \text{m}$$

Patent Owner Manufacturing Resources International, Inc.
Exhibit 2017 - Page 533 of 999

and the thermal entrance length may be obtained from Equation 8.23, yielding

$$x_{fd,t} \approx x_{fd,h} Pr = 34.2 \times 10^{-6}\ \text{m} \times 45.2 = 1.55 \times 10^{-3}\ \text{m}$$

Both entrance lengths occupy less than 10% of the total microchannel length, $L = 20$ mm. Therefore, use of fully developed values of f are justified, and the mass flow rate for the $T = 125°C$ microchannel is

$$\dot{m} = \rho A_c u_m = \rho a b u_m = 1085\ \text{kg/m}^3 \times 40 \times 10^{-6}\ \text{m} \times 160 \times 10^{-6}\ \text{m} \times 0.657\ \text{m/s}$$
$$= 4.56 \times 10^{-6}\ \text{kg/s}$$

Equation 8.42 may now be used to determine the distance from the entrance of the microchannel to the location, x_c, where $T_{m,c} = 124°C$, that is, within 1°C of the surface temperature. The average heat transfer coefficient, $\bar{h}$, is replaced by the fully developed value of the heat transfer coefficient, h, because of the relatively short thermal entrance length. From Table 8.1, we see that for $b/a = 4$, $Nu_D = hD_h/k = 4.44$. Therefore,

$$\bar{h} \approx h = Nu_D \frac{k}{D_h} = 4.44 \times \frac{0.261\ \text{W/m} \cdot \text{K}}{64 \times 10^{-6}\ \text{m}} = 1.81 \times 10^4\ \text{W/m}^2 \cdot \text{K}$$

As expected from our discussion of microscale flows, the convection coefficient is extremely large.

Rearranging Equation 8.42 yields

$$x_c = \frac{\dot{m} c_p}{Ph} \ln\left[\frac{T_s - T_{m,i}}{T_s - T_{m,c}}\right] = \frac{4.56 \times 10^{-6}\ \text{kg/s} \times 2583\ \text{J/kg} \cdot \text{K}}{0.4 \times 10^{-3}\ \text{m} \times 1.81 \times 10^4\ \text{W/m}^2 \cdot \text{K}} \ln\left[\frac{(125 - 5)°C}{(125 - 124)°C}\right]$$
$$= 7.79 \times 10^{-3}\ \text{m}$$

Therefore, the time needed for the reactant to reach a mean temperature that is within 1°C of the processing temperature is

$$t_c = x_c/u_m = 7.79 \times 10^{-3}\ \text{m}/0.657\ \text{m/s} = 0.012\ \text{s} \quad \triangleleft$$

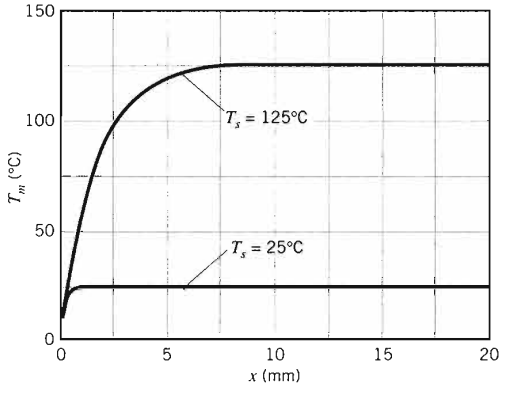
Repeating the calculations for the microchannel associated with the smallest processing temperature of 25°C yields $u_m = 0.0995$ m/s, $Re_D = 0.253$, $x_{fd,h} = 8.09 \times 10^{-7}$ m, $x_{fd,t} = 0.218 \times 10^{-3}$ m, $h = 1.71 \times 10^4$ W/m$^2 \cdot$ K, $x_c = 0.73 \times 10^{-3}$ m, and $t_c = 0.007$ s.

Comments:

1. The total thickness of the glass (2 mm) is 50 times greater than the depth of each microchannel, while the thermal conductivity of the glass, $k_{glass} \approx 1.4$ W/m $\cdot$ K (Table A.3), is 5 times greater than that of the fluid. The presence of such a small amount of fluid is expected to have a negligible effect on the linear temperature distribution that is established across the chip. The temperature difference across the bottom or top surface of each channel is approximately $\Delta T = (T_1 - T_2)b/L = (125 - 25)°C \times (160 \times 10^{-6}\ \text{m})/(20 \times 10^{-3}\ \text{m}) = 0.8°C$.

Patent Owner Manufacturing Resources International, Inc.
Exhibit 2017 - Page 534 of 999

2. Solving Equation 8.42 over the range $0 \leq x \leq L$ yields the axial variation of the mean temperature for the two extreme processing temperature channels, as shown below.



8.9 *Convection Mass Transfer*

Mass transfer by convection may also occur for internal flows. For example, a gas may flow through a tube whose surface has been wetted or is sublimable. Evaporation or sublimation will then occur, and a concentration boundary layer will develop. Just as the mean temperature is the appropriate reference temperature for heat transfer, the mean species concentration $\rho_{A,m}$ plays an analogous role for mass transfer. Defining the mass flow rate of species A in a duct of arbitrary cross section A_c as $\dot{m}_A = \rho_{A,m} u_m A_c = \int_{A_c} (\rho_A u) dA_c$, the mean species density is, accordingly,

$$\rho_{A,m} = \frac{\int_{A_c} (\rho_A u) dA_c}{u_m A_c} \tag{8.78a}$$

or for a circular tube,

$$\rho_{A,m} = \frac{2}{u_m r_o^2} \int_0^{r_o} (\rho_A u r)\, dr \tag{8.78b}$$

The concentration boundary layer development is characterized by entrance and fully developed regions, and Equation 8.23 may be used (with Pr replaced by Sc) to determine the *concentration entry length* $x_{fd,c}$ for laminar flow. Equation 8.4 may again be used as a first approximation for turbulent flow. Moreover, by analogy to Equation 8.28, for both laminar and turbulent flows, fully developed conditions exist when

$$\frac{\partial}{\partial x}\left[\frac{\rho_{A,s} - \rho_A(r, x)}{\rho_{A,s} - \rho_{A,m}(x)}\right]_{fd,c} = 0 \tag{8.79}$$

where a uniform species concentration $\rho_{A,s}$ is presumed to exist at the surface.

Patent Owner Manufacturing Resources International, Inc.
Exhibit 2017 - Page 535 of 999

The local mass flux of species A from the surface may be computed from an expression of the form

$$n''_A = h_m(\rho_{A,s} - \rho_{A,m}) \tag{8.80}$$

while the total rate of species transfer for a duct of surface area A_s may be expressed as

$$n_A = \bar{h}_m A_s \Delta\rho_{A,lm} \tag{8.81}$$

where the *log mean concentration difference*

$$\Delta\rho_{A,lm} = \frac{\Delta\rho_{A,o} - \Delta\rho_{A,i}}{\ln(\Delta\rho_{A,o}/\Delta\rho_{A,i})} \tag{8.82}$$

is analogous to the log mean temperature difference of Equation 8.44 and the concentration difference is defined as $\Delta\rho_A = \rho_{A,s} - \rho_{A,m}$. From application of conservation of species A to a control volume about the duct, the total rate of species transfer may also be expressed as

$$n_A = \frac{\dot{m}}{\rho}(\rho_{A,o} - \rho_{A,i}) \tag{8.83}$$

where ρ and $\dot{m}$ are the total mass density and flow rate, respectively, and $\dot{m}/\rho = u_m A_c$. Equations 8.81 and 8.83 are the mass transfer equivalents of Equations 8.43 and 8.34, respectively, for heat transfer. In addition, the analog to Equation 8.42 that characterizes the variation of the mean vapor density with distance x from the duct entrance may be expressed as

$$\frac{\rho_{A,s} - \rho_{A,m}(x)}{\rho_{A,s} - \rho_{A,m,i}} = \exp\left(-\frac{\bar{h}_m \rho P}{\dot{m}} x\right) \tag{8.84}$$

where P is the duct perimeter.

The convection mass transfer coefficients, h_m and $\bar{h}_m$, may be obtained from appropriate correlations for the corresponding Sherwood numbers, which are defined as $Sh_D = h_m D/D_{AB}$ and $\overline{Sh}_D = \bar{h}_m D/D_{AB}$. The specific form of a correlation may be inferred from the foregoing heat transfer results by invoking the heat and mass transfer analogy, with Sh_D and Sc substituted for Nu_D and Pr, respectively. For example, with a uniform vapor density at the surface of a circular duct and fully developed laminar flow through the duct,

$$Sh_D = 3.66 \tag{8.85}$$

For fully developed turbulent flow, the mass transfer analog to the Dittus–Boelter equation is

$$Sh_D = 0.023\, Re_D^{4/5}\, Sc^{0.4} \tag{8.86}$$

Microscale conditions for mass transfer are similar to those discussed for heat transfer in Section 8.8.

EXAMPLE 8.8

A thin liquid film of ammonia (NH_3), which has formed on the inner surface of a tube of diameter $D = 10$ mm and length $L = 1$ m, is removed by passing dry air

Patent Owner Manufacturing Resources International, Inc.
Exhibit 2017 - Page 536 of 999

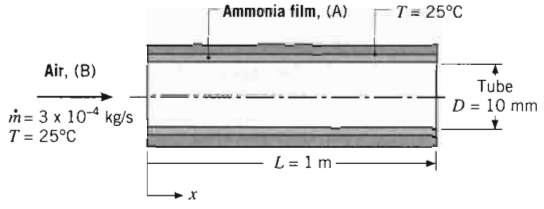
through the tube at a flow rate of 3×10^{-4} kg/s. The tube and the air are at 25°C. What is the average mass transfer convection coefficient?

SOLUTION

Known: Liquid ammonia on the inner surface of a tube is removed by evaporation into an airstream.

Find: Average mass transfer convection coefficient for the tube.

Schematic:



Assumptions:

1. Thin ammonia film with smooth surface.
2. Heat and mass transfer analogy is applicable.

Properties: Table A.4, air (25°C): $\nu = 15.7 \times 10^{-6}$ m²/s, $\mu = 183.6 \times 10^{-7}$ N · s/m². Table A.8, ammonia–air (25°C): $D_{AB} = 0.28 \times 10^{-4}$ m²/s, $Sc = (\nu/D_{AB}) = 0.56$.

Analysis: From Equation 8.6

$$Re_D = \frac{4 \times 3 \times 10^{-4}\ \text{kg/s}}{\pi \times 0.01\ \text{m} \times 183.6 \times 10^{-7}\ \text{N} \cdot \text{s/m}^2} = 2080$$

in which case the flow is laminar. Hence, since a constant ammonia vapor concentration is maintained at the surface of the film, which is analogous to a constant surface temperature, it follows from Equation 8.57 that

$$\overline{Sh}_D = 1.86\left(\frac{Re_D\, Sc}{L/D}\right)^{1/3} = 1.86 \times 2.27 = 4.22$$

Since $\overline{Sh}_D = 4.22 > 3.66$, use of Equation 8.57 is valid. Finally,

$$\overline{h}_m = \overline{Sh}_D \frac{D_{AB}}{D} = \frac{4.22 \times 0.28 \times 10^{-4}\ \text{m}^2/\text{s}}{0.01\ \text{m}} = 0.012\ \text{m/s}$$

Comments: From Equation 8.23, $x_{fd,c} \approx (0.05 Re_D\, Sc)D = 0.58$ m, and fully developed conditions exist over approximately 40% of the tube length. An assumption of fully developed conditions over the entire tube would provide a value of $\overline{Sh}_D = 3.66$, which is 13% less than the above result.

Patent Owner Manufacturing Resources International, Inc.
Exhibit 2017 - Page 537 of 999

8.10 Summary

In this chapter we have considered forced convection heat and mass transfer for an important class of problems involving *internal flow*. Such flows are encountered in numerous applications, and you should be able to perform engineering calculations that involve an energy balance and appropriate convection correlations. The methodology involves determining whether the flow is laminar or turbulent and establishing the length of the entry region. After deciding whether you are interested in local conditions (at a particular axial location) or in average conditions (for the entire tube), the convection correlation may be selected and used with the appropriate form of the energy balance to solve the problem. A summary of the correlations is provided in Table 8.4.

You should test your understanding of related concepts by addressing the following questions.

- What are the salient features of a *hydrodynamic entry region*? A *thermal entry region*? Are hydrodynamic and thermal entry lengths equivalent? If not, on what do the relative lengths depend?
- What are the salient *hydrodynamic* features of *fully developed flow*? How is the friction factor for fully developed flow affected by wall roughness?
- To what important characteristic of an internal flow is the *mean* or *bulk temperature* linked?
- What are the salient *thermal* features of *fully developed flow*?
- If fluid enters a tube at a uniform temperature and there is heat transfer to or from the surface of the tube, how does the convection coefficient vary with distance along the tube?
- For fluid flow through a tube with a uniform surface heat flux, how does the mean temperature of the fluid vary with distance from the tube entrance in (a) the entrance region and (b) the fully developed region? How does the surface temperature vary with distance in the entrance and fully developed regions?
- For heat transfer to or from a fluid flowing through a tube with a uniform surface temperature, how does the mean temperature of the fluid vary with distance from the entrance? How does the surface heat flux vary with distance from the entrance?
- Why is a *log mean temperature difference*, rather than an arithmetic mean temperature difference, used to calculate the total rate of heat transfer to or from a fluid flowing through a tube with a constant surface temperature?
- What two equations may be used to calculate the total heat rate to a fluid flowing through a tube with a uniform surface heat flux? What two equations may be used to calculate the total heat rate to or from a fluid flowing through a tube with a uniform surface temperature?
- Under what conditions is the Nusselt number associated with internal flow equal to a constant value, independent of Reynolds number and Prandtl number?
- Is the average Nusselt number associated with flow through a tube larger than, equal to, or less than the Nusselt number for fully developed conditions? Why?
- How is the characteristic length defined for a noncircular tube?
- What are the salient features of a *concentration entry region*?

Patent Owner Manufacturing Resources International, Inc.
Exhibit 2017 - Page 538 of 999

TABLE 8.4 Summary of convection correlations for flow in a circular tube[a,b,e]

Correlation		Conditions
$f = 64/Re_D$	(8.19)	Laminar, fully developed
$Nu_D = 4.36$	(8.53)	Laminar, fully developed, uniform q_s''
$Nu_D = 3.66$	(8.55)	Laminar, fully developed, uniform T_s
$\overline{Nu}_D = 3.66 + \dfrac{0.0668(D/L)Re_D\,Pr}{1 + 0.04[(D/L)Re_D\,Pr]^{2/3}}$	(8.56)	Laminar, thermal entry (or combined entry with $Pr \gtrsim 5$), uniform T_s
or		
$\overline{Nu}_D = 1.86\left(\dfrac{Re_D\,Pr}{L/D}\right)^{1/3}\left(\dfrac{\mu}{\mu_s}\right)^{0.14}$	(8.57)	Laminar, combined entry, $0.6 \lesssim Pr \lesssim 5$, $0.0044 \lesssim (\mu/\mu_s) \lesssim 9.75$, uniform T_s
$f = 0.316Re_D^{-1/4}$	(8.20a)[c]	Turbulent, fully developed, $Re_D \lesssim 2 \times 10^4$
$f = 0.184Re_D^{-1/5}$	(8.20b)[c]	Turbulent, fully developed, $Re_D \gtrsim 2 \times 10^4$
or		
$f = (0.790 \ln Re_D - 1.64)^{-2}$	(8.21)[c]	Turbulent, fully developed, $3000 \lesssim Re_D \lesssim 5 \times 10^6$
$Nu_D = 0.023Re_D^{4/5}\,Pr^n$	(8.60)[d]	Turbulent, fully developed, $0.6 \lesssim Pr \lesssim 160$, $Re_D \gtrsim 10{,}000$, $(L/D) \gtrsim 10$, $n = 0.4$ for $T_s > T_m$ and $n = 0.3$ for $T_s < T_m$
or		
$Nu_D = 0.027Re_D^{4/5}\,Pr^{1/3}\left(\dfrac{\mu}{\mu_s}\right)^{0.14}$	(8.61)[d]	Turbulent, fully developed, $0.7 \lesssim Pr \lesssim 16{,}700$, $Re_D \gtrsim 10{,}000$, $L/D \gtrsim 10$
or		
$Nu_D = \dfrac{(f/8)(Re_D - 1000)Pr}{1 + 12.7(f/8)^{1/2}(Pr^{2/3} - 1)}$	(8.62)[d]	Turbulent, fully developed, $0.5 \lesssim Pr \lesssim 2000$, $3000 \lesssim Re_D \lesssim 5 \times 10^6$, $(L/D) \gtrsim 10$
$Nu_D = 4.82 + 0.0185(Re_D\,Pr)^{0.827}$	(8.64)	Liquid metals, turbulent, fully developed, uniform q_s'', $3.6 \times 10^3 \lesssim Re_D \lesssim 9.05 \times 10^5$, $10^2 \lesssim Pe_D \lesssim 10^4$
$Nu_D = 5.0 + 0.025(Re_D\,Pr)^{0.8}$	(8.65)	Liquid metals, turbulent, fully developed, uniform T_s, $Pe_D \gtrsim 100$

[a]The mass transfer correlations may be obtained by replacing Nu_D and Pr by Sh_D and Sc, respectively.
[b]Properties in Equations 8.53, 8.55, 8.60, 8.61, 8.62, 8.64, and 8.65 are based on T_m; properties in Equations 8.19, 8.20, and 8.21 are based on $T_f \equiv (T_s + T_m)/2$; properties in Equations 8.56 and 8.57 are based on $\overline{T}_m \equiv (T_{m,i} + T_{m,o})/2$.
[c]Equations 8.20 and 8.21 pertain to smooth tubes. For rough tubes, Equation 8.62 should be used with the results of Figure 8.3.
[d]As a first approximation, Equations 8.60, 8.61, or 8.62 may be used to evaluate the average Nusselt number $\overline{Nu}_D$ over the entire tube length, if $(L/D) \gtrsim 10$. The properties should then be evaluated at the average of the mean temperature, $\overline{T}_m \equiv (T_{m,i} + T_{m,o})/2$.
[e]For tubes of noncircular cross section, $Re_D \equiv D_h u_m/\nu$, $D_h \equiv 4A_c/P$, and $u_m = \dot{m}/\rho A_c$. Results for fully developed laminar flow are provided in Table 8.1. For turbulent flow, Equation 8.60 may be used as a first approximation.

References

1. Langhaar, H. L.,
2. Kays, W. M., an *Mass Transfer*, 3
3. Moody, L. F., *Tr*
4. Petukhov, B. S., *Advances in He* New York, 1970
5. Chen, M. M., ar **335**, 137, 1980.
6. Chato, J. C., *J. B*
7. Kays, W. M., *Tr*
8. Hausen, H., *Z. V.*
9. Sieder, E. N., an 1936.
10. Whitaker, S., *AI*
11. Shah, R. K., an *Convection in D*
12. Shah, R. K., and and W. Aung, Ed *Heat Transfer*, (1987.
13. Colburn, A. P., *T*
14. Winterton, R. H. 1998.
15. Bhatti, M. S., ar and W. Aung, E *tive Heat Trans* York, 1987.
16. Gnielinski, V., *I*
17. Kakac, S., in S. *Handbook of S* Chap. 18, Wiley-

Patent Owner Manufacturing Resources International, Inc.
Exhibit 2017 - Page 539 of 999

- What are the salient features of fully developed flow for mass transfer?
- How may convection mass transfer correlations be inferred?

Several features that complicate internal flows have not been considered in this chapter. For example, a situation may exist for which there is a prescribed axial variation in T_s or q_s'', rather than uniform surface conditions. Among other things, such a variation would preclude the existence of a fully developed region. There may also exist surface roughness effects, circumferential heat flux or temperature variations, widely varying fluid properties, or transition flow conditions. For a complete discussion of these effects, the literature should be consulted [11, 12, 15, 17, 24].

References

1. Langhaar, H. L., *J. Appl. Mech.*, **64**, A-55, 1942.
2. Kays, W. M., and M. E. Crawford, *Convective Heat and Mass Transfer*, 3rd ed. McGraw-Hill, New York, 1993.
3. Moody, L. F., *Trans. ASME*, **66**, 671, 1944.
4. Petukhov, B. S., in T. F. Irvine and J. P. Hartnett, Eds., *Advances in Heat Transfer*, Vol. 6, Academic Press, New York, 1970.
5. Chen, M. M., and K. R. Holmes, *Ann. N. Y. Acad. Sci.*, **335**, 137, 1980.
6. Chato, J. C., *J. Biomech. Eng.*, **102**, 110, 1980.
7. Kays, W. M., *Trans. ASME*, **77**, 1265, 1955.
8. Hausen, H., *Z. VDI Beih. Verfahrenstech.*, **4**, 91, 1943.
9. Sieder, E. N., and G. E. Tate, *Ind. Eng. Chem.*, **28**, 1429, 1936.
10. Whitaker, S., *AIChE J.*, **18**, 361, 1972.
11. Shah, R. K., and A. L. London, *Laminar Flow Forced Convection in Ducts*, Academic Press, New York, 1978.
12. Shah, R. K., and M. S. Bhatti, in S. Kakac, R. K. Shah, and W. Aung, Eds., *Handbook of Single-Phase Convective Heat Transfer*, Chap. 3, Wiley-Interscience, New York, 1987.
13. Colburn, A. P., *Trans. AIChE*, **29**, 174, 1933.
14. Winterton, R. H. S., *Int. J. Heat Mass Transfer*, **41**, 809, 1998.
15. Bhatti, M. S., and R. K. Shah, in S. Kakac, R. K. Shah, and W. Aung, Eds., *Handbook of Single-Phase Convective Heat Transfer*, Chap. 4, Wiley-Interscience, New York, 1987.
16. Gnielinski, V., *Int. Chem. Eng.*, **16**, 359, 1976.
17. Kakac, S., in S. Kakac, R. K. Shah, and W. Aung, Eds., *Handbook of Single-Phase Convective Heat Transfer*, Chap. 18, Wiley-Interscience, New York, 1987.
18. Ghajar, A. J., and L.-M. Tam, *Exp. Thermal and Fluid Science*, **8**, 79, 1994.
19. Norris, R. H., in A. E. Bergles and R. L. Webb, Eds., *Augmentation of Convective Heat and Mass Transfer*, ASME, New York, 1970.
20. Molki, M., and E. M. Sparrow, *J. Heat Transfer*, **108**, 482, 1986.
21. Skupinski, E. S., J. Tortel, and L. Vautrey, *Int. J. Heat Mass Transfer*, **8**, 937, 1965.
22. Seban, R. A., and T. T. Shimazaki, *Trans. ASME*, **73**, 803, 1951.
23. Reed, C. B., in S. Kakac, R. K. Shah, and W. Aung, Eds., *Handbook of Single-Phase Convective Heat Transfer*, Chap. 8, Wiley-Interscience, New York, 1987.
24. Kays, W. M., and H. C. Perkins, in W. M. Rohsenow, J. P. Hartnett, and E. N. Ganic, Eds., *Handbook of Heat Transfer, Fundamentals*, Chap. 7, McGraw-Hill, New York, 1985.
25. Bergles, A. E., "Principles of Heat Transfer Augmentation," *Heat Exchangers, Thermal-Hydraulic Fundamentals and Design*, Hemisphere Publishing, New York, 1981, pp. 819–842.
26. Webb, R. L., in S. Kakac, R. K. Shah, and W. Aung, Eds., *Handbook of Single-Phase Convective Heat Transfer*, Chap. 17, Wiley-Interscience, New York, 1987.
27. Webb, R. L., *Principles of Enhanced Heat Transfer*, Wiley, New York, 1993.
28. Manglik, R. M., and A. E. Bergles, in J. P. Hartnett, T. F. Irvine, Y. I. Cho, and R. E. Greene, Eds., *Advances in Heat Transfer*, Vol. 36, Academic Press, New York, 2002.
29. Shah, R. K., and S. D. Joshi, in *Handbook of Single-Phase Convective Heat Transfer*, Chap. 5, Wiley-Interscience, New York, 1987.

Patent Owner Manufacturing Resources International, Inc.
Exhibit 2017 - Page 540 of 999

30. Jensen, K. F., *Chem. Eng. Sci.*, **56**, 293, 2001.
31. Kaviany, M., *Principles of Convective Heat Transfer*, Springer-Verlag, New York, 1994.
32. Sharp, K. V., and R. J. Adrian, *Exp. Fluids*, **36**, 741, 2004.
33. Travis, K. P., B. D. Todd, and D. J. Evans, *Phys. Rev. E*, **55**, 4288, 1997.

Problems

Hydrodynamic Considerations

8.1 Fully developed conditions are known to exist for water flowing through a 25-mm-diameter tube at 0.01 kg/s and 27°C. What is the maximum velocity of the water in the tube? What is the pressure gradient associated with the flow?

8.2 What is the pressure drop associated with water at 27°C flowing with a mean velocity of 0.2 m/s through a 600-m-long cast iron pipe of 0.15-m inside diameter?

8.3 Water at 27°C flows with a mean velocity of 1 m/s through a 1-km-long pipe of 0.25-m inside diameter.

(a) Determine the pressure drop over the pipe length and the corresponding pump power requirement, if the pipe surface is smooth.

(b) If the pipe is made of cast iron and its surface is clean, determine the pressure drop and pump power requirement.

(c) For the smooth pipe condition, generate a plot of pressure drop and pump power requirement for mean velocities in the range from 0.05 to 1.5 m/s.

8.4 An engine oil cooler consists of a bundle of 25 smooth tubes, each of length $L = 2.5$ m and diameter $D = 10$ mm.

(a) If oil at 300 K and a total flow rate of 24 kg/s is in fully developed flow through the tubes, what is the pressure drop and the pump power requirement?

(b) Compute and plot the pressure drop and pump power requirement as a function of flow rate for $10 \leq \dot{m} \leq 30$ kg/s.

8.5 For fully developed laminar flow through a parallel-plate channel, the x-momentum equation has the form

$$\mu\left(\frac{d^2u}{dy^2}\right) = \frac{dp}{dx} = \text{constant}$$

The purpose of this problem is to develop expressions for the velocity distribution and pressure gradient analogous to those for the circular tube in Section 8.1.

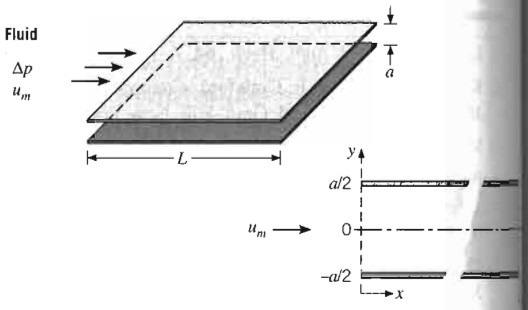
(a) Show that the velocity profile, $u(y)$, is parabolic and of the form

$$u(y) = \frac{3}{2}u_m\left[1 - \frac{y^2}{(a/2)^2}\right]$$

where u_m is the mean velocity

$$u_m = -\frac{a^2}{12\mu}\left(\frac{dp}{dx}\right)$$

and $-dp/dx = \Delta p/L$, where Δp is the pressure drop across the channel of length L.



(b) Write an expression defining the friction factor, f, using the hydraulic diameter D_h as the characteristic length. What is the hydraulic diameter for the parallel-plate channel?

(c) The friction factor is estimated from the expression $f = C/Re_{D_h}$, where C depends upon the flow cross section, as shown in Table 8.1. What is the coefficient C for the parallel-plate channel?

(d) Air flow in a parallel-plate channel with a separation of 5 mm and a length of 200 mm experiences a pressure drop of $\Delta p = 3.75$ N/m^2. Calculate the mean velocity and the Reynolds number for air at atmospheric pressure and 300 K. Is the assumption of fully developed flow reasonable for this application? If not, what is the effect on the estimate for u_m?

Thermal Entry Length and Energy Balance Considerations

8.6 Consider pressurized water, engine oil (unused), and NaK (22%/78%) flowing in a 20-mm-diameter tube.

(a) Determine the mean velocity, the hydrodynamic entry length, and the thermal entry length for each of the fluids when the fluid temperature is 366 K and the flow rate is 0.01 kg/s.

(b) Determine th
entry length,
and engine oi
of 0.02 m/s.

8.7 Velocity and tem
tube of radius r_o =

$u(r) = 0.$
$T(r) = 3$

with units of m/s
responding value
at this axial positi

8.8 At a particular a
profiles for lamin
the form

$u(y) = 0.$
$T(y) = 5.$

with units of m/s

Fluid

Determine corre
u_m, and mean (o
ity and temperat
and T_m appear re

8.9 In Chapter 1, it
uids, flow work
steady-flow ener
trans-Alaska pip
long distances ca
reasonable to que
nificant. Consider
eter $D = 1.2$ m, v
properties are ρ =
0.765 N · s/m^2. (
work, and the ter

8.10 When viscous d
(multiplied by ρc_p

$$\rho c_p u\frac{\partial T}{\partial x}$$

This problem ex
pation. The condi
fully developed f
Equation 8.15.

Patent Owner Manufacturing Resources International, Inc.
Exhibit 2017 - Page 541 of 999

(b) Determine the mass flow rate, the hydrodynamic entry length, and the thermal entry length for water and engine oil at 300 and 400 K and a mean velocity of 0.02 m/s.

8.7 Velocity and temperature profiles for laminar flow in a tube of radius $r_o = 10$ mm have the form

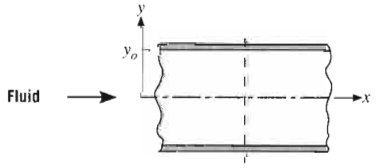
$$u(r) = 0.1[1 - (r/r_o)^2]$$
$$T(r) = 344.8 + 75.0(r/r_o)^2 - 18.8(r/r_o)^4$$

with units of m/s and K, respectively. Determine the corresponding value of the mean (or bulk) temperature, T_m, at this axial position.

8.8 At a particular axial station, velocity and temperature profiles for laminar flow in a parallel plate channel have the form

$$u(y) = 0.75[1 - (y/y_o)^2]$$
$$T(y) = 5.0 + 95.66(y/y_o)^2 - 47.83(y/y_o)^4$$

with units of m/s and °C, respectively.



Determine corresponding values of the mean velocity, u_m, and mean (or bulk) temperature, T_m. Plot the velocity and temperature distributions. Do your values of u_m and T_m appear reasonable?

8.9 In Chapter 1, it was stated that for incompressible liquids, flow work could usually be neglected in the steady-flow energy equation (Equation 1.11d). In the trans-Alaska pipeline, the high viscosity of the oil and long distances cause significant pressure drops, and it is reasonable to question whether flow work would be significant. Consider a $L = 100$ km length of pipe of diameter $D = 1.2$ m, with oil flow rate $\dot{m} = 500$ kg/s. The oil properties are $\rho = 900$ kg/m^3, $c_p = 2000$ J/kg · K, $\mu = 0.765$ N · s/m^2. Calculate the pressure drop, the flow work, and the temperature rise caused by the flow work.

8.10 When viscous dissipation is included, Equation 8.48 (multiplied by ρc_p) becomes

$$\rho c_p u \frac{\partial T}{\partial x} = \frac{k}{r}\frac{\partial}{\partial r}\left(r\frac{\partial T}{\partial r}\right) + \mu\left(\frac{du}{dr}\right)^2$$

This problem explores the importance of viscous dissipation. The conditions under consideration are laminar, fully developed flow in a circular pipe, with u given by Equation 8.15.

(a) By integrating the left-hand side over a section of a pipe of length L and radius r_o, show that this term yields the right-hand side of Equation 8.34.

(b) Integrate the viscous dissipation term over the same volume.

(c) Find the temperature rise caused by viscous dissipation by equating the two terms calculated above. Use the same conditions as in Problem 8.9.

8.11 Water enters a tube at 27°C with a flow rate of 450 kg/h. The heat transfer from the tube wall to the fluid is given as q_s' (W/m) $= ax$, where the coefficient a is 20 W/m^2 and x (m) is the axial distance from the tube entrance.

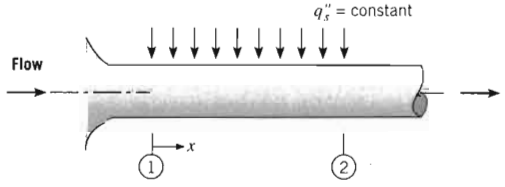
(a) Beginning with a properly defined differential control volume in the tube, derive an expression for the temperature distribution $T_m(x)$ of the water.

(b) What is the outlet temperature of the water for a heated section 30 m long?

(c) Sketch the mean fluid temperature, $T_m(x)$, and the tube wall temperature, $T_s(x)$, as a function of distance along the tube for fully developed *and* developing flow conditions.

(d) What value of a uniform wall heat flux, q_s'' (instead of $q_s' = ax$), would provide the same fluid outlet temperature as that determined in part (b)? For this type of heating, sketch the temperature distributions requested in part (c).

8.12 Consider flow in a circular tube. Within the test section length (between 1 and 2) a constant heat flux q_s'' is maintained.

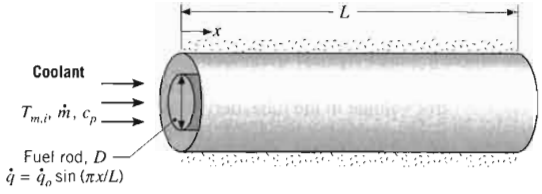


(a) For the following two cases, sketch the surface temperature $T_s(x)$ and the fluid mean temperature $T_m(x)$ as a function of distance along the test section x. In case A, flow is hydrodynamically and thermally fully developed. In case B, flow is not developed.

(b) Assuming that the surface flux q_s'' and the inlet mean temperature $T_{m,1}$ are identical for both cases, will the exit mean temperature $T_{m,2}$ for case A be greater than, equal to, or less than $T_{m,2}$ for case B? Briefly explain why.

Patent Owner Manufacturing Resources International, Inc.
Exhibit 2017 - Page 542 of 999

8.13 Consider a cylindrical nuclear fuel rod of length L and diameter D that is encased in a concentric tube. Pressurized water flows through the annular region between the rod and the tube at a rate $\dot{m}$, and the outer surface of the tube is well insulated. Heat generation occurs within the fuel rod, and the volumetric generation rate is known to vary sinusoidally with distance along the rod. That is, $\dot{q}(x) = \dot{q}_o \sin(\pi x/L)$, where $\dot{q}_o$ (W/m^3) is a constant. A uniform convection coefficient h may be assumed to exist between the surface of the rod and the water.



(a) Obtain expressions for the local heat flux $q''(x)$ and the total heat transfer q from the fuel rod to the water.

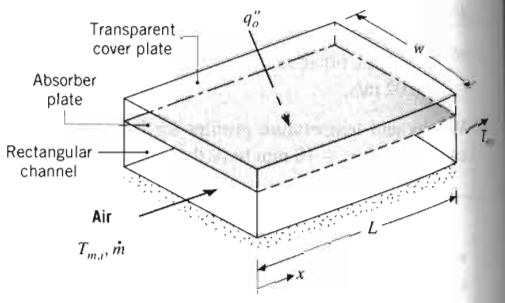
(b) Obtain an expression for the variation of the mean temperature $T_m(x)$ of the water with distance x along the tube.

(c) Obtain an expression for the variation of the rod surface temperature $T_s(x)$ with distance x along the tube. Develop an expression for the x location at which this temperature is maximized.

8.14 In a particular application involving fluid flow at a rate $\dot{m}$ through a circular tube of length L and diameter D, the surface heat flux is known to have a sinusoidal variation with x, which is of the form $q''_s(x) = q''_{s,m} \sin(\pi x/L)$. The maximum flux, $q''_{s,m}$, is a known constant, and the fluid enters the tube at a known temperature, $T_{m,i}$. Assuming the convection coefficient to be constant, how do the mean temperature of the fluid and the surface temperature vary with x?

8.15 A flat-plate solar collector is used to heat atmospheric air flowing through a rectangular channel. The bottom surface of the channel is well insulated, while the top surface is subjected to a uniform heat flux q''_o, which is due to the net effect of solar radiation absorption and heat exchange between the absorber and cover plates.

(a) Beginning with an appropriate differential control volume, obtain an equation that could be used to determine the mean air temperature $T_m(x)$ as a function of distance along the channel. Solve this equation to obtain an expression for the mean temperature of the air leaving the collector.



(b) With air inlet conditions of $\dot{m} = 0.1$ kg/s and $T_{m,i} = 40°C$, what is the air outlet temperature if $L = 3$ m, $w = 1$ m, and $q''_o = 700$ W/m^2? The specific heat of air is $c_p = 1008$ J/kg · K.

8.16 Atmospheric air enters the heated section of a circular tube at a flow rate of 0.005 kg/s and a temperature of 20°C. The tube is of diameter $D = 50$ mm, and fully developed conditions with $h = 25$ W/m^2 · K exist over the entire length of $L = 3$ m.

(a) For the case of uniform surface heat flux at $q''_s = 1000$ W/m^2, determine the total heat transfer rate q and the mean temperature of the air leaving the tube $T_{m,o}$. What is the value of the surface temperature at the tube inlet $T_{s,i}$ and outlet $T_{s,o}$? Sketch the axial variation of T_s and T_m. On the same figure, also sketch (qualitatively) the axial variation of T_s and T_m for the more realistic case in which the local convection coefficient varies with x.

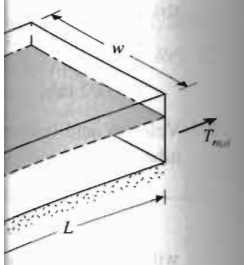
(b) If the surface heat flux varies linearly with x, such that q''_s (W/m^2) = 500x (m), what are the values of q, $T_{m,o}$, $T_{s,i}$, and $T_{s,o}$? Sketch the axial variation of T_s and T_m. On the same figure, also sketch (qualitatively) the axial variation of T_s and T_m for the more realistic case in which the local convection coefficient varies with x.

(c) For the two heating conditions of parts (a) and (b), plot the mean fluid and surface temperatures, $T_m(x)$ and $T_s(x)$, respectively, as functions of distance along the tube. What effect will a fourfold increase in the convection coefficient have on the temperature distributions?

(d) For each type of heating process, what heat fluxes are required to achieve an air outlet temperature of 125°C? Plot the temperature distributions.

8.17 Water at 300 K and a flow rate of 5 kg/s enters a black, thin-walled tube, which passes through a large furnace whose walls and air are at a temperature of 700 K. The diameter and length of the tube are 0.25 m and 8 m, respectively. Convection coefficients associated with

Patent Owner Manufacturing Resources International, Inc.
Exhibit 2017 - Page 543 of 999



s of $\dot{m} = 0.1$ kg/s and air outlet temperature if $''_o = 700$ W/m^2? The spe- 08 J/kg · K.

ated section of a circular g/s and a temperature of r $D = 50$ mm, and fully = 25 W/m^2 · K exist over

surface heat flux at $q''_s =$ total heat transfer rate q e of the air leaving the e of the surface tempera- nd outlet $T_{s,o}$? Sketch the T_m. On the same figure, the axial variation of T_s ic case in which the local ies with x.

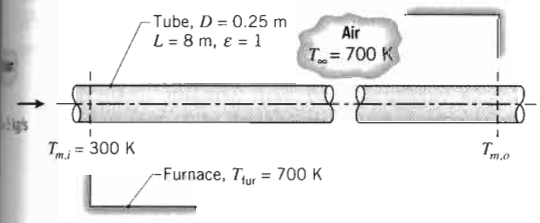
ries linearly with x, such), what are the values of h the axial variation of T_s ure, also sketch (qualita- of T_s and T_m for the more local convection coeffi-

tions of parts (a) and (b), rface temperatures, $T_m(x)$ as functions of distance t will a fourfold increase ent have on the tempera-

process, what heat fluxes an air outlet temperature erature distributions.

of 5 kg/s enters a black, s through a large furnace mperature of 700 K. The ube are 0.25 m and 8 m, fficients associated with

water flow through the tube and air flow over the tube are 300 W/m^2 · K and 50 W/m^2 · K, respectively.



(a) Write an expression for the linearized radiation coefficient corresponding to radiation exchange between the outer surface of the pipe and the furnace walls. Explain how to calculate this coefficient if the surface temperature of the tube is represented by the arithmetic mean of its inlet and outlet values.

(b) Determine the outlet temperature of the water, $T_{m,o}$.

8.18 Slug flow is an idealized tube flow condition for which the velocity is assumed to be uniform over the entire tube cross section. For the case of laminar slug flow with a uniform surface heat flux, determine the form of the fully developed temperature distribution $T(r)$ and the Nusselt number Nu_D.

8.19 Superimposing a control volume that is differential in x on the tube flow conditions of Figure 8.8, derive Equation 8.45a.

8.20 An experimental nuclear core simulation apparatus consists of a long thin-walled metallic tube of diameter D and length L, which is electrically heated to produce the sinusoidal heat flux distribution

$$q''_s(x) = q''_o \sin\left(\frac{\pi x}{L}\right)$$

where x is the distance measured from the tube inlet. Fluid at an inlet temperature $T_{m,i}$ flows through the tube at a rate of $\dot{m}$. Assuming the flow is turbulent and fully developed over the entire length of the tube, develop expressions for:

(a) the total rate of heat transfer, q, from the tube to the fluid;

(b) the fluid outlet temperature, $T_{m,o}$;

(c) the axial distribution of the wall temperature, $T_s(x)$; and

(d) the magnitude and position of the highest wall temperature.

(e) Consider a 40-mm-diameter tube of 4-m length with a sinusoidal heat flux distribution for which $q''_o = 10{,}000$ W/m^2. Fluid passing through the tube has a flow rate of 0.025 kg/s, a specific heat of 4180 J/kg · K, an entrance temperature of 25°C, and a convection coefficient of 1000 W/m^2 · K. Plot the mean fluid and surface temperatures as a function of distance along the tube. Identify important features of the distributions. Explore the effect of ±25% changes in the convection coefficient and the heat flux on the distributions.

8.21 Water at 20°C and a flow rate of 0.1 kg/s enters a heated, thin-walled tube with a diameter of 15 mm and length of 2 m. The wall heat flux provided by the heating elements depends on the wall temperature according to the relation

$$q''_s(x) = q''_{s,o}[1 + \alpha(T_s - T_{ref})]$$

where $q''_{s,o} = 10^4$ W/m^2, $\alpha = 0.2$ K^{-1}, $T_{ref} = 20$°C, and T_s is the wall temperature in °C. Assume fully developed flow and thermal conditions with a convection coefficient of 3000 W/m^2 · K.

(a) Beginning with a properly defined differential control volume in the tube, derive expressions for the variation of the water, $T_m(x)$, and the wall, $T_s(x)$, temperatures as a function of distance from the tube inlet.

(b) Using a numerical integration scheme, calculate and plot the temperature distributions, $T_m(x)$ and $T_s(x)$, on the same graph. Identify and comment on the main features of the distributions. *Hint*: The *IHT* integral function *DER*(T_m,x) can be used to perform the integration along the length of the tube.

(c) Calculate the total rate of heat transfer to the water.

Heat Transfer Correlations: Circular Tubes

8.22 Engine oil is heated by flowing through a circular tube of diameter $D = 50$ mm and length $L = 25$ m and whose surface is maintained at 150°C.

(a) If the flow rate and inlet temperature of the oil are 0.5 kg/s and 20°C, what is the outlet temperature $T_{m,o}$? What is the total heat transfer rate q for the tube?

(b) For flow rates in the range $0.5 \le \dot{m} \le 2.0$ kg/s, compute and plot the variations of $T_{m,o}$ and q with $\dot{m}$. For what flow rate(s) are q and $T_{m,o}$ maximized? Explain your results.

8.23 Engine oil flows through a 25-mm-diameter tube at a rate of 0.5 kg/s. The oil enters the tube at a temperature of 25°C, while the tube surface temperature is maintained at 100°C.

(a) Determine the oil outlet temperature for a 5-m and for a 100-m long tube. For each case, compare the

Patent Owner Manufacturing Resources International, Inc.
Exhibit 2017 - Page 544 of 999

log mean temperature difference to the arithmetic mean temperature difference.

(b) For $5 \le L \le 100$ m, compute and plot the average Nusselt number $\overline{Nu}_D$ and the oil outlet temperature as a function of L.

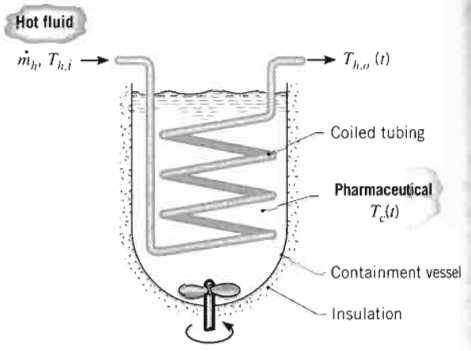
8.24 An oil preheater consists of a single tube of 10 mm diameter and 5 m length, with its surface maintained at 175°C by swirling combustion gases. The engine oil (new) enters at 75°C. What flow rate must be supplied to maintain an oil outlet temperature of 100°C ? What is the corresponding heat transfer rate ?

8.25 Engine oil flows at a rate of 1 kg/s through a 5-mm-diameter straight tube. The oil has an inlet temperature of 45°C and it is desired to heat the oil to a mean temperature of 80°C at the exit of the tube. The surface of the tube is maintained at 150°C. Determine the required length of the tube. *Hint*: Calculate the Reynolds numbers at the entrance and exit of the tube before proceeding with your analysis.

8.26 Ethylene glycol flows at 0.01 kg/s through a 3-mm-diameter, thin-walled tube. The tube is coiled and submerged in a well-stirred water bath maintained at 25°C. If the fluid enters the tube at 85°C, what heat rate and tube length are required for the fluid to leave at 35°C? Neglect heat transfer enhancement associated with the coiling.

8.27 In the final stages of production, a pharmaceutical is sterilized by heating it from 25 to 75°C as it moves at 0.2 m/s through a straight thin-walled stainless steel tube of 12.7-mm diameter. A uniform heat flux is maintained by an electric resistance heater wrapped around the outer surface of the tube. If the tube is 10 m long, what is the required heat flux? If fluid enters the tube with a fully developed velocity profile and a uniform temperature profile, what is the surface temperature at the tube exit and at a distance of 0.5 m from the entrance? Fluid properties may be approximated as $\rho = 1000$ kg/m^3, $c_p = 4000$ J/kg · K, $\mu = 2 \times 10^{-3}$ kg/s · m, $k = 0.8$ W/m · K, and $Pr = 10$.

8.28 *Batch processes* are often used in chemical and pharmaceutical operations to achieve a desired chemical composition for the final product. Related heat transfer processes are typically transient, involving a liquid of fixed volume that may be heated from room temperature to a desired process temperature, or cooled from the process temperature to room temperature. Consider a batch process for which a pharmaceutical (the cold fluid, c) is poured into an insulated, highly agitated vessel (a *stirred reactor*) and heated by passing a hot fluid (h) through a submerged heat exchanger coil of thin-walled tubing and surface area A_s. The flow rate, $\dot{m}_h$, mean inlet temperature, $T_{h,i}$, and specific heat, $c_{p,h}$, of the hot fluid are known, as are the initial temperature, $T_{c,i} < T_{h,i}$, the volume, V_c, mass density, ρ_c, and specific heat, $c_{v,c}$, of the pharmaceutical. Heat transfer from the hot fluid to the pharmaceutical is governed by an overall heat transfer coefficient U.



(a) Starting from basic principles, derive expressions that can be used to determine the variation of T_c and $T_{h,o}$ with time during the heating process. *Hint*: Two equations may be written for the rate of heat transfer, $q(t)$, to the pharmaceutical, one based on the log-mean temperature difference and the other on an energy balance for flow of the hot fluid through the tube. Equate these expressions to determine $T_{h,o}(t)$ as a function of $T_c(t)$ and prescribed parameters. Use the expression for $T_{h,o}(t)$ and the energy balance for flow through the tube with an energy balance for a control volume containing the pharmaceutical to obtain an expression for $T_c(t)$.

(b) Consider a pharmaceutical of volume $V_c = 1$ m^3, density $\rho_c = 1100$ kg/m^3, specific heat $c_{v,c} = 2000$ J/kg · K, and an initial temperature of $T_{c,i} = 25$°C. A coiled tube of length $L = 40$ m, diameter $D = 50$ mm, and coil diameter $C = 500$ mm is submerged in the vessel, and hot fluid enters the tubing at $T_{h,i} = 200$°C and $\dot{m}_h = 2.4$ kg/s. The convection coefficient at the outer surface of the tubing may be approximated as $h_o = 1000$ W/m^2 · K, and the fluid properties are $c_{p,h} = 2500$ J/kg · K, $\mu_h = 0.002$ N · s/m^2, $k_h = 0.260$ W/m · K, and $Pr_h = 20$. For the foregoing conditions, compute and plot the pharmaceutical temperature T_c and the outlet temperature $T_{h,o}$ as a function of time over the range $0 \le t \le 3600$ s. How long does it take to reach a batch temperature of $T_c = 160$°C? The process operator may control the heating time by varying $\dot{m}_h$. For $1 \le \dot{m}_h \le 5$ kg/s, explore the effect of the

flow rate on
$T_c = 160$°C.

8.29 The mold that is
constructed of m
The mold, to be
thermoplastic n
before ejection
30°C is availabl
50 mm × 100
must specify inc
ter 5 mm, to be
can be placed e
the mold, the d
100-mm-long p
The total mass
among the char
($N = 5$ long pa
the mold desig
faster and, in tu
be manufacture
ing of the mol
channel is full
mold. Neglect t

8.30 The evaporator
large tank of w
ing the winter.
begins to freez
which may be u
mer. Consider
is passed throu
inside diameter

(a) If air ente
$T_{m,i} = 24$°C
tube length
ture of $T_{m,o}$
a tank of
contains 80
to complet
heat of fu
10^5 J/kg, re

(b) The air o
adjusting
length det
as a funct
the dwellin
imately 0.
operating
system?

8.31 To cool a st
compression re
a plastic pipe

Patent Owner Manufacturing Resources International, Inc.
Exhibit 2017 - Page 545 of 999

flow rate on the time t_c required to reach a value of $T_c = 160°C$.

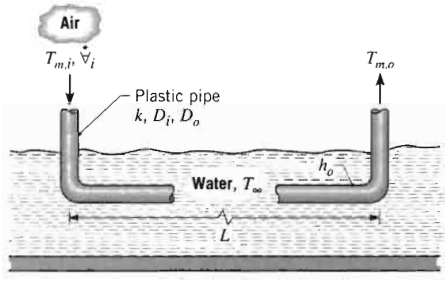
8.29 The mold that is used in an injection molding process is constructed of metal ($\rho = 7800$ kg/m^3, $c = 450$ J/kg · K). The mold, to be heated to 190°C prior to injection of the thermoplastic material, must be subsequently cooled before ejection of the finished part. Pressurized water at 30°C is available for cooling. The mold has dimensions 50 mm × 100 mm × 40 mm and the mold designer must specify inclusion of N cooling passages, of diameter 5 mm, to be machined into the mold. If one passage can be placed every 10 mm along the length or width of the mold, the designer can therefore specify either five 100-mm-long passages or ten 50-mm-long passages. The total mass flow rate of water, divided equally among the channels, is 0.02 kg/s. Which configuration ($N = 5$ long passages or $N = 10$ short passages) should the mold designer specify in order to cool the mold faster and, in turn, increase the number of parts that can be manufactured daily? What is the initial rate of cooling of the mold (°C/s)? The velocity profile in each channel is fully developed prior to entering the hot mold. Neglect the mass of the thermoplastic part.

8.30 The evaporator section of a heat pump is installed in a large tank of water, which is used as a heat source during the winter. As energy is extracted from the water, it begins to freeze, creating an ice/water bath at 0°C, which may be used for air conditioning during the summer. Consider summer cooling conditions for which air is passed through an array of copper tubes, each of inside diameter $D = 50$ mm, submerged in the bath.

(a) If air enters each tube at a mean temperature of $T_{m,i} = 24°C$ and a flow rate of $\dot{m} = 0.01$ kg/s, what tube length L is needed to provide an exit temperature of $T_{m,o} = 14°C$? With 10 tubes passing through a tank of total volume $V = 10$ m^3, which initially contains 80% ice by volume, how long would it take to completely melt the ice? The density and latent heat of fusion of ice are 920 kg/m^3 and 3.34×10^5 J/kg, respectively.

(b) The air outlet temperature may be regulated by adjusting the tube mass flow rate. For the tube length determined in part (a), compute and plot $T_{m,o}$ as a function of $\dot{m}$ for $0.005 \leq \dot{m} \leq 0.05$ kg/s. If the dwelling cooled by this system requires approximately 0.05 kg/s of air at 16°C, what design and operating conditions should be prescribed for the system?

8.31 To cool a summer home without using a vapor-compression refrigeration cycle, air is routed through a plastic pipe ($k = 0.15$ W/m · K, $D_i = 0.15$ m, $D_o = 0.17$ m) that is submerged in an adjoining body of water. The water temperature is nominally at $T_\infty = 17°C$, and a convection coefficient of $h_o \approx 1500$ W/m^2 · K is maintained at the outer surface of the pipe.



If air from the home enters the pipe at a temperature of $T_{m,i} = 29°C$ and a volumetric flow rate of $\forall_i = 0.025$ m^3/s, what pipe length L is needed to provide a discharge temperature of $T_{m,o} = 21°C$? What is the fan power required to move the air through this length of pipe if its inner surface is smooth?

8.32 Water flowing at 2 kg/s through a 40-mm-diameter tube is to be heated from 25 to 75°C by maintaining the tube surface temperature at 100°C.

(a) What is the required tube length for these conditions?

(b) In order to design a water heating system, we wish to consider using tube diameters in the range from 30 to 50 mm. What are the required tube lengths for water flow rates of 1, 2, and 3 kg/s? Represent this design information graphically.

(c) Plot the pressure gradient as a function of tube diameter for the three flow rates. Assume the tube wall is smooth.

8.33 Consider the conditions associated with the hot water pipe of Problem 7.56, but now account for the convection resistance associated with water flow at a mean velocity of $u_m = 0.5$ m/s in the pipe. What is the corresponding daily cost of heat loss per meter of the uninsulated pipe?

8.34 A thick-walled, stainless steel (AISI 316) pipe of inside and outside diameters $D_i = 20$ mm and $D_o = 40$ mm is heated electrically to provide a uniform heat generation rate of $\dot{q} = 10^6$ W/m^3. The outer surface of the pipe is insulated, while water flows through the pipe at a rate of $\dot{m} = 0.1$ kg/s.

(a) If the water inlet temperature is $T_{m,i} = 20°C$ and the desired outlet temperature is $T_{m,o} = 40°C$, what is the required pipe length?

Patent Owner Manufacturing Resources International, Inc.
Exhibit 2017 - Page 546 of 999

(b) What are the location and value of the maximum pipe temperature?

8.35 Consider the encased pipe of Problem 4.29, but now allow for the difference between the mean temperature of the fluid, which changes along the pipe length, and that of the pipe.

(a) For the prescribed values of k, D, w, h, and T_∞ and a pipe of length $L = 100$ m, what is the outlet temperature $T_{m,o}$ of water that enters the pipe at a temperature of $T_{m,i} = 90°C$ and a flow rate of $\dot{m} = 2$ kg/s?

(b) What is the pressure drop of the water and the corresponding pump power requirement?

(c) Subject to the constraint that the width of the duct is fixed at $w = 0.30$ m, explore the effects of the flow rate and the pipe diameter on the outlet temperature.

8.36 Water flows through a thick-walled tube with an inner diameter of 12 mm and a length of 8 m. The tube is immersed in a well-stirred, hot reaction tank maintained at 85°C, and the conduction resistance of the tube wall (based on the inner surface area) is $R''_{cd} = 0.002$ m$^2 \cdot$ K/W. The inlet temperature of the process fluid is $T_{m,i} = 20°C$, and the flow rate is 33 kg/h.

(a) Estimate the outlet temperature of the process fluid, $T_{m,o}$. Assume, and then justify, fully developed flow and thermal conditions within the tube.

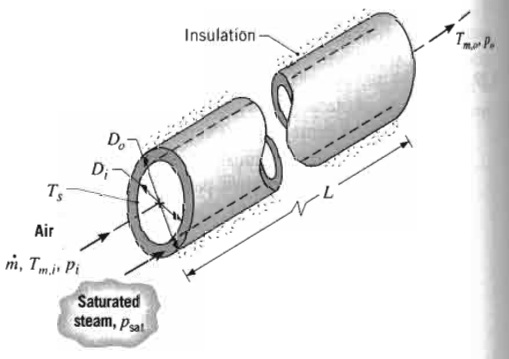
(b) Do you expect $T_{m,o}$ to increase or decrease if combined thermal and hydrodynamic entry conditions exist within the tube? Estimate the outlet temperature of the water for this condition.

8.37 Atmospheric air enters a 10-m-long, 150-mm-diameter uninsulated heating duct at 60°C and 0.04 kg/s. The duct surface temperature is approximately constant at $T_s = 15°C$.

(a) What are the outlet air temperature, the heat rate q, and pressure drop Δp for these conditions?

(b) To illustrate the tradeoff between heat transfer rate and pressure drop considerations, calculate q and Δp for diameters in the range from 0.1 to 0.2 m. In your analysis, maintain the total surface area, $A_s = \pi DL$, at the value computed for part (a). Plot q, Δp, and L as a function of the duct diameter.

8.38 An air heater for an industrial application consists of an insulated, concentric tube annulus, for which air flows through a thin-walled inner tube. Saturated steam flows through the outer annulus, and condensation of the steam maintains a uniform temperature T_s on the tube surface.



Consider conditions for which air enters a 50-mm-diameter tube at a pressure of 5 atm, a temperature of $T_{m,i} = 17°C$, and a flow rate of $\dot{m} = 0.03$ kg/s, while saturated steam at 2.455 bars condenses on the outer surface of the tube. If the length of the annulus is $L = 5$ m, what are the outlet temperature $T_{m,o}$ and pressure p_o of the air? What is the mass rate at which condensate leaves the annulus?

8.39 The products of combustion from a burner are routed to an industrial application through a thin-walled metallic duct of diameter $D_i = 1$ m and length $L = 100$ m. The gas enters the duct at atmospheric pressure and a mean temperature and velocity of $T_{m,i} = 1600$ K and $u_{m,i} = 10$ m/s, respectively. It must exit the duct at a temperature that is no less than $T_{m,o} = 1400$ K. What is the minimum thickness of an alumina-silica insulation ($k_{ins} = 0.125$ W/m$\cdot$K) needed to meet the outlet requirement under worst case conditions for which the duct is exposed to ambient air at $T_\infty = 250$ K and a cross-flow velocity of $V = 15$ m/s? The properties of the gas may be approximated as those of air, and as a first estimate, the effect of the insulation thickness on the convection coefficient and thermal resistance associated with the cross flow may be neglected.

8.40 Liquid mercury at 0.5 kg/s is to be heated from 300 to 400 K by passing it through a 50-mm-diameter tube whose surface is maintained at 450 K. Calculate the required tube length by using an appropriate liquid metal convection heat transfer correlation. Compare your result with that which would have been obtained by using a correlation appropriate for $Pr \gtrsim 0.7$.

8.41 The surface of a 50-mm-diameter, thin-walled tube is maintained at 100°C. In one case air is in cross flow over the tube with a temperature of 25°C and a velocity of 30 m/s. In another case air is in fully developed flow through the tube with a temperature of 25°C and a mean velocity of 30 m/s. Compare the heat flux from the tube to the air for the two cases.

8.42 Cooling wate
thin-walled tul
surface temper
densing steam
and the tubes a

(a) What is the
properties
$\overline{T}_m = 300$

(b) Was the a
repeat the
a more ap

(c) A range o
to the eng
a plot to
possible if
at the valu
remain the

8.43 The air passag
approximated
length. The op
and air enters t

(a) For an air
outlet tem
vane.

(b) Generate
function
Compare
2- and 4-n
tions rema

8.44 The core of
reactor has coo
mm length. He
when the flow

(a) Determine
ture for the

(b) If the cool
rate if the
temperatur
temperatur

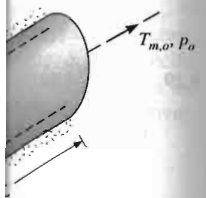
8.45 Air at 200 kPa
25-mm diamet
condenses on th

(a) Determine
of the air, a

(b) Calculate t
of the air is

8.46 Heated air requ
ated by passing
lar tubes ($D =$

Patent Owner Manufacturing Resources International, Inc.
Exhibit 2017 - Page 547 of 999



air enters a 50-mm-
atm, a temperature of
= 0.03 kg/s, while sat-
nses on the outer sur-
he annulus is $L = 5$ m,
$T_{m,o}$ and pressure p_o of
at which condensate

a burner are routed to
a thin-walled metallic
th $L = 100$ m. The gas
ssure and a mean tem-
0 K and $u_{m,i} = 10$ m/s,
t a temperature that is
is the minimum thick-
on ($k_{ins} = 0.125$ W/m ·
ment under worst case
posed to ambient air at
ity of $V = 15$ m/s? The
timated as those of air,
f the insulation thick-
and thermal resistance
e neglected.

e heated from 300 to
50-mm-diameter tube
450 K. Calculate the
propriate liquid metal
. Compare your result
obtained by using a

, thin-walled tube is
air is in cross flow
25°C and a velocity
fully developed flow
of 25°C and a mean
at flux from the tube

8.42 Cooling water flows through the 25.4-mm-diameter thin-walled tubes of a steam condenser at 1 m/s, and a surface temperature of 350 K is maintained by the condensing steam. The water inlet temperature is 290 K, and the tubes are 5 m long.

(a) What is the water outlet temperature? Evaluate water properties at an assumed average mean temperature, $\overline{T}_m = 300$ K.

(b) Was the assumed value for $\overline{T}_m$ reasonable? If not, repeat the calculation using properties evaluated at a more appropriate temperature.

(c) A range of tube lengths from 4 to 7 m is available to the engineer designing this condenser. Generate a plot to show what coolant mean velocities are possible if the water outlet temperature is to remain at the value found for part (b). All other conditions remain the same.

8.43 The air passage for cooling a gas turbine vane can be approximated as a tube of 3-mm diameter and 75-mm length. The operating temperature of the vane is 650°C, and air enters the tube at 427°C.

(a) For an air flow rate of 0.18 kg/h, calculate the air outlet temperature and the heat removed from the vane.

(b) Generate a plot of the air outlet temperature as a function of flow rate for $0.1 \leq \dot{m} \leq 0.6$ kg/h. Compare this result with those for vanes having 2- and 4-mm-diameter tubes, with all other conditions remaining the same.

8.44 The core of a high-temperature, gas-cooled nuclear reactor has coolant tubes of 20-mm diameter and 780-mm length. Helium enters at 600 K and exits at 1000 K when the flow rate is 8×10^{-3} kg/s per tube.

(a) Determine the uniform tube wall surface temperature for these conditions.

(b) If the coolant gas is air, determine the required flow rate if the heat removal rate and tube wall surface temperature remain the same. What is the outlet temperature of the air?

8.45 Air at 200 kPa enters a 2-m-long, thin-walled tube of 25-mm diameter at 150°C and 6 m/s. Steam at 20 bars condenses on the outer surface.

(a) Determine the outlet temperature and pressure drop of the air, as well as the rate of heat transfer to the air.

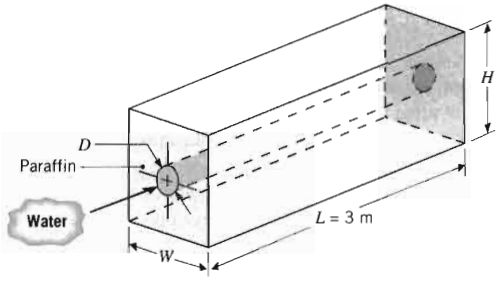
(b) Calculate the parameters of part (a) if the pressure of the air is doubled.

8.46 Heated air required for a food-drying process is generated by passing ambient air at 20°C through long, circular tubes ($D = 50$ mm, $L = 5$ m) housed in a steam condenser. Saturated steam at atmospheric pressure condenses on the outer surface of the tubes, maintaining a uniform surface temperature of 100°C.

(a) If an air flow rate of 0.01 kg/s is maintained in each tube, determine the air outlet temperature $T_{m,o}$ and the total heat rate q for the tube.

(b) The air outlet temperature may be controlled by adjusting the tube mass flow rate. Compute and plot $T_{m,o}$ as a function of $\dot{m}$ for $0.005 \leq \dot{m} \leq 0.050$ kg/s. If a particular drying process requires approximately 1 kg/s of air at 75°C, what design and operating conditions should be prescribed for the air heater, subject to the constraint that the tube diameter and length be fixed at 50 mm and 5 m, respectively?

8.47 Consider a horizontal, thin-walled circular tube of diameter $D = 0.025$ m submerged in a container of *n*-octadecane (paraffin), which is used to store thermal energy. As hot water flows through the tube, heat is transferred to the paraffin, converting it from the solid to liquid state at the phase change temperature of $T_\infty = 27.4$°C. The latent heat of fusion and density of paraffin are $h_{sf} = 244$ kJ/kg and $\rho = 770$ kg/m^3, respectively, and thermophysical properties of the water may be taken as $c_p = 4.185$ kJ/kg · K, $k = 0.653$ W/m · K, $\mu = 467 \times 10^{-6}$ kg/s · m, and $Pr = 2.99$.



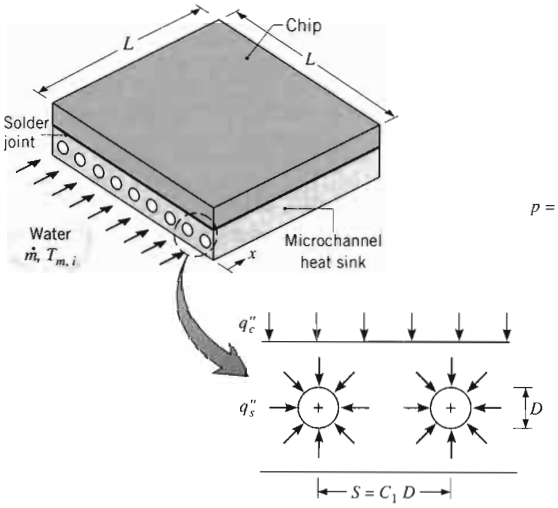
(a) Assuming the tube surface to have a uniform temperature corresponding to that of the phase change, determine the water outlet temperature and total heat transfer rate for a water flow rate of 0.1 kg/s and an inlet temperature of 60°C. If $H = W = 0.25$ m, how long would it take to completely liquefy the paraffin, from an initial state for which all the paraffin is solid and at 27.4°C?

(b) The liquefaction process can be accelerated by increasing the flow rate of the water. Compute and plot the heat rate and outlet temperature as a function of flow rate for $0.1 \leq \dot{m} \leq 0.5$ kg/s. How long would it take to melt the paraffin for $\dot{m} = 0.5$ kg/s?

8.48 A common procedure for cooling a high-performance computer chip involves joining the chip to a heat sink

Patent Owner Manufacturing Resources International, Inc.
Exhibit 2017 - Page 548 of 999

within which circular microchannels are machined. During operation, the chip produces a uniform heat flux q_c'' at its interface with the heat sink, while a liquid coolant (water) is routed through the channels. Consider a square chip and heat sink, each $L \times L$ on a side, with microchannels of diameter D and pitch $S = C_1 D$, where the constant C_1 is greater than unity. Water is supplied at an inlet temperature $T_{m,i}$ and a total mass flow rate $\dot{m}$ (for the entire heat sink).

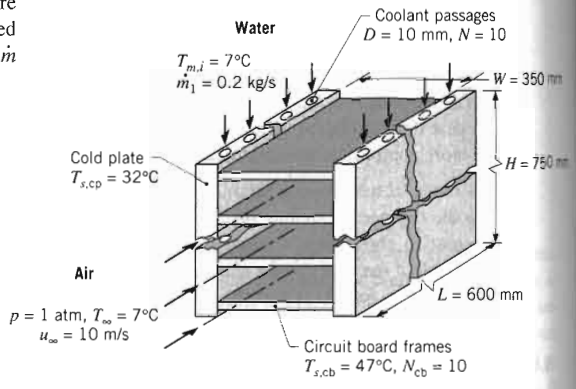


(a) Assuming that q_c'' is dispersed in the heat sink such that a uniform heat flux q_s'' is maintained at the surface of each channel, obtain expressions for the longitudinal distributions of the mean fluid, $T_m(x)$, and surface, $T_s(x)$, temperatures in each channel. Assume laminar, fully developed flow throughout each channel, and express your results in terms of $\dot{m}$, q_c'', C_1, D, and/or L, as well as appropriate thermophysical properties.

(b) For $L = 12$ mm, $D = 1$ mm, $C_1 = 2$, $q_c'' = 20$ W/cm^2, $\dot{m} = 0.010$ kg/s, and $T_{m,i} = 290$ K, compute and plot the temperature distributions $T_m(x)$ and $T_s(x)$.

(c) A common objective in designing such heat sinks is to maximize q_c'' while maintaining the heat sink at an acceptable temperature. Subject to prescribed values of $L = 12$ mm and $T_{m,i} = 290$ K and the constraint that $T_{s,\max} \leq 50°C$, explore the effect on q_c'' of variations in heat sink design and operating conditions.

8.49 One way to cool chips mounted on the circuit boards of a computer is to encapsulate the boards in metal frames that provide efficient pathways for conduction to supporting *cold plates*. Heat generated by the chips is then dissipated by transfer to water flowing through passages drilled in the plates. Because the plates are made from a metal of large thermal conductivity (typically aluminium or copper), they may be assumed to be at a temperature, $T_{s,cp}$.



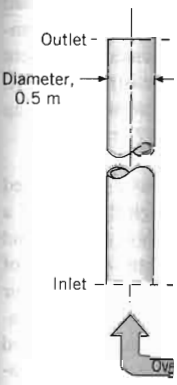
(a) Consider circuit boards attached to cold plates of height $H = 750$ mm and width $L = 600$ mm, each with $N = 10$ holes of diameter $D = 10$ mm. If operating conditions maintain plate temperatures of $T_{s,cp} = 32°C$ with water flow at $\dot{m}_1 = 0.2$ kg/s per passage and $T_{m,i} = 7°C$, how much heat may be dissipated by the circuit boards?

(b) To enhance cooling, thereby allowing increased power generation without an attendant increase in system temperatures, a hybrid cooling scheme may be used. The scheme involves forced air flow over the encapsulated circuit boards, as well as water flow through the cold plates. Consider conditions for which $N_{cb} = 10$ circuit boards of width $W = 350$ mm are attached to the cold plates and their average surface temperature is $T_{s,cb} = 47°C$ when $T_{s,cp} = 32°C$. If air is in parallel flow over the plates with $u_\infty = 10$ m/s and $T_\infty = 7°C$, how much of the heat generated by the circuit boards is transferred to the air?

8.50 Refrigerant-134a is being transported at 0.1 kg/s through a Teflon tube of inside diameter $D_i = 25$ mm and outside diameter $D_o = 28$ mm, while atmospheric air at $V = 25$ m/s and 300 K is in cross flow over the tube. What is the heat transfer per unit length of tube to Refrigerant-134a at 240 K?

8.51 Oil at 150°C flows *slowly* through a long, thin-walled pipe of 30-mm inner diameter. The pipe is suspended in a room for which the air temperature is 20°C and the convection coefficient at the outer tube surface is 11 W/m$^2 \cdot$ K. Estimate the heat loss per unit length of tube.

8.52 Exhaust gase
charged into a
temperatures
mated. Knowl
useful for pre
thermal plume
face temperatu
the gas produc
stack is 0.5 m
gas flow rate
600°C.



(a) Consider c
perature a
respectivel
properties
mate the c
for the giv

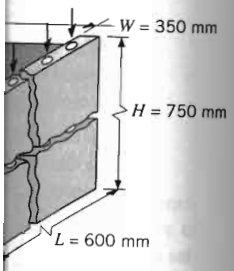
(b) The gas o
in the am
For T_∞ =
the gas o
velocity fc

8.53 A hot fluid pas
diameter and
is in cross flo
$\dot{m}$ = 18 kg/h a
the outlet temp
Assuming
ditions in the
$T_{m,o}$, if the flo
is, $\dot{m}$ = 36 kg
The thermopl

Patent Owner Manufacturing Resources International, Inc.
Exhibit 2017 - Page 549 of 999

water flowing through
Because the plates are
mal conductivity (typi-
may be assumed to be

Coolant passages
= 10 mm, $N = 10$



rd frames
C, $N_{cb} = 10$

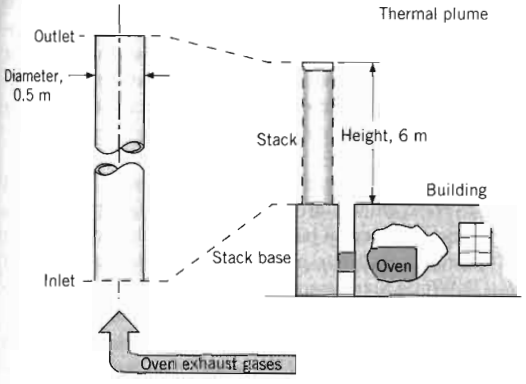
hed to cold plates of
th $L = 600$ mm, each
$D = 10$ mm. If oper-
late temperatures of
at $\dot{m}_1 = 0.2$ kg/s per
uch heat may be dis-

allowing increased
ttendant increase in
cooling scheme may
forced air flow over
ds, as well as water
Consider conditions
boards of width
the cold plates and
ture is $T_{s,cb} = 47°C$
arallel flow over the
$_\infty = 7°C$, how much
rcuit boards is trans-

ported at 0.1 kg/s
ameter $D_i = 25$ mm
while atmospheric
cross flow over the
nit length of tube to

a long, thin-walled
pipe is suspended
rature is 20°C and
r tube surface is 11
nit length of tube.

8.52 Exhaust gases from a wire processing oven are discharged into a tall stack, and the gas and stack surface temperatures at the outlet of the stack must be estimated. Knowledge of the outlet gas temperature $T_{m,o}$ is useful for predicting the dispersion of effluents in the thermal plume, while knowledge of the outlet stack surface temperature $T_{s,o}$ indicates whether condensation of the gas products will occur. The thin-walled, cylindrical stack is 0.5 m in diameter and 6.0 m high. The exhaust gas flow rate is 0.5 kg/s, and the inlet temperature is 600°C.

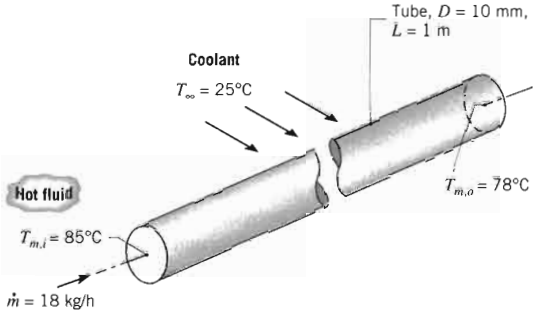


(a) Consider conditions for which the ambient air temperature and wind velocity are 4°C and 5 m/s, respectively. Approximating the thermophysical properties of the gas as those of atmospheric air, estimate the outlet gas and stack surface temperatures for the given conditions.

(b) The gas outlet temperature is sensitive to variations in the ambient air temperature and wind velocity. For $T_\infty = -25°C$, 5°C, and 35°C, compute and plot the gas outlet temperature as a function of wind velocity for $2 \le V \le 10$ m/s.

8.53 A hot fluid passes through a thin-walled tube of 10-mm diameter and 1-m length, and a coolant at $T_\infty = 25°C$ is in cross flow over the tube. When the flow rate is $\dot{m} = 18$ kg/h and the inlet temperature is $T_{m,i} = 85°C$, the outlet temperature is $T_{m,o} = 78°C$.

Assuming fully developed flow and thermal conditions in the tube, determine the outlet temperature, $T_{m,o}$, if the flow rate is increased by a factor of 2. That is, $\dot{m} = 36$ kg/h, with all other conditions the same. The thermophysical properties of the hot fluid are $\rho = 1079$ kg/m^3, $c_p = 2637$ J/kg · K, $\mu = 0.0034$ N · s/m^2, and $k = 0.261$ W/m · K.



8.54 Consider a thin-walled tube of 10-mm diameter and 2-m length. Water enters the tube from a large reservoir at $\dot{m} = 0.2$ kg/s and $T_{m,i} = 47°C$.

(a) If the tube surface is maintained at a uniform temperature of 27°C, what is the outlet temperature of the water, $T_{m,o}$? To obtain the properties of water, assume an average mean temperature of $\overline{T}_m = 300$ K.

(b) What is the exit temperature of the water if it is heated by passing air at $T_\infty = 100°C$ and $V = 10$ m/s in cross flow over the tube? The properties of air may be evaluated at an assumed film temperature of $T_f = 350$ K.

(c) In the foregoing calculations, were the assumed values of $\overline{T}_m$ and T_f appropriate? If not, use properly evaluated properties and recompute $T_{m,o}$ for the conditions of part (b).

8.55 Water at a flow rate of $\dot{m} = 0.215$ kg/s is cooled from 70°C to 30°C by passing it through a thin-walled tube of diameter $D = 50$ mm and maintaining a coolant at $T_\infty = 15°C$ in cross flow over the tube.

(a) What is the required tube length if the coolant is air and its velocity is $V = 20$ m/s?

(b) What is the tube length if the coolant is water and $V = 2$ m/s?

8.56 Consider a thin-walled, metallic tube of length $L = 1$ m and inside diameter $D_i = 3$ mm. Water enters the tube at $\dot{m} = 0.015$ kg/s and $T_{m,i} = 97°C$.

(a) What is the outlet temperature of the water if the tube surface temperature is maintained at 27°C?

(b) If a 0.5-mm-thick layer of insulation of $k = 0.05$ W/m · K is applied to the tube and its outer surface is maintained at 27°C, what is the outlet temperature of the water?

(c) If the outer surface of the insulation is no longer maintained at 27°C but is allowed to exchange heat

Patent Owner Manufacturing Resources International, Inc.
Exhibit 2017 - Page 550 of 999

by free convection with ambient air at 27°C, what is the outlet temperature of the water? The free convection heat transfer coefficient is 5 W/m² · K.

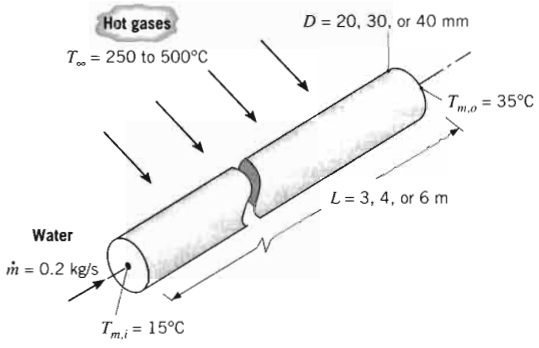
8.57 A thick-walled steel pipe ($k = 60$ W/m · K) carrying hot water is cooled externally by a cross-flow airstream at a velocity of 20 m/s and a temperature of 25°C. The inner and outer diameters of the pipe are $D_i = 20$ mm and $D_o = 25$ mm, respectively. At a certain location along the pipe, the mean temperature of the water is 80°C. Assuming the flow inside the tube is fully developed with a Reynolds number of 20,000, find the heat transfer rate to the airstream per unit pipe length.

8.58 Heat is to be removed from a reaction vessel operating at 75°C by supplying water at 27°C and 0.12 kg/s through a thin-walled tube of 15-mm diameter. The convection coefficient between the tube outer surface and the fluid in the vessel is 3000 W/m² · K.

(a) If the outlet water temperature cannot exceed 47°C, what is the maximum rate of heat transfer from the vessel?

(b) What tube length is required to accomplish the heat transfer rate of part (a)?

8.59 A heating contractor must heat 0.2 kg/s of water from 15°C to 35°C using hot gases in cross flow over a thin-walled tube.



Your assignment is to develop a series of design graphs that can be used to demonstrate acceptable combinations of tube dimensions (D and L) and of hot gas conditions (T_∞ and V) that satisfy this requirement. In your analysis, consider the following parameter ranges: $D = 20$, 30, or 40 mm; $L = 3$, 4, or 6 m; $T_\infty = 250$, 375, or 500°C; and $20 \leq V \leq 40$ m/s.

8.60 A thin-walled tube with a diameter of 6 mm and length of 20 m is used to carry exhaust gas from a smoke stack to the laboratory in a nearby building for analysis. The gas enters the tube at 200°C and with a mass flow rate of 0.003 kg/s. Autumn winds at a temperature of 15°C blow directly across the tube at a velocity of 5 m/s. Assume the thermophysical properties of the exhaust gas are those of air.

(a) Estimate the average heat transfer coefficient for the exhaust gas flowing inside the tube.

(b) Estimate the heat transfer coefficient for the air flowing across the outside of the tube.

(c) Estimate the overall heat transfer coefficient U and the temperature of the exhaust gas when it reaches the laboratory.

8.61 A 50-mm-diameter, thin-walled metal pipe covered with a 25-mm-thick layer of insulation (0.085 W/m · K) and carrying superheated steam at atmospheric pressure is suspended from the ceiling of a large room. The steam temperature entering the pipe is 120°C, and the air temperature is 20°C. The convection heat transfer coefficient on the outer surface of the covered pipe is 10 W/m² · K. If the velocity of the steam is 10 m/s, at what point along the pipe will the steam begin condensing?

8.62 A thin-walled, uninsulated 0.3-m-diameter duct is used to route chilled air at 0.05 kg/s through the attic of a large commercial building. The attic air is at 37°C, and natural circulation provides a convection coefficient of 2 W/m² · K at the outer surface of the duct. If chilled air enters a 15-m-long duct at 7°C, what is its exit temperature and the rate of heat gain? Properties of the chilled air may be evaluated at an assumed average temperature of 300 K.

8.63 The problem of heat losses from a fluid moving through a buried pipeline has received considerable attention. Practical applications include the trans-Alaska pipeline, as well as power plant steam and water distribution lines. Consider a steel pipe of diameter D that is used to transport oil flowing at a rate $\dot{m}_o$ through a cold region. The pipe is covered with a layer of insulation of thickness t and thermal conductivity k_i and is buried in soil to a depth z (distance from the soil surface to the pipe centerline). Each section of pipe is of length L and extends between pumping stations in which the oil is heated to ensure low viscosity and hence low pump power requirements. The temperature of the oil entering the pipe from a pumping station and the temperature of the ground above the pipe are designated as $T_{m,i}$ and T_s, respectively, and are known.

Consider conditions for which the oil (o) properties may be approximated as $\rho_o = 900$ kg/m³, $c_{p,o} = 2000$ J/kg · K, $\nu_o = 8.5 \times 10^{-4}$ m²/s, $k_o = 0.140$ W/m · K, $Pr_o = 10^4$; the oil flow rate is $\dot{m}_o = 500$ kg/s; and the pipe diameter is 1.2 m.

(a) Expressing $T_{m,i}$, and T_s, lation (i), expressions of the oil le

(b) If $T_s = -$ 0.05 W/m · $L = 100$ km total rate c pipeline?

(c) The operat between th thickness c graphical r

8.64 In order to mai flow rate belov pipeline of the straint that the For the values Problem 8.63, and affect $T_{m,o}$ and the flow ra tion and moist tive variations $\dot{m}_o \leq 500$ kg/s Problem 8.63. variations on worst case o adjustments c for the worst c

8.65 You are desig device to cool to 30°C by pas in a vat of wa ($\forall$) is 10^{-4} m and $T_{m,i}$ and T tures of the b associated wit

(a) At what properties

(b) If the pro ture for p m²/s, k = is the Pra

(c) Is the blo

(d) Neglectir develope heat trans

(e) What is t passes th

Patent Owner Manufacturing Resources International, Inc.
Exhibit 2017 - Page 551 of 999

(a) Expressing your results in terms of D, L, z, t, $\dot{m}_o$, $T_{m,i}$, and T_s, as well as the appropriate oil (o), insulation (i), and soil (s) properties, obtain all the expressions needed to estimate the temperature $T_{m,o}$ of the oil leaving the pipe.

(b) If $T_s = -40°C$, $T_{m,i} = 120°C$, $t = 0.15$ m, $k_i = 0.05$ W/m · K, $k_s = 0.5$ W/m · K, $z = 3$ m, and $L = 100$ km, what is the value of $T_{m,o}$? What is the total rate of heat transfer q from a section of the pipeline?

(c) The operations manager wants to know the tradeoff between the burial depth of the pipe and insulation thickness on the heat loss from the pipe. Develop a graphical representation of this design information.

8.64 In order to maintain pump power requirements per unit flow rate below an acceptable level, operation of the oil pipeline of the preceding problem is subject to the constraint that the oil exit temperature $T_{m,o}$ exceed 110°C. For the values of $T_{m,i}$, T_s, D, t_i, z, L, and k_i prescribed in Problem 8.63, operating parameters that are variable and affect $T_{m,o}$ are the thermal conductivity of the soil and the flow rate of the oil. Depending on soil composition and moisture and the demand for oil, representative variations are $0.25 \leq k_s \leq 1.0$ W/m · K and $250 \leq \dot{m}_o \leq 500$ kg/s. Using the properties prescribed in Problem 8.63, determine the effect of the foregoing variations on $T_{m,o}$ and the total heat rate q. What is the worst case operating condition? If necessary, what adjustments could be made to ensure that $T_{m,o} \geq 110°C$ for the worst case conditions?

8.65 You are designing an operating room heat exchange device to cool blood (bypassed from a patient) from 40 to 30°C by passing the fluid through a coiled tube sitting in a vat of water–ice mixture. The volumetric flow rate ($\forall$) is 10^{-4} m^3/min; the tube diameter (D) is 2.5 mm; and $T_{m,i}$ and $T_{m,o}$ represent the inlet and outlet temperatures of the blood. Neglect heat transfer enhancement associated with the coiling.

(a) At what temperature would you evaluate the fluid properties in determining $\bar{h}$ for the entire tube length?

(b) If the properties of blood evaluated at the temperature for part (a) are $\rho = 1000$ kg/m^3, $\nu = 7 \times 10^{-7}$ m^2/s, $k = 0.5$ W/m · K, and $c_p = 4.0$ kJ/kg · K, what is the Prandtl number for the blood?

(c) Is the blood flow laminar or turbulent?

(d) Neglecting all entrance effects and assuming fully developed conditions, calculate the value of $\bar{h}$ for heat transfer from the blood.

(e) What is the total heat rate loss from the blood as it passes through the tube?

(f) When free convection effects on the outside of the tube are included, the average overall heat transfer coefficient $\overline{U}$ between the blood and the ice–water mixture can be approximated as 300 W/m^2 · K. Determine the tube length L required to obtain the outlet temperature $T_{m,o}$.

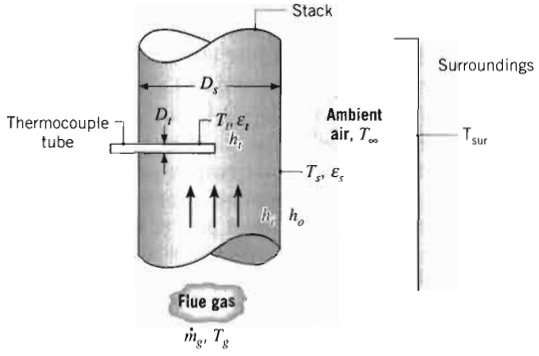
8.66 Pressurized water at $T_{m,i} = 200°C$ is pumped at $\dot{m} = 2$ kg/s from a power plant to a nearby industrial user through a thin-walled, round pipe of inside diameter $D = 1$ m. The pipe is covered with a layer of insulation of thickness $t = 0.15$ m and thermal conductivity $k = 0.05$ W/m · K. The pipe, which is of length $L = 500$ m, is exposed to a cross flow of air at $T_\infty = -10°C$ and $V = 4$ m/s. Obtain a differential equation that could be used to solve for the variation of the mixed mean temperature of the water $T_m(x)$ with the axial coordinate. As a first approximation, the internal flow may be assumed to be fully developed throughout the pipe. Express your results in terms of $\dot{m}$, V, T_∞, D, t, k, and appropriate water (w) and air (a) properties. Evaluate the heat loss per unit length of the pipe at the inlet. What is the mean temperature of the water at the outlet?

8.67 Water at 290 K and 0.2 kg/s flows through a Teflon tube ($k = 0.35$ W/m · K) of inner and outer radii equal to 10 and 13 mm, respectively. A thin electrical heating tape wrapped around the outer surface of the tube delivers a uniform surface heat flux of 2000 W/m^2, while a convection coefficient of 25 W/m^2 · K is maintained on the outer surface of the tape by ambient air at 300 K. What is the fraction of the power dissipated by the tape, which is transferred to the water? What is the outer surface temperature of the Teflon tube?

8.68 The temperature of flue gases flowing through the large stack of a boiler is measured by means of a thermocouple enclosed within a cylindrical tube as shown. The tube axis is oriented normal to the gas flow, and the thermocouple senses a temperature T_t corresponding to that of the tube surface. The gas flow rate and temperature are designated as $\dot{m}_g$ and T_g, respectively, and the gas flow may be assumed to be fully developed. The stack is fabricated from sheet metal that is at a uniform temperature T_s and is exposed to ambient air at T_∞ and large surroundings at T_{sur}. The convection coefficient associated with the outer surface of the duct is designated as h_o, while those associated with the inner surface of the duct and the tube surface are designated as h_i and h_t, respectively. The tube and duct surface emissivities are designated as ε_t and ε_s, respectively.

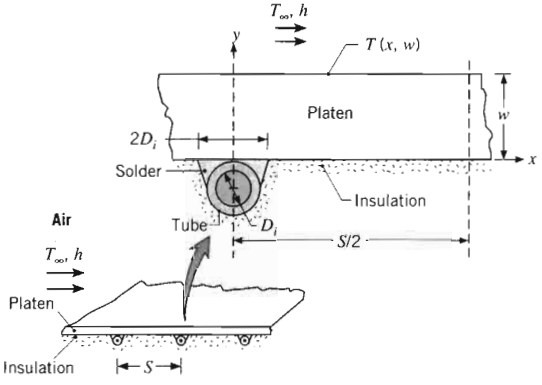
(a) Neglecting conduction losses along the thermocouple tube, develop an analysis that could be used to predict the error ($T_g - T_t$) in the temperature measurement.

Patent Owner Manufacturing Resources International, Inc.
Exhibit 2017 - Page 552 of 999



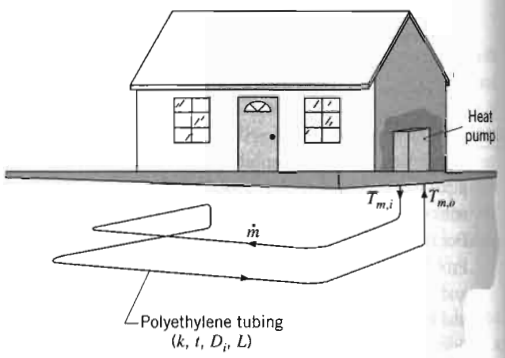
(b) Assuming the flue gas to have the properties of atmospheric air, evaluate the error for $T_t = 300°C$, $D_s = 0.6$ m, $D_t = 10$ mm, $\dot{m}_g = 1$ kg/s, $T_\infty = T_{sur} = 27°C$, $\varepsilon_t = \varepsilon_s = 0.8$, and $h_o = 25$ W/m$^2 \cdot$ K.

8.69 In a biomedical supplies manufacturing process, a requirement exists for a large platen that is to be maintained at $45 \pm 0.25°C$. The proposed design features the attachment of heating tubes to the platen at a relative spacing S. The thick-walled, copper tubes have an inner diameter of $D_i = 8$ mm and are attached to the platen with a high thermal conductivity solder, which provides a contact width of $2D_i$. The heating fluid (ethylene glycol) flows through each tube at a fixed rate of $\dot{m} = 0.06$ kg/s. The platen has a thickness of $w = 25$ mm and is fabricated from a stainless steel with a thermal conductivity of 15 W/m $\cdot$ K.



Considering the two-dimensional cross section of the platen shown in the inset, perform an analysis to determine the heating fluid temperature T_m and the tube spacing S required to maintain the surface temperature of the platen, $T(x, w)$, at $45 \pm 0.25°C$, when the ambient temperature is 25°C and the convection coefficient is 100 W/m$^2 \cdot$ K.

8.70 Ground source heat pumps operate by using a liquid, rather than ambient air, as the heat source (or sink) for winter heating (or summer cooling). The liquid flows in a closed loop through plastic tubing that is buried at a depth for which annual variations in the temperature of the soil are much less than those of the ambient air. For example, at a location such as South Bend, Indiana, deep-ground temperatures may remain at approximately 11°C, while annual excursions in the ambient air temperature may range from −25°C to +37°C.



Consider winter conditions for which the liquid is discharged from the heat pump into high-density polyethylene tubing of thickness $t = 8$ mm and thermal conductivity $k = 0.47$ W/m $\cdot$ K. The tubing is routed through soil that maintains a uniform temperature of approximately 10°C at the tube outer surface. The properties of the fluid may be approximated as those of water.

(a) For a tube inner diameter and flow rate of $D_i = 25$ mm and $\dot{m} = 0.03$ kg/s and a fluid inlet temperature of $T_{m,i} = 0°C$, determine the tube outlet temperature (heat pump inlet temperature), $T_{m,o}$, as a function of the tube length L for $10 \le L \le 50$ m.

(b) Recommend an appropriate length for the system. How would your recommendation be affected by variations in the liquid flow rate?

8.71 Compare Nusselt predictions based on the Colburn, Dittus–Boelter, Sieder and Tate, and Gnielinski correlations for the fully developed turbulent flow of water in a smooth circular tube at Reynolds numbers of 4000, 10^4, and 10^5 when the average mean temperature is 295 K and the surface temperature is 305 K.

8.72 For a sharp-edged inlet and a combined entry region, the average Nusselt number may be computed from Equation 8.63, with $C = 24Re_D^{-0.23}$ and $m = 0.815 - 2.08 \times 10^{-6} Re_D$ [20]. Determine $\overline{Nu}_D / Nu_{D,fd}$ at $x/D = 10$ and 60 for $Re_D = 10^4$ and 10^5.

8.73 Fluid enters a 2-m length with ture of $T_{m,i} = 8$ temperature of tion, the outlet outlet tempera developed, turb both cases, and independent of

Noncircular Du

8.74 Air at $3 \times 10^$ that is 1 m lon form heat flux face. What is surface at the

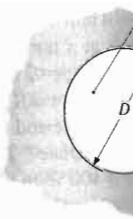
8.75 Air at $4 \times 10^$ that is 20 mm maintained at throughout the

8.76 Air at 25°C f long channels metal mold. thermally full

(a) Determin lar chann ture is 50

(b) Using ne 8.99), ch readily f molds. C tions as mented flow area case B. I the segm

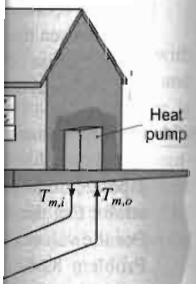
(c) Compare



Case

Patent Owner Manufacturing Resources International, Inc.
Exhibit 2017 - Page 553 of 999

rate by using a liquid, eat source (or sink) for g). The liquid flows in ping that is buried at a s in the temperature of of the ambient air. For South Bend, Indiana, remain at approxi- rsions in the ambient −25°C to +37°C.



which the liquid is nto high-density poly- mm and thermal con- ubing is routed through mperature of approxi- face. The properties of hose of water.

nd flow rate of D_i = d a fluid inlet temper- e the tube outlet tem- mperature), $T_{m,o}$, as a for $10 \leq L \leq 50$ m.

length for the system. dation be affected by ate?

sed on the Colburn, nd Gnielinski correla- ent flow of water in a numbers of 4000, 10^4, temperature is 295 K K.

mbined entry region, y be computed from 0.23 and $m = 0.815 -$ $\overline{Nu}_D/Nu_{D,fd}$ at $x/D =$

8.73 Fluid enters a thin-walled tube of 5-mm diameter and 2-m length with a flow rate of 0.04 kg/s and a temperature of $T_{m,i} = 85°C$. The tube surface is maintained at a temperature of $T_s = 25°C$, and for this operating condition, the outlet temperature is $T_{m,o} = 31.1°C$. What is the outlet temperature if the flow rate is doubled? Fully developed, turbulent flow may be assumed to exist in both cases, and the fluid properties may be assumed to be independent of temperature.

Noncircular Ducts

8.74 Air at 3×10^{-4} kg/s and 27°C enters a rectangular duct that is 1 m long and 4 mm by 16 mm on a side. A uniform heat flux of 600 W/m^2 is imposed on the duct surface. What is the temperature of the air and of the duct surface at the outlet?

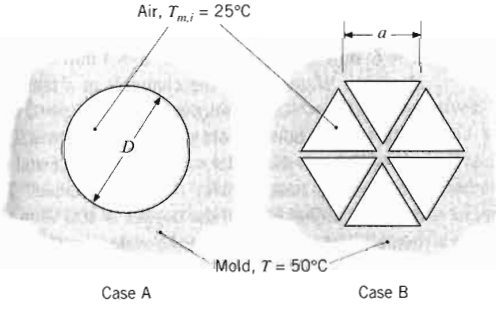
8.75 Air at 4×10^{-4} kg/s and 27°C enters a triangular duct that is 20 mm on a side and 2 m long. The duct surface is maintained at 100°C. Assuming fully developed flow throughout the duct, determine the air outlet temperature.

8.76 Air at 25°C flows at 30×10^{-6} kg/s within 100-mm-long channels used to cool a high thermal conductivity metal mold. Assume the flow is hydrodynamically and thermally fully developed.

(a) Determine the heat transferred to the air for a circular channel ($D = 10$ mm) when the mold temperature is 50°C (case A).

(b) Using new manufacturing methods (see Problem 8.99), channels of complex cross section can be readily fabricated within metal objects, such as molds. Consider air flowing under the same conditions as in case A, except now the channel is segmented into six smaller triangular sections. The flow area of case A is equal to the total flow area of case B. Determine the heat transferred to the air for the segmented channel.

(c) Compare the pressure drops for cases A and B.



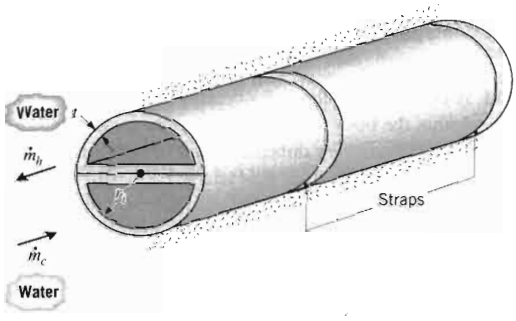
8.77 A device that recovers heat from high-temperature combustion products involves passing the combustion gas between parallel plates, each of which is maintained at 350 K by water flow on the opposite surface. The plate separation is 40 mm, and the gas flow is fully developed. The gas may be assumed to have the properties of atmospheric air, and its mean temperature and velocity are 1000 K and 60 m/s, respectively.

(a) What is the heat flux at the plate surface?

(b) If a third plate, 20 mm thick, is suspended midway between the original plates, what is the surface heat flux for the original plates? Assume the temperature and *flow rate* of the gas to be unchanged and radiation effects to be negligible.

8.78 Air at 1 atm and 285 K enters a 2-m-long rectangular duct with cross section 75 mm by 150 mm. The duct is maintained at a constant surface temperature of 400 K, and the air mass flow rate is 0.10 kg/s. Determine the heat transfer rate from the duct to the air and the air outlet temperature.

8.79 A double-wall heat exchanger is used to transfer heat between liquids flowing through semicircular copper tubes. Each tube has a wall thickness of $t = 3$ mm and an inner radius of $r_i = 20$ mm, and good contact is maintained at the plane surfaces by tightly wound straps. The tube outer surfaces are well insulated.



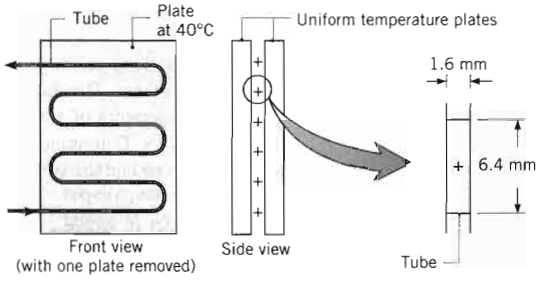
(a) If hot and cold water at mean temperatures of $T_{h,m} = 330$ K and $T_{c,m} = 290$ K flow through the adjoining tubes at $\dot{m}_h = \dot{m}_c = 0.2$ kg/s, what is the rate of heat transfer per unit length of tube? The wall contact resistance is 10^{-5} m$^2 \cdot$ K/W. Approximate the properties of both the hot and cold water as $\mu = 800 \times 10^{-6}$ kg/s $\cdot$ m, $k = 0.625$ W/m $\cdot$ K, and $Pr = 5.35$. *Hint*: Heat transfer is enhanced by conduction through the semicircular portions of the tube walls, and each portion may be subdivided into two straight fins with adiabatic tips.

(b) Using the thermal model developed for part (a), determine the heat transfer rate per unit length

Patent Owner Manufacturing Resources International, Inc.
Exhibit 2017 - Page 554 of 999

when the fluids are ethylene glycol. Also, what effect will fabricating the exchanger from an aluminum alloy have on the heat rate? Will increasing the thickness of the tube walls have a beneficial effect?

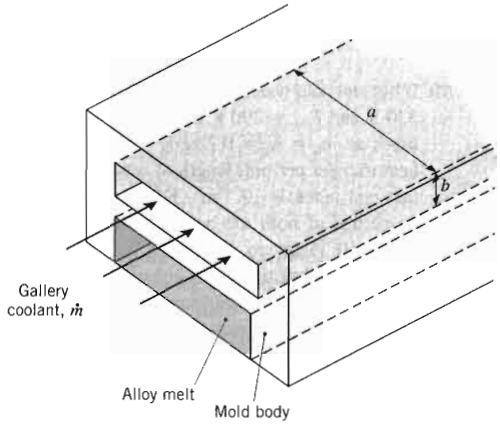
8.80 You have been asked to perform a feasibility study on the design of a blood warmer to be used during the transfusion of blood to a patient. This exchanger is to heat blood taken from the bank at 10°C to 37°C at a flow rate of 200 ml/min. The blood passes through a rectangular cross-section tube, 6.4 mm by 1.6 mm, which is sandwiched between two plates held at a constant temperature of 40°C.



(a) Compute the length of the tubing required to achieve the desired outlet conditions at the specified flow rate. Assume the flow is fully developed and the blood has the same properties as water.

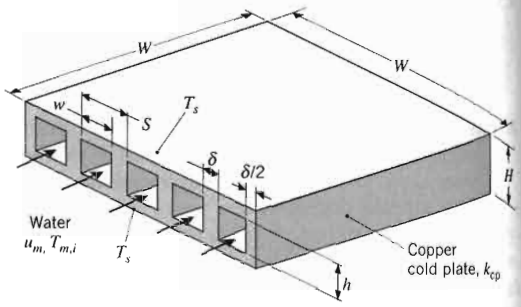
(b) Assess your assumptions and indicate whether your analysis over- or underestimates the necessary length.

8.81 A coolant flows through a rectangular channel (*gallery*) within the body of a mold used to form metal injection parts. The *gallery* dimensions are $a = 90$ mm and $b = 9.5$ mm, and the fluid flow rate is 1.3×10^{-3} m^3/s. The coolant temperature is 15°C, and the mold wall is at an approximately uniform temperature of 140°C.



To minimize corrosion damage to the expensive mold, it is customary to use a heat transfer fluid such as ethylene glycol, rather than process water. Compare the convection coefficients of water and ethylene glycol for this application. What is the trade-off between thermal performance and minimizing corrosion?

8.82 A *cold plate* is an active cooling device that is attached to a heat-generating system in order to dissipate the heat while maintaining the system at an acceptable temperature. It is typically fabricated from a material of high thermal conductivity, k_{cp}, within which channels are machined and a coolant is passed. Consider a copper cold plate of height H and width W on a side, within which water passes through square channels of width $w = h$. The transverse spacing between channels δ is twice the spacing between the sidewall of an outer channel and the sidewall of the cold plate.



Consider conditions for which *equivalent* heat-generating systems are attached to the top and bottom of the cold plate, maintaining the corresponding surfaces at the same temperature T_s. The mean velocity and inlet temperature of the coolant are u_m and $T_{m,i}$, respectively.

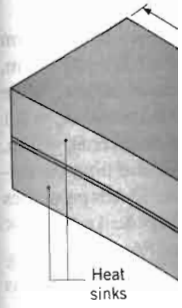
(a) Assuming fully developed turbulent flow throughout each channel, obtain a system of equations that may be used to evaluate the total rate of heat transfer to the cold plate, q, and the outlet temperature of the water, $T_{m,o}$, in terms of the specified parameters.

(b) Consider a cold plate of width $W = 100$ mm and height $H = 10$ mm, with 10 square channels of width $w = 6$ mm and a spacing of $\delta = 4$ mm between channels. Water enters the channels at a temperature of $T_{m,i} = 300$ K and a velocity of $u_m = 2$ m/s. If the top and bottom cold plate surfaces are at $T_s = 360$ K, what is the outlet water temperature and the total rate of heat transfer to the cold plate? The thermal conductivity of the copper is 400 W/m · K, while average properties of the water may be taken to be $\rho = 984$ kg/m^3, $c_p = 4184$ J/kg · K, $\mu = 489 \times 10^{-6}$ N · s/m^2, $k = 0.65$ W/m · K, and $Pr = 3.15$. Is

this a good
formance be

8.83 The cold plate de
mized with resp
and we wish to e
heat transfer ma
and height of th
100 mm and H =
spacing betwee
$\delta = 4$ mm. The
the water are ma
while equivalent
top and bottom
sponding surfac
changing the ch
channels, on the
Include conside
$w = 96$ mm (on

8.84 An electronic c
wiched betwee
sinks. The sinks
tangular passag
a volumetric flo
through the sin
temperature of
the sinks.



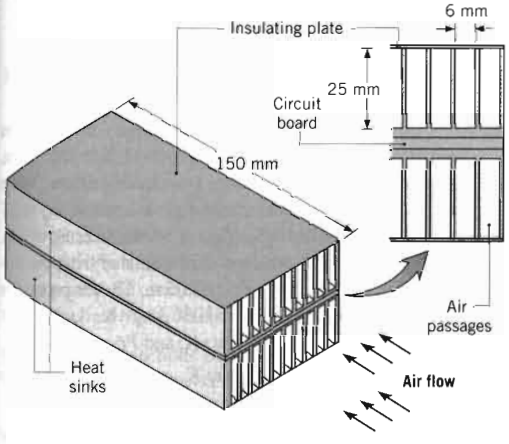
8.85 To slow down
process terme
switch the trac
mechanical po
and used to ge
schematic, the
tor grid (*a*),
blades electric

Patent Owner Manufacturing Resources International, Inc.
Exhibit 2017 - Page 555 of 999

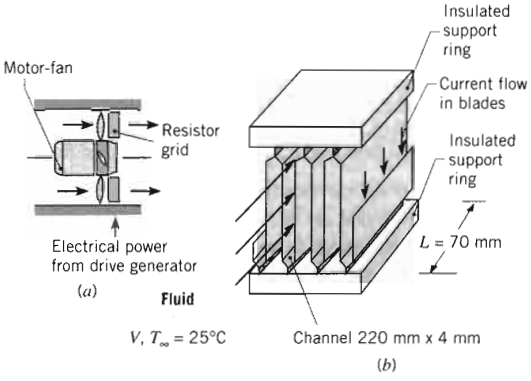
this a good cold plate design? How could its performance be improved?

8.83 The cold plate design of Problem 8.82 has not been optimized with respect to selection of the channel width, and we wish to explore conditions for which the rate of heat transfer may be enhanced. Assume that the width and height of the copper cold plate are fixed at $W = 100$ mm and $H = 10$ mm, while the channel height and spacing between channels are fixed at $h = 6$ mm and $\delta = 4$ mm. The mean velocity and inlet temperature of the water are maintained at $u_m = 2$ m/s and $T_{m,i} = 300$ K, while equivalent heat-generating systems attached to the top and bottom of the cold plate maintain the corresponding surfaces at 360 K. Evaluate the effect of changing the channel width, and hence the number of channels, on the rate of heat transfer to the cold plate. Include consideration of the limiting case for which $w = 96$ mm (one channel).

8.84 An electronic circuit board dissipating 50 W is sandwiched between two ducted, forced-air-cooled heat sinks. The sinks are 150 mm in length and have 24 rectangular passages 6 mm by 25 mm. Atmospheric air at a volumetric flow rate of 0.060 m^3/s and 27°C is drawn through the sinks by a blower. Estimate the operating temperature of the board and the pressure drop across the sinks.



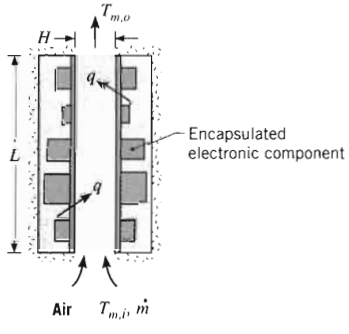
8.85 To slow down large prime movers like locomotives, a process termed dynamic electric braking is used to switch the traction motor to a generator mode in which mechanical power from the drive wheels is absorbed and used to generate electrical current. As shown in the schematic, the electric power is passed through a resistor grid (*a*), which consists of an array of metallic blades electrically connected in series (*b*). The blade material is a high-temperature, high electrical resistivity alloy, and the electrical power is dissipated as heat by internal volumetric generation. To cool the blades, a motor-fan moves high-velocity air through the grid.



(a) Treating the space between the blades as a rectangular channel of 220-mm × 4-mm cross section and 70-mm length, estimate the heat removal rate per blade if the air stream has an inlet temperature and velocity of 25°C and 50 m/s, respectively, while the blade has an operating temperature of 600°C.

(b) On a locomotive pulling a 10-car train, there may be 2000 of these blades. Based on your result from part (a), how long will it take to slow a train whose total mass is 10^6 kg from a speed of 120 km/h to 50 km/h using dynamic electric braking?

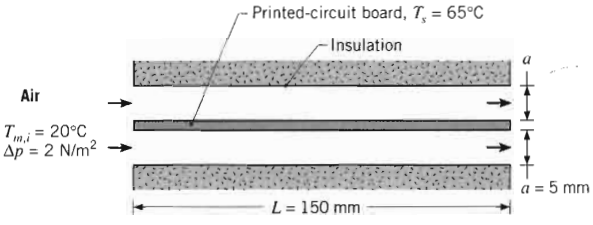
8.86 To cool electronic components that are mounted to a printed circuit board and hermetically sealed from their surroundings, two boards may be joined to form an intermediate channel through which the coolant is passed. Termed a hollow-core PCB, all of the heat generated by the components may be assumed to be transferred to the coolant.



Patent Owner Manufacturing Resources International, Inc.
Exhibit 2017 - Page 556 of 999

Consider a hollow-core PCB of length $L = 300$ mm and equivalent width W (normal to the page). Under normal operating conditions, 40 W of power are dissipated on each side of the PCB and a uniform distribution of the attendant heat transfer may be assumed for each of the hollow-core surfaces. If air enters a core of height $H = 4$ mm at a temperature of $T_{m,i} = 20°C$ and a flow rate of $\dot{m} = 0.002$ kg/s, what is its outlet temperature $T_{m,o}$? What are the surface temperatures at the inlet and outlet of the core? What are the foregoing temperatures if the flow rate is increased by a factor of five?

8.87 A printed circuit board (PCB) is cooled by laminar, fully developed air flow in adjoining, parallel-plate channels of length L and separation distance a. The channels may be assumed to be of infinite extent in the transverse direction, and the upper and lower surfaces are insulated. The temperature T_s of the PCB board is uniform, and air flow with an inlet temperature of $T_{m,i}$ is driven by a pressure difference, Δp.



Calculate the average heat removal rate per unit area (W/m^2) from the PCB.

8.88 Referring to Figure 8.11, consider conditions in an annulus having an outer surface that is insulated ($q''_o = 0$) and a uniform heat flux q''_i at the inner surface. Fully developed, laminar flow may be assumed to exist.

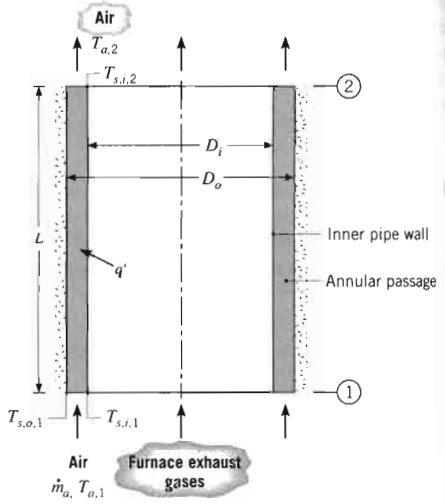
(a) Determine the velocity profile $u(r)$ in the annular region.

(b) Determine the temperature profile $T(r)$ and obtain an expression for the Nusselt number Nu_i associated with the inner surface.

8.89 Consider the air heater of Problem 8.38, but now with air flow through the annulus and steam flow through the inner tube. For the prescribed conditions and an outer tube diameter of $D_o = 65$ mm, determine the outlet temperature and pressure of the air, as well as the mass rate of steam condensation.

8.90 Consider a concentric tube annulus for which the inner and outer diameters are 25 and 50 mm. Water enters the annular region at 0.04 kg/s and 25°C. If the inner tube wall is heated electrically at a rate (per unit length) of $q' = 4000$ W/m, while the outer tube wall is insulated, how long must the tubes be for the water to achieve an outlet temperature of 85°C? What is the inner tube surface temperature at the outlet, where fully developed conditions may be assumed?

8.91 It is common practice to recover waste heat from an oil- or gas-fired furnace by using the exhaust gases to preheat the combustion air. A device commonly used for this purpose consists of a concentric pipe arrangement for which the exhaust gases are passed through the inner pipe, while the cooler combustion air flows through an annular passage around the pipe.



Consider conditions for which there is a uniform heat transfer rate per unit length, $q'_i = 1.25 \times 10^5$ W/m, from the exhaust gases to the pipe inner surface, while air flows through the annular passage at a rate of $\dot{m}_a = 2.1$ kg/s. The thin-walled inner pipe is of diameter $D_i = 2$ m, while the outer pipe, which is well insulated from the surroundings, is of diameter $D_o = 2.05$ m. The air properties may be taken to be $c_p = 1030$ J/kg · K, $\mu = 270 \times 10^{-7}$ N · s/m^2, $k = 0.041$ W/m · K, and $Pr = 0.68$.

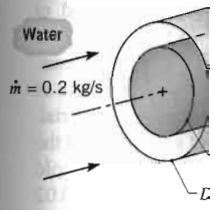
(a) If air enters at $T_{a,1} = 300$ K and $L = 7$ m, what is the air outlet temperature $T_{a,2}$?

(b) If the airflow is fully developed throughout the annular region, what is the temperature of the inner pipe at the inlet ($T_{s,i,1}$) and outlet ($T_{s,i,2}$) sections of the device? What is the outer surface temperature $T_{s,o,1}$ at the inlet?

8.92 A concentric tube arrangement, for which the inner and outer diameters are 80 mm and 100 mm, respectively, is used to remove heat from a biochemical reaction occurring in a 1-m-long settling tank. Heat is generated uniformly within the tank

plied to the ann

Reaction
$\dot{q} = 1 \times$
$L = 1$ m



(a) Determine
that will m
ture of 37°
mal condit

(b) It is desire
ent on the
chemical
Sketch the
temperatu
ing two ca
part (a),
effects are
temperatu
tem or op
reduce the

8.93 Water at $\dot{m}$ =
lar region for
25 mm and a
Saturated stea
ing its surface
while the out
lated. If fully
throughout th
provide an o
the heat flux f

8.94 For the condit
annulus be if
0.02 kg/s?

Heat Transfer

8.95 Consider the a
lem 8.31, but

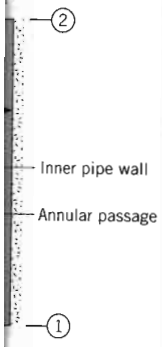
(a) What is
the fan p

(b) The con
in the pi

Patent Owner Manufacturing Resources International, Inc.
Exhibit 2017 - Page 557 of 999

the water to achieve an
at is the inner tube sur-
where fully developed

waste heat from an oil-
e exhaust gases to pre-
ice commonly used for
entric pipe arrangement
passed through the inner
on air flows through an



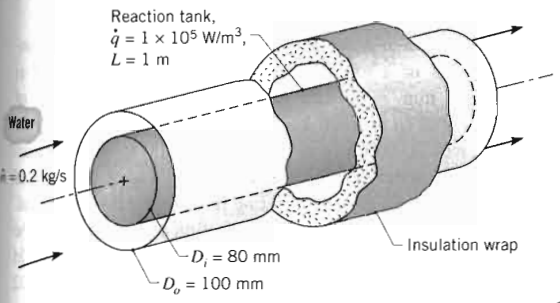
ich there is a uniform
$q_i' = 1.25 \times 10^5$ W/m,
pe inner surface, while
ge at a rate of $\dot{m}_a = 2.1$
s of diameter $D_i = 2$ m,
insulated from the sur-
5 m. The air properties
0 J/kg · K, $\mu = 270 \times$
and $Pr = 0.68$.

and $L = 7$ m, what is
?

loped throughout the
mperature of the inner
utlet ($T_{s,i,2}$) sections of
r surface temperature

r which the inner and
0 mm, respectively, is
ical reaction occurring
s generated uniformly

within the tank at a rate of 10^5 W/m^3, and water is supplied to the annular region at a rate of 0.2 kg/s.



(a) Determine the inlet temperature of the supply water that will maintain an average tank surface temperature of 37°C. Assume fully developed flow and thermal conditions. Is this assumption reasonable?

(b) It is desired to have a slight, axial temperature gradient on the tank surface, since the rate of the biochemical reaction is highly temperature dependent. Sketch the axial variation of the water and surface temperatures along the flow direction for the following two cases: (i) the fully developed conditions of part (a), and (ii) conditions for which entrance effects are important. Comment on features of the temperature distributions. What change to the system or operating conditions would you make to reduce the surface temperature gradient?

8.93 Water at $\dot{m} = 0.02$ kg/s and $T_{m,i} = 20$°C enters an annular region formed by an inner tube of diameter $D_i = 25$ mm and an outer tube of diameter $D_o = 100$ mm. Saturated steam flows through the inner tube, maintaining its surface at a uniform temperature of $T_{s,i} = 100$°C, while the outer surface of the outer tube is well insulated. If fully developed conditions may be assumed throughout the annulus, how long must the system be to provide an outlet water temperature of 75°C? What is the heat flux from the inner tube at the outlet?

8.94 For the conditions of Problem 8.93, how long must the annulus be if the water flow rate is 0.30 kg/s instead of 0.02 kg/s?

Heat Transfer Enhancement

8.95 Consider the air cooling system and conditions of Problem 8.31, but with a prescribed pipe length of $L = 15$ m.

(a) What is the air outlet temperature, $T_{m,o}$? What is the fan power requirement?

(b) The convection coefficient associated with airflow in the pipe may be increased twofold by inserting a coiled spring along the length of the pipe to disrupt flow conditions near the inner surface. If such a heat transfer enhancement scheme is adopted, what is the attendant value of $T_{m,o}$? Use of the insert would not come without a corresponding increase in the fan power requirement. What is the power requirement if the friction factor is increased by 50%?

(c) After extended exposure to the water, a thin coating of organic matter forms on the outer surface of the pipe, and its thermal resistance (for a unit area of the outer surface) is $R_{t,o}'' = 0.050$ m$^2 \cdot$ K/W. What is the corresponding value of $T_{m,o}$ without the insert of part (b)?

8.96 Consider sterilization of the pharmaceutical product of Problem 8.27. To avoid any possibility of heating the product to an unacceptably high temperature, atmospheric steam is condensed on the exterior of the tube instead of using the resistance heater, providing a uniform surface temperature, $T_s = 100$°C.

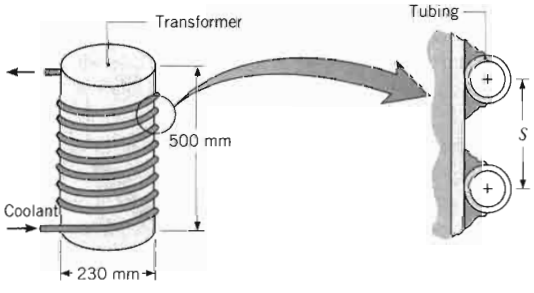
(a) For the conditions of Problem 8.27, determine the required length of straight tube, L_s, that would be needed to increase the mean temperature of the pharmaceutical product from 25°C to 75°C.

(b) Consider replacing the straight tube with a coiled tube characterized by a coil diameter $C = 100$ mm and a coil pitch $S = 25$ mm. Determine the overall length of the coiled tube, L_{cl} (i.e., the product of the tube pitch and the number of coils), necessary to increase the mean temperature of the pharmaceutical to the desired value.

(c) Calculate the pressure drop through the straight tube and through the coiled tube.

(d) Calculate the steam condensation rate.

8.97 An electrical power transformer of diameter 230 mm and height 500 mm dissipates 1000 W. It is desired to maintain its surface temperature at 47°C by supplying ethylene glycol at 24°C through thin-walled tubing of 20-mm diameter welded to the lateral surface of the transformer. All the heat dissipated by the transformer is assumed to be transferred to the ethylene glycol.



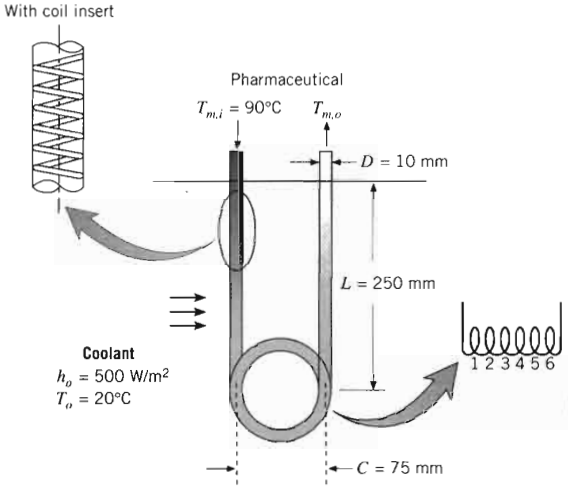
Patent Owner Manufacturing Resources International, Inc.
Exhibit 2017 - Page 558 of 999

Assuming the maximum allowable temperature rise of the coolant to be 6°C, determine the required coolant flow rate, the total length of tubing, and the coil pitch S between turns of the tubing.

8.98 A *bayonet cooler* is used to reduce the temperature of a pharmaceutical fluid. The pharmaceutical fluid flows through the cooler, which is fabricated of 10-mm-diameter, thin-walled tubing with two 250-mm-long straight sections and a coil with six and a half turns and a coil diameter of 75 mm. A coolant flows outside the cooler, with a convection coefficient at the outside surface of $h_o = 500\ \text{W/m}^2 \cdot \text{K}$ and a coolant temperature of 20°C. Consider the situation where the pharmaceutical fluid enters at 90°C with a mass flow rate of 0.005 kg/s. The pharmaceutical has the following properties: $\rho = 1200\ \text{kg/m}^3$, $\mu = 4 \times 10^{-3}\ \text{N} \cdot \text{s/m}^2$, $c_p = 2000\ \text{J/kg} \cdot \text{K}$, and $k = 0.5\ \text{W/m} \cdot \text{K}$.

(a) Determine the outlet temperature of the pharmaceutical fluid.

(b) It is desired to further reduce the outlet temperature of the pharmaceutical. However, because the cooling process is just one part of an intricate processing operation, flow rates cannot be changed. A young engineer suggests that the outlet temperature might be reduced by inserting stainless steel coiled springs into the straight sections of the cooler with the notion that the springs will disturb the flow adjacent to the inner tube wall and, in turn, increase the heat transfer coefficient at the inner tube wall. A senior engineer asserts that insertion of the springs should double the heat transfer coefficient at the straight inner tube walls. Determine the outlet temperature of the pharmaceutical fluid with the springs inserted into the tubes, assuming the senior engineer is correct in his assertion.



(c) Would you expect the outlet temperature of the pharmaceutical to depend on whether the springs have a left-hand or right-hand spiral? Why?

8.99 The mold used in an injection molding process consists of a top half and a bottom half. Each half is 60 mm × 60 mm × 20 mm and is constructed of metal ($\rho = 7800\ \text{kg/m}^3$, $c = 450\ \text{J/kg} \cdot \text{K}$). The cold mold (100°C) is to be heated to 200°C with pressurized water (available at 275°C and a total flow rate of 0.02 kg/s) prior to injecting the thermoplastic material. The injection takes only a fraction of a second, and the hot mold (200°C) is subsequently cooled with cold water (available at 25°C and a total flow rate of 0.02 kg/s) prior to ejecting the molded part. After part ejection, which also takes a fraction of a second, the process is repeated.

(a) In conventional mold design, straight cooling (heating) passages are bored through the mold in a location where the passages will not interfere with the molded part. Determine the initial heating rate and the initial cooling rate of the mold when five 5-mm-diameter, 60-mm-long passages are bored in each half of the mold (10 passages total). The velocity distribution of the water is fully developed at the entrance of each passage in the hot (or cold) mold.

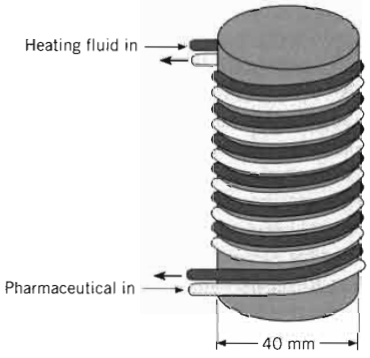
(b) New additive manufacturing processes, known as *selective freeform fabrication*, or *SFF*, are used to construct molds that are configured with *conformal cooling passages*. Consider the same mold as before, but now a 5-mm-diameter, coiled, conformal cooling passage is designed within each half of the SFF-manufactured mold. Each of the two coiled passages has $N = 2$ turns. The coiled passage does not interfere with the molded part. The conformal channels have a coil diameter $C = 50$ mm. The total water flow remains the same as in part (a) (0.01 kg/s per coil). Determine the initial heating rate and the initial cooling rate of the mold.

(c) Compare the surface areas of the conventional and conformal cooling passages. Compare the rate at which the mold temperature changes for molds configured with the conventional and conformal heating and cooling passages. Which cooling passage, conventional or conformal, will enable production of more parts per day? Neglect the presence of the thermoplastic material.

8.100 Consider the pharmaceutical product of Problem 8.27. Prior to finalizing the manufacturing process, test trials are performed to experimentally determine the dependence of the shelf life of the drug as a

Patent Owner Manufacturing Resources International, Inc.
Exhibit 2017 - Page 559 of 999

function of the sterilization temperature. Hence, the sterilization temperature must be carefully controlled in the trials. To promote good mixing of the pharmaceutical and, in turn, relatively uniform outlet temperatures across the exit tube area, experiments are performed using a device that is constructed of two interwoven coiled tubes, each of 10-mm diameter. The thin-walled tubing is welded to a solid high thermal conductivity rod of diameter $D_r = 40$ mm. One tube carries the pharmaceutical product at a mean velocity of $u_p = 0.1$ m/s and inlet temperature of 25°C, while the second tube carries pressurized liquid water at $u_w = 0.12$ m/s with an inlet temperature of 127°C. The tubes do not contact each other but are each welded to the solid metal rod, with each tube making 20 turns around the rod. The exterior of the apparatus is well insulated.

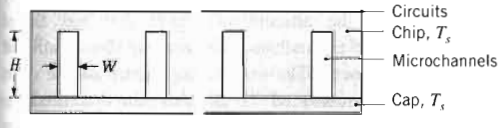


(a) Determine the outlet temperature of the pharmaceutical product. Evaluate the liquid water properties at 380 K.

(b) Investigate the sensitivity of the pharmaceutical's outlet temperature to the velocity of the pressurized water over the range $0.10 < u_w < 0.25$ m/s.

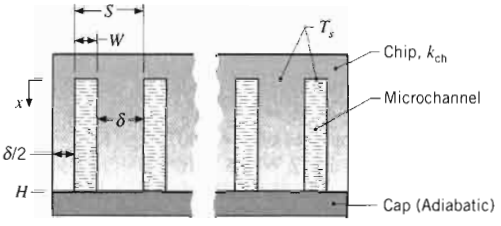
Microscale Internal Flow

8.101 An extremely effective method of cooling high-power-density silicon chips involves etching microchannels in the back (noncircuit) surface of the chip. The channels are covered with a silicon cap, and cooling is maintained by passing water through the channels.



Consider a chip that is 10 mm by 10 mm on a side and in which fifty 10-mm-long rectangular microchannels, each of width $W = 50$ μm and height $H = 200$ μm, have been etched. Consider operating conditions for which water enters each microchannel at a temperature of 290 K and a flow rate of 10^{-4} kg/s, while the chip and cap are at a uniform temperature of 350 K. Assuming fully developed flow in the channel and that all the heat dissipated by the circuits is transferred to the water, determine the water outlet temperature and the chip power dissipation. Water properties may be evaluated at 300 K.

8.102 Consider the microchannel cooling arrangement of Problem 8.101. However, instead of assuming the entire chip and cap to be at a uniform temperature, adopt a more conservative (and realistic) approach that prescribes a temperature of $T_s = 350$ K at the base of the channels ($x = 0$) and allows for a decrease in temperature with increasing x along the side walls of each channel.



(a) For the operating conditions prescribed in Problem 8.101 and a chip thermal conductivity of $k_{ch} = 140$ W/m · K, determine the water outlet temperature and the chip power dissipation. Heat transfer from the sides of the chip to the surroundings and from the side walls of a channel to the cap may be neglected. Note that the spacing between channels, $\delta = S - W$, is twice the spacing between the side wall of an outer channel and the outer surface of the chip. The channel pitch is $S = L/N$, where $L = 10$ mm is the chip width and $N = 50$ is the number of channels.

(b) The channel geometry prescribed in Problem 8.101 and considered in part (a) is not optimized, and larger heat rates may be dissipated by adjusting related dimensions. Consider the effect of reducing the pitch to a value of $S = 100$ μm, while retaining a width of $W = 50$ μm and a flow rate per channel of $\dot{m}_1 = 10^{-4}$ kg/s.

8.103 Due to its comparatively large thermal conductivity, water is a preferred fluid for convection cooling. However, in applications involving electronic devices, water must not come into contact with the devices, which would therefore have to be hermetically sealed. To circumvent related design and operational complexities

Patent Owner Manufacturing Resources International, Inc.
Exhibit 2017 - Page 560 of 999

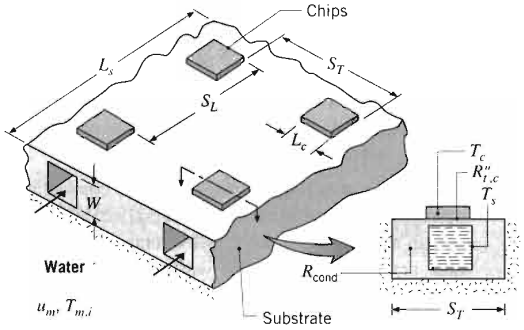
and to ensure that the devices are not rendered inoperable by contact with the coolant, a dielectric fluid is commonly used in lieu of water. Many gases have excellent dielectric characteristics, and despite its poor heat transfer properties, air is the common choice for electronic cooling. However, there is an alternative, which involves a class of *perfluorinated liquids* that are excellent dielectrics and have heat transfer properties superior to those of gases.

Consider the microchannel chip cooling application of Problem 8.102, but now for a perfluorinated liquid with properties of $c_p = 1050$ J/kg · K, $k = 0.065$ W/m · K, $\mu = 0.0012$ N · s/m^2 and $Pr = 15$.

(a) For channel dimensions of $H = 200\ \mu$m, $W = 50\ \mu$m and $S = 200\ \mu$m, a chip thermal conductivity of $k_{ch} = 140$ W/m · K and width $L = 10$ mm, a channel base temperature ($x = 0$) of $T_s = 350$ K, a channel inlet temperature of $T_{m,i} = 290$ K, and a flow rate of $\dot{m}_l = 10^{-4}$ kg/s per channel, determine the outlet temperature and the chip power dissipation for the dielectric liquid.

(b) Consider the foregoing conditions, but with air at a flow rate of $\dot{m}_l = 10^{-6}$ kg/s used as the coolant. Using properties of $c_p = 1007$ J/kg · K, $k = 0.0263$ W/m · K, and $\mu = 185 \times 10^{-7}$ N · s/m^2, determine the air outlet temperature and the chip power dissipation.

8.104 A novel scheme for dissipating heat from the chips of a multichip array involves machining coolant channels in the ceramic substrate to which the chips are attached. The square chips ($L_c = 5$ mm) are aligned above each of the channels, with longitudinal and transverse pitches of $S_L = S_T = 20$ mm. Water flows through the square cross section ($W = 5$ mm) of each channel with a mean velocity of $u_m = 1$ m/s, and its properties may be approximated as $\rho = 1000$ kg/m^3, $c_p = 4180$ J/kg · K, $\mu = 855 \times 10^{-6}$ kg/s · m, $k = 0.610$ W/m · K, and $Pr = 5.8$. Symmetry in the transverse direction dictates the existence of equivalent conditions for each substrate section of length L_s and width S_T.



(a) Consider a substrate whose length in the flow direction is $L_s = 200$ mm, thereby providing a total of $N_L = 10$ chips attached in-line above each flow channel. To a good approximation, all the heat dissipated by the chips above a channel may be assumed to be transferred to the water flowing through the channel. If each chip dissipates 5 W, what is the temperature rise of the water passing through the channel?

(b) The chip–substrate contact resistance is $R''_{t,c} = 0.5 \times 10^{-4}$ m^2 · K/W, and the three-dimensional conduction resistance for the $L_s \times S_T$ substrate section is $R_{cond} = 0.120$ K/W. If water enters the substrate at 25°C and is in fully developed flow, estimate the temperature T_c of the chips and the temperature T_s of the substrate channel surface.

8.105 An experiment is designed to study microscale forced convection. Water at $T_{m,i} = 300$ K is to be heated in a straight, circular glass tube with a 50-μm inner diameter and a wall thickness of 1 mm. Warm water at $T_\infty = 350$ K, $V = 2$ m/s is in cross flow over the exterior tube surface. The experiment is to be designed to cover the operating range $1 \le Re_D \le 2000$, where Re_D is the Reynolds number associated with the internal flow.

(a) Determine the tube length L that meets a design requirement that the tube be twice as long as the thermal entrance length associated with the highest Reynolds number of interest. Evaluate water properties at 305 K.

(b) Determine the water outlet temperature, $T_{m,o}$, that is expected to be associated with $Re_D = 2000$. Evaluate the heating water (water in cross flow over the tube) properties at 330 K.

(c) Calculate the pressure drop from the entrance to the exit of the tube for $Re_D = 2000$.

(d) Based on the calculated flow rate and pressure drop in the tube, estimate the height of a column of water (at 300 K) necessary to supply the necessary pressure at the tube entrance and the time needed to collect 0.1 liter of water. Discuss how the outlet temperature of the water flowing from the tube, $T_{m,o}$, might be measured.

8.106 An experiment is devised to measure liquid flow and convective heat transfer rates in microscale channels. The mass flow rate through a channel is determined by measuring the amount of liquid that has flowed through the channel and dividing by the duration of the experiment. The mean temperature of the outlet fluid is also measured. To minimize the time needed to perform the experiment (that is, to collect a significant amount of liquid so that its mass and temperature can be accurately measured), *arrays* of microchannels are

typically used
circular cross
50 μm, fabric
are 20 mm lor
at an inlet te
channels from
difference of
the exit of eac

In many
dimensions a
controlled du
apparatus. He
of machining
ing the experi

(a) Consider
are mach
diameters
turing co
45 μm, 5(
the mass
nels, alon
each chan

(b) If the wa
collected
late the a
channels
water that

(c) The enthu
flow rate
to analyze
diameter
and heat
decreased
convectio
the validit

Mass Transfer

8.107 In the process
inside diamet
Reynolds nun
plastic materi
developed co
400 K, and th
plastic vapor
mass transfer

8.108 Air at 300 K
through a 30-
film of water,
the inner surfa

Determi
cient for this

Patent Owner Manufacturing Resources International, Inc.
Exhibit 2017 - Page 561 of 999

typically used. Consider an array of microchannels of circular cross section, each with a nominal diameter of 50 μm, fabricated into a copper block. The channels are 20 mm long, and the block is held at 310 K. Water at an inlet temperature of 300 K is forced into the channels from a pressurized plenum, so that a pressure difference of 2.5×10^6 Pa exists from the entrance to the exit of each channel.

In many microscale systems, the characteristic dimensions are similar to the tolerances that can be controlled during the manufacture of the experimental apparatus. Hence, careful consideration of the effect of machining tolerances must be made when interpreting the experimental results.

(a) Consider the case in which three microchannels are machined in the copper block. The channel diameters exhibit some deviation due to manufacturing constraints and are of actual diameter 45 μm, 50 μm, and 55 μm, respectively. Calculate the mass flow rate through each of the three channels, along with the mean outlet temperature of each channel.

(b) If the water exiting each of the three channels is collected and mixed in a single container, calculate the average flow rate through each of the three channels and the average mixed temperature of the water that is collected from all three channels.

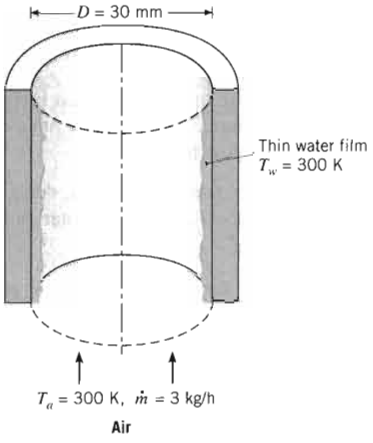
(c) The enthusiastic experimentalist uses the average flow rate and the average mixed outlet temperature to analyze the performance of the average (50 μm) diameter channel and concludes that flow rates and heat transfer coefficients are increased and decreased, respectively, by about 5% when forced convection occurs in microchannels. Comment on the validity of the experimentalist's conclusion.

Mass Transfer

8.107 In the processing of very long plastic tubes of 2-mm inside diameter, air flows inside the tubing with a Reynolds number of 1000. The interior layer of the plastic material evaporates into the air under fully developed conditions. Both plastic and air are at 400 K, and the Schmidt number for the mixture of the plastic vapor and air is 2.0. Determine the convection mass transfer coefficient.

8.108 Air at 300 K and a flow rate of 3 kg/h passes upward through a 30-mm tube, as shown in the sketch. A thin film of water, also at 300 K, slowly falls downward on the inner surface of the tube.

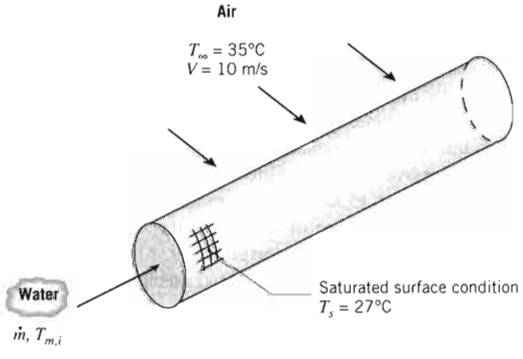
Determine the convection mass transfer coefficient for this situation.



8.109 What is the convection mass transfer coefficient associated with fully developed atmospheric airflow at 27°C and 0.04 kg/s through a 50-mm-diameter tube whose surface has been coated with a thin layer of naphthalene? Determine the velocity and concentration entry lengths.

8.110 Air flowing through a tube of 75-mm diameter passes over a 150-mm-long roughened section that is constructed from naphthalene having the properties $\mathcal{M}$ = 128.16 kg/kmol and $p_{sat}(300\ \text{K}) = 1.31 \times 10^{-4}$ bar. The air is at 1 atm and 300 K, and the Reynolds number is Re_D = 35,000. In an experiment for which flow was maintained for 3 h, mass loss due to sublimation from the roughened surface was determined to be 0.01 kg. What is the associated convection mass transfer coefficient? What would be the corresponding convection heat transfer coefficient? Contrast these results with those predicted by conventional smooth tube correlations.

8.111 Dry air at 35°C and a velocity of 10 m/s flows over a thin-walled tube of 20-mm diameter and 200-mm length, having a fibrous coating that is water-saturated.



Patent Owner Manufacturing Resources International, Inc.
Exhibit 2017 - Page 562 of 999

To maintain an approximately uniform surface temperature of 27°C, water at a prescribed flow rate and temperature passes through the tube.

(a) Considering the heat and mass transfer processes on the external surface of the tube, determine the heat rate from the tube.

(b) For a flow rate of 0.025 kg/s, determine the inlet temperature, $T_{m,i}$, at which water must be supplied to the tube.

8.112 Consider gas flow of mass density ρ and rate $\dot{m}$ through a tube whose inner surface is coated with a liquid or a sublimable solid of uniform vapor density $\rho_{A,s}$. Derive Equation 8.84 for variation of the mean vapor density, $\rho_{A,m}$, with distance x from the tube entrance and Equation 8.81 for the total rate of vapor transfer from a tube of length L.

8.113 Atmospheric air at 25°C and 3×10^{-4} kg/s flows through a 10-mm-diameter, 1-m-long circular tube whose inner surface is wetted with a water film. Determine the water vapor density at the tube outlet, assuming the inlet air to be dry. What is the rate at which vapor is added to the air?

8.114 Air at 25°C and 1 atm is in fully developed flow at $\dot{m} = 10^{-3}$ kg/s through a 10-mm-diameter circular tube whose inner surface is wetted with water. Determine the tube length required for the water vapor in the air to reach 99% of saturation. The inlet air is dry.

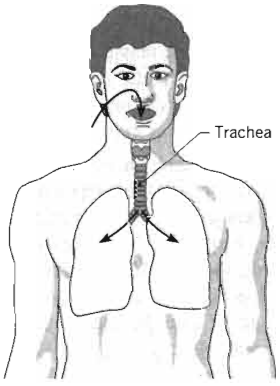
8.115 A humidifier consists of a bundle of vertical tubes, each of 20-mm diameter, through which dry atmospheric air is in fully developed flow at 10^{-3} kg/s and 298 K. The inner tube surface is wetted with a water film. Determine the tube length required for the water vapor to reach 99% of saturation. What is the rate at which energy must be supplied to each tube to maintain its temperature at 298 K?

8.116 The final step of a manufacturing process in which a protective coating is applied to the inner surface of a circular tube involves passage of dry, atmosphere air through the tube to remove a residual liquid associated with the process. Consider a coated 5-m-long tube with an inner diameter of 50 mm. The tube is maintained at a temperature of 300 K, and the residual liquid exists as a thin film whose corresponding vapor pressure is 15 mm Hg. The molecular weight and diffusion coefficient of the vapor are $\mathcal{M}_A = 70$ kg/kmol and $D_{AB} = 10^{-5}$ m^2/s, respectively. Air enters the tube at a mean velocity of 0.5 m/s and a temperature of 300 K.

(a) Estimate the partial pressure and mass density of vapor in the air exiting the tube.

(b) What is the rate of liquid removal from the tube in kg/s?

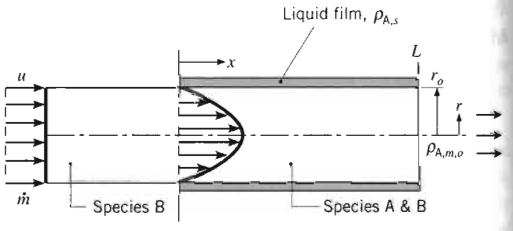
8.117 Dry air is inhaled at a rate of 10 liter/min through a trachea with a diameter of 20 mm and a length of 125 mm. The inner surface of the trachea is at a normal body temperature of 37°C and may be assumed to be saturated with water.



(a) Assuming steady, fully developed flow in the trachea, estimate the mass transfer convection coefficient.

(b) Estimate the daily water loss (liter/day) associated with evaporation in the trachea.

8.118 A mass transfer operation is preceded by laminar flow of a gaseous species B through a circular tube that is sufficiently long to achieve a fully developed velocity profile. Once the fully developed condition is reached, the gas enters a section of the tube that is wetted with a liquid film (A). The film maintains a uniform vapor density $\rho_{A,s}$ along the tube surface.



(a) Write the differential equation and boundary conditions that govern the species A mass density distribution, $\rho_A(x, r)$, for $x > 0$.

(b) What is the heat transfer analog to this problem? From this analog, write an expression for the

average Sh
exchange o

(c) Beginning
species to a
$\pi r_o^2\, dx$, der
may be use
$\rho_{A,m,o}$ at $x =$

Patent Owner Manufacturing Resources International, Inc.
Exhibit 2017 - Page 563 of 999

removal from the tube

10 liter/min through a
) mm and a length of
the trachea is at a nor-
and may be assumed to

– Trachea

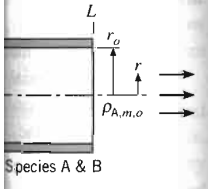


developed flow in the
ss transfer convection

ss (liter/day) associated
hea.

eceded by laminar flow
a circular tube that is
ully developed velocity
ed condition is reached,
be that is wetted with a
ntains a uniform vapor
ace.

l film, $\rho_{A,s}$



tion and boundary con-
ies A mass density dis-
0.

analog to this problem?
an expression for the

average Sherwood number associated with mass exchange over the region $0 \leq x \leq L$.

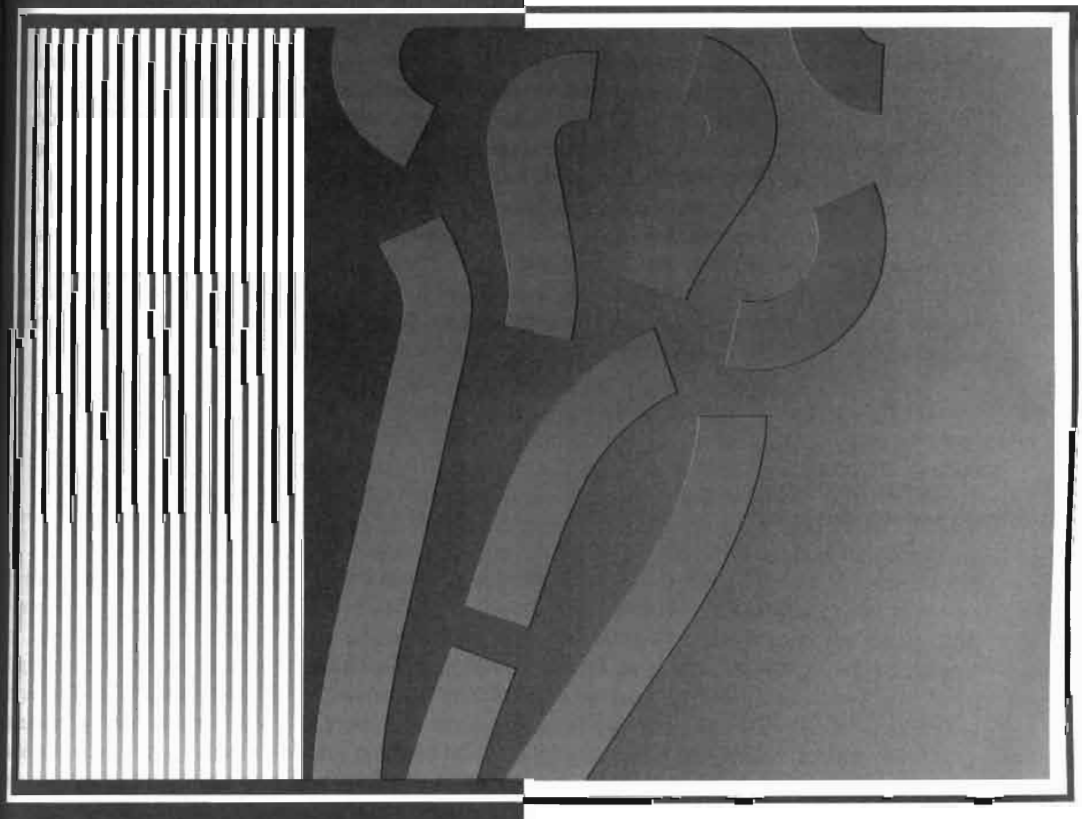
(c) Beginning with application of conservation of species to a differential control volume of extent $\pi r_o^2\, dx$, derive an expression (Equation 8.84) that may be used to determine the mean vapor density $\rho_{A,m,o}$ at $x = L$.

(d) Consider conditions for which species B is air at 25°C and 1 atm and the liquid film consists of water, also at 25°C. The flow rate is $\dot{m} = 2.5 \times 10^{-4}$ kg/s, and the tube diameter is $D = 10$ mm. What is the mean vapor density at the tube outlet if $L = 1$ m?

Patent Owner Manufacturing Resources International, Inc.
Exhibit 2017 - Page 564 of 999

CHAPTER 9

Free Convection



Patent Owner Manufacturing Resources International, Inc.
Exhibit 2017 - Page 565 of 999

In preceding chapters we considered convection transfer in fluid flows that originate from an *external forcing* condition. For example, fluid motion may be induced by a fan or a pump, or it may result from propulsion of a solid through the fluid. In the presence of a temperature gradient, *forced convection* heat transfer will occur.

Now we consider situations for which there is no *forced* velocity, yet convection currents exist within the fluid. Such situations are referred to as *free* or *natural convection,* and they originate when a *body force* acts on a fluid in which there are *density gradients.* The net effect is a *buoyancy force,* which induces free convection currents. In the most common case, the density gradient is due to a temperature gradient, and the body force is due to the gravitational field.

Since free convection flow velocities are generally much smaller than those associated with forced convection, the corresponding convection transfer rates are also smaller. It is perhaps tempting to therefore attach less significance to free convection processes. This temptation should be resisted. In many systems involving multimode heat transfer effects, free convection provides the largest resistance to heat transfer and therefore plays an important role in the design or performance of the system. Moreover, when it is desirable to minimize heat transfer rates or to minimize operating cost, free convection is often preferred to forced convection.

There are, of course, many applications. Free convection strongly influences the operating temperatures of power generating and electronic devices. It plays a major role in a vast array of thermal manufacturing applications. Free convection is important in establishing temperature distributions within buildings and in determining heat losses or heat loads for heating, ventilating, and air conditioning systems. Free convection distributes the poisonous products of combustion during fires and is relevant to the environmental sciences, where it drives oceanic and atmospheric motions, as well as the related heat transfer and mass transfer processes.

In this chapter our objectives are to obtain an appreciation for the physical origins and nature of buoyancy-driven flows and to acquire tools for performing related heat transfer calculations.

9.1 *Physical Considerations*

In free convection fluid motion is due to buoyancy forces within the fluid, while in forced convection it is externally imposed. *Buoyancy is due to the combined presence of a fluid density gradient* and *a body force that is proportional to density.* In practice, the body force is usually *gravitational,* although it may be a centrifugal force in rotating fluid machinery or a Coriolis force in atmospheric and oceanic rotational motions. There are also several ways in which a mass density gradient may arise in a fluid, but for the most common situation it is due to the presence of a temperature gradient. We know that the density of gases and liquids depends on temperature, generally decreasing (due to fluid expansion) with increasing temperature ($\partial\rho/\partial T < 0$).

In this text we focus on free convection problems in which the density gradient is due to a temperature gradient and the body force is gravitational. However, the

Patent Owner Manufacturing Resources International, Inc.
Exhibit 2017 - Page 566 of 999

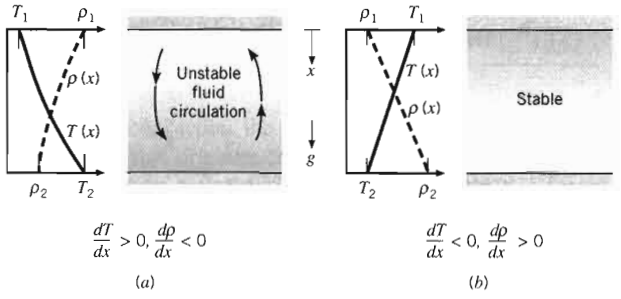


FIGURE 9.1 Conditions in a fluid between large horizontal plates at different temperatures. (*a*) Unstable temperature gradient. (*b*) Stable temperature gradient.

presence of a fluid density gradient in a gravitational field does not ensure the existence of free convection currents. Consider the conditions of Figure 9.1. A fluid is enclosed by two large, horizontal plates of different temperature ($T_1 \neq T_2$). In case *a* the temperature of the lower plate exceeds that of the upper plate, and the density decreases in the direction of the gravitational force. If the temperature difference exceeds a critical value, conditions are *unstable* and buoyancy forces are able to overcome the retarding influence of viscous forces. The gravitational force on the denser fluid in the upper layers exceeds that acting on the lighter fluid in the lower layers, and the designated circulation pattern will exist. The heavier fluid will descend, being warmed in the process, while the lighter fluid will rise, cooling as it moves. However, this condition does not characterize case *b*, for which $T_1 > T_2$ and the density no longer decreases in the direction of the gravitational force. Conditions are now *stable,* and there is no bulk fluid motion. In case *a* heat transfer occurs from the bottom to the top surface by free convection; for case *b* heat transfer (from top to bottom) occurs by conduction.

Free convection flows may be classified according to whether the flow is bounded by a surface. In the absence of an adjoining surface, *free boundary flows* may occur in the form of a *plume* or a *buoyant jet* (Figure 9.2). A plume is associated with fluid rising from a submerged heated object. Consider the heated wire of Figure 9.2*a*, which is immersed in an *extensive, quiescent* fluid.[1] Fluid that is heated by the wire rises due to buoyancy forces, entraining fluid from the quiescent region. Although the width of the plume increases with distance from the wire, the plume itself will eventually dissipate as a result of viscous effects and a reduction in the buoyancy force caused by cooling of the fluid in the plume. The distinction between a plume and a buoyant jet is generally made on the basis of the *initial* fluid velocity. This velocity is zero for the plume, but finite for the buoyant jet. Figure 9.2*b* shows a heated fluid being discharged as a horizontal jet into a quiescent medium of lower temperature. The vertical motion that the jet begins to assume is due to the buoyancy force. Such a condition occurs when warm water

[1]An extensive medium is, in principle, an infinite medium. Since a quiescent fluid is one that is otherwise at rest, the velocity of fluid far from the heated wire is zero.

Patent Owner Manufacturing Resources International, Inc.
Exhibit 2017 - Page 567 of 999

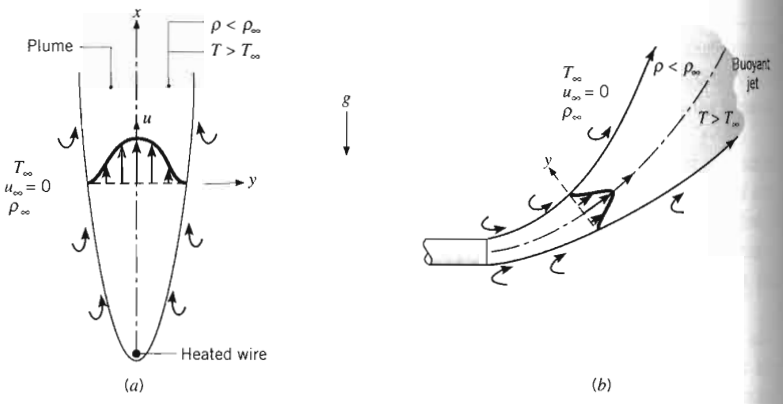


FIGURE 9.2 Buoyancy-driven free boundary layer flows in an extensive, quiescent medium. (*a*) Plume formation above a heated wire. (*b*) Buoyant jet associated with a heated discharge.

from the condenser of a central power station is discharged into a reservoir of cooler water. Free boundary flows are discussed in considerable detail by Jaluria [1] and Gebhart et al. [2].

In this text we focus on free convection flows bounded by a surface, and a classic example relates to boundary layer development on a heated vertical plate (Figure 9.3). The plate is immersed in an extensive, quiescent fluid, and with $T_s > T_\infty$ the fluid close to the plate is less dense than fluid that is further removed. Buoyancy forces therefore induce a free convection boundary layer in which the heated fluid rises vertically, entraining fluid from the quiescent region. The resulting velocity distribution is unlike that associated with forced convection boundary layers. In particular, the velocity is zero as $y \rightarrow \infty$, as well as at $y = 0$. A free convection boundary layer also develops if $T_s < T_\infty$. In this case, however, fluid motion is downward.

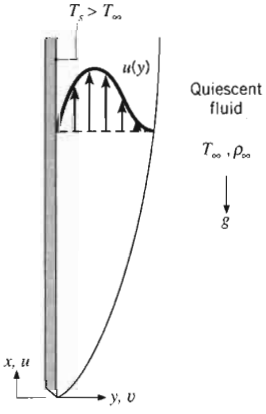
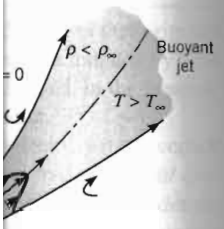


FIGURE 9.3
Boundary layer development on a heated vertical plate.

Patent Owner Manufacturing Resources International, Inc.
Exhibit 2017 - Page 568 of 999



(*b*)

sive, quiescent medium.
ith a heated discharge.

to a reservoir of cooler
tail by Jaluria [1] and

d by a surface, and a
a heated vertical plate
scent fluid, and with
at is further removed.
ary layer in which the
ent region. The result-
l convection boundary
s at $y = 0$. A free con-
however, fluid motion

eated vertical

9.2 The Governing Equations

As for forced convection, the equations that describe momentum and energy transfer in free convection originate from the related conservation principles. Moreover, the specific processes are much like those that dominate in forced convection. Inertia and viscous forces remain important, as does energy transfer by advection and diffusion. The difference between the two flows is that, in free convection, a major role is played by buoyancy forces. It is such forces that, in fact, sustain the flow.

Consider a laminar boundary layer flow (Figure 9.3) that is driven by buoyancy forces. Assume steady, two-dimensional, constant property conditions in which the gravity force acts in the negative x direction. Also, with one exception, assume the fluid to be incompressible. The exception involves accounting for the effect of variable density in the buoyancy force, since it is this variation that induces fluid motion. Finally, assume that the boundary layer approximations are valid.

With the foregoing simplifications the x-momentum equation (Equation D.2) reduces to the boundary layer equation (Equation 6.28), except that the body force term X is retained. If the only contribution to this force is made by gravity, the body force per unit volume is $X = -\rho g$, where g is the local acceleration due to gravity. The appropriate form of the x-momentum equation is then

$$u\frac{\partial u}{\partial x} + v\frac{\partial u}{\partial y} = -\frac{1}{\rho}\frac{dp_\infty}{dx} - g + \nu\frac{\partial^2 u}{\partial y^2} \tag{9.1}$$

where dp_∞/dx is the free stream pressure gradient in the quiescent region *outside* the boundary layer. In this region, $u = 0$ and Equation 9.1 reduces to

$$\frac{dp_\infty}{dx} = -\rho_\infty g \tag{9.2}$$

Substituting Equation 9.2 into 9.1, we obtain the following expression:

$$u\frac{\partial u}{\partial x} + v\frac{\partial u}{\partial y} = g\,(\Delta\rho/\rho) + \nu\frac{\partial^2 u}{\partial y^2} \tag{9.3}$$

where $\Delta\rho = \rho_\infty - \rho$. This expression must apply at every point in the free convection boundary layer.

The first term on the right-hand side of Equation 9.3 is the buoyancy force, and flow originates because the density ρ is a variable. If density variations are due only to temperature variations, the term may be related to a fluid property known as the *volumetric thermal expansion coefficient*

$$\beta = -\frac{1}{\rho}\left(\frac{\partial\rho}{\partial T}\right)_p \tag{9.4}$$

This *thermodynamic* property of the fluid provides a measure of the amount by which the density changes in response to a change in temperature at constant pressure. If it is expressed in the following approximate form,

$$\beta \approx -\frac{1}{\rho}\frac{\Delta\rho}{\Delta T} = -\frac{1}{\rho}\frac{\rho_\infty - \rho}{T_\infty - T}$$

Patent Owner Manufacturing Resources International, Inc.
Exhibit 2017 - Page 569 of 999

it follows that

$$(\rho_\infty - \rho) \approx \rho\beta(T - T_\infty)$$

This simplification is known as the *Boussinesq approximation*, and substituting into Equation 9.3, the x-momentum equation becomes

$$u\frac{\partial u}{\partial x} + v\frac{\partial u}{\partial y} = g\beta(T - T_\infty) + \nu\frac{\partial^2 u}{\partial y^2} \tag{9.5}$$

where it is now apparent how the buoyancy force, which drives the flow, is related to the temperature difference.

Since buoyancy effects are confined to the momentum equation, the mass and energy conservation equations are unchanged from forced convection. Equations 6.27 and 6.29 may then be used to complete the problem formulation. The set of governing equations is then

$$\frac{\partial u}{\partial x} + \frac{\partial v}{\partial y} = 0 \tag{9.6}$$

$$u\frac{\partial u}{\partial x} + v\frac{\partial u}{\partial y} = g\beta(T - T_\infty) + \nu\frac{\partial^2 u}{\partial y^2} \tag{9.7}$$

$$u\frac{\partial T}{\partial x} + v\frac{\partial T}{\partial y} = \alpha\frac{\partial^2 T}{\partial y^2} \tag{9.8}$$

Note that viscous dissipation has been neglected in the energy equation, (9.8), an assumption that is certainly reasonable for the small velocities associated with free convection. In the mathematical sense the appearance of the buoyancy term in Equation 9.7 complicates matters. No longer may the hydrodynamic problem, given by Equations 9.6 and 9.7, be uncoupled from and solved to the exclusion of the thermal problem, given by Equation 9.8. The solution to the momentum equation depends on knowledge of T, and hence on the solution to the energy equation. Equations 9.6 through 9.8 are therefore strongly coupled and must be solved simultaneously.

Free convection effects obviously depend on the expansion coefficient β. The manner in which β is obtained depends on the fluid. For an ideal gas, $\rho = p/RT$ and

$$\beta = -\frac{1}{\rho}\left(\frac{\partial \rho}{\partial T}\right)_p = \frac{1}{\rho}\frac{p}{RT^2} = \frac{1}{T} \tag{9.9}$$

where T is the *absolute* temperature. For liquids and nonideal gases, β must be obtained from appropriate property tables (Appendix A).

9.3 *Similarity Considerations*

Let us now consider the dimensionless parameters that govern free convective flow and heat transfer. As for forced convection (Chapter 6), the parameters may be obtained by nondimensionalizing the governing equations. Introducing

$$x^* \equiv \frac{x}{L} \qquad y^* \equiv \frac{y}{L}$$

Patent Owner Manufacturing Resources International, Inc.
Exhibit 2017 - Page 570 of 999

$$u^* \equiv \frac{u}{u_0} \qquad v^* \equiv \frac{v}{u_0} \qquad T^* \equiv \frac{T - T_\infty}{T_s - T_\infty}$$

where L is a characteristic length and u_0 is an *arbitrary* reference velocity,[2] the x-momentum and energy equations (9.7 and 9.8) reduce to

$$u^* \frac{\partial u^*}{\partial x^*} + v^* \frac{\partial u^*}{\partial y^*} = \frac{g\beta (T_s - T_\infty)L}{u_0^2} T^* + \frac{1}{Re_L} \frac{\partial^2 u^*}{\partial y^{*2}} \tag{9.10}$$

$$u^* \frac{\partial T^*}{\partial x^*} + v^* \frac{\partial T^*}{\partial y^*} = \frac{1}{Re_L\, Pr} \frac{\partial^2 T^*}{\partial y^{*2}} \tag{9.11}$$

The dimensionless parameter in the first term on the right-hand side of Equation 9.10 is a direct consequence of the buoyancy force. Since the reference velocity u_0 is arbitrary, it can be chosen to simplify the form of the equation. It is convenient to choose $u_0^2 = g\beta(T_s - T_\infty)L$, so that the term multiplying T^* becomes unity. Then, Re_L becomes $[g\beta(T_s - T_\infty)L^3/\nu^2]^{1/2}$. It is customary to define the *Grashof number* Gr_L as the square of this Reynolds number:

$$Gr_L \equiv \frac{g\beta(T_s - T_\infty)L^3}{\nu^2} \tag{9.12}$$

As a result, Re_L in Equations 9.10 and 9.11 is replaced by $Gr_L^{1/2}$, and we see that the Grashof number (or more precisely, $Gr_L^{1/2}$) plays the same role in free convection that the Reynolds number plays in forced convection. Based on the resulting form of Equations 9.10 and 9.11, we expect heat transfer correlations of the form $Nu_L = f(Gr_L, Pr)$ in free convection. Recall that the *Reynolds number* provides a measure of the *ratio of the inertial to viscous forces* acting on a fluid element. In contrast, the *Grashof number* is a measure of the *ratio of the buoyancy forces to the viscous forces* acting on the fluid.

When forced and free convection effects are comparable, the situation is more complex. For example, consider the boundary layer of Figure 9.3, but with a non zero free stream velocity, u_∞. In this case, it is more convenient to choose the characteristic velocity as u_∞ (so that the free stream boundary condition for the dimensionless velocity, u^*, is simply $u^*(y^* \to \infty) \to 1$). Then the T^* term in Equation 9.10 will be multiplied by Gr_L/Re_L^2, and the resulting Nusselt number expressions will be of the form $Nu_L = f(Re_L, Gr_L, Pr)$. Generally, the combined effects of free and forced convection must be considered when $Gr_L/Re_L^2 \approx 1$. If the inequality $Gr_L/Re_L^2 \ll 1$ is satisfied, free convection effects may be neglected and $Nu_L = f(Re_L, Pr)$. Conversely, if $Gr_L/Re_L^2 \gg 1$, forced convection effects may be neglected and $Nu = f(Gr_L, Pr)$, as indicated in the preceding paragraph for pure free convection.

[2]Since free stream conditions are quiescent in free convection, there is no logical external reference velocity (V or u_∞), as in forced convection.

Patent Owner Manufacturing Resources International, Inc.
Exhibit 2017 - Page 571 of 999

9.4 *Laminar Free Convection on a Vertical Surface*

Numerous solutions to the laminar free convection boundary layer equations have been obtained, and a special case that has received much attention involves free convection from an isothermal vertical surface in an extensive quiescent medium (Figure 9.3). For this geometry Equations 9.6 through 9.8 must be solved subject to boundary conditions of the form[3]

$$y = 0: \qquad u = v = 0 \qquad T = T_s$$
$$y \to \infty: \qquad u \to 0 \qquad T \to T_\infty$$

A similarity solution to the foregoing problem has been obtained by Ostrach [3]. The solution involves transforming variables by introducing a *similarity parameter* of the form

$$\eta \equiv \frac{y}{x}\left(\frac{Gr_x}{4}\right)^{1/4} \tag{9.13}$$

and representing the velocity components in terms of a stream function defined as

$$\psi(x,y) \equiv f(\eta)\left[4\nu\left(\frac{Gr_x}{4}\right)^{1/4}\right] \tag{9.14}$$

With the foregoing definition of the stream function, the x-velocity component may be expressed as

$$u = \frac{\partial\psi}{\partial y} = \frac{\partial\psi}{\partial\eta}\frac{\partial\eta}{\partial y} = 4\nu\left(\frac{Gr_x}{4}\right)^{1/4} f'(\eta)\frac{1}{x}\left(\frac{Gr_x}{4}\right)^{1/4}$$
$$= \frac{2\nu}{x}Gr_x^{1/2} f'(\eta) \tag{9.15}$$

where primed quantities indicate differentiation with respect to η. Hence $f'(\eta) \equiv df/d\eta$. Evaluating the y-velocity component $v = -\partial\psi/\partial x$ in a similar fashion and introducing the dimensionless temperature

$$T^* \equiv \frac{T - T_\infty}{T_s - T_\infty} \tag{9.16}$$

the three original partial differential equations (9.6 through 9.8) may then be reduced to two ordinary differential equations of the form

$$f''' + 3ff'' - 2(f')^2 + T^* = 0 \tag{9.17}$$

$$T^{*\prime\prime} + 3Prf T^{*\prime} = 0 \tag{9.18}$$

[3]The boundary layer approximations are assumed in using Equations 9.6 through 9.8. However, the approximations are only valid for $(Gr_x\, Pr) \gtrsim 10^4$. Below this value (close to the leading edge) the boundary layer thickness is too large relative to the characteristic length x to ensure the validity of the approximations.

Patent Owner Manufacturing Resources International, Inc.
Exhibit 2017 - Page 572 of 999

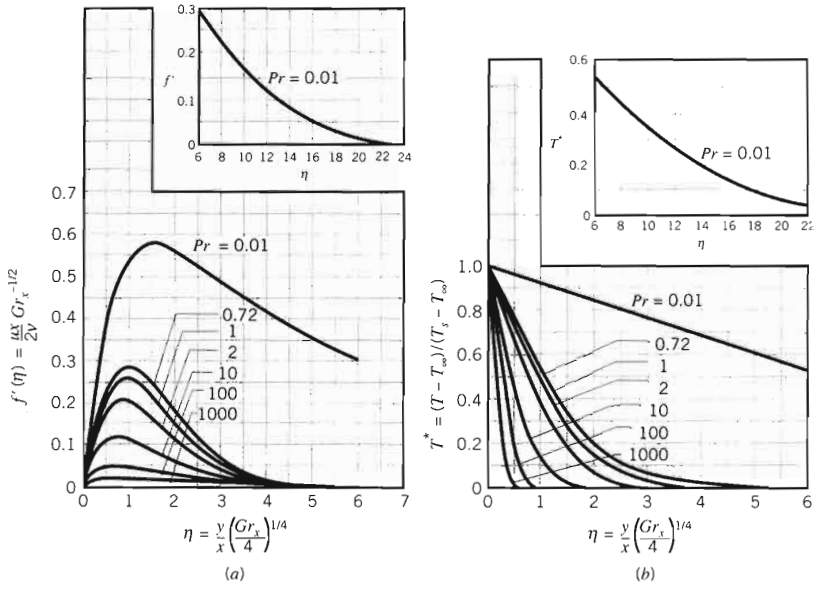


FIGURE 9.4 Laminar, free convection boundary layer conditions on an isothermal, vertical surface. (*a*) Velocity profiles. (*b*) Temperature profiles [3].

where f and T^* are functions of only η and the double and triple primes, respectively, refer to second and third derivatives with respect to η. Note that f is the key dependent variable for the velocity boundary layer and that the continuity equation (9.6) is automatically satisfied through introduction of the stream function.

The transformed boundary conditions required to solve the momentum and energy equations (9.17 and 9.18) are of the form

$$\eta = 0: \qquad f = f' = 0 \qquad T^* = 1$$
$$\eta \to \infty: \qquad f' \to 0 \qquad T^* \to 0$$

A numerical solution has been obtained by Ostrach [3], and selected results are shown in Figure 9.4. Note that the x-velocity component u may readily be obtained from Figure 9.4*a* through the use of Equation 9.15. Note also that, through the definition of the similarity parameter η, Figure 9.4 may be used to obtain values of u and T for any value of x and y.

Figure 9.4*b* may also be used to infer the appropriate form of the heat transfer correlation. Using Newton's law of cooling for the local convection coefficient h, the local Nusselt number may be expressed as

$$Nu_x = \frac{hx}{k} = \frac{[q_s''/(T_s - T_\infty)]x}{k}$$

Patent Owner Manufacturing Resources International, Inc.
Exhibit 2017 - Page 573 of 999

Using Fourier's law to obtain q_s'' and expressing the surface temperature gradient in terms of η, Equation 9.13, and T^*, Equation 9.16, it follows that

$$q_s'' = -k\frac{\partial T}{\partial y}\bigg|_{y=0} = -\frac{k}{x}(T_s - T_\infty)\left(\frac{Gr_x}{4}\right)^{1/4}\frac{dT^*}{d\eta}\bigg|_{\eta=0}$$

Hence

$$Nu_x = \frac{hx}{k} = -\left(\frac{Gr_x}{4}\right)^{1/4}\frac{dT^*}{d\eta}\bigg|_{\eta=0} = \left(\frac{Gr_x}{4}\right)^{1/4} g(Pr) \tag{9.19}$$

which acknowledges that the dimensionless temperature gradient at the surface is a function of the Prandtl number $g(Pr)$. This dependence is evident from Figure 9.4*b* and has been determined numerically for selected values of Pr [3]. The results have been correlated to within 0.5% by an interpolation formula of the form [4]

$$g(Pr) = \frac{0.75Pr^{1/2}}{(0.609 + 1.221Pr^{1/2} + 1.238Pr)^{1/4}} \tag{9.20}$$

which applies for $0 \leq Pr \leq \infty$.

Using Equation 9.19 for the local convection coefficient and substituting for the local Grashof number,

$$Gr_x = \frac{g\beta(T_s - T_\infty)x^3}{\nu^2}$$

the average convection coefficient for a surface of length L is then

$$\bar{h} = \frac{1}{L}\int_0^L h\,dx = \frac{k}{L}\left[\frac{g\beta(T_s - T_\infty)}{4\nu^2}\right]^{1/4} g(Pr)\int_0^L \frac{dx}{x^{1/4}}$$

Integrating, it follows that

$$\overline{Nu}_L = \frac{\bar{h}L}{k} = \frac{4}{3}\left(\frac{Gr_L}{4}\right)^{1/4} g(Pr) \tag{9.21}$$

or substituting from Equation 9.19, with $x = L$,

$$\overline{Nu}_L = \tfrac{4}{3}Nu_L \tag{9.22}$$

The foregoing results apply irrespective of whether $T_s > T_\infty$ or $T_s < T_\infty$. If $T_s < T_\infty$, conditions are inverted from those of Figure 9.3. The leading edge is at the top of the plate, and positive x is defined in the direction of the gravity force.

9.5 *The Effects of Turbulence*

It is important to note that free convection boundary layers are not restricted to laminar flow. As with forced convection, *hydrodynamic instabilities* may arise. That is,

Patent Owner Manufacturing Resources International, Inc.
Exhibit 2017 - Page 574 of 999

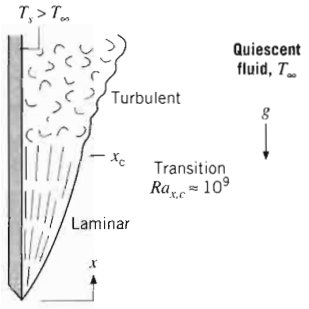


FIGURE 9.5
Free convection boundary layer transition on a vertical plate.

disturbances in the flow may be amplified, leading to transition from laminar to turbulent flow. This process is shown schematically in Figure 9.5 for a heated vertical plate.

Transition in a free convection boundary layer depends on the relative magnitude of the buoyancy and viscous forces in the fluid. It is customary to correlate its occurrence in terms of the *Rayleigh number,* which is simply the product of the Grashof and Prandtl numbers. For vertical plates the critical Rayleigh number is

$$Ra_{x,c} = Gr_{x,c}\,Pr = \frac{g\beta(T_s - T_\infty)x^3}{\nu\alpha} \approx 10^9 \tag{9.23}$$

An extensive discussion of stability and transition effects is provided by Gebhart et al. [2].

As in forced convection, transition to turbulence has a strong effect on heat transfer. Hence the results of the foregoing section apply only if $Ra_L \lesssim 10^9$. To obtain appropriate correlations for turbulent flow, emphasis is placed on experimental results.

EXAMPLE 9.1

Consider a 0.25-m-long vertical plate that is at 70°C. The plate is suspended in air that is at 25°C. Estimate the boundary layer thickness at the trailing edge of the plate if the air is quiescent. How does this thickness compare with that which would exist if the air were flowing over the plate at a free stream velocity of 5 m/s?

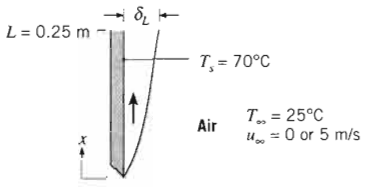
SOLUTION

Known: Vertical plate is in quiescent air at a lower temperature.

Find: Boundary layer thickness at trailing edge. Compare with thickness corresponding to an air speed of 5 m/s.

Patent Owner Manufacturing Resources International, Inc.
Exhibit 2017 - Page 575 of 999

Schematic:



Assumptions:

1. Constant properties.
2. Buoyancy effects negligible when $u_\infty = 5$ m/s.

Properties: Table A.4, air ($T_f = 320.5$ K): $\nu = 17.95 \times 10^{-6}$ m^2/s, $Pr = 0.7$, $\beta = T_f^{-1} = 3.12 \times 10^{-3}$ K^{-1}.

Analysis: For the quiescent air, Equation 9.12 gives

$$Gr_L = \frac{g\beta(T_s - T_\infty)L^3}{\nu^2}$$

$$= \frac{9.8 \text{ m/s}^2 \times (3.12 \times 10^{-3} \text{ K}^{-1})(70 - 25)°\text{C}(0.25 \text{ m})^3}{(17.95 \times 10^{-6} \text{ m}^2/\text{s})^2} = 6.69 \times 10^7$$

Hence $Ra_L = Gr_L\, Pr = 4.68 \times 10^7$ and, from Equation 9.23, the free convection boundary layer is laminar. The analysis of Section 9.4 is therefore applicable. From the results of Figure 9.4, it follows that, for $Pr = 0.7$, $\eta \approx 6.0$ at the edge of the boundary layer, that is, at $y \approx \delta$. Hence

$$\delta_L \approx \frac{6L}{(Gr_L/4)^{1/4}} = \frac{6(0.25 \text{ m})}{(1.67 \times 10^7)^{1/4}} = 0.024 \text{ m}$$

For airflow at $u_\infty = 5$ m/s

$$Re_L = \frac{u_\infty L}{\nu} = \frac{(5 \text{ m/s}) \times 0.25 \text{ m}}{17.95 \times 10^{-6} \text{ m}^2/\text{s}} = 6.97 \times 10^4$$

and the boundary layer is laminar. Hence, from Equation 7.19,

$$\delta_L \approx \frac{5L}{Re_L^{1/2}} = \frac{5(0.25 \text{ m})}{(6.97 \times 10^4)^{1/2}} = 0.0047 \text{ m}$$

Comments:

1. Boundary layer thicknesses are typically larger for free convection than for forced convection.
2. $(Gr_L/Re_L^2) = 0.014 \ll 1$, and the assumption of negligible buoyancy effects for $u_\infty = 5$ m/s is justified.

9.6
Empirical Co
External Free

Patent Owner Manufacturing Resources International, Inc.
Exhibit 2017 - Page 576 of 999

9.6 *Empirical Correlations: External Free Convection Flows*

In this section we summarize empirical correlations that have been developed for common *immersed* (external flow) geometries. The correlations are suitable for most engineering calculations and are generally of the form

$$\overline{Nu}_L = \frac{\bar{h}L}{k} = C\,Ra_L^n \tag{9.24}$$

where the Rayleigh number,

$$Ra_L = Gr_L\,Pr = \frac{g\beta(T_s - T_\infty)L^3}{\nu\alpha} \tag{9.25}$$

is based on the characteristic length L of the geometry. Typically, $n = \frac{1}{4}$ and $\frac{1}{3}$ for laminar and turbulent flows, respectively. For turbulent flow it then follows that $\bar{h}_L$ is independent of L. Note that all properties are evaluated at the film temperature, $T_f \equiv (T_s + T_\infty)/2$.

9.6.1 The Vertical Plate

Expressions of the form given by Equation 9.24 have been developed for the vertical plate [5–7]. For laminar flow ($10^4 \lesssim Ra_L \lesssim 10^9$), $C = 0.59$ and $n = 1/4$, and for turbulent flow ($10^9 \lesssim Ra_L \lesssim 10^{13}$), $C = 0.10$ and $n = 1/3$. A correlation that may be applied over the *entire* range of Ra_L has been recommended by Churchill and Chu [8] and is of the form

$$\overline{Nu}_L = \left\{0.825 + \frac{0.387Ra_L^{1/6}}{[1 + (0.492/Pr)^{9/16}]^{8/27}}\right\}^2 \tag{9.26}$$

Although Equation 9.26 is suitable for most engineering calculations, slightly better accuracy may be obtained for laminar flow by using [8]

$$\overline{Nu}_L = 0.68 + \frac{0.670Ra_L^{1/4}}{[1 + (0.492/Pr)^{9/16}]^{4/9}} \qquad Ra_L \lesssim 10^9 \tag{9.27}$$

When the Rayleigh number is moderately large, the second term on the right-hand side of Equations 9.26 and 9.27 dominates, and the correlations are the same form as Equation 9.24, except that the constant, C, is replaced by a function of Pr. Equation 9.27 is then in excellent quantitative agreement with the analytical solution given by Equations 9.21 and 9.20. In contrast, when the Rayleigh number is small, the first term on the right-hand side of Equations 9.26 and 9.27 dominates, and the

Patent Owner Manufacturing Resources International, Inc.
Exhibit 2017 - Page 577 of 999

equations yield the same behavior since $0.825^2 \approx 0.68$. The presence of leading constants in Equations 9.26 and 9.27 accounts for the fact that, for small Rayleigh number, the boundary layer assumption becomes invalid and conduction parallel to the plate is important.

It is important to recognize that the foregoing results have been obtained for an isothermal plate (constant T_s). If the surface condition is, instead, one of uniform heat flux (constant q_s''), the temperature difference $(T_s - T_\infty)$ will vary with x, increasing from a value of zero at the leading edge. An approximate procedure for determining this variation may be based on results [8, 9] showing that $\overline{Nu}_L$ correlations obtained for the isothermal plate may still be used to an excellent approximation, if $\overline{Nu}_L$ and Ra_L are defined in terms of the temperature difference at the midpoint of the plate, $\Delta T_{L/2} = T_s(L/2) - T_\infty$. Hence, with $\bar{h} \equiv q_s''/\Delta T_{L/2}$, a correlation such as Equation 9.27 could be used to determine $\Delta T_{L/2}$ (for example, using a trial-and-error technique), and hence the midpoint surface temperature $T_s(L/2)$. If it is assumed that $Nu_x \propto Ra_x^{1/4}$ over the entire plate, it follows that

$$\frac{q_s'' x}{k \Delta T} \propto \Delta T^{1/4} x^{3/4}$$

or

$$\Delta T \propto x^{1/5}$$

Hence the temperature difference at any x is

$$\Delta T_x \approx \frac{x^{1/5}}{(L/2)^{1/5}} \Delta T_{L/2} = 1.15 \left(\frac{x}{L}\right)^{1/5} \Delta T_{L/2} \tag{9.28}$$

A more detailed discussion of constant heat flux results is provided by Churchill [10].

The foregoing results may also be applied to *vertical* cylinders of height L, if the boundary layer thickness δ is much less than the cylinder diameter D. This condition is known to be satisfied [11] when

$$\frac{D}{L} \gtrsim \frac{35}{Gr_L^{1/4}}$$

Cebeci [12] and Minkowycz and Sparrow [13] present results for slender, vertical cylinders not meeting this condition, where transverse curvature influences boundary layer development and enhances the rate of heat transfer.

EXAMPLE 9.2

A glass-door firescreen, used to reduce exfiltration of room air through a chimney, has a height of 0.71 m and a width of 1.02 m and reaches a temperature of 232°C. If the room temperature is 23°C, estimate the convection heat rate from the fireplace to the room.

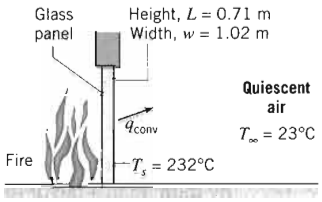
SOLUTION

Known: Glass screen situated in fireplace opening.

Patent Owner Manufacturing Resources International, Inc.
Exhibit 2017 - Page 578 of 999

Find: Heat transfer by convection between screen and room air.

Schematic:



Assumptions:

1. Screen is at a uniform temperature T_s.
2. Room air is quiescent.

Properties: Table A.4, air ($T_f = 400$ K): $k = 33.8 \times 10^{-3}$ W/m · K, $\nu = 26.4 \times 10^{-6}$ m^2/s, $\alpha = 38.3 \times 10^{-6}$ m^2/s, $Pr = 0.690$, $\beta = (1/T_f) = 0.0025$ K^{-1}.

Analysis: The rate of heat transfer by free convection from the panel to the room is given by Newton's law of cooling

$$q = \bar{h} A_s (T_s - T_\infty)$$

where $\bar{h}$ may be obtained from knowledge of the Rayleigh number. Using Equation 9.25,

$$Ra_L = \frac{g\beta(T_s - T_\infty)L^3}{\alpha\nu}$$

$$= \frac{9.8 \text{ m/s}^2 \times 1/400 \text{ K } (232 - 23)°\text{C} \times (0.71 \text{ m})^3}{38.3 \times 10^{-6} \text{ m}^2/\text{s} \times 26.4 \times 10^{-6} \text{ m}^2/\text{s}} = 1.813 \times 10^9$$

and from Equation 9.23 it follows that transition to turbulence occurs on the panel. The appropriate correlation is then given by Equation 9.26

$$\overline{Nu}_L = \left\{0.825 + \frac{0.387 Ra_L^{1/6}}{[1 + (0.492/Pr)^{9/16}]^{8/27}}\right\}^2$$

$$\overline{Nu}_L = \left\{0.825 + \frac{0.387(1.813 \times 10^9)^{1/6}}{[1 + (0.492/0.690)^{9/16}]^{8/27}}\right\}^2 = 147$$

Hence

$$\bar{h} = \frac{\overline{Nu}_L \cdot k}{L} = \frac{147 \times 33.8 \times 10^{-3} \text{ W/m} \cdot \text{K}}{0.71 \text{ m}} = 7.0 \text{ W/m}^2 \cdot \text{K}$$

and

$$q = 7.0 \text{ W/m}^2 \cdot \text{K } (1.02 \times 0.71) \text{ m}^2 (232 - 23)°\text{C} = 1060 \text{ W} \quad \triangleleft$$

Patent Owner Manufacturing Resources International, Inc.
Exhibit 2017 - Page 579 of 999

Comments:

1. Radiation heat transfer effects are often significant relative to free convection. Using Equation 1.7 and assuming $\varepsilon = 1.0$ for the glass surface and $T_{sur} = 23°C$, the net rate of radiation heat transfer between the glass and the surroundings is

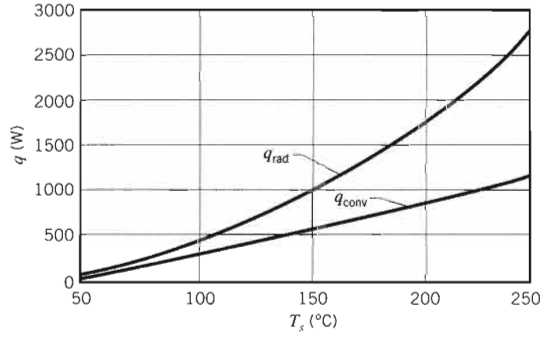
$$q_{rad} = \varepsilon A_s \sigma (T_s^4 - T_{sur}^4)$$

$$q_{rad} = 1(1.02 \times 0.71)\,m^2 \times 5.67 \times 10^{-8}\,W/m^2 \cdot K^4\,(505^4 - 296^4)\,K^4$$

$$q_{rad} = 2355\,W$$

   Hence in this case radiation heat transfer exceeds free convection heat transfer by more than a factor of 2.

2. The effects of radiation and free convection on heat transfer from the glass depend strongly on its temperature. With $q \propto T_s^4$ for radiation and $q \propto T_s^n$ for free convection, where $1.25 < n < 1.33$, we expect the relative influence of radiation to increase with increasing temperature. This behavior is revealed by computing and plotting the heat rates as a function of temperature for $50 \leq T_s \leq 250°C$.



   For each value of T_s used to generate the foregoing free convection results, air properties were determined at the corresponding value of T_f.

9.6.2 Inclined and Horizontal Plates

For a vertical plate, heated (or cooled) relative to an ambient fluid, the plate is aligned with the gravitational vector, and the buoyancy force acts exclusively to induce fluid motion in the upward (or downward) direction. However, if the plate is inclined with respect to gravity, the buoyancy force has a component normal, as well as parallel, to the plate surface. With a reduction in the buoyancy force parallel to the surface, there is a reduction in fluid velocities along the plate, and one might expect there to be an attendant reduction in convection heat transfer. Whether, in fact, there is such a reduction depends on whether one is interested in heat transfer from the top or bottom surface of the plate.

Patent Owner Manufacturing Resources International, Inc.
Exhibit 2017 - Page 580 of 999

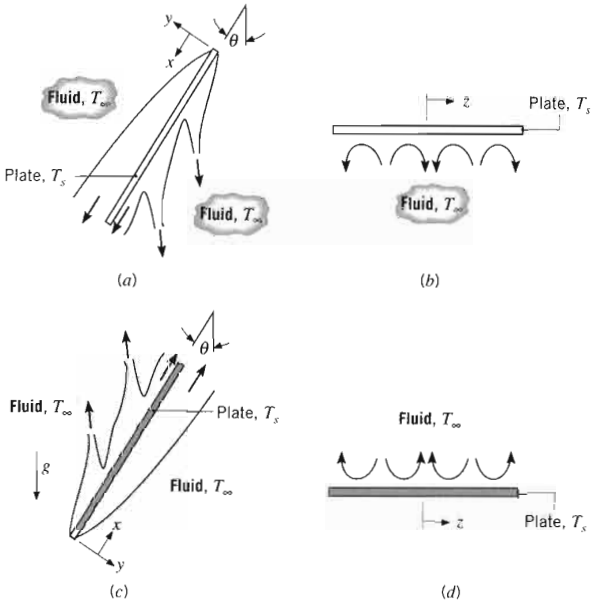


FIGURE 9.6 Buoyancy-driven flows on an inclined plate: (*a*) side view of flows at top and bottom surfaces of a cold plate ($T_s < T_\infty$), (*b*) end view of flow at bottom surface of cold plate, (*c*) side view of flows at top and bottom surfaces of a hot plate ($T_s > T_\infty$), and (*d*) end view of flow at top surface of hot plate.

As shown in Figure 9.6*a*, if the plate is cooled, the y component of the buoyancy force, which is normal to the plate, acts to maintain the descending boundary layer flow in contact with the top surface of the plate. Since the x component of the gravitational acceleration is reduced to $g \cos \theta$, fluid velocities along the plate are reduced and there is an attendant reduction in convection heat transfer to the top surface. However, at the bottom surface, the y component of the buoyancy force acts to move fluid from the surface, and boundary layer development is interrupted by the discharge of parcels of cool fluid from the surface (Figure 9.6*a*). The resulting flow is three-dimensional, and, as shown by the spanwise (z-direction) variations of Figure 9.6*b*, the cool fluid discharged from the bottom surface is continuously replaced by the warmer ambient fluid. The displacement of cool boundary layer fluid by the warmer ambient and the attendant reduction in the thermal boundary layer thickness act to increase convection heat transfer to the bottom surface. In fact, heat transfer enhancement due to the three-dimensional flow typically exceeds the reduction associated with the reduced x component of g, and the combined effect is to increase heat transfer to the bottom surface. Similar trends characterize a heated plate (Figure 9.6*c*,*d*), and the three-dimensional flow is now associated with the upper surface, from which parcels of warm fluid are discharged. Such flows have been observed by several investigators [14–16].

In an early study of heat transfer from inclined plates, Rich [17] suggested that convection coefficients could be determined from vertical plate correlations, if g is

Patent Owner Manufacturing Resources International, Inc.
Exhibit 2017 - Page 581 of 999

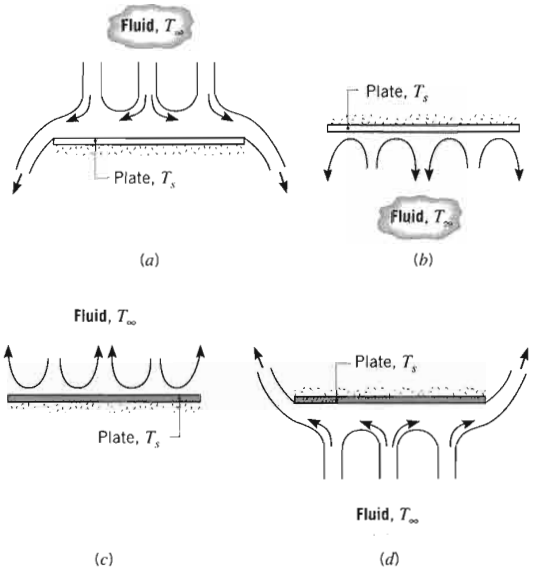


FIGURE 9.7
Buoyancy-driven flows on horizontal cold ($T_s < T_\infty$) and hot ($T_s > T_\infty$) plates: (*a*) top surface of cold plate, (*b*) bottom surface of cold plate, (*c*) top surface of hot plate, and (*d*) bottom surface of hot plate.

replaced by $g \cos \theta$ in computing the plate Rayleigh number. Since then, however, it has been determined that this approach is only satisfactory for the top and bottom surfaces of cooled and heated plates, respectively. It is not appropriate for the top and bottom surfaces of heated and cooled plates, respectively, where the three-dimensionality of the flow has limited the ability to develop generalized correlations. At the top and bottom surfaces of cooled and heated inclined plates, respectively, it is therefore recommended that, for $0 \leq \theta \lesssim 60°$, g be replaced by $g \cos \theta$ and that Equation 9.26 or 9.27 be used to compute the average Nusselt number. For the opposite surfaces, no recommendations are made and the literature should be consulted [14–16].

If the plate is horizontal, the buoyancy force is exclusively normal to the surface. As for the inclined plate, flow patterns and heat transfer depend strongly on whether the surface is cooled or heated and on whether it is facing upward or downward. For a cold surface facing upward (Figure 9.7*a*) and a hot surface facing downward (Figure 9.7*d*), the tendency of the fluid to descend and ascend, respectively, is impeded by the plate. The flow must move horizontally before it can descend or ascend from the edges of the plate, and convection heat transfer is somewhat ineffective. In contrast, for a cold surface facing downward (Figure 9.7*b*) and a hot surface facing upward (Figure 9.7*c*), flow is driven by descending and ascending parcels of fluid, respectively. Conservation of mass dictates that cold (warm) fluid descending (ascending) from a surface be replaced by ascending (descending) warmer (cooler) fluid from the ambient, and heat transfer is much more effective.

Although correlations suggested by McAdams [5] are widely used for horizontal plates, improved accuracy may be obtained by altering the form of the

Patent Owner Manufacturing Resources International, Inc.
Exhibit 2017 - Page 582 of 999

characteristic length on which the correlations are based [18, 19]. In particular with the characteristic length defined as

$$L \equiv \frac{A_s}{P} \tag{9.29}$$

where A_s and P are the plate surface area and perimeter, respectively, recommended correlations for the average Nusselt number are

Upper Surface of Hot Plate or Lower Surface of Cold Plate:

$$\overline{Nu}_L = 0.54 Ra_L^{1/4} \quad (10^4 \lesssim Ra_L \lesssim 10^7) \tag{9.30}$$

$$\overline{Nu}_L = 0.15 Ra_L^{1/3} \quad (10^7 \lesssim Ra_L \lesssim 10^{11}) \tag{9.31}$$

Lower Surface of Hot Plate or Upper Surface of Cold Plate:

$$\overline{Nu}_L = 0.27 Ra_L^{1/4} \quad (10^5 \lesssim Ra_L \lesssim 10^{10}) \tag{9.32}$$

URE 9.7
yancy-driven flows on
izontal cold ($T_s < T_\infty$)
hot ($T_s > T_\infty$) plates:
top surface of cold plate,
bottom surface of cold
e, (c) top surface of hot
e, and (d) bottom
face of hot plate.

Since then, however,
for the top and bottom
ppropriate for the top
ely, where the three-
p generalized correla-
eated inclined plates,
60°, g be replaced by
average Nusselt num-
ade and the literature

ely normal to the sur-
er depend strongly on
cing upward or down-
a hot surface facing
d and ascend, respec-
zontally before it can
ction heat transfer is
wnward (Figure 9.7*b*)
en by descending and
ass dictates that cold
eplaced by ascending
heat transfer is much

widely used for hori-
ring the form of the

EXAMPLE 9.3

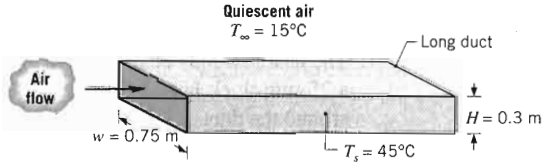
Airflow through a long rectangular heating duct that is 0.75 m wide and 0.3 m high maintains the outer duct surface at 45°C. If the duct is uninsulated and exposed to air at 15°C in the crawlspace beneath a home, what is the heat loss from the duct per meter of length?

SOLUTION

Known: Surface temperature of a long rectangular duct.

Find: Heat loss from duct per meter of length.

Schematic:



Assumptions:

1. Ambient air is quiescent.
2. Surface radiation effects are negligible.

Properties: Table A.4, air ($T_f = 303$ K): $\nu = 16.2 \times 10^{-6}$ m^2/s, $\alpha = 22.9 \times 10^{-6}$ m^2/s, $k = 0.0265$ W/m · K, $\beta = 0.0033$ K^{-1}, $Pr = 0.71$.

Patent Owner Manufacturing Resources International, Inc.
Exhibit 2017 - Page 583 of 999

Analysis: Surface heat loss is by free convection from the vertical sides and the horizontal top and bottom. From Equation 9.25

$$Ra_L = \frac{g\beta(T_s - T_\infty)L^3}{\nu\alpha} = \frac{(9.8\ \text{m/s}^2)(0.0033\ \text{K}^{-1})(30\ \text{K})\,L^3\,(\text{m}^3)}{(16.2 \times 10^{-6}\ \text{m}^2/\text{s})(22.9 \times 10^{-6}\ \text{m}^2/\text{s})}$$

$$Ra_L = 2.62 \times 10^9 L^3$$

For the two sides, $L = H = 0.3$ m. Hence $Ra_L = 7.07 \times 10^7$. The free convection boundary layer is therefore laminar, and from Equation 9.27

$$\overline{Nu}_L = 0.68 + \frac{0.670 Ra_L^{1/4}}{[1 + (0.492/Pr)^{9/16}]^{4/9}}$$

The convection coefficient associated with the sides is then

$$\bar{h}_s = \frac{k}{H}\overline{Nu}_L$$

$$\bar{h}_s = \frac{0.0265\ \text{W/m} \cdot \text{K}}{0.3\ \text{m}}\left\{0.68 + \frac{0.670(7.07 \times 10^7)^{1/4}}{[1 + (0.492/0.71)^{9/16}]^{4/9}}\right\} = 4.23\ \text{W/m}^2 \cdot \text{K}$$

For the top and bottom, $L = (A_s/P) \approx (w/2) = 0.375$ m. Hence $Ra_L = 1.38 \times 10^8$, and from Equations 9.31 and 9.32, respectively,

$$\bar{h}_t = [k/(w/2)] \times 0.15\, Ra_L^{1/3} = \frac{0.0265\ \text{W/m} \cdot \text{K}}{0.375\ \text{m}} \times 0.15(1.38 \times 10^8)^{1/3}$$
$$= 5.47\ \text{W/m}^2 \cdot \text{K}$$

$$\bar{h}_b = [k/(w/2)] \times 0.27\, Ra_L^{1/4} = \frac{0.0265\ \text{W/m} \cdot \text{K}}{0.375\ \text{m}} \times 0.27(1.38 \times 10^8)^{1/4}$$
$$= 2.07\ \text{W/m}^2 \cdot \text{K}$$

The rate of heat loss per unit length of duct is then

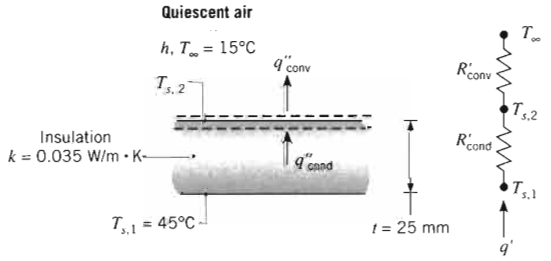
$$q' = 2q_s' + q_t' + q_b' = (2\bar{h}_s \cdot H + \bar{h}_t \cdot w + \bar{h}_b \cdot w)(T_s - T_\infty)$$

$$q' = (2 \times 4.23 \times 0.3 + 5.47 \times 0.75 + 2.07 \times 0.75)(45 - 15)\ \text{W/m}$$

$$q' = 246\ \text{W/m}$$

Comments:

1. The heat loss may be reduced by insulating the duct. We consider this option for a 25-mm-thick layer of blanket insulation ($k = 0.035$ W/m · K) that is wrapped around the duct.



Patent Owner Manufacturing Resources International, Inc.
Exhibit 2017 - Page 584 of 999

The heat loss at each surface may be expressed as

$$q' = \frac{T_{s,1} - T_\infty}{R'_{\text{cond}} + R'_{\text{conv}}}$$

where R'_{conv} is associated with free convection from the outer surface and hence depends on the unknown temperature $T_{s,2}$. This temperature may be determined by applying an energy balance to the outer surface, from which it follows that

$$q''_{\text{cond}} = q''_{\text{conv}}$$

or

$$\frac{(T_{s,1} - T_{s,2})}{(t/k)} = \frac{(T_{s,2} - T_\infty)}{(1/\bar{h})}$$

Since different convection coefficients are associated with the sides, top, and bottom ($\bar{h}_s$, $\bar{h}_t$, and $\bar{h}_b$), a separate solution to this equation must be obtained for each of the three surfaces. The solutions are iterative, since the properties of air and the convection coefficients depend on T_s. Performing the calculations, we obtain

Sides	$T_{s,2} = 24°\text{C}$,	$\bar{h}_s = 3.18\ \text{W/m}^2 \cdot \text{K}$
Top	$T_{s,2} = 23°\text{C}$,	$\bar{h}_t = 3.66\ \text{W/m}^2 \cdot \text{K}$
Bottom	$T_{s,2} = 29°\text{C}$,	$\bar{h}_b = 1.71\ \text{W/m}^2 \cdot \text{K}$

Neglecting heat loss through the corners of the insulation, the total heat rate per unit length of duct is then

$$q' = 2q'_s + q'_t + q'_b$$

$$q' = \frac{2H(T_{s,1} - T_\infty)}{(t/k) + (1/\bar{h}_s)} + \frac{w(T_{s,1} - T_\infty)}{(t/k) + (1/\bar{h}_t)} + \frac{w(T_{s,1} - T_\infty)}{(t/k) + (1/\bar{h}_b)}$$

which yields

$$q' = (17.5 + 22.8 + 17.3)\ \text{W/m} = 57.6\ \text{W/m}$$

The insulation therefore provides a 77% reduction in heat loss to the ambient air by natural convection.

2. Although they have been neglected, radiation losses may still be significant. From Equation 1.7 with ε assumed to be unity and $T_{\text{sur}} = 288$ K, $q'_{\text{rad}} = 398$ W/m for the uninsulated duct. Inclusion of radiation effects in the energy balance for the insulated duct would reduce the outer surface temperatures, thereby reducing the convection heat rates. With radiation, however, the total heat rate ($q'_{\text{conv}} + q'_{\text{rad}}$) would increase.

9.6.3 The Long Horizontal Cylinder

This important geometry has been studied extensively, and many existing correlations have been reviewed by Morgan [20]. For an isothermal cylinder, Morgan suggests an expression of the form

$$\overline{Nu}_D = \frac{\bar{h}D}{k} = C\,Ra_D^n \tag{9.33}$$

Patent Owner Manufacturing Resources International, Inc.
Exhibit 2017 - Page 585 of 999

where C and n are given in Table 9.1 and Ra_D and $\overline{Nu}_D$ are based on the cylinder diameter. In contrast, Churchill and Chu [21] have recommended a single correlation for a wide Rayleigh number range:

$$\overline{Nu}_D = \left\{0.60 + \frac{0.387\, Ra_D^{1/6}}{[1 + (0.559/Pr)^{9/16}]^{8/27}}\right\}^2 \qquad Ra_D \lesssim 10^{12} \tag{9.34}$$

TABLE 9.1 Constants of Equation 9.33 for free convection on a horizontal circular cylinder [20]

Ra_D	C	n
10^{-10}–10^{-2}	0.675	0.058
10^{-2}–10^{2}	1.02	0.148
10^{2}–10^{4}	0.850	0.188
10^{4}–10^{7}	0.480	0.250
10^{7}–10^{12}	0.125	0.333

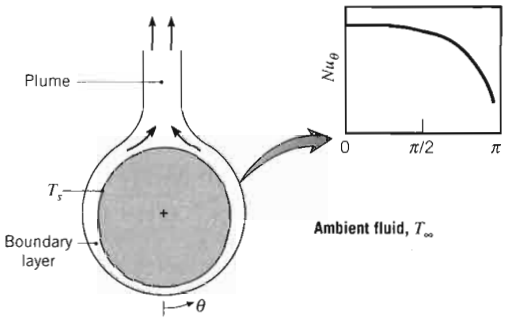


FIGURE 9.8 Boundary layer development and Nusselt number distribution on a heated horizontal cylinder.

The foregoing correlations provide the average Nusselt number over the entire circumference of an isothermal cylinder. As shown in Figure 9.8 for a heated cylinder, local Nusselt numbers are influenced by boundary layer development, which begins at $\theta = 0$ and concludes at $\theta < \pi$ with formation of a plume ascending from the cylinder. If the flow remains laminar over the entire surface, the distribution of the local Nusselt number with θ is characterized by a maximum at $\theta = 0$ and a monotonic decay with increasing θ. This decay would be disrupted at Rayleigh numbers sufficiently large ($Ra_D \gtrsim 10^9$) to permit transition to turbulence within the boundary layer. If the cylinder is cooled relative to the ambient fluid, boundary layer development begins at $\theta = \pi$, the local Nusselt number is a maximum at this location, and the plume descends from the cylinder.

EXAMPLE 9.4

A horizontal, high-pressure steam pipe of 0.1-m outside diameter passes through a large room whose wall and air temperatures are 23°C. The pipe has an outside

Patent Owner Manufacturing Resources International, Inc.
Exhibit 2017 - Page 586 of 999

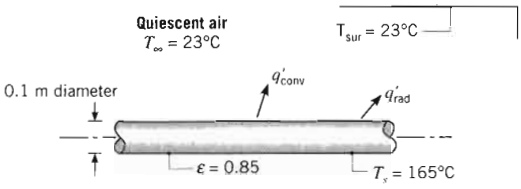
surface temperature of 165°C and an emissivity of $\varepsilon = 0.85$. Estimate the heat loss from the pipe per unit length.

SOLUTION

Known: Surface temperature of a horizontal steam pipe.

Find: Heat loss from the pipe per unit length q' (W/m).

Schematic:



Assumptions:

1. Pipe surface area is small compared to surroundings.
2. Room air is quiescent.

Properties: Table A.4, air ($T_f = 367$ K): $k = 0.0313$ W/m · K, $\nu = 22.8 \times 10^{-6}$ m²/s, $\alpha = 32.8 \times 10^{-6}$ m²/s, $Pr = 0.697$, $\beta = 2.725 \times 10^{-3}$ K^{-1}.

Analysis: The total heat loss per unit length of pipe is

$$q' = q'_{conv} + q'_{rad} = \bar{h}\pi D(T_s - T_\infty) + \varepsilon\pi D\sigma(T_s^4 - T_{sur}^4)$$

The convection coefficient may be obtained from Equation 9.34

$$\overline{Nu}_D = \left\{0.60 + \frac{0.387\, Ra_D^{1/6}}{[1 + (0.559/Pr)^{9/16}]^{8/27}}\right\}^2$$

where

$$Ra_D = \frac{g\beta(T_s - T_\infty)D^3}{\nu\alpha}$$

$$Ra_D = \frac{9.8\ \text{m/s}^2 \times 2.725 \times 10^{-3}\ \text{K}^{-1}\,(165 - 23)°\text{C}\,(0.1\ \text{m})^3}{22.8 \times 10^{-6}\ \text{m}^2/\text{s} \times 32.8 \times 10^{-6}\ \text{m}^2/\text{s}} = 5.073 \times 10^6$$

Hence

$$\overline{Nu}_D = \left\{0.60 + \frac{0.387(5.073 \times 10^6)^{1/6}}{[1 + (0.559/0.697)^{9/16}]^{8/27}}\right\}^2 = 23.3$$

and

$$\bar{h} = \frac{k}{D}\overline{Nu}_D = \frac{0.0313\ \text{W/m} \cdot \text{K}}{0.1\ \text{m}} \times 23.3 = 7.29\ \text{W/m}^2 \cdot \text{K}$$

Patent Owner Manufacturing Resources International, Inc.
Exhibit 2017 - Page 587 of 999

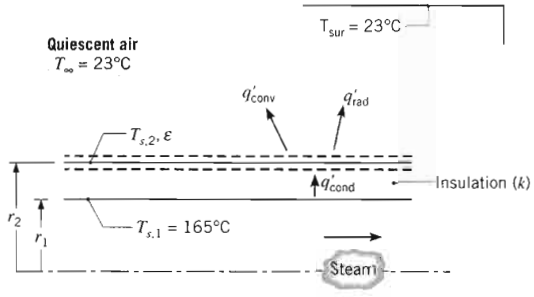
The total heat loss is then

$$q' = 7.29\ \text{W/m}^2 \cdot \text{K}\,(\pi \times 0.1\ \text{m})(165 - 23)^\circ\text{C} + 0.85(\pi \times 0.1\ \text{m})5.67 \times 10^{-8}\ \text{W/m}^2 \cdot \text{K}^4\,(438^4 - 296^4)\ \text{K}^4$$

$$q' = (325 + 441)\ \text{W/m} = 766\ \text{W/m}$$

Comments:

1. Equation 9.33 could also be used to estimate the Nusselt number, with the result that $\overline{Nu}_D = 22.8$.
2. To explore the effect of an insulating layer on heat loss from the pipe, we consider a 25-mm-thick layer of urethane for which $k = 0.026$ W/m · K and $\varepsilon = 0.85$.



Free convection heat transfer to the ambient air and net radiation transfer to the surroundings depend on the temperature $T_{s,2}$ of the insulation, which may be obtained by performing an energy balance at the outer surface:

$$q'_{cond} = q'_{conv} + q'_{rad}$$

Substituting from Equations 1.7 and 3.27, it follows that

$$\frac{2\pi k(T_{s,1} - T_{s,2})}{\ln(r_2/r_1)} = \bar{h}(2\pi r_2)(T_{s,2} - T_\infty) + \varepsilon 2\pi r_2 \sigma(T_{s,2}^4 - T_{sur}^4)$$

The unknown temperature is determined from an iterative solution for which Equation 9.34 is used to reevaluate the convection coefficient, and hence the properties of air, at each step of the iteration. For the prescribed conditions, the solution yields $T_{s,2} = 35.3^\circ$C and $\bar{h} = 3.71$ W/m^2 · K, from which it follows that

$$q' = q'_{conv} + q'_{rad}$$

$$q' = 3.71\ \text{W/m}^2 \cdot \text{K}(\pi \times 0.15\ \text{m})(35.3 - 23)^\circ\text{C} + 0.85(\pi \times 0.15\ \text{m})5.67 \times 10^{-8}\ \text{W/m}^2 \cdot \text{K}^4\,(308.3^4 - 296^4)\ \text{K}^4$$

$$q' = (21.5 + 30.8)\ \text{W/m} = 52.3\ \text{W/m}$$

As expected, the insulation significantly reduces heat loss from the pipe.

Patent Owner Manufacturing Resources International, Inc.
Exhibit 2017 - Page 588 of 999

9.6.4 Spheres

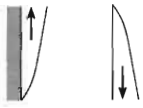
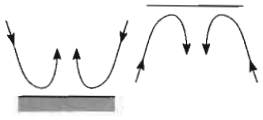
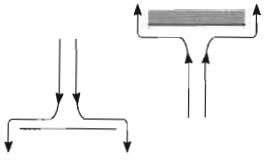
The following correlation due to Churchill [10] is recommended for spheres in fluids of $Pr \gtrsim 0.7$ and for $Ra_D \lesssim 10^{11}$.

$$\overline{Nu}_D = 2 + \frac{0.589 Ra_D^{1/4}}{[1 + (0.469/Pr)^{9/16}]^{4/9}} \tag{9.35}$$

In the limit as $Ra_D \to 0$, Equation 9.35 reduces to $\overline{Nu}_D = 2$, which corresponds to heat transfer by conduction between a spherical surface and a stationary infinite medium, in a manner consistent with Equations 7.56 and 7.57.

Recommended correlations from this section are summarized in Table 9.2. Results for other immersed geometries and special conditions are presented in comprehensive reviews by Churchill [10] and Raithby and Hollands [22].

TABLE 9.2 Summary of free convection empirical correlations for immersed geometries

Geometry	Recommended Correlation	Restrictions
1. Vertical plates[a] 	Equation 9.26	None
2. Inclined plates Cold surface up or hot surface down 	Equation 9.26 $g \longrightarrow g \cos\theta$	$0 \lesssim \theta \lesssim 60°$
3. Horizontal plates (a) Hot surface up or cold surface down 	Equation 9.30 Equation 9.31	$10^4 \lesssim Ra_L \lesssim 10^7$ $10^7 \lesssim Ra_L \lesssim 10^{11}$
(b) Cold surface up or hot surface down 	Equation 9.32	$10^5 \lesssim Ra_L \lesssim 10^{10}$

Patent Owner Manufacturing Resources International, Inc.
Exhibit 2017 - Page 589 of 999

TABLE 9.2 *Continued*

Geometry	Recommended Correlation	Restrictions
4. Horizontal cylinder 	Equation 9.34	$Ra_D \lesssim 10^{12}$
5. Sphere 	Equation 9.35	$Ra_D \lesssim 10^{11}$ $Pr \gtrsim 0.7$

[a] The correlation may be applied to a vertical cylinder if $(D/L) \gtrsim (35/Gr_L^{1/4})$.

9.7 *Free Convection within Parallel Plate Channels*

A common free convection geometry involves vertical (or inclined) parallel plate channels that are open to the ambient at opposite ends (Figure 9.9). The plates could constitute a fin array used to enhance free convection heat transfer from a base surface to which the fins are attached, or they could constitute an array of circuit boards with heat-dissipating electronic components. Surface thermal conditions may be idealized as being isothermal or isoflux and symmetrical ($T_{s,1} = T_{s,2}$; $q''_{s,1} = q''_{s,2}$) or asymmetrical ($T_{s,1} \neq T_{s,2}$; $q''_{s,1} \neq q''_{s,2}$).

For vertical channels ($\theta = 0$) buoyancy acts exclusively to induce motion in the streamwise (x) direction and, beginning at $x = 0$, boundary layers develop on each surface. For short channels and/or large spacings (small L/S), independent boundary layer development occurs at each surface and conditions correspond to those for an *isolated plate* in an infinite, quiescent medium. For large L/S, however, boundary

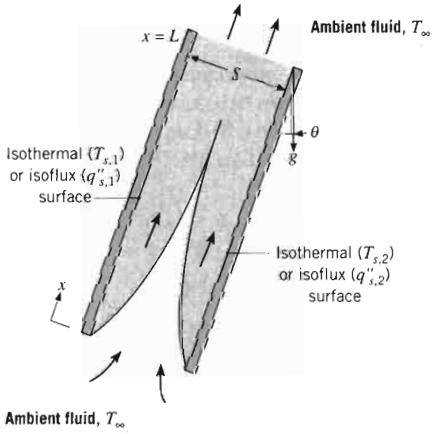


FIGURE 9.9
Free convection flow between heated parallel plates with opposite ends exposed to a quiescent fluid.

Patent Owner Manufacturing Resources International, Inc.
Exhibit 2017 - Page 590 of 999

layers developing on opposing surfaces eventually merge to yield a fully developed condition. If the channel is inclined, there is a component of the buoyancy force normal, as well as parallel, to the streamwise direction, and conditions may strongly be influenced by development of a three-dimensional, secondary flow.

9.7.1 Vertical Channels

Beginning with the benchmark paper by Elenbaas [23], the vertical orientation has been studied extensively for symmetrically and asymmetrically heated plates with isothermal or isoflux surface conditions. For *symmetrically heated, isothermal plates,* Elenbaas obtained the following semiempirical correlation:

$$\overline{Nu}_S = \frac{1}{24} Ra_S \left(\frac{S}{L}\right)\left\{1 - \exp\left[-\frac{35}{Ra_S(S/L)}\right]\right\}^{3/4} \tag{9.36}$$

where the average Nusselt and Rayleigh numbers are defined as

$$\overline{Nu}_S = \left(\frac{q/A}{T_s - T_\infty}\right)\frac{S}{k} \tag{9.37}$$

and

$$Ra_S = \frac{g\beta(T_s - T_\infty)S^3}{\alpha\nu} \tag{9.38}$$

Equation 9.36 was developed for air as the working fluid, and its range of applicability is

$$\left[10^{-1} \lesssim \frac{S}{L} Ra_S \lesssim 10^5\right]$$

Knowledge of the average Nusselt number for a plate therefore permits determination of the total heat rate for the plate. In the fully developed limit ($S/L \longrightarrow 0$), Equation 9.36 reduces to

$$\overline{Nu}_{S(\mathrm{fd})} = \frac{Ra_S(S/L)}{24} \tag{9.39}$$

Retention of the L dependence results from defining $\overline{Nu}_S$ in terms of the fixed inlet (ambient) temperature and not in terms of the fluid mixed-mean temperature, which is not explicitly known. For the common condition corresponding to adjoining isothermal ($T_{s,1}$) and insulated ($q''_{s,2} = 0$) plates, the fully developed limit yields the following expression for the isothermal surface [24]:

$$\overline{Nu}_{S(\mathrm{fd})} = \frac{Ra_S(S/L)}{12} \tag{9.40}$$

For isoflux surfaces, it is more convenient to define a local Nusselt number as

$$Nu_{S,L} = \left(\frac{q''_s}{T_{s,L} - T_\infty}\right)\frac{S}{k} \tag{9.41}$$

and to correlate results in terms of a modified Rayleigh number defined as

$$Ra^*_S = \frac{g\beta q''_s S^4}{k\alpha\nu} \tag{9.42}$$

Patent Owner Manufacturing Resources International, Inc.
Exhibit 2017 - Page 591 of 999

The subscript L refers to conditions at $x = L$, where the plate temperature is a maximum. For symmetric, isoflux plates the fully developed limit corresponds to [24]

$$Nu_{S,L(\mathrm{fd})} = 0.144[Ra_S^*(S/L)]^{1/2} \tag{9.43}$$

and for asymmetric isoflux conditions with one surface insulated ($q''_{s,2} = 0$) the limit is

$$Nu_{S,L(\mathrm{fd})} = 0.204[Ra_S^*(S/L)]^{1/2} \tag{9.44}$$

Combining the foregoing relations for the fully developed limit with available results for the isolated plate limit, Bar-Cohen and Rohsenow [24] obtained Nusselt number correlations applicable to the complete range of S/L. For isothermal and isoflux conditions, respectively, the correlations are of the form

$$\overline{Nu}_S = \left[\frac{C_1}{(Ra_S\,S/L)^2} + \frac{C_2}{(Ra_S\,S/L)^{1/2}}\right]^{-1/2} \tag{9.45}$$

$$Nu_{S,L} = \left[\frac{C_1}{Ra_S^*\,S/L} + \frac{C_2}{(Ra_S^*\,S/L)^{2/5}}\right]^{-1/2} \tag{9.46}$$

where the constants C_1 and C_2 are given in Table 9.3 for the different surface thermal conditions. In each case the fully developed and isolated plate limits correspond to Ra_S (or Ra_S^*)$S/L \lesssim 10$ and Ra_S (or Ra_S^*)$S/L \gtrsim 100$, respectively.

Bar-Cohen and Rohsenow [24] used the foregoing correlations to infer the optimum plate spacing S_{opt} for maximizing heat transfer from an array of isothermal plates, as well as the spacing S_{max} needed to maximize heat transfer from each plate in the array. Existence of an optimum for the array results from the fact that, although heat transfer from each plate decreases with decreasing S, the number of plates that may be placed in a prescribed volume increases. Hence S_{opt} maximizes heat transfer from the array by yielding a maximum for the product of $\bar{h}$ and the total plate surface area. In contrast, to maximize heat transfer from each plate, S_{max} must be large enough to preclude overlap of adjoining boundary layers, such that the isolated plate limit remains valid over the entire plate.

Consideration of the optimum plate spacing is particularly important for vertical parallel plates used as fins to enhance heat transfer by natural convection from a base surface of fixed width W. With the temperature of the fins exceeding that of the ambient fluid, flow between the fins is induced by buoyancy forces. However, resistance to the flow is associated with viscous forces imposed by the surface of the

TABLE 9.3 Heat transfer parameters for free convection between vertical parallel plates

Surface Condition	C_1	C_2	S_{opt}	$S_{\mathrm{max}}/S_{\mathrm{opt}}$
Symmetric isothermal plates ($T_{s,1} = T_{s,2}$)	576	2.87	$2.71(Ra_S/S^3L)^{-1/4}$	1.71
Symmetric isoflux plates ($q''_{s,1} = q''_{s,2}$)	48	2.51	$2.12(Ra_S^*/S^4L)^{-1/5}$	4.77
Isothermal/adiabatic plates ($T_{s,1}$, $q''_{s,2} = 0$)	144	2.87	$2.15(Ra_S/S^3L)^{-1/4}$	1.71
Isoflux/adiabatic plates ($q''_{s,1}$, $q''_{s,2} = 0$)	24	2.51	$1.69(Ra_S^*/S^4L)^{-1/5}$	4.77

9.8 Empirical Co

Patent Owner Manufacturing Resources International, Inc.
Exhibit 2017 - Page 592 of 999

fins, and the rate of mass flow between adjoining fins is governed by a balance between buoyancy and viscous forces. Since viscous forces increase with decreasing S, there is an accompanying reduction in the flow rate, and hence $\bar{h}$. However, for fixed W, the attendant increase in the number of fins increases the total surface area A_s and yields a maximum in $\bar{h}A_s$ for $S = S_{opt}$. For $S < S_{opt}$, the amount by which $\bar{h}$ is diminished by viscous effects exceeds the increase in A_s; for $S > S_{opt}$, the amount by which A_s is diminished exceeds the increase in $\bar{h}$.

For isoflux plates, the total volumetric heat rate simply increases with decreasing S. However, the need to maintain T_s below prescribed limits precludes reducing S to extremely small values. Hence S_{opt} may be defined as that value of S which yields the maximum volumetric heat dissipation per unit temperature difference, $T_s(L) - T_\infty$. The spacing S_{max} that yields the lowest possible surface temperature for a prescribed heat flux, without regard to volumetric considerations, is again the value of S that precludes boundary layer merger. Values of S_{opt} and S_{max}/S_{opt} are presented in Table 9.3 for plates of negligible thickness.

In using the foregoing correlations, fluid properties are evaluated at average temperatures of $\overline{T} = (T_s + T_\infty)/2$ for isothermal surfaces and $\overline{T} = (T_{s,L} + T_\infty)/2$ for isoflux surfaces.

9.7.2 Inclined Channels

Experiments have been performed by Azevedo and Sparrow [16] for inclined channels in water. Symmetric isothermal plates and isothermal–insulated plates were considered for $0 \leq \theta \leq 45°$ and conditions within the isolated plate limit, $Ra_S(S/L) > 200$. Although three-dimensional secondary flows were observed at the lower plate, when it was heated, data for all experimental conditions were correlated to within $\pm 10\%$ by

$$\overline{Nu}_S = 0.645[Ra_S(S/L)]^{1/4} \tag{9.47}$$

Departures of the data from the correlation were most pronounced at large tilt angles with bottom surface heating and were attributed to heat transfer enhancement by the three-dimensional secondary flow. Fluid properties are evaluated at $\overline{T} = (T_s + T_\infty)/2$.

9.8 *Empirical Correlations: Enclosures*

The foregoing results pertain to free convection between a surface and an extensive fluid medium. However, engineering applications frequently involve heat transfer between surfaces that are at different temperatures and are separated by an *enclosed* fluid. In this section we present correlations that are pertinent to the most common geometries.

9.8.1 Rectangular Cavities

The rectangular cavity (Figure 9.10) has been studied extensively, and comprehensive reviews of both experimental and theoretical results are available [25, 26]. Two

Patent Owner Manufacturing Resources International, Inc.
Exhibit 2017 - Page 593 of 999

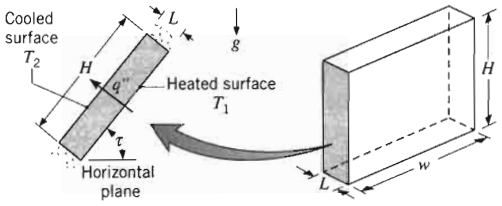


FIGURE 9.10
Free convection in a rectangular cavity.

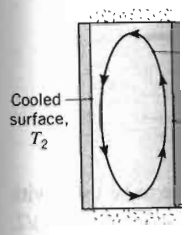


FIGURE 9.12
Cellular flow in a ve cavity with different temperatures.

of the opposing walls are maintained at different temperatures ($T_1 > T_2$), while the remaining walls are insulated from the surroundings. The tilt angle τ between the heated and cooled surfaces and the horizontal can vary from 0° (*horizontal cavity* with bottom heating) to 90° (*vertical cavity* with sidewall heating) to 180° (*horizontal cavity* with top heating). The heat flux across the cavity, which is expressed as

$$q'' = h(T_1 - T_2) \tag{9.48}$$

can depend strongly on the aspect ratio H/L, as well as the value of τ. For large values of the aspect ratio w/L, its dependence on w/L is small and may be neglected for the purposes of this text.

The horizontal cavity heated from below ($\tau = 0$) has been considered by many investigators. For H/L, $w/L \gg 1$, and Rayleigh numbers less than a critical value of $Ra_{L,c} = 1708$, buoyancy forces cannot overcome the resistance imposed by viscous forces and there is no advection within the cavity. Hence heat transfer from the bottom to the top surface occurs by conduction or, for a gas, by conduction and radiation. Since conditions correspond to one-dimensional conduction through a plane fluid layer, the convection coefficient is $h = k/L$ and $Nu_L = 1$. However, for

$$Ra_L \equiv \frac{g\beta(T_1 - T_2)L^3}{\alpha\nu} > 1708$$

conditions are thermally unstable and there is advection within the cavity. For Rayleigh numbers in the range $1708 < Ra_L \lesssim 5 \times 10^4$, fluid motion consists of regularly spaced roll cells (Figure 9.11), while for larger Rayleigh numbers, the cells break down and the fluid motion is turbulent.

As a first approximation, convection coefficients for the horizontal cavity heated from below may be obtained from the following correlation proposed by Globe and Dropkin [27]:

$$\overline{Nu}_L = \frac{\bar{h}L}{k} = 0.069 Ra_L^{1/3} Pr^{0.074} \qquad 3 \times 10^5 \lesssim Ra_L \lesssim 7 \times 10^9 \tag{9.49}$$

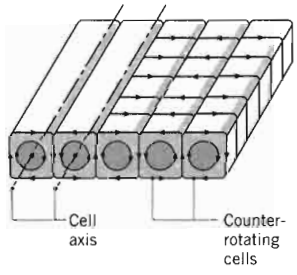


FIGURE 9.11
Longitudinal roll cells characteristic of advection in a horizontal fluid layer heated from below ($1708 < Ra_L \lesssim 5 \times 10^4$).

Patent Owner Manufacturing Resources International, Inc.
Exhibit 2017 - Page 594 of 999

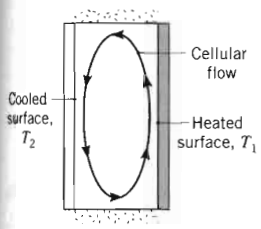


FIGURE 9.12
Cellular flow in a vertical cavity with different sidewall temperatures.

where all properties are evaluated at the average temperature, $\overline{T} \equiv (T_1 + T_2)/2$. The correlation applies for values of L/H sufficiently small to ensure a negligible effect of the sidewalls. More detailed correlations, which apply over a wider range of Ra_L, have been proposed [28, 29]. In concluding the discussion of horizontal cavities, it is noted that in the absence of radiation, for $\tau = 180°$, heat transfer from the top to bottom surface is exclusively by conduction ($Nu_L = 1$), irrespective of the value of Ra_L.

In the vertical rectangular cavity ($\tau = 90°$), the vertical surfaces are heated and cooled, while the horizontal surfaces are adiabatic. As shown in Figure 9.12, fluid motion is characterized by a recirculating or cellular flow for which fluid ascends along the hot wall and descends along the cold wall. For small Rayleigh numbers, $Ra_L \lesssim 10^3$, the buoyancy-driven flow is weak and heat transfer is primarily by conduction across the fluid. Hence, from Fourier's law, the Nusselt number is again $Nu_L = 1$. With increasing Rayleigh number, the cellular flow intensifies and becomes concentrated in thin boundary layers adjoining the sidewalls. The core becomes nearly stagnant, although additional cells can develop in the corners and the sidewall boundary layers eventually undergo transition to turbulence. For aspect ratios in the range $1 \lesssim (H/L) \lesssim 10$, the following correlations have been suggested [26]:

$$\overline{Nu}_L = 0.22\left(\frac{Pr}{0.2 + Pr}Ra_L\right)^{0.28}\left(\frac{H}{L}\right)^{-1/4} \qquad (9.50)$$

$$\begin{bmatrix} 2 \lesssim \dfrac{H}{L} \lesssim 10 \\ Pr \lesssim 10^5 \\ 10^3 \lesssim Ra_L \lesssim 10^{10} \end{bmatrix}$$

$$\overline{Nu}_L = 0.18\left(\frac{Pr}{0.2 + Pr}Ra_L\right)^{0.29} \qquad (9.51)$$

$$\begin{bmatrix} 1 \lesssim \dfrac{H}{L} \lesssim 2 \\ 10^{-3} \lesssim Pr \lesssim 10^5 \\ 10^3 \lesssim \dfrac{Ra_L Pr}{0.2 + Pr} \end{bmatrix}$$

while for larger aspect ratios, the following correlations have been proposed [30]:

$$\overline{Nu}_L = 0.42 Ra_L^{1/4}\, Pr^{0.012}\left(\frac{H}{L}\right)^{-0.3} \qquad \begin{bmatrix} 10 \lesssim \dfrac{H}{L} \lesssim 40 \\ 1 \lesssim Pr \lesssim 2 \times 10^4 \\ 10^4 \lesssim Ra_L \lesssim 10^7 \end{bmatrix} \qquad (9.52)$$

$$\overline{Nu}_L = 0.046 Ra_L^{1/3} \qquad \begin{bmatrix} 1 \lesssim \dfrac{H}{L} \lesssim 40 \\ 1 \lesssim Pr \lesssim 20 \\ 10^6 \lesssim Ra_L \lesssim 10^9 \end{bmatrix} \qquad (9.53)$$

Patent Owner Manufacturing Resources International, Inc.
Exhibit 2017 - Page 595 of 999

TABLE 9.4 Critical angle for inclined rectangular cavities

(H/L)	1	3	6	12	>12
τ^*	25°	53°	60°	67°	70°

Convection coefficients computed from the foregoing expressions are to be used with Equation 9.48. Again, all properties are evaluated at the mean temperature, $(T_1 + T_2)/2$.

Studies of free convection in tilted cavities are often stimulated by applications involving flat-plate solar collectors [31–36]. For such cavities, the fluid motion consists of a combination of the roll structure of Figure 9.11 and the cellular structure of Figure 9.12. Typically, transition between the two types of fluid motion occurs at a critical tilt angle, τ^*, with a corresponding change in the value of $\overline{Nu}_L$. For large aspect ratios, $(H/L) \gtrsim 12$, and tilt angles less than the critical value τ^* given in Table 9.4, the following correlation due to Hollands et al. [36] is in excellent agreement with available data:

$$\overline{Nu}_L = 1 + 1.44\left[1 - \frac{1708}{Ra_L \cos\tau}\right]^{\cdot}\left[1 - \frac{1708(\sin 1.8\tau)^{1.6}}{Ra_L \cos\tau}\right] + \left[\left(\frac{Ra_L \cos\tau}{5830}\right)^{1/3} - 1\right]^{\cdot} \qquad \begin{bmatrix} \frac{H}{L} \gtrsim 12 \\ 0 < \tau \lesssim \tau^* \end{bmatrix} \tag{9.54}$$

The notation $[\quad]^{\cdot}$ implies that, if the quantity in brackets is negative, it must be set equal to zero. The implication is that, if the Rayleigh number is less than a critical value $Ra_{L,c} = 1708/\cos\tau$, there is no flow within the cavity. For small aspect ratios Catton [26] suggests that reasonable results may be obtained from a correlation of the form

$$\overline{Nu}_L = \overline{Nu}_L(\tau = 0)\left[\frac{\overline{Nu}_L(\tau = 90°)}{\overline{Nu}_L(\tau = 0)}\right]^{\tau/\tau^*} (\sin\tau^*)^{(\tau/4\tau^*)} \qquad \begin{bmatrix} \frac{H}{L} \lesssim 12 \\ 0 < \tau \lesssim \tau^* \end{bmatrix} \tag{9.55}$$

Beyond the critical tilt angle, the following correlations due to Ayyaswamy and Catton [31] and Arnold et al. [34], respectively, have been recommended [26] for all aspect ratios (H/L):

$$\overline{Nu}_L = \overline{Nu}_L(\tau = 90°)(\sin\tau)^{1/4} \qquad \tau^* \lesssim \tau < 90° \tag{9.56}$$

$$\overline{Nu}_L = 1 + [\overline{Nu}_L(\tau = 90°) - 1]\sin\tau \qquad 90° < \tau < 180° \tag{9.57}$$

9.8.2 Concentric Cylinders

Free convection heat transfer in the annular space between *long*, horizontal concentric cylinders (Figure 9.13) has been considered by Raithby and Hollands [37]. Flow in the annular region is characterized by two cells that are symmetric about the vertical midplane. If the inner cylinder is heated and the outer cylinder is cooled $(T_i > T_o)$, fluid ascends and descends along the inner and outer cylinders, respectively. If $T_i < T_o$, the cellular flows are reversed. The heat transfer rate (W) between

Patent Owner Manufacturing Resources International, Inc.
Exhibit 2017 - Page 596 of 999

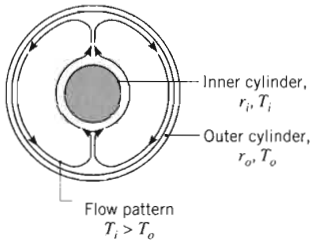


FIGURE 9.13
Free convection flow in the annular space between long, horizontal, concentric cylinders or concentric spheres of inner radius r_i and outer radius r_o.

the two cylinders, each of length L, is expressed by Equation 3.27 (with an *effective thermal conductivity*, k_{eff}, replacing the molecular thermal conductivity, k) as

$$q = \frac{2\pi L k_{\text{eff}}(T_i - T_o)}{\ln(r_o/r_i)} \tag{9.58}$$

We see that the effective conductivity of a fictitious *stationary* fluid will transfer the same amount of heat as the actual *moving* fluid. The suggested correlation for k_{eff} is

$$\frac{k_{\text{eff}}}{k} = 0.386\left(\frac{Pr}{0.861 + Pr}\right)^{1/4} Ra_c^{1/4} \tag{9.59}$$

where the length scale in Ra_c is given by

$$L_c = \frac{2[\ln(r_o/r_i)]^{4/3}}{(r_i^{-3/5} + r_o^{-3/5})^{5/3}} \tag{9.60}$$

Equation 9.59 may be used for the range $0.7 \lesssim Pr \lesssim 6000$ and $Ra_c \lesssim 10^7$. Properties are evaluated at the mean temperature, $T_m = (T_i + T_o)/2$. Of course, the minimum heat transfer rate between the cylinders cannot fall below the conduction limit; therefore, $k_{\text{eff}} = k$ if the value of k_{eff}/k predicted by Equation 9.59 is less than unity. A more detailed correlation, which accounts for cylinder eccentricity effects, has been developed by Kuehn and Goldstein [38].

9.8.3 Concentric Spheres

Raithby and Hollands [37] have also considered free convection heat transfer between concentric spheres (Figure 9.14) and express the total heat transfer rate by Equation 3.35 (with an effective thermal conductivity, k_{eff}, replacing the molecular thermal conductivity, k) as

$$q = \frac{4\pi k_{\text{eff}}(T_i - T_o)}{(1/r_i) - (1/r_o)} \tag{9.61}$$

The effective thermal conductivity is

$$\frac{k_{\text{eff}}}{k} = 0.74\left(\frac{Pr}{0.861 + Pr}\right)^{1/4} Ra_s^{1/4} \tag{9.62}$$

Patent Owner Manufacturing Resources International, Inc.
Exhibit 2017 - Page 597 of 999

where the length scale in Ra_s is given by

$$L_s = \frac{\left(\frac{1}{r_i} - \frac{1}{r_o}\right)^{4/3}}{2^{1/3}(r_i^{-7/5} + r_o^{-7/5})^{5/3}} \tag{9.63}$$

The result may be used to a reasonable approximation for $0.7 \lesssim Pr \lesssim 4000$ and $Ra_s \lesssim 10^4$. Properties are evaluated at $T_m = (T_i + T_o)/2$, and $k_{\text{eff}} = k$ if the value of k_{eff}/k predicted by Equation 9.62 is less than unity.

EXAMPLE 9.5

A long tube of 0.1-m diameter is maintained at 120°C by passing steam through its interior. A radiation shield is installed concentric to the tube with an air gap of 10 mm. If the shield is at 35°C, estimate the heat transfer by free convection from the tube per unit length. What is the heat loss if the space between the tube and the shield is filled with glass-fiber blanket insulation?

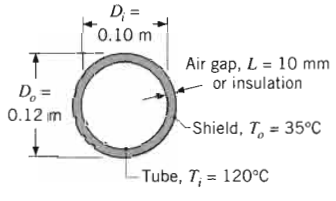
SOLUTION

Known: Temperatures and diameters of a steam tube and a concentric radiation shield.

Find:

1. Heat loss per unit length of tube.
2. Heat loss if air space is filled with glass-fiber blanket insulation.

Schematic:



Assumptions:

1. Radiation heat transfer may be neglected.
2. Contact resistance with insulation is negligible.

Properties: Table A.4, air [$T = (T_i + T_o)/2 = 350$ K]: $k = 0.030$ W/m·K, $\nu = 20.92 \times 10^{-6}$ m²/s, $\alpha = 29.9 \times 10^{-6}$ m²/s, $Pr = 0.70$, $\beta = 0.00285$ K⁻¹. Table A.3, insulation, glass-fiber ($T \approx 300$ K): $k = 0.038$ W/m · K.

9.9 Combined Fr

Patent Owner Manufacturing Resources International, Inc.
Exhibit 2017 - Page 598 of 999

Analysis:

1. From Equation 9.58, the heat loss per unit length by free convection is

$$q' = \frac{2\pi k_{\text{eff}}(T_i - T_o)}{\ln(r_o/r_i)}$$

where k_{eff} may be obtained from Equations 9.59 and 9.60. With

$$L_c = \frac{2[\ln(r_o/r_i)]^{4/3}}{(r_i^{-3/5} + r_o^{-3/5})^{5/3}} = \frac{2[\ln(0.06\text{ m}/0.05\text{ m})]^{4/3}}{(0.05^{-3/5} + 0.06^{-3/5})^{5/3}\text{m}^{-1}} = 0.00117\text{ m}$$

we find

$$Ra_c = \frac{g\beta(T_i - T_o)L_c^3}{\nu\alpha} = \frac{9.8\text{ m/s}^2 \times 0.00285\text{ K}^{-1} \times (120 - 35)^\circ\text{C} \times (0.00117\text{ m})^3}{20.92 \times 10^{-6}\text{ m}^2/\text{s} \times 29.9 \times 10^{-6}\text{ m}^2/\text{s}}$$
$$= 171$$

The effective thermal conductivity is then

$$k_{\text{eff}} = 0.386k\left(\frac{Pr}{0.861 + Pr}\right)^{1/4} Ra_c^{1/4}$$
$$= 0.386 \times 0.030\text{ W/m} \cdot \text{K}\left(\frac{0.70}{0.861 + 0.70}\right)^{1/4}(171)^{1/4} = 0.0343\text{ W/m} \cdot \text{K}$$

and the heat loss is

$$q' = \frac{2\pi k_{\text{eff}}(T_i - T_o)}{\ln(r_o/r_i)} = \frac{2\pi(0.0343\text{ W/m} \cdot \text{K})}{\ln(0.06\text{ m}/0.05\text{ m})}(120 - 35)^\circ\text{C} = 100\text{ W/m}$$

2. With insulation in the space between the tube and the shield, heat loss is by conduction; comparing Equation 3.27 and Equation 9.58,

$$q'_{\text{ins}} = q'\frac{k_{\text{ins}}}{k_{\text{eff}}} = 100\text{ W/m}\frac{0.038\text{ W/m} \cdot \text{K}}{0.0343\text{ W/m} \cdot \text{K}} = 111\text{ W/m}$$

Comments: Although there is slightly more heat loss by conduction through the insulation than by free convection across the air space, the total heat loss across the air space may exceed that through the insulation because of the effects of radiation. The heat loss due to radiation may be minimized by using a radiation shield of low emissivity, and the means for calculating the loss will be developed in Chapter 13.

9.9 *Combined Free and Forced Convection*

In dealing with forced convection (Chapters 6 through 8), we ignored the effects of free convection. This was, of course, an assumption; for, as we now know, free convection is likely when there is an unstable temperature gradient. Similarly, in the preceding sections of this chapter, we assumed that forced convection was negligible.

Patent Owner Manufacturing Resources International, Inc.
Exhibit 2017 - Page 599 of 999

It is now time to acknowledge that situations may arise for which free and forced convection effects are comparable, in which case it is inappropriate to neglect either process. In Section 9.3 we indicated that free convection is negligible if $(Gr_L/Re_L^2) \ll 1$ and that forced convection is negligible if $(Gr_L/Re_L^2) \gg 1$. Hence the *combined free* and *forced* (or *mixed*) *convection* regime is generally one for which $(Gr_L/Re_L^2) \approx 1$.

The effect of buoyancy on heat transfer in a forced flow is strongly influenced by the direction of the buoyancy force relative to that of the flow. Three special cases that have been studied extensively correspond to buoyancy-induced and forced motions having the same direction (*assisting* flow), opposite directions (*opposing* flow), and perpendicular directions (*transverse* flow). Upward and downward forced motions over a heated vertical plate are examples of assisting and opposing flows, respectively. Examples of transverse flow include horizontal motion over a heated cylinder, sphere, or horizontal plate. In assisting and transverse flows, buoyancy acts to enhance the rate of heat transfer associated with pure forced convection; in opposing flows, it acts to decrease this rate.

It has become common practice to correlate mixed convection heat transfer results for external and internal flows by an expression of the form

$$Nu^n = Nu_F^n \pm Nu_N^n \tag{9.64}$$

For the specific geometry of interest, the Nusselt numbers Nu_F and Nu_N are determined from existing correlations for pure forced and natural (free) convection, respectively. The plus sign on the right-hand side of Equation 9.64 applies for assisting and transverse flows, while the minus sign applies for opposing flow. The best correlation of data is often obtained for $n = 3$, although values of 7/2 and 4 may be better suited for transverse flows involving horizontal plates and cylinders (or spheres), respectively.

Equation 9.64 should be viewed as a first approximation, and any serious treatment of a mixed convection problem should be accompanied by an examination of the open literature. Mixed convection flows received considerable attention in the late 1970s to middle 1980s, and comprehensive literature reviews are available [39–42]. The flows are endowed with a variety of rich and unusual features that can complicate heat transfer predictions. For example, in a horizontal, parallel-plate channel, three-dimensional flows in the form of longitudinal vortices are induced by bottom heating, and the longitudinal variation of the Nusselt number is characterized by a decaying oscillation [43, 44]. Moreover, in channel flows, significant asymmetries may be associated with convection heat transfer at top and bottom surfaces [45]. Finally, we note that, although buoyancy effects can significantly enhance heat transfer for laminar forced convection flows, enhancement is typically negligible if the forced flow is turbulent [46].

9.11 Summary

9.10 Convection Mass Transfer

The buoyancy term on the right-hand side of Equation 9.3 is due to density variations in the fluid, which may arise from species concentration gradients, as well as

Patent Owner Manufacturing Resources International, Inc.
Exhibit 2017 - Page 600 of 999

temperature gradients. Hence, a more general form of the Grashof number, Equation 9.12, is

$$Gr_L = \frac{g(\Delta\rho/\rho)\,L^3}{\nu^2} = \frac{g(\rho_s - \rho_\infty)\,L^3}{\rho\nu^2} \tag{9.65}$$

which may be applied to natural convection flows driven by concentration gradients and/or temperature gradients. As shown in Section 9.2, if density variations are due only to temperature gradients, $(\Delta\rho/\rho) = -\beta\Delta T$. However, if there are no temperature gradients, motion may still be induced by spatial variations in the species composition, and similarity considerations lead to the conclusion that $Sh_L = f(Gr_L, Sc)$. Moreover, correlations for convection mass transfer may be inferred from those for heat transfer by invoking the heat and mass transfer analogy. For example, if species A is evaporating or sublimating from a vertical surface into a quiescent ambient fluid B, the convection mass transfer coefficient may be obtained from the analogous form of Equation 9.24. That is,

$$\overline{Sh}_L = \frac{\overline{h}_m L}{D_{AB}} = C(Gr_L\,Sc)^n \tag{9.66}$$

where Gr_L is given by Equation 9.65. If the molecular weight of species A is less than that of species B, $\rho_s < \rho_\infty$ and the buoyancy-induced flow is upward along the surface. If the opposite is true, $\rho_s > \rho_\infty$ and the flow is descending.

The analogy may only be applied in the foregoing manner for isothermal conditions. If there are gradients in both temperature and species concentration, heat and mass transfer will occur concurrently by natural convection. Similarity considerations then yield $\overline{Nu}_L = f(Gr_L, Pr, Sc)$ and $\overline{Sh}_L = f(Gr_L, Sc, Pr)$, where the density difference $\Delta\rho$ is due to both temperature and concentration variations. As a first approximation, existing correlations of the form $\overline{Nu}_L = f(Gr_L, Pr)$ and $\overline{Sh}_L = f(Gr_L, Sc)$ may be used to determine the convection transfer coefficients, so long as the value of $\Delta\rho = \rho_s - \rho_\infty$ is calculated by including the effects of both temperature and concentration variations on ρ_s and ρ_∞ and $Le = Pr/Sc \approx 1$. In a binary mixture of species A and B, the surface and free stream densities are defined as $\rho_s = \rho_{s,A} + \rho_{s,B}$ and $\rho_\infty = \rho_{\infty,A} + \rho_{\infty,B}$, respectively, where the species densities depend on the surface and free stream temperatures. The average density across the boundary layer(s) is $\rho = (\rho_s + \rho_\infty)/2$.

9.11 *Summary*

We have considered convective flows that originate in part or exclusively from buoyancy forces, and we have introduced the dimensionless parameters needed to characterize such flows. You should be able to discern when free convection effects are important and to quantify the associated heat transfer rates. An assortment of empirical correlations has been provided for this purpose.

To test your understanding of related concepts, consider the following questions.

- What is an *extensive, quiescent* fluid?
- What conditions are required for a buoyancy-driven flow?

Patent Owner Manufacturing Resources International, Inc.
Exhibit 2017 - Page 601 of 999

- How does the velocity profile in the free convection boundary layer on a heated vertical plate differ from the velocity profile in the boundary layer associated with forced flow over a parallel plate?
- What is the general form of the buoyancy term in the x-momentum equation for a free convection boundary layer? How may it be approximated if the flow is due to temperature variations? What is the name of the approximation?
- What is the physical interpretation of the *Grashof number*? What is the *Rayleigh number*? How does each parameter depend on the characteristic length?
- For a heated horizontal plate in quiescent air, do you expect heat transfer to be larger for the top or bottom surface? Why? For a cooled horizontal plate in quiescent air, do you expect heat transfer to be larger for the top or bottom surface? Why?
- For free convection within a vertical parallel plate channel, what kind of force balance governs the flow rate in the channel?
- For a vertical channel with isothermal plates, what is the physical basis for existence of an optimum spacing?
- What is the nature of flow in a cavity whose vertical surfaces are heated and cooled? What is the nature of flow in an annular space between concentric cylindrical surfaces that are heated and cooled?
- What is meant by the term *mixed convection*? How can one determine if mixed convection effects should be considered in a heat transfer analysis? Under what conditions is heat transfer enhanced by mixed convection? Under what conditions is it reduced?
- Consider transport of species A from a horizontal surface facing upward in a quiescent fluid B. If $T_s = T_\infty$ and the molecular weight of A is less than that of B, what is the analogous heat transfer problem? What is the analogous heat transfer problem if the molecular weight of A exceeds that of B?

References

1. Jaluria, Y., *Natural Convection Heat and Mass Transfer*, Pergamon Press, New York, 1980.
2. Gebhart, B., Y. Jaluria, R. L. Mahajan, and B. Sammakia, *Buoyancy-Induced Flows and Transport*, Hemisphere Publishing, Washington, DC, 1988.
3. Ostrach, S., "An Analysis of Laminar Free Convection Flow and Heat Transfer About a Flat Plate Parallel to the Direction of the Generating Body Force," National Advisory Committee for Aeronautics, Report 1111, 1953.
4. LeFevre, E. J., "Laminar Free Convection from a Vertical Plane Surface," *Proc. Ninth Int. Congr. Appl. Mech.*, Brussels, Vol. 4, 168, 1956.
5. McAdams, W. H., *Heat Transmission*, 3rd ed., McGraw-Hill, New York, 1954, Chap. 7.
6. Warner, C. Y., and V. S. Arpaci, *Int. J. Heat Mass Transfer*, **11,** 397, 1968.
7. Bayley, F. J., *Proc. Inst. Mech. Eng.*, **169,** 361, 1955.
8. Churchill, S. W., and H. H. S. Chu, *Int. J. Heat Mass Transfer*, **18,** 1323, 1975.
9. Sparrow, E. M., and J. L. Gregg, *Trans. ASME*, **78,** 435, 1956.
10. Churchill, S. W., "Free Convection Around Immersed Bodies," in G. F. Hewitt, Exec. Ed., *Heat Exchanger Design Handbook*, Section 2.5.7, Begell House, New York, 2002.
11. Sparrow, E. M., and J. L. Gregg, *Trans. ASME*, **78,** 1823, 1956.
12. Cebeci, T., "Laminar-Free-Convective Heat Transfer from the Outer Surface of a Vertical Slender Circular Cylinder," *Proc. Fifth Int. Heat Transfer Conf.*, Paper NC1.4, pp. 15–19, 1974.
13. Minkowycz, W. J., and E. M. Sparrow, *J. Heat Transfer*, **96,** 178, 1974.
14. Vliet, G. C., *Trans. ASME*, **91C,** 511, 1969.
15. Fujii, T., and H. 755, 1972.
16. Azevedo, L. F. **107,** 893, 1985.
17. Rich, B. R., *Tra*
18. Goldstein, R. J., *Heat Mass Trans*
19. Lloyd, J. R., an Adjacent to Hor ASME Paper 74-
20. Morgan, V. T., from Smooth Cir Hartnett, Eds., *A* demic Press, New
21. Churchill, S. W. *Transfer*, **18,** 10
22. Raithby, G. D., Rohsenow, J. P. *of Heat Transfer* New York, 1998
23. Elenbaas, W., *Ph*
24. Bar-Cohen, A., a **106,** 116, 1984.
25. Ostrach, S., "Nat Hartnett and T. F. Vol. 8, Academic
26. Catton, I., "Natu *Int. Heat Transfe* pp. 13–31.
27. Globe, S., and D 1959.
28. Hollands, K. G. *J. Heat Mass Tra*
29. Churchill, S. W., sures," in G. F. *Design Handboo* York, 2002.
30. MacGregor, R. K **91,** 391, 1969.
31. Ayyaswamy, P. S 543, 1973.

Problems

Properties and

9.1 Using the value culate the volu

Patent Owner Manufacturing Resources International, Inc.
Exhibit 2017 - Page 602 of 999

15. Fujii, T., and H. Imura, *Int. J. Heat Mass Transfer,* **15,** 755, 1972.
16. Azevedo, L. F. A., and E. M. Sparrow, *J. Heat Transfer,* **107,** 893, 1985.
17. Rich, B. R., *Trans. ASME,* **75,** 489, 1953.
18. Goldstein, R. J., E. M. Sparrow, and D. C. Jones, *Int. J. Heat Mass Transfer,* **16,** 1025, 1973.
19. Lloyd, J. R., and W. R. Moran, "Natural Convection Adjacent to Horizontal Surfaces of Various Planforms," ASME Paper 74-WA/HT-66, 1974.
20. Morgan, V. T., "The Overall Convective Heat Transfer from Smooth Circular Cylinders," in T. F. Irvine and J. P. Hartnett, Eds., *Advances in Heat Transfer,* Vol. 11, Academic Press, New York, 1975, pp. 199–264.
21. Churchill, S. W., and H. H. S. Chu, *Int. J. Heat Mass Transfer,* **18,** 1049, 1975.
22. Raithby, G. D., and K. G. T. Hollands, in W. M. Rohsenow, J. P. Hartnett, and Y. I. Cho, Eds., *Handbook of Heat Transfer Fundamentals,* Chap. 4, McGraw-Hill, New York, 1998.
23. Elenbaas, W., *Physica,* **9,** 1, 1942.
24. Bar-Cohen, A., and W. M. Rohsenow, *J. Heat Transfer,* **106,** 116, 1984.
25. Ostrach, S., "Natural Convection in Enclosures," in J. P. Hartnett and T. F. Irvine, Eds., *Advances in Heat Transfer,* Vol. 8, Academic Press, New York, 1972, pp. 161–227.
26. Catton, I., "Natural Convection in Enclosures," *Proc. 6th Int. Heat Transfer Conf.*, Toronto, Canada, 1978, Vol. 6, pp. 13–31.
27. Globe, S., and D. Dropkin, *J. Heat Transfer,* **81C,** 24, 1959.
28. Hollands, K. G. T., G. D. Raithby, and L. Konicek, *Int. J. Heat Mass Transfer,* **18,** 879, 1975.
29. Churchill, S. W., "Free Convection in Layers and Enclosures," in G. F. Hewitt, Exec. Ed., *Heat Exchanger Design Handbook*, Section 2.5.8, Begell House, New York, 2002.
30. MacGregor, R. K., and A. P. Emery, *J. Heat Transfer,* **91,** 391, 1969.
31. Ayyaswamy, P. S., and I. Catton, *J. Heat Transfer,* **95,** 543, 1973.
32. Catton, I., P. S. Ayyaswamy, and R. M. Clever, *Int. J. Heat Mass Transfer,* **17,** 173, 1974.
33. Clever, R. M., *J. Heat Transfer,* **95,** 407, 1973.
34. Arnold, J. N., I. Catton, and D. K. Edwards, "Experimental Investigation of Natural Convection in Inclined Rectangular Regions of Differing Aspect Ratios," ASME Paper 75-HT-62, 1975.
35. Buchberg, H., I. Catton, and D. K. Edwards, *J. Heat Transfer,* **98,** 182, 1976.
36. Hollands, K. G. T., S. E. Unny, G. D. Raithby, and L. Konicek, *J. Heat Transfer,* **98,** 189, 1976.
37. Raithby, G. D., and K. G. T. Hollands, "A General Method of Obtaining Approximate Solutions to Laminar and Turbulent Free Convection Problems," in T. F. Irvine and J. P. Hartnett, Eds., *Advances in Heat Transfer,* Vol. 11, Academic Press, New York, 1975, pp. 265–315.
38. Kuehn, T. H., and R. J. Goldstein, *Int. J. Heat Mass Transfer,* **19,** 1127, 1976.
39. Churchill, S. W., "Combined Free and Forced Convection around Immersed Bodies," in G. F. Hewitt, Exec. Ed., *Heat Exchanger Design Handbook*, Section 2.5.9, Begell House, New York, 2002.
40. Churchill, S. W., "Combined Free and Forced Convection in Channels," in G. F. Hewitt, Exec. Ed., *Heat Exchanger Design Handbook*, Section 2.5.10, Begell House, New York, 2002.
41. Chen, T. S., and B. F. Armaly, in S. Kakac, R. K. Shah, and W. Aung, Eds., *Handbook of Single-Phase Convective Heat Transfer,* Chap. 14, Wiley-Interscience, New York, 1987.
42. Aung, W., in S. Kakac, R. K. Shah, and W. Aung, Eds., *Handbook of Single-Phase Convective Heat Transfer,* Chap. 15, Wiley-Interscience, New York, 1987.
43. Incropera, F. P., A. J. Knox, and J. R. Maughan, *J. Heat Transfer,* **109,** 434, 1987.
44. Maughan, J. R., and F. P. Incropera, *Int. J. Heat Mass Transfer,* **30,** 1307, 1987.
45. Osborne, D. G., and F. P. Incropera, *Int. J. Heat Mass Transfer,* **28,** 207, 1985.
46. Osborne, D. G., and F. P. Incropera, *Int. J. Heat Mass Transfer,* **28,** 1337, 1985.

Problems

Properties and General Considerations

9.1 Using the values of density for water in Table A.6, calculate the volumetric thermal expansion coefficient at 300 K from its definition, Equation 9.4, and compare your result with the tabulated value.

9.2 Consider an object of characteristic length 0.01 m and a situation for which the temperature difference is 30°C.

Patent Owner Manufacturing Resources International, Inc.
Exhibit 2017 - Page 603 of 999

Evaluating thermophysical properties at the prescribed conditions, determine the Rayleigh number for the following fluids: air (1 atm, 400 K), helium (1 atm, 400 K), glycerin (285 K), and water (310 K).

9.3 To assess the efficacy of different liquids for cooling by natural convection, it is convenient to introduce a *figure of merit*, F_N, which combines the influence of all pertinent fluid properties on the convection coefficient. If the Nusselt number is governed by an expression of the form, $Nu_L \sim Ra^n$, obtain the corresponding relationship between F_N and the fluid properties. For a representative value of $n = 0.33$, calculate values of F_N for air ($k = 0.026$ W/m · K, $\beta = 0.0035\ K^{-1}$, $\nu = 1.5 \times 10^{-5}\ m^2/s$, $Pr = 0.70$), water ($k = 0.600$ W/m · K, $\beta = 2.7 \times 10^{-4}\ K^{-1}$, $\nu = 10^{-6}\ m^2/s$, $Pr = 5.0$), and a dielectric liquid ($k = 0.064$ W/m · K, $\beta = 0.0014\ K^{-1}$, $\nu = 10^{-6}\ m^2/s$, $Pr = 25$). What fluid is the most effective cooling agent?

9.4 In many cases, we are concerned with free convection involving gases that are contained within sealed enclosures. Consider air at 27°C and pressures of 1, 10, and 100 bars. Determine the *figure of merit* described in Problem 9.3 for each of these three pressures. Which air pressure will provide the most effective cooling?
Hint: See Problem 6.17.

Vertical Plates

9.5 The heat transfer rate due to free convection from a vertical surface, 1 m high and 0.6 m wide, to quiescent air that is 20 K colder than the surface is known. What is the ratio of the heat transfer rate for that situation to the rate corresponding to a vertical surface, 0.6 m high and 1 m wide, when the quiescent air is 20 K warmer than the surface? Neglect heat transfer by radiation and any influence of temperature on the relevant thermophysical properties of air.

9.6 Consider a large vertical plate with a uniform surface temperature of 130°C suspended in quiescent air at 25°C and atmospheric pressure.

(a) Estimate the boundary layer thickness at a location 0.25 m measured from the lower edge.

(b) What is the maximum velocity in the boundary layer at this location and at what position in the boundary layer does the maximum occur?

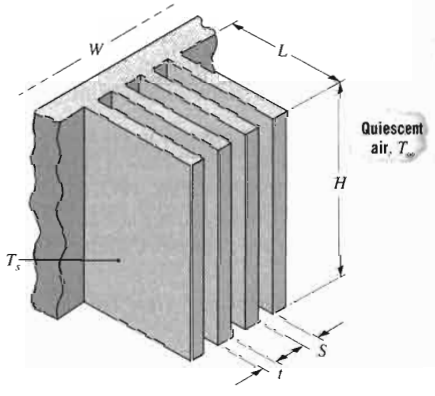
(c) Using the similarity solution result, Equation 9.19, determine the heat transfer coefficient 0.25 m from the lower edge.

(d) At what location on the plate measured from the lower edge will the boundary layer become turbulent?

9.7 A number of thin plates are to be cooled by vertically suspending them in a water bath at a temperature of 20°C. If the plates are initially at 54°C and are 0.15 m long, what minimum spacing would prevent interference between their free convection boundary layers?

9.8 A square aluminum plate 5 mm thick and 200 mm on a side is heated while vertically suspended in quiescent air at 40°C. Determine the average heat transfer coefficient for the plate when its temperature is 15°C by two methods: using results from the similarity solution to the boundary layer equations, and using results from an empirical correlation.

9.9 Consider an array of vertical rectangular fins, which is to be used to cool an electronic device mounted in quiescent, atmospheric air at $T_\infty = 27$°C. Each fin has $L = 20$ mm and $H = 150$ mm and operates at an approximately uniform temperature of $T_s = 77$°C.



(a) Viewing each fin surface as a vertical plate in an infinite, quiescent medium, briefly describe why there exists an optimum fin spacing S. Using Figure 9.4, estimate the optimum value of S for the prescribed conditions.

(b) For the optimum value of S and a fin thickness of $t = 1.5$ mm, estimate the rate of heat transfer from the fins for an array of width $W = 355$ mm.

9.10 Determine the average convection heat transfer coefficient for the 2.5-m-high vertical walls of a home having respective interior air and wall surface temperatures of (a) 20 and 10°C and (b) 27 and 37°C.

9.11 Beginning with the free convection correlation of the form given by Equation 9.24, show that for air at atmospheric pressure and a film temperature of 400 K,

the average
can be expre

$\bar{h}_L =$

$\bar{h}_L =$

9.12 A solid objec
escent fluid,
cient is giver
$\Delta T = T - T_$

(a) Invokin
obtain a
object t
final tem

(b) Conside
minum
tially at
25°C. U
tion fro
required

(c) Plot the
part (b)
lumped
convecti
appropri
temperat

9.13 A household
width reache
during opera
with ambient
of 1.0 and th
on the heat l
radiation.

9.14 An aluminun
temperature
cally suspenc
surroundings
with a thickn

(a) Develop
of the pl
to be uni

(b) Determir
plate tem

(c) Justify th

(d) Compute
plate fro
temperat
sponding
heat trans

Patent Owner Manufacturing Resources International, Inc.
Exhibit 2017 - Page 604 of 999

the average heat transfer coefficient for a vertical plate can be expressed as

$$\bar{h}_L = 1.40\left(\frac{\Delta T}{L}\right)^{1/4} \qquad 10^4 < Ra_L < 10^9$$

$$\bar{h}_L = 0.98\Delta T^{1/3} \qquad 10^9 < Ra_L < 10^{13}$$

9.12 A solid object is to be cooled by submerging it in a quiescent fluid, and the associated free convection coefficient is given by $\bar{h} = C\Delta T^{1/4}$, where C is a constant and $\Delta T = T - T_\infty$.

(a) Invoking the lumped capacitance approximation, obtain an expression for the time required for the object to cool from an initial temperature T_i to a final temperature T_f.

(b) Consider a highly polished, 150-mm square aluminum alloy (2024) plate of 5-mm thickness, initially at 225°C, and suspended in ambient air at 25°C. Using the appropriate approximate correlation from Problem 9.11, determine the time required for the plate to reach 80°C.

(c) Plot the temperature–time history obtained from part (b) and compare with the results from a lumped capacitance analysis using a constant free convection coefficient, $\bar{h}_o$. Evaluate $\bar{h}_o$ from an appropriate correlation based on an average surface temperature of $\bar{T} = (T_i + T_f)/2$.

9.13 A household oven door of 0.5-m height and 0.7-m width reaches an average surface temperature of 32°C during operation. Estimate the heat loss to the room with ambient air at 22°C. If the door has an emissivity of 1.0 and the surroundings are also at 22°C, comment on the heat loss by free convection relative to that by radiation.

9.14 An aluminum alloy (2024) plate, heated to a uniform temperature of 227°C, is allowed to cool while vertically suspended in a room where the ambient air and surroundings are at 27°C. The plate is 0.3 m square with a thickness of 15 mm and an emissivity of 0.25.

(a) Develop an expression for the time rate of change of the plate temperature, assuming the temperature to be uniform at any time.

(b) Determine the initial rate of cooling (K/s) when the plate temperature is 227°C.

(c) Justify the uniform plate temperature assumption.

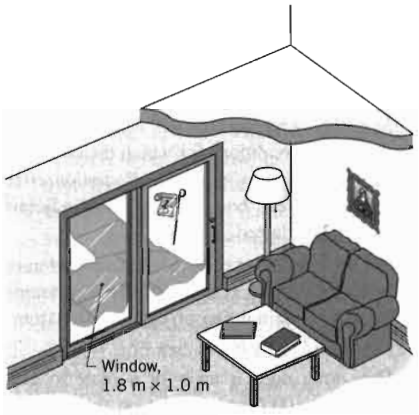
(d) Compute and plot the temperature history of the plate from $t = 0$ to the time required to reach a temperature of 30°C. Compute and plot the corresponding variations in the convection and radiation heat transfer rates.

9.15 The plate described in Problem 9.14 has been used in an experiment to determine the free convection heat transfer coefficient. At an instant of time when the plate temperature was 127°C, the time rate of change of this temperature was observed to be −0.0465 K/s. What is the corresponding free convection heat transfer coefficient? Compare this result with an estimate based on a standard empirical correlation.

9.16 The ABC Evening News Report in a news segment on hypothermia research studies at the University of Minnesota claimed that heat loss from the body is 30 times faster in 10°C water than in air at the same temperature. Is that a realistic statement?

9.17 Consider a vertical, single-pane window of equivalent width and height ($W = L = 1$ m). The interior surface is exposed to the air and walls of a room, which are each at 18°C. Under cold ambient conditions for which a thin layer of frost has formed on the inner surface, what is the heat loss through the window? How would your analysis be affected by a frost layer whose thickness is not negligible? During incipience of frost formation, where would you expect the frost to begin to develop on the window? The frost may be assumed to have an emissivity of $\varepsilon = 0.90$.

9.18 During a winter day, the window of a patio door with a height of 1.8 m and width of 1.0 m shows a frost line near its base. The room wall and air temperatures are 15°C.



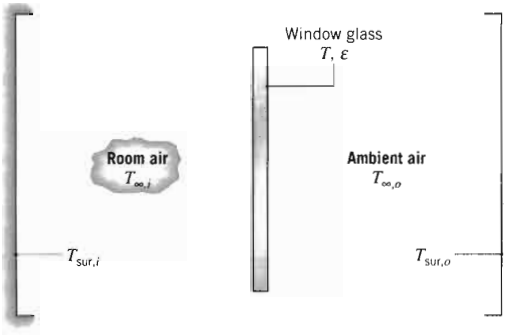
(a) Explain why the window would show a frost layer at the base rather than at the top.

(b) Estimate the heat loss through the window due to free convection and radiation. Assume the window has a uniform temperature of 0°C and the

Patent Owner Manufacturing Resources International, Inc.
Exhibit 2017 - Page 605 of 999

emissivity of the glass surface is 0.94. If the room has electric baseboard heating, estimate the corresponding daily cost of the window heat loss for a utility rate of 0.08 \$/kW · h.

9.19 A vertical, thin pane of window glass that is 1 m on a side separates quiescent room air at $T_{\infty,i} = 20°C$ from quiescent ambient air at $T_{\infty,o} = -20°C$. The walls of the room and the external surroundings (landscape, buildings, etc.) are also at $T_{sur,i} = 20°C$ and $T_{sur,o} = -20°C$, respectively.



If the glass has an emissivity of $\varepsilon = 1$, what is its temperature T? What is the rate of heat loss through the glass?

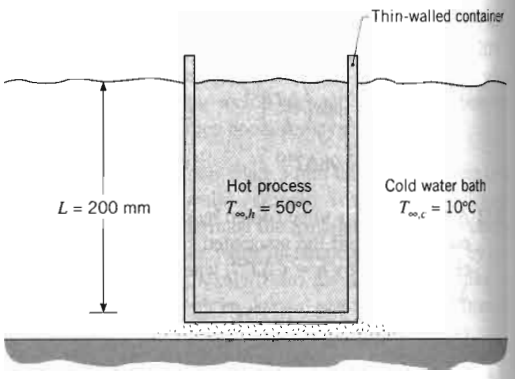
9.20 Consider the conditions of Problem 9.19, but now allow for a difference between the inner and outer surface temperatures, $T_{s,i}$ and $T_{s,o}$, of the window. For a glass thickness and thermal conductivity of $t_g = 10$ mm and $k_g = 1.4$ W/m · K, respectively, evaluate $T_{s,i}$ and $T_{s,o}$. What is the heat loss through the window?

9.21 Consider the conveyor system described in Problem 7.24, but under conditions for which the conveyor is not moving and the air is quiescent. Radiation effects and interactions between boundary layers on adjoining surfaces may be neglected.

(a) For the prescribed plate dimensions and initial temperature, as well as the prescribed air temperature, what is the initial rate of heat transfer from one of the plates?

(b) How long does it take for a plate to cool from 300°C to 100°C? Comment on the assumption of negligible radiation.

9.22 A thin-walled container with a hot process fluid at 50°C is placed in a quiescent, cold water bath at 10°C. Heat transfer at the inner and outer surfaces of the container may be approximated by free convection from a vertical plate.



(a) Determine the overall heat transfer coefficient between the hot process fluid and the cold water bath. Assume the properties of the hot process fluid are those of water.

(b) Generate a plot of the overall heat transfer coefficient as a function of the hot process fluid temperature $T_{\infty,h}$ for the range 20 to 60°C, with all other conditions remaining the same.

9.23 Consider an experiment to investigate the transition to turbulent flow in a free convection boundary layer that develops along a vertical plate suspended in a large room. The plate is constructed of a thin heater that is sandwiched between two aluminum plates and may be assumed to be isothermal. The heated plate is 1 m high and 2 m wide. The quiescent air and the surroundings are both at 25°C.

(a) The exposed surfaces of the aluminum plate are painted with a very thin coating of high emissivity ($\varepsilon = 0.95$) paint. Determine the electrical power that must be supplied to the heater to sustain the plate at a temperature of $T_s = 35°C$. How much of the plate is exposed to turbulent conditions in the free convection boundary layer?

(b) The experimentalist speculates that the roughness of the paint is affecting the transition to turbulence in the boundary layer and decides to remove the paint and polish the aluminum surface ($\varepsilon = 0.05$). If the same power is supplied to the plate as in part (a), what is the steady-state plate temperature? How much of the plate is exposed to turbulent conditions in the free convection boundary layer?

9.24 A square plate of pure aluminum, 0.5 m on a side and 16 mm thick, is initially at 300°C and is suspended in a large chamber. The walls of the chamber are maintained at 27°C, as is the enclosed air. If the surface emissivity of the plate is 0.25, what is the initial cooling rate? Is it

reasonable to
ing the cooli

9.25 The vertical
ness $L = 8$ r
fine-meshed
form volume

(a) Consider
interior s
cent air
exposed
over the
mine the
tain the i

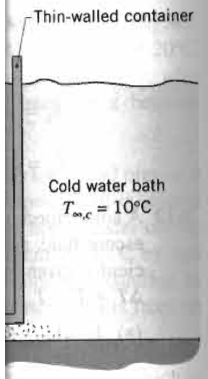
(b) The inter
and $T_{s,o}$,
temperat
ity u_z of
the volur
straint th
to develc
in respor
If $T_{\infty,i}$ is
vary with
20, and
maintaine
$T_{s,o}$ vary
$-25, -1($

9.26 Determine the
that may be i
if the maxim
when the ambi

9.27 The componen
side, dissipate
and the front s

Assuming a un
imum tempera
ture of the boa

Patent Owner Manufacturing Resources International, Inc.
Exhibit 2017 - Page 606 of 999



t transfer coefficient
id and the cold water
of the hot process fluid

ll heat transfer coeffi-
process fluid tempera-
60°C, with all other
ne.

tigate the transition to
on boundary layer that
suspended in a large
f a thin heater that is
um plates and may be
eated plate is 1 m high
and the surroundings

e aluminum plate are
ting of high emissivity
the electrical power
e heater to sustain the
= 35°C. How much of
ulent conditions in the
er?

tes that the roughness
transition to turbulence
decides to remove the
um surface ($\varepsilon = 0.05$).
d to the plate as in part
late temperature? How
to turbulent conditions
ary layer?

n, 0.5 m on a side and
C and is suspended in a
chamber are maintained
f the surface emissivity
nitial cooling rate? Is it

reasonable to assume a uniform plate temperature during the cooling process?

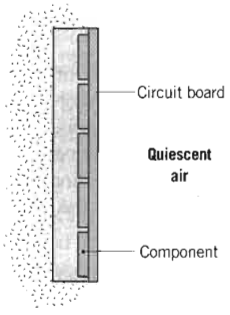
9.25 The vertical rear window of an automobile is of thickness $L = 8$ mm and height $H = 0.5$ m and contains fine-meshed heating wires that can induce nearly uniform volumetric heating, $\dot{q}$ (W/m^3).

(a) Consider steady-state conditions for which the interior surface of the window is exposed to quiescent air at 10°C, while the exterior surface is exposed to air at −10°C moving in parallel flow over the surface with a velocity of 20 m/s. Determine the volumetric heating rate needed to maintain the interior window surface at $T_{s,i} = 15°C$.

(b) The interior and exterior window temperatures, $T_{s,i}$ and $T_{s,o}$, depend on the compartment and ambient temperatures, $T_{\infty,i}$ and $T_{\infty,o}$, as well as on the velocity u_∞ of air flowing over the exterior surface and the volumetric heating rate $\dot{q}$. Subject to the constraint that $T_{s,i}$ is to be maintained at 15°C, we wish to develop guidelines for varying the heating rate in response to changes in $T_{\infty,i}$, $T_{\infty,o}$, and/or u_∞. If $T_{\infty,i}$ is maintained at 10°C, how will $\dot{q}$ and $T_{s,o}$ vary with $T_{\infty,o}$ for $-25 \le T_{\infty,o} \le 5°C$ and $u_\infty = 10$, 20, and 30 m/s? If a constant vehicle speed is maintained, such that $u_\infty = 30$ m/s, how will $\dot{q}$ and $T_{s,o}$ vary with $T_{\infty,i}$ for $5 \le T_{\infty,i} \le 20°C$ and $T_{\infty,o} = -25$, −10, and 5°C?

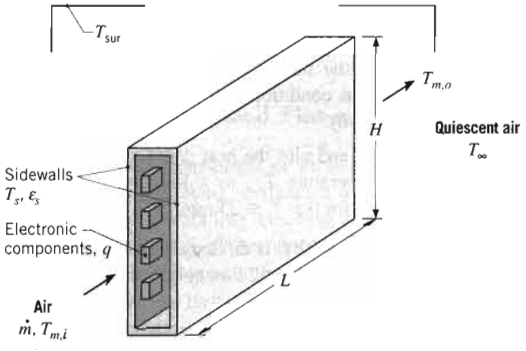
9.26 Determine the maximum allowable uniform heat flux that may be imposed at a wall heating panel 1 m high if the maximum temperature is not to exceed 37°C when the ambient air temperature is 25°C.

9.27 The components of a vertical circuit board, 150 mm on a side, dissipate 5 W. The back surface is well insulated and the front surface is exposed to quiescent air at 27°C.



Assuming a uniform surface heat flux, what is the maximum temperature of the board? What is the temperature of the board for an isothermal surface condition?

9.28 Circuit boards are mounted to interior vertical surfaces of a rectangular duct of height $H = 400$ mm and length $L = 800$ mm. Although the boards are cooled by forced convection heat transfer to air flowing through the duct, not all of the heat dissipated by the electronic components is transferred to the flow. Some of the heat is instead transferred by conduction to the vertical walls of the duct and then by natural convection and radiation to the ambient (atmospheric) air and surroundings, which are at equivalent temperatures of $T_\infty = T_{sur} = 20°C$. The walls are metallic and, to a first approximation, may be assumed to be isothermal at a temperature T_s.



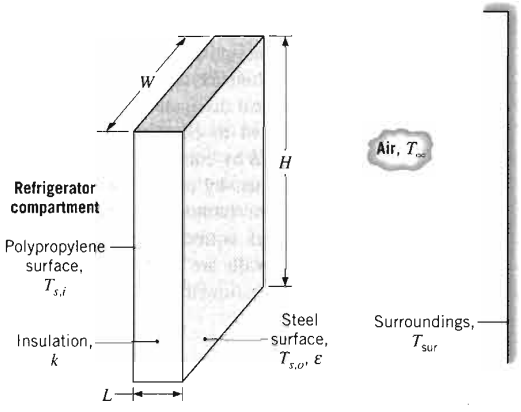
(a) Consider conditions for which the electronic components dissipate 200 W and air enters the duct at a flow rate of $\dot{m} = 0.015$ kg/s and a temperature of $T_{m,i} = 20°C$. If the emissivity of the side walls is $\varepsilon_s = 0.15$ and the outlet temperature of the air is $T_{m,o} = 30°C$, what is the surface temperature T_s?

(b) To reduce the temperature of the electronic components, it is desirable to enhance heat transfer from the side walls. Assuming no change in the air flow conditions, what is the effect on T_s of applying a high emissivity coating ($\varepsilon_s = 0.90$) to the side walls?

(c) If there is a loss of air flow while power continues to be dissipated, what are the resulting values of T_s for $\varepsilon_s = 0.15$ and $\varepsilon_s = 0.90$?

9.29 A refrigerator door has a height and width of $H = 1$ m and $W = 0.65$ m, respectively, and is situated in a large room for which the air and walls are at $T_\infty = T_{sur} = 25°C$. The door consists of a layer of polystyrene insulation ($k = 0.03$ W/m · K) sandwiched between thin sheets of steel ($\varepsilon = 0.6$) and polypropylene. Under normal operating conditions, the inner surface of the door is maintained at a fixed temperature of $T_{s,i} = 5°C$.

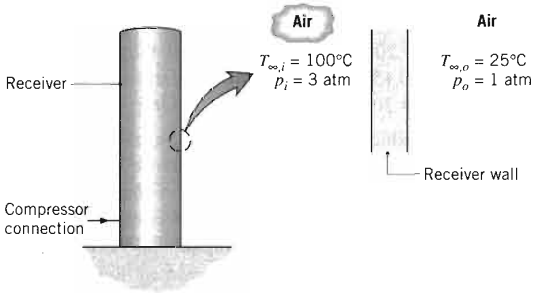
Patent Owner Manufacturing Resources International, Inc.
Exhibit 2017 - Page 607 of 999



(a) Estimate the heat gain through the door for the worst case condition corresponding to no insulation ($L = 0$).

(b) Compute and plot the heat gain and the outer surface temperature $T_{s,o}$ as a function of insulation thickness for $0 \leq L \leq 25$ mm.

9.30 Air at 3 atm and 100°C is discharged from a compressor into a vertical receiver of 2.5-m height and 0.75-m diameter. Assume that the receiver wall has negligible thermal resistance, is at a uniform temperature, and that heat transfer at its inner and outer surfaces is by free convection from a vertical plate. Neglect radiation exchange and any losses from the top.

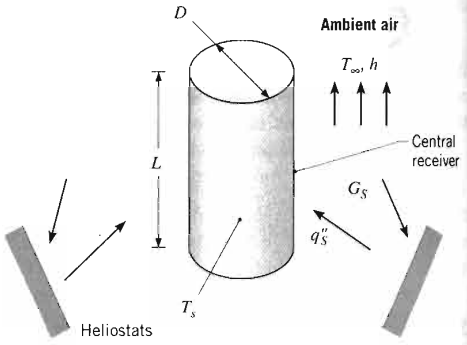


(a) Estimate the receiver wall temperature and the heat transfer to the ambient air at 25°C. To facilitate use of the free convection correlations with appropriate film temperatures, assume that the receiver wall temperature is 60°C.

(b) Were the assumed film temperatures of part (a) reasonable? If not, use an iteration procedure to find consistent values.

(c) Now consider two features of the receiver neglected in the previous analysis: (i) radiation exchange from the exterior surface of emissivity 0.85 to large surroundings, also at 25°C; and (ii) the thermal resistance of a 20-mm-thick wall with a thermal conductivity of 0.25 W/m · K. Represent the system by a thermal circuit and estimate the wall temperatures and the heat transfer rate.

9.31 In the *central receiver* concept of a solar power plant, many heliostats at ground level are used to direct a concentrated solar flux q''_S to the receiver, which is positioned at the top of a tower. However, even with absorption of all the solar flux by the outer surface of the receiver, losses due to free convection and radiation reduce the collection efficiency below the maximum possible value of 100%. Consider a cylindrical receiver of diameter $D = 7$ m, length $L = 12$ m, and emissivity $\varepsilon = 0.20$.

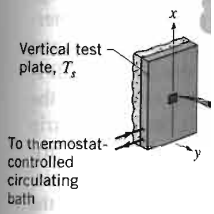


(a) If all of the solar flux is absorbed by the receiver and a surface temperature of $T_s = 800$ K is maintained, what is the rate of heat loss from the receiver? The ambient air is quiescent at a temperature of $T_\infty = 300$ K, and irradiation from the surroundings may be neglected. If the corresponding value of the solar flux is $q''_S = 10^5$ W/m^2, what is the collector efficiency?

(b) The surface temperature of the receiver is affected by design and operating conditions within the power plant. Over the range from 600 to 1000 K, plot the variation of the convection, radiation, and total heat rates as a function of T_s. For a fixed value of $q''_S = 10^5$ W/m^2, plot the corresponding variation of the receiver efficiency.

9.32 An experimental apparatus is shown in the schematic for measuring the local convection coefficient and the boundary layer temperature distribution for a heated vertical plate immersed in an extensive, quiescent fluid. The plate is maintained at a uniform temperature by circulating a thermostatically controlled fluid through imbedded

flow channels.
measured at di
ture sensors u
The fluid temp
using a micro
mounted withi
the series of ot
air and room w
to process the
them to results
free convection



The following
heat flux sen
plate–air temp

x (mm)	25	7
q''_{tot} (W/m^2)	41.4	2

Measurements
probe are pro
at two x-locati
sponding to t
simplify your

	G
y(mm)	2.5
$T(x, y) - T_\infty$(K)	5.5

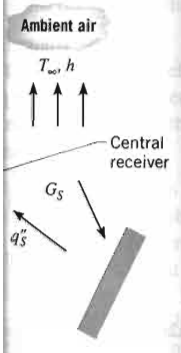
(a) The surfaces
convection
roundings.
radiation he
the surface
roundings, a

(b) Using the e
correction t

Patent Owner Manufacturing Resources International, Inc.
Exhibit 2017 - Page 608 of 999

sivity 0.85 to large sur-
d (ii) the thermal resis-
wall with a thermal
K. Represent the system
imate the wall tempera-
te.

of a solar power plant,
are used to direct a con-
eceiver, which is posi-
However, even with
by the outer surface of
onvection and radiation
below the maximum
r a cylindrical receiver
= 12 m, and emissivity

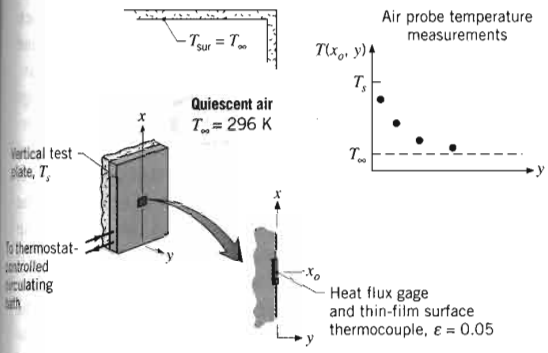


bed by the receiver and
= 800 K is maintained,
from the receiver? The
at a temperature of
from the surroundings
esponding value of the
what is the collector

he receiver is affected
conditions within the
from 600 to 1000 K,
vection, radiation, and
of T_s. For a fixed value
orresponding variation

wn in the schematic for
coefficient and the
bution for a heated ver-
ve, quiescent fluid. The
emperature by circulat-
luid through imbedded

flow channels. The heat flux and surface temperature are measured at discrete locations along the x-axis by miniature sensors using thin-film thermocouple technology. The fluid temperature in the boundary layer is measured using a microwire thermocouple probe. The plate is mounted within a room under stable climate control. For the series of observations tabulated below, the quiescent air and room wall temperatures were 296 K. Your task is to process the experimental observations and compare them to results from the similarity solution for laminar free convection (Section 9.4).



The following table provides measurements from the heat flux sensor at six x-locations for the specified plate–air temperature difference.

$T_s - T_\infty = 7.7$ K

x (mm)	25	75	175	275	375	475
q''_{tot} (W/m^2)	41.4	27.2	22.0	20.1	18.3	17.2

Measurements obtained from the air temperature probe are provided next for three discrete y-locations at two x-locations. The local Grashof numbers corresponding to the x-locations have been calculated to simplify your analysis.

$T_s - T_\infty = 7.3$ K

	x = 200 mm, $Gr_x = 7.6 \times 10^6$			x = 400 mm, $Gr_x = 6.0 \times 10^7$		
y(mm)	2.5	5.0	10.0	2.5	5.0	10.0
$T(x, y) - T_\infty$(K)	5.5	3.8	1.6	5.9	4.5	2.0

(a) The surfaces of the heat flux sensors experience free convection and radiation exchange with the surroundings. Write an expression for estimating the radiation heat flux from the sensor as a function of the surface emissivity, the temperature of the surroundings, and the temperature difference ($T_s - T_\infty$).

(b) Using the expression derived in part (a), apply a correction to the measured total heat flux, q''_{tot}, to obtain the convection heat flux, q''_{cv}, and calculate the convection coefficient. Extend the first table above to include the results of your analysis.

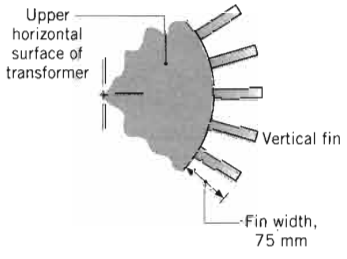
(c) Calculate and plot the local convection coefficient, $h_x(x)$, as a function of the x-coordinate using the similarity solution, Eqs. 9.19 and 9.20. On the same graph, plot the experimental points. Comment on the comparison between the experimental and analytical results.

(d) For the conditions in the second table, compare the experimental boundary-layer air temperature measurements with those from the similarity solution, Figure 9.4*b*. Summarize the results of your analysis using the similarity parameter, η, and the dimensionless temperature, T^*. Comment on the comparison between the experimental and analytical results.

Horizontal and Inclined Plates

9.33 Consider the transformer of Problem 8.97, whose lateral surface is being maintained at 47°C by a forced convection coolant line removing 1000 W. It is desired to explore cooling of the transformer by free convection and radiation, assuming the surface to have an emissivity of 0.80.

(a) Determine how much power could be removed by free convection and radiation from the lateral *and* the upper horizontal surfaces when the ambient temperature and the surroundings are at 27°C.



(b) Vertical fins, 5 mm thick, 75 mm wide, and 500 mm long, can easily be welded to the lateral surface. What is the heat removal rate by free convection if 30 such fins are attached?

9.34 Airflow through a long, 0.2-m-square air conditioning duct maintains the outer duct surface temperature at 10°C. If the horizontal duct is uninsulated and exposed to air at 35°C in the crawlspace beneath a home, what is the heat gain per unit length of the duct?

9.35 Consider the conditions of Example 9.3, including the effect of adding insulation of thickness t and thermal

Patent Owner Manufacturing Resources International, Inc.
Exhibit 2017 - Page 609 of 999

conductivity $k = 0.035$ W/m · K to the duct. We wish to now include the effect of radiation on the outer surface temperatures and the total heat loss per unit length of duct.

(a) If $T_{s,1} = 45°C$, $t = 25$ mm, $\varepsilon = 1$, and $T_{sur} = 288$ K, what are the temperatures of the side, top, and bottom surfaces? What are the corresponding heat losses per unit length of duct?

(b) For the top surface, compute and plot $T_{s,2}$ and q' as a function of insulation thickness for $0 \leq t \leq 50$ mm. The exposed duct surface ($t = 0$) may also be assumed to have an emissivity of $\varepsilon = 1$.

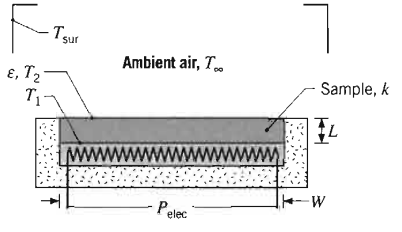
9.36 An electrical heater in the form of a horizontal disk of 400-mm diameter is used to heat the bottom of a tank filled with engine oil at a temperature of 5°C. Calculate the power required to maintain the heater surface temperature at 70°C.

9.37 Consider a horizontal 6-mm-thick, 100-mm-long straight fin fabricated from plain carbon steel ($k = 57$ W/m · K, $\varepsilon = 0.5$). The base of the fin is maintained at 150°C, while the quiescent ambient air and the surroundings are at 25°C. Assume the fin tip is adiabatic.

(a) Estimate the fin heat rate per unit width, q_f'. Use an average fin surface temperature of 125°C to estimate the free convection coefficient and the linearized radiation coefficient. How sensitive is your estimate to the choice of the average fin surface temperature?

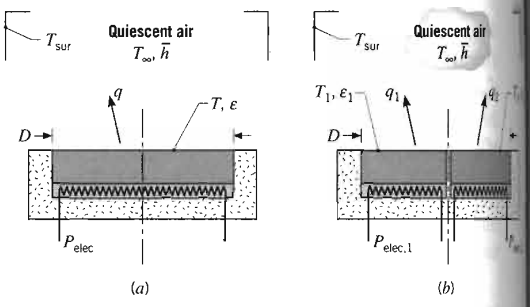
(b) Generate a plot of q_f' as a function of the fin emissivity for $0.05 \leq \varepsilon \leq 0.95$. On the same coordinates, show the fraction of the total heat rate due to radiation exchange.

9.38 The thermal conductivity and surface emissivity of a material may be determined by heating its bottom surface and exposing its top surface to quiescent air and large surroundings of equivalent temperatures, $T_\infty = T_{sur} = 25°C$. The remaining surfaces of the sample/heater are well insulated.



Consider a sample of thickness $L = 25$ mm and a square planform of width $W = 250$ mm. In an experiment performed under steady-state conditions, temperature measurements made at the lower and upper surface of the sample yield values of $T_1 = 150°C$ and $T_2 = 100°C$, respectively, for a power input of $P_{elec} = 70$ W. What are the thermal conductivity and emissivity of the sample?

9.39 Convection heat transfer coefficients for a heated horizontal surface facing upward may be determined by a gage whose specific features depend on whether the temperature of the surroundings is known. For configuration A, a copper disk, which is electrically heated from below, is encased in an insulating material such that all of the heat is transferred by convection and radiation from the top surface. If the surface emissivity and the temperatures of the air and surroundings are known, the convection coefficient may be determined from measurement of the electrical power and the surface temperature of the disk. Configuration B is used in situations for which the temperature of the surroundings is not known. A thin, insulating strip separates semicircular disks with independent electrical heaters and different emissivities. If the emissivities and temperature of the air are known, the convection coefficient may be determined from measurement of the electrical power supplied to each of the disks in order to maintain them at a common temperature.



(a) In an application of configuration A to a disk of diameter $D = 160$ mm and emissivity $\varepsilon = 0.8$, values of $P_{elec} = 10.8$ W and $T = 67°C$ are measured for $T_\infty = T_{sur} = 27°C$. What is the corresponding value of the average convection coefficient? How does it compare with predictions based on a standard correlation?

(b) Now consider an application of configuration *B* for which $T_\infty = 17°C$ and T_{sur} is unknown. With $D = 160$ mm, $\varepsilon_1 = 0.8$ and $\varepsilon_2 = 0.1$, values of $P_{elec,1} = 9.70$ W and $P_{elec,2} = 5.67$ W are measured when $T_1 = T_2 = 77°C$. Determine the corresponding

values of the
ature of the s
coefficient c
priate correla

9.40 A circular grill o
maintained at a
What electrical
and surrounding

9.41 Many laptop con
agement system
tral processing u
to the back of th
tion of heat fro
way of a flat, is
uid is recirculate
Consider an alu
$w = 275$ mm a
assembly is orie
cal direction, ar
$t = 3$ mm thick p
ing adhesive. Th
tivity of $k = 0.2$
The contact resis
housing interfac
CPU generates,
what is the temp
$T_{sur} = 23°C$? W
duction, radiatio

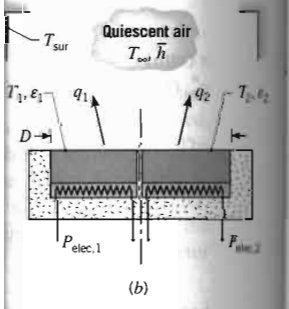
9.42 Consider the roc
described in Pr
which the truck
remain unchange
surface temperat
the refrigeration
$Ra_L > 10^7$.

9.43 The 4-m by 4-n
minum melting
fireclay brick re
(AISI 1010) pl
the furnace gas
ation, while the
the air and wall
ity of the steel i
(a) What is the
(b) If a 20-mm
(64 kg/m^3)
steel, what
roof? What
of the insul
(c) One of the
perature at

Patent Owner Manufacturing Resources International, Inc.
Exhibit 2017 - Page 610 of 999

tate conditions, tempera-
lower and upper surface
f $T_1 = 150°C$ and $T_2 =$
er input of $P_{elec} = 70$ W.
ity and emissivity of the

cients for a heated hori-
nay be determined by a
depend on whether the
gs is known. For config-
ch is electrically heated
insulating material such
rred by convection and
. If the surface emissiv-
ie air and surroundings
efficient may be deter-
he electrical power and
disk. Configuration B is
the temperature of the
A thin, insulating strip
ith independent electri-
issivities. If the emis-
the air are known, the
determined from mea-
wer supplied to each of
in them at a common



(b)

guration A to a disk of
emissivity $\varepsilon = 0.8$, val-
$T = 67°C$ are measured
at is the corresponding
rection coefficient? How
ictions based on a stan-

tion of configuration B
T_{sur} is unknown. With
nd $\varepsilon_2 = 0.1$, values of
= 5.67 W are measured
ermine the corresponding

values of the convection coefficient and the temperature of the surroundings. How does the convection coefficient compare with predictions by an appropriate correlation?

9.40 A circular grill of diameter 0.25 m and emissivity 0.9 is maintained at a constant surface temperature of 130°C. What electrical power is required when the room air and surroundings are at 24°C?

9.41 Many laptop computers are equipped with thermal management systems that involve liquid cooling of the central processing unit (CPU), transfer of the heated liquid to the back of the laptop screen assembly, and dissipation of heat from the back of the screen assembly by way of a flat, isothermal heat spreader. The cooled liquid is recirculated to the CPU and the process continues. Consider an aluminum heat spreader that is of width $w = 275$ mm and height $L = 175$ mm. The screen assembly is oriented at an angle $\theta = 30°$ from the vertical direction, and the heat spreader is attached to the $t = 3$ mm thick plastic housing with a thermally conducting adhesive. The plastic housing has a thermal conductivity of $k = 0.21$ W/m · K and emissivity of $\varepsilon = 0.85$. The contact resistance associated with the heat spreader-housing interface is $R''_{t,c} = 2.0 \times 10^{-4}$ m^2 · K/W. If the CPU generates, on average, 15 W of thermal energy, what is the temperature of the heat spreader when $T_\infty = T_{sur} = 23°C$? Which thermal resistance (contact, conduction, radiation, or free convection) is the largest?

9.42 Consider the roof of the refrigerated truck compartment described in Problem 7.20, but under conditions for which the truck is parked ($V = 0$). All other conditions remain unchanged. For $\alpha_S = \varepsilon = 0.5$, determine the outer surface temperature, $T_{s,o}$, and the heat load imposed on the refrigeration system. *Hint*: Assume $T_{s,o} > T_\infty$ and $Ra_L > 10^7$.

9.43 The 4-m by 4-m horizontal roof of an uninsulated aluminum melting furnace is comprised of a 0.08-m-thick fireclay brick refractory covered by a 5-mm-thick steel (AISI 1010) plate. The refractory surface exposed to the furnace gases is maintained at 1700 K during operation, while the outer surface of the steel is exposed to the air and walls of a large room at 25°C. The emissivity of the steel is $\varepsilon = 0.3$.

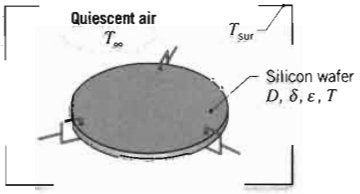
(a) What is the rate of heat loss from the roof?

(b) If a 20-mm-thick layer of alumina–silica insulation (64 kg/m^3) is placed between the refractory and the steel, what is the new rate of heat loss from the roof? What is the temperature at the inner surface of the insulation?

(c) One of the process engineers claims that the temperature at the inner surface of the insulation found in part (b) is too high for safe, long-term operation. What thickness of fireclay brick would reduce this temperature to 1350 K?

9.44 A stereo receiver/amplifier is enclosed in a thin metallic case for which the top, horizontal surface is 0.5 m × 0.5 m on a side. The surface, which is not vented, has an emissivity of $\varepsilon = 0.8$ and is exposed to quiescent ambient air and large surroundings for which $T_\infty = T_{sur} = 25°C$. For surface temperatures in the range $50 \le T_s \le 75°C$, compute and plot the total heat rate from the surface, as well as the contributions due to convection and radiation.

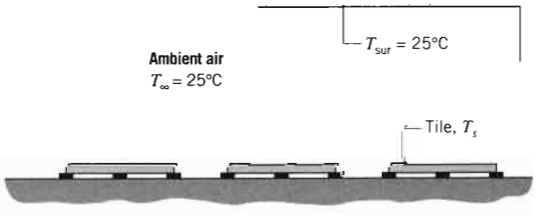
9.45 At the end of its manufacturing process, a silicon wafer of diameter $D = 150$ mm, thickness $\delta = 1$ mm, and emissivity $\varepsilon = 0.65$ is at an initial temperature of $T_i = 325°C$ and is allowed to cool in quiescent, ambient air and large surroundings for which $T_\infty = T_{sur} = 25°C$.



(a) What is the initial rate of cooling?

(b) How long does it take for the wafer to reach a temperature of 50°C? Comment on how the relative effects of convection and radiation vary with time during the cooling process.

9.46 A 200-mm-square, 10-mm-thick tile has the thermophysical properties of pyrex ($\varepsilon = 0.80$) and emerges from a curing process at an initial temperature of $T_i = 140°C$. The backside of the tile is insulated while the upper surface is exposed to ambient air and surroundings at 25°C.



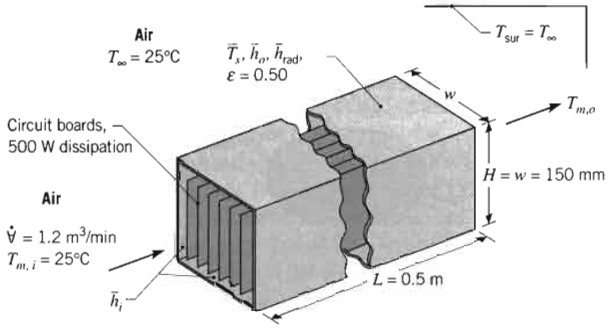
(a) Estimate the time required for the tile to cool to a final, safe-to-touch temperature of $T_f = 40°C$. Use

Patent Owner Manufacturing Resources International, Inc.
Exhibit 2017 - Page 611 of 999

an average tile surface temperature of $\overline{T} = (T_i + T_f)/2$ to estimate the average free convection coefficient and the linearized radiation coefficient. How sensitive is your estimate to the assumed value for $\overline{T}$?

(b) Estimate the required cooling time if ambient air is blown in parallel flow over the tile with a velocity of 10 m/s.

9.47 Integrated circuit (IC) boards are stacked within a duct and dissipate a total of 500 W. The duct has a square cross section with $w = H = 150$ mm and a length of 0.5 m. Air flows into the duct at 25°C and 1.2 m³/min, and the convection coefficient between the air and the inner surfaces of the duct is $\overline{h}_i = 50\ \text{W/m}^2 \cdot \text{K}$. The entire outer surface of the duct, which is anodized with an emissivity of 0.5, is exposed to ambient air and large surroundings at 25°C.



Your assignment is to develop a model to estimate the outlet temperature of the air, $T_{m,o}$, and the average surface temperature of the duct, $\overline{T}_s$.

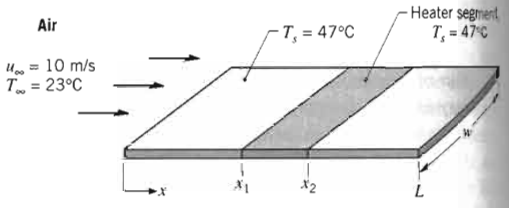
(a) Assuming a surface temperature of 37°C, estimate the average free convection coefficient, $\overline{h}_o$, for the outer surface of the duct.

(b) Assuming a surface temperature of 37°C, estimate the average linearized radiation coefficient, $\overline{h}_{rad}$, for the outer surface of the duct.

(c) Perform an energy balance on the duct by considering the dissipation of electrical power in the ICs, the rate of change in the energy of air flowing through the duct, and the rate of heat transfer from the air in the duct to the surroundings. Express the last process in terms of thermal resistances between the mean temperature, $\overline{T}_m$, of the air in the duct and the temperature of the ambient air and the surroundings.

(d) Substitute numerical values into the expression of part (c) and calculate the air outlet temperature, $T_{m,o}$. Estimate the corresponding value of $\overline{T}_s$. Comment on your results and the assumptions inherent in your model.

9.48 A highly polished aluminum plate of length 0.5 m and width 0.2 m is subjected to an airstream at a temperature of 23°C and a velocity of 10 m/s. Because of upstream conditions, the flow is turbulent over the entire length of the plate. A series of segmented, independently controlled heaters is attached to the lower side of the plate to maintain approximately isothermal conditions over the entire plate. The electrical heater covering the section between the positions $x_1 = 0.2$ m and $x_2 = 0.3$ m is shown in the schematic.



(a) Estimate the electrical power that must be supplied to the designated heater segment to maintain the plate surface temperature at $T_s = 47°C$.

(b) If the blower that maintains the airstream velocity over the plate malfunctions, but the power to the heaters remains constant, estimate the surface temperature of the designated segment. Assume that the ambient air is extensive, quiescent, and at 23°C.

9.49 The average free convection coefficient for the exterior surfaces of a long, horizontal rectangular duct exposed to a quiescent fluid can be estimated from the Hahn–Didion (H–D) correlation [ASHRAE Proceedings, Part 1, pp. 262–67, 1972]

$$\overline{Nu}_P = 0.55\text{Ra}_P^{1/4}\left(\frac{H}{P}\right)^{1/8} \qquad \text{Ra}_P \le 10^7$$

where the characteristic length is the half-perimeter, $P = (w + H)$, and w and H are the horizontal width and vertical height, respectively, of the duct. The thermophysical properties are evaluated at the film temperature.

(a) Consider a horizontal 0.15-m-square duct with a surface temperature of 35°C in ambient air at 15°C. Calculate the average convection coefficient and the heat rate per unit length using the H–D correlation.

(b) Calculate the average convection coefficient and the heat rate per unit length considering the duct as formed by vertical plates (sides) and horizontal plates (top and bottom). Do you expect this estimate to be lower or higher than that obtained with the H–D correlation? Explain the difference, if any.

(c) Using an appropriate correlation, calculate the average convection coefficient and the heat rate per unit

length for a
perimeter eq
tangular duc
mate to be l
the H–D cor

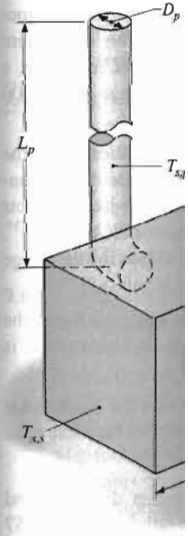
9.50 It is desired to es
straight fin of re
a surface operati
the surroundings
is to be fabric
with an anodize
and 100 mm long

(a) Considering
face and est
cient, determ

(b) Estimate th
the influen
surrounding

(c) Using a n
difference
ness. The f
modes shou
age, values

9.51 Certain wood s
transfer by radia
roundings. Cons
sure, $L_s = 1$ m
walls of the stov
at an operating t



Patent Owner Manufacturing Resources International, Inc.
Exhibit 2017 - Page 612 of 999

length for a duct of circular cross section having a perimeter equal to the wetted perimeter of the rectangular duct of part (a). Do you expect this estimate to be lower or higher than that obtained with the H–D correlation? Explain the difference, if any.

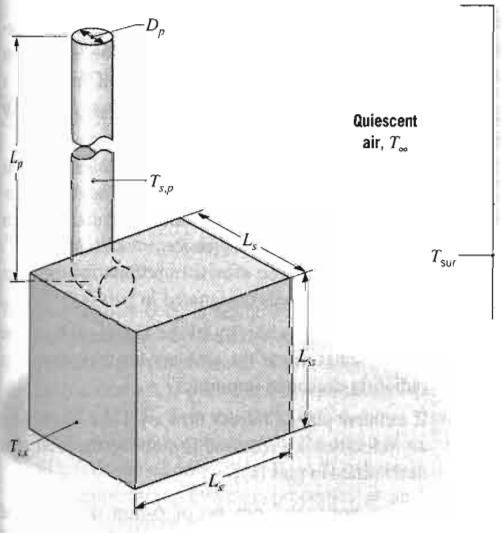
9.50 It is desired to estimate the effectiveness of a horizontal, straight fin of rectangular cross section when applied to a surface operating at 45°C in an environment for which the surroundings and ambient air are at 25°C. The fin is to be fabricated from aluminum alloy (2024-T6) with an anodized finish ($\varepsilon = 0.82$) and is 2 mm thick and 100 mm long.

(a) Considering only free convection from the fin surface and estimating an average heat transfer coefficient, determine the effectiveness of the fin.

(b) Estimate the effectiveness of the fin, including the influence of radiation exchange with the surroundings.

(c) Using a numerical method, develop the finite-difference equations and obtain the fin effectiveness. The free convection and radiation exchange modes should be based on local, rather than average, values for the fin.

9.51 Certain wood stove designs rely exclusively on heat transfer by radiation and natural convection to the surroundings. Consider a stove that forms a cubical enclosure, $L_s = 1$ m on a side, in a large room. The exterior walls of the stove have an emissivity of $\varepsilon = 0.8$ and are at an operating temperature of $T_{s,s} = 500$ K.



The stove pipe, which may be assumed to be isothermal at an operating temperature of $T_{s,p} = 400$ K, has a diameter of $D_p = 0.25$ m and a height of $L_p = 2$ m, extending from stove to ceiling. The stove is in a large room whose air and walls are at $T_\infty = T_{sur} = 300$ K. Neglecting heat transfer from the small horizontal section of the pipe and radiation exchange between the pipe and stove, estimate the rate at which heat is transferred from the stove and pipe to the surroundings.

9.52 A plate 1 m by 1 m, inclined at an angle of 45°, is exposed to a net radiation heat flux of 300 W/m^2 at its bottom surface. If the top surface of the plate is well insulated, estimate the temperature the plate reaches when the ambient air is quiescent and at a temperature of 0°C.

Horizontal Cylinders and Spheres

9.53 A horizontal rod 5 mm in diameter is immersed in water maintained at 18°C. If the rod surface temperature is 56°C, estimate the free convection heat transfer rate per unit length of the rod.

9.54 A horizontal uninsulated steam pipe passes through a large room whose walls and ambient air are at 300 K. The pipe of 150-mm diameter has an emissivity of 0.85 and an outer surface temperature of 400 K. Calculate the heat loss per unit length from the pipe.

9.55 Examine the conditions of Example 9.4, including the effect of adding insulation of thickness t, thermal conductivity $k = 0.026$ W/m · K, and emissivity $\varepsilon = 0.85$. Compute and plot the surface temperature $T_{s,2}$ and the heat loss q' as a function of insulation thickness for $0 \leq t \leq 50$ mm. In addition to adding insulation, the heat loss may be reduced by decreasing the surface emissivity of the insulation. For $t = 25$ mm compute and plot $T_{s,2}$ and q' as a function of the emissivity for $0.1 \leq \varepsilon \leq 1.0$.

9.56 Beverage in cans 150 mm long and 60 mm in diameter is initially at 27°C and is to be cooled by placement in a refrigerator compartment at 4°C. In the interest of maximizing the cooling rate, should the cans be laid horizontally or vertically in the compartment? As a first approximation, neglect heat transfer from the ends.

9.57 Consider Problem 8.47. A more realistic solution would account for the resistance to heat transfer due to free convection in the paraffin during melting. Assuming the tube surface to have a uniform temperature of 55°C and the paraffin to be an infinite, quiescent liquid, determine the convection coefficient associated with the outer surface. Using this result and recognizing that the tube surface temperature is not known, determine the water outlet temperature, the total heat transfer rate, and the

Patent Owner Manufacturing Resources International, Inc.
Exhibit 2017 - Page 613 of 999

time required to completely liquefy the paraffin, for the prescribed conditions. Thermophysical properties associated with the liquid state of the paraffin are $k = 0.15$ W/m · K, $\beta = 8 \times 10^{-4}$ K^{-1}, $\rho = 770$ kg/m^3, $\nu = 5 \times 10^{-6}$ m^2/s, and $\alpha = 8.85 \times 10^{-8}$ m^2/s.

9.58 A long, uninsulated steam line with a diameter of 89 mm and a surface emissivity of 0.8 transports steam at 200°C and is exposed to atmospheric air and large surroundings at an equivalent temperature of 20°C.

(a) Calculate the heat loss per unit length for a calm day.

(b) Calculate the heat loss on a breezy day when the wind speed is 8 m/s.

(c) For the conditions of part (a), calculate the heat loss with a 20-mm-thick layer of insulation ($k = 0.08$ W/m · K). Would the heat loss change significantly with an appreciable wind speed?

9.59 A horizontal tube of 12.5-mm diameter with an outer surface temperature of 240°C is located in a room with an air temperature of 20°C. Estimate the heat transfer rate per unit length of the tube due to free convection.

9.60 Saturated steam at 4 bars absolute pressure with a mean velocity of 3 m/s flows through a horizontal pipe whose inner and outer diameters are 55 and 65 mm, respectively. The heat transfer coefficient for the steam flow is known to be 11,000 W/m^2 · K.

(a) If the pipe is covered with a 25-mm-thick layer of 85% magnesia insulation and is exposed to atmospheric air at 25°C, determine the rate of heat transfer by free convection to the room per unit length of the pipe. If the steam is saturated at the inlet of the pipe, estimate its quality at the outlet of a pipe 30 m long.

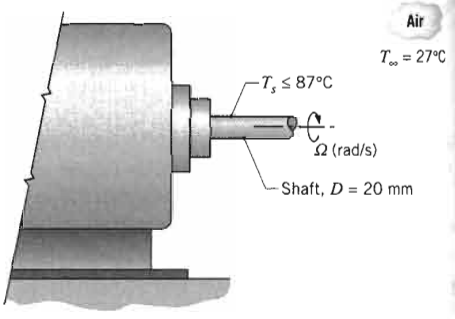
(b) Net radiation to the surroundings also contributes to heat loss from the pipe. If the insulation has a surface emissivity of $\varepsilon = 0.8$ and the surroundings are at $T_{sur} = T_\infty = 25$°C, what is the rate of heat transfer to the room per unit length of pipe? What is the quality of the outlet flow?

(c) The heat loss may be reduced by increasing the insulation thickness and/or reducing its emissivity. What is the effect of increasing the insulation thickness to 50 mm if $\varepsilon = 0.8$? Of decreasing the emissivity to 0.2 if the insulation thickness is 25 mm? Of reducing the emissivity to 0.2 and increasing the insulation thickness to 50 mm?

9.61 A horizontal electrical cable of 25-mm diameter has a heat dissipation rate of 30 W/m. If the ambient air temperature is 27°C, estimate the surface temperature of the cable.

9.62 An electric immersion heater, 10 mm in diameter and 300 mm long, is rated at 550 W. If the heater is horizontally positioned in a large tank of water at 20°C, estimate its surface temperature. Estimate the surface temperature if the heater is accidentally operated in air at 20°C.

9.63 The maximum surface temperature of the 20-mm-diameter shaft of a motor operating in ambient air at 27°C should not exceed 87°C. Because of power dissipation within the motor housing, it is desirable to reject as much heat as possible through the shaft to the ambient air. In this problem, we will investigate several methods for heat removal.



(a) For horizontal rotating cylinders, a suitable correlation for estimating the convection coefficient is of the form

$$\overline{Nu}_D = 0.133 Re_D^{2/3} Pr^{1/3}$$
$$(Re_D < 4.3 \times 10^5, \quad 0.7 < Pr < 670)$$

where $Re_D \equiv \Omega D^2/\nu$ and Ω is the rotational velocity (rad/s). Determine the convection coefficient and the maximum heat rate per unit length as a function of rotational speed in the range from 5000 to 15,000 rpm.

(b) Estimate the free convection coefficient and the maximum heat rate per unit length for the stationary shaft. Mixed free and forced convection effects may become significant for $Re_D < 4.7(Gr_D^3/Pr)^{0.137}$. Are free convection effects important for the range of rotational speeds designated in part (a)?

(c) Assuming the emissivity of the shaft is 0.8 and the surroundings are at the ambient air temperature, is radiation exchange important?

(d) If ambient air is in cross flow over the shaft, what air velocities are required to remove the heat rates determined in part (a)?

9.64 Consider a horizontal pin fin of 6-mm diameter and 60-mm length fabricated from plain carbon steel ($k = 57$

W/m · K, $\varepsilon = 0.$
150°C, while th
roundings are at

(a) Estimate th
surface tem
convection
coefficient.
choice of th

(b) Use the fi
obtain q_f w
cients are b
peratures fo
with the ana

9.65 Consider the ho
conditions for w
over the pipe an
the effect of ra
0.6, what is the
per unit length c

9.66 Common practi
clad pipe insulat
The functions o
tion and to redu
roundings. Bec
chlorine or seas
which is initially
time. Typically
0.12 at installati
300-mm-diamet
perature is 90°C
degradation of t
heat loss from t
roundings and a
(b) a cross-wind

9.67 Consider the el
blower were to
the heater conti
perature would
take to come w
for radiation ex
the duct walls,

9.68 A computer coo
mm-diameter,
ambient air ter
convection whil
at $T_\infty = 27$°C.
80°C, derive an
as a function of
sor temperature
film temperatur
tion has on the c

Patent Owner Manufacturing Resources International, Inc.
Exhibit 2017 - Page 614 of 999

W/m · K, $\varepsilon = 0.5$). The base of the fin is maintained at 150°C, while the quiescent ambient air and the surroundings are at 25°C. Assume the fin tip is adiabatic.

(a) Estimate the fin heat rate, q_f. Use an average fin surface temperature of 125°C in estimating the free convection coefficient and the linearized radiation coefficient. How sensitive is this estimate to your choice of the average fin surface temperature?

(b) Use the finite-difference method of solution to obtain q_f when the convection and radiation coefficients are based on local, rather than average, temperatures for the fin. How does your result compare with the analytical solution of part (a)?

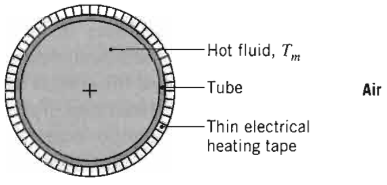
9.65 Consider the hot water pipe of Problem 7.56, but under conditions for which the ambient air is not in cross flow over the pipe and is, instead, quiescent. Accounting for the effect of radiation with a pipe emissivity of $\varepsilon_p = 0.6$, what is the corresponding daily cost of heat loss per unit length of the uninsulated pipe?

9.66 Common practice in chemical processing plants is to clad pipe insulation with a durable, thick aluminum foil. The functions of the foil are to confine the batt insulation and to reduce heat transfer by radiation to the surroundings. Because of the presence of chlorine (at chlorine or seaside plants), the aluminum foil surface, which is initially bright, becomes etched with in-service time. Typically, the emissivity might change from 0.12 at installation to 0.36 with extended service. For a 300-mm-diameter foil-covered pipe whose surface temperature is 90°C, will this increase in emissivity due to degradation of the foil finish have a significant effect on heat loss from the pipe? Consider two cases with surroundings and ambient air at 25°C: (a) quiescent air and (b) a cross-wind velocity of 10 m/s.

9.67 Consider the electrical heater of Problem 7.43. If the blower were to malfunction, terminating airflow while the heater continued to operate at 1000 W/m, what temperature would the heater assume? How long would it take to come within 10°C of this temperature? Allow for radiation exchange between the heater ($\varepsilon = 0.8$) and the duct walls, which are also at 27°C.

9.68 A computer code is being developed to analyze a 12.5-mm-diameter, cylindrical sensor used to determine ambient air temperature. The sensor experiences free convection while positioned horizontally in quiescent air at $T_\infty = 27$°C. For the temperature range from 30 to 80°C, derive an expression for the convection coefficient as a function of only $\Delta T = T_s - T_\infty$, where T_s is the sensor temperature. Evaluate properties at an appropriate film temperature and show what effect this approximation has on the convection coefficient estimate.

9.69 A thin-walled tube of 20-mm diameter passes hot fluid at a mean temperature of 45°C in an experimental flow loop. The tube is mounted horizontally in quiescent air at a temperature of 15°C. To satisfy the stringent temperature control requirements of the experiment, it was decided to wind thin electrical heating tape on the outer surface of the tube to prevent heat loss from the hot fluid to the ambient air.



(a) Neglecting radiation heat loss, calculate the heat flux q_e'' that must be supplied by the electrical tape to ensure a uniform fluid temperature.

(b) Assuming the emissivity of the tape is 0.95 and the surroundings are also at 15°C, calculate the required heat flux.

(c) The heat loss may be reduced by wrapping the heating tape in a layer of insulation. For 85% magnesia insulation ($k = 0.050$ W/m · K) having a surface emissivity of $\varepsilon = 0.60$, compute and plot the required heat flux q_e'' as a function of insulation thickness in the range from 0 to 20 mm. For this range, compute and plot the convection and radiation heat rates per unit tube length as a function of insulation thickness.

9.70 A billet of stainless steel, AISI 316, with a diameter of 150 mm and a length of 500 mm emerges from a heat treatment process at 200°C and is placed in an unstirred oil bath maintained at 20°C.

(a) Determine whether it is advisable to position the billet in the bath with its centerline horizontal or vertical in order to decrease the cooling time.

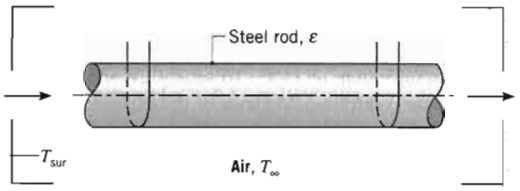
(b) Estimate the time for the billet to cool to 30°C for the preferred arrangement.

9.71 Long stainless steel rods of 50-mm diameter are preheated to a uniform temperature of 1000 K before being suspended from an overhead conveyor for transport to a hot forming operation. The conveyor is in a large room whose walls and air are at 300 K.

(a) Assuming the linear motion of the rod to have a negligible effect on convection heat transfer from its surface, determine the average convection coefficient at the start of the transport process.

(b) If the surface emissivity of the rod is $\varepsilon = 0.40$, what is the effective radiation heat transfer coefficient at the start of the transport process?

Patent Owner Manufacturing Resources International, Inc.
Exhibit 2017 - Page 615 of 999



(c) Assuming a constant cumulative (radiation plus convection) heat transfer coefficient corresponding to the results of parts (a) and (b), what is the maximum allowable conveyor transit time, if the centerline temperature of the rod must exceed 900 K for the forming operation? Properties of the steel are $k = 25$ W/m · K and $\alpha = 5.2 \times 10^{-6}$ m²/s.

(d) Heat transfer by convection and radiation are actually decreasing during the transfer operation. Accounting for this reduction, reconsider the conditions of part (c) and obtain a more accurate estimate of the maximum allowable conveyor transit time.

9.72 Hot air flows from a furnace through a 0.15-m-diameter, thin-walled steel duct with a velocity of 3 m/s. The duct passes through the crawlspace of a house, and its uninsulated exterior surface is exposed to quiescent air and surroundings at 0°C.

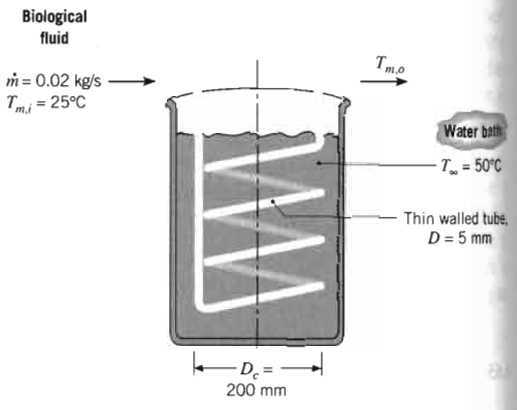
(a) At a location in the duct for which the mean air temperature is 70°C, determine the heat loss per unit duct length and the duct wall temperature. The duct outer surface has an emissivity of 0.5.

(b) If the duct is wrapped with a 25-mm-thick layer of 85% magnesia insulation ($k = 0.050$ W/m · K) having a surface emissivity of $\varepsilon = 0.60$, what are the duct wall temperature, the outer surface temperature, and the heat loss per unit length?

9.73 A biological fluid moves at a flow rate of $\dot{m} = 0.02$ kg/s through a coiled, thin-walled, 5-mm-diameter tube submerged in a large water bath maintained at 50°C. The fluid enters the tube at 25°C.

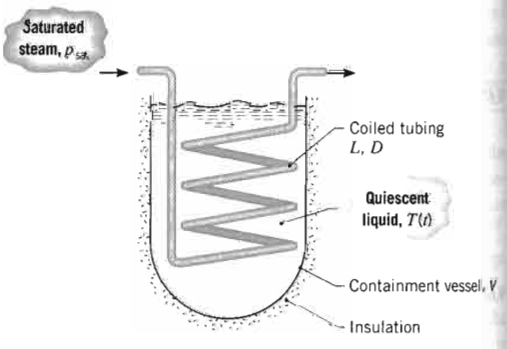
(a) Estimate the length of the tube and the number of coil turns required to provide an exit temperature of $T_{m,o} = 38$°C for the biological fluid. Assume that the water bath is an extensive, quiescent medium, that the coiled tube approximates a horizontal tube, and that the biological fluid has the thermophysical properties of water.

(b) The flow rate through the tube is controlled by a pump that experiences throughput variations of approximately ±10% at any one setting. This condition is of concern to the project engineer because the



corresponding variation of the exit temperature of the biological fluid could influence the downstream process. What variation would you expect in $T_{m,o}$ for a ±10% change in $\dot{m}$?

9.74 Consider a batch process in which 200 liters of a pharmaceutical are heated from 25°C to 70°C by saturated steam condensing at 2.455 bars as it flows through a coiled tube of 15-mm diameter and 15-m length. At any time during the process, the liquid may be approximated as an infinite, quiescent medium of uniform temperature and may be assumed to have constant properties of $\rho = 1100$ kg/m³, $c = 2000$ J/kg · K, $k = 0.25$ W/m · K, $\nu = 4.0 \times 10^{-6}$ m²/s, $Pr = 10$, and $\beta = 0.002$ K⁻¹. The thermal resistances of the condensing steam and tube wall may be neglected.



(a) What is the initial rate of heat transfer to the pharmaceutical?

(b) Neglecting heat transfer between the tank and its surroundings, how long does it take to heat the pharmaceutical to 70°C? Plot the corresponding variation with time of the fluid temperature and the

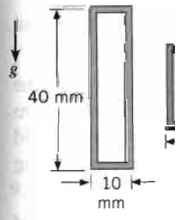
convectio
tube. How
heating pr

9.75 In the analytic
sectional area,
transfer coeffi
fin. Consider
and 50-mm le
conditions for
27°C, and ε =

(a) Estimate
coefficien
exchange
temperatu

(b) Use a nur
foregoing
radiation
than aver

9.76 A hot fluid at
horizontally p
of the tube sh
would you us
ambient air by



Use the follo
Mass Transf
laminar conv
on which the
the surface,

The characte
fluid in the
Compare this
test its utility.

9.77 Consider a 2
at 300 K and

(a) If the flui
sive, sho
from the
Hint: Be
resistanc

Patent Owner Manufacturing Resources International, Inc.
Exhibit 2017 - Page 616 of 999

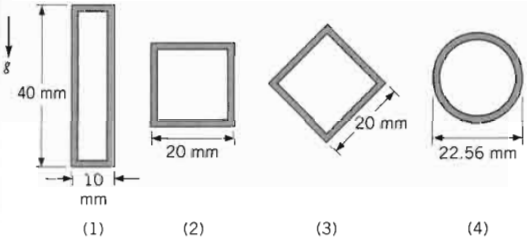
convection coefficient at the outer surface of the tube. How much steam is condensed during the heating process?

9.75 In the analytical treatment of the fin with uniform cross-sectional area, it was assumed that the convection heat transfer coefficient is constant along the length of the fin. Consider an AISI 316 steel fin of 6-mm diameter and 50-mm length (with insulated tip) operating under conditions for which $T_b = 125°C$, $T_\infty = 27°C$, $T_{sur} = 27°C$, and $\varepsilon = 0.6$.

(a) Estimate average values of the fin heat transfer coefficients for free convection (h_c) and radiation exchange (h_r). Use these values to predict the tip temperature and fin effectiveness.

(b) Use a numerical method of solution to estimate the foregoing parameters when the convection and radiation coefficients are based on local, rather than average, values for the fin.

9.76 A hot fluid at 35°C is to be transported through a tube horizontally positioned in quiescent air at 25°C. Which of the tube shapes, each of equal cross-sectional area, would you use in order to minimize heat losses to the ambient air by free convection?



Use the following correlation of Lienhard (*Int. J. Heat Mass Transfer,* **16,** 2121, 1973) to approximate the laminar convection coefficient for an immersed body on which the boundary layer does not separate from the surface,

$$\overline{Nu}_l = 0.52 Ra_l^{1/4}$$

The characteristic length l is the length of travel of the fluid in the boundary layer across the shape surface. Compare this correlation to that given for a sphere to test its utility.

9.77 Consider a 2-mm-diameter sphere immersed in a fluid at 300 K and 1 atm.

(a) If the fluid around the sphere is quiescent and extensive, show that the conduction limit of heat transfer from the sphere can be expressed as $Nu_{D,\,cond} = 2$. *Hint:* Begin with the expression for the thermal resistance of a hollow sphere, Equation 3.36, letting $r_2 \to \infty$, and then expressing the result in terms of the Nusselt number.

(b) Considering free convection, at what surface temperature will the Nusselt number be twice that for the conduction limit? Consider air and water as the fluids.

(c) Considering forced convection, at what velocity will the Nusselt number be twice that for the conduction limit? Consider air and water as the fluids.

9.78 A sphere of 25-mm diameter contains an embedded electrical heater. Calculate the power required to maintain the surface temperature at 94°C when the sphere is exposed to a quiescent medium at 20°C for: (a) air at atmospheric pressure, (b) water, and (c) ethylene glycol.

9.79 Under steady-state operation the surface temperature of a small 20-W incandescent light bulb is 125°C when the temperature of the room air and walls is 25°C. Approximating the bulb as a sphere 40 mm in diameter with a surface emissivity of 0.8, what is the rate of heat transfer from the surface of the bulb to the surroundings?

9.80 A 25-mm-diameter copper sphere with a low emissivity coating is removed from an oven at a uniform temperature of 85°C and allowed to cool in a quiescent fluid maintained at 25°C.

(a) Calculate convection coefficients associated with the initial condition for immersion in air and water.

(b) Using two different approaches, estimate the time for the sphere to reach 30°C when immersed in air and water. In the simpler, but more approximate, approach, use an average convection coefficient based on the average temperature of the sphere during the cooling process. In the more accurate method, treat the convection coefficient as a variable and numerically integrate the energy balance equation.

Parallel Plate Channels

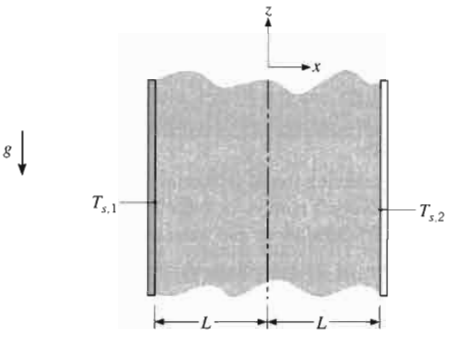
9.81 Consider two long vertical plates maintained at uniform temperatures $T_{s,1} > T_{s,2}$. The plates are open at their ends and are separated by the distance $2L$.

(a) Sketch the velocity distribution in the space between the plates.

(b) Write appropriate forms of the continuity, momentum, and energy equations for laminar flow between the plates.

(c) Evaluate the temperature distribution, and express your result in terms of the mean temperature, $T_m = (T_{s,1} + T_{s,2})/2$.

Patent Owner Manufacturing Resources International, Inc.
Exhibit 2017 - Page 617 of 999

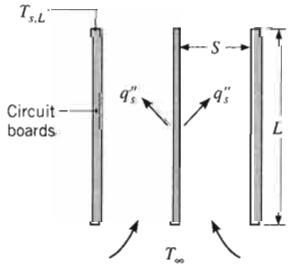


(d) Estimate the vertical pressure gradient by assuming the density to be a constant ρ_m corresponding to T_m. Substituting from the Boussinesq approximation, obtain the resulting form of the momentum equation.

(e) Determine the velocity distribution.

9.82 Consider the conditions of Problem 9.9, but now view the problem as one involving free convection between vertical, parallel plate channels. What is the optimum fin spacing S? For this spacing and the prescribed values of t and W, what is the rate of heat transfer from the fins?

9.83 A vertical array of circuit boards is immersed in quiescent ambient air at $T_\infty = 17°C$. Although the components protrude from their substrates, it is reasonable, as a first approximation, to assume *flat* plates with uniform surface heat flux q_s''. Consider boards of length and width $L = W = 0.4$ m and spacing $S = 25$ mm. If the maximum allowable board temperature is 77°C, what is the maximum allowable power dissipation per board?

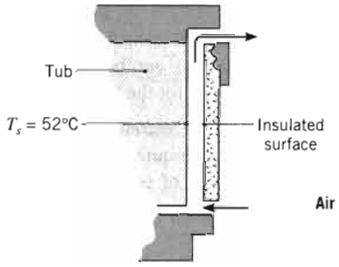


9.84 Determined to reduce the $3 per week cost associated with heat loss through their patio window by convection and radiation, the tenants of Problem 9.18 cover the inside of the window with a 50-mm-thick sheet of extruded insulation. Because they are not very handy around the house, the insulation is installed poorly, resulting in a $S = 5$ mm gap between the extruded insulation and the window pane, allowing the room air to infiltrate into the space between the pane and the insulation.

(a) Determine the window heat loss and associated weekly cost with the ill-fitting insulation in place. The insulation will significantly reduce the radiation losses through the window. Losses will be due almost entirely to convection.

(b) Plot the heat loss through the patio window as a function of the gap spacing for 1 mm $\leq S \leq$ 20 mm.

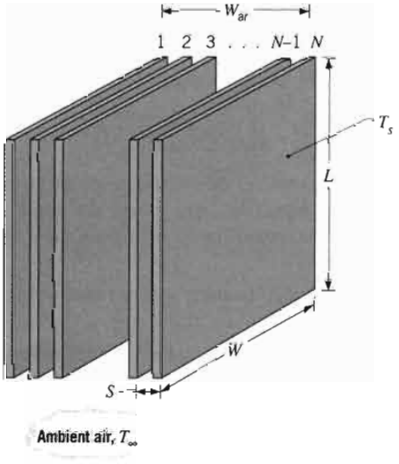
9.85 The front door of a dishwasher of width 580 mm has a vertical air vent that is 500 mm in height with a 20-mm spacing between the inner tub operating at 52°C and an outer plate that is thermally insulated.



(a) Determine the heat loss from the tub surface when the ambient air is 27°C.

(b) A change in the design of the door provides the opportunity to increase or decrease the 20-mm spacing by 10 mm. What recommendations would you offer with regard to how the change in spacing will alter heat losses?

9.86 A natural convection air heater consists of an array of parallel, equally spaced vertical plates, which may be



maintained a
electrical hea
$L = W = 300$
air at $T_\infty = 2$
exceed a valu
For T_s =
maximizes he
ing, how mar
the correspon

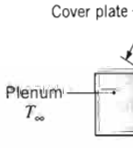
9.87 A bank of dryi
with an ambie
ovens are 500
the ovens is 15



(a) Estimate
oven wh

(b) Explore
At what
Describe
tion. Car
side of a

9.88 A solar collec
is connected
and to a heat
$\theta = 30°$ from
plate. Solar
plate and the

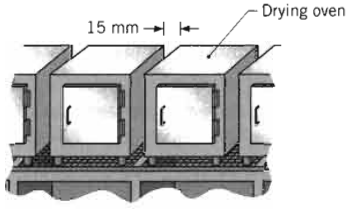


Patent Owner Manufacturing Resources International, Inc.
Exhibit 2017 - Page 618 of 999

maintained at a fixed temperature T_s by embedded electrical heaters. The plates are of length and width $L = W = 300$ mm and are in quiescent, atmospheric air at $T_\infty = 20°C$. The total width of the array cannot exceed a value of $W_{ar} = 150$ mm.

For $T_s = 75°C$, what is the plate spacing S that maximizes heat transfer from the array? For this spacing, how many plates comprise the array and what is the corresponding rate of heat transfer from the array?

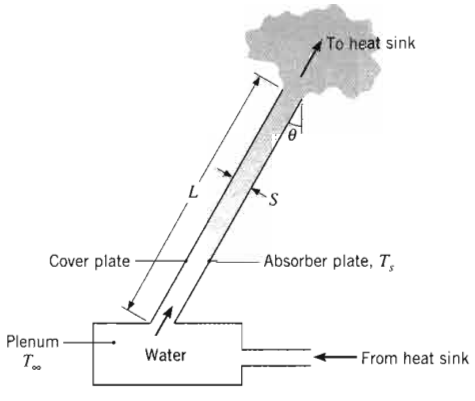
9.87 A bank of drying ovens is mounted on a rack in a room with an ambient air temperature of 27°C. The cubical ovens are 500 mm to a side, and the spacing between the ovens is 15 mm.



(a) Estimate the heat loss from a facing side of an oven when its surface temperature is 47°C.

(b) Explore the effect of the spacing on the heat loss. At what spacing is the heat loss a maximum? Describe the boundary layer behavior for this condition. Can this condition be analyzed by treating the side of an oven as an isolated vertical plate?

9.88 A solar collector consists of a parallel plate channel that is connected to a water storage plenum at the bottom and to a heat sink at the top. The channel is inclined $\theta = 30°$ from the vertical and has a transparent cover plate. Solar radiation transmitted through the cover plate and the water maintains the isothermal absorber plate at a temperature $T_s = 67°C$, while water returned to the reservoir from the heat sink is at $T_\infty = 27°C$. The system operates as a *thermosyphon,* for which water flow is driven exclusively by buoyancy forces. The plate spacing and length are $S = 15$ mm and $L = 1.5$ m.



Assuming the cover plate to be adiabatic with respect to convection heat transfer to or from the water, estimate the rate of heat transfer per unit width normal to the flow direction (W/m) from the absorber plate to the water.

Rectangular Cavities

9.89 As is evident from the property data of Tables A.3 and A.4, the thermal conductivity of glass at room temperature is more than 50 times larger than that of air. It is therefore desirable to use windows of double-pane construction, for which the two panes of glass enclose an air space. If heat transfer across the air space is by conduction, the corresponding thermal resistance may be increased by increasing the thickness L of the space. However, there are limits to the efficacy of such a measure, since convection currents are induced if L exceeds a critical value, beyond which the thermal resistance decreases.

Consider atmospheric air enclosed by vertical panes at temperatures of $T_1 = 22°C$ and $T_2 = -20°C$. If the critical Rayleigh number for the onset of convection is $Ra_L \approx 2000$, what is the maximum allowable spacing for conduction across the air? How is this spacing affected by the temperatures of the panes? How is it affected by the pressure of the air, as, for example, by partial evacuation of the space?

9.90 A building window pane that is 1.2 m high and 0.8 m wide is separated from the ambient air by a storm window of the same height and width. The air space between the two windows is 0.06 m thick. If the building and storm windows are at 20 and −10°C, respectively, what is the rate of heat loss by free convection across the air space?

9.91 The absorber plate and the adjoining cover plate of a flat-plate solar collector are at 70 and 35°C, respectively, and are separated by an air space of 0.05 m. What is the rate of free convection heat transfer per unit surface area between the two plates if they are inclined at an angle of 60° from the horizontal?

9.92 Consider a thermal storage system in which the phase change material (paraffin) is housed in a large container whose bottom, horizontal surface is maintained at $T_s = 50°C$ by warm water delivered from a solar collector.

(a) Neglecting the change in sensible energy of the liquid phase, estimate the amount of paraffin that is melted over a five-hour period beginning with an

Patent Owner Manufacturing Resources International, Inc.
Exhibit 2017 - Page 619 of 999

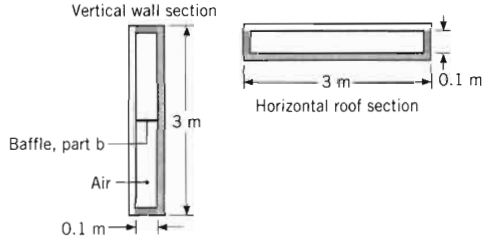
initial liquid layer at the bottom of the container of thickness $s_i = 10$ mm. The paraffin of Problems 8.47 and 9.57 is used as the phase change material and is initially at the phase change temperature, $T_{mp} = 27.4°C$. The bottom surface area of the container is $A = 2.5\ m^2$.

(b) Compare the amount of energy needed to melt the paraffin to the amount of energy required to increase the temperature of the same amount of liquid from the phase change temperature to the average liquid temperature, $(T_s + T_{mp})/2$.

(c) Neglecting the change in sensible energy of the liquid phase, estimate the amount of paraffin that would melt over a five-hour time period if the hot plate is placed at the top of the container and $s_i = 10$ mm.

9.93 A rectangular cavity consists of two parallel, 0.5-m-square plates separated by a distance of 50 mm, with the lateral boundaries insulated. The heated plate is maintained at 325 K and the cooled plate at 275 K. Estimate the heat flux between the surfaces for three orientations of the cavity using the notation of Figure 9.6: vertical with $\tau = 90°$, horizontal with $\tau = 0°$, and horizontal with $\tau = 180°$.

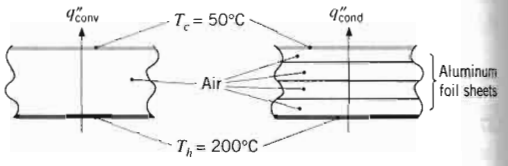
9.94 Consider a horizontal flat roof section having the same dimensions as a vertical wall section. For both sections, the surfaces exposed to the air gap are at 18°C (inside) and −10°C (outside).



(a) Estimate the ratio of the convection heat rate for the horizontal section to that of the vertical section.

(b) What effect will inserting a baffle at the mid-height of the vertical section have on the convection heat rate for that section?

9.95 A 50-mm-thick air gap separates two horizontal metal plates that form the top surface of an industrial furnace. The bottom plate is at $T_h = 200°C$ and the top plate is at $T_c = 50°C$. The plant operator wishes to provide insulation between the plates to minimize heat loss. The relatively hot temperatures preclude use of foamed or felt insulation materials. Evacuated insulation materials cannot be used due to the harsh industrial environment and their expense. A young engineer suggests that equally spaced, extremely thin horizontal sheets of aluminum foil may be inserted in the gap to eliminate natural convection and minimize heat loss through the air gap.



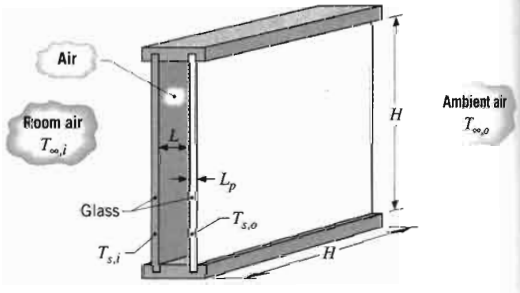
(a) Determine the convective heat flux across the gap when no insulation is in place.

(b) Determine the minimum number of foil sheets that must be inserted in the gap to eliminate free convection.

(c) Determine the conduction heat flux across the air gap with the foil sheets in place.

9.96 The space between the panes of a double-glazed window can be filled with either air or carbon dioxide at atmospheric pressure. The window is 1.5 m high and the spacing between the panes can be varied. Develop an analysis to predict the convection heat transfer rate across the window as a function of pane spacing and determine, under otherwise identical conditions, whether air or carbon dioxide will yield the smaller rate. Illustrate the results of your analysis for two conditions: winter (−10°C, 20°C) and summer (35°C, 25°C).

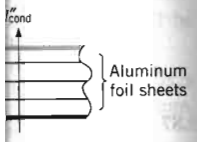
9.97 A vertical, double-pane window, which is 1 m on a side and has a 25-mm gap filled with atmospheric air, separates quiescent room air at $T_{\infty,i} = 20°C$ from quiescent ambient air at $T_{\infty,o} = -20°C$. Radiation exchange between the window panes, as well as between each pane and its surroundings, may be neglected.



(a) Neglecting the thermal resistance associated with conduction heat transfer across each pane, determine the corresponding temperature of each pane and the rate of heat transfer through the window.

Patent Owner Manufacturing Resources International, Inc.
Exhibit 2017 - Page 620 of 999

suggests that equally
sheets of aluminum
eliminate natural con-
ough the air gap.



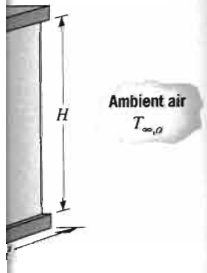
at flux across the gap
e.

umber of foil sheets
gap to eliminate free

eat flux across the air
ace.

double-glazed window
rbon dioxide at atmo-
s 1.5 m high and the
be varied. Develop an
ion heat transfer rate
of pane spacing and
cal conditions, whether
the smaller rate. Illus-
or two conditions: win-
5°C, 25°C).

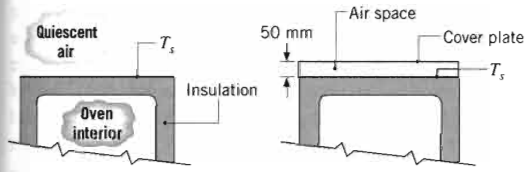
which is 1 m on a side
atmospheric air, sepa-
= 20°C from quiescent
Radiation exchange
well as between each
e neglected.



istance associated with
ross each pane, deter-
nperature of each pane
through the window.

(b) Comment on the validity of neglecting the conduction resistance of the panes if each is of thickness $L_p = 6$ mm.

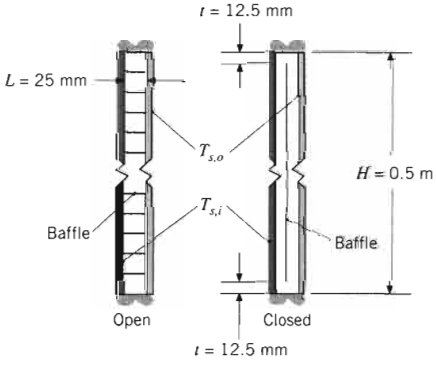
9.98 The top surface (0.5 m × 0.5 m) of an oven is 60°C for a particular operating condition when the room air is 23°C. To reduce heat loss from the oven and to minimize burn hazard, it is proposed to create a 50-mm air space by adding a cover plate.



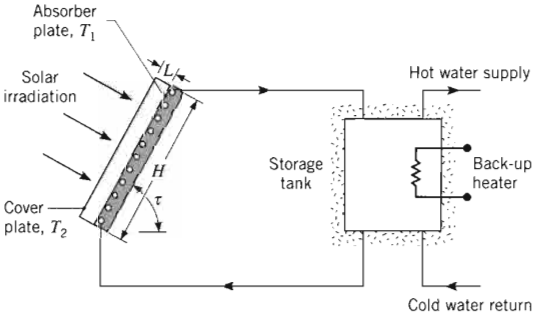
(a) Assuming the same oven surface temperature T_s for both situations, estimate the reduction in the convection heat loss resulting from installation of the cover plate. What is the temperature of the cover plate?

(b) Explore the effect of the cover plate spacing on the convection heat loss and the cover plate temperature for spacings in the range $5 \leq L \leq 50$ mm. Is there an optimum spacing?

9.99 Consider window blinds that are installed in the air space between the two panes of a vertical double-pane window. The window is $H = 0.5$ m high and $w = 0.5$ m wide, and includes $N = 19$ individual blinds that are each $L = 25$ mm wide. When the blinds are open, 20 smaller, square enclosures are formed along the height of the window. In the closed position, the blinds form a nearly continuous sheet with two $t = 12.5$ mm open gaps at the top and bottom of the enclosure. Determine the convection heat transfer rate between the inner pane, which is held at $T_{s,i} = 20$°C, and the outer pane, which is at $T_{s,o} = -20$°C, when the blinds are in the open and closed positions, respectively. Explain why the closed blinds have little effect on the convection heat transfer rate across the cavity.



9.100 A solar water heater consists of a flat-plate collector that is coupled to a storage tank. The collector consists of a transparent cover plate and an absorber plate that are separated by an air gap.



Although much of the solar energy collected by the absorber plate is transferred to a working fluid passing through a coiled tube brazed to the back of the absorber, some of the energy is lost by free convection and net radiation transfer across the air gap. In Chapter 13, we will evaluate the contribution of radiation exchange to this loss. For now, we restrict our attention to the free convection effect.

(a) Consider a collector that is inclined at an angle of $\tau = 60°$ and has dimensions of $H = w = 2$ m on a side, with an air gap of $L = 30$ mm. If the absorber and cover plates are at $T_1 = 70$°C and $T_2 = 30$°C, respectively, what is the rate of heat transfer by free convection from the absorber plate?

(b) The heat loss by free convection depends on the spacing between the plates. Compute and plot the heat loss as a function of spacing for $5 \leq L \leq 50$ mm. Is there an optimum spacing?

Concentric Cylinders and Spheres

9.101 Consider the cylindrical, 0.12-m-diameter radiation shield of Example 9.5 that is installed concentric with a 0.10-m-diameter tube carrying steam. The spacing provides an air gap of $L = 10$ mm.

(a) Calculate the heat loss per unit length of the tube by convection when a second shield of 0.14-m diameter is installed, with the second shield maintained at 35°C. Compare the result to that for the single shield of the example.

(b) In the two-shield configuration of part (a), the air gaps formed by the annular concentric tubes are $L = 10$ mm. Calculate the heat loss per unit length if the gap dimension is $L = 15$ mm. Do you expect the heat loss to increase or decrease?

Patent Owner Manufacturing Resources International, Inc.
Exhibit 2017 - Page 621 of 999

9.102 A solar collector design consists of an inner tube enclosed concentrically in an outer tube that is transparent to solar radiation. The tubes are thin walled with inner and outer diameters of 0.10 and 0.15 m, respectively. The annular space between the tubes is completely enclosed and filled with air at atmospheric pressure. Under operating conditions for which the inner and outer tube surface temperatures are 70 and 30°C, respectively, what is the convective heat loss per meter of tube length across the air space?

9.103 It has been proposed to use large banks of rechargeable, lithium ion batteries to power hybrid electric vehicles. The cylindrical batteries, each of which is of radius r_i = 9 mm and length L = 65 mm, undergo exothermic electrochemical reactions while being discharged. Since excessively high temperatures damage the batteries, it is proposed to encase them in a phase change material that melts when the batteries discharge (and resolidifies when the batteries are charged; charging is associated with an endothermic electrochemical reaction). Consider the paraffin of Problems 8.47 and 9.57.

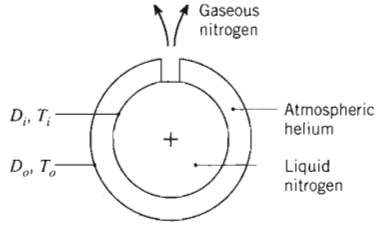
(a) At an instant in time during the discharge of a battery, liquid paraffin occupies an annular region of outer radius r_o = 19 mm around the battery, which is generating $\dot{E}_g$ = 1 W of thermal energy. Determine the surface temperature of the battery.

(b) At the time of interest in part (a), what is the rate at which the liquid annulus radius is increasing?

(c) Graph the battery surface temperature versus the outer radius of the liquid-filled annulus. Explain the relative insensitivity of the battery surface temperature to the size of the annulus for 15 mm ≤ $r_o \leq$ 30 mm.

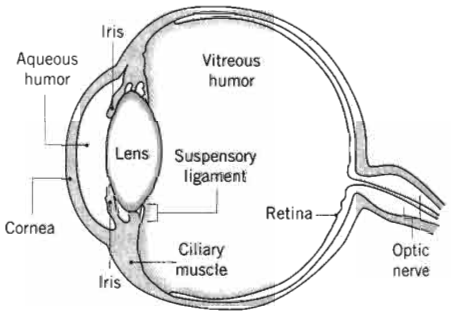
9.104 The surfaces of two long, horizontal, concentric thin-walled tubes having radii of 100 and 125 mm are maintained at 300 and 400 K, respectively. If the annular space is pressurized with nitrogen at 5 atm, estimate the convection heat transfer rate per unit length of the tubes.

9.105 Liquid nitrogen is stored in a thin-walled spherical vessel of diameter D_i = 1 m. The vessel is positioned concentrically within a larger, thin-walled spherical container of diameter D_o = 1.10 m, and the intervening cavity is filled with atmospheric helium.



Under normal operating conditions, the inner and outer surface temperatures are T_i = 77 K and T_o = 283 K. If the latent heat of vaporization of nitrogen is 2 × 10^5 J/kg, what is the mass rate $\dot{m}$ (kg/s) at which gaseous nitrogen is vented from the system?

9.106 The human eye contains aqueous humor, which separates the external cornea and the internal iris–lens structure. It is hypothesized that, in some individuals, small flakes of pigment are intermittently liberated from the iris and migrate to, and subsequently damage, the cornea. Approximating the geometry of the enclosure formed by the cornea and iris–lens structure as a pair of concentric hemispheres of outer radius r_o = 10 mm and inner radius r_i = 7 mm, respectively, investigate whether free convection can occur in the aqueous humor by evaluating the effective thermal conductivity ratio, k_{eff}/k. If free convection can occur, it is possible that the damaging particles are advected from the iris to the cornea. The iris–lens structure is at the core temperature, T_i = 37°C, while the cornea temperature is measured to be T_o = 34°C. The properties of the aqueous humor are ρ = 990 kg/m^3, k = 0.58 W/m · K, c_p = 4.2 × 10^3 J/kg · K, μ = 7.1 × 10^{-4} N · s/m^2, and β = 3.2 × 10^{-4} K^{-1}.



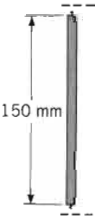
Mixed Convection

9.107 Water at 35°C with a velocity of 0.05 m/s flows over a horizontal, 50-mm-diameter cylinder maintained at a uniform surface temperature of 20°C. Do you anticipate that heat transfer by free convection will be significant? What would be the situation if the fluid were air at atmospheric pressure?

9.108 According to experimental results for parallel airflow over a uniform temperature, heated vertical plate, the effect of free convection on the heat transfer convection coefficient will be 5% when Gr_L/Re_L^2 = 0.08. Consider a heated vertical plate 0.3 m long, maintained at a surface temperature of 60°C in atmospheric air at 25°C. What is the minimum vertical velocity

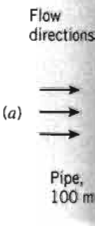
required of
effects will be

9.109 A vertical arra
be air cooled
exceed 60°C v



Assuming isc
the allowable
for the cooling
(a) Free conv
(b) Airflow w
(c) Airflow w
(d) Airflow w
5 m/s.

9.110 A horizontal 1(
be used in th
Based on a typ
pipe is 0.5 m/s
temperature at

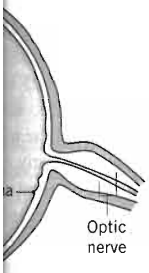


Investigate th
rate (W/m) f
(c) upward flo

Patent Owner Manufacturing Resources International, Inc.
Exhibit 2017 - Page 622 of 999

tions, the inner and
T_i = 77 K and T_o =
orization of nitrogen
ass rate $\dot{m}$ (kg/s) at
d from the system?

humor, which sepa-
nternal iris–lens struc-
me individuals, small
dly liberated from the
quently damage, the
etry of the enclosure
s structure as a pair of
adius r_o = 10 mm and
ly, investigate whether
queous humor by eval-
uctivity ratio, k_{eff}/k. If
ssible that the damag-
iris to the cornea. The
mperature, T_i = 37°C,
measured to be T_o =
us humor are ρ = 990
= 4.2 × 10³ J/kg · K,
3.2 × 10⁻⁴ K⁻¹.

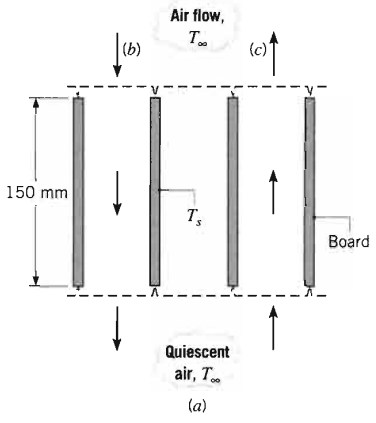


0.05 m/s flows over a
nder maintained at a
0°C. Do you anticipate
ion will be significant?
the fluid were air at

lts for parallel airflow
ated vertical plate, the
heat transfer convec-
when Gr_L/Re_L^2 = 0.08.
te 0.3 m long, main-
f 60°C in atmospheric
num vertical velocity

required of the airflow such that free convection effects will be less than 5% of the heat transfer rate?

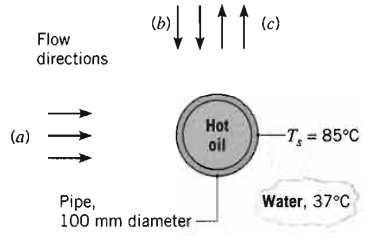
9.109 A vertical array of circuit boards of 150-mm height is to be air cooled such that the board temperature does not exceed 60°C when the ambient temperature is 25°C.



Assuming isothermal surface conditions, determine the allowable electrical power dissipation per board for the cooling arrangements:

(a) Free convection only (no forced airflow).
(b) Airflow with a downward velocity of 0.6 m/s.
(c) Airflow with an upward velocity of 0.3 m/s.
(d) Airflow with a velocity (upward or downward) of 5 m/s.

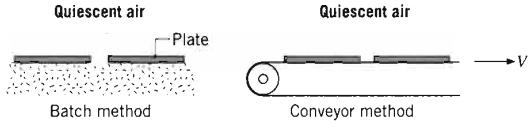
9.110 A horizontal 100-mm-diameter pipe passing hot oil is to be used in the design of an industrial water heater. Based on a typical water draw rate, the velocity over the pipe is 0.5 m/s. The hot oil maintains the outer surface temperature at 85°C and the water temperature is 37°C.



Investigate the effect of flow direction on the heat rate (W/m) for (a) horizontal, (b) downward, and (c) upward flow.

9.111 Determine the heat transfer rate from the steel plates of Problem 7.24 accounting for free convection from the plate surfaces. What is the corresponding rate of change of the plate temperature? Plot the heat transfer coefficient associated with free convection, forced convection, and mixed convection for air velocities ranging from $2 \leq u_\infty \leq 10$ m/s. The velocity of the plate is small compared to the air velocity.

9.112 Square panels (250 mm × 250 mm) with a decorative, highly reflective plastic finish are cured in an oven at 125°C and cooled in quiescent air at 29°C. Quality considerations dictate that the panels remain horizontal and that the cooling rate be controlled. To increase productivity in the plant, it is proposed to replace the batch cooling method with a conveyor system having a velocity of 0.5 m/s.



Compare the initial (immediately after leaving the oven) convection heat transfer rates for the two methods.

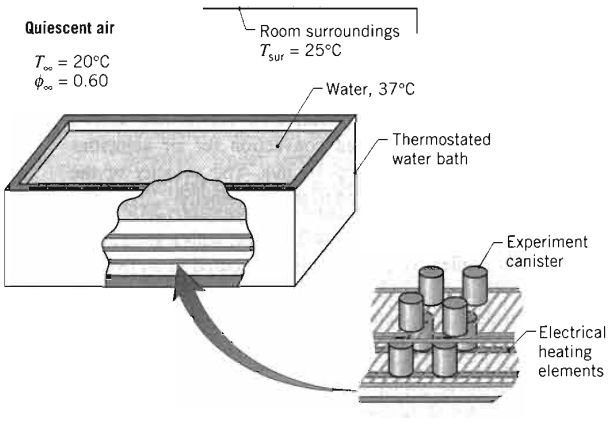
Mass Transfer

9.113 A garment soaked with water is hung up to dry in a warm room at atmospheric pressure. The still air is dry and at a temperature of 40°C. The garment may be assumed to have a temperature of 25°C and a characteristic length of 1 m in the vertical direction. Estimate the drying rate per unit width of the garment.

9.114 A water bath is used to maintain canisters containing experimental biological reactions at a uniform temperature of 37°C. The top of the bath has a width and length of 0.25 m and 0.50 m, respectively, and is uncovered to allow easy access for removal or insertion of the canisters. The bath is located in a draft-free laboratory with air at atmospheric pressure, a temperature of 20°C, and a relative humidity of 60%. The walls of the laboratory are at a uniform temperature of 25°C.

(a) Estimate the heat loss from the surface of the bath by radiation exchange with the surroundings.
(b) Calculate the Grashof number using Equation 9.65, which can be applied to natural convection flows driven by temperature and concentration gradients. Use a characteristic length L that is appropriate for the exposed surface of the water bath.
(c) Estimate the free convection heat transfer coefficient using the result for Gr_L obtained in part (b).

Patent Owner Manufacturing Resources International, Inc.
Exhibit 2017 - Page 623 of 999



(d) Invoke the heat and mass transfer analogy and use an appropriate correlation to estimate the mass transfer coefficient using Gr_L. Calculate the water evaporation rate on a daily basis and the heat loss by evaporation.

(e) Calculate the total heat loss from the surface, and compare the relative contributions of the sensible, latent, and radiative effects. Review the assumptions made in your analysis, especially those relating to the heat and mass transfer analogy.

9.115 On a very still morning, the surface temperature of a lake used to cool the condenser of a power plant is 30°C while the air temperature is 23°C with a relative humidity of 80%. Assume a surroundings temperature of 285 K. The lake is nominally circular in shape with a diameter of approximately 4 km. Determine the heat loss from the surface of the lake by radiation, free convection, and evaporation. This heat loss determines the capacity of the lake to cool the condenser. Justify why the heat transfer correlation you select is useful, even though Ra_L is outside of its specified range. *Hint:* See Problem 9.114.

9.116 Fuel cells similar to the PEM cell of Example 1.4 operate with a mixture of liquid water and methanol instead of hydrogen; the anode is placed in direct contact with the liquid fuel. Oxygen (species A) is delivered to the exposed cathode by free convection. Hence, no fans or pumps are needed to operate the device. The power output of *passive, direct methanol fuel cells* (DMFCs) can become *mass transfer limited*, since the electric current produced by the DMFC is related to the rate at which oxygen is consumed at the cathode by the expression $I = 4n_A\mathcal{F}\mathcal{M}_A$, where $\mathcal{F}$ is Faraday's constant, $\mathcal{F} = 96489$ coulombs/mol. Consider a passive DMFC with a 120 mm × 120 mm membrane. Determine the maximum possible electric current produced by the DMFC when the oxygen mass fraction at the cathode is $m_{A,s} = 0.10$ for cases where the cathode is facing up or is vertical. As a first approximation and to illustrate the sensitivity of the device to its orientation relative to the vertical direction, assume buoyancy forces are dominated by the difference in density associated with the change in the oxygen mass fraction between the cathode surface and the quiescent environment, which is atmospheric air at $T_\infty = 25$°C. Assume the quiescent air is composed of nitrogen and oxygen, with an oxygen mass fraction $m_{A,\infty} = 0.233$.

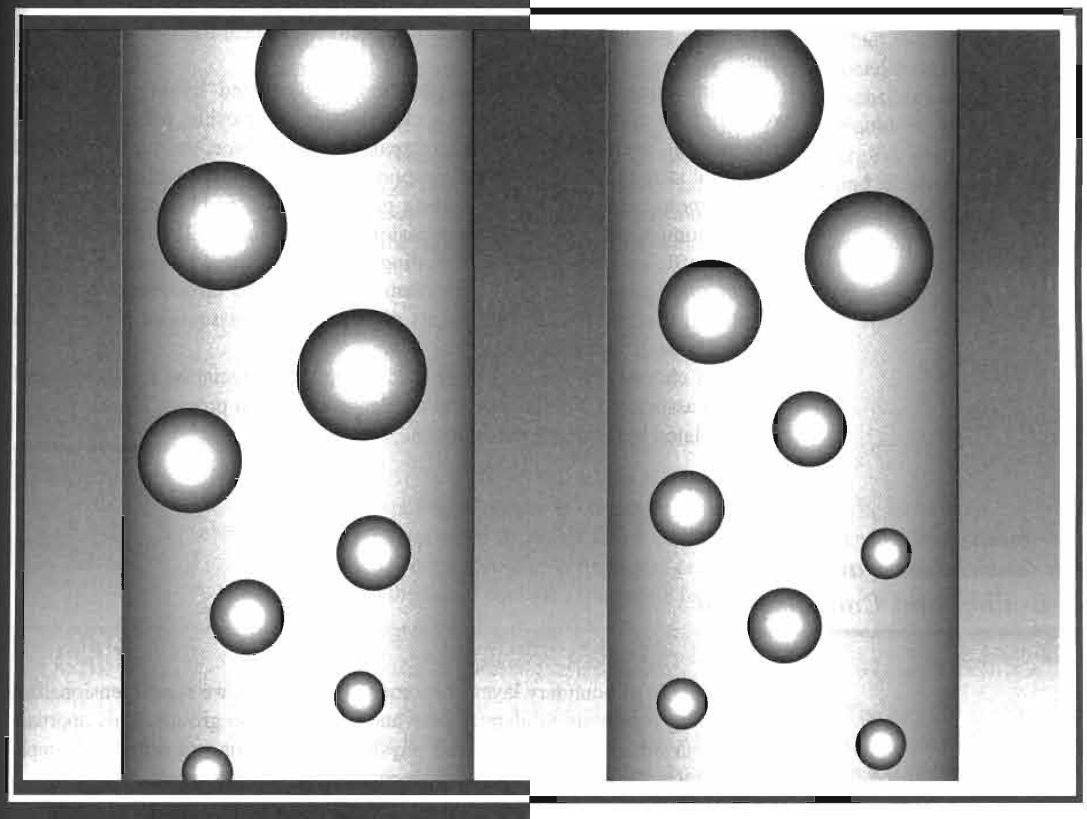
Patent Owner Manufacturing Resources International, Inc.
Exhibit 2017 - Page 624 of 999

m. Determine the heat
by radiation, free con-
eat loss determines the
ondenser. Justify why
select is useful, even
cified range. *Hint:* See

l of Example 1.4 oper-
r and methanol instead
l in direct contact with
A) is delivered to the
ion. Hence, no fans or
ne device. The power
ol fuel cells (DMFCs)
ted, since the electric
is related to the rate at
the cathode by the
$\mathcal{F}$ is Faraday's con-
. Consider a passive
nm membrane. Deter-
ctric current produced
mass fraction at the
where the cathode is
approximation and to
vice to its orientation
n, assume buoyancy
rence in density asso-
oxygen mass fraction
the quiescent environ-
t $T_\infty = 25°C$. Assume
nitrogen and oxygen,
$_\infty = 0.233$.

CHAPTER **10**

Boiling and Condensation



Patent Owner Manufacturing Resources International, Inc.
Exhibit 2017 - Page 625 of 999

In this chapter we focus on convection processes associated with the change in phase of a fluid. In particular, we consider processes that can occur at a solid–liquid or solid–vapor interface, namely, *boiling* and *condensation*. For these cases *latent* heat effects associated with the phase change are significant. The change from the liquid to the vapor state due to boiling is sustained by heat transfer from the solid surface; conversely, condensation of a vapor to the liquid state results in heat transfer to the solid surface.

Since they involve fluid motion, boiling and condensation are classified as forms of the convection mode of heat transfer. However, they are characterized by unique features. Because there is a phase change, heat transfer to or from the fluid can occur without influencing the fluid temperature. In fact, through boiling or condensation, large heat transfer rates may be achieved with small temperature differences. In addition to the *latent heat* h_{fg}, two other parameters are important in characterizing the processes, namely, the *surface tension* σ at the liquid–vapor interface and the *density difference* between the two phases. This difference induces a *buoyancy force*, which is proportional to $g(\rho_l - \rho_v)$. Because of combined latent heat and buoyancy-driven flow effects, boiling and condensation heat transfer coefficients and rates are generally much larger than those characteristic of convection heat transfer without phase change.

Many engineering applications that are characterized by high heat fluxes involve boiling and condensation. In a closed-loop power cycle, pressurized liquid is converted to vapor in a *boiler*. After expansion in a turbine, the vapor is restored to its liquid state in a *condenser*, whereupon it is pumped to the boiler to repeat the cycle. *Evaporators*, in which the boiling process occurs, and condensers are also essential components in vapor-compression refrigeration cycles. The high heat transfer coefficients associated with boiling make it attractive to consider for purposes of managing the thermal performance of advanced electronics equipment. The rational design of such components dictates that the associated phase change processes be well understood.

In this chapter our objectives are to develop an appreciation for the physical conditions associated with boiling and condensation and to provide a basis for performing related heat transfer calculations.

10.1 *Dimensionless Parameters in Boiling and Condensation*

In our treatment of boundary layer phenomena (Chapter 6), we nondimensionalized the governing equations to identify relevant dimensionless groups. This approach enhanced our understanding of related physical mechanisms and suggested simplified procedures for generalizing and representing heat transfer results.

Since it is difficult to develop governing equations for boiling and condensation processes, the appropriate dimensionless parameters can be obtained by using the Buckingham pi theorem [1]. For either process, the convection coefficient could depend on the difference between the surface and saturation temperatures,

10.2 *Boiling Mod*

Patent Owner Manufacturing Resources International, Inc.
Exhibit 2017 - Page 626 of 999

$\Delta T = |T_s - T_{sat}|$, the body force arising from the liquid–vapor density difference, $g(\rho_l - \rho_v)$, the latent heat h_{fg}, the surface tension σ, a characteristic length L, and the thermophysical properties of the liquid or vapor: ρ, c_p, k, μ. That is,

$$h = h\,[\Delta T, g(\rho_l - \rho_v), h_{fg}, \sigma, L, \rho, c_p, k, \mu] \tag{10.1}$$

Since there are 10 variables in 5 dimensions (m, kg, s, J, K), there are $(10 - 5) = 5$ pi-groups, which can be expressed in the following forms:

$$\frac{hL}{k} = f\left[\frac{\rho g(\rho_l - \rho_v)L^3}{\mu^2}, \frac{c_p\,\Delta T}{h_{fg}}, \frac{\mu c_p}{k}, \frac{g(\rho_l - \rho_v)L^2}{\sigma}\right] \tag{10.2a}$$

or, defining the dimensionless groups,

$$Nu_L = f\left[\frac{\rho g\,(\rho_l - \rho_v)L^3}{\mu^2}, Ja, Pr, Bo\right] \tag{10.2b}$$

The Nusselt and Prandtl numbers are familiar from our earlier single-phase convection analyses. The new dimensionless parameters are the Jakob number *Ja*, the Bond number *Bo*, and a nameless parameter that bears a strong resemblance to the Grashof number (see Equation 9.12 and recall that $\beta\Delta T \approx \Delta\rho/\rho$). This unnamed parameter represents the effect of buoyancy-induced fluid motion on heat transfer. The Jakob number is the ratio of the maximum sensible energy absorbed by the liquid (vapor) to the latent energy absorbed by the liquid (vapor) during condensation (boiling). In many applications, the sensible energy is much less than the latent energy and *Ja* has a small numerical value. The Bond number is the ratio of the buoyancy force to the surface tension force. In subsequent sections, we will delineate the role of these parameters in boiling and condensation.

10.2 *Boiling Modes*

When evaporation occurs at a solid–liquid interface, it is termed *boiling*. The process occurs when the temperature of the surface T_s exceeds the saturation temperature T_{sat} corresponding to the liquid pressure. Heat is transferred from the solid surface to the liquid, and the appropriate form of Newton's law of cooling is

$$q_s'' = h(T_s - T_{sat}) = h\,\Delta T_e \tag{10.3}$$

where $\Delta T_e \equiv T_s - T_{sat}$ is termed the *excess temperature*. The process is characterized by the formation of vapor bubbles, which grow and subsequently detach from the surface. Vapor bubble growth and dynamics depend, in a complicated manner, on the excess temperature, the nature of the surface, and thermophysical properties of the fluid, such as its surface tension. In turn, the dynamics of vapor bubble formation affect liquid motion near the surface and therefore strongly influence the heat transfer coefficient.

Patent Owner Manufacturing Resources International, Inc.
Exhibit 2017 - Page 627 of 999

Boiling may occur under various conditions. For example, in *pool boiling* the liquid is quiescent and its motion near the surface is due to free convection and to mixing induced by bubble growth and detachment. In contrast, for *forced convection boiling,* fluid motion is induced by external means, as well as by free convection and bubble-induced mixing. Boiling may also be classified according to whether it is *subcooled* or *saturated.* In subcooled boiling, the temperature of the liquid is below the saturation temperature and bubbles formed at the surface may condense in the liquid. In contrast, the temperature of the liquid slightly exceeds the saturation temperature in *saturated boiling.* Bubbles formed at the surface are then propelled through the liquid by buoyancy forces, eventually escaping from a free surface.

10.3 *Pool Boiling*

Saturated pool boiling, as shown in Figure 10.1, has been studied extensively. Although there is a sharp increase in the liquid temperature close to the solid surface, the temperature through most of the liquid remains slightly above saturation. Bubbles generated at the liquid–solid interface therefore rise to and are transported across the liquid–vapor interface. An appreciation for the underlying physical mechanisms may be obtained by examining the *boiling curve.*

10.3.1 The Boiling Curve

Nukiyama [2] was the first to identify different regimes of pool boiling using the apparatus of Figure 10.2. The heat flux from a horizontal *nichrome* wire to saturated water was determined by measuring the current flow I and potential drop E. The wire temperature was determined from knowledge of the manner in which its electrical resistance varied with temperature. This arrangement is termed *power-controlled* heating, wherein the wire temperature T_s (hence the excess temperature ΔT_e) is the dependent variable and the power setting (hence the heat flux q_s'') is the independent variable. Following the arrows of the *heating curve* of Figure 10.3, it is evident that as power is applied, the heat flux increases, at first slowly and then very rapidly, with excess temperature.

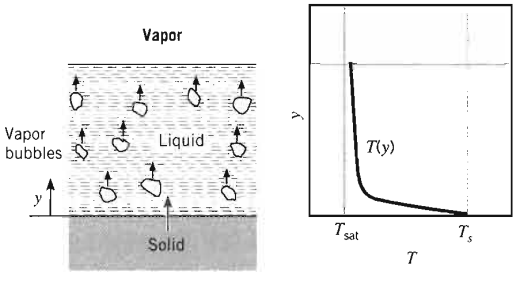


FIGURE 10.1
Temperature distribution in saturated pool boiling with a liquid–vapor interface.

Patent Owner Manufacturing Resources International, Inc.
Exhibit 2017 - Page 628 of 999

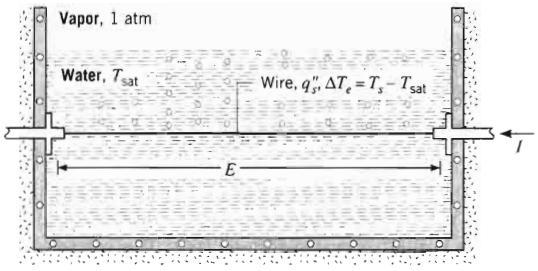


FIGURE 10.2 Nukiyama's power-controlled heating apparatus for demonstrating the boiling curve.

Nukiyama observed that boiling, as evidenced by the presence of bubbles, did not begin until $\Delta T_e \approx 5°C$. With further increase in power, the heat flux increased to very high levels until *suddenly,* for a value slightly larger than q''_{max}, the wire temperature jumped to the melting point and burnout occurred. However, repeating the experiment with a *platinum* wire having a higher melting point (2045 K vs. 1500 K), Nukiyama was able to maintain heat fluxes above q''_{max} without burnout. When he subsequently reduced the power, the variation of ΔT_e with q_s'' followed the *cooling curve* of Figure 10.3. When the heat flux reached the minimum point q''_{min}, a further decrease in power caused the excess temperature to drop abruptly, and the process followed the original heating curve back to the saturation point.

Nukiyama believed that the hysteresis effect of Figure 10.3 was a consequence of the power-controlled method of heating, where ΔT_e is a dependent variable. He also believed that by using a heating process permitting the independent control of ΔT_e, the missing (dashed) portion of the curve could be obtained. His conjecture was subsequently confirmed by Drew and Mueller [3]. By condensing steam inside a tube at different pressures, they were able to control the value of ΔT_e for boiling of

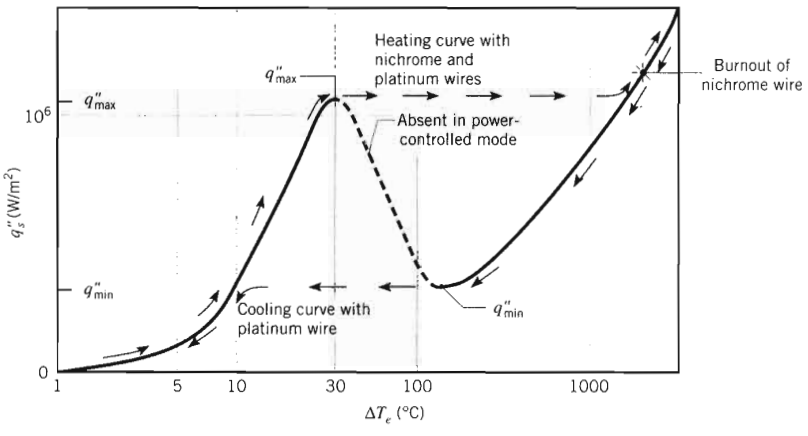


FIGURE 10.3 Nukiyama's boiling curve for saturated water at atmospheric pressure.

Patent Owner Manufacturing Resources International, Inc.
Exhibit 2017 - Page 629 of 999

a low boiling point organic fluid at the tube outer surface and thereby obtain the missing portion of the boiling curve.

10.3.2 Modes of Pool Boiling

An appreciation for the underlying physical mechanisms may be obtained by examining the different modes, or regimes, of pool boiling. These regimes are identified in the boiling curve of Figure 10.4. The specific curve pertains to water at 1 atm, although similar trends characterize the behavior of other fluids. From Equation 10.3 we note that q_s'' depends on the convection coefficient h, as well as on the excess temperature ΔT_e. Different boiling regimes may be delineated according to the value of ΔT_e.

Free Convection Boiling Free convection boiling is said to exist if $\Delta T_e \leq \Delta T_{e,A}$, where $\Delta T_{e,A} \approx 5°C$. The surface temperature must be somewhat above the saturation temperature in order to sustain bubble formation. As the excess temperature is increased, bubble inception will eventually occur, but below point A (referred to as

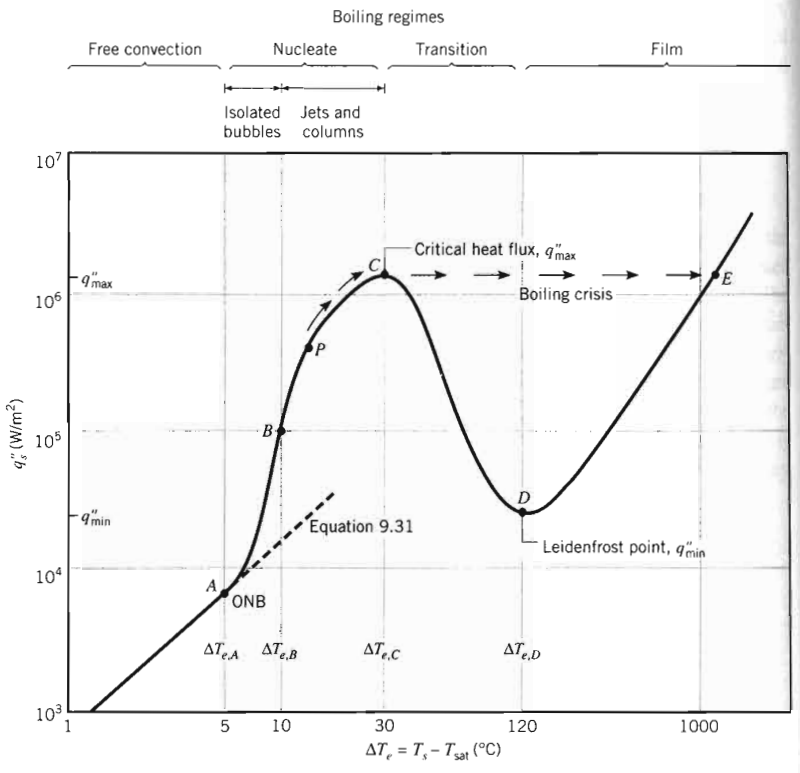


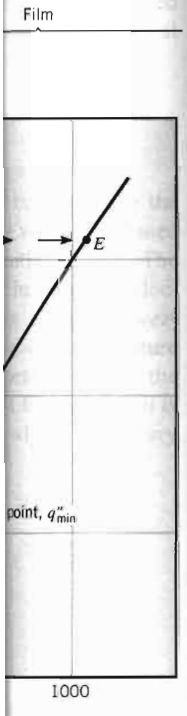
FIGURE 10.4 Typical boiling curve for water at 1 atm: surface heat flux q_s'' as a function of excess temperature, $\Delta T_e \equiv T_s - T_{sat}$.

Patent Owner Manufacturing Resources International, Inc.
Exhibit 2017 - Page 630 of 999

thereby obtain the

obtained by exam-
imes are identified
to water at 1 atm,
ds. From Equation
as well as on the
eated according to

to exist if $\Delta T_e \leq$
what above the sat-
excess temperature
int A (referred to as



q''_s as a

the *onset of nucleate boiling,* ONB), fluid motion is determined principally by free convection effects. According to whether the flow is laminar or turbulent, h varies as ΔT_e to the $\frac{1}{4}$ or $\frac{1}{3}$ power, respectively, in which case q''_s varies as ΔT_e to the $\frac{5}{4}$ or $\frac{4}{3}$ power. For a large horizontal plate, the fluid flow is turbulent and Equation 9.31 can be used to predict the free convection portion of the boiling curve, as shown in Figure 10.4.

Nucleate Boiling Nucleate boiling exists in the range $\Delta T_{e,A} \leq \Delta T_e \leq \Delta T_{e,C}$, where $\Delta T_{e,C} \approx 30°C$. In this range, two different flow regimes may be distinguished. In region *A–B, isolated bubbles* form at nucleation sites and separate from the surface, as illustrated in Figure 10.2. This separation induces considerable fluid mixing near the surface, substantially increasing h and q''_s. In this regime most of the heat exchange is through direct transfer from the surface to liquid in motion at the surface, and not through the vapor bubbles rising from the surface. As ΔT_e is increased beyond $\Delta T_{e,B}$, more nucleation sites become active and increased bubble formation causes bubble interference and coalescence. In the region *B–C*, the vapor escapes as *jets* or *columns,* which subsequently merge into slugs of the vapor. This condition is illustrated in Figure 10.5*a*. Interference between the densely populated bubbles inhibits the motion of liquid near the surface. Point *P* of Figure 10.4 corresponds to an inflection in the boiling curve at which the heat transfer coefficient is a maximum. At this point h begins to decrease with increasing ΔT_e, although q''_s, which is the product of h and ΔT_e, continues to increase. This trend results because, for $\Delta T_e > \Delta T_{e,P}$, the relative increase in ΔT_e exceeds the relative reduction in h. At point *C*, however, further increase in ΔT_e is balanced by the reduction in h. The maximum heat flux, $q''_{s,C} = q''_{max}$, is usually termed the *critical heat flux,* and in water at atmospheric pressure it exceeds 1 MW/m^2. At the point of this maximum, considerable vapor is being formed, making it difficult for liquid to continuously wet the surface.

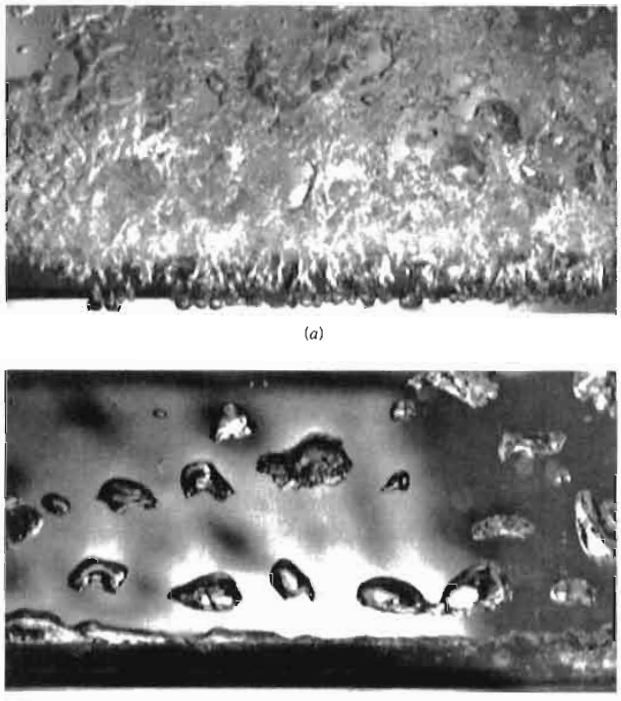
Because high heat transfer rates and convection coefficients are associated with small values of the excess temperature, it is desirable to operate many engineering devices in the nucleate boiling regime. The approximate magnitude of the convection coefficient may be inferred by using Equation 10.3 with the boiling curve of Figure 10.4. Dividing q''_s by ΔT_e, it is evident that convection coefficients in excess of 10^4 W/m$^2 \cdot$ K are characteristic of this regime. These values are considerably larger than those normally corresponding to convection with no phase change.

Transition Boiling The region corresponding to $\Delta T_{e,C} \leq \Delta T_e \leq \Delta T_{e,D}$, where $\Delta T_{e,D} \approx 120°C$, is termed *transition boiling, unstable film boiling,* or *partial film boiling.* Bubble formation is now so rapid that a vapor film or blanket begins to form on the surface. At any point on the surface, conditions may oscillate between film and nucleate boiling, but the fraction of the total surface covered by the film increases with increasing ΔT_e. Because the thermal conductivity of the vapor is much less than that of the liquid, h (and q''_s) must decrease with increasing ΔT_e.

Film Boiling Film boiling exists for $\Delta T_e \geq \Delta T_{e,D}$. At point *D* of the boiling curve, referred to as the *Leidenfrost point,* the heat flux is a minimum, $q''_{s,D} = q''_{min}$, and the surface is completely covered by a *vapor blanket.* Heat transfer from the surface to the liquid occurs by conduction and radiation through the vapor. It was Leidenfrost who in 1756 observed that water droplets supported by the vapor film

Patent Owner Manufacturing Resources International, Inc.
Exhibit 2017 - Page 631 of 999

10.4 *Pool Boiling*



(*a*)

(*b*)

FIGURE 10.5 Boiling of methanol on a horizontal tube. (*a*) Nucleate boiling in the jets and columns regime. (*b*) Film boiling. Photographs courtesy of Professor J. W. Westwater, University of Illinois at Champaign-Urbana.

slowly boil away as they move about a hot surface. As the surface temperature is increased, radiation through the vapor film becomes more significant and the heat flux increases with increasing ΔT_e.

Figure 10.5 illustrates the nature of the vapor formation and bubble dynamics associated with nucleate and film boiling. The photographs were obtained for the boiling of methanol on a horizontal tube.

Although the foregoing discussion of the boiling curve assumes that control may be maintained over T_s, it is important to remember the Nukiyama experiment and the many applications that involve controlling q_s'' (e.g., in a nuclear reactor or in an electric resistance heating device). Consider starting at some point P in Figure 10.4 and gradually increasing q_s''. The value of ΔT_e, and hence the value of T_s, will also increase, following the boiling curve to point C. However, any increase in q_s'' beyond this point will induce a sharp departure from the boiling curve in which surface conditions change abruptly from $\Delta T_{e,C}$ to $\Delta T_{e,E} \equiv T_{s,E} - T_{\text{sat}}$. Because $T_{s,E}$ may exceed the melting point of the solid, destruction or failure of the system may occur. For this reason point C is often termed the *burnout point* or the *boiling crisis,* and accurate knowledge of the *critical heat flux* (CHF), $q_{s,C}'' \equiv q_{\max}''$, is important. We may want to operate a heat transfer surface close to this value, but rarely would we want to exceed it.

Patent Owner Manufacturing Resources International, Inc.
Exhibit 2017 - Page 632 of 999

10.4 *Pool Boiling Correlations*

From the shape of the boiling curve and the fact that various physical mechanisms characterize the different regimes, it is no surprise that a multiplicity of heat transfer correlations exist for the boiling process. For the region below $\Delta T_{e,A}$ of the boiling curve (Figure 10.4), appropriate free convection correlations from Chapter 9 can be used to estimate heat transfer coefficients and heat rates. In this section we review some of the more widely used correlations for nucleate and film boiling.

10.4.1 Nucleate Pool Boiling

The analysis of nucleate boiling requires prediction of the number of surface nucleation sites and the rate at which bubbles originate from each site. While mechanisms associated with this boiling regime have been studied extensively, complete and reliable mathematical models have yet to be developed. Yamagata et al. [4] were the first to show the influence of nucleation sites on the heat rate and to demonstrate that q_s'' is approximately proportional to ΔT_e^3. It is desirable to develop correlations that reflect this relationship between the surface heat flux and the excess temperature.

In Section 10.3.2 we noted that within region *A*-*B* of Figure 10.4, most of the heat exchange is due to direct transfer from the heated surface to the liquid. Hence, the boiling phenomena in this region may be thought of as a type of liquid phase forced convection in which the fluid motion is induced by the rising bubbles. We have seen that forced convection correlations are generally of the form

$$\overline{Nu}_L = C_{fc} Re_L^{m_{fc}} Pr^{n_{fc}} \tag{7.1}$$

and Equation 7.1 may provide insight into how pool boiling data can be correlated, provided that a length scale and a characteristic velocity can be identified for inclusion in the Nusselt and Reynolds numbers. The subscript *fc* is added to the constants that appear in Equation 7.1 to remind us that they apply to this *forced convection* expression. As we saw in Chapter 7, these constants are determined experimentally for complicated flows. Because it is postulated that the rising bubbles mix the liquid, an appropriate length scale for relatively large heater surfaces is the bubble diameter, D_b. The diameter of the bubble upon its departure from the heated surface may be determined from a force balance in which the buoyancy force (which promotes bubble departure and is proportional to D_b^3) is equal to the surface tension force (which adheres the bubble to the surface and is proportional to D_b), resulting in the expression

$$D_b \propto \sqrt{\frac{\sigma}{g(\rho_l - \rho_v)}} \tag{10.4a}$$

The constant of proportionality depends on the angle of contact between the liquid, its vapor, and the solid surface; the contact angle depends on the particular liquid and solid surface that is considered. The subscripts l and v denote the saturated liquid and vapor states, respectively and σ (N/m) is the surface tension.

Patent Owner Manufacturing Resources International, Inc.
Exhibit 2017 - Page 633 of 999

A characteristic velocity for the agitation of the liquid may be found by dividing the distance the liquid travels to fill in behind a departing bubble (proportional to D_b) by the time between bubble departures, t_b. The time t_b is equal to the energy it takes to form a vapor bubble (proportional to D_b^3), divided by the rate at which heat is added over the solid–vapor contact area (proportional to D_b^2). Thus,

$$V \propto \frac{D_b}{t_b} \propto \frac{D_b}{\left(\dfrac{\rho_l h_{fg} D_b^3}{q_s'' D_b^2}\right)} \propto \frac{q_s''}{\rho_l h_{fg}} \tag{10.4b}$$

Substituting Equations 10.4a and 10.4b into Equation 7.1, absorbing the proportionalities into the constant C_{fc}, and substituting the resulting expression for h into Equation 10.3 provides the following expression, where the constants $C_{s,f}$ and n are newly introduced and the exponent m_{fc} in Equation 7.1 has an experimentally determined value of 2/3:

$$q_s'' = \mu_l h_{fg} \left[\frac{g(\rho_l - \rho_v)}{\sigma}\right]^{1/2} \left(\frac{c_{p,l}\,\Delta T_e}{C_{s,f} h_{fg} Pr_l^n}\right)^3 \tag{10.5}$$

Equation 10.5 was developed by Rohsenow [5] and is the first and most widely used correlation for nucleate boiling. The coefficient $C_{s,f}$ and the exponent n depend on the solid–liquid combination, and representative experimentally determined values are presented in Table 10.1. Values for other surface–liquid combinations may be obtained from the literature [6–8]. Values of the surface tension and the latent heat of vaporization for water are presented in Table A.6 and for selected fluids in Table A.5. Values for other liquids may be obtained from any recent edition of the

TABLE 10.1 Values of $C_{s,f}$ for various surface–fluid combinations [5–7]

Surface–Fluid Combination	$C_{s,f}$	n
Water–copper		
Scored	0.0068	1.0
Polished	0.0128	1.0
Water–stainless steel		
Chemically etched	0.0133	1.0
Mechanically polished	0.0132	1.0
Ground and polished	0.0080	1.0
Water–brass	0.0060	1.0
Water–nickel	0.006	1.0
Water–platinum	0.0130	1.0
n-Pentane–copper		
Polished	0.0154	1.7
Lapped	0.0049	1.7
Benzene–chromium	0.0101	1.7
Ethyl alcohol–chromium	0.0027	1.7

Patent Owner Manufacturing Resources International, Inc.
Exhibit 2017 - Page 634 of 999

Handbook of Chemistry and Physics. If Equation 10.5 is rewritten in terms of a Nusselt number based on an arbitrary length scale L, it will be in the form $Nu_L \propto Ja^2\, Pr^{1-3n}\, Bo^{1/2}$, with all the properties being for the liquid, except for ρ_v. Comparing with Equation 10.2b, we see that only the first dimensionless parameter does not appear. If the Nusselt number is based on the characteristic bubble diameter given in Equation 10.4a, the expression reduces to the simpler form $Nu_{D_b} \propto Ja^2\, Pr^{1-3n}$.

The Rohsenow correlation applies only for clean surfaces. When it is used to estimate the heat flux, errors can amount to ±100%. However, since $\Delta T_e \propto (q_s'')^{1/3}$, this error is reduced by a factor of 3 when the expression is used to estimate ΔT_e from knowledge of q_s''. Also, since $q_s'' \propto h_{fg}^{-2}$ and h_{fg} decreases with increasing saturation pressure (temperature), the nucleate boiling heat flux will increase as the liquid is pressurized.

10.4.2 Critical Heat Flux for Nucleate Pool Boiling

We recognize that the critical heat flux, $q_{s,C}'' = q_{\max}''$, represents an important point on the boiling curve. We may wish to operate a boiling process close to this point, but we appreciate the danger of dissipating heat in excess of this amount. Kutateladze [9], through dimensional analysis, and Zuber [10], through a hydrodynamic stability analysis, obtained an expression which can be approximated as

$$q_{\max}'' = C h_{fg} \rho_v \left[\frac{\sigma g(\rho_l - \rho_v)}{\rho_v^2} \right]^{1/4} \tag{10.6}$$

which is independent of surface material and is weakly dependent upon the heated surface geometry through the leading constant, C. For large horizontal cylinders, for spheres, and for many large finite heated surfaces, use of a leading constant with the value $C = \pi/24 \approx 0.131$ (the Zuber constant) agrees with experimental data to within 16% [11]. For large horizontal plates, a value of $C = 0.149$ gives better agreement with experimental data. The properties in Equation 10.6 are evaluated at the saturation temperature. Equation 10.6 applies when the characteristic length of the heater surface, L, is large relative to the bubble diameter, D_b. However, when the heater is small, such that the Confinement number, $Co = \sqrt{\sigma/(g[\rho_l - \rho_v])}/L = Bo^{-1/2}$ [12], is greater than approximately 0.2, a correction factor must be applied to account for the small size of the heater. Lienhard [11] reports correction factors for various geometries, including horizontal plates, cylinders, spheres, and vertically and horizontally oriented ribbons.

It is important to note that the critical heat flux depends strongly on pressure, mainly through the pressure dependence of surface tension and the heat of vaporization. Cichelli and Bonilla [13] have experimentally demonstrated that the peak flux increases with pressure up to one-third of the critical pressure, after which it falls to zero at the critical pressure.

10.4.3 Minimum Heat Flux

The transition boiling regime is of little practical interest, as it may be obtained only by controlling the surface heater temperature. While no adequate theory has been

Patent Owner Manufacturing Resources International, Inc.
Exhibit 2017 - Page 635 of 999

developed for this regime, conditions can be characterized by periodic, *unstable* contact between the liquid and the heated surface. However, the upper limit of this regime is of interest because it corresponds to formation of a *stable* vapor blanket or film and to a minimum heat flux condition. If the heat flux drops below this minimum, the film will collapse, causing the surface to cool and nucleate boiling to be reestablished.

Zuber [10] used stability theory to derive the following expression for the minimum heat flux, $q''_{s,D} = q''_{\min}$, from a large horizontal plate.

$$q''_{\min} = C\rho_v h_{fg}\left[\frac{g\sigma(\rho_l - \rho_v)}{(\rho_l + \rho_v)^2}\right]^{1/4} \tag{10.7}$$

where the properties are evaluated at the saturation temperature. The constant, $C = 0.09$, has been experimentally determined by Berenson [14]. This result is accurate to approximately 50% for most fluids at moderate pressures but provides poorer estimates at higher pressures [15]. A similar result has been obtained for horizontal cylinders [16].

10.4.4 Film Pool Boiling

At excess temperatures beyond the Leidenfrost point, a continuous vapor film blankets the surface and there is no contact between the liquid phase and the surface. Because conditions in the stable vapor film bear a strong resemblance to those of laminar film condensation (Section 10.7), it is customary to base film boiling correlations on results obtained from condensation theory. One such result, which applies to film boiling on a cylinder or sphere of diameter D, is of the form

$$\overline{Nu}_D = \frac{\bar{h}_{\text{conv}} D}{k_v} = C\left[\frac{g(\rho_l - \rho_v)h'_{fg}D^3}{v_v k_v (T_s - T_{\text{sat}})}\right]^{1/4} \tag{10.8}$$

The correlation constant C is 0.62 for horizontal cylinders [17] and 0.67 for spheres [11]. The corrected latent heat h'_{fg} accounts for the sensible energy required to maintain temperatures within the vapor blanket above the saturation temperature. Although it may be approximated as $h'_{fg} = h_{fg} + 0.80c_{p,v}(T_s - T_{\text{sat}})$, it is known to depend weakly on the Prandtl number of the vapor [18]. Vapor properties are evaluated at the film temperature, $T_f = (T_s + T_{\text{sat}})/2$, and the liquid density is evaluated at the saturation temperature.

At elevated surface temperatures ($T_s \gtrsim 300°\text{C}$), radiation heat transfer across the vapor film becomes significant. Since radiation acts to increase the film thickness, it is not reasonable to assume that the radiative and convective processes are simply additive. Bromley [17] investigated film boiling from the outer surface of horizontal tubes and suggested calculating the total heat transfer coefficient from a transcendental equation of the form

$$\bar{h}^{4/3} = \bar{h}^{4/3}_{\text{conv}} + \bar{h}_{\text{rad}}\bar{h}^{1/3} \tag{10.9}$$

If $\bar{h}_{\text{rad}} < \bar{h}_{\text{conv}}$, a simpler form may be used:

$$\bar{h} = \bar{h}_{\text{conv}} + \tfrac{3}{4}\bar{h}_{\text{rad}} \tag{10.10}$$

Patent Owner Manufacturing Resources International, Inc.
Exhibit 2017 - Page 636 of 999

The effective radiation coefficient $\bar{h}_{rad}$ is expressed as

$$\bar{h}_{rad} = \frac{\varepsilon\sigma(T_s^4 - T_{sat}^4)}{T_s - T_{sat}} \tag{10.11}$$

where ε is the emissivity of the solid (Table A.11) and σ is the Stefan–Boltzmann constant.

Note that the analogy between film boiling and film condensation does not hold for small surfaces with high curvature because of the large disparity between vapor and liquid film thicknesses for the two processes. The analogy is also questionable for a vertical surface, although satisfactory predictions have been obtained for limited conditions.

10.4.5 Parametric Effects on Pool Boiling

In this section we briefly consider other parameters that can affect pool boiling, confining our attention to the gravitational field, liquid subcooling, and solid surface conditions.

The influence of the *gravitational field* on boiling must be considered in applications involving space travel and rotating machinery. This influence is evident from appearance of the gravitational acceleration g in the foregoing expressions. Siegel [19], in his review of low gravity effects, confirms that the $g^{1/4}$ dependence in Equations 10.6, 10.7, and 10.8 (for the maximum and minimum heat fluxes and for film boiling) is correct for values of g as low as 0.10 m/s^2. For nucleate boiling, however, evidence indicates that the heat flux is nearly independent of gravity, which is in contrast to the $g^{1/2}$ dependence of Equation 10.5. Above-normal gravitational forces show similar effects, although near the ONB, gravity can influence bubble-induced convection.

If liquid in a pool boiling system is maintained at a temperature that is less than the saturation temperature, the liquid is said to be *subcooled*, where $\Delta T_{sub} \equiv T_{sat} - T_l$. In the natural convection regime, the heat flux increases typically as $(T_s - T_l)^{5/4}$ or $(\Delta T_e + \Delta T_{sub})^{5/4}$. In contrast, for nucleate boiling, the influence of subcooling is considered to be negligible, although the maximum and minimum heat fluxes, q''_{max} and q''_{min}, are known to increase linearly with ΔT_{sub}. For film boiling, the heat flux increases strongly with increasing ΔT_{sub}.

The influence of *surface roughness* (by machining, grooving, scoring or sandblasting) on the maximum and minimum heat fluxes and on film boiling is negligible. However, as demonstrated by Berensen [20], increased surface roughness can cause a large increase in heat flux for the nucleate boiling regime. As Figure 10.6 illustrates, a roughened surface has numerous cavities that serve to trap vapor, providing more and larger sites for bubble growth. It follows that the nucleation site density for a rough surface can be substantially larger than that for a smooth surface. However, under prolonged boiling, the effects of surface roughness generally diminish, indicating that the new, large sites created by roughening are not stable sources of vapor entrapment.

Special surface arrangements that provide stable *augmentation* (*enhancement*) of nucleate boiling are available commercially and have been reviewed by Webb [21]. *Enhancement surfaces* are of two types: (1) coatings of very porous material

Patent Owner Manufacturing Resources International, Inc.
Exhibit 2017 - Page 637 of 999

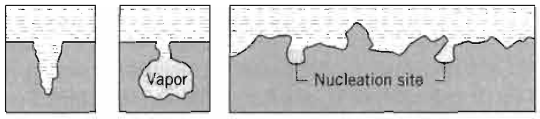


FIGURE 10.6 Formation of nucleation sites. (*a*) Wetted cavity with no trapped vapor. (*b*) Reentrant cavity with trapped vapor. (*c*) Enlarged profile of a roughened surface.

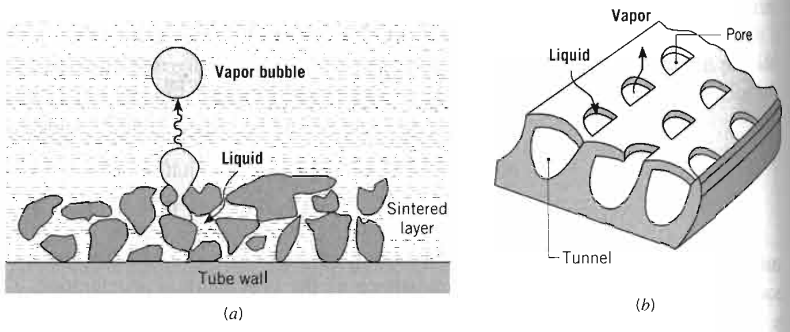


FIGURE 10.7 Typical structured enhancement surfaces for augmentation of nucleate boiling. (*a*) Sintered metallic coating. (*b*) Mechanically formed double-reentrant cavity.

formed by sintering, brazing, flame spraying, electrolytic deposition, or foaming, and (2) mechanically machined or formed double-reentrant cavities to ensure continuous vapor trapping (see Figure 10.7). Such surfaces provide for continuous renewal of vapor at the nucleation sites and heat transfer augmentation by more than an order of magnitude. Active augmentation techniques, such as surface wiping–rotation, surface vibration, fluid vibration, and electrostatic fields, have also been reviewed by Bergles [22, 23]. However, because such techniques complicate the boiling system and, in many instances, impair reliability, they have found little practical application.

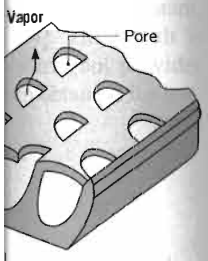
EXAMPLE 10.1

The bottom of a copper pan, 0.3 m in diameter, is maintained at 118°C by an electric heater. Estimate the power required to boil water in this pan. What is the evaporation rate? Estimate the critical heat flux.

SOLUTION

Known: Water boiling in a copper pan of prescribed surface temperature.

Patent Owner Manufacturing Resources International, Inc.
Exhibit 2017 - Page 638 of 999



(*b*)

ion of nucleate boiling.
cavity.

osition, or foaming,
ies to ensure contin-
continuous renewal
y more than an order
wiping–rotation, sur-
o been reviewed by
e the boiling system
practical application.

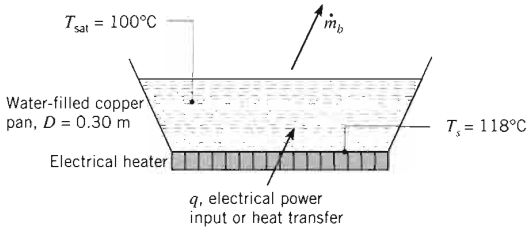
t 118°C by an elec-
. What is the evapo-

temperature.

Find:

1. Power required by electric heater to cause boiling.
2. Rate of water evaporation due to boiling.
3. Critical heat flux corresponding to the burnout point.

Schematic:



Assumptions:

1. Steady-state conditions.
2. Water exposed to standard atmospheric pressure, 1.01 bar.
3. Water at uniform temperature $T_{sat} = 100°C$.
4. Large pan bottom surface of polished copper.
5. Negligible losses from heater to surroundings.

Properties: Table A.6, saturated water, liquid (100°C): $\rho_l = 1/v_f = 957.9$ kg/m^3, $c_{p,l} = c_{p,f} = 4.217$ kJ/kg · K, $\mu_l = \mu_f = 279 \times 10^{-6}$ N · s/m^2, $Pr_l = Pr_f = 1.76$, $h_{fg} = 2257$ kJ/kg, $\sigma = 58.9 \times 10^{-3}$ N/m. Table A.6, saturated water, vapor (100°C): $\rho_v = 1/v_g = 0.5956$ kg/m^3.

Analysis:

1. From knowledge of the saturation temperature T_{sat} of water boiling at 1 atm and the temperature of the heated copper surface T_s, the excess temperature ΔT_e is

$$\Delta T_e \equiv T_s - T_{sat} = 118°C - 100°C = 18°C$$

According to the boiling curve of Figure 10.4, nucleate pool boiling will occur and the recommended correlation for estimating the heat transfer rate per unit area of plate surface is given by Equation 10.5.

$$q_s'' = \mu_l h_{fg} \left[\frac{g(\rho_l - \rho_v)}{\sigma}\right]^{1/2} \left(\frac{c_{p,l}\,\Delta T_e}{C_{s,f} h_{fg} Pr_l^n}\right)^3$$

The values of $C_{s,f}$ and n corresponding to the polished copper surface–water combination are determined from the experimental results of Table 10.1,

Patent Owner Manufacturing Resources International, Inc.
Exhibit 2017 - Page 639 of 999

where $C_{s,f} = 0.0128$ and $n = 1.0$. Substituting numerical values, the boiling heat flux is

$$q_s'' = 279 \times 10^{-6}\ \text{N} \cdot \text{s/m}^2 \times 2257 \times 10^3\ \text{J/kg} \times \left[\frac{9.8\ \text{m/s}^2\,(957.9 - 0.5956)\ \text{kg/m}^3}{58.9 \times 10^{-3}\ \text{N/m}}\right]^{1/2} \times \left(\frac{4.217 \times 10^3\ \text{J/kg} \cdot \text{K} \times 18°\text{C}}{0.0128 \times 2257 \times 10^3\ \text{J/kg} \times 1.76}\right)^3 = 836\ \text{kW/m}^2$$

Hence the boiling heat transfer rate is

$$q_s = q_s'' \times A = q_s'' \times \frac{\pi D^2}{4}$$

$$q_s = 8.36 \times 10^5\ \text{W/m}^2 \times \frac{\pi(0.30\ \text{m})^2}{4} = 59.1\ \text{kW}$$ ◁

2. Under steady-state conditions all heat addition to the pan will result in water evaporation from the pan. Hence

$$q_s = \dot{m}_b h_{fg}$$

where $\dot{m}_b$ is the rate at which water evaporates from the free surface to the room. It follows that

$$\dot{m}_b = \frac{q_s}{h_{fg}} = \frac{5.91 \times 10^4\ \text{W}}{2257 \times 10^3\ \text{J/kg}} = 0.0262\ \text{kg/s} = 94\ \text{kg/h}$$ ◁

3. The critical heat flux for nucleate pool boiling can be estimated from Equation 10.6:

$$q''_{\max} = 0.149 h_{fg} \rho_v \left[\frac{\sigma g(\rho_l - \rho_v)}{\rho_v^2}\right]^{1/4}$$

Substituting the appropriate numerical values,

$$q''_{\max} = 0.149 \times 2257 \times 10^3\ \text{J/kg} \times 0.5956\ \text{kg/m}^3 \times \left[\frac{58.9 \times 10^{-3}\ \text{N/m} \times 9.8\ \text{m/s}^2\,(957.9 - 0.5956)\ \text{kg/m}^3}{(0.5956)^2(\text{kg/m}^3)^2}\right]^{1/4}$$

$$q''_{\max} = 1.26\ \text{MW/m}^2$$ ◁

Comments:

1. Note that the critical heat flux $q''_{\max} = 1.26\ \text{MW/m}^2$ represents the maximum heat flux for boiling water at normal atmospheric pressure. Operation of the heater at $q_s'' = 0.836\ \text{MW/m}^2$ is therefore below the critical condition.
2. Using Equation 10.7, the minimum heat flux at the Leidenfrost point is $q''_{\min} = 18.9\ \text{kW/m}^2$. Note from Figure 10.4 that, for this condition, $\Delta T_e \approx 120°\text{C}$.

Patent Owner Manufacturing Resources International, Inc.
Exhibit 2017 - Page 640 of 999

l values, the boiling

W/m²

W ◁

will result in water

free surface to the

kg/h ◁

timated from Equa-

956) kg/m³]^1/4

◁

sents the maximum
re. Operation of the
condition.
Leidenfrost point is
lition, $\Delta T_e \approx 120°C$.

EXAMPLE 10.2

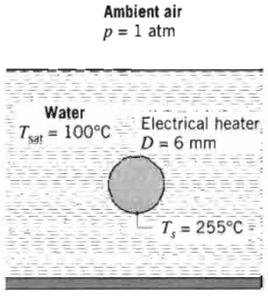
A metal-clad heating element of 6-mm diameter and emissivity $\varepsilon = 1$ is horizontally immersed in a water bath. The surface temperature of the metal is 255°C under steady-state boiling conditions. Estimate the power dissipation per unit length of the heater.

SOLUTION

Known: Boiling from outer surface of horizontal cylinder in water.

Find: Power dissipation per unit length for the cylinder, q_s'.

Schematic:



Assumptions:

1. Steady-state conditions.
2. Water exposed to standard atmospheric pressure and at uniform temperature T_{sat}.

Properties: Table A.6, saturated water, liquid (100°C): $\rho_l = 1/v_f = 957.9$ kg/m³, $h_{fg} = 2257$ kJ/kg. Table A.4, water vapor at atmospheric pressure ($T_f \approx 450$ K): $\rho_v = 0.4902$ kg/m³, $c_{p,v} = 1.980$ kJ/kg · K, $k_v = 0.0299$ W/m · K, $\mu_v = 15.25 \times 10^{-6}$ N · s/m².

Analysis: The excess temperature is

$$\Delta T_e = T_s - T_{sat} = 255°C - 100°C = 155°C$$

According to the boiling curve of Figure 10.4, film pool boiling conditions are achieved, in which case heat transfer is due to both convection and radiation. The heat transfer rate follows from Equation 10.3, written on a per unit length basis for a cylindrical surface of diameter D:

$$q_s' = q_s'' \pi D = \bar{h} \pi D \, \Delta T_e$$

The heat transfer coefficient $\bar{h}$ is calculated from Equation 10.9,

$$\bar{h}^{4/3} = \bar{h}_{conv}^{4/3} + \bar{h}_{rad} \bar{h}^{1/3}$$

Patent Owner Manufacturing Resources International, Inc.
Exhibit 2017 - Page 641 of 999

where the convection and radiation heat transfer coefficients follow from Equations 10.8 and 10.11, respectively. For the convection coefficient:

$$\bar{h}_{conv} = 0.62\left[\frac{k_v^3\rho_v(\rho_l - \rho_v)g(h_{fg} + 0.8c_{p,v}\,\Delta T_e)}{\mu_v D\,\Delta T_e}\right]^{1/4}$$

$$\bar{h}_{conv} = 0.62 \times \left[\frac{(0.0299)^3(\mathrm{W/m\cdot K})^3 \times 0.4902\ \mathrm{kg/m^3}\,(957.9 - 0.4902)\ \mathrm{kg/m^3} \times 9.8\ \mathrm{m/s^2}}{1}\right.$$

$$\left. \times \frac{(2257 \times 10^3\ \mathrm{J/kg} + 0.8 \times 1.98 \times 10^3\ \mathrm{J/kg\cdot K} \times 155°\mathrm{C})}{15.25 \times 10^{-6}\ \mathrm{N\cdot s/m^2} \times 6 \times 10^{-3}\ \mathrm{m} \times 155°\mathrm{C}}\right]^{1/4}$$

$$\bar{h}_{conv} = 238\ \mathrm{W/m^2\cdot K}$$

For the radiation heat transfer coefficient:

$$\bar{h}_{rad} = \frac{\varepsilon\sigma(T_s^4 - T_{sat}^4)}{T_s - T_{sat}}$$

$$\bar{h}_{rad} = \frac{5.67 \times 10^{-8}\ \mathrm{W/m^2\cdot K^4}\,(528^4 - 373^4)\mathrm{K}^4}{(528 - 373)\ \mathrm{K}} = 21.3\ \mathrm{W/m^2\cdot K}$$

Solving Equation 10.9 by trial and error,

$$\bar{h}^{4/3} = 238^{4/3} + 21.3\bar{h}^{1/3}$$

it follows that

$$\bar{h} = 254.1\ \mathrm{W/m^2\cdot K}$$

Hence the heat transfer rate per unit length of heater element is

$$q_s' = 254.1\ \mathrm{W/m^2\cdot K} \times \pi \times 6 \times 10^{-3}\ \mathrm{m} \times 155°\mathrm{C} = 742\ \mathrm{W/m}$$ ◁

Comments: Equation 10.10 is appropriate for estimating $\bar{h}$; it provides a value of 254.0 $\mathrm{W/m^2\cdot K}$.

10.5 *Forced Convection Boiling*

In *pool boiling* fluid flow is due primarily to the buoyancy-driven motion of bubbles originating from the heated surface. In contrast, for *forced convection boiling,* flow is due to a directed (bulk) motion of the fluid, as well as to buoyancy effects. Conditions depend strongly on geometry, which may involve *external* flow over heated plates and cylinders or *internal* (duct) flow. Internal, forced convection boiling is commonly referred to as *two-phase flow* and is characterized by rapid changes from liquid to vapor in the flow direction.

Patent Owner Manufacturing Resources International, Inc.
Exhibit 2017 - Page 642 of 999

10.5.1 External Forced Convection Boiling

For external flow over a heated plate, the heat flux can be estimated by standard forced convection correlations up to the inception of boiling. As the temperature of the heated plate is increased, nucleate boiling will occur, causing the heat flux to increase. If vapor generation is not extensive and the liquid is subcooled, Bergles and Rohsenow [24] suggest a method for estimating the total heat flux in terms of components associated with pure forced convection and pool boiling.

Both forced convection and subcooling are known to increase the critical heat flux q''_{max} for nucleate boiling. Experimental values as high as 35 MW/m^2 (compared with 1.3 MW/m^2 for pool boiling of water at 1 atm) have been reported [25]. For a liquid of velocity V moving in cross flow over a cylinder of diameter D, Lienhard and Eichhorn [26] have developed the following expressions for low- and high-velocity flows, where properties are evaluated at the saturation temperature.

Low Velocity:

$$\frac{q''_{max}}{\rho_v h_{fg} V} = \frac{1}{\pi}\left[1 + \left(\frac{4}{We_D}\right)^{1/3}\right] \tag{10.12}$$

High Velocity:

$$\frac{q''_{max}}{\rho_v h_{fg} V} = \frac{(\rho_l/\rho_v)^{3/4}}{169\pi} + \frac{(\rho_l/\rho_v)^{1/2}}{19.2\pi\, We_D^{1/3}} \tag{10.13}$$

The Weber number We_D is the ratio of inertia to surface tension forces and has the form

$$We_D \equiv \frac{\rho_v V^2 D}{\sigma} \tag{10.14}$$

The high- and low-velocity regions, respectively, are determined by whether the heat flux parameter $q''_{max}/\rho_v h_{fg} V$ is less than or greater than $[(0.275/\pi)\,(\rho_l/\rho_v)^{1/2} + 1]$. In most cases, Equations 10.12 and 10.13 correlate q''_{max} data within 20%.

10.5.2 Two-Phase Flow

Internal forced convection boiling is associated with bubble formation at the inner surface of a heated tube through which a liquid is flowing. Bubble growth and separation are strongly influenced by the flow velocity, and hydrodynamic effects differ significantly from those corresponding to pool boiling. The process is accompanied by the existence of a variety of two-phase flow patterns.

Consider flow development in a vertical tube that is subjected to a constant surface heat flux, as shown in Figure 10.8. Heat transfer to the subcooled liquid that enters the tube is initially by *single-phase forced convection* and may be predicted using the correlations of Chapter 8. Farther down the tube, the wall temperature exceeds the saturation temperature of the liquid, and vaporization is initiated in the *subcooled flow boiling region*. This region is characterized by significant radial

Patent Owner Manufacturing Resources International, Inc.
Exhibit 2017 - Page 643 of 999

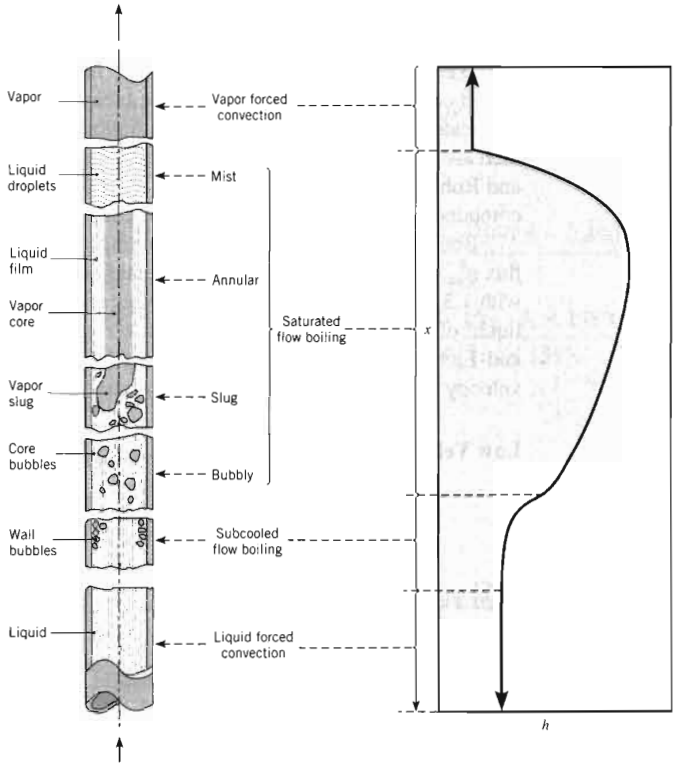


FIGURE 10.8 Flow regimes for forced convection boiling in a tube.

temperature gradients, with bubbles forming adjacent to the heated wall and subcooled liquid flowing near the center of the tube. The thickness of the bubble region increases farther downstream, and eventually, the core of the liquid reaches the saturation temperature of the fluid. Bubbles can then exist at any radial location, and the time-averaged mass fraction of vapor in the fluid,[1] X, exceeds zero at any radial location. This marks the beginning of the *saturated flow boiling region*. Within the saturated flow boiling region, the mean vapor mass fraction defined as

$$\overline{X} \equiv \frac{\int_{A_c} \rho u(r,x) X dA_c}{\dot{m}}$$

increases and, due to the large density difference between the vapor and liquid phases, the mean velocity of the fluid, u_m, increases significantly.

The first stage of the saturated flow boiling region corresponds to the *bubbly flow regime*. As $\overline{X}$ increases further, individual bubbles coalesce to form slugs of

[1]This term is often referred to as the *quality* of a two-phase fluid.

Patent Owner Manufacturing Resources International, Inc.
Exhibit 2017 - Page 644 of 999

vapor. This *slug-flow regime* is followed by an *annular-flow regime* in which the liquid forms a film on the tube wall. This film moves along the inner surface of the tube, while vapor moves at a larger velocity through the core of the tube. Dry spots eventually appear on the inner surface of the tube and grow in size within a *transition regime*. Eventually, the entire tube surface is completely dry, and all remaining liquid is in the form of droplets that travel at high velocity within the core of the tube in the *mist regime*. After the droplets are completely vaporized, the fluid consists of superheated vapor in a *second* single-phase forced convection region. The increase in the vapor fraction along the tube length, along with the significant difference in the densities of the liquid and vapor phases, increases the mean velocity of the fluid by several orders of magnitude between the first and the second single-phase forced convection regions.

The local heat transfer coefficient varies significantly as $\overline{X}$ and u_m decrease and increase, respectively, along the length of the tube, x. In general, the heat transfer coefficient can increase by approximately an order of magnitude through the subcooled flow boiling region. Heat transfer coefficients are further increased in the early stages of the saturated flow boiling region. Conditions become more complex deeper in the saturated flow boiling region since the convection coefficient, defined in Equation 10.3, *either* increases or decreases with increasing $\overline{X}$, depending on the fluid and tube wall material. Typically, the smallest convection coefficients exist in the second (vapor) forced convection region owing to the low thermal conductivity of the vapor relative to that of the liquid.

The following correlation has been developed for the saturated flow boiling region in smooth circular tubes [27, 28]:

$$\frac{h}{h_{sp}} = 0.6683\left(\frac{\rho_l}{\rho_v}\right)^{0.1}\overline{X}^{0.16}(1-\overline{X})^{0.64}f(Fr) + 1058\left(\frac{q''_s}{\dot{m}''h_{fg}}\right)^{0.7}(1-\overline{X})^{0.8}G_{s,f} \tag{10.15a}$$

or

$$\frac{h}{h_{sp}} = 1.136\left(\frac{\rho_l}{\rho_v}\right)^{0.45}\overline{X}^{0.72}(1-\overline{X})^{0.08}f(Fr) + 667.2\left(\frac{q''_s}{\dot{m}''h_{fg}}\right)^{0.7}(1-\overline{X})^{0.8}G_{s,f} \tag{10.15b}$$

$$0 < \overline{X} \lesssim 0.8$$

where $\dot{m}'' = \dot{m}/A_c$ is the mass flow rate per unit cross-sectional area. In utilizing Equation 10.15, the larger value of the heat transfer coefficient, h, should be used. In this expression, the liquid phase *Froude number* is $Fr = (\dot{m}''/\rho_l)^2/gD$ and the coefficient $G_{s,f}$ depends on the surface–liquid combination, with representative values given in Table 10.2. Equation 10.15 applies for horizontal as well as vertical tubes, where the *stratification parameter*, $f(Fr)$, accounts for stratification of the liquid and vapor phases that may occur for horizontal tubes. Its value is unity for vertical tubes and for horizontal tubes with $Fr \gtrsim 0.04$. For horizontal tubes with $Fr \lesssim 0.04$, $f(Fr) = 2.63Fr^{0.3}$. All properties are evaluated at the saturation temperature, T_{sat}. The single-phase convection coefficient, h_{sp}, is associated with the liquid forced convection region of Figure 10.8 and is obtained from Equation 8.62 with properties evaluated at T_{sat}. Because Equation 8.62 is for turbulent flow, it is recommended that Equation 10.15 not be applied to situations where the liquid single-phase

Patent Owner Manufacturing Resources International, Inc.
Exhibit 2017 - Page 645 of 999

10.6 Condensation

TABLE 10.2 Values of $G_{s,f}$ for various surface–liquid combinations [27, 28].

Fluid in Commercial Copper Tubing	$G_{s,f}$
Kerosene	0.488
Refrigerant R-134a	1.63
Refrigerant R-152a	1.10
Water	1.00
For stainless steel tubing, use $G_{s,f} = 1$.	

convection is laminar. Equation 10.15 is applicable when the channel dimension is large relative to the bubble diameter, that is, for Confinement numbers, $Co = \sqrt{\sigma/(g[\rho_l - \rho_v])}/D_h \lesssim 1/2$ [3].

In order to use Equation 10.15, the mean vapor mass fraction, $\overline{X}$, must be known. For negligible changes in the fluid's kinetic and potential energy as well as negligible work, Equation 1.11d may be rearranged to yield

$$\overline{X}(x) = \frac{q_s'' \pi D x}{\dot{m} h_{fg}} \tag{10.16}$$

where the origin of the x-coordinate, $x = 0$, corresponds to the axial location where $\overline{X}$ begins to exceed zero, and the change in enthalpy, $u_l + pv$, is equal to the change in $\overline{X}$ multiplied by the enthalpy of vaporization, h_{fg}.

Correlations for the subcooled flow boiling region and annular as well as mist regimes are available in the literature [28]. For constant heat flux conditions, critical heat fluxes may occur in the subcooled flow boiling region, in the saturated flow boiling region where $\overline{X}$ is large, or in the vapor forced convection region. Critical heat flux conditions may lead to melting of the tube material in extreme conditions [29]. Additional discussions of flow boiling are available in the literature [7, 30–33]. Extensive databases consisting of thousands of experimentally measured values of the critical heat flux for wide ranges of operating conditions are also available [34, 35].

10.5.3 Two-Phase Flow in Microchannels

Two-phase microchannels feature forced convection boiling of a liquid through circular or noncircular tubes having hydraulic diameters ranging from 10 to 1000 μm, resulting in extremely high heat transfer rates [36]. In these situations, the characteristic bubble size can occupy a significant fraction of the tube diameter and the Confinement number can become very large. Hence, different types of flow regimes exist, including regimes where the bubbles occupy nearly the full diameter of the heated tube [37]. This can lead to a dramatic increase in the convection coefficient, h, corresponding to the peak in Figure 10.8. Thereafter, h decreases with increasing x as it does in Figure 10.8. Equation 10.15 cannot be used to predict correct values of the heat transfer coefficient and does not even predict correct trends for microchannel flow boiling cases. Recourse must be made to more sophisticated modeling [38].

Patent Owner Manufacturing Resources International, Inc.
Exhibit 2017 - Page 646 of 999

10.6
Condensation: Physical Mechanisms

Condensation occurs when the temperature of a vapor is reduced below its saturation temperature. In industrial equipment, the process commonly results from contact between the vapor and a cool *surface* (Figures 10.9*a*, *b*). The latent energy of the vapor is released, heat is transferred to the surface, and the condensate is formed. Other common modes are *homogeneous* condensation (Figure 10.9*c*), where vapor condenses out as droplets suspended in a gas phase to form a fog, and *direct contact* condensation (Figure 10.9*d*), which occurs when vapor is brought into contact with a cold liquid. In this chapter we will consider only surface condensation.

As shown in Figures 10.9*a*, *b*, condensation may occur in one of two ways, depending on the condition of the surface. The dominant form of condensation is one in which a liquid film covers the entire condensing surface, and under the action of gravity the film flows continuously from the surface. *Film condensation* is generally characteristic of clean, uncontaminated surfaces. However, if the surface is coated with a substance that inhibits wetting, it is possible to maintain *dropwise condensation.* The drops form in cracks, pits, and cavities on the surface and may grow and coalesce through continued condensation. Typically, more than 90% of the surface is covered by drops, ranging from a few micrometers in diameter to

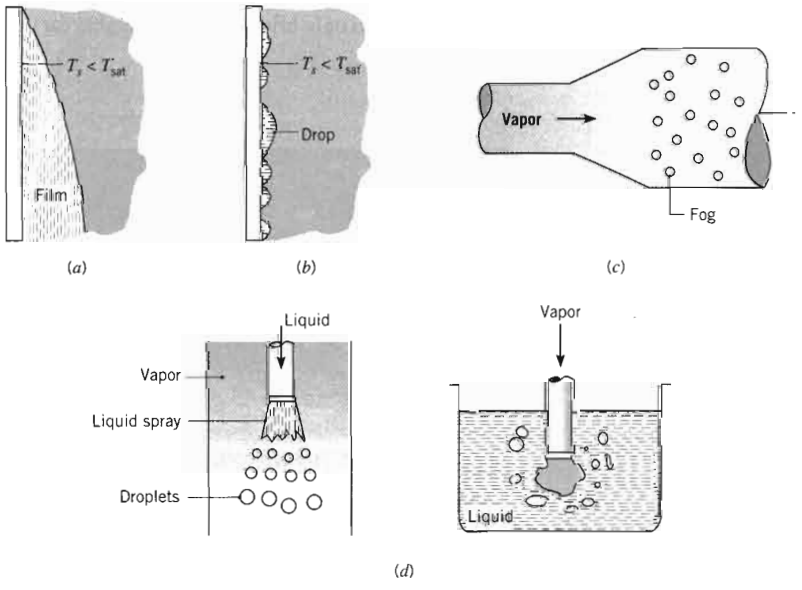


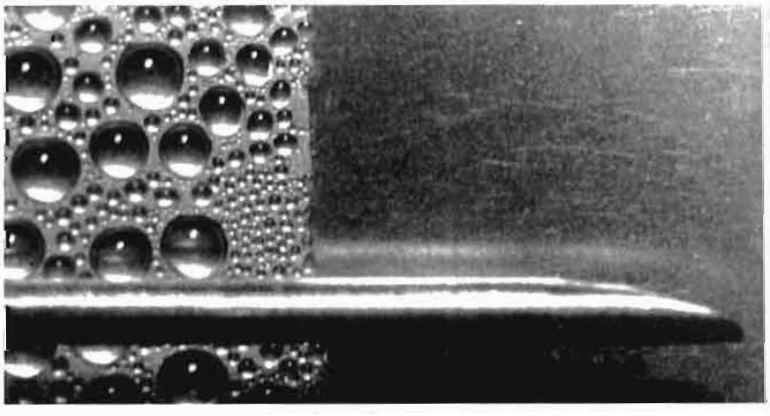
FIGURE 10.9 Modes of condensation. (*a*) Film. (*b*) Dropwise condensation on a surface. (*c*) Homogeneous condensation or fog formation resulting from increased pressure due to expansion. (*d*) Direct contact condensation.

Patent Owner Manufacturing Resources International, Inc.
Exhibit 2017 - Page 647 of 999

agglomerations visible to the naked eye. The droplets flow from the surface due to the action of gravity. Film and dropwise condensation of steam on a vertical copper surface are shown in Figure 10.10. A thin coating of cupric oleate was applied to the left-hand portion of the surface to promote the dropwise condensation. A thermocouple probe of 1-mm diameter extends across the photograph.

Regardless of whether it is in the form of a film or droplets, the condensate provides a resistance to heat transfer between the vapor and the surface. Because this resistance increases with condensate thickness, which increases in the flow direction, it is desirable to use short vertical surfaces or horizontal cylinders in situations involving film condensation. Most condensers therefore consist of horizontal tube bundles through which a liquid coolant flows and around which the vapor to be condensed is circulated. In terms of maintaining high condensation and heat transfer rates, droplet formation is superior to film formation. In dropwise condensation most of the heat transfer is through drops of less than 100-μm diameter, and transfer rates that are more than an order of magnitude larger than those associated with film condensation may be achieved. It is therefore common practice to use surface coatings that inhibit wetting, and hence stimulate dropwise condensation. Silicones, Teflon, and an assortment of waxes and fatty acids are often used for this purpose. However, such coatings gradually lose their effectiveness due to oxidation, fouling, or outright removal, and film condensation eventually occurs.

Although it is desirable to achieve dropwise condensation in industrial applications, it is often difficult to maintain this condition. For this reason and because the convection coefficients for film condensation are smaller than those for the dropwise case, condenser design calculations are often based on the assumption of film condensation. In the remaining sections of this chapter, we focus on film condensation and mention only briefly results available for dropwise condensation.



(*a*) (*b*)

FIGURE 10.10 Condensation on a vertical surface. (*a*) Dropwise. (*b*) Film. Photograph courtesy of Professor J. W. Westwater, University of Illinois at Champaign-Urbana.

10.7 *Laminar Film on a Vertical*

Patent Owner Manufacturing Resources International, Inc.
Exhibit 2017 - Page 648 of 999

m the surface due to
on a vertical copper
leate was applied to
ondensation. A ther-
oh.
lets, the condensate
he surface. Because
creases in the flow
tal cylinders in situ-
consist of horizon-
nd which the vapor
ndensation and heat
n dropwise conden-
100-μm diameter,
e larger than those
re common practice
e dropwise conden-
tty acids are often
their effectiveness
ensation eventually

n industrial applica-
son and because the
those for the drop-
assumption of film
s on film condensa-
lensation.



m.

10.7 *Laminar Film Condensation on a Vertical Plate*

As shown in Figure 10.11*a*, there may be several complicating features associated with film condensation. The film originates at the top of the plate and flows downward under the influence of gravity. The thickness δ and the condensate mass flow rate $\dot{m}$ increase with increasing x because of continuous condensation at the liquid–vapor interface, which is at T_{sat}. There is then heat transfer from this interface through the film to the surface, which is maintained at $T_s < T_{sat}$. In the most general case the vapor may be superheated ($T_{v,\infty} > T_{sat}$) and may be part of a mixture containing one or more noncondensable gases. Moreover, there exists a finite shear stress at the liquid–vapor interface, contributing to a velocity gradient in the vapor, as well as in the film [39, 40].

Despite the complexities associated with film condensation, useful results may be obtained by making assumptions that originated with an analysis by Nusselt [41].

1. Laminar flow and constant properties are assumed for the liquid film.
2. The gas is assumed to be a pure vapor and at a uniform temperature equal to T_{sat}. With no temperature gradient in the vapor, heat transfer to the liquid–vapor

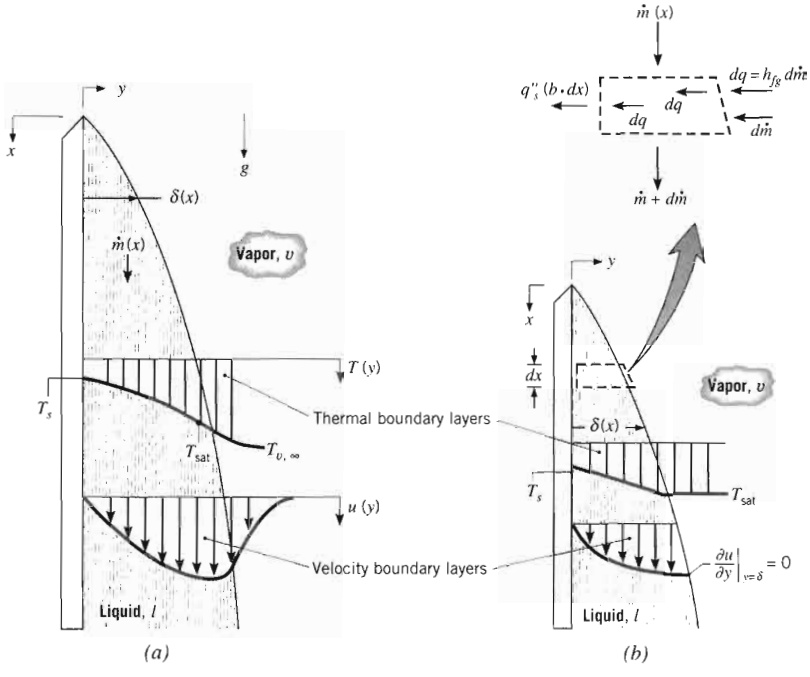


FIGURE 10.11 Boundary layer effects related to film condensation on a vertical surface. (*a*) Without approximation. (*b*) With assumptions associated with Nusselt's analysis, for a vertical plate of width b.

Patent Owner Manufacturing Resources International, Inc.
Exhibit 2017 - Page 649 of 999

interface can occur only by condensation at the interface and not by conduction from the vapor.

3. The shear stress at the liquid–vapor interface is assumed to be negligible, in which case $\partial u/\partial y|_{y=\delta} = 0$. With this assumption and the foregoing assumption of a uniform vapor temperature, there is no need to consider the vapor velocity or thermal boundary layers shown in Figure 10.11*a*.
4. Momentum and energy transfer by advection in the condensate film are assumed to be negligible. This assumption is reasonable by virtue of the low velocities associated with the film. It follows that heat transfer across the film occurs only by conduction, in which case the liquid temperature distribution is linear.

Film conditions resulting from the assumptions are shown in Figure 10.11*b*.

The x-momentum equation for the film can be found from Equation 9.1, with $\rho = \rho_l$ and $\nu = \nu_l$ for the liquid, and with the sign of the gravity term changed since x is now in the direction of gravity. The pressure gradient is obtained from Equation 9.2 and is $dp_\infty/dx = +\rho_v g$, since the free stream density is the vapor density. From the fourth approximation, momentum advection terms may be neglected, and the x-momentum equation may be expressed as

$$\frac{\partial^2 u}{\partial y^2} = -\frac{g}{\mu_l}(\rho_l - \rho_v) \tag{10.17}$$

Integrating twice and applying boundary conditions of the form $u(0) = 0$ and $\partial u/\partial y|_{y=\delta} = 0$, the velocity profile in the film becomes

$$u(y) = \frac{g(\rho_l - \rho_v)\delta^2}{\mu_l}\left[\frac{y}{\delta} - \frac{1}{2}\left(\frac{y}{\delta}\right)^2\right] \tag{10.18}$$

From this result the condensate mass flow rate per unit width $\Gamma(x)$ may be obtained in terms of an integral involving the velocity profile:

$$\frac{\dot{m}(x)}{b} = \int_0^{\delta(x)} \rho_l u(y)\, dy \equiv \Gamma(x) \tag{10.19}$$

Substituting from Equation 10.18, it follows that

$$\Gamma(x) = \frac{g\rho_l(\rho_l - \rho_v)\delta^3}{3\mu_l} \tag{10.20}$$

The specific variation with x of δ, and hence of Γ, may be obtained by first applying the conservation of energy requirement to the differential element shown in Figure 10.11*b*. At a portion of the liquid–vapor interface of unit width and length dx, the rate of heat transfer into the film, dq, must equal the rate of energy release due to condensation at the interface. Hence

$$dq = h_{fg}\, d\dot{m} \tag{10.21}$$

Since advection is neglected, it also follows that the rate of heat transfer across the interface must equal the rate of heat transfer to the surface. Hence

$$dq = q_s''(b \cdot dx) \tag{10.22}$$

Patent Owner Manufacturing Resources International, Inc.
Exhibit 2017 - Page 650 of 999

Since the liquid temperature distribution is linear, Fourier's law may be used to express the surface heat flux as

$$q_s'' = \frac{k_l(T_{sat} - T_s)}{\delta} \tag{10.23}$$

Combining Equations 10.19 and 10.21 through 10.23, we then obtain

$$\frac{d\Gamma}{dx} = \frac{k_l(T_{sat} - T_s)}{\delta h_{fg}} \tag{10.24}$$

Differentiating Equation 10.20, we also obtain

$$\frac{d\Gamma}{dx} = \frac{g\rho_l(\rho_l - \rho_v)\delta^2}{\mu_l}\frac{d\delta}{dx} \tag{10.25}$$

Combining Equations 10.24 and 10.25, it follows that

$$\delta^3\, d\delta = \frac{k_l\mu_l(T_{sat} - T_s)}{g\rho_l(\rho_l - \rho_v)h_{fg}}\, dx$$

Integrating from $x = 0$, where $\delta = 0$, to any x location of interest on the surface,

$$\delta(x) = \left[\frac{4k_l\mu_l(T_{sat} - T_s)x}{g\rho_l(\rho_l - \rho_v)h_{fg}}\right]^{1/4} \tag{10.26}$$

This result may then be substituted into Equation 10.20 to obtain $\Gamma(x)$.

An improvement to the foregoing result for $\delta(x)$ was made by Nusselt [41] and Rohsenow [42], who showed that, with the inclusion of thermal advection effects, a term is added to the latent heat of vaporization. In lieu of h_{fg}, Rohsenow recommended using a modified latent heat of the form $h_{fg}' = h_{fg} + 0.68c_{p,l}(T_{sat} - T_s)$, or in terms of the Jakob number,

$$h_{fg}' = h_{fg}(1 + 0.68Ja) \tag{10.27}$$

More recently, Sadasivan and Lienhard [18] have shown that the modified latent heat depends weakly on the Prandtl number of the liquid.

The surface heat flux may be expressed as

$$q_s'' = h_x(T_{sat} - T_s) \tag{10.28}$$

Substituting from Equation 10.23, the local convection coefficient is then

$$h_x = \frac{k_l}{\delta} \tag{10.29}$$

or, from Equation 10.26, with h_{fg} replaced by h_{fg}',

$$h_x = \left[\frac{g\rho_l(\rho_l - \rho_v)k_l^3 h_{fg}'}{4\mu_l(T_{sat} - T_s)x}\right]^{1/4} \tag{10.30}$$

Since h_x depends on $x^{-1/4}$, it follows that the average convection coefficient for the entire plate is

$$\bar{h}_L = \frac{1}{L}\int_0^L h_x\, dx = \frac{4}{3}h_L$$

Patent Owner Manufacturing Resources International, Inc.
Exhibit 2017 - Page 651 of 999

or

$$\bar{h}_L = 0.943 \left[\frac{g\rho_l(\rho_l - \rho_v)k_l^3 h'_{fg}}{\mu_l(T_{sat} - T_s)L} \right]^{1/4} \tag{10.31}$$

The average Nusselt number then has the form

$$\overline{Nu}_L = \frac{\bar{h}_L L}{k_l} = 0.943 \left[\frac{\rho_l g(\rho_l - \rho_v)h'_{fg}L^3}{\mu_l k_l(T_{sat} - T_s)} \right]^{1/4} \tag{10.32}$$

In using this equation all liquid properties should be evaluated at the film temperature $T_f = (T_{sat} + T_s)/2$, and ρ_v and h_{fg} should be evaluated at T_{sat}.

A more detailed boundary layer analysis of film condensation on a vertical plate has been performed by Sparrow and Gregg [39]. Their results, confirmed by Chen [43], indicate that errors associated with using Equation 10.32 are less than 3% for $Ja \leq 0.1$ and $1 \leq Pr \leq 100$. Dhir and Lienhard [44] have also shown that Equation 10.32 may be used for inclined plates, if g is replaced by $g \cdot \cos\theta$, where θ is the angle between the vertical and the surface. However, it must be used with caution for large values of θ and does not apply if $\theta = \pi/2$. The expression may be used for condensation on the inner or outer surface of a vertical tube of radius R, if $R \gg \delta$.

The total heat transfer to the surface may be obtained by using Equation 10.31 with the following form of Newton's law of cooling:

$$q = \bar{h}_L A(T_{sat} - T_s) \tag{10.33}$$

The total condensation rate may then be determined from the relation

$$\dot{m} = \frac{q}{h'_{fg}} = \frac{\bar{h}_L A(T_{sat} - T_s)}{h'_{fg}} \tag{10.34}$$

Equations 10.33 and 10.34 are generally applicable to any surface geometry, although the form of $\bar{h}_L$ will vary according to geometry and flow conditions.

10.8 *Turbulent Film Condensation*

As for all previously discussed convection phenomena, turbulent flow conditions may exist in film condensation. Consider the vertical surface of Figure 10.12*a*. The transition criterion may be expressed in terms of a Reynolds number defined as

$$Re_\delta \equiv \frac{4\Gamma}{\mu_l} \tag{10.35}$$

With the condensate mass flow rate given by $\dot{m} = \rho_l u_m b\delta$, the Reynolds number may be expressed as

$$Re_\delta = \frac{4\dot{m}}{\mu_l b} = \frac{4\rho_l u_m \delta}{\mu_l} \tag{10.36}$$

Patent Owner Manufacturing Resources International, Inc.
Exhibit 2017 - Page 652 of 999

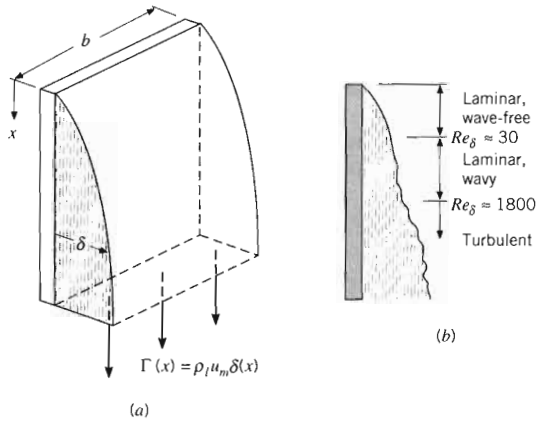


FIGURE 10.12 Film condensation on a vertical plate. (*a*) Condensate rate for plate of width *b*. (*b*) Flow regimes.

where u_m is the average velocity in the film and δ, the film thickness, is the characteristic length. As in the case of single-phase boundary layers, the Reynolds number is an indicator of flow conditions. As shown in Figure 10.12*b*, for $Re_\delta \lesssim 30$, the film is laminar and wave free. For increased Re_δ, ripples or waves form on the condensate film, and at $Re_\delta \approx 1800$ the transition from laminar to turbulent flow is complete.

For the wave-free laminar region ($Re_\delta \lesssim 30$), Equations 10.35 and 10.20 may be combined to yield

$$Re_\delta = \frac{4g\rho_l(\rho_l - \rho_v)\delta^3}{3\mu_l^2} \tag{10.37}$$

Assuming $\rho_l \gg \rho_v$ and substituting from Equations 10.26 and 10.31, Equation 10.37 can be expressed in terms of a modified Nusselt number:

$$\frac{\bar{h}_L(\nu_l^2/g)^{1/3}}{k_l} = 1.47Re_\delta^{-1/3} \qquad Re_\delta \lesssim 30 \tag{10.38}$$

In the laminar wavy region, Kutateladze [45] recommends a correlation of the form

$$\frac{\bar{h}_L(\nu_l^2/g)^{1/3}}{k_l} = \frac{Re_\delta}{1.08Re_\delta^{1.22} - 5.2} \qquad 30 \lesssim Re_\delta \lesssim 1800 \tag{10.39}$$

and for the turbulent region, Labuntsov [46] recommends

$$\frac{\bar{h}_L(\nu_l^2/g)^{1/3}}{k_l} = \frac{Re_\delta}{8750 + 58Pr_l^{-0.5}(Re_\delta^{0.75} - 253)} \qquad Re_\delta \gtrsim 1800 \tag{10.40}$$

Graphical representation of the foregoing correlations is provided in Figure 10.13, and the trends have been verified experimentally by Gregorig et al. [47] for water over the range $1 < Re_\delta < 7200$. All properties are evaluated as for laminar film condensation, as explained beneath Equation 10.32.

The Reynolds number in Equations 10.38 through 10.40 is associated with the film thickness that exists at the bottom of the condensing surface, $x = L$. To use

Patent Owner Manufacturing Resources International, Inc.
Exhibit 2017 - Page 653 of 999

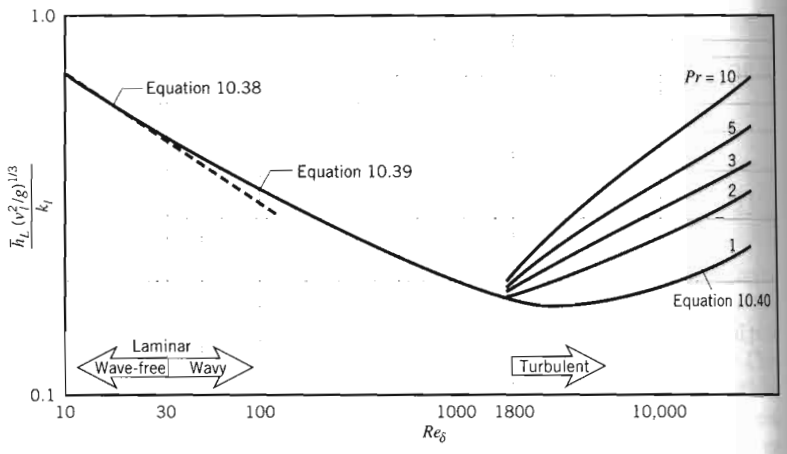


FIGURE 10.13 Modified Nusselt number for condensation on a vertical plate.

these equations, it is necessary to determine the value of the Reynolds number, Re_δ. To do so, Equations 10.34 and 10.36 may be combined to provide

$$\bar{h}_L = \frac{Re_\delta \mu_l h'_{fg}}{4L(T_{sat} - T_s)} \tag{10.41}$$

and expressions for $\bar{h}_L$ may be determined from Equations 10.38, 10.39, and 10.40 and substituted into Equation 10.41 to yield

$$Re_\delta = 3.78\left[\frac{k_l L(T_{sat} - T_s)}{\mu_l h'_{fg}(v_l^2/g)^{1/3}}\right]^{3/4} \qquad Re_\delta \lesssim 30 \tag{10.42}$$

$$Re_\delta = \left[\frac{3.70 k_l L(T_{sat} - T_s)}{\mu_l h'_{fg}(v_l^2/g)^{1/3}} + 4.8\right]^{0.82} \qquad 30 \lesssim Re_\delta \lesssim 1800 \tag{10.43}$$

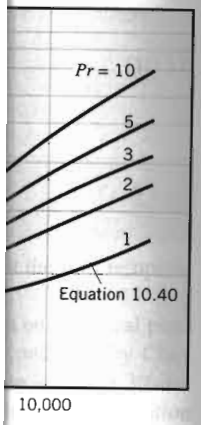
$$Re_\delta = \left[\frac{0.069 k_l L(T_{sat} - T_s)}{\mu_l h'_{fg}(v_l^2/g)^{1/3}} Pr_l^{0.5} - 151 Pr_l^{0.5} + 253\right]^{4/3} \qquad Re_\delta \gtrsim 1800 \tag{10.44}$$

For a particular problem, Equations 10.42 through 10.44 may each be solved for Re_δ, yielding three possible values of the Reynolds number. The correct value is the one that lies within the range of application listed with the equation. Once Re_δ is known, the average convection coefficient can be found most readily from Equation 10.41.

EXAMPLE 10.3

The outer surface of a vertical tube, which is 1 m long and has an outer diameter of 80 mm, is exposed to saturated steam at atmospheric pressure and is maintained at 50°C by the flow of cool water through the tube. What is the rate of heat transfer to the coolant, and what is the rate at which steam is condensed at the surface?

Patent Owner Manufacturing Resources International, Inc.
Exhibit 2017 - Page 654 of 999



l plate.

ynolds number, Re_δ.
le

(10.41)

8, 10.39, and 10.40

30 (10.42)

$Re_\delta \lesssim 1800$ (10.43)

800 (10.44)

h be solved for Re_δ,
ect value is the one
Once Re_δ is known,
n Equation 10.41.

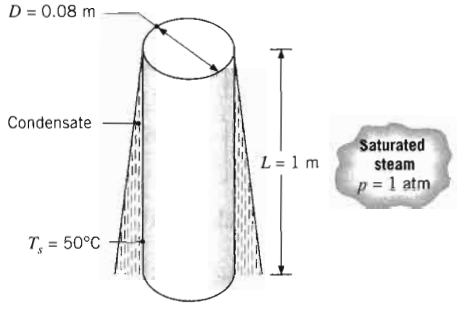
n outer diameter of
ıd is maintained at
of heat transfer to
surface?

SOLUTION

Known: Dimensions and temperature of a vertical tube experiencing condensation of steam at its outer surface.

Find: Heat transfer and condensation rates.

Schematic:



Assumptions: The condensate film thickness is small relative to the cylinder diameter.

Properties: Table A.6, saturated vapor (p = 1.0133 bars): T_{sat} = 100°C, $\rho_v = (1/v_g) = 0.596$ kg/m^3, $h_{fg} = 2257$ kJ/kg. Table A.6, saturated liquid (T_f = 75°C): $\rho_l = (1/v_f) = 975$ kg/m^3, $\mu_l = 375 \times 10^{-6}$ N · s/m^2, $k_l = 0.668$ W/m · K, $c_{p,l} = 4193$ J/kg · K, $\nu_l = \mu_l/\rho_l = 385 \times 10^{-9}$ m^2/s.

Analysis: Since we assume the film thickness is small relative to the cylinder diameter, we may use the correlations of Sections 10.7 and 10.8. With

$$Ja = \frac{c_{p,l}(T_{sat} - T_s)}{h_{fg}} = \frac{4193 \text{ J/kg} \cdot \text{K}(100 - 50) \text{ K}}{2257 \times 10^3 \text{ J/kg}} = 0.0929$$

it follows that

$$h'_{fg} = h_{fg}(1 + 0.68Ja) = 2257 \text{ kJ/kg } (1.0632) = 2400 \text{ kJ/kg}$$

Equations 10.42, 10.43, and 10.44 may each be solved for possible values of Re_δ. In particular, Equation 10.43 yields

$$Re_\delta = \left[\frac{3.70 \times 0.668 \text{ W/m} \cdot \text{K} \times 1 \text{ m} \times (100 - 50)\text{K}}{375 \times 10^{-6} \text{ N} \cdot \text{s/m}^2 \times 2.4 \times 10^6 \text{ J/kg} \left(\frac{(385 \times 10^{-9} \text{ m}^2/\text{s})^2}{9.8 \text{ m/s}^2} \right)^{1/3}} + 4.8 \right]^{0.82}$$

$$= 1177$$

Since the range of applicability of Equation 10.43 is $30 \lesssim Re_\delta \lesssim 1800$, the correct Reynolds number is 1177. It follows from Equation 10.41 that

$$\bar{h}_L = \frac{1177 \times 375 \times 10^{-6} \text{kg/s} \cdot \text{m} \times 2.4 \times 10^6 \text{ J/kg}}{4 \times 1 \text{ m } (100 - 50) \text{ K}} = 5300 \text{ W/m}^2 \cdot \text{K}$$

Patent Owner Manufacturing Resources International, Inc.
Exhibit 2017 - Page 655 of 999

and from Equations 10.33 and 10.34

$$q = \bar{h}_L(\pi DL)(T_{sat} - T_s) = 5300\ \text{W/m}^2 \cdot \text{K} \times \pi \times 0.08\ \text{m} \times 1\ \text{m}\ (100 - 50)\ \text{K} = 66.6\ \text{kW}$$

$$\dot{m} = \frac{q}{h'_{fg}} = \frac{66.6 \times 10^3\ \text{W}}{2.4 \times 10^6\ \text{J/kg}} = 0.0276\ \text{kg/s}$$

Note that using Equation 10.26, with the corrected latent heat, the film thickness at the bottom of the tube $\delta(L)$ for the wave-free laminar assumption is

$$\delta(L) = \left[\frac{4k_l\mu_l(T_{sat} - T_s)L}{g\rho_l(\rho_l - \rho_v)h'_{fg}}\right]^{1/4}$$

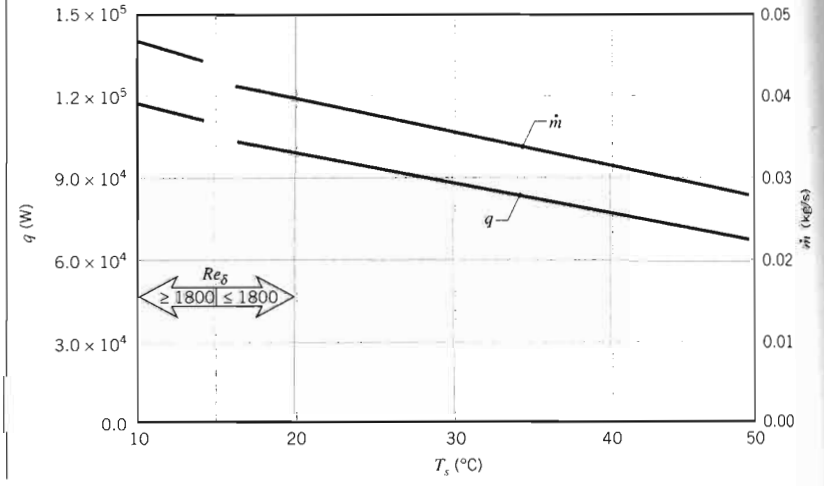
$$\delta(L) = \left[\frac{4 \times 0.668\ \text{W/m} \cdot \text{K} \times 375 \times 10^{-6}\ \text{kg/s} \cdot \text{m}\ (100 - 50)\ \text{K} \times 1\ \text{m}}{9.8\ \text{m/s}^2 \times 975\ \text{kg/m}^3\ (975 - 0.596)\ \text{kg/m}^3 \times 2.4 \times 10^6\ \text{J/kg}}\right]^{1/4}$$

$$\delta(L) = 2.18 \times 10^{-4}\ \text{m} = 0.218\ \text{mm}$$

Hence $\delta(L) \ll (D/2)$, and use of the vertical plate correlation for a vertical cylinder is justified.

Comments:

1. Equations 10.43 and 10.45 yield Reynolds number values of 910 and 1019, respectively. These Reynolds number values lie outside the ranges of applicability of these equations, and therefore Equations 10.43 and 10.45 are not appropriate for use in this problem.
2. The condensation heat and mass rates may be increased by reducing the temperature of the water flowing through the tube. For $10 \leq T_s \leq 50°\text{C}$, the calculations yield the following variations:



10.9 Film Conden

Patent Owner Manufacturing Resources International, Inc.
Exhibit 2017 - Page 656 of 999

for which $1969 \geq Re_\delta \geq 1173$ and $5155 \leq \bar{h}_L \leq 5285$ W/m$^2 \cdot$ K. Due to an increase in the condensation rate, Re_δ increases with decreasing T_s. However, a corresponding increase in the thickness of the film causes a slight reduction in the average convection coefficient. The foregoing calculations were performed by using the wavy-laminar correlation, Equation 10.39, under conditions for which $Re_\delta < 1800$ ($T_s > 15$°C) and the turbulent correlation, Equation 10.40, for $Re_\delta > 1800$. Note, however, that the correlations do not provide equivalent results at $Re_\delta = 1800$. Moreover, there is a narrow Reynolds number range about 1800 for which values of Re_δ computed from Equation 10.39 slightly exceed 1800, while values of Re_δ computed from Equation 10.40 are slightly less than 1800.

10.9 *Film Condensation on Radial Systems*

The Nusselt analysis may be extended to laminar film condensation on the outer surface of a sphere and a horizontal tube (Figures 10.14*a*, *b*), and the average convection coefficient may be expressed as

$$\bar{h}_D = C\left[\frac{g\rho_l(\rho_l - \rho_v)k_l^3 h'_{fg}}{\mu_l(T_{sat} - T_s)D}\right]^{1/4} \tag{10.45}$$

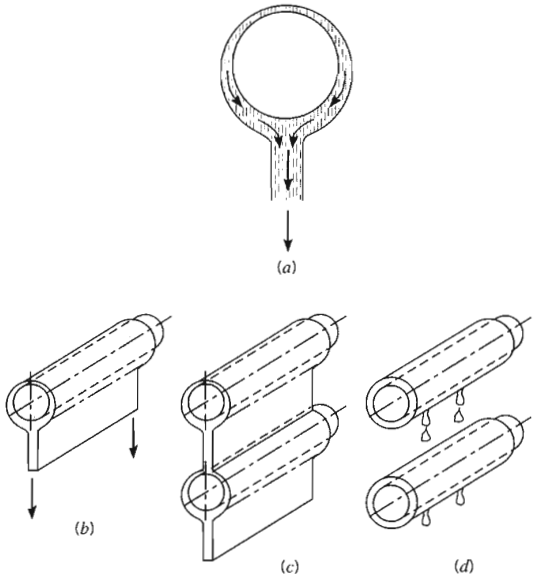


FIGURE 10.14 Film condensation on (*a*) a sphere, (*b*) a single horizontal tube, (*c*) a vertical tier of horizontal tubes with a continuous condensate sheet, and (*d*) with dripping condensate.

Patent Owner Manufacturing Resources International, Inc.
Exhibit 2017 - Page 657 of 999

where $C = 0.826$ for the sphere [48] and 0.729 for the tube [44]. The properties in this equation and the one below are evaluated as explained beneath Equation 10.32.

For a vertical tier of N horizontal tubes, Figure 10.14*c*, the average convection coefficient (over the N tubes) may be expressed as

$$\bar{h}_{D,N} = 0.729 \left[\frac{g\rho_l(\rho_l - \rho_v)k_l^3 h'_{fg}}{N\mu_l(T_{sat} - T_s)D} \right]^{1/4} \tag{10.46}$$

That is, $\bar{h}_{D,N} = \bar{h}_D N^{-1/4}$, where $\bar{h}_D$ is the heat transfer coefficient for the first (upper) tube. Such an arrangement is often used in condenser design. The reduction in $\bar{h}$ with increasing N may be attributed to an increase in the average film thickness for each successive tube. Equations 10.45 and 10.46 are generally in agreement with or slightly lower than experimental results for pure vapors. Departures may be attributed to ripples in the liquid surface for the single horizontal tube. For the tube bank, it is assumed that the condensate falls in a continuous sheet (Figure 10.14*c*) and two effects are neglected: heat transfer to the condensate sheet between the tubes and momentum gain as the sheet falls freely under gravity. These effects enhance heat transfer, and Chen [49] has accounted for their influence in terms of the Jakob number and the number of tubes. For $Ja < 0.1$, however, heat transfer is enhanced by less than 15%. Despite this correction, experimental results tend to be higher than the predictions. A plausible explanation for the discrepancy is that, rather than flow as a continuous sheet, the condensate drips from tube to tube, as illustrated in Figure 10.14*d*. Dripping reduces the sheet thickness and promotes turbulence, thereby enhancing heat transfer.

If the length-to-diameter ratio exceeds $1.8 \tan\theta$ [50], the foregoing equations may be applied to inclined tubes by replacing g with $g\cos\theta$, where the angle θ is measured from the horizontal position. In the presence of noncondensable gases, however, the convection coefficient will be less than predictions based on the foregoing correlations.

EXAMPLE 10.4

A steam condenser consists of a square array of 400 tubes, each 6 mm in diameter. If the tubes are exposed to saturated steam at a pressure of 0.15 bar and the tube surface temperature is maintained at 25°C, what is the rate at which steam is condensed per unit length of the tubes?

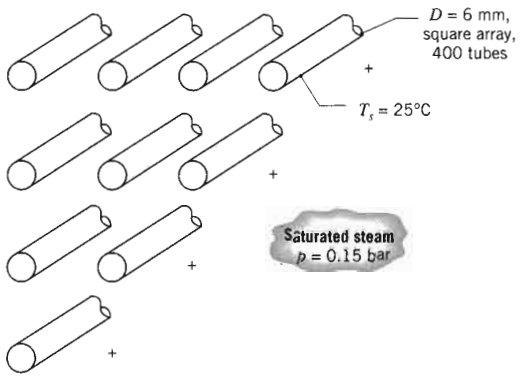
SOLUTION

Known: Configuration and surface temperature of condenser tubes exposed to saturated steam at 0.15 bar.

Find: Condensation rate per unit length of tubes.

Patent Owner Manufacturing Resources International, Inc.
Exhibit 2017 - Page 658 of 999

Schematic:



Assumptions:

1. Negligible concentration of noncondensable gases in the steam.
2. Laminar film condensation on the tubes.

Properties: Table A.6, saturated vapor ($p = 0.15$ bar): $T_{sat} = 327$ K = 54°C, $\rho_v = (1/v_g) = 0.098$ kg/m^3, $h_{fg} = 2373$ kJ/kg. Table A.6, saturated water ($T_f = 312.5$ K): $\rho_l = (1/v_f) = 992$ kg/m^3, $\mu_l = 663 \times 10^{-6}$ N · s/m^2, $k_l = 0.631$ W/m · K, $c_{p,l} = 4178$ J/kg · K.

Analysis: The *average* condensation rate for a single tube of the array may be obtained from Equation 10.34, where for a unit length of the tube,

$$\dot{m}_1' = \frac{q_1'}{h_{fg}'} = \frac{\bar{h}_{D,N}(\pi D)(T_{sat} - T_s)}{h_{fg}'}$$

From Equation 10.46

$$\bar{h}_{D,N} = 0.729 \left[\frac{g\rho_l(\rho_l - \rho_v)k_l^3 h_{fg}'}{N\mu_l(T_{sat} - T_s)D} \right]^{1/4}$$

or with $N = 20$, $Ja = 0.051$, and $h_{fg}' = 2455$ kJ/kg,

$$\begin{aligned}\bar{h}_{D,N} = 0.729 \{ &[9.8 \text{ m/s}^2 \times 992 \text{ kg/m}^3 (992 - 0.098) \text{ kg/m}^3 \\ &\times (0.631 \text{ W/m} \cdot \text{K})^3 2.455 \times 10^6 \text{ J/kg}] \\ &\div [20 \times 663 \times 10^{-6} \text{ kg/s} \cdot \text{m} (54 - 25) \text{ K} \times 0.006 \text{ m}] \}^{1/4}\end{aligned}$$

$$\bar{h}_{D,N} = 5194 \text{ W/m}^2 \cdot \text{K}$$

Hence the average condensation rate for a single tube is

$$\dot{m}_1' = \frac{5194 \text{ W/m}^2 \cdot \text{K}(\pi \times 0.006 \text{ m})(54 - 25) \text{ K}}{2.455 \times 10^6 \text{ J/kg}} = 1.16 \times 10^{-3} \text{ kg/s} \cdot \text{m}$$

For the complete array, the condensation rate per unit length is then

$$\dot{m}' = N^2 \dot{m}_1' = 400 \times 1.16 \times 10^{-3} \text{ kg/s} \cdot \text{m} = 0.464 \text{ kg/s} \cdot \text{m} \quad \triangleleft$$

Patent Owner Manufacturing Resources International, Inc.
Exhibit 2017 - Page 659 of 999

Comments: Since $Ja < 0.1$, Equation 10.46 provides a reliable estimate of the average heat transfer coefficient.

10.10 *Film Condensation in Horizontal Tubes*

Condensers used for refrigeration and air-conditioning systems generally involve vapor condensation inside horizontal or vertical tubes. Conditions within the tube are complicated and depend strongly on the velocity of the vapor flowing through the tube. If this velocity is small, condensation occurs in the manner depicted by Figure 10.15*a* for a horizontal tube. That is, the condensate flow is from the upper portion of the tube to the bottom, from whence it flows in a longitudinal direction with the vapor. For low vapor velocities such that

$$Re_{v,i} = \left(\frac{\rho_v u_{m,v} D}{\mu_v}\right)_i < 35{,}000$$

where i refers to the tube inlet, Chato [51] recommends an expression of the form

$$\overline{h}_D = 0.555\left[\frac{g\rho_l(\rho_l - \rho_v)k_l^3 h'_{fg}}{\mu_l(T_{\text{sat}} - T_s)D}\right]^{1/4} \tag{10.47}$$

where, for this case, the modified latent heat is

$$h'_{fg} \equiv h_{fg} + \tfrac{3}{8}c_{p,l}(T_{\text{sat}} - T_s) \tag{10.48}$$

The properties in these equations are evaluated as explained beneath Equation 10.32.

At higher vapor velocities the two-phase flow regime becomes annular (Figure 10.15*b*). The vapor occupies the core of the annulus, diminishing in diameter as the thickness of the outer condensate layer increases in the flow direction. Results for this flow condition are provided by Marto [52].

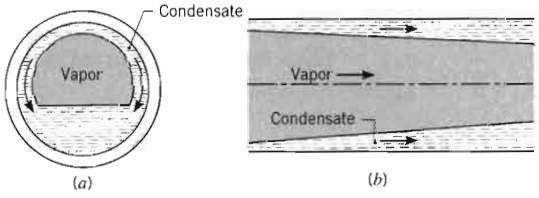


FIGURE 10.15 Film condensation in a horizontal tube. (*a*) Cross section of condensate flow for low vapor velocities. (*b*) Longitudinal section of condensate flow for large vapor velocities.

10.11 *Dropwise Con*

10.12 *Summary*

Patent Owner Manufacturing Resources International, Inc.
Exhibit 2017 - Page 660 of 999

liable estimate of the

ns generally involve
tions within the tube
apor flowing through
manner depicted by
ow is from the upper
ongitudinal direction

ssion of the form

(10.47)

(10.48)

heath Equation 10.32.
omes annular (Figure
ng in diameter as the
direction. Results for

10.11 *Dropwise Condensation*

Typically, heat transfer coefficients for dropwise condensation are an order of magnitude larger than those for film condensation. In fact, in heat exchanger applications for which dropwise condensation is promoted, other thermal resistances may be significantly larger than that due to condensation and, therefore, reliable correlations for the condensation process are not needed.

Of the many surface–fluid systems studied [53], most of the data are for steam condensation on well-promoted copper surfaces—that is, surfaces for which wetting is inhibited—and are correlated by an expression of the form [54]

$$\bar{h}_{dc} = 51{,}104 + 2044T_{sat}(°C) \qquad 22°C \lesssim T_{sat} \lesssim 100°C \tag{10.49}$$

$$\bar{h}_{dc} = 255{,}510 \qquad 100°C \lesssim T_{sat} \tag{10.50}$$

where the heat transfer coefficient has units of $(W/m^2 \cdot K)$. The heat transfer rate and condensation rate can be calculated from Equations 10.33 and 10.34, where h'_{fg} is given by Equation 10.27, and properties are evaluated as explained beneath Equation 10.32. The effect of subcooling, $T_{sat} - T_s$, on $\bar{h}_{dc}$ is small and may be neglected.

The effect of noncondensable vapors in the steam can be very important and has been studied by Shade and Mikic [55]. In addition, if the condensing surface material does not conduct as well as copper or silver, its thermal resistance becomes a factor. Since all the heat is transferred to the drops, which are very small and widely distributed over the surface, heat flow lines within the surface material near the active areas of condensation will *crowd,* inducing a *constriction* resistance. This effect has been studied by Hannemann and Mikic [56].

10.12 *Summary*

It is apparent that boiling and condensation are complicated processes for which the existence of generalized relations is somewhat limited. This chapter identifies the essential physical features of the processes and presents correlations suitable for approximate engineering calculations. However, a great deal of additional information is available, and much of it has been summarized in several extensive reviews of the subject [7, 15, 25, 30–33, 52, 54, 56–61].

You may test your understanding of heat transfer with phase change by addressing the following questions.

- What is *pool boiling*? *Forced convection boiling*? *Subcooled boiling*? *Saturated boiling*?
- How is the *excess temperature* defined?
- Sketch the *boiling curve* and identify key regimes and features. What is the *critical heat flux*? What is the *Leidenfrost point*? How does progression along the boiling curve occur if the surface heat flux is controlled? What is the nature

Patent Owner Manufacturing Resources International, Inc.
Exhibit 2017 - Page 661 of 999

of the hysteresis effect? How does progression along the boiling curve occur if the surface temperature is controlled?

- How does heat flux depend on the excess temperature in the *nucleate boiling* regime?
- What modes of heat transfer are associated with *film boiling*?
- How is the amount of liquid *subcooling* defined?
- To what extent is the boiling heat flux influenced by the magnitude of the gravitational field, liquid subcooling, and surface roughness?
- How do two-phase flow and heat transfer in microchannels differ from two-phase flow and heat transfer in larger tubes?
- How does *dropwise condensation* differ from *film condensation*? Which mode of condensation is characterized by larger heat transfer rates?
- For laminar film condensation on a vertical surface, how do the local and average convection coefficients vary with distance from the leading edge?
- How is the Reynolds number defined for film condensation on a vertical surface? What are the corresponding flow regimes?

References

1. Fox, R. W., A. T. McDonald, and P. J. Pritchard, *Introduction to Fluid Mechanics*, 6th ed. Wiley, New York, 2003.
2. Nukiyama, S., *J. Japan Soc. Mech. Eng.*, **37**, 367, 1934 (Translation: *Int. J. Heat Mass Transfer*, **9**, 1419, 1966).
3. Drew, T. B., and C. Mueller, *Trans. AIChE*, **33**, 449, 1937.
4. Yamagata, K., F. Kirano, K. Nishiwaka, and H. Matsuoka, *Mem. Fac. Eng. Kyushu*, **15**, 98, 1955.
5. Rohsenow, W. M., *Trans. ASME*, **74**, 969, 1952.
6. Vachon, R. I., G. H. Nix, and G. E. Tanger, *J. Heat Transfer*, **90**, 239, 1968.
7. Collier, J. G., and J. R. Thome, *Convective Boiling and Condensation*, 3rd ed., Oxford University Press, New York, 1996.
8. Pioro I. L., *Int. J. Heat Mass Transfer*, **42**, 2003, 1999.
9. Kutateladze, S. S., *Kotloturbostroenie*, **3**, 10, 1948.
10. Zuber, N., *Trans. ASME*, **80**, 711, 1958.
11. Lienhard, J. H., *A Heat Transfer Textbook*, 2nd ed., Prentice-Hall, Englewood Cliffs, NJ, 1987.
12. Nakayama, W., A. Yabe, P. Kew, K. Cornwell, S. G. Kandlikar, and V. K. Dhir, in S. G. Kandlikar, M. Shoji, and V. K. Dhir, Eds., *Handbook of Phase Change: Boiling and Condensation*, Chap. 16, Taylor & Francis, New York, 1999.
13. Cichelli, M. T., and C. F. Bonilla, *Trans. AIChE*, **41**, 755, 1945.
14. Berenson, P. J., *J. Heat Transfer*, **83**, 351, 1961.
15. Hahne, E., and U. Grigull, *Heat Transfer in Boiling*, Hemisphere/Academic Press, New York, 1977.
16. Lienhard, J. H., and P. T. Y. Wong, *J. Heat Transfer*, **86**, 220, 1964.
17. Bromley, L. A., *Chem. Eng. Prog.*, **46**, 221, 1950.
18. Sadasivan, P., and J. H. Lienhard, *J. Heat Transfer*, **109**, 545, 1987.
19. Siegel, R., *Adv. Heat Transfer*, **4**, 143, 1967.
20. Berensen, P. J., *Int. J. Heat Mass Transfer*, **5**, 985, 1962.
21. Webb, R. L., *Heat Transfer Eng.*, **2**, 46, 1981, and *Heat Transfer Eng.*, **4**, 71, 1983.
22. Bergles, A. E., "Enhancement of Heat Transfer," *Heat Transfer 1978*, Vol. 6, pp. 89–108, Hemisphere Publishing, New York, 1978.
23. Bergles, A. E., in G. F. Hewitt, Exec. Ed., *Heat Exchanger Design Handbook*, Section 2.7.9, Begell House, New York, 2002.
24. Bergles, A. E., and W. H. Rohsenow, *J. Heat Transfer*, **86**, 365, 1964.
25. van Stralen, S., and R. Cole, *Boiling Phenomena*, McGraw-Hill/Hemisphere, New York, 1979.
26. Lienhard, J. H., and R. Eichhorn, *Int. J. Heat Mass Transfer*, **19**, 1135, 1976.
27. Kandlikar, S. G., *J. Heat Transfer*, **112**, 219, 1990.
28. Kandlikar, S. G., and H. Nariai, in S. G. Kandlikar, M. Shoji, and V. K. Dhir, Eds., *Handbook of Phase Change: Boiling and Condensation*, Chap. 15, Taylor & Francis, New York, 1999.
29. Celata, G. P., and
and V. K. Dhir, Ed
and Condensation
1999.
30. Tong, L. S., and Y
Phase Flow, 2nd e
31. Rohsenow, W. M
nett, Eds., *Han*
McGraw-Hill, N
32. Griffith, P., in W
Handbook of H
New York, 1973
33. Ginoux, J. N.,
McGraw-Hill/H
34. Hall, D. D., and
43, 2573, 2000.
35. Hall, D. D., and
43, 2605, 2000.
36. Qu, W., and I. M
2755, 2003.
37. Ghiaasiaan, S. M
T. F. Irvine, Y. I
Heat Transfer, V
38. Qu, W., and I. I
2773, 2003.
39. Sparrow, E. M
13, 1959.
40. Koh, J. C. Y.,
Heat Mass Tra
41. Nusselt, W., Z.
42. Rohsenow, W.
43. Chen, M. M.,
44. Dhir, V. K., ar
1971.
45. Kutateladze, S
demic Press, N
46. Labuntsov, D.

Problems

General Cons

10.1 Show that,
$T_{sat} = 10°C$,
What is the
that this con

Patent Owner Manufacturing Resources International, Inc.
Exhibit 2017 - Page 662 of 999

29. Celata, G. P., and A. Mariani, in S. G. Kandlikar, M. Shoji, and V. K. Dhir, Eds., *Handbook of Phase Change: Boiling and Condensation*, Chap. 17, Taylor & Francis, New York, 1999.

30. Tong, L. S., and Y. S. Tang, *Boiling Heat Transfer and Two Phase Flow*, 2nd ed., Taylor & Francis, New York, 1997.

31. Rohsenow, W. M., in W. M. Rohsenow and J. P. Hartnett, Eds., *Handbook of Heat Transfer*, Chap. 13, McGraw-Hill, New York, 1973.

32. Griffith, P., in W. M. Rohsenow and J. P. Hartnett, Eds., *Handbook of Heat Transfer*, Chap. 14, McGraw-Hill, New York, 1973.

33. Ginoux, J. N., *Two-Phase Flow and Heat Transfer*, McGraw-Hill/Hemisphere, New York, 1978.

34. Hall, D. D., and I. Mudawar, *Int. J. Heat Mass Transfer*, **43**, 2573, 2000.

35. Hall, D. D., and I. Mudawar, *Int. J. Heat Mass Transfer*, **43**, 2605, 2000.

36. Qu, W., and I. Mudawar, *Int. J. Heat Mass Transfer*, **46**, 2755, 2003.

37. Ghiaasiaan, S. M., and S. I. Abdel-Khalik, in J. P. Hartnett, T. F. Irvine, Y. I. Cho, and G. A. Greene, Eds., *Advances in Heat Transfer*, Vol. 34, Academic Press, New York, 2001.

38. Qu, W., and I. Mudawar, *Int. J. Heat Mass Transfer*, **46**, 2773, 2003.

39. Sparrow, E. M., and J. L. Gregg, *J. Heat Transfer*, **81**, 13, 1959.

40. Koh, J. C. Y., E. M. Sparrow, and J. P. Hartnett, *Int. J. Heat Mass Transfer*, **2**, 69, 1961.

41. Nusselt, W., *Z. Ver. Deut. Ing.*, **60**, 541, 1916.

42. Rohsenow, W. M., *Trans. ASME*, **78**, 1645, 1956.

43. Chen, M. M., *J. Heat Transfer*, **83**, 48, 1961.

44. Dhir, V. K., and J. H. Lienhard, *J. Heat Transfer*, **93**, 97, 1971.

45. Kutateladze, S. S., *Fundamentals of Heat Transfer*, Academic Press, New York, 1963.

46. Labuntsov, D. A., *Teploenergetika*, **4**, 72, 1957.

47. Gregorig, R., J. Kern, and K. Turek, *Wärme Stoffübertrag.*, **7**, 1, 1974.

48. Popiel, Cz. O., and L. Boguslawski, *Int. J. Heat Mass Transfer*, **18**, 1486, 1975.

49. Chen, M. M., *J. Heat Transfer*, **83**, 55, 1961.

50. Selin, G., "Heat Transfer by Condensing Pure Vapours Outside Inclined Tubes," *International Developments in Heat Transfer*, Part 2, International Heat Transfer Conference, University of Colorado, pp. 278–289, ASME, New York, 1961.

51. Chato, J. C., *J. ASHRAE*, **4**, 52, 1962.

52. Marto, P. J., in W. M. Rohsenow, J. P. Hartnett, and Y. I. Cho, Eds., *Handbook of Heat Transfer*, 3rd ed., Chap. 14, McGraw-Hill, New York, 1998.

53. Tanner, D. W., D. Pope, C. J. Potter, and D. West, *Int. J. Heat Mass Transfer*, **11**, 181, 1968.

54. Griffith, P., in G. F. Hewitt, Exec. Ed., *Heat Exchanger Design Handbook*, Section 2.6.5, Hemisphere Publishing, New York, 1990.

55. Shade, R., and B. Mikic, "The Effects of Non-condensable Gases on Heat Transfer During Dropwise Condensation," Paper 67b presented at the 67th Annual Meeting of the American Institute of Chemical Engineers, Washington, DC, 1974.

56. Hannemann, R., and B. Mikic, *Int. J. Heat Mass Transfer*, **19**, 1309, 1976.

57. Collier, J. G., and V. Wadekar, in G. F. Hewitt, Exec. Ed., *Heat Exchanger Design Handbook*, Section 2.7.2, Begell House, New York, 2002.

58. Butterworth, D., in D. Butterworth and G. F. Hewitt, Eds., *Two-Phase Flow and Heat Transfer*, Oxford University Press, London, 1977, pp. 426–462.

59. McNaught, J., and D. Butterworth, in G. F. Hewitt, Exec. Ed., *Heat Exchanger Design Handbook*, Section 2.6.2, Begell House, New York, 2002.

60. Rose, J. W., *Int. J. Heat Mass Transfer*, **24**, 191, 1981.

61. Pioro, L. S., and I. L. Pioro, *Industrial Two-Phase Thermosyphons*, Begell House, New York, 1997.

Problems

General Considerations

10.1 Show that, for water at 1-atm pressure with $T_s - T_{sat} = 10°C$, the Jakob number is much less than unity. What is the physical significance of this result? Verify that this conclusion applies to other fluids.

10.2 The surface of a horizontal, 20-mm-diameter cylinder is maintained at an excess temperature of 5°C in saturated water at 1 atm. Estimate the heat flux using the appropriate free convection correlation and compare your result with the boiling curve of Figure 10.4. For nucleate boiling, estimate the

Patent Owner Manufacturing Resources International, Inc.
Exhibit 2017 - Page 663 of 999

maximum value of the heat transfer coefficient from the boiling curve.

10.3 The role of surface tension in bubble formation can be demonstrated by considering a spherical bubble of pure saturated vapor in *mechanical* and *thermal* equilibrium with its superheated liquid.

(a) Beginning with an appropriate free-body diagram of the bubble, perform a force balance to obtain an expression of the bubble radius,

$$r_b = \frac{2\sigma}{p_{sat} - p_l}$$

where p_{sat} is the pressure of the saturated vapor and p_l is the pressure of the superheated liquid outside the bubble.

(b) On a p–v diagram, represent the bubble and liquid states. Discuss what changes in these conditions will cause the bubble to grow or collapse.

(c) Calculate the bubble size under equilibrium conditions for which the vapor is saturated at 101°C and the liquid pressure corresponds to a saturation temperature of 100°C.

Nucleate Boiling and Critical Heat Flux

10.4 A long, 1-mm-diameter wire passes an electrical current dissipating 3150 W/m and reaches a surface temperature of 126°C when submerged in water at 1 atm. What is the boiling heat transfer coefficient? Estimate the value of the correlation coefficient $C_{s,f}$.

10.5 Estimate the nucleate pool boiling heat transfer coefficient for water boiling at atmospheric pressure on the outer surface of a platinum-plated 10-mm-diameter tube maintained 10°C above the saturation temperature.

10.6 Plot the nucleate boiling heat flux for saturated water at atmospheric pressure on a large, horizontal polished copper plate, over the excess temperature range $5°C \leq \Delta T_e \leq 30°C$. Compare your results with Figure 10.4. Also find the excess temperature corresponding to the critical heat flux.

10.7 A simple expression to account for the effect of pressure on the nucleate boiling convection coefficient in water (W/m^2 · K) is

$$h = C(\Delta T_e)^n \left(\frac{p}{p_a}\right)^{0.4}$$

where p and p_a are the system pressure and standard atmospheric pressure, respectively. For a horizontal plate and the range $15 < q_s'' < 235$ kW/m^2, $C = 5.56$ and $n = 3$. Units of ΔT_e are kelvins. Compare predictions from this expression with the Rohsenow correlation ($C_{s,f} = 0.013$, $n = 1$) for pressures of 2 and 5 bars with $\Delta T_e = 10°C$.

10.8 In Example 10.1 we considered conditions for which vigorous boiling occurs in a pan of water, and we determined the electric power (heat rate) required to maintain a prescribed temperature for the bottom of the pan. However, the electric power is, in fact, the control (independent) variable, from which the temperature of the pan follows.

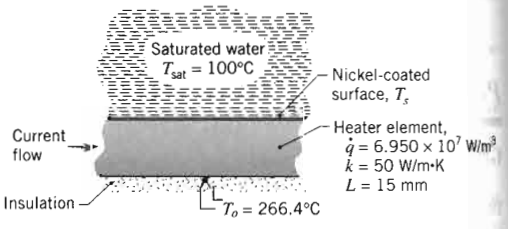
(a) For nucleate boiling in the copper pan of Example 10.1, compute and plot the temperature of the pan as a function of the heat rate for $1 \leq q \leq 100$ kW.

(b) If the water is initially at room temperature, it must, of course, be heated for a period of time before it will boil. Consider conditions shortly after heating is initiated and the water is at 20°C. Estimate the temperature of the pan bottom for a heat rate of 8 kW.

10.9 Calculate the critical heat flux on a large horizontal surface for the following fluids at 1 atm: mercury, ethanol, and refrigerant R-134a. Compare these results to the critical heat flux for water at 1 atm.

10.10 The bottom of a copper pan, 150 mm in diameter, is maintained at 115°C by the heating element of an electric range. Estimate the power required to boil the water in this pan. Determine the evaporation rate. What is the ratio of the surface heat flux to the critical heat flux? What pan temperature is required to achieve the critical heat flux?

10.11 A nickel-coated heater element with a thickness of 15 mm and a thermal conductivity of 50 W/m · K is exposed to saturated water at atmospheric pressure. A thermocouple is attached to the back surface, which is well insulated. Measurements at a particular operating condition yield an electrical power dissipation in the heater element of 6.950×10^7 W/m^3 and a temperature of $T_o = 266.4°C$.



(a) From the foregoing data, calculate the surface temperature, T_s, and the heat flux at the exposed surface.

Patent Owner Manufacturing Resources International, Inc.
Exhibit 2017 - Page 664 of 999

(b) Using the surface heat flux determined in part (a), estimate the surface temperature by applying an appropriate boiling correlation.

10.12 Advances in very large scale integration (VLSI) of electronic devices on a chip are often restricted by the ability to cool the chip. For mainframe computers, an array of several hundred chips, each of area 25 mm^2, may be mounted on a ceramic substrate. A method of cooling the array is by immersion in a low boiling point fluid such as refrigerant R-134a. At 1 atm and 247 K, properties of the saturated liquid are $\mu = 1.46 \times 10^{-4}$ N · s/m^2, $c_p = 1551$ J/kg · K, and $Pr = 3.2$. Assume values of $C_{s,f} = 0.004$ and $n = 1.7$.

(a) Estimate the power dissipated by a single chip if it is operating at 50% of the critical heat flux. What is the corresponding value of the chip temperature?

(b) Compute and plot the chip temperature as a function of surface heat flux for $0.25 \leq q''_s/q''_{max} \leq 0.90$.

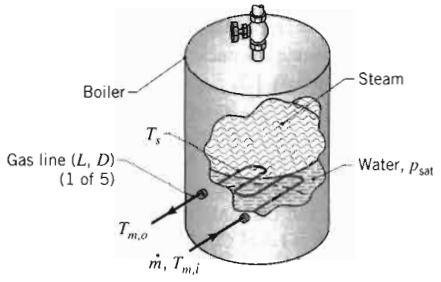
10.13 Saturated ethylene glycol at 1 atm is heated by a horizontal chromium-plated surface which has a diameter of 200 mm and is maintained at 480 K. Estimate the heating power requirement and the rate of evaporation. What fraction is the power requirement of the maximum power associated with the critical heat flux? At 470 K, properties of the saturated liquid are $\mu = 0.38 \times 10^{-3}$ N · s/m^2, $c_p = 3280$ J/kg · K, and $Pr = 8.7$. The saturated vapor density is $\rho = 1.66$ kg/m^3. Assume nucleate boiling constants of $C_{s,f} = 0.01$ and $n = 1.0$.

10.14 Copper tubes 25 mm in diameter and 0.75 m long are used to boil saturated water at 1 atm.

(a) If the tubes are operated at 75% of the critical heat flux, how many tubes are needed to provide a vapor production rate of 750 kg/h? What is the corresponding tube surface temperature?

(b) Compute and plot the tube surface temperature as a function of heat flux for $0.25 \leq q''_s/q''_{max} \leq 0.90$. On the same graph, plot the corresponding number of tubes needed to provide the prescribed vapor production rate.

10.15 Consider a gas-fired boiler in which five coiled, thin-walled, copper tubes of 25-mm diameter and 8-m length are submerged in pressurized water at 4.37 bars. The walls of the tubes are polished and may be assumed to be isothermal. Combustion gases enter each of the tubes at a temperature of $T_{m,i} = 700$°C and a flow rate of $\dot{m} = 0.08$ kg/s, respectively.



Determine the tube wall temperature T_s and the gas outlet temperature $T_{m,o}$ for the prescribed conditions. As a first approximation, the properties of the combustion gases may be taken as those of air at 700 K.

10.16 Estimate the current at which a 1-mm-diameter nickel wire will burn out when submerged in water at atmospheric pressure. The electrical resistance of the wire is 0.129 Ω/m.

10.17 Estimate the power (W/m^2) required to maintain a brass plate at $\Delta T_e = 15$°C while boiling saturated water at 1 atm. What is the power requirement if the water is pressurized to 10 atm? At what fraction of the critical heat flux is the plate operating?

10.18 It has been demonstrated experimentally that the critical heat flux is highly dependent on pressure, primarily through the pressure dependence of the fluid surface tension and latent heat of vaporization. Using Equation 10.6, calculate values of q''_{max} for water on a large horizontal surface as a function of pressure. Demonstrate that the peak critical heat flux occurs at approximately one-third the critical pressure ($p_c = 221$ bars). Since all common fluids have this characteristic, suggest what coordinates should be used to plot critical heat flux–pressure values to obtain a universal curve.

10.19 In applying dimensional analysis, Kutateladze [9] postulated that the critical heat flux varies with the heat of vaporization, vapor density, surface tension, and the bubble diameter parameter given in Equation 10.4a. Verify that dimensional analysis would yield the following expression for the critical heat flux:

$$q''_{max} = Ch_{fg}\rho_v^{1/2}D_b^{-1/2}\sigma^{1/2}$$

10.20 A dielectric fluid at atmospheric pressure is heated with a 0.5-mm-diameter, horizontal platinum wire. Determine the temperature of the wire when the wire is heated at 50% of the critical heat flux. The properties of the fluid are $c_{p,l} = 1300$ J/kg · K, $h_{fg} = 142$ kJ/kg,

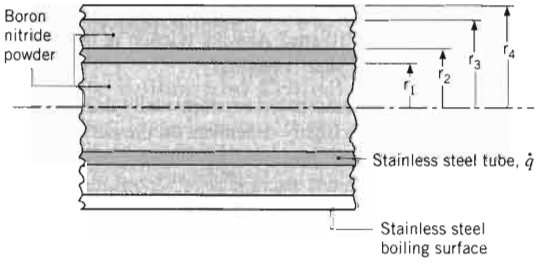
Patent Owner Manufacturing Resources International, Inc.
Exhibit 2017 - Page 665 of 999

$k_l = 0.075$ W/m · K, $\nu_l = 0.32 \times 10^{-6}$ m²/s, $\rho_l = 1400$ kg/m³, $\rho_v = 7.2$ kg/m³, $\sigma = 12.4 \times 10^{-3}$ N/m, $T_{sat} = 34$°C. Assume the nucleate boiling constants are $C_{s,f} = 0.005$ and $n = 1.7$. For small horizontal cylinders, the critical heat flux is found by multiplying the value associated with large horizontal cylinders by a correction factor F, where $F = 0.89 + 2.27 \exp(-3.44 Co^{-1/2})$. The Confinement number is based on the radius of the cylinder, and the range of applicability for the correction factor is $1.3 \lesssim Co \lesssim 6.7$ [11].

10.21 What is the critical heat flux for boiling water at 1 atm on a large horizontal surface on the surface of the moon, where the gravitational acceleration is one-sixth that of the earth?

10.22 A heater for boiling a saturated liquid consists of two concentric stainless steel tubes packed with dense boron nitride powder. Electrical current is passed through the inner tube, creating uniform volumetric heating $\dot{q}$ (W/m³). The exposed surface of the outer tube is in contact with the liquid and the boiling heat flux is given as

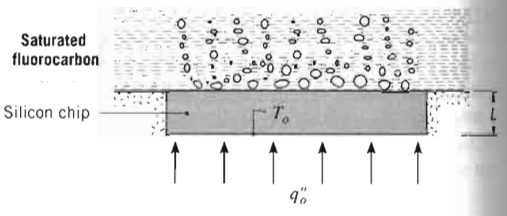
$$q_s'' = C(T_s - T_{sat})^3$$



It is feared that under high-power operation the stainless steel tubes would severely oxidize if temperatures exceed $T_{ss,x}$ or that the boron nitride would deteriorate if its temperature exceeds $T_{bn,x}$. Presuming that the saturation temperature of the liquid (T_{sat}) and the boiling surface temperature (T_s) are prescribed, derive expressions for the maximum temperatures in the stainless steel (ss) tubes and in the boron nitride (bn). Express your results in terms of geometric parameters (r_1, r_2, r_3, r_4), thermal conductivities (k_{ss}, k_{bn}), and the boiling parameters (C, T_{sat}, T_s).

10.23 A silicon chip of thickness $L = 2.5$ mm and thermal conductivity $k_s = 135$ W/m · K is cooled by boiling a saturated fluorocarbon liquid ($T_{sat} = 57$°C) on its surface. The electronic circuits on the bottom of the chip produce a uniform heat flux of $q_o'' = 5 \times 10^4$ W/m², while the sides of the chip are perfectly insulated.

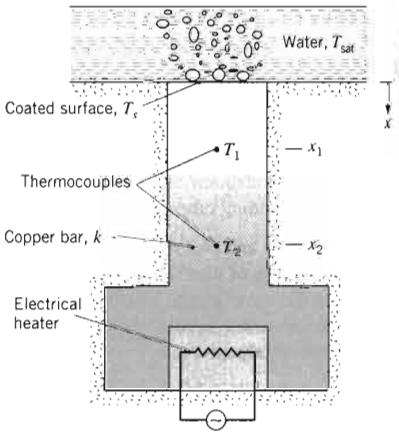
Properties of the saturated fluorocarbon are $c_{p,l} = 1100$ J/kg · K, $h_{fg} = 84{,}400$ J/kg, $\rho_l = 1619.2$ kg/m³, $\rho_v = 13.4$ kg/m³, $\sigma = 8.1 \times 10^{-3}$ kg/s², $\mu_l = 440 \times 10^{-6}$ kg/m · s, and $Pr_l = 9.01$. In addition, the nucleate boiling constants are $C_{s,f} = 0.005$ and $n = 1.7$.



(a) What is the steady-state temperature T_o at the bottom of the chip? If, during testing of the chip, q_o'' is increased to 90% of the critical heat flux, what is the new steady-state value of T_o?

(b) Compute and plot the chip surface temperatures (top and bottom) as a function of heat flux for $0.20 \leq q_o''/q_{max}'' \leq 0.90$. If the maximum allowable chip temperature is 80°C, what is the maximum allowable value of q_o''?

10.24 A device for performing boiling experiments consists of a copper bar ($k = 400$ W/m · K), which is exposed to a boiling liquid at one end, encapsulates an electrical heater at the other end, and is well insulated from its surroundings at all but the exposed surface. Thermocouples inserted in the bar are used to measure temperatures at distances of $x_1 = 10$ mm and $x_2 = 25$ mm from the surface.



(a) An experiment is performed to determine the boiling characteristics of a special coating applied to the exposed surface. Under steady-state conditions, nucleate boiling is maintained in saturated water at

atmospheri
and T_2 =
value of th
Rohsenow

(b) Assuming
with the
(a), compu
as a funct
$q_s'' \leq 10^6$ V
of T_1 an
increased
results be
values of

Minimum Heat

10.25 A small coppe
temperature T
fluid bath mai
the sphere ex
ing to the tem

(a) Sketch th
ature, $\overline{T}$(
process.
T_i, T_D, an
sition, ar
single-ph
the tempe

(b) At what
expect th
deviate r
your ans

10.26 A sphere m
eter of 20 m
suddenly ir
tained at a
sphere has

(a) Calculat
initial co
cient is

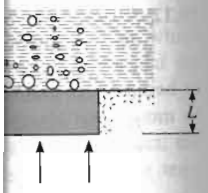
(b) Estimat
is imme

10.27 A steel bar,
an emissivit
455°C and
water bath
initial heat t

10.28 Electrical cu
diameter co
in water unc

Patent Owner Manufacturing Resources International, Inc.
Exhibit 2017 - Page 666 of 999

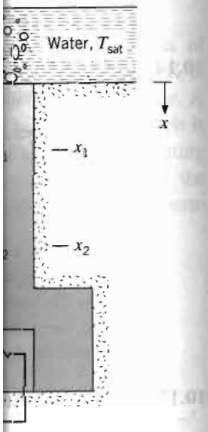
kg/s², $\mu_l = 440 \times 10^{-6}$
tion, the nucleate boil-
d $n = 1.7$.



nperature T_o at the bot-
esting of the chip, q''_o is
tical heat flux, what is
f T_o?

p surface temperatures
action of heat flux for
ne maximum allowable
what is the maximum

g experiments consists
· K), which is exposed
ncapsulates an electri-
is well insulated from
exposed surface. Ther-
e used to measure tem-
0 mm and $x_2 = 25$ mm



d to determine the boil-
ial coating applied to the
steady-state conditions,
ed in saturated water at

atmospheric pressure, and values of $T_1 = 133.7$°C and $T_2 = 158.6$°C are recorded. If $n = 1$, what value of the coefficient $C_{s,f}$ is associated with the Rohsenow correlation?

(b) Assuming applicability of the Rohsenow correlation with the value of $C_{s,f}$ determined from part (a), compute and plot the excess temperature ΔT_e as a function of the boiling heat flux for $10^5 \leq q''_s \leq 10^6$ W/m². What are the corresponding values of T_1 and T_2 for $q''_s = 10^6$ W/m²? If q''_s were increased to 1.5×10^6 W/m², could the foregoing results be extrapolated to infer the corresponding values of ΔT_e, T_1, and T_2?

Minimum Heat Flux and Film Boiling

10.25 A small copper sphere, initially at a uniform, elevated temperature $T(0) = T_i$, is suddenly immersed in a large fluid bath maintained at T_{sat}. The initial temperature of the sphere exceeds the Leidenfrost point corresponding to the temperature T_D of Figure 10.4.

(a) Sketch the variation of the average sphere temperature, $\overline{T}(t)$, with time during the quenching process. Indicate on this sketch the temperatures T_i, T_D, and T_{sat}, as well as the regimes of film, transition, and nucleate boiling and the regime of single-phase convection. Identify key features of the temperature history.

(b) At what time(s) in this cooling process do you expect the surface temperature of the sphere to deviate most from its center temperature? Explain your answer.

10.26 A sphere made of aluminum alloy 2024 with a diameter of 20 mm and a uniform temperature of 500°C is suddenly immersed in a saturated water bath maintained at atmospheric pressure. The surface of the sphere has an emissivity of 0.25.

(a) Calculate the total heat transfer coefficient for the initial condition. What fraction of the total coefficient is contributed by radiation?

(b) Estimate the temperature of the sphere 30 s after it is immersed in the bath.

10.27 A steel bar, 20 mm in diameter and 200 mm long, with an emissivity of 0.9, is removed from a furnace at 455°C and suddenly submerged horizontally in a water bath under atmospheric pressure. Estimate the initial heat transfer rate from the bar.

10.28 Electrical current passes through a horizontal, 2-mm-diameter conductor of emissivity 0.5 when immersed in water under atmospheric pressure.

(a) Estimate the power dissipation per unit length of the conductor required to maintain the surface temperature at 555°C.

(b) For conductor diameters of 1.5, 2.0, and 2.5 mm, compute and plot the power dissipation per unit length as a function of surface temperature for $250 \leq T_s \leq 650$°C. On a separate figure, plot the percentage contribution of radiation as a function of T_s.

10.29 Consider a horizontal, $D = 1$-mm-diameter platinum wire suspended in saturated water at atmospheric pressure. The wire is heated by an electrical current. Determine the heat flux from the wire at the instant when the surface of the wire reaches its melting point. Determine the corresponding centerline temperature of the wire. Due to oxidation at very high temperature, the wire emissivity is $\varepsilon = 0.80$ when it burns out. The water vapor properties at the film temperature of 1209 K are $\rho_v = 0.189$ kg/m³, $c_{p,v} = 2404$ J/kg · K, $\nu_v = 231 \times 10^{-6}$ m²/s, $k_v = 0.113$ W/m · K.

10.30 A heater element of 5-mm diameter is maintained at a surface temperature of 350°C when immersed horizontally in water under atmospheric pressure. The element sheath is stainless steel with a mechanically polished finish having an emissivity of 0.25.

(a) Calculate the electrical power dissipation and the rate of vapor production per unit heater length.

(b) If the heater were operated at the same power dissipation rate in the nucleate boiling regime, what temperature would the surface achieve? Calculate the rate of vapor production per unit length for this operating condition.

(c) Sketch the boiling curve and represent the two operating conditions of parts (a) and (b). Compare the results of your analysis. If the heater element is operated in the power-controlled mode, explain how you would achieve these two operating conditions beginning with a cold element.

10.31 The thermal energy generated by a silicon chip increases in proportion to its clock speed. The silicon chip of Problem 10.23 is designed to operate in the nucleate boiling regime at approximately 30% of the critical heat flux. A sudden surge in the chip's clock speed triggers film boiling, after which the clock speed and power dissipation return to their design values.

(a) In which boiling regime does the chip operate after the power dissipation returns to its design value?

(b) To return to the nucleate boiling regime, how much must the clock speed be reduced relative to the design value?

Patent Owner Manufacturing Resources International, Inc.
Exhibit 2017 - Page 667 of 999

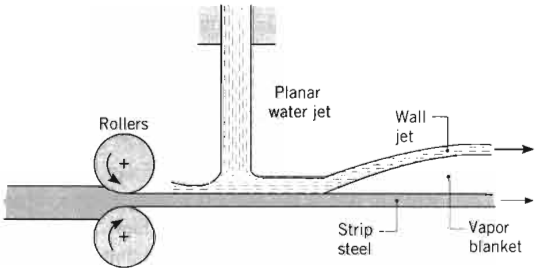
10.32 A cylinder of 120-mm diameter at 1000 K is quenched in saturated water at 1 atm. Describe the quenching process and estimate the maximum heat removal rate per unit length during the process.

10.33 A 1-mm-diameter horizontal platinum wire of emissivity $\varepsilon = 0.25$ is operated in saturated water at 1-atm pressure.

(a) What is the surface heat flux if the surface temperature is $T_s = 800$ K?

(b) For emissivities of 0.1, 0.25, and 0.95, generate a log–log plot of the heat flux as a function of surface excess temperature, $\Delta T_e \equiv T_s - T_{sat}$, for $150 \leq \Delta T_e \leq 550$ K. Show the critical heat flux and the Leidenfrost point on your plot. Separately, plot the percentage contribution of radiation to the total heat flux for $150 \leq \Delta T_e \leq 550$ K.

10.34 As strip steel leaves the last set of rollers in a hot rolling mill, it is quenched by planar water jets before being coiled. Due to the large plate temperatures, film boiling is achieved shortly downstream of the jet impingement region.



Consider conditions for which the strip steel beneath the vapor blanket is at a temperature of 907 K and has an emissivity of 0.35. Neglecting the effects of the strip and jet motions and assuming boiling within the film to be approximated by that associated with a large horizontal cylinder of 1-m diameter, estimate the rate of heat transfer per unit surface area from the strip to the wall jet.

10.35 A copper sphere of 10-mm diameter, initially at a prescribed elevated temperature T_i, is quenched in a saturated (1 atm) water bath. Using the lumped capacitance method, estimate the time for the sphere to cool (a) from $T_i = 130$°C to 110°C and (b) from $T_i = 550$°C to 220°C. Plot the temperature history for each quenching process.

Forced Convection Boiling

10.36 A tube of 2-mm diameter is used to heat saturated water at 1 atm, which is in cross flow over the tube. Calculate and plot the critical heat flux as a function of water velocity over the range 0 to 2 m/s. On your plot, identify the pool boiling region and the transition region between the low- and high-velocity ranges. *Hint:* Problem 10.20 contains relevant information for pool boiling on small-diameter cylinders.

10.37 Saturated water at 1 atm and velocity 2 m/s flows over a cylindrical heating element of diameter 5 mm. What is the maximum heating rate (W/m) for nucleate boiling?

10.38 A vertical steel tube carries water at a pressure of 10 bars. Saturated liquid water is pumped into the $D = 0.1$ m diameter tube at its bottom end ($x = 0$) with a mean velocity of $u_m = 0.05$ m/s. The tube is exposed to combusting pulverized coal, providing a uniform heat flux of $q'' = 100{,}000$ W/m^2.

(a) Determine the tube wall temperature and the quality of the flowing water at $x = 15$ m. Assume $G_{s,f} = 1$.

(b) Determine the tube wall temperature at a location beyond $x = 15$ m where single-phase flow of the vapor exists at a mean temperature of T_m. Assume the vapor at this location is also at a pressure of 10 bars.

(c) Plot the tube wall temperature in the range -5 m $\leq x \leq 30$ m.

10.39 Consider refrigerant R-134a flowing in a smooth, horizontal, 10-mm-inner-diameter tube of wall thickness 2 mm. The refrigerant is at a saturation temperature of 15°C (for which $\rho_{v,sat} = 23.75$ kg/m^3) and flows at a rate of 0.01 kg/s. Determine the maximum wall temperature associated with a heat flux of 10^5 W/m^2 at the inner wall at a location 0.4 m downstream from the onset of boiling for tubes fabricated of (a) pure copper and (b) AISI 316 stainless steel.

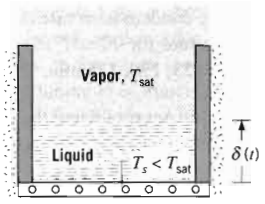
10.40 Determine the tube diameter associated with $p = 1$ atm and a critical Confinement number of 0.5 for ethanol, mercury, water, R-134a, and the dielectric fluid of Problem 10.23.

Film Condensation

10.41 Saturated steam at 0.1 bar condenses with a convection coefficient of 6800 W/m$^2 \cdot$ K on the outside of a brass tube having inner and outer diameters of 16.5 and 19 mm, respectively. The convection coefficient for water flowing inside the tube is 5200 W/m$^2 \cdot$ K. Estimate the steam condensation rate per unit length of the tube when the mean water temperature is 30°C.

10.42 Consider a container exposed to a saturated vapor, T_{sat}, having a cold bottom surface, $T_s < T_{sat}$, and with insulated sidewalls.

Patent Owner Manufacturing Resources International, Inc.
Exhibit 2017 - Page 668 of 999



Assuming a linear temperature distribution for the liquid, perform a surface energy balance on the liquid–vapor interface to obtain the following expression for the growth rate of the liquid layer:

$$\delta(t) = \left[\frac{2k_l(T_{sat} - T_s)}{\rho_l h_{fg}} t\right]^{1/2}$$

Calculate the thickness of the liquid layer formed in 1 h for a 200-mm^2 bottom surface maintained at 80°C and exposed to saturated steam at 1 atm. Compare this result with the condensate formed by a *vertical* plate of the same dimensions for the same period of time.

10.43 Saturated steam at 1 atm condenses on the outer surface of a vertical, 100-mm-diameter pipe 1 m long, having a uniform surface temperature of 94°C. Estimate the total condensation rate and the heat transfer rate to the pipe.

10.44 Determine the total condensation rate and the heat transfer rate for Problem 10.43 when the steam is saturated at 1.5 bars.

10.45 A vertical plate 500 mm high and 200 mm wide is to be used to condense saturated steam at 1 atm.

(a) At what surface temperature must the plate be maintained to achieve a condensation rate of $\dot{m} = 25$ kg/h?

(b) Compute and plot the surface temperature as a function of condensation rate for $15 \leq \dot{m} \leq 50$ kg/h.

(c) On the same graph and for the same range of $\dot{m}$, plot the surface temperature as a function of condensation rate if the plate is 200 mm high and 500 mm wide.

10.46 A 2 m × 2 m vertical plate is exposed on one side to saturated steam at atmospheric pressure and on the other side to cooling water that maintains a plate temperature of 50°C.

(a) What is the rate of heat transfer to the coolant? What is the rate at which steam condenses on the plate?

(b) For plates inclined at an angle θ from the vertical, the average convection coefficient for condensation on the upper surface, $\bar{h}_{L(\text{incl})}$, may be approximated by an expression of the form, $\bar{h}_{L(\text{incl})} \approx (\cos\theta)^{1/4}\,\bar{h}_{L(\text{vert})}$, where $\bar{h}_{L(\text{vert})}$ is the average coefficient for the vertical orientation. If the 2 m × 2 m plate is inclined 45° from the normal, what are the rates of heat transfer and condensation?

10.47 Saturated ethylene glycol vapor at 1 atm is exposed to a vertical plate 300 mm high and 100 mm wide having a uniform temperature of 420 K. Estimate the heat transfer rate to the plate and the condensation rate. Approximate the liquid properties as those corresponding to saturated conditions at 373 K (Table A.5).

10.48 A vertical plate 2.5 m high, maintained at a uniform temperature of 54°C, is exposed to saturated steam at atmospheric pressure.

(a) Estimate the condensation and heat transfer rates per unit width of the plate.

(b) If the plate height were halved, would the flow regime stay the same or change?

(c) For $54 \leq T_s \leq 90$°C, plot the condensation rate as a function of plate temperature for the two plate heights of parts (a) and (b).

10.49 Two configurations are being considered in the design of a condensing system for steam at 1 atm employing a vertical plate maintained at 90°C. The first configuration is a single vertical plate $L \times w$ and the second consists of two vertical plates $(L/2) \times w$, where L and w are the vertical and horizontal dimensions, respectively. Which configuration would you choose?

10.50 The condenser of a steam power plant consists of a square (in-line) array of 625 tubes, each of 25-mm diameter. Consider conditions for which saturated steam at 0.105 bars condenses on the outer surface of each tube, while a tube wall temperature of 17°C is maintained by the flow of cooling water through the tubes. What is the rate of heat transfer to the water per unit length of the tube array? What is the corresponding condensation rate?

10.51 The condenser of a steam power plant consists of AISI 302 stainless steel tubes ($k_s = 15$ W/m · K), each of outer and inner diameters $D_o = 30$ mm and $D_i = 26$ mm, respectively. Saturated steam at 0.135 bar condenses on the outer surface of a tube, while water at a mean temperature of $T_m = 290$ K is in fully developed flow through the tube.

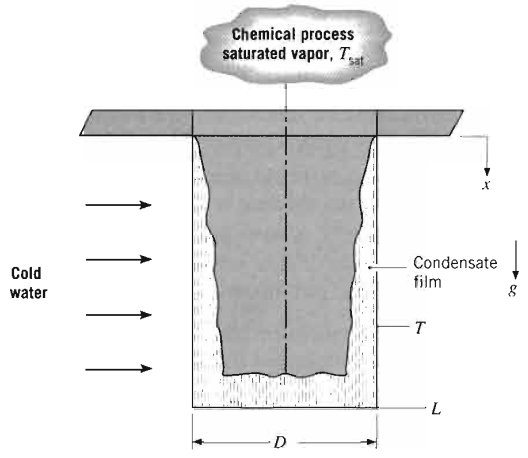
(a) For a water flow rate of $\dot{m} = 0.25$ kg/s, what is the outer surface temperature $T_{s,o}$ of the tube and the rates of heat transfer and steam condensation per unit tube length? As a first estimate, you may

Patent Owner Manufacturing Resources International, Inc.
Exhibit 2017 - Page 669 of 999

evaluate the properties of the liquid film at the saturation temperature. If one wishes to increase the transfer rates, what is the limiting factor that should be addressed?

(b) Explore the effect of the water flow rate on $T_{s,o}$ and the rate of heat transfer per unit length.

10.52 Saturated vapor from a chemical process condenses at a slow rate on the inner surface of a vertical, thin-walled cylindrical container of length L and diameter D. The container wall is maintained at a uniform temperature T_s by flowing cold water across its outer surface.



Derive an expression for the time, t_f, required to fill the container with condensate, assuming that the condensate film is laminar. Express your result in terms of D, L, $(T_{sat} - T_s)$, g, and appropriate fluid properties.

10.53 Determine the total condensation rate and heat transfer rate for the condensation process of Problem 10.43 when the pipe is horizontal.

10.54 An uninsulated, 25-mm-diameter pipe with a surface temperature of 15°C passes through a room having an air temperature of 37°C and relative humidity of 75%. Estimate the condensation rate per unit length of the pipe assuming film, rather than dropwise, condensation.

10.55 A horizontal tube of 50-mm diameter, with a surface temperature of 34°C, is exposed to steam at 0.2 bar. Estimate the condensation rate and heat transfer rate per unit length of the tube.

10.56 A horizontal tube 1 m long with a surface temperature of 70°C is used to condense saturated steam at 1 atm.

(a) What diameter is required to achieve a condensation rate of 125 kg/h?

(b) Plot the condensation rate as a function of surface temperature for $70 \leq T_s \leq 90$°C and tube diameters of 125, 150, 175 mm.

10.57 The Clean Air Act prohibited the production of chlorofluorocarbons (CFCs) in the United States as of 1996. One widely used CFC, refrigerant R-12, has been replaced by R-134a in many applications because of their similar properties, including a low boiling point at atmospheric pressure, $T_{sat} = 243$ K and 246.9 K for R-12 and R-134a, respectively. Compare the performance of these two refrigerants under the following conditions. The saturated refrigerant vapor at 310 K is condensed as it flows through a 30-mm-diameter, 0.8-m-long tube whose wall temperature is maintained at 290 K. If vapor enters the tube at a flow rate of 0.010 kg/s, what is the rate of condensation and the flow rate of vapor leaving the tube? The relevant properties of R-12 at $T_{sat} = 310$ K are $\rho_v = 50.1$ kg/m^3, $h_{fg} = 160$ kJ/kg, and $\mu_v = 150 \times 10^{-7}$ N · s/m^2 and those of liquid R-12 at $T_f = 300$ K are $\rho_l = 1306$ kg/m^3, $c_{p,l} = 978$ J/kg · K, $\mu_l = 2.54 \times 10^{-4}$ N · s/m^2, $k_l = 0.072$ W/m · K. The properties of the saturated R-134a vapor are $\rho_v = 46.1$ kg/m^3, $h_{fg} = 166$ kJ/kg, and $\mu_v = 136 \times 10^{-7}$ N · s/m^2.

10.58 Saturated steam at a pressure of 0.1 bar is condensed over a square array of 100 tubes each of diameter 8 mm.

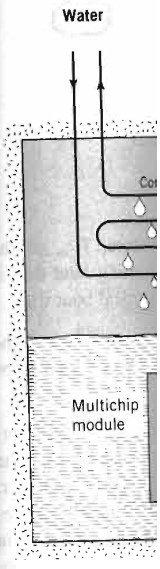
(a) If the tube surfaces are maintained at 27°C, estimate the condensation rate per unit tube length.

(b) Subject to the requirement that the total number of tubes and the tube diameter are fixed at 100 and 8 mm, respectively, what options are available for increasing the condensation rate? Assess these options quantitatively.

10.59 A thin-walled concentric tube heat exchanger of 0.19-m length is to be used to heat deionized water from 40 to 60°C at a flow rate of 5 kg/s. The deionized water flows through the inner tube of 30-mm diameter while saturated steam at 1 atm is supplied to the annulus formed with the outer tube of 60-mm diameter. The thermophysical properties of the deionized water are $\rho = 982.3$ kg/m^3, $c_p = 4181$ J/kg · K, $k = 0.643$ W/m · K, $\mu = 548 \times 10^{-6}$ N · s/m^2, and $Pr = 3.56$. Estimate the convection coefficients for both sides of the tube and determine the inner tube wall outlet temperature. Does condensation provide a fairly uniform inner tube wall temperature equal approximately to the saturation temperature of the steam?

10.60 A technique for cooling a multichip module involves submerging the module in a saturated fluorocarbon

liquid. Vapor
surface is con
tubing suspen
The thin-walle
is coiled in a
that enters at
dissipated by
from a 100-m
the flux is 10^5
is at $T_{sat} = 5$
W/m · K, $c_{p,l}$
$\rho_l = 1619.2$ k
kg/s^2, $\mu_l = 4$



(a) For the
require
flowrat

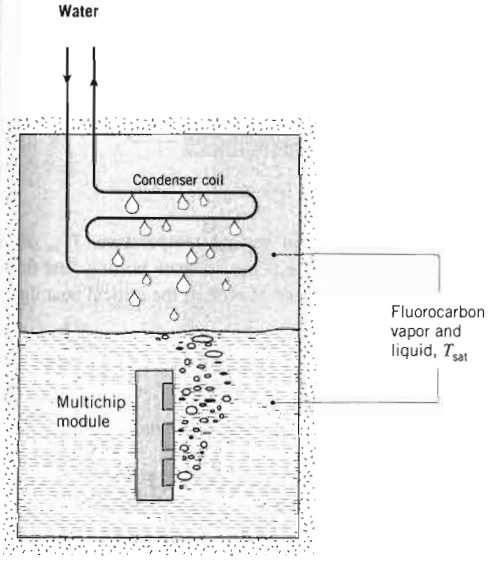
(b) Assum
tube,
the coi

(c) Assum
$T_s = 5$
coil.

10.61 Determine
diameter sp
saturated e
the liquid p
conditions

Patent Owner Manufacturing Resources International, Inc.
Exhibit 2017 - Page 670 of 999

liquid. Vapor generated due to boiling at the module surface is condensed on the outer surface of copper tubing suspended in the vapor space above the liquid. The thin-walled tubing is of diameter $D = 10$ mm and is coiled in a horizontal plane. It is cooled by water that enters at 285 K and leaves at 315 K. All the heat dissipated by the chips within the module is transferred from a 100-mm by 100-mm boiling surface, at which the flux is 10^5 W/m^2, to the fluorocarbon liquid, which is at $T_{sat} = 57°C$. Liquid properties are $k_l = 0.0537$ W/m · K, $c_{p,l} = 1100$ J/kg · K, $h'_{fg} \approx h_{fg} = 84{,}400$ J/kg, $\rho_l = 1619.2$ kg/m^3, $\rho_v = 13.4$ kg/m^3, $\sigma = 8.1 \times 10^{-3}$ kg/s^2, $\mu_l = 440 \times 10^{-6}$ kg/m · s, and $Pr_l = 9$.



(a) For the prescribed heat dissipation, what is the required condensation rate (kg/s) and water flowrate (kg/s)?

(b) Assuming fully developed flow throughout the tube, determine the tube surface temperature at the coil inlet and outlet.

(c) Assuming a uniform tube surface temperature of $T_s = 53.0°C$, determine the required length of the coil.

10.61 Determine the rate of condensation on a 100-mm-diameter sphere with a surface temperature of 150°C in saturated ethylene glycol vapor at 1 atm. Approximate the liquid properties as those corresponding to saturated conditions at 373 K (Table A.5).

10.62 A 10-mm-diameter copper sphere, initially at a uniform temperature of 50°C, is placed in a large container filled with saturated steam at 1 atm. Using the lumped capacitance method, estimate the time required for the sphere to reach an equilibrium condition. How much condensate (kg) was formed during this period?

10.63 Saturated steam at 1.5 bars condenses inside a horizontal, 75-mm-diameter pipe whose surface is maintained at 100°C. Assuming low vapor velocities and film condensation, estimate the heat transfer coefficient and the condensation rate per unit length of the pipe.

Dropwise Condensation

10.64 Consider Problem 10.41. In an effort to increase the condensation rate, an engineer proposes to apply a $L = 100$ μm thick Teflon coating to the exterior surface of the brass tube to promote dropwise condensation. Estimate the new condensation convection coefficient and the steam condensation rate per unit length of the tube after application of the coating. Comment on the proposed scheme's effect on the condensation rate (the condensation rate per unit length in Problem 10.41 is approximately 1×10^{-3} kg/s).

10.65 Consider the conditions of Problem 10.54. Estimate the condensation rate for dropwise condensation.

10.66 A beverage can with a diameter of 65 mm and a height of 120 mm has a uniform temperature of 5°C when it is removed from the refrigerator. The can is set on a table in a room with an ambient air temperature of 32°C and a relative humidity of 75%.

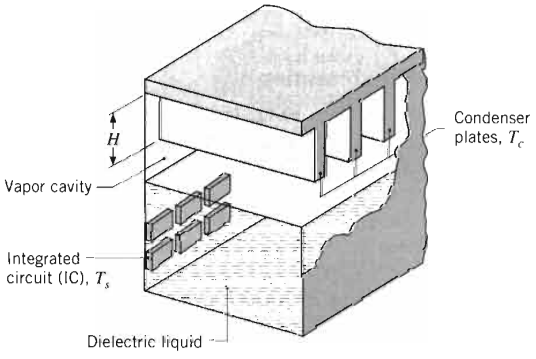
Estimate the condensation rate assuming (a) dropwise condensation and (b) film condensation. Compare the rates and explain under what conditions dropwise condensation can occur.



Patent Owner Manufacturing Resources International, Inc.
Exhibit 2017 - Page 671 of 999

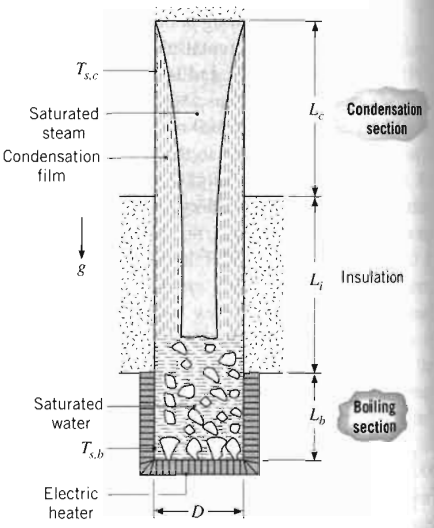
Combined Boiling/Condensation

10.67 A passive technique for cooling heat-dissipating integrated circuits involves submerging the ICs in a low boiling point dielectric fluid. Vapor generated in cooling the circuits is condensed on vertical plates suspended in the vapor cavity above the liquid. The temperature of the plates is maintained below the saturation temperature, and during steady-state operation a balance is established between the rate of heat transfer to the condenser plates and the rate of heat dissipation by the ICs.



Consider conditions for which the 25-mm^2 surface area of each IC is submerged in a fluorocarbon liquid for which $T_{sat} = 50°C$, $\rho_l = 1700$ kg/m^3, $c_{p,l} = 1005$ J/kg · K, $\mu_l = 6.80 \times 10^{-4}$ kg/s · m, $k_l = 0.062$ W/m · K, $Pr_l = 11.0$, $\sigma = 0.013$ kg/s^2, $h_{fg} = 1.05 \times 10^5$ J/kg, $C_{s,f} = 0.004$, and $n = 1.7$. If the integrated circuits are operated at a surface temperature of $T_s = 75°C$, what is the rate at which heat is dissipated by each circuit? If the condenser plates are of height $H = 50$ mm and are maintained at a temperature of $T_c = 15°C$ by an internal coolant, how much condenser surface area must be provided to balance the heat generated by 500 integrated circuits?

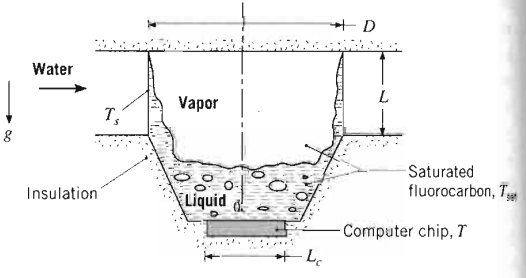
10.68 A thermosyphon consists of a closed container that absorbs heat along its boiling section and rejects heat along its condensation section. Consider a thermosyphon made from a thin-walled mechanically polished stainless steel cylinder of diameter D. Heat supplied to the thermosyphon boils saturated water at atmospheric pressure on the surfaces of the lower boiling section of length L_b and is then rejected by condensing vapor into a thin film, which falls by gravity along the wall of the condensation section of length L_c back into the boiling section. The two sections are separated by an insulated section of length L_i. The top surface of the condensation section may be treated as being insulated. The thermosyphon dimensions are $D = 20$ mm, $L_b = 20$ mm, $L_c = 40$ mm, and $L_i = 40$ mm.



(a) Find the mean surface temperature, $T_{s,b}$, of the boiling surface if the nucleate boiling heat flux is to be maintained at 30% of the critical heat flux.

(b) Find the total condensation flow rate, $\dot{m}$, and the mean surface temperature of the condensation section, $T_{s,c}$.

10.69 A novel scheme for cooling computer chips uses a thermosyphon containing a saturated fluorocarbon. The chip is brazed to the bottom of a cuplike container, within which heat is dissipated by boiling and subsequently transferred to an external coolant (water) via condensation on the inner surface of a thin-walled tube.

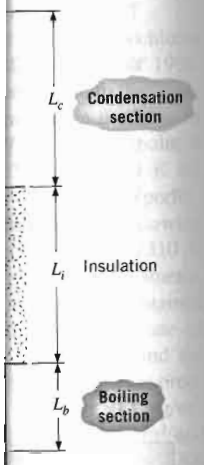


The nucleate boiling constants and the properties of the fluorocarbon are provided in Problem 10.23. In addition, $k_l = 0.054$ W/m · K.

(a) If the chip operates under steady-state conditions and its surface heat flux is maintained at 90% of

Patent Owner Manufacturing Resources International, Inc.
Exhibit 2017 - Page 672 of 999

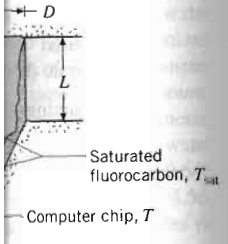
sions are $D = 20$ mm,
$= 40$ mm.



mperature, $T_{s,b}$, of the
eate boiling heat flux is
f the critical heat flux.

n flow rate, $\dot{m}$, and the
e of the condensation

mputer chips uses a ther-
ated fluorocarbon. The
of a cuplike container,
d by boiling and subse-
rnal coolant (water) via
ce of a thin-walled tube.



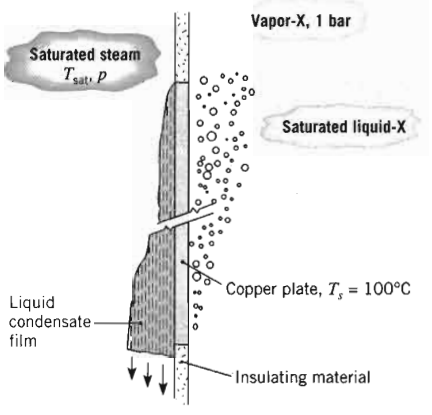
ts and the properties of
d in Problem 10.23. In

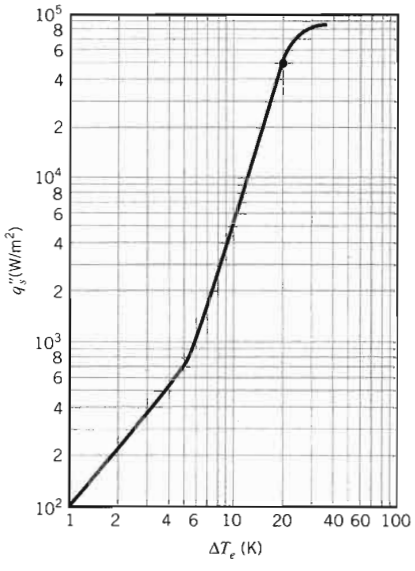
r steady-state conditions
is maintained at 90% of

the critical heat flux, what is its temperature T? What is the total power dissipation if the chip width is $L_c = 20$ mm on a side?

(b) If the tube diameter is $D = 30$ mm and its surface is maintained at $T_s = 25°C$ by the water, what tube length L is required to maintain the designated conditions?

10.70 A condenser–boiler section contains a 2-m × 2-m copper plate operating at a uniform temperature of $T_s = 100°C$ and separating saturated steam, which is condensing, from a saturated liquid-X, which experiences nucleate pool boiling. A portion of the boiling curve for liquid-X is shown as follows. Both saturated steam and saturated liquid-X are supplied to the system, while water condensate and vapor-X are removed by means not shown in the sketch. At a pressure of 1 bar, fluid-X has a saturation temperature and a latent heat of vaporization of $T_{sat} = 80°C$ and $h_{fg} = 700{,}000$ J/kg, respectively.

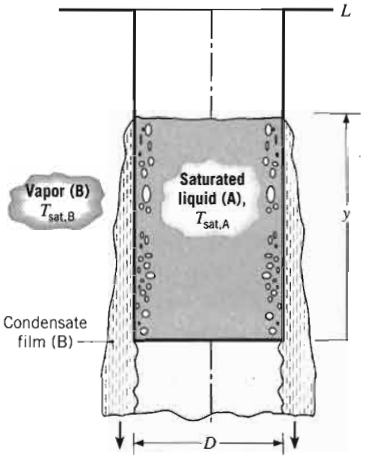




(a) Estimate the rates of evaporation and condensation (kg/s) for the two fluids.

(b) Determine the saturation temperature T_{sat} and pressure p for the steam, assuming that film condensation occurs.

10.71 A thin-walled cylindrical container of diameter D and height L is filled to a height y with a low boiling point liquid (A) at $T_{sat,A}$. The container is located in a large chamber filled with the vapor of a high boiling point fluid (B). Vapor-B condenses into a laminar film on the outer surface of the cylindrical container, extending from the location of the liquid-A free surface. The condensation process sustains nucleate boiling in liquid-A along the container wall according to the relation $q'' = C(T_s - T_{sat})^3$, where C is a known empirical constant.



(a) For the portion of the wall covered with the condensate film, derive an equation for the average temperature of the container wall, T_s. Assume that the properties of fluids A and B are known.

(b) At what rate is heat supplied to liquid-A?

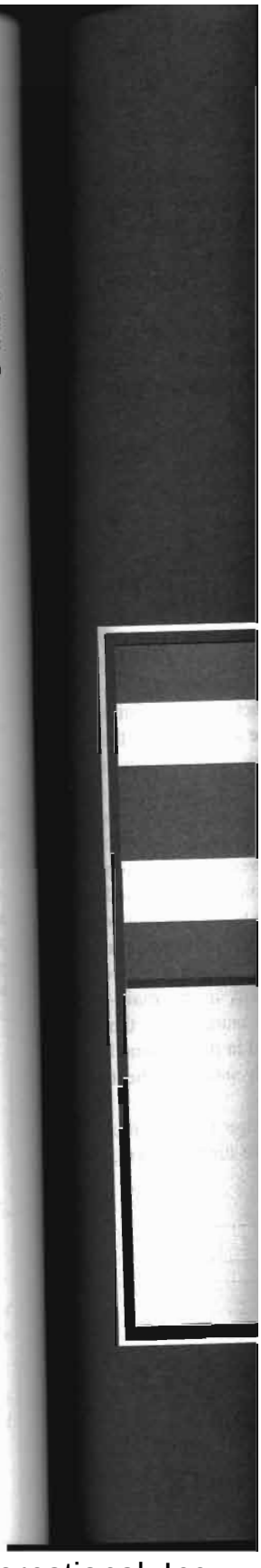
(c) Assuming the container is initially filled completely with liquid, that is, $y = L$, derive an expression for the time required to evaporate all the liquid in the container.

Patent Owner Manufacturing Resources International, Inc.
Exhibit 2017 - Page 673 of 999

10.72 It has been proposed that the very hot air trapped inside the attic of a house in the summer may be used as the energy source for a *passive* water heater installed in the attic. Energy costs associated with heating the cool water and air conditioning the house are both reduced. Ten thermosyphons, similar to that of Problem 10.68, are inserted in the bottom of a well-insulated water heater. Each thermosyphon has a condensing section that is $L_c = 50$ mm long, an insulated section that is of length $L_i = 40$ mm, and a boiling section that is $L_b = 30$ mm long. The diameter of each thermosyphon is $D = 20$ mm. The working fluid within the thermosyphons is water at a pressure of $p = 0.047$ bars.

(a) Determine the heating rate delivered by the 10 thermosyphons when boiling occurs at 25% of the CHF. What are the mean temperatures of the boiling and condensing sections?

(b) At night the attic air temperature drops below the temperature of the water. Estimate the heat loss from the hot water tank to the cool attic, assuming losses through the tank insulation are negligible and the stainless steel tube wall thickness of each thermosyphon is very small.



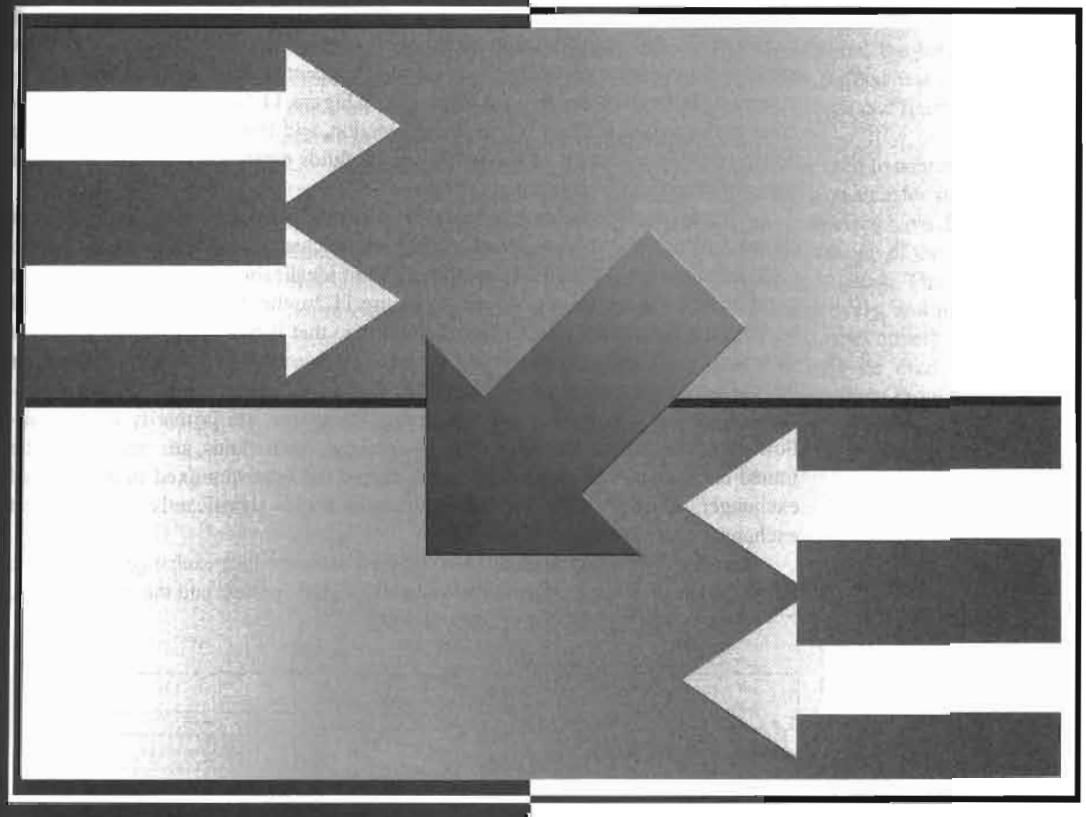
Patent Owner Manufacturing Resources International, Inc.
Exhibit 2017 - Page 674 of 999

delivered by the 10
g occurs at 25% of the
mperatures of the boil-
s?

rature drops below the
Estimate the heat loss
he cool attic, assuming
sulation are negligible
wall thickness of each
l.

CHAPTER 11

Heat Exchangers



Patent Owner Manufacturing Resources International, Inc.
Exhibit 2017 - Page 675 of 999

The process of heat exchange between two fluids that are at different temperatures and separated by a solid wall occurs in many engineering applications. The device used to implement this exchange is termed a *heat exchanger*, and specific applications may be found in space heating and air-conditioning, power production, waste heat recovery, and chemical processing.

In this chapter our objectives are to introduce performance parameters for assessing the efficacy of a heat exchanger and to develop methodologies for designing a heat exchanger or for predicting the performance of an existing exchanger operating under prescribed conditions.

11.1 *Heat Exchanger Types*

Heat exchangers are typically classified according to *flow arrangement* and *type of construction*. The simplest heat exchanger is one for which the hot and cold fluids move in the same or opposite directions in a *concentric tube* (or *double-pipe*) construction. In the *parallel-flow* arrangement of Figure 11.1*a*, the hot and cold fluids enter at the same end, flow in the same direction, and leave at the same end. In the *counterflow* arrangement of Figure 11.1*b*, the fluids enter at opposite ends, flow in opposite directions, and leave at opposite ends.

Alternatively, the fluids may move in *cross flow* (perpendicular to each other), as shown by the *finned* and *unfinned* tubular heat exchangers of Figure 11.2. The two configurations are typically differentiated by an idealization that treats fluid motion over the tubes as *unmixed* or *mixed*. In Figure 11.2*a*, the fluid is said to be unmixed because the fins inhibit motion in a direction (y) that is transverse to the main-flow direction (x). In this case the fluid temperature varies with x and y. In contrast, for the unfinned tube bundle of Figure 11.2*b*, fluid motion, hence mixing, in the transverse direction is possible, and temperature variations are primarily in the main-flow direction. Since the tube flow is unmixed, both fluids are unmixed in the finned exchanger, while one fluid is mixed and the other unmixed in the unfinned exchanger. The nature of the mixing condition can significantly influence heat exchanger performance.

Another common configuration is the *shell-and-tube* heat exchanger [1]. Specific forms differ according to the number of shell-and-tube passes, and the simplest form,

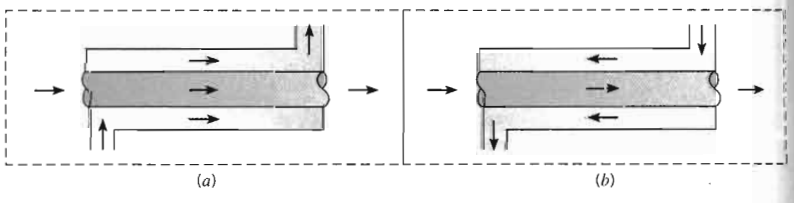


FIGURE 11.1 Concentric tube heat exchangers. (*a*) Parallel flow. (*b*) Counterflow.

Patent Owner Manufacturing Resources International, Inc.
Exhibit 2017 - Page 676 of 999

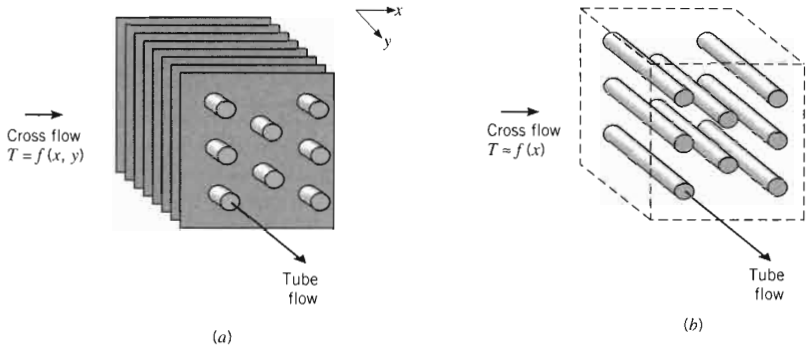


FIGURE 11.2 Cross-flow heat exchangers. (*a*) Finned with both fluids unmixed. (*b*) Unfinned with one fluid mixed and the other unmixed.

which involves single tube and shell *passes*, is shown in Figure 11.3. Baffles are usually installed to increase the convection coefficient of the shell-side fluid by inducing turbulence and a cross-flow velocity component. In addition, the baffles physically support the tubes, reducing flow-induced tube vibration. Baffled heat exchangers with one shell pass and two tube passes and with two shell passes and four tube passes are shown in Figures 11.4*a* and 11.4*b*, respectively.

A special and important class of heat exchangers is used to achieve a very large ($\gtrsim 400$ m^2/m^3 for liquids and $\gtrsim 700$ m^2/m^3 for gases) heat transfer surface area per unit volume. Termed *compact heat exchangers*, these devices have dense arrays of finned tubes or plates and are typically used when at least one of the fluids is a gas, and is hence characterized by a small convection coefficient. The tubes may be *flat* or *circular*, as in Figures 11.5*a* and 11.5*b*, *c*, respectively, and the fins may be *plate* or *circular*, as in Figures 11.5*a*, *b* and 11.5*c*, respectively. Parallel-plate heat exchangers may be finned or corrugated and may be used in single-pass (Figure 11.5*d*) or multipass (Figure 11.5*e*) modes of operation. Flow passages associated with compact heat exchangers are typically small ($D_h \lesssim 5$ mm), and the flow is usually laminar.

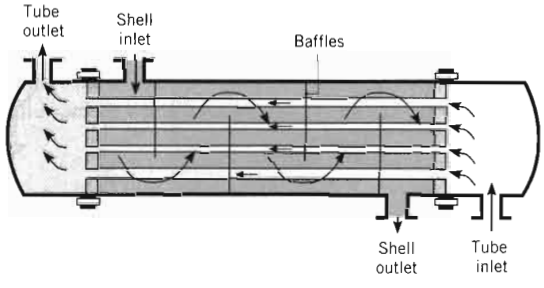


FIGURE 11.3 Shell-and-tube heat exchanger with one shell pass and one tube pass (cross-counterflow mode of operation).

Patent Owner Manufacturing Resources International, Inc.
Exhibit 2017 - Page 677 of 999

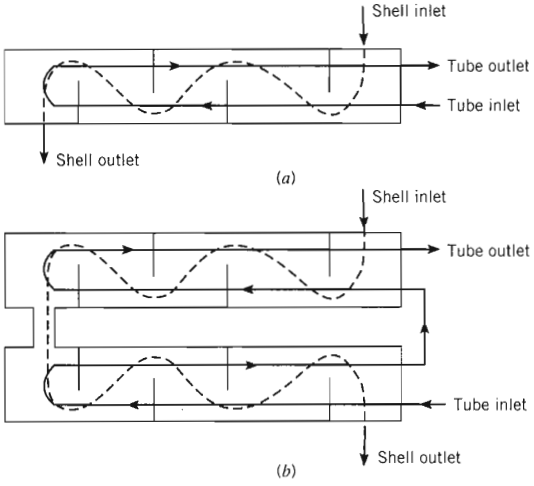


FIGURE 11.4 Shell-and-tube heat exchangers. (*a*) One shell pass and two tube passes. (*b*) Two shell passes and four tube passes.

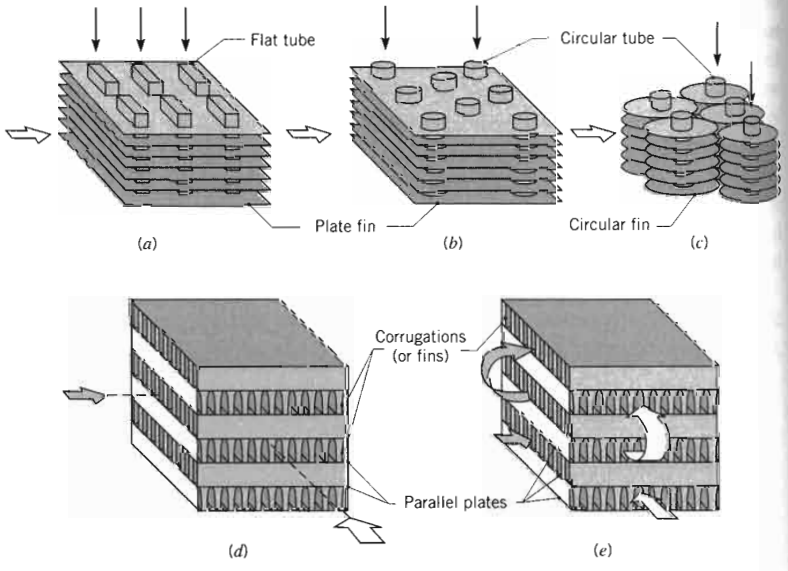


FIGURE 11.5 Compact heat exchanger cores. (*a*) Fin–tube (flat tubes, continuous plate fins). (*b*) Fin–tube (circular tubes, continuous plate fins). (*c*) Fin–tube (circular tubes, circular fins). (*d*) Plate–fin (single pass). (*e*) Plate–fin (multipass).

Patent Owner Manufacturing Resources International, Inc.
Exhibit 2017 - Page 678 of 999

11.2
The Overall Heat Transfer Coefficient

An essential, and often the most uncertain, part of any heat exchanger analysis is determination of the *overall heat transfer coefficient.* Recall from Equation 3.19 that this coefficient is defined in terms of the total thermal resistance to heat transfer between two fluids. In Equations 3.18 and 3.31, the coefficient was determined by accounting for conduction and convection resistances between fluids separated by composite plane and cylindrical walls, respectively. It is important to acknowledge, however, that such results apply only to *clean, unfinned* surfaces.

During normal heat exchanger operation, surfaces are often subject to fouling by fluid impurities, rust formation, or other reactions between the fluid and the wall material. The subsequent deposition of a film or scale on the surface can greatly increase the resistance to heat transfer between the fluids. This effect can be treated by introducing an additional thermal resistance, termed the *fouling factor,* R_f. Its value depends on the operating temperature, fluid velocity, and length of service of the heat exchanger.

In addition, we know that fins are often added to surfaces exposed to either or both fluids and that, by increasing the surface area, they reduce the resistance to convection heat transfer. Accordingly, with inclusion of surface fouling and fin (extended surface) effects, the overall heat transfer coefficient may be expressed as

$$\frac{1}{UA} = \frac{1}{U_c A_c} = \frac{1}{U_h A_h}$$

$$= \frac{1}{(\eta_o hA)_c} + \frac{R''_{f,c}}{(\eta_o A)_c} + R_w + \frac{R''_{f,h}}{(\eta_o A)_h} + \frac{1}{(\eta_o hA)_h} \tag{11.1}$$

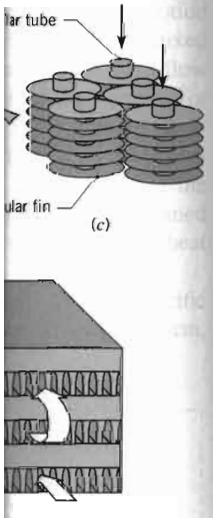
where c and h refer to the cold and hot fluids, respectively. Note that calculation of the UA product does not require designation of the hot or cold side ($U_c A_c = U_h A_h$). However, calculation of an overall coefficient depends on whether it is based on the cold or hot side surface area, since $U_c \neq U_h$ if $A_c \neq A_h$. The conduction resistance R_w is obtained from Equation 3.6 for a plane wall or Equation 3.28 for a cylindrical wall. Although representative fouling factors are listed in Table 11.1, the factor is a variable during heat exchanger operation (increasing from zero for a clean surface, as deposits accumulate on the surface). Comprehensive discussions of fouling are provided in References 2 through 4.

The quantity η_o in Equation 11.1 is termed the *overall surface efficiency* or *temperature effectiveness* of a finned surface. It is defined such that, for the hot or cold surface without fouling, the heat transfer rate is

$$q = \eta_o hA(T_b - T_\infty) \tag{11.2}$$

where T_b is the base surface temperature (Figure 3.20) and A is the total (fin plus exposed base) surface area. The quantity was introduced in Section 3.6.5, and the following expression was derived:

$$\eta_o = 1 - \frac{A_f}{A}(1 - \eta_f) \tag{11.3}$$



, continuous plate fins).
r tubes, circular fins).

Patent Owner Manufacturing Resources International, Inc.
Exhibit 2017 - Page 679 of 999

TABLE 11.1 Representative Fouling Factors [1]

Fluid	R''_f (m² · K/W)
Seawater and treated boiler feedwater (below 50°C)	0.0001
Seawater and treated boiler feedwater (above 50°C)	0.0002
River water (below 50°C)	0.0002–0.001
Fuel oil	0.0009
Refrigerating liquids	0.0002
Steam (nonoil bearing)	0.0001

where A_f is the entire fin surface area and η_f is the efficiency of a single fin. To be consistent with the nomenclature commonly used in heat exchanger analysis, the ratio of fin surface area to the total surface area has been expressed as A_f/A. This representation differs from that of Section 3.6.5, where the ratio is expressed as NA_f/A_t, with A_f representing the area of a single fin and A_t the total surface area. If a straight or pin fin of length L (Figure 3.16) is used and an adiabatic tip is assumed, Equations 3.76 and 3.86 yield

$$\eta_f = \frac{\tanh(mL)}{mL} \tag{11.4}$$

where $m = (2h/kt)^{1/2}$ and t is the fin thickness. For several common fin shapes, the efficiency may be obtained from Table 3.5.

Note that, as written, Equation 11.2 corresponds to negligible fouling. However, if fouling is significant, the convection coefficient in Equation 11.2 must be replaced by a *partial* overall heat transfer coefficient of the form $U_p = h/(1 + hR''_f)$. In contrast to Equation 11.1, which provides the overall heat transfer coefficient between the hot and cold fluids, U_p is termed a partial coefficient because it only includes the convection coefficient and fouling factor associated with one fluid and its adjoining surface. Partial coefficients for the hot and cold sides are then $U_{p,h} = h_h/(1 + h_h R''_{f,h})$ and $U_{p,c} = h_c/(1 + h_c R''_{f,c})$, respectively. Equation 11.3 may still be used to evaluate η_o for the hot and/or cold side, but U_p must be used in lieu of h to evaluate the corresponding fin efficiency. Moreover, it is readily shown that the second and fourth terms on the right-hand side of Equation 11.1 may be deleted if the convection coefficients in the first and fifth terms are replaced by $U_{p,c}$ and $U_{p,h}$, respectively.

The wall conduction term in Equation 11.1 may often be neglected, since a thin wall of large thermal conductivity is generally used. Also, one of the convection coefficients is often much smaller than the other and hence dominates determination of the overall coefficient. For example, if one of the fluids is a gas and the other is a liquid or a liquid–vapor mixture experiencing boiling or condensation, the gas-side convection coefficient is much smaller. It is in such situations that fins are used to enhance gas-side convection. Representative values of the overall coefficient are summarized in Table 11.2.

11.3 *Heat Excha Mean Temp*

Patent Owner Manufacturing Resources International, Inc.
Exhibit 2017 - Page 680 of 999

TABLE 11.2 Representative Values of the Overall Heat Transfer Coefficient

Fluid Combination	U (W/m^2 · K)
Water to water	850–1700
Water to oil	110–350
Steam condenser (water in tubes)	1000–6000
Ammonia condenser (water in tubes)	800–1400
Alcohol condenser (water in tubes)	250–700
Finned-tube heat exchanger (water in tubes, air in cross flow)	25–50

For the unfinned, tubular heat exchangers of Figures 11.1 through 11.4, Equation 11.1 reduces to

$$\frac{1}{UA} = \frac{1}{U_i A_i} = \frac{1}{U_o A_o}$$
$$= \frac{1}{h_i A_i} + \frac{R''_{f,i}}{A_i} + \frac{\ln (D_o/D_i)}{2\pi kL} + \frac{R''_{f,o}}{A_o} + \frac{1}{h_o A_o} \tag{11.5}$$

where subscripts i and o refer to inner and outer tube surfaces ($A_i = \pi D_i L$, $A_o = \pi D_o L$), which may be exposed to either the hot or the cold fluid.

The overall heat transfer coefficient may be determined from knowledge of the hot and cold fluid convection coefficients and fouling factors and from appropriate geometric parameters. For unfinned surfaces, the convection coefficients may be estimated from correlations presented in Chapters 7 and 8. For standard fin configurations, the coefficients may be obtained from results compiled by Kays and London [5].

11.3 *Heat Exchanger Analysis: Use of the Log Mean Temperature Difference*

To design or to predict the performance of a heat exchanger, it is essential to relate the total heat transfer rate to quantities such as the inlet and outlet fluid temperatures, the overall heat transfer coefficient, and the total surface area for heat transfer. Two such relations may readily be obtained by applying overall energy balances to the hot and cold fluids, as shown in Figure 11.6. In particular, if q is the total rate of heat transfer between the hot and cold fluids and there is negligible heat transfer between the exchanger and its surroundings, as well as negligible potential and kinetic energy changes, application of the steady flow energy equation, Equation 1.11d, gives

$$q = \dot{m}_h (i_{h,i} - i_{h,o}) \tag{11.6a}$$

Patent Owner Manufacturing Resources International, Inc.
Exhibit 2017 - Page 681 of 999

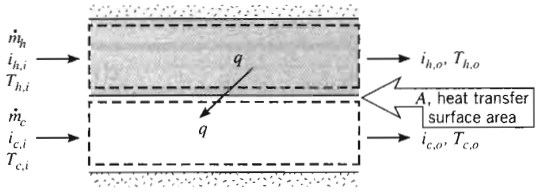


FIGURE 11.6 Overall energy balances for the hot and cold fluids of a two-fluid heat exchanger.

and

$$q = \dot{m}_c(i_{c,o} - i_{c,i}) \tag{11.7a}$$

where i is the fluid enthalpy. The subscripts h and c refer to the hot and cold fluids, whereas i and o designate the fluid inlet and outlet conditions. If the fluids are not undergoing a phase change and constant specific heats are assumed, these expressions reduce to

$$q = \dot{m}_h c_{p,h}(T_{h,i} - T_{h,o}) \tag{11.6b}$$

and

$$q = \dot{m}_c c_{p,c}(T_{c,o} - T_{c,i}) \tag{11.7b}$$

where the temperatures appearing in the expressions refer to the *mean* fluid temperatures at the designated locations. Note that Equations 11.6 and 11.7 are independent of the flow arrangement and heat exchanger type.

Another useful expression may be obtained by relating the total heat transfer rate q to the temperature difference ΔT between the hot and cold fluids, where

$$\Delta T \equiv T_h - T_c \tag{11.8}$$

Such an expression would be an extension of Newton's law of cooling, with the overall heat transfer coefficient U used in place of the single convection coefficient h. However, since ΔT varies with position in the heat exchanger, it is necessary to work with a rate equation of the form

$$q = UA\,\Delta T_m \tag{11.9}$$

where ΔT_m is an appropriate *mean* temperature difference. Equation 11.9 may be used with Equations 11.6 and 11.7 to perform a heat exchanger analysis. Before this can be done, however, the specific form of ΔT_m must be established.

11.3.1 The Parallel-Flow Heat Exchanger

The hot and cold fluid temperature distributions associated with a parallel-flow heat exchanger are shown in Figure 11.7. The temperature difference ΔT is initially large but decays with increasing x, approaching zero asymptotically. It is important to note that, for such an exchanger, the outlet temperature of the cold fluid never exceeds that of the hot fluid. In Figure 11.7 the subscripts 1 and 2 designate opposite ends of the

Patent Owner Manufacturing Resources International, Inc.
Exhibit 2017 - Page 682 of 999

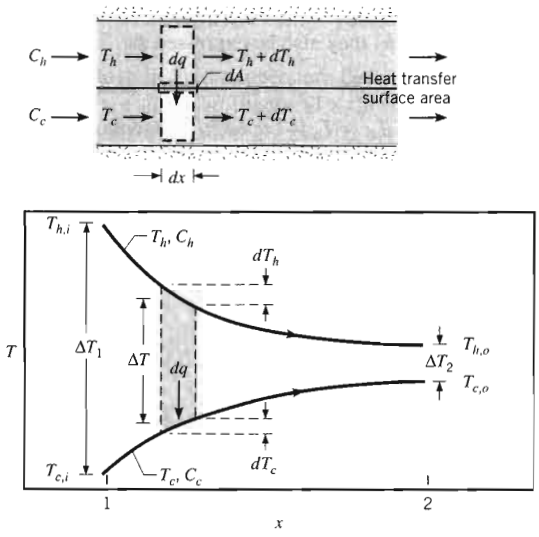


FIGURE 11.7 Temperature distributions for a parallel-flow heat exchanger.

heat exchanger. This convention is used for all types of heat exchangers considered. For parallel flow, it follows that $T_{h,i} = T_{h,1}$, $T_{h,o} = T_{h,2}$, $T_{c,i} = T_{c,1}$, and $T_{c,o} = T_{c,2}$.

The form of ΔT_m may be determined by applying an energy balance to differential elements in the hot and cold fluids. Each element is of length dx and heat transfer surface area dA, as shown in Figure 11.7. The energy balances and the subsequent analysis are subject to the following assumptions.

1. The heat exchanger is insulated from its surroundings, in which case the only heat exchange is between the hot and cold fluids.
2. Axial conduction along the tubes is negligible.
3. Potential and kinetic energy changes are negligible.
4. The fluid specific heats are constant.
5. The overall heat transfer coefficient is constant.

The specific heats may of course change as a result of temperature variations, and the overall heat transfer coefficient may change because of variations in fluid properties and flow conditions. However, in many applications such variations are not significant, and it is reasonable to work with average values of $c_{p,c}$, $c_{p,h}$, and U for the heat exchanger.

Applying an energy balance to each of the differential elements of Figure 11.7, it follows that

$$dq = -\dot{m}_h c_{p,h}\, dT_h \equiv -C_h\, dT_h \tag{11.10}$$

and

$$dq = \dot{m}_c c_{p,c}\, dT_c \equiv C_c\, dT_c \tag{11.11}$$

where C_h and C_c are the hot and cold fluid *heat capacity rates*, respectively. These expressions may be integrated across the heat exchanger to obtain the overall

Patent Owner Manufacturing Resources International, Inc.
Exhibit 2017 - Page 683 of 999

energy balances given by Equations 11.6b and 11.7b. The heat transfer across the surface area dA may also be expressed as

$$dq = U\,\Delta T\,dA \tag{11.12}$$

where $\Delta T = T_h - T_c$ is the *local* temperature difference between the hot and cold fluids.

To determine the integrated form of Equation 11.12, we begin by substituting Equations 11.10 and 11.11 into the differential form of Equation 11.8

$$d(\Delta T) = dT_h - dT_c$$

to obtain

$$d(\Delta T) = -dq\left(\frac{1}{C_h} + \frac{1}{C_c}\right)$$

Substituting for dq from Equation 11.12 and integrating across the heat exchanger, we obtain

$$\int_1^2 \frac{d(\Delta T)}{\Delta T} = -U\left(\frac{1}{C_h} + \frac{1}{C_c}\right)\int_1^2 dA$$

or

$$\ln\left(\frac{\Delta T_2}{\Delta T_1}\right) = -UA\left(\frac{1}{C_h} + \frac{1}{C_c}\right) \tag{11.13}$$

Substituting for C_h and C_c from Equations 11.6b and 11.7b, respectively, it follows that

$$\ln\left(\frac{\Delta T_2}{\Delta T_1}\right) = -UA\left(\frac{T_{h,i} - T_{h,o}}{q} + \frac{T_{c,o} - T_{c,i}}{q}\right)$$
$$= -\frac{UA}{q}[(T_{h,i} - T_{c,i}) - (T_{h,o} - T_{c,o})]$$

Recognizing that, for the parallel-flow heat exchanger of Figure 11.7, $\Delta T_1 = (T_{h,i} - T_{c,i})$ and $\Delta T_2 = (T_{h,o} - T_{c,o})$, we then obtain

$$q = UA\,\frac{\Delta T_2 - \Delta T_1}{\ln(\Delta T_2/\Delta T_1)}$$

Comparing the above expression with Equation 11.9, we conclude that the appropriate average temperature difference is a *log mean temperature difference*, ΔT_{lm}. Accordingly, we may write

$$q = UA\,\Delta T_{lm} \tag{11.14}$$

where

$$\Delta T_{lm} = \frac{\Delta T_2 - \Delta T_1}{\ln(\Delta T_2/\Delta T_1)} = \frac{\Delta T_1 - \Delta T_2}{\ln(\Delta T_1/\Delta T_2)} \tag{11.15}$$

Remember that, for the *parallel-flow exchanger*,

$$\begin{bmatrix} \Delta T_1 \equiv T_{h,1} - T_{c,1} = T_{h,i} - T_{c,i} \\ \Delta T_2 \equiv T_{h,2} - T_{c,2} = T_{h,o} - T_{c,o} \end{bmatrix} \tag{11.16}$$

Patent Owner Manufacturing Resources International, Inc.
Exhibit 2017 - Page 684 of 999

11.3.2 The Counterflow Heat Exchanger

The hot and cold fluid temperature distributions associated with a counterflow heat exchanger are shown in Figure 11.8. In contrast to the parallel-flow exchanger, this configuration provides for heat transfer between the hotter portions of the two fluids at one end, as well as between the colder portions at the other. For this reason, the change in the temperature difference, $\Delta T = T_h - T_c$, with respect to x is nowhere as large as it is for the inlet region of the parallel-flow exchanger. Note that the outlet temperature of the cold fluid may now exceed the outlet temperature of the hot fluid.

Equations 11.6b and 11.7b apply to any heat exchanger and hence may be used for the counterflow arrangement. Moreover, from an analysis like that performed in Section 11.3.1, it may be shown that Equations 11.14 and 11.15 also apply. However, for the *counterflow exchanger* the endpoint temperature differences must now be defined as

$$\begin{bmatrix} \Delta T_1 \equiv T_{h,1} - T_{c,1} = T_{h,i} - T_{c,o} \\ \Delta T_2 \equiv T_{h,2} - T_{c,2} = T_{h,o} - T_{c,i} \end{bmatrix} \tag{11.17}$$

Note that, for the same inlet and outlet temperatures, the log mean temperature difference for counterflow exceeds that for parallel flow, $\Delta T_{lm,CF} > \Delta T_{lm,PF}$. Hence the surface area required to effect a prescribed heat transfer rate q is smaller for the counterflow than for the parallel-flow arrangement, assuming the same value of U. Also note that $T_{c,o}$ can exceed $T_{h,o}$ for counterflow but not for parallel flow.

11.3.3 Special Operating Conditions

It is useful to note certain special conditions under which heat exchangers may be operated. Figure 11.9*a* shows temperature distributions for a heat exchanger in

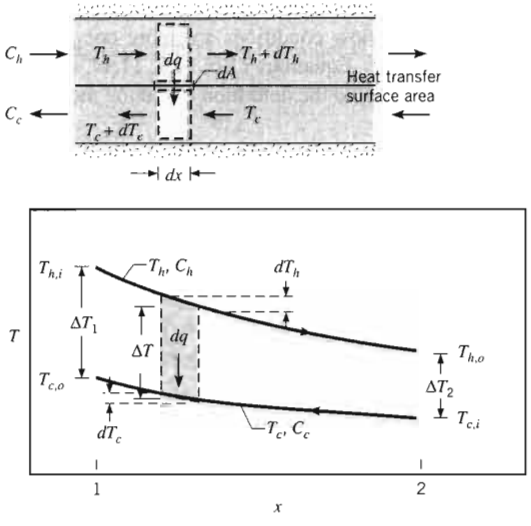


FIGURE 11.8 Temperature distributions for a counterflow heat exchanger.

Patent Owner Manufacturing Resources International, Inc.
Exhibit 2017 - Page 685 of 999

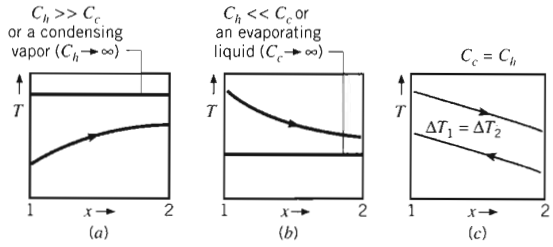


FIGURE 11.9 Special heat exchanger conditions. (*a*) $C_h \gg C_c$ or a condensing vapor. (*b*) An evaporating liquid or $C_h \ll C_c$. (*c*) A counterflow heat exchanger with equivalent fluid heat capacities ($C_h = C_c$).

which the hot fluid has a heat capacity rate, $C_h \equiv \dot{m}_h c_{p,h}$, which is much larger than that of the cold fluid, $C_c \equiv \dot{m}_c c_{p,c}$. For this case the temperature of the hot fluid remains approximately constant throughout the heat exchanger, while the temperature of the cold fluid increases. The same condition is achieved if the hot fluid is a condensing vapor. Condensation occurs at constant temperature, and, for all practical purposes, $C_h \to \infty$. Conversely, in an evaporator or a boiler (Figure 11.9*b*), it is the cold fluid that experiences a change in phase and remains at a nearly uniform temperature ($C_c \to \infty$). The same effect is achieved without phase change if $C_h \ll C_c$. Note that, with condensation or evaporation, the heat rate is given by Equation 11.6a or 11.7a. The third special case (Figure 11.9*c*) involves a counterflow heat exchanger for which the heat capacity rates are equal ($C_h = C_c$). The temperature difference ΔT must then be a constant throughout the exchanger, in which case $\Delta T_1 = \Delta T_2 = \Delta T_{lm}$.

Methodologies for using the LMTD method for other heat exchanger types are included in Section 11S.1.

Although flow conditions are more complicated in multipass and cross-flow heat exchangers, Equations 11.6, 11.7, 11.14, and 11.15 may still be used if modifications are made to the definition of the log mean temperature difference [6].

EXAMPLE 11.1

A counterflow, concentric tube heat exchanger is used to cool the lubricating oil for a large industrial gas turbine engine. The flow rate of cooling water through the inner tube ($D_i = 25$ mm) is 0.2 kg/s, while the flow rate of oil through the outer annulus ($D_o = 45$ mm) is 0.1 kg/s. The oil and water enter at temperatures of 100 and 30°C, respectively. How long must the tube be made if the outlet temperature of the oil is to be 60°C?

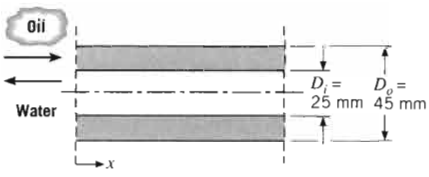
SOLUTION

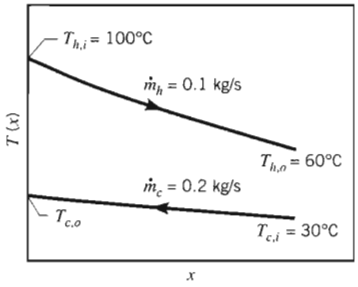
Known: Fluid flow rates and inlet temperatures for a counterflow, concentric tube heat exchanger of prescribed inner and outer diameter.

Find: Tube length to achieve a desired hot fluid outlet temperature.

Patent Owner Manufacturing Resources International, Inc.
Exhibit 2017 - Page 686 of 999

Schematic:





Assumptions:

1. Negligible heat loss to the surroundings.
2. Negligible kinetic and potential energy changes.
3. Constant properties.
4. Negligible tube wall thermal resistance and fouling factors.
5. Fully developed conditions for the water and oil (U independent of x).

Properties: Table A.5, unused engine oil ($\overline{T}_h = 80°C = 353$ K): $c_p = 2131$ J/kg · K, $\mu = 3.25 \times 10^{-2}$ N · s/m^2, $k = 0.138$ W/m · K. Table A.6, water ($\overline{T}_c \approx 35°C$): $c_p = 4178$ J/kg · K, $\mu = 725 \times 10^{-6}$ N · s/m^2, $k = 0.625$ W/m · K, $Pr = 4.85$.

Analysis: The required heat transfer rate may be obtained from the overall energy balance for the hot fluid, Equation 11.6b.

$$q = \dot{m}_h c_{p,h}(T_{h,i} - T_{h,o})$$

$$q = 0.1 \text{ kg/s} \times 2131 \text{ J/kg} \cdot \text{K}\,(100 - 60)°C = 8524 \text{ W}$$

Applying Equation 11.7b, the water outlet temperature is

$$T_{c,o} = \frac{q}{\dot{m}_c c_{p,c}} + T_{c,i}$$

$$T_{c,o} = \frac{8524 \text{ W}}{0.2 \text{ kg/s} \times 4178 \text{ J/kg} \cdot \text{K}} + 30°C = 40.2°C$$

Accordingly, use of $\overline{T}_c = 35°C$ to evaluate the water properties was a good choice. The required heat exchanger length may now be obtained from Equation 11.14,

$$q = UA\,\Delta T_{lm}$$

where $A = \pi D_i L$ and from Equations 11.15 and 11.17

$$\Delta T_{lm} = \frac{(T_{h,i} - T_{c,o}) - (T_{h,o} - T_{c,i})}{\ln\left[(T_{h,i} - T_{c,o})/(T_{h,o} - T_{c,i})\right]} = \frac{59.8 - 30}{\ln(59.8/30)} = 43.2°C$$

From Equation 11.5 the overall heat transfer coefficient is

$$U = \frac{1}{(1/h_i) + (1/h_o)}$$

Patent Owner Manufacturing Resources International, Inc.
Exhibit 2017 - Page 687 of 999

For water flow through the tube,

$$Re_D = \frac{4\dot{m}_c}{\pi D_i \mu} = \frac{4 \times 0.2 \text{ kg/s}}{\pi(0.025 \text{ m})725 \times 10^{-6} \text{ N} \cdot \text{s/m}^2} = 14{,}050$$

Accordingly, the flow is turbulent and the convection coefficient may be computed from Equation 8.60

$$Nu_D = 0.023\, Re_D^{4/5}\, Pr^{0.4}$$
$$Nu_D = 0.023\,(14{,}050)^{4/5}\,(4.85)^{0.4} = 90$$

Hence

$$h_i = Nu_D \frac{k}{D_i} = \frac{90 \times 0.625 \text{ W/m} \cdot \text{K}}{0.025 \text{ m}} = 2250 \text{ W/m}^2 \cdot \text{K}$$

For the flow of oil through the annulus, the hydraulic diameter is, from Equation 8.71, $D_h = D_o - D_i = 0.02$ m, and the Reynolds number is

$$Re_D = \frac{\rho u_m D_h}{\mu} = \frac{\rho(D_o - D_i)}{\mu} \times \frac{\dot{m}_h}{\rho\pi(D_o^2 - D_i^2)/4}$$

$$Re_D = \frac{4\dot{m}_h}{\pi\,(D_o + D_i)\,\mu} = \frac{4 \times 0.1 \text{ kg/s}}{\pi(0.045 + 0.025) \text{ m} \times 3.25 \times 10^{-2} \text{ kg/s} \cdot \text{m}} = 56.0$$

The annular flow is therefore laminar. Assuming uniform temperature along the inner surface of the annulus and a perfectly insulated outer surface, the convection coefficient at the inner surface may be obtained from Table 8.2. With $(D_i/D_o) = 0.56$, linear interpolation provides

$$Nu_i = \frac{h_o D_h}{k} = 5.63$$

and

$$h_o = 5.63 \frac{0.138 \text{ W/m} \cdot \text{K}}{0.020 \text{ m}} = 38.8 \text{ W/m}^2 \cdot \text{K}$$

The overall convection coefficient is then

$$U = \frac{1}{(1/2250 \text{ W/m}^2 \cdot \text{K}) + (1/38.8 \text{ W/m}^2 \cdot \text{K})} = 38.1 \text{ W/m}^2 \cdot \text{K}$$

and from the rate equation it follows that

$$L = \frac{q}{U\pi D_i \Delta T_{\text{lm}}} = \frac{8524 \text{ W}}{38.1 \text{ W/m}^2 \cdot \text{K}\, \pi\, (0.025 \text{ m})\, (43.2°\text{C})} = 65.9 \text{ m} \quad \triangleleft$$

Comments:

1. The hot side convection coefficient controls the rate of heat transfer between the two fluids, and the low value of h_o is responsible for the large value of L. Incorporation of heat transfer enhancement methods, such as described in Section 8.8, could be used to decrease the size of the heat exchanger.
2. Because $h_i \gg h_o$, the tube wall temperature will follow closely that of the coolant water. Accordingly, the assumption of uniform wall temperature, which is inherent in the use of Table 8.2 to obtain h_o, is reasonable.

Patent Owner Manufacturing Resources International, Inc.
Exhibit 2017 - Page 688 of 999

EXAMPLE 11.2

The counterflow, concentric tube heat exchanger of Example 11.1 is replaced with a compact, plate-type heat exchanger that consists of a stack of thin metal sheets, separated by N gaps of width a. The oil and water flows are subdivided into $N/2$ individual flow streams, with the oil and water moving in opposite directions within alternating gaps. It is desirable for the stack to be of a cubical geometry, with a characteristic exterior dimension L. Determine the exterior dimensions of the heat exchanger as a function of the number of gaps if the flow rates, inlet temperatures, and desired oil outlet temperature are the same as in Example 11.1. Compare the pressure drops of the water and oil streams within the plate-type heat exchanger to the pressure drops of the flow streams in Example 11.1, if 60 gaps are specified.

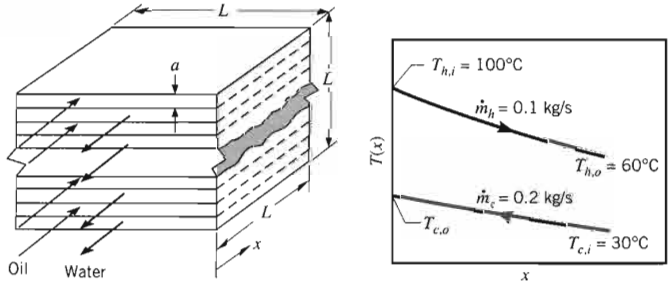
SOLUTION

Known: Configuration of a plate-type heat exchanger. Fluid flow rates, inlet temperatures, and desired oil outlet temperature.

Find:

1. Exterior dimensions of the heat exchanger.
2. Pressure drops within the plate-type heat exchanger with $N = 60$ gaps, and the concentric tube heat exchanger of Example 11.1.

Schematic:



Assumptions:

1. Negligible heat loss to the surroundings.
2. Negligible kinetic and potential energy changes.
3. Constant properties.
4. Negligible plate thermal resistance and fouling factors.
5. Fully developed conditions for the water and oil.
6. Identical gap-to-gap heat transfer coefficients.
7. Heat exchanger exterior dimension is large compared to the gap width.

Properties: See Example 11.1. In addition, Table A.5, unused engine oil ($\overline{T}_h$ = 353 K): $\rho = 852.1$ kg/m^3. Table A.6, water ($\overline{T}_c \approx 35$°C): $\rho = v_f^{-1} = 994$ kg/m^3.

Patent Owner Manufacturing Resources International, Inc.
Exhibit 2017 - Page 689 of 999

Analysis:

1. The gap width may be related to the overall dimension of the heat exchanger by the expression $a = L/N$, and the total heat transfer area is $A = L^2 (N - 1)$. Assuming $a \ll L$ and the existence of laminar flow, the Nusselt number for each interior gap is provided in Table 8.1 and is

$$Nu_D = \frac{hD_h}{k} = 7.54$$

From Equation 8.66, the hydraulic diameter is $D_h = 2a$. Combining the preceding expressions yields for the water:

$$h_c = 7.54k/2L = 7.54 \times 0.625 \text{ W/m} \cdot \text{K} \times N/2L = (2.36 \text{ W/m} \cdot \text{K})N/L$$

Likewise, for the oil:

$$h_h = 7.54k/2L = 7.54 \times 0.138 \text{ W/m} \cdot \text{K} \times N/2L = (0.520 \text{ W/m} \cdot \text{K})N/L$$

and the overall convection coefficient is

$$U = \frac{1}{1/h_c + 1/h_h}$$

From Example 11.1, the required log mean temperature difference and heat transfer rate are $\Delta T_{lm} = 43.2°\text{C}$ and $q = 8524$ W, respectively. From Equation 11.14 it follows that

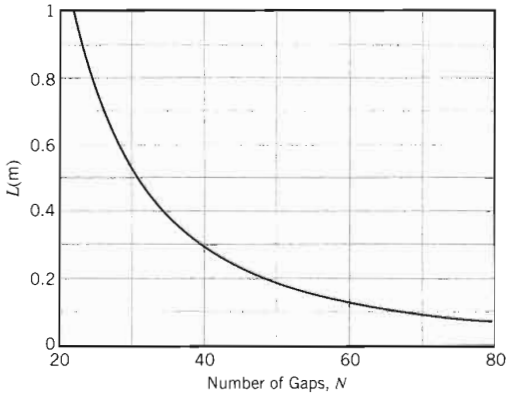
$$UA = \frac{L^2(N-1)}{1/h_c + 1/h_h} = \frac{q}{\Delta T_{lm}}$$

which may be rearranged to yield

$$L = \frac{q}{\Delta T_{lm}(N-1)}\left[\frac{1}{h_c L} + \frac{1}{h_h L}\right]$$

$$= \frac{8524 \text{ W}}{43.2°\text{C}(N-1)N}\left[\frac{1}{2.36 \text{ W/m} \cdot \text{K}} + \frac{1}{0.520 \text{ W/m} \cdot \text{K}}\right] = \frac{463 \text{ m}}{N(N-1)} \quad \triangleleft$$

The size of the compact heat exchanger decreases as the number of gaps is increased, as shown in the figure below.



Patent Owner Manufacturing Resources International, Inc.
Exhibit 2017 - Page 690 of 999

heat exchanger by
$A = L^2 (N - 1)$.
Nusselt number for

nbining the preced-

W/m · K)N/L

W/m · K)N/L

rence and heat trans-
rom Equation 11.14

$= \dfrac{463 \text{ m}}{N(N-1)}$ ◁

e number of gaps is



2. For $N = 60$ gaps, the stack dimension is $L = 0.131$ m from the results of part 1, and the gap width is $a = L/N = 0.131 \text{ m}/60 = 0.00218$ m.

The hydraulic diameter is $D_h = 0.00436$ m, and the mean velocity in each water-filled gap is

$$u_m = \frac{\dot{m}}{\rho L^2/2} = \frac{2 \times 0.2 \text{ kg/s}}{994 \text{ kg/m}^3 \times 0.131^2 \text{ m}^2} = 0.0235 \text{ m/s}$$

providing a Reynolds number of

$$Re_D = \frac{\rho u_m D_h}{\mu} = \frac{994 \text{ kg/m}^3 \times 0.0235 \text{ m/s} \times 0.00436 \text{ m}}{725 \times 10^{-6} \text{ N} \cdot \text{s/m}^2} = 141$$

For the oil-filled gaps

$$u_m = \frac{\dot{m}}{\rho L^2/2} = \frac{2 \times 0.1 \text{ kg/s}}{852.1 \text{ kg/m}^3 \times 0.131^2 \text{ m}^2} = 0.0137 \text{ m/s}$$

yielding a Reynolds number of

$$Re_D = \frac{\rho u_m D_h}{\mu} = \frac{852.1 \text{ kg/m}^3 \times 0.0137 \text{ m/s} \times 0.00436 \text{ m}}{3.25 \times 10^{-2} \text{ N} \cdot \text{s/m}^2} = 1.57$$

Therefore, the flow is laminar for both fluids, as assumed in part 1. Equations 8.19 and 8.22a may be used to calculate the pressure drop for the water:

$$\Delta p = \frac{64}{Re_D} \cdot \frac{\rho u_m^2}{2D_h} \cdot L = \frac{64}{141} \times \frac{994 \text{ kg/m}^3 \times 0.0235^2 \text{ m}^2/\text{s}^2}{2 \times 0.00436 \text{ m}} \times 0.131 \text{ m}$$
$$= 3.76 \text{ N/m}^2 \quad \triangleleft$$

Similarly, for the oil

$$\Delta p = \frac{64}{Re_D} \cdot \frac{\rho u_m^2}{2D_h} \cdot L = \frac{64}{1.57} \times \frac{852.1 \text{ kg/m}^3 \times 0.0137^2 \text{ m}^2/\text{s}^2}{2 \times 0.00436 \text{ m}} \times 0.131 \text{ m}$$
$$= 98.2 \text{ N/m}^2 \quad \triangleleft$$

For Example 11.1, the friction factor associated with the water flow may be calculated using Equation 8.21, and for a smooth surface condition is $f = (0.790 \ln(14{,}050) - 1.64)^{-2} = 0.0287$. The mean velocity is $u_m = 4\dot{m}/[\rho\pi D_i^2 = 4 \times 0.2 \text{ kg/s}/(994 \text{ kg/m}^3 \times \pi \times 0.025^2 \text{ m}^2)] = 0.410$ m/s, and the pressure drop is

$$\Delta p = f \cdot \frac{\rho u_m^2}{2D_h} \cdot L = 0.0287 \times \frac{994 \text{ kg/m}^3 \times 0.410^2 \text{ m}^2/\text{s}^2}{2 \times 0.025 \text{ m}} \times 65.9 \text{ m}$$
$$= 6310 \text{ N/m}^2$$

For the oil flowing in the annular region, the mean velocity is $u_m = 4\dot{m}/[\rho\pi (D_o^2 - D_i^2)] = 4 \times 0.1 \text{ kg/s}/[852.1 \text{ kg/m}^3 \times \pi \times (0.045^2 - 0.025^2)\text{m}^2] = 0.107$ m/s, and the pressure drop is

$$\Delta p = \frac{64}{Re_D} \cdot \frac{\rho u_m^2}{2D_h} \cdot L = \frac{64}{56} \times \frac{852.1 \text{ kg/m}^3 \times 0.107^2 \text{ m}^2/\text{s}^2}{2 \times 0.020 \text{ m}} \times 65.9 \text{ m}$$
$$= 18{,}300 \text{ N/m}^2 \quad \triangleleft$$

Patent Owner Manufacturing Resources International, Inc.
Exhibit 2017 - Page 691 of 999

Comments:

1. Increasing the number of gaps increases the UA product by simultaneously providing more surface area and increasing the heat transfer coefficients associated with the flow of the fluids through smaller passages.
2. The area-to-volume ratio of the $N = 60$ heat exchanger is $L^2(N-1)/L^3 = (N-1)/L = (60-1)/0.131\ \text{m} = 451\ \text{m}^2/\text{m}^3$.
3. The volume occupied by the concentric tube heat exchanger is $V = \pi D_o^2 L/4 = \pi \times 0.045^2\ \text{m}^2 \times 65.9\ \text{m}/4 = 0.10\ \text{m}^3$, while the volume of the compact plate-type exchanger is $V = L^3 = 0.131^3\ \text{m}^3 = 0.0022\ \text{m}^3$. Use of the plate-type heat exchanger results in a 97.8% reduction in volume relative to the conventional, concentric tube heat exchanger.
4. The pressure drops associated with use of the compact heat exchanger are significantly less than for a conventional concentric tube configuration. Pressure drops are reduced by 99.9% and 99.5% for the water and oil flows, respectively.
5. Fouling of the heat transfer surfaces may result in a decrease in the gap width, as well as an associated reduction in heat transfer rate and increase in pressure drop.
6. Because $h_c > h_h$, the temperatures of the thin metal sheets will follow closely that of the water, and, as in Example 11.1, the assumption of uniform temperature conditions to obtain h_c and h_h is reasonable.
7. One method to fabricate such a heat exchanger is presented in C. F. McDonald, *Appl. Thermal Engin.*, **20**, 471, 2000.

11.4 *Heat Exchanger Analysis: The Effectiveness–NTU Method*

It is a simple matter to use the log mean temperature difference (LMTD) method of heat exchanger analysis when the fluid inlet temperatures are known and the outlet temperatures are specified or readily determined from the energy balance expressions, Equations 11.6b and 11.7b. The value of ΔT_{lm} for the exchanger may then be determined. However, if only the inlet temperatures are known, use of the LMTD method requires a cumbersome iterative procedure. It is therefore preferable to use an alternative approach termed the *effectiveness*–NTU (or NTU) method.

11.4.1 Definitions

To define the *effectiveness of a heat exchanger*, we must first determine the *maximum possible heat transfer rate*, q_{max}, for the exchanger. This heat transfer rate could, in principle, be achieved in a counterflow heat exchanger (Figure 11.8) of infinite length. In such an exchanger, one of the fluids would experience the maximum possible temperature difference, $T_{h,i} - T_{c,i}$. To illustrate this point, consider a situation for which $C_c < C_h$, in which case, from Equations 11.10 and 11.11, $|dT_c| > |dT_h|$. The cold fluid would then experience the larger temperature change, and since $L \to \infty$, it would be heated to the inlet temperature of the hot fluid ($T_{c,o} = T_{h,i}$). Accordingly, from Equation 11.7b,

Patent Owner Manufacturing Resources International, Inc.
Exhibit 2017 - Page 692 of 999

$$C_c < C_h: \qquad q_{max} = C_c(T_{h,i} - T_{c,i})$$

Similarly, if $C_h < C_c$, the hot fluid would experience the larger temperature change and would be cooled to the inlet temperature of the cold fluid ($T_{h,o} = T_{c,i}$). From Equation 11.6b, we then obtain

$$C_h < C_c: \qquad q_{max} = C_h(T_{h,i} - T_{c,i})$$

From the foregoing results we are then prompted to write the general expression

$$q_{max} = C_{min}(T_{h,i} - T_{c,i}) \tag{11.18}$$

where C_{min} is equal to C_c or C_h, whichever is smaller. For prescribed hot and cold fluid inlet temperatures, Equation 11.18 provides the maximum heat transfer rate that could possibly be delivered by the exchanger. A quick mental exercise should convince the reader that the maximum possible heat transfer rate is *not* equal to $C_{max}(T_{h,i} - T_{c,i})$. If the fluid having the larger heat capacity rate were to experience the maximum possible temperature change, conservation of energy in the form $C_c(T_{c,o} - T_{c,i}) = C_h(T_{h,i} - T_{h,o})$ would require that the other fluid experience yet a larger temperature change. For example, if $C_{max} = C_c$ and one argues that it is possible for $T_{c,o}$ to be equal to $T_{h,i}$, it follows that $(T_{h,i} - T_{h,o}) = (C_c/C_h)(T_{h,i} - T_{c,i})$, in which case $(T_{h,i} - T_{h,o}) > (T_{h,i} - T_{c,i})$. Such a condition is clearly impossible.

It is now logical to define the *effectiveness*, ε, as the ratio of the actual heat transfer rate for a heat exchanger to the maximum possible heat transfer rate:

$$\varepsilon \equiv \frac{q}{q_{max}} \tag{11.19}$$

From Equations 11.6b, 11.7b, and 11.18, it follows that

$$\varepsilon = \frac{C_h(T_{h,i} - T_{h,o})}{C_{min}(T_{h,i} - T_{c,i})} \tag{11.20}$$

or

$$\varepsilon = \frac{C_c(T_{c,o} - T_{c,i})}{C_{min}(T_{h,i} - T_{c,i})} \tag{11.21}$$

By definition the effectiveness, which is dimensionless, must be in the range $0 \leq \varepsilon \leq 1$. It is useful because, if ε, $T_{h,i}$, and $T_{c,i}$ are known, the actual heat transfer rate may readily be determined from the expression

$$q = \varepsilon C_{min}(T_{h,i} - T_{c,i}) \tag{11.22}$$

For any heat exchanger it can be shown that [5]

$$\varepsilon = f\left(\text{NTU}, \frac{C_{min}}{C_{max}}\right) \tag{11.23}$$

where C_{min}/C_{max} is equal to C_c/C_h or C_h/C_c, depending on the relative magnitudes of the hot and cold fluid heat capacity rates. The *number of transfer units* (NTU) is a dimensionless parameter that is widely used for heat exchanger analysis and is defined as

$$\text{NTU} \equiv \frac{UA}{C_{min}} \tag{11.24}$$

Patent Owner Manufacturing Resources International, Inc.
Exhibit 2017 - Page 693 of 999

11.4.2 Effectiveness–NTU Relations

To determine a specific form of the effectiveness–NTU relation, Equation 11.23, consider a *parallel-flow* heat exchanger for which $C_{min} = C_h$. From Equation 11.20 we then obtain

$$\varepsilon = \frac{T_{h,i} - T_{h,o}}{T_{h,i} - T_{c,i}} \tag{11.25}$$

and from Equations 11.6b and 11.7b it follows that

$$\frac{C_{min}}{C_{max}} = \frac{\dot{m}_h c_{p,h}}{\dot{m}_c c_{p,c}} = \frac{T_{c,o} - T_{c,i}}{T_{h,i} - T_{h,o}} \tag{11.26}$$

Now consider Equation 11.13, which may be expressed as

$$\ln\left(\frac{T_{h,o} - T_{c,o}}{T_{h,i} - T_{c,i}}\right) = -\frac{UA}{C_{min}}\left(1 + \frac{C_{min}}{C_{max}}\right)$$

or from Equation 11.24

$$\frac{T_{h,o} - T_{c,o}}{T_{h,i} - T_{c,i}} = \exp\left[-\text{NTU}\left(1 + \frac{C_{min}}{C_{max}}\right)\right] \tag{11.27}$$

Rearranging the left-hand side of this expression as

$$\frac{T_{h,o} - T_{c,o}}{T_{h,i} - T_{c,i}} = \frac{T_{h,o} - T_{h,i} + T_{h,i} - T_{c,o}}{T_{h,i} - T_{c,i}}$$

and substituting for $T_{c,o}$ from Equation 11.26, it follows that

$$\frac{T_{h,o} - T_{c,o}}{T_{h,i} - T_{c,i}} = \frac{(T_{h,o} - T_{h,i}) + (T_{h,i} - T_{c,i}) - (C_{min}/C_{max})(T_{h,i} - T_{h,o})}{T_{h,i} - T_{c,i}}$$

or from Equation 11.25

$$\frac{T_{h,o} - T_{c,o}}{T_{h,i} - T_{c,i}} = -\varepsilon + 1 - \left(\frac{C_{min}}{C_{max}}\right)\varepsilon = 1 - \varepsilon\left(1 + \frac{C_{min}}{C_{max}}\right)$$

Substituting the above expression into Equation 11.27 and solving for ε, we obtain for the *parallel-flow heat exchanger*

$$\varepsilon = \frac{1 - \exp\{-\text{NTU}[1 + (C_{min}/C_{max})]\}}{1 + (C_{min}/C_{max})} \tag{11.28a}$$

Since precisely the same result may be obtained for $C_{min} = C_c$, Equation 11.28a applies for any parallel-flow heat exchanger, irrespective of whether the minimum heat capacity rate is associated with the hot or cold fluid.

Similar expressions have been developed for a variety of heat exchangers [5], and representative results are summarized in Table 11.3, where C_r is the *heat capacity ratio* $C_r \equiv C_{min}/C_{max}$. In deriving Equation 11.31a for a shell-and-tube heat exchanger with multiple shell passes, it is assumed that the total NTU is equally distributed between shell passes of the same arrangement, $\text{NTU} = n(\text{NTU})_1$. In order to determine ε, $(\text{NTU})_1$ would first be calculated using the heat transfer area for one shell, ε_1 would then be calculated from Equation 11.30a, and ε would finally be

Patent Owner Manufacturing Resources International, Inc.
Exhibit 2017 - Page 694 of 999

TABLE 11.3 Heat Exchanger Effectiveness Relations [5]

Flow Arrangement	Relation		
Concentric tube			
Parallel flow	$\varepsilon = \dfrac{1 - \exp[-\text{NTU}(1 + C_r)]}{1 + C_r}$		(11.28a)
Counterflow	$\varepsilon = \dfrac{1 - \exp[-\text{NTU}(1 - C_r)]}{1 - C_r \exp[-\text{NTU}(1 - C_r)]}$	$(C_r < 1)$	
	$\varepsilon = \dfrac{\text{NTU}}{1 + \text{NTU}}$	$(C_r = 1)$	(11.29a)
Shell-and-tube			
One shell pass (2, 4, . . . tube passes)	$\varepsilon_1 = 2\left\{1 + C_r + (1 + C_r^2)^{1/2} \times \dfrac{1 + \exp[-(\text{NTU})_1(1 + C_r^2)^{1/2}]}{1 - \exp[-(\text{NTU})_1(1 + C_r^2)^{1/2}]}\right\}^{-1}$		(11.30a)
n Shell passes (2n, 4n, . . . tube passes)	$\varepsilon = \left[\left(\dfrac{1 - \varepsilon_1 C_r}{1 - \varepsilon_1}\right)^n - 1\right]\left[\left(\dfrac{1 - \varepsilon_1 C_r}{1 - \varepsilon_1}\right)^n - C_r\right]^{-1}$		(11.31a)
Cross-flow (single pass)			
Both fluids unmixed	$\varepsilon = 1 - \exp\left[\left(\dfrac{1}{C_r}\right)(\text{NTU})^{0.22}\{\exp[-C_r(\text{NTU})^{0.78}] - 1\}\right]$		(11.32)
$C_{\max}$ (mixed), $C_{\min}$ (unmixed)	$\varepsilon = \left(\dfrac{1}{C_r}\right)(1 - \exp\{-C_r[1 - \exp(-\text{NTU})]\})$		(11.33a)
$C_{\min}$ (mixed), $C_{\max}$ (unmixed)	$\varepsilon = 1 - \exp(-C_r^{-1}\{1 - \exp[-C_r(\text{NTU})]\})$		(11.34a)
All exchangers ($C_r = 0$)	$\varepsilon = 1 - \exp(-\text{NTU})$		(11.35a)

calculated from Equation 11.31a. Note that for $C_r = 0$, as in a boiler or condenser, ε is given by Equation 11.35a for *all flow arrangements. Hence, for this special case, it follows that heat exchanger behavior is independent of flow arrangement.* For the cross-flow heat exchanger with both fluids unmixed, Equation 11.32 is exact only for $C_r = 1$. However, it may be used to a good approximation for all $0 < C_r \leq 1$. For $C_r = 0$, Equation 11.35a must be used.

In heat exchanger design calculations (Section 11.5), it is more convenient to work with ε–NTU relations of the form

$$\text{NTU} = f\left(\varepsilon, \frac{C_{\min}}{C_{\max}}\right)$$

Explicit relations for NTU as a function of ε and C_r are provided in Table 11.4. Note that Equation 11.32 may not be manipulated to yield a direct relationship for NTU as a function of ε and C_r. Note also that to determine the NTU for a shell-and-tube heat exchanger with multiple shell passes, ε would first be calculated for the entire heat exchanger. The variables F and ε_1 would then be calculated using Equations 11.31c and 11.31b, respectively. The parameter E would subsequently be determined from Equation 11.30c and substituted into Equation 11.30b to find

Patent Owner Manufacturing Resources International, Inc.
Exhibit 2017 - Page 695 of 999

TABLE 11.4 Heat Exchanger NTU Relations

Flow Arrangement	Relation	
Concentric tube		
Parallel flow	$\text{NTU} = -\dfrac{\ln[1-\varepsilon(1+C_r)]}{1+C_r}$	(11.28b)
Counterflow	$\text{NTU} = \dfrac{1}{C_r-1}\ln\left(\dfrac{\varepsilon-1}{\varepsilon C_r-1}\right) \quad (C_r<1)$	
	$\text{NTU} = \dfrac{\varepsilon}{1-\varepsilon} \quad (C_r=1)$	(11.29b)
Shell-and-tube		
One shell pass (2, 4, . . . tube passes)	$(\text{NTU})_1 = -(1+C_r^2)^{-1/2}\ln\left(\dfrac{E-1}{E+1}\right)$	(11.30b)
	$E = \dfrac{2/\varepsilon_1-(1+C_r)}{(1+C_r^2)^{1/2}}$	(11.30c)
n Shell passes ($2n$, $4n$, . . . tube passes)	Use Equations 11.30b and 11.30c with $\varepsilon_1 = \dfrac{F-1}{F-C_r} \quad F = \left(\dfrac{\varepsilon C_r-1}{\varepsilon-1}\right)^{1/n} \quad \text{NTU} = n(\text{NTU})_1$	(11.31b, c, d)
Cross-flow (single pass)		
C_{max} (mixed), C_{min} (unmixed)	$\text{NTU} = -\ln\left[1+\left(\dfrac{1}{C_r}\right)\ln(1-\varepsilon C_r)\right]$	(11.33b)
C_{min} (mixed), C_{max} (unmixed)	$\text{NTU} = -\left(\dfrac{1}{C_r}\right)\ln[C_r\ln(1-\varepsilon)+1]$	(11.34b)
All exchangers ($C_r = 0$)	$\text{NTU} = -\ln(1-\varepsilon)$	(11.35b)

$(\text{NTU})_1$. Finally, this result would be multiplied by n to obtain the NTU for the entire exchanger, as indicated in Equation 11.31d.

The foregoing expressions are represented graphically in Figures 11.10 through 11.15. When using Figure 11.13, the abscissa corresponds to the total number of

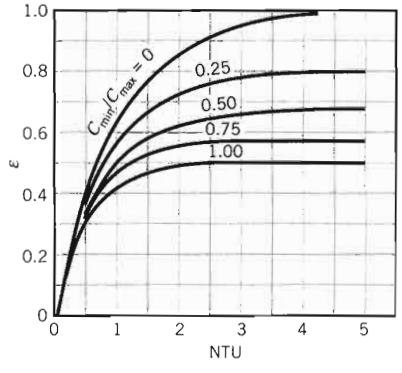


FIGURE 11.10 Effectiveness of a parallel-flow heat exchanger (Equation 11.28).

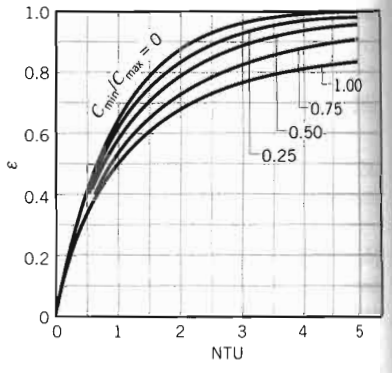


FIGURE 11.11 Effectiveness of a counterflow heat exchanger (Equation 11.29).

Patent Owner Manufacturing Resources International, Inc.
Exhibit 2017 - Page 696 of 999

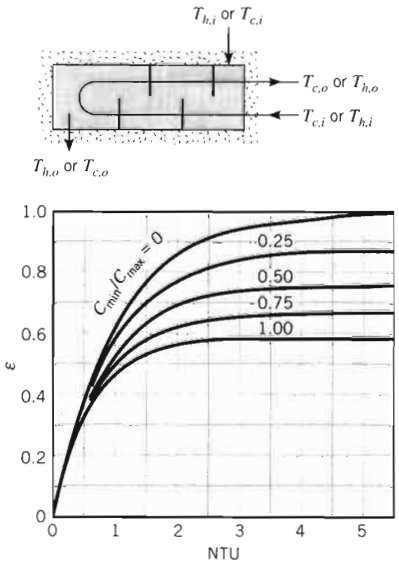


FIGURE 11.12 Effectiveness of a shell-and-tube heat exchanger with one shell and any multiple of two tube passes (two, four, etc. tube passes) (Equation 11.30).

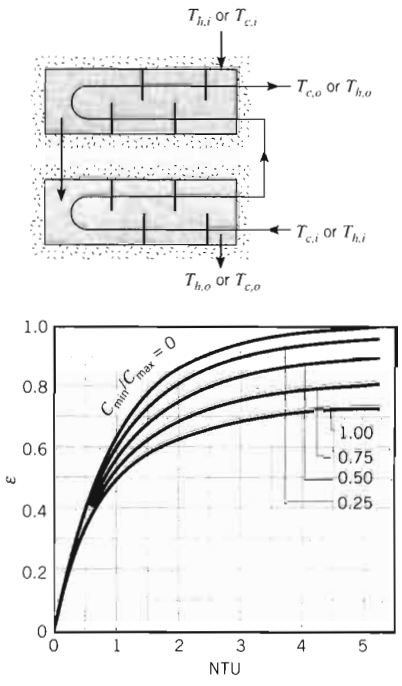


FIGURE 11.13 Effectiveness of a shell-and-tube heat exchanger with two shell passes and any multiple of four tube passes (four, eight, etc. tube passes) (Equation 11.31 with $n = 2$).

transfer units, NTU $= n(\text{NTU})_1$. For Figure 11.15 the solid curves correspond to C_{min} mixed and C_{max} unmixed, while the dashed curves correspond to C_{min} unmixed and C_{max} mixed. Note that for $C_r = 0$, all heat exchangers have the same effectiveness, which may be computed from Equation 11.35a. Moreover, if NTU $\lesssim 0.25$, all heat exchangers have approximately the same effectiveness, regardless of the value of C_r, and ε may again be computed from Equation 11.35a. More generally, for $C_r > 0$ and NTU $\gtrsim 0.25$, the counterflow exchanger is the most effective. For any exchanger, maximum and minimum values of the effectiveness are associated with $C_r = 0$ and $C_r = 1$, respectively.

As noted previously, in the context of cross-flow heat exchangers, the terms *mixed* and *unmixed* are idealizations representing limiting cases of actual flow conditions. That is, most flows are neither completely mixed nor unmixed, but exhibit partial degrees of mixing. This issue has been addressed by DiGiovanni and Webb [7], and algebraic expressions have been developed to determine the $\varepsilon-$NTU relationship for arbitrary values of partial mixing.

We also note that both the LMTD and $\varepsilon-$NTU methods approach heat exchanger analysis from a global perspective and provide no information concerning conditions within the exchanger. Although flow and temperature variations within a

Patent Owner Manufacturing Resources International, Inc.
Exhibit 2017 - Page 697 of 999

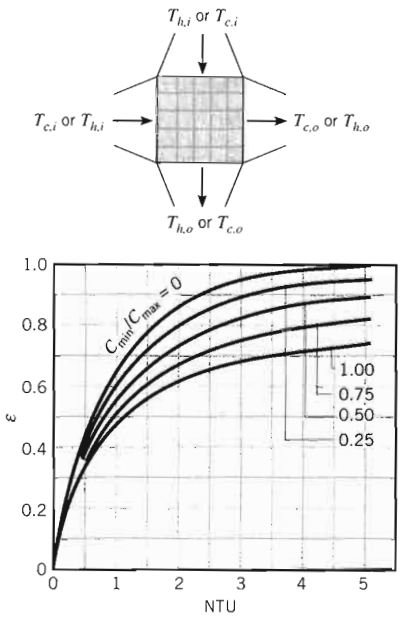


FIGURE 11.14 Effectiveness of a single-pass, cross-flow heat exchanger with both fluids unmixed (Equation 11.32).

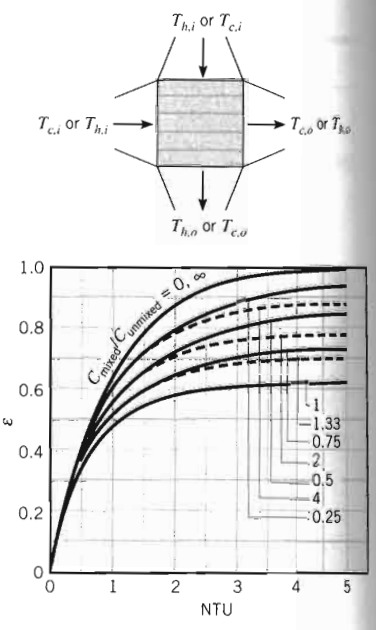


FIGURE 11.15 Effectiveness of a single-pass, cross-flow heat exchanger with one fluid mixed and the other unmixed (Equations 11.33, 11.34).

heat exchanger may be determined using commercial CFD (computational fluid dynamic) computer codes, simpler numerical procedures may be adopted. Such procedures have been applied by Ribando et al. to determine temperature variations in concentric tube and shell-and-tube heat exchangers [8].

EXAMPLE 11.3

Hot exhaust gases, which enter a finned-tube, cross-flow heat exchanger at 300°C and leave at 100°C, are used to heat pressurized water at a flow rate of 1 kg/s from 35 to 125°C. The exhaust gas specific heat is approximately 1000 J/kg · K, and the overall heat transfer coefficient based on the gas-side surface area is U_h = 100 W/m^2 · K. Determine the required gas-side surface area A_h using the NTU method.

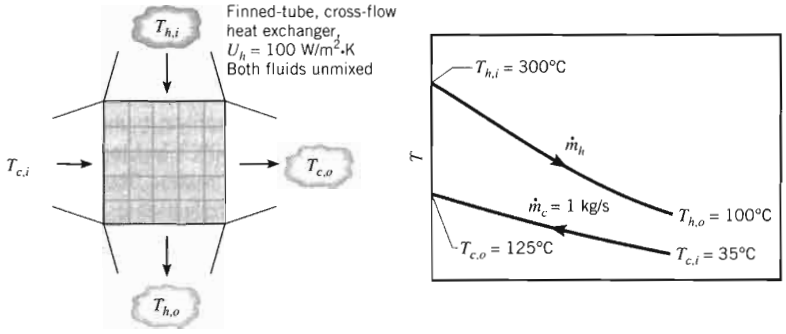
SOLUTION

Known: Inlet and outlet temperatures of hot gases and water used in a finned-tube, cross-flow heat exchanger. Water flow rate and gas-side overall heat transfer coefficient.

Find: Required gas-side surface area.

Patent Owner Manufacturing Resources International, Inc.
Exhibit 2017 - Page 698 of 999

Schematic:



Assumptions:

1. Negligible heat loss to the surroundings and kinetic and potential energy changes.
2. Constant properties.

Properties: Table A.6, water ($\overline{T}_c$ = 80°C): $c_{p,c}$ = 4197 J/kg · K. Exhaust gases: $c_{p,h}$ = 1000 J/kg · K.

Analysis: The required surface area may be obtained from knowledge of the number of transfer units, which, in turn, may be obtained from knowledge of the ratio of heat capacity rates and the effectiveness. To determine the minimum heat capacity rate, we begin by computing

$$C_c = \dot{m}_c c_{p,c} = 1 \text{ kg/s} \times 4197 \text{ J/kg} \cdot \text{K} = 4197 \text{ W/K}$$

Since $\dot{m}_h$ is not specified, C_h is obtained by combining the overall energy balances, Equations 11.6b and 11.7b:

$$C_h = \dot{m}_h c_{p,h} = C_c \frac{T_{c,o} - T_{c,i}}{T_{h,i} - T_{h,o}} = 4197 \frac{125 - 35}{300 - 100} = 1889 \text{ W/K} = C_{\min}$$

From Equation 11.18

$$q_{\max} = C_{\min}(T_{h,i} - T_{c,i}) = 1889 \text{ W/K}\,(300 - 35)^\circ\text{C} = 5.00 \times 10^5 \text{ W}$$

From Equation 11.7b the actual heat transfer rate is

$$q = \dot{m}_c c_{p,c}(T_{c,o} - T_{c,i}) = 1 \text{ kg/s} \times 4197 \text{ J/kg} \cdot \text{K}\,(125 - 35)^\circ\text{C}$$
$$q = 3.78 \times 10^5 \text{ W}$$

Hence from Equation 11.19 the effectiveness is

$$\varepsilon = \frac{q}{q_{\max}} = \frac{3.78 \times 10^5 \text{ W}}{5.00 \times 10^5 \text{ W}} = 0.75$$

With

$$\frac{C_{\min}}{C_{\max}} = \frac{1889}{4197} = 0.45$$

it follows from Figure 11.14 that

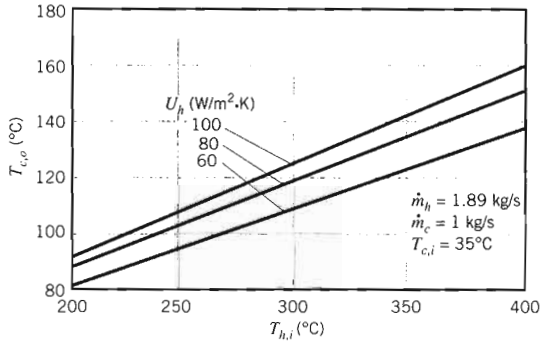
$$\text{NTU} = \frac{U_h A_h}{C_{\min}} \approx 2.1$$

Patent Owner Manufacturing Resources International, Inc.
Exhibit 2017 - Page 699 of 999

or

$$A_h = \frac{2.1(1889\ \text{W/K})}{100\ \text{W/m}^2 \cdot \text{K}} = 39.7\ \text{m}^2$$

Comments: With the heat exchanger sized ($A_h = 39.7\ \text{m}^2$) and placed into operation, its actual performance is subject to uncontrolled variations in the exhaust gas inlet temperature ($200 \leq T_{h,i} \leq 400°\text{C}$) and to gradual degradation of the heat exchanger surfaces due to fouling (U_h decreasing from 100 to 60 $\text{W/m}^2 \cdot \text{K}$). For a fixed value of $C_{\min} = C_h = 1889\ \text{W/K}$, the reduction in U_h corresponds to a reduction in the NTU (to NTU $\approx$ 1.26) and hence to a reduction in the heat exchanger effectiveness, which can be computed from Equation 11.32. The effect of the variations on the water outlet temperature has been computed and is plotted as follows:



If the intent is to maintain a fixed water outlet temperature of $T_{c,o} = 125°\text{C}$, adjustments in the flow rates, $\dot{m}_c$ and $\dot{m}_h$, could be made to compensate for the variations. The model equations could be used to determine the adjustments and hence as a basis for designing the requisite *controller*.

11.5 *Heat Exchanger Design and Performance Calculations: Using the Effectiveness–NTU Method*

Two general types of heat exchanger problems are commonly encountered by the practicing engineer.

In the *heat exchanger design problem*, the fluid inlet temperatures and flow rates, as well as a desired hot or cold fluid outlet temperature, are prescribed. The design problem is then one of specifying a specific heat exchanger type and determining its size—that is, the heat transfer surface area A—required to achieve the desired outlet temperature. The design problem is commonly encountered when a heat exchanger is to be custom-built for a specific application. Alternatively, in a *heat exchanger performance calculation*, an existing heat exchanger is analyzed to determine the heat transfer rate and the fluid outlet temperatures for prescribed flow

Patent Owner Manufacturing Resources International, Inc.
Exhibit 2017 - Page 700 of 999

rates and inlet temperatures. The performance calculation is commonly associated with the use of off-the-shelf heat exchanger types and sizes available from a vendor.

For heat exchanger design problems, the NTU method may be used by first calculating ε and (C_{min}/C_{max}). The appropriate equation (or chart) may then be used to obtain the NTU value, which in turn may be used to determine A. For a performance calculation, the NTU and (C_{min}/C_{max}) values may be computed and ε may then be determined from the appropriate equation (or chart) for a particular exchanger type. Since q_{max} may also be computed from Equation 11.18, it is a simple matter to determine the actual heat transfer rate from the requirement that $q = \varepsilon q_{max}$. Both fluid outlet temperatures may then be determined from Equations 11.6b and 11.7b.

EXAMPLE 11.4

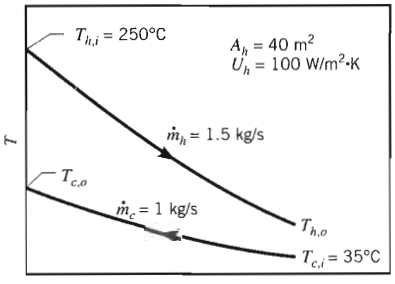
Consider the heat exchanger design of Example 11.3, that is, a finned-tube, cross-flow heat exchanger with a gas-side overall heat transfer coefficient and area of 100 $W/m^2 \cdot K$ and 40 m^2, respectively. The water flow rate and inlet temperature remain at 1 kg/s and 35°C. However, a change in operating conditions for the hot gas generator causes the gases to now enter the heat exchanger with a flow rate of 1.5 kg/s and a temperature of 250°C. What is the rate of heat transfer by the exchanger, and what are the gas and water outlet temperatures?

SOLUTION

Known: Hot and cold fluid inlet conditions for a finned-tube, cross-flow heat exchanger of known surface area and overall heat transfer coefficient.

Find: Heat transfer rate and fluid outlet temperatures.

Schematic:



Assumptions:

1. Negligible heat loss to surroundings and kinetic and potential energy changes.
2. Constant properties (unchanged from Example 11.3).

Analysis: The problem may be classified as one requiring a heat exchanger *performance calculation.* The heat capacity rates are

$$C_c = \dot{m}_c c_{p,c} = 1 \text{ kg/s} \times 4197 \text{ J/kg} \cdot \text{K} = 4197 \text{ W/K}$$

$$C_h = \dot{m}_h c_{p,h} = 1.5 \text{ kg/s} \times 1000 \text{ J/kg} \cdot \text{K} = 1500 \text{ W/K} = C_{min}$$

Patent Owner Manufacturing Resources International, Inc.
Exhibit 2017 - Page 701 of 999

in which case

$$\frac{C_{\min}}{C_{\max}} = \frac{1500}{4197} = 0.357$$

The number of transfer units is

$$\text{NTU} = \frac{U_h A_h}{C_{\min}} = \frac{100\ \text{W/m}^2 \cdot \text{K} \times 40\ \text{m}^2}{1500\ \text{W/K}} = 2.67$$

From Figure 11.14 the heat exchanger effectiveness is then $\varepsilon \approx 0.82$, and from Equation 11.18 the maximum possible heat transfer rate is

$$q_{\max} = C_{\min}(T_{h,i} - T_{c,i}) = 1500\ \text{W/K}\,(250 - 35)^\circ\text{C} = 3.23 \times 10^5\ \text{W}$$

Accordingly, from the definition of ε, Equation 11.19, the actual heat transfer rate is

$$q = \varepsilon q_{\max} = 0.82 \times 3.23 \times 10^5\ \text{W} = 2.65 \times 10^5\ \text{W}$$

It is now a simple matter to determine the outlet temperatures from the overall energy balances. From Equation 11.6b

$$T_{h,o} = T_{h,i} - \frac{q}{\dot{m}_h c_{p,h}} = 250^\circ\text{C} - \frac{2.65 \times 10^5\ \text{W}}{1500\ \text{W/K}} = 73.3^\circ\text{C}$$

and from Equation 11.7b

$$T_{c,o} = T_{c,i} + \frac{q}{\dot{m}_c c_{p,c}} = 35^\circ\text{C} + \frac{2.65 \times 10^5\ \text{W}}{4197\ \text{W/K}} = 98.1^\circ\text{C}$$

Comments:

1. From Equation 11.32, $\varepsilon = 0.845$, which is in good agreement with the estimate obtained from the charts.
2. The overall heat transfer coefficient has tacitly been assumed to be unaffected by the change in $\dot{m}_h$. In fact, with an approximately 20% reduction in $\dot{m}_h$, there would be a significant, albeit smaller percentage, reduction in U_h.
3. As discussed in the Comment of Example 11.3, flow rate adjustments could be made to maintain a fixed water outlet temperature. If, for example, the outlet temperature must be maintained at $T_{c,o} = 125^\circ\text{C}$, the water flow rate could be reduced to an amount prescribed by Equation 11.7b. That is,

$$\dot{m}_c = \frac{q}{c_{p,c}(T_{c,o} - T_{c,i})} = \frac{2.65 \times 10^5\ \text{W}}{4197\ \text{J/kg} \cdot \text{K}\,(125 - 35)^\circ\text{C}} = 0.702\ \text{kg/s}$$

The change in flow rate has again been presumed to have a negligible effect on U_h. In this case the assumption is good, since the dominant contribution to U_h is made by the gas-side, and not the water-side, convection coefficient.

EXAMPLE 11.5

The condenser of a large steam power plant is a heat exchanger in which steam is condensed to liquid water. Assume the condenser to be a *shell-and-tube* heat exchanger consisting of a single shell and 30,000 tubes, each executing two passes. The tubes are of thin wall construction with $D = 25$ mm, and steam condenses on their outer surface with an associated convection coefficient of $h_o = 11{,}000\ \text{W/m}^2 \cdot \text{K}$. The heat transfer rate that must be effected by the exchanger is $q = 2 \times 10^9$ W, and

Patent Owner Manufacturing Resources International, Inc.
Exhibit 2017 - Page 702 of 999

this is accomplished by passing cooling water through the tubes at a rate of 3×10^4 kg/s (the flow rate per tube is therefore 1 kg/s). The water enters at 20°C, while the steam condenses at 50°C. What is the temperature of the cooling water emerging from the condenser? What is the required tube length L per pass?

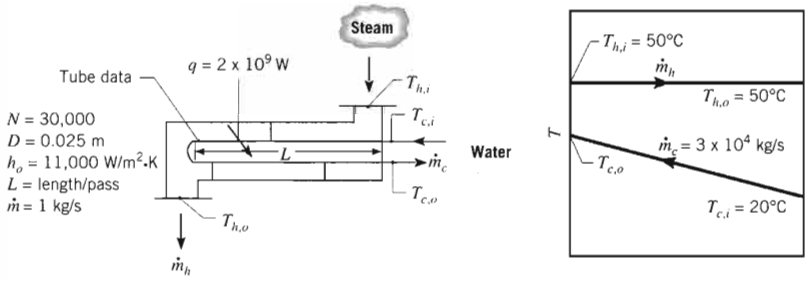
SOLUTION

Known: Heat exchanger consisting of single shell and 30,000 tubes with two passes each.

Find:

1. Outlet temperature of the cooling water.
2. Tube length per pass to achieve required heat transfer.

Schematic:



Assumptions:

1. Negligible heat transfer between exchanger and surroundings and negligible kinetic and potential energy changes.
2. Tube internal flow and thermal conditions fully developed.
3. Negligible thermal resistance of tube material and fouling effects.
4. Constant properties.

Properties: Table A.6, water (assume $\overline{T}_c \approx 27°C = 300$ K): $\rho = 997$ kg/m^3, $c_p = 4179$ J/kg · K, $\mu = 855 \times 10^{-6}$ N · s/m^2, $k = 0.613$ W/m · K, $Pr = 5.83$.

Analysis:

1. The cooling water outlet temperature may be obtained from the overall energy balance, Equation 11.7b. Accordingly,

$$T_{c,o} = T_{c,i} + \frac{q}{\dot{m}_c c_{p,c}} = 20°C + \frac{2 \times 10^9 \text{ W}}{3 \times 10^4 \text{ kg/s} \times 4179 \text{ J/kg} \cdot \text{K}}$$

$$T_{c,o} = 36.0°C \quad \triangleleft$$

2. The problem may be classified as one requiring a *heat exchanger design calculation.* First, we determine the overall heat transfer coefficient for use in the NTU method.

From Equation 11.5

$$U = \frac{1}{(1/h_i) + (1/h_o)}$$

Patent Owner Manufacturing Resources International, Inc.
Exhibit 2017 - Page 703 of 999

where h_i may be estimated from an internal flow correlation. With

$$Re_D = \frac{4\dot{m}}{\pi D\mu} = \frac{4 \times 1 \text{ kg/s}}{\pi(0.025 \text{ m})855 \times 10^{-6} \text{ N} \cdot \text{s/m}^2} = 59{,}567$$

the flow is turbulent and from Equation 8.60

$$Nu_D = 0.023\, Re_D^{4/5} Pr^{0.4} = 0.023(59{,}567)^{0.8}(5.83)^{0.4} = 308$$

Hence

$$h_i = Nu_D \frac{k}{D} = 308 \frac{0.613 \text{ W/m} \cdot \text{K}}{0.025 \text{ m}} = 7543 \text{ W/m}^2 \cdot \text{K}$$

$$U = \frac{1}{[(1/7543) + (1/11{,}000)] \text{ m}^2 \cdot \text{K/W}} = 4474 \text{ W/m}^2 \cdot \text{K}$$

Using the design calculation methodology, we note that

$$C_h = C_{\max} = \infty$$

and

$$C_{\min} = \dot{m}_c c_{p,c} = 3 \times 10^4 \text{ kg/s} \times 4179 \text{ J/kg} \cdot \text{K} = 1.25 \times 10^8 \text{ W/K}$$

from which

$$\frac{C_{\min}}{C_{\max}} = C_r = 0$$

The maximum possible heat transfer rate is

$$q_{\max} = C_{\min}(T_{h,i} - T_{c,i}) = 1.25 \times 10^8 \text{ W/K} \times (50 - 20) \text{ K} = 3.76 \times 10^9 \text{ W}$$

from which

$$\varepsilon = \frac{q}{q_{\max}} = \frac{2 \times 10^9 \text{ W}}{3.76 \times 10^9 \text{ W}} = 0.532$$

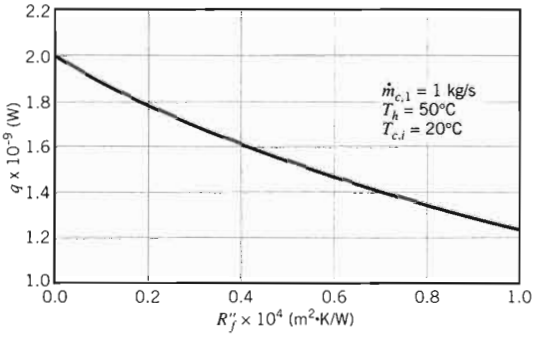
From Equation 11.35b or Figure 11.12, we find NTU = 0.759. From Equation 11.24, it follows that the tube length per pass is

$$L = \frac{\text{NTU} \cdot C_{\min}}{U(N2\pi D)} = \frac{0.759 \times 1.25 \times 10^8 \text{ W/K}}{4474 \text{ W/m}^2 \cdot \text{K}\,(30{,}000 \times 2 \times \pi \times 0.025 \text{ m})} = 4.51 \text{ m} \quad \triangleleft$$

Comments:

1. Recognize that L is the tube length per pass, in which case the total length per tube is 9.0 m. The entire length of tubing in the condenser is $N \times L \times 2 = 30{,}000 \times 4.51 \text{ m} \times 2 = 271{,}000$ m or 271 km.
2. Over time, the performance of the heat exchanger would be degraded by fouling on both the inner and outer tube surfaces. A representative maintenance schedule would call for taking the heat exchanger off-line and cleaning the tubes when fouling factors reached values of $R''_{f,i} = R''_{f,o} = 10^{-4}$ m$^2 \cdot$ K/W. To determine the effect of fouling on performance, the ε–NTU method may be used to calculate the total heat rate as a function of the fouling factor, with $R''_{f,o}$ assumed to equal $R''_{f,i}$. The following results are obtained:

Patent Owner Manufacturing Resources International, Inc.
Exhibit 2017 - Page 704 of 999



To maintain the requirement of $q = 2 \times 10^9$ W with the maximum allowable fouling and the restriction of $\dot{m}_{c,1} = 1$ kg/s, the tube length or the number of tubes would have to be increased. Keeping the length per pass at $L = 4.51$ m, $N = 48{,}300$ tubes would be needed to transfer 2×10^9 W for $R''_{f,i} = R''_{f,o} = 10^{-4}$ m²·K/W. The corresponding increase in the total flow rate to $\dot{m}_c = N\dot{m}_{c,1} = 48{,}300$ kg/s would have the beneficial effect of reducing the water outlet temperature to $T_{c,o} = 29.9°C$, thereby ameliorating potentially harmful effects associated with discharge into the environment. The additional tube length associated with increasing the number of tubes to $N = 48{,}300$ is 165 km, which would result in a significant increase in the capital cost of the condenser.

3. The steam plant generates 1250 MW of electricity with a wholesale value of \$0.05 per kW·h. If the plant is shut down for 48 hours to clean the condenser tubes, the loss in revenue for the plant's owner is 48 h × 1250 × 10^6 W × \$0.05/(1 × 10^3 W·h) = \$3 million.
4. Assuming a smooth surface condition within each tube, the friction factor may be determined from Equation 8.20b, $f = 0.184(59{,}567)^{-0.2} = 0.020$. The pressure drop within one tube of length $L = 9$ m may be determined from Equation 8.22a, where $u_m = 4\dot{m}/(\rho\pi D^2) = (4 \times 1 \text{ kg/s})/(997 \text{ kg/m}^3 \times \pi \times 0.025^2 \text{m}^2) = 2.04$ m/s.

$$\Delta p = f\frac{\rho u_m^2}{2D}L = 0.020\frac{997 \text{ kg/m}^3(2.04 \text{ m/s})^2}{2(0.025 \text{ m})}9.0 \text{ m} = 15{,}300 \text{ N/m}^2$$

Therefore, the power required to pump the cooling water through the 48,300 tubes may be found by using Equation 8.22b and is

$$P = \frac{\Delta p\dot{m}}{\rho} = \frac{15{,}300 \text{ N/m}^2 \times 48{,}300 \text{ kg/s}}{997 \text{ kg/m}^3} = 742{,}000 \text{ W} = 0.742 \text{ MW}$$

The cooling water pump is driven by an electric motor. If the combined efficiency of the pump and motor is 87%, the annual cost to overcome friction losses in the condenser tubes is 24 h/day × 365 days/yr × 0.742 × 10^6 W × \$0.05/1 × 10^3 W·h/0.87 = \$374,000.

5. Optimal condenser designs are based on the desired thermal performance and environmental considerations as well as on the capital cost, operating cost, and maintenance cost associated with the device.

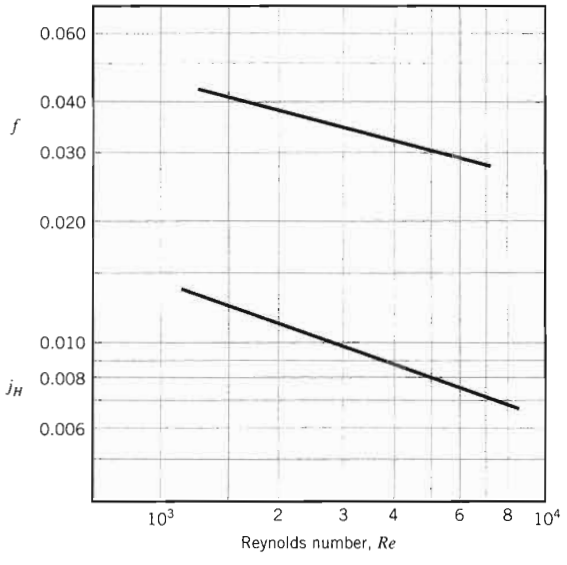
Patent Owner Manufacturing Resources International, Inc.
Exhibit 2017 - Page 705 of 999

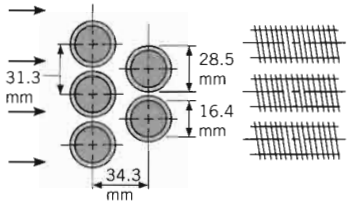
11.6 *Compact Heat Exchangers*

As discussed in Section 11.1, *compact heat exchangers* are typically used when a large heat transfer surface area per unit volume is desired and at least one of the fluids is a gas. Many different tubular and plate configurations have been considered, where differences are due primarily to fin design and arrangement. Heat transfer and flow characteristics have been determined for specific configurations and are typically presented in the format of Figures 11.16 and 11.17. Heat transfer results are correlated in terms of the Colburn j factor $j_H = St\,Pr^{2/3}$ and the Reynolds number, where both the Stanton ($St = h/Gc_p$) and Reynolds ($Re = GD_h/\mu$) numbers are based on the maximum mass velocity

$$G \equiv \rho V_{max} = \frac{\rho V A_{fr}}{A_{ff}} = \frac{\dot{m}}{A_{ff}} = \frac{\dot{m}}{\sigma A_{fr}} \tag{11.36}$$

The quantity σ is the ratio of the minimum free-flow area of the finned passages (cross-sectional area perpendicular to flow direction), A_{ff}, to the frontal area, A_{fr}, of the exchanger. Values of σ, D_h (the hydraulic diameter of the flow passage), α (the heat transfer surface area per total heat exchanger volume), A_f/A (the ratio of fin to total heat transfer surface area), and other geometrical parameters are listed for each configuration. The ratio A_f/A is used in Equation 11.3 to evaluate the temperature effectiveness η_o. In a design calculation, α would be used to determine the required heat exchanger volume, after the total heat transfer surface area has been found; in a performance calculation it would be used to determine the surface area from knowledge of the heat exchanger volume.





Tube outside diameter, D_o = 16.4 mm
Fin pitch = 275 per meter
Flow passage hydraulic diameter, D_h = 6.68 mm
Fin thickness, t = 0.254 mm
Free-flow area/frontal area, σ = 0.449
Heat transfer area/total volume, α = 269 m²/m³
Fin area/total area, A_f/A = 0.830
Note: Minimum free-flow area is in spaces transverse to flow.

FIGURE 11.16 Heat transfer and friction factor for a circular tube–circular fin heat exchanger, surface CF-7.0-5/8J from Kays and London [5].

Patent Owner Manufacturing Resources International, Inc.
Exhibit 2017 - Page 706 of 999

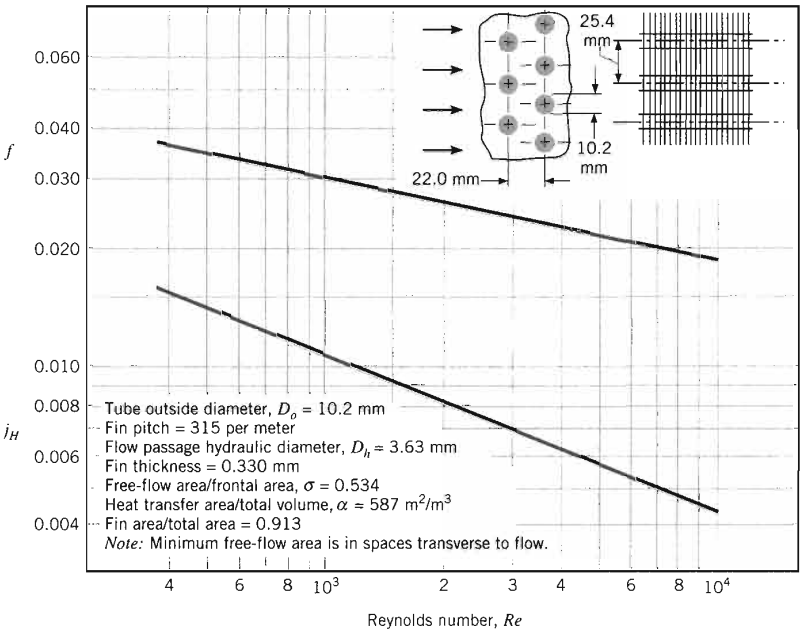


FIGURE 11.17 Heat transfer and friction factor for a circular tube–continuous fin heat exchanger, surface 8.0-3/8T from Kays and London [5].

In a compact heat exchanger calculation, empirical information, such as that provided in Figures 11.16 and 11.17, would first be used to determine the average convection coefficient of the finned surfaces. The overall heat transfer coefficient would then be determined, and using the ε–NTU method, the heat exchanger design or performance calculations would be performed.

The pressure drop associated with flow across finned-tube banks, such as those of Figures 11.16 and 11.17, may be computed from the expression

$$\Delta p = \frac{G^2 v_i}{2}\left[(1+\sigma^2)\left(\frac{v_o}{v_i}-1\right)+f\frac{A}{A_{ff}}\frac{v_m}{v_i}\right] \tag{11.37}$$

where v_i and v_o are the fluid inlet and outlet specific volumes and $v_m = (v_i + v_o)/2$. The first term on the right-hand side of Equation 11.37 accounts for the cumulative effects of pressure change due to inviscid fluid acceleration and deceleration at the exchanger inlet and outlet, respectively. The effects are *reversible*, and if fluid density variations may be neglected ($v_o \simeq v_i$), the term is negligible. The second term accounts for losses due to fluid friction in the heat exchanger core, with fully developed conditions presumed to exist throughout the core. For a prescribed core configuration, the friction factor is known as a function of Reynolds number, as, for example, from Figures 11.16 and 11.17; and for a prescribed heat exchanger size, the area ratio may be evaluated from the relation $(A/A_{ff}) = (\alpha V/\sigma A_{fr})$, where V is the total heat exchanger volume.

Equation 11.37 does not account for irreversible losses due to viscous effects at the inlet and outlet of the heat exchanger. The losses depend on the nature of the ductwork used to transport fluids to and from the heat exchanger core. If the

Patent Owner Manufacturing Resources International, Inc.
Exhibit 2017 - Page 707 of 999

transition between the ductwork and the core occurs with little flow separation, the losses are small. However, if there are abrupt changes between the duct cross-sectional area and the free-flow area of the heat exchanger, separation is pronounced and the attendant losses are large. Inlet and exit losses may be estimated from empirical *contraction* and *expansion coefficients* obtained for a variety of core geometries [5].

The classic work of Kays and London [5] provides Colburn j and friction factor data for many different compact heat exchanger cores, which include flat tube (Figure 11.5*a*) and plate–fin (Figure 11.5*d*, *e*) configurations, as well as other circular tube configurations (Figure 11.5*b*, *c*). Other excellent sources of information are provided by References 3, 4, 9, and 10.

EXAMPLE 11.6

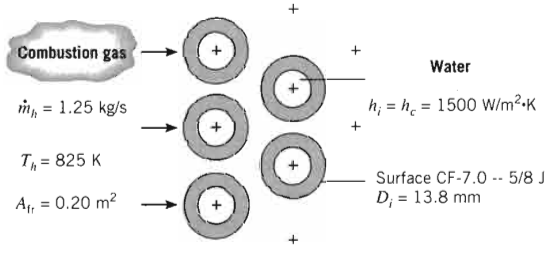
Consider a finned-tube, compact heat exchanger having the core configuration of Figure 11.16. The core is fabricated from aluminum, and the tubes have an inside diameter of 13.8 mm. In a waste heat recovery application, water flow through the tubes provides an inside convection coefficient of $h_i = 1500\ \text{W/m}^2 \cdot \text{K}$, while combustion gases at 1 atm and 825 K are in cross flow over the tubes. If the gas flow rate is 1.25 kg/s and the frontal area is 0.20 m^2, what is the gas-side overall heat transfer coefficient? If a water flow rate of 1 kg/s is to be heated from 290 to 370 K, what is the required heat exchanger volume?

SOLUTION

Known: Compact heat exchanger geometry, gas-side flow rate and temperature, and water-side convection coefficient. Water flow rate and inlet and outlet temperatures.

Find: Gas-side overall heat transfer coefficient. Heat exchanger volume.

Schematic:



Assumptions:

1. Gas has properties of atmospheric air at an assumed mean temperature of 700 K.
2. Fouling is negligible.

Properties: Table A.1, aluminum ($T \approx 300$ K): $k = 237\ \text{W/m} \cdot \text{K}$. Table A.4, air ($p = 1$ atm, $\overline{T} = 700$ K): $c_p = 1075\ \text{J/kg} \cdot \text{K}$, $\mu = 338.8 \times 10^{-7}\ \text{N} \cdot \text{s/m}^2$, Pr = 0.695. Table A.6, water ($\overline{T} = 330$ K): $c_p = 4184\ \text{J/kg} \cdot \text{K}$.

Patent Owner Manufacturing Resources International, Inc.
Exhibit 2017 - Page 708 of 999

Analysis: Referring to Equation 11.1, the combustion gas and the water are the hot and cold fluids, respectively. Hence, neglecting fouling effects and acknowledging that the tube inner surface is not finned ($\eta_{o,c} = 1$), the overall heat transfer coefficient based on the gas- (hot) side surface area is given by

$$\frac{1}{U_h} = \frac{1}{h_c(A_c/A_h)} + A_h R_w + \frac{1}{\eta_{o,h} h_h}$$

where A_h and A_c are the total gas-side (hot) and water-side (cold) surface areas, respectively. If the fin thickness is assumed to be negligible, it is readily shown that

$$\frac{A_c}{A_h} \approx \frac{D_i}{D_o}\left(1 - \frac{A_{f,h}}{A_h}\right)$$

where $A_{f,h}$ is that portion of the total gas-side area associated with the fins. The approximation is valid to within 10%, and for the heat exchanger core conditions (Figure 11.16)

$$\frac{A_c}{A_h} \approx \frac{13.8}{16.4}(1 - 0.830) = 0.143$$

Obtaining the wall conduction resistance from Equation 3.28, it follows that

$$A_h R_w = \frac{\ln (D_o/D_i)}{2\pi L k/A_h} = \frac{D_i \ln (D_o/D_i)}{2k(A_c/A_h)}$$

Hence

$$A_h R_w = \frac{(0.0138\ \text{m}) \ln (16.4/13.8)}{2(237\ \text{W/m} \cdot \text{K})(0.143)} = 3.51 \times 10^{-5}\ \text{m}^2 \cdot \text{K/W}$$

The gas-side convection coefficient may be obtained by first using Equation 11.36 to evaluate the mass velocity:

$$G = \frac{\dot{m}}{\sigma A_{\text{fr}}} = \frac{1.25\ \text{kg/s}}{0.449 \times 0.20\ \text{m}^2} = 13.9\ \text{kg/s} \cdot \text{m}^2$$

Hence

$$Re = \frac{13.9\ \text{kg/s} \cdot \text{m}^2 \times 6.68 \times 10^{-3}\ \text{m}}{338.8 \times 10^{-7}\ \text{kg/s} \cdot \text{m}} = 2740$$

and from Figure 11.16, $j_H \approx 0.010$. Hence

$$h_h \approx 0.010 \frac{G c_p}{Pr^{2/3}} = 0.010 \frac{(13.9\ \text{kg/s} \cdot \text{m}^2)(1075\ \text{J/kg} \cdot \text{K})}{(0.695)^{2/3}}$$

$$= 190\ \text{W/m}^2 \cdot \text{K}$$

To obtain the hot-side temperature effectiveness from Equation 11.3, the fin efficiency must first be determined from Figure 3.19. With $r_{2c} = 14.38$ mm, $r_{2c}/r_1 = 1.75$, $L_c = 6.18$ mm, $A_p = 1.57 \times 10^{-6}\ \text{m}^2$, and $L_c^{3/2}(h_h/kA_p)^{1/2} = 0.34$, it follows that $\eta_f \approx 0.89$. Hence

$$\eta_{o,h} = 1 - \frac{A_f}{A}(1 - \eta_f) = 1 - 0.830(1 - 0.89) = 0.91$$

We then obtain

$$\frac{1}{U_h} = \left(\frac{1}{1500 \times 0.143} + 3.51 \times 10^{-5} + \frac{1}{0.91 \times 190}\right) \text{m}^2 \cdot \text{K/W}$$

Patent Owner Manufacturing Resources International, Inc.
Exhibit 2017 - Page 709 of 999

$$\frac{1}{U_h} = (4.66 \times 10^{-3} + 3.51 \times 10^{-5} + 5.78 \times 10^{-3}) = 0.010\ \text{m}^2 \cdot \text{K/W}$$

or

$$U_h = 100\ \text{W/m}^2 \cdot \text{K}$$ ◁

With $C_c = \dot{m}_c c_{p,c} = 1\ \text{kg/s} \times 4184\ \text{J/kg} \cdot \text{K} = 4184\ \text{W/K}$, the heat exchanger must be large enough to transfer heat in the amount

$$q = C_c(T_{c,o} - T_{c,i}) = 4184\ \text{W/K}\ (370 - 290)\ \text{K} = 3.35 \times 10^5\ \text{W}$$

With $C_h = \dot{m}_h c_{p,h} = 1.25\ \text{kg/s} \times 1075\ \text{J/kg} \cdot \text{K} = 1344\ \text{W/K}$, the minimum heat capacity rate corresponds to the hot fluid and the maximum possible heat transfer rate is

$$q_{\max} = C_{\min}(T_{h,i} - T_{c,i}) = 1344\ \text{W/K}\ (825 - 290)\ \text{K} = 7.19 \times 10^5\ \text{W}$$

It follows that

$$\varepsilon = \frac{q}{q_{\max}} = \frac{3.35 \times 10^5\ \text{W}}{7.19 \times 10^5\ \text{W}} = 0.466$$

Hence, with $(C_{\min}/C_{\max}) = 0.321$, Figure 11.14 (cross-flow heat exchanger with both fluids unmixed) yields

$$\text{NTU} = \frac{U_h A_h}{C_{\min}} \approx 0.65$$

The required gas-side heat transfer surface area is then

$$A_h = \frac{0.65 \times 1344\ \text{W/K}}{100\ \text{W/m}^2 \cdot \text{K}} = 8.7\ \text{m}^2$$

With the gas-side surface area per unit heat exchanger volume corresponding to $\alpha = 269\ \text{m}^2/\text{m}^3$ (Figure 11.16), the required heat exchanger volume is

$$V = \frac{A_h}{\alpha} = \frac{8.7\ \text{m}^2}{269\ \text{m}^2/\text{m}^3} = 0.032\ \text{m}^3$$ ◁

Comments:

1. The effect of the tube wall thermal conduction resistance is negligible, while contributions due to the cold- and hot-side convection resistances are comparable.
2. Knowledge of the heat exchanger volume yields the heat exchanger length in the gas-flow direction, $L = V/A_{\text{fr}} = 0.032\ \text{m}^3/0.20\ \text{m}^2 = 0.16\ \text{m}$, from which the number of tube rows in the flow direction may be determined.

$$N_L \approx \frac{L - D_f}{S_L} + 1 = \frac{(160 - 28.5)\ \text{mm}}{34.3\ \text{mm}} + 1 = 4.8 \approx 5$$

3. The temperature of the gas leaving the heat exchanger is

$$T_{h,o} = T_{h,i} - \frac{q}{C_h} = 825\ \text{K} - \frac{3.35 \times 10^5\ \text{W}}{1344\ \text{W/K}} = 576\ \text{K}$$

Hence the assumption of $\bar{T}_h = 700\ \text{K}$ is excellent.

11.7 Summary

Patent Owner Manufacturing Resources International, Inc.
Exhibit 2017 - Page 710 of 999

4. From Figure 11.16, the friction factor is $f \approx 0.033$. With $(A/A_{ff}) = (\alpha V/\sigma A_{ff}) = (269 \times 0.032/0.449 \times 0.20) = 96$, $v_i(825\ \text{K}) = 2.37\ \text{m}^3/\text{kg}$, $v_o(576\ \text{K}) = 1.65\ \text{m}^3/\text{kg}$, and $v_m = 2.01\ \text{m}^3/\text{kg}$, Equation 11.37 yields a pressure drop of

$$\Delta p = \frac{(13.9\ \text{kg/s} \cdot \text{m}^2)^2(2.37\ \text{m}^3/\text{kg})}{2}[(1 + 0.202)(0.696 - 1) + 0.033 \times 96 \times 0.848]$$

$$\Delta p = 530\ \text{kg/s}^2 \cdot \text{m} = 530\ \text{N/m}^2$$

11.7 *Summary*

Because there are many important applications, heat exchanger research and development has had a long history. Such activity is by no means complete, however, as many talented workers continue to seek ways of improving design and performance. In fact, with heightened concern for energy conservation, there has been a steady and substantial increase in activity. A focal point for this work has been *heat transfer enhancement,* which includes the search for special heat exchanger surfaces through which enhancement may be achieved. In this chapter we have attempted to develop tools that will allow you to perform approximate heat exchanger calculations. More detailed considerations of the subject are available in the literature, including treatment of the uncertainties associated with heat exchanger analysis [3, 4, 7, 9–15].

Although we have restricted ourselves to heat exchangers involving separation of hot and cold fluids by a stationary wall, there are other important options. For example, *evaporative* heat exchangers enable *direct contact* between a liquid and a gas (there is no separating wall), and because of latent energy effects, large heat transfer rates per unit volume are possible. Also, for gas-to-gas heat exchange, use is often made of *regenerators* in which the same space is alternately occupied by the hot and cold gases. In a fixed regenerator such as a packed bed, the hot and cold gases alternately enter a stationary, porous solid. In a rotary regenerator, the porous solid is a rotating wheel, which alternately exposes its surfaces to the continuously flowing hot and cold gases. Detailed descriptions of such heat exchangers are available in the literature [3, 4, 9, 12, 16–19].

You should test your understanding of fundamental issues by addressing the following questions.

- What are the two possible arrangements for a *concentric tube heat exchanger*? For each arrangement, what restrictions are associated with the fluid outlet temperatures?
- As applied to a *cross-flow heat exchanger*, what is meant by the terms *mixed* and *unmixed*? In what sense are they idealizations of actual conditions?
- Why are baffles used in a *shell-and-tube heat exchanger*?
- What is the principal distinguishing feature of a *compact heat exchanger*?
- What effect does *fouling* have on the overall heat transfer coefficient and hence the performance of a heat exchanger?

Patent Owner Manufacturing Resources International, Inc.
Exhibit 2017 - Page 711 of 999

- What effect do *finned surfaces* have on the overall heat transfer coefficient and hence the performance of a heat exchanger? When is the use of fins most appropriate?
- When can the overall heat transfer coefficient be expressed as $U = (h_i^{-1} + h_o^{-1})^{-1}$?
- What is the appropriate form of the mean temperature difference for the two fluids of a parallel or counter-flow heat exchanger?
- What can be said about the change in temperature of a saturated fluid undergoing evaporation or condensation in a heat exchanger?
- Will the fluid having the minimum or the maximum heat capacity rate experience the largest temperature change in a heat exchanger?
- Why is the maximum possible heat rate for a heat exchanger *not* equal to $C_{\max}(T_{h,i} - T_{c,i})$? Can the outlet temperature of the cold fluid ever exceed the inlet temperature of the hot fluid?
- What is the *effectiveness* of a heat exchanger? What is its range of possible values? What is the *number of transfer units*? What is its range of possible values?
- Generally, how does the effectiveness change if the size (surface area) of a heat exchanger is increased? If the overall heat transfer coefficient is increased? If the ratio of heat capacity rates is decreased? As manifested by the number of transfer units, are there limitations to the foregoing trends? What penalty is associated with increasing the size of a heat exchanger? With increasing the overall heat transfer coefficient?

References

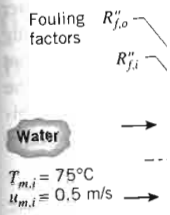
1. *Standards of the Tubular Exchange Manufacturers Association*, 6th ed., Tubular Exchanger Manufacturers Association, New York, 1978.
2. Chenoweth, J. M., and M. Impagliazzo, Eds., *Fouling in Heat Exchange Equipment*, American Society of Mechanical Engineers Symposium Volume HTD-17, ASME, New York, 1981.
3. Kakac, S., A. E. Bergles, and F. Mayinger, Eds., *Heat Exchangers*, Hemisphere Publishing, New York, 1981.
4. Kakac, S., R. K. Shah, and A. E. Bergles, Eds., *Low Reynolds Number Flow Heat Exchangers*, Hemisphere Publishing, New York, 1983.
5. Kays, W. M., and A. L. London, *Compact Heat Exchangers*, 3rd ed., McGraw-Hill, New York, 1984.
6. Bowman, R. A., A. C. Mueller, and W. M. Nagle, *Trans. ASME*, **62**, 283, 1940.
7. DiGiovanni, M. A., and R. L. Webb, *Heat Transfer Eng.*, **10**, 61, 1989.
8. Ribando, R. J., G. W. O'Leary, and S. Carlson-Skalak, *Comp. Appl. Eng. Educ.*, **5**, 231, 1997.
9. Shah, R. K., C. F. McDonald, and C. P. Howard, Eds., *Compact Heat Exchangers*, American Society of Mechanical Engineers Symposium Volume HTD-10, ASME, New York, 1980.
10. Webb, R. L., in G. F. Hewitt, Exec. Ed., *Heat Exchanger Design Handbook*, Section 3.9, Begell House, New York, 2002.
11. Marner, W. J., A. E. Bergles, and J. M. Chenoweth, *Trans. ASME, J. Heat Transfer*, **105**, 358, 1983.
12. G. F. Hewitt, Exec. Ed., *Heat Exchanger Design Handbook*, Vols. 1–5, Begell House, New York, 2002.
13. Webb, R. L., and N.-H. Kim, *Principles of Enhanced Heat Transfer*, 2nd ed., Taylor & Francis, New York, 2005.
14. Andrews, M. J., and L. S. Fletcher, *ASME/JSME Thermal Eng. Conf.*, **4**, 359, 1995.
15. James, C. A., R. P. Taylor, and B. K. Hodge, *ASME/JSME Thermal Eng. Conf.*, **4**, 337, 1995.
16. Coppage, J. E., and A. L. London, *Trans. ASME*, **75**, 779, 1953.
17. Treybal, R. E., *Mass-Transfer Operations*, 3rd ed., McGraw-Hill, New York, 1980.
18. Sherwood, T. K., R. L. Pigford, and C. R. Wilkie, *Mass Transfer*, McGraw-Hill, New York, 1975.
19. Schmidt, F. W., and A. J. Willmott, *Thermal Energy Storage and Regeneration*, Hemisphere Publishing, New York, 1981.

Problems

Overall Heat Tr

11.1 In a fire-tube
ing through a
boil water fl
installation, t
400 W/m^2 · K
tube surfaces
factors of R''_f
respectively.
ing of the tub

11.2 A type-302 st
ters $D_i = 22$
in a cross-flo
for the inner
0.0004 and 0



(a) Deter
based
pare
tube

(b) Instea
uatio
15°C
the o
outsi
resist
tion,

(c) For t
velo
over
the

(d) For
cros
the
of th

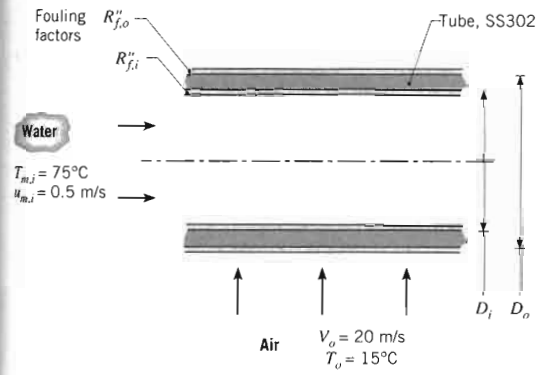
Patent Owner Manufacturing Resources International, Inc.
Exhibit 2017 - Page 712 of 999

Problems

Overall Heat Transfer Coefficient

11.1 In a fire-tube boiler, hot products of combustion flowing through an array of thin-walled tubes are used to boil water flowing over the tubes. At the time of installation, the overall heat transfer coefficient was 400 W/m^2 · K. After 1 year of use, the inner and outer tube surfaces are fouled, with corresponding fouling factors of $R''_{f,i} = 0.0015$ and $R''_{f,o} = 0.0005$ m^2 · K/W, respectively. Should the boiler be scheduled for cleaning of the tube surfaces?

11.2 A type-302 stainless steel tube of inner and outer diameters $D_i = 22$ mm and $D_o = 27$ mm, respectively, is used in a cross-flow heat exchanger. The fouling factors, R''_f, for the inner and outer surfaces are estimated to be 0.0004 and 0.0002 m^2 · K/W, respectively.



(a) Determine the overall heat transfer coefficient based on the outside area of the tube, U_o. Compare the thermal resistances due to convection, tube wall conduction, and fouling.

(b) Instead of air flowing over the tube, consider a situation for which the cross-flow fluid is water at 15°C with a velocity of $V_o = 1$ m/s. Determine the overall heat transfer coefficient based on the outside area of the tube, U_o. Compare the thermal resistances due to convection, tube wall conduction, and fouling.

(c) For the water–air conditions of part (a) and mean velocities, $u_{m,i}$, of 0.2, 0.5, and 1.0 m/s, plot the overall heat transfer coefficient as a function of the cross-flow velocity for $5 \leq V_o \leq 30$ m/s.

(d) For the water–water conditions of part (b) and cross-flow velocities, V_o, of 1, 3, and 8 m/s, plot the overall heat transfer coefficient as a function of the mean velocity for $0.5 \leq u_{m,i} \leq 2.5$ m/s.

11.3 A shell-and-tube heat exchanger is to heat an acidic liquid that flows in unfinned tubes of inside and outside diameters $D_i = 10$ mm and $D_o = 11$ mm, respectively. A hot gas flows on the shell side. To avoid corrosion of the tube material, the engineer may specify either a Ni-Cr-Mo corrosion-resistant metal alloy ($\rho_m = 8900$ kg/m^3, $k_m = 8$ W/m · K) or a polyvinylidene fluoride (PVDF) plastic ($\rho_p = 1780$ kg/m^3, $k_p = 0.17$ W/m · K). The inner and outer heat transfer coefficients are $h_i = 1500$ W/m^2 · K and $h_o = 200$ W/m^2 · K, respectively.

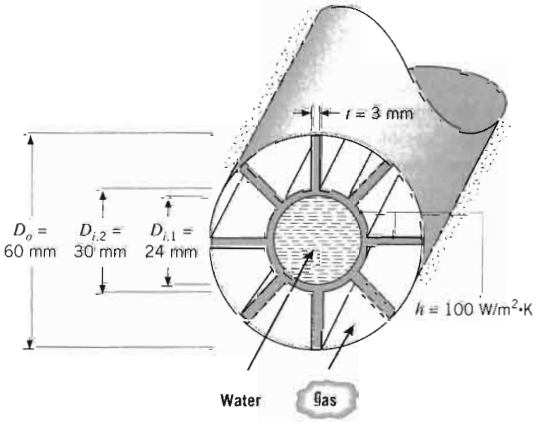
(a) Determine the ratio of plastic to metal tube surface areas needed to transfer the same amount of heat.

(b) Determine the ratio of plastic to metal mass associated with the two heat exchanger designs.

(c) The cost of the metal alloy per unit mass is three times that of the plastic. Determine which tube material should be specified on the basis of cost.

11.4 A steel tube ($k = 50$ W/m · K) of inner and outer diameters $D_i = 20$ mm and $D_o = 26$ mm, respectively, is used to transfer heat from hot gases flowing over the tube ($h_h = 200$ W/m^2 · K) to cold water flowing through the tube ($h_c = 8000$ W/m^2 · K). What is the cold-side overall heat transfer coefficient U_c? To enhance heat transfer, 16 straight fins of rectangular profile are installed longitudinally along the outer surface of the tube. The fins are equally spaced around the circumference of the tube, each having a thickness of 2 mm and a length of 15 mm. What is the corresponding overall heat transfer coefficient U_c?

11.5 A heat recovery device involves transferring energy from the hot flue gases passing through an annular

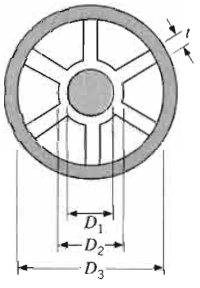


Patent Owner Manufacturing Resources International, Inc.
Exhibit 2017 - Page 713 of 999

region to pressurized water flowing through the inner tube of the annulus. The inner tube has inner and outer diameters of 24 and 30 mm and is connected by eight struts to an insulated outer tube of 60-mm diameter. Each strut is 3 mm thick and is integrally fabricated with the inner tube from carbon steel ($k = 50$ W/m · K).

Consider conditions for which water at 300 K flows through the inner tube at 0.161 kg/s while flue gases at 800 K flow through the annulus, maintaining a convection coefficient of 100 W/m^2 · K on both the struts and the outer surface of the inner tube. What is the rate of heat transfer per unit length of tube from gas to the water?

11.6 A novel design for a condenser consists of a tube of thermal conductivity 200 W/m · K with longitudinal fins snugly fitted into a larger tube. Condensing refrigerant at 45°C flows axially through the inner tube, while water at a flow rate of 0.012 kg/s passes through the six channels around the inner tube. The pertinent diameters are $D_1 = 10$ mm, $D_2 = 14$ mm, and $D_3 = 50$ mm, while the fin thickness is $t = 2$ mm. Assume that the convection coefficient associated with the condensing refrigerant is extremely large.



Determine the heat removal rate per unit tube length in a section of the tube for which the water is at 15°C.

11.7 The condenser of a steam power plant contains $N = 1000$ brass tubes ($k_t = 110$ W/m · K), each of inner and outer diameters, $D_i = 25$ mm and $D_o = 28$ mm, respectively. Steam condensation on the outer surfaces of the tubes is characterized by a convection coefficient of $h_o = 10{,}000$ W/m^2 · K.

(a) If cooling water from a large lake is pumped through the condenser tubes at $\dot{m}_c = 400$ kg/s, what is the overall heat transfer coefficient U_o based on the outer surface area of a tube? Properties of the water may be approximated as $\mu = 9.60 \times 10^{-4}$ N · s/m^2, $k = 0.60$ W/m · K, and Pr = 6.6.

(b) If, after extended operation, fouling provides a resistance of $R''_{f,i} = 10^{-4}$ m^2 · K/W, at the inner surface, what is the value of U_o?

(c) If water is extracted from the lake at 15°C and 10 kg/s of steam at 0.0622 bars are to be condensed, what is the corresponding temperature of the water leaving the condenser? The specific heat of the water is 4180 J/kg · K.

11.8 Thin-walled aluminum tubes of diameter $D = 10$ mm are used in the condenser of an air conditioner. Under normal operating conditions, a convection coefficient of $h_i = 5000$ W/m^2 · K is associated with condensation on the inner surface of the tubes, while a coefficient of $h_o = 100$ W/m^2 · K is maintained by airflow over the tubes.

(a) What is the overall heat transfer coefficient if the tubes are unfinned?

(b) What is the overall heat transfer coefficient based on the inner surface, U_i, if aluminum annular fins of thickness $t = 1.5$ mm, outer diameter $D_o = 20$ mm, and pitch $S = 3.5$ mm are added to the outer surface? Base your calculations on a 1-m-long section of tube. Subject to the requirements that $t \geq 1$ mm and $(S - t) \geq 1.5$ mm, explore the effect of variations in t and S on U_i. What combination of t and S would yield the best heat transfer performance?

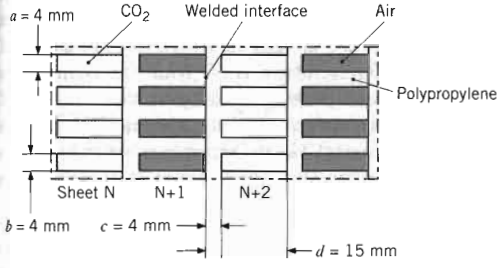
11.9 A finned-tube, cross-flow heat exchanger is to use the exhaust of a gas turbine to heat pressurized water. Laboratory measurements are performed on a prototype version of the exchanger, which has a surface area of 10 m^2, to determine the overall heat transfer coefficient as a function of operating conditions. Measurements made under particular conditions, for which $\dot{m}_h = 2$ kg/s, $T_{h,i} = 325$°C, $\dot{m}_c = 0.5$ kg/s, and $T_{c,i} = 25$°C, reveal a water outlet temperature of $T_{c,o} = 150$°C. What is the overall heat transfer coefficient of the exchanger?

11.10 Water at a rate of 45,500 kg/h is heated from 80 to 150°C in a heat exchanger having two shell passes and eight tube passes with a total surface area of 925 m^2. Hot exhaust gases having approximately the same thermophysical properties as air enter at 350°C and exit at 175°C. Determine the overall heat transfer coefficient.

11.11 A novel heat exchanger concept consists of a large number of extruded polypropylene sheets ($k = 0.17$ W/m · K), each having a fin-like geometry, that are subsequently stacked and melted together to form the heat exchanger core. Besides being inexpensive, the heat exchanger can be easily recycled at the end of its life. Carbon dioxide at a mean temperature of 10°C and pressure of 2 atm flows in the cool channels at a

Patent Owner Manufacturing Resources International, Inc.
Exhibit 2017 - Page 714 of 999

mean velocity of $u_m = 0.1$ m/s. Air at 30°C and 2 atm flows at 0.2 m/s in the warm channels. Neglecting the thermal contact resistance at the welded interface, determine the product of the overall heat transfer coefficient and heat transfer area, UA, for a heat exchanger core consisting of 200 cool channels and 200 warm channels.



Design and Performance Calculations

11.12 The properties and flow rates for the hot and cold fluids of a heat exchanger are shown in the following table. Which fluid limits the heat transfer rate of the exchanger? Explain your choice.

	Hot fluid	Cold fluid
Density, kg/m^3	997	1247
Specific heat, J/kg · K	4179	2564
Thermal conductivity, W/m · K	0.613	0.287
Viscosity, N · s/m^2	8.55×10^{-4}	1.68×10^{-4}
Flow rate, m^3/h	14	16

11.13 A process fluid having a specific heat of 3500 J/kg · K and flowing at 2 kg/s is to be cooled from 80°C to 50°C with chilled water, which is supplied at a temperature of 15°C and a flow rate of 2.5 kg/s. Assuming an overall heat transfer coefficient of 2000 W/m^2 · K, calculate the required heat transfer areas for the following exchanger configurations: (a) parallel flow, (b) counterflow, (c) shell-and-tube, one shell pass and 2 tube passes, and (d) cross-flow, single pass, both fluids unmixed. Compare the results of your analysis. Your work can be reduced by using the *Tools/Heat Exchanger* models of *IHT*.

11.14 A shell-and-tube exchanger (two shells, four tube passes) is used to heat 10,000 kg/h of pressurized water from 35 to 120°C with 5000 kg/h pressurized water entering the exchanger at 300°C. If the overall heat transfer coefficient is 1500 W/m^2 · K, determine the required heat exchanger area.

11.15 Consider the heat exchanger of Problem 11.14. After several years of operation, it is observed that the outlet temperature of the cold water reaches only 95°C rather than the desired 120°C for the same flow rates and inlet temperatures of the fluids. Determine the cumulative (inner and outer surface) fouling factor that is the cause of the poorer performance.

11.16 A counterflow, concentric tube heat exchanger is designed to heat water from 20 to 80°C using hot oil, which is supplied to the annulus at 160°C and discharged at 140°C. The thin-walled inner tube has a diameter of $D_i = 20$ mm, and the overall heat transfer coefficient is 500 W/m^2 · K. The design condition calls for a total heat transfer rate of 3000 W.

(a) What is the length of the heat exchanger?

(b) After 3 years of operation, performance is degraded by fouling on the water side of the exchanger, and the water outlet temperature is only 65°C for the same fluid flow rates and inlet temperatures. What are the corresponding values of the heat transfer rate, the outlet temperature of the oil, the overall heat transfer coefficient, and the water-side fouling factor, $R''_{f,c}$?

11.17 Consider the counterflow, concentric tube heat exchanger of Example 11.1. The designer wishes to consider the effect of the cooling water flow rate on the tube length. All other conditions, including the outlet oil temperature of 60°C, remain the same.

(a) From the analysis of Example 11.1, we saw that the overall coefficient U is dominated by the hot-side convection coefficient. Assuming the water properties are independent of temperature, calculate U as a function of the water flow rate. Justify a constant value of U in the calculations of part (b).

(b) Calculate and plot the required exchanger tube length L and the water outlet temperature $T_{c,o}$ as a function of the cooling water flow rate for $0.15 \leq \dot{m}_c \leq 0.30$ kg/s.

11.18 Consider a concentric tube heat exchanger with an area of 50 m^2 operating under the following conditions:

	Hot fluid	Cold fluid
Heat capacity rate, kW/K	6	3
Inlet temperature, °C	60	30
Outlet temperature, °C	—	54

(a) Determine the outlet temperature of the hot fluid.

(b) Is the heat exchanger operating in counterflow or parallel flow, or can't you tell from the available information?

(c) Calculate the overall heat transfer coefficient.

(d) Calculate the effectiveness of this exchanger.

Patent Owner Manufacturing Resources International, Inc.
Exhibit 2017 - Page 715 of 999

(e) What would be the effectiveness of this exchanger if its length were made very large?

11.19 For a senior project, a student was given the assignment to design a heat exchanger that meets the following specifications:

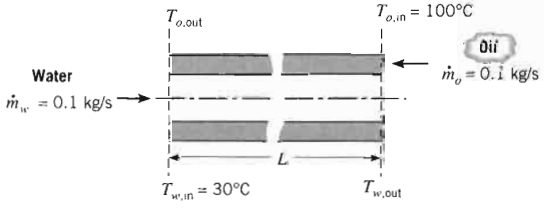
	$\dot{m}$ (kg/s)	$T_{m,i}$ (°C)	$T_{m,o}$ (°C)
Hot water	28	90	—
Cold water	27	34	60

Like many real-world situations, the customer hasn't revealed, or doesn't know, additional requirements that would allow you to proceed directly to a final configuration. At the outset, it is helpful to make a first-cut design based upon simplifying assumptions, which can be evaluated to determine what additional requirements and trade-offs should be considered by the customer.

(a) Design a heat exchanger to meet the foregoing specifications. List and explain your assumptions. *Hint:* Begin by finding the required value for UA and using representative values of U to determine A.

(b) Evaluate your design by identifying what features and configurations could be explored with your customer in order to develop more complete specifications.

11.20 A concentric tube heat exchanger for cooling lubricating oil is comprised of a thin-walled inner tube of 25-mm diameter carrying water and an outer tube of 45-mm diameter carrying the oil. The exchanger operates in counterflow with an overall heat transfer coefficient of 60 W/m^2 · K and the tabulated average properties.



Properties	Water	Oil
ρ (kg/m^3)	1000	800
c_p (J/kg · K)	4200	1900
ν (m^2/s)	7×10^{-7}	1×10^{-5}
k (W/m · K)	0.64	0.134
Pr	4.7	140

(a) If the outlet temperature of the oil is 60°C, determine the total heat transfer and the outlet temperature of the water.

(b) Determine the length required for the heat exchanger.

11.21 A counterflow, concentric tube heat exchanger used for engine cooling has been in service for an extended period of time. The heat transfer surface area of the exchanger is 5 m^2, and the *design value* of the overall convection coefficient is 38 W/m^2 · K. During a test run, engine oil flowing at 0.1 kg/s is cooled from 110°C to 66°C by water supplied at a temperature of 25°C and a flow rate of 0.2 kg/s. Determine whether fouling has occurred during the service period. If so, calculate the fouling factor, R''_f (m^2 · K/W).

11.22 A shell-and-tube heat exchanger must be designed to heat 2.5 kg/s of water from 15 to 85°C. The heating is to be accomplished by passing hot engine oil, which is available at 160°C, through the shell side of the exchanger. The oil is known to provide an average convection coefficient of h_o = 400 W/m^2 · K on the outside of the tubes. Ten tubes pass the water through the shell. Each tube is thin walled, of diameter D = 25 mm, and makes eight passes through the shell. If the oil leaves the exchanger at 100°C, what is its flow rate? How long must the tubes be to accomplish the desired heating?

11.23 An automobile radiator may be viewed as a cross-flow heat exchanger with both fluids unmixed. Water, which has a flow rate of 0.05 kg/s, enters the radiator at 400 K and is to leave at 330 K. The water is cooled by air that enters at 0.75 kg/s and 300 K.

(a) If the overall heat transfer coefficient is 200 W/m^2 · K, what is the required heat transfer surface area?

(b) A manufacturing engineer claims ridges can be stamped on the finned surface of the exchanger, which could greatly increase the overall heat transfer coefficient. With all other conditions remaining the same and the heat transfer surface area determined from part (a), generate a plot of the air and water outlet temperatures as a function of U for 200 ≤ U ≤ 400 W/m^2 · K. What benefits result from increasing the overall convection coefficient for this application?

11.24 Hot air for a large-scale drying operation is to be produced by routing the air over a tube bank (unmixed), while products of combustion are routed through the tubes. The surface area of the cross-flow heat exchanger is A = 25 m^2, and for the proposed operating conditions, the manufacturer specifies an overall heat transfer coefficient of U = 35 W/m^2 · K. The air

and the com
have a specif
conditions f
1 kg/s enter
5 kg/s has an
(a) What ar
(b) After e
tube su
resistan
ation be
(c) The hea
by incr
heat tr
such cl
500 ≤

11.25 In a dairy
liter/hour a
be chilled
less. Groun
0.72 m^3/h.
1030 kg/m^3
(a) Deter
excha
Deter
pipe h
transf
(b) Deter
(c) Using
mine
rate i
the fl

11.26 A shell-a
and two t
heat milk
regenerat
complete
$T_{h,i}$ = 70°
milk ente
temperat
(a) A re
proc
$\dot{m}_c$ =
ture
tran
desi
wha
the
flui
to h

Patent Owner Manufacturing Resources International, Inc.
Exhibit 2017 - Page 716 of 999

and the combustion gases may each be assumed to have a specific heat of $c_p = 1040$ J/kg · K. Consider conditions for which combustion gases flowing at 1 kg/s enter the heat exchanger at 800 K, while air at 5 kg/s has an inlet temperature of 300 K.

(a) What are the air and gas outlet temperatures?

(b) After extended operation, deposits on the inner tube surfaces are expected to provide a fouling resistance of $R''_f = 0.004$ m² · K/W. Should operation be suspended in order to clean the tubes?

(c) The heat exchanger performance may be improved by increasing the surface area and/or the overall heat transfer coefficient. Explore the effect of such changes on the air outlet temperature for $500 \leq UA \leq 2500$ W/K.

11.25 In a dairy operation, milk at a flow rate of 250 liter/hour and a *cow-body* temperature of 38.6°C must be chilled to a safe-to-store temperature of 13°C or less. Ground water at 10°C is available at a flow rate of 0.72 m³/h. The density and specific heat of milk are 1030 kg/m³ and 3860 J/kg · K, respectively.

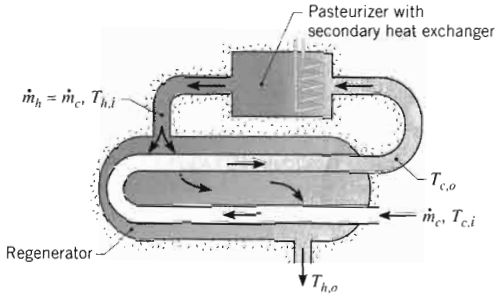
(a) Determine the UA product of a counterflow heat exchanger required for the chilling process. Determine the length of the exchanger if the inner pipe has a 50-mm diameter and the overall heat transfer coefficient is $U = 1000$ W/m² · K.

(b) Determine the outlet temperature of the water.

(c) Using the value of UA found in part (a), determine the milk outlet temperature if the water flow rate is doubled. What is the outlet temperature if the flow rate is halved?

11.26 A shell-and-tube heat exchanger with one shell pass and two tube passes is used as a *regenerator,* to preheat milk before it is pasteurized. Cold milk enters the regenerator at $T_{c,i} = 5$°C, while hot milk, which has completed the pasteurization process, enters at $T_{h,i} = 70$°C. After leaving the regenerator, the heated milk enters a second heat exchanger, which raises its temperature from $T_{c,o}$ to 70°C.

(a) A regenerator is to be used in a pasteurization process for which the flow rate of the milk is $\dot{m}_c = \dot{m}_h = 5$ kg/s. For this flow rate, the manufacturer of the regenerator specifies an overall heat transfer coefficient of 2000 W/m² · K. If the desired effectiveness of the regenerator is 0.5, what is the requisite heat transfer area? What are the corresponding rate of heat recovery and the fluid outlet temperatures? Milk may be assumed to have the properties of water.



(b) If the hot fluid in the secondary heat exchanger derives its energy from the combustion of natural gas and the burner has an efficiency of 90%, what would be the annual savings in energy and fuel costs associated with installation of the regenerator? The facility operates continuously throughout the year, and the cost of natural gas is $C_{ng} = \$0.0075$/MJ.

11.27 The compartment heater of an automobile exchanges heat between warm radiator fluid and cooler outside air. The flow rate of water is large compared to the air, and the effectiveness, ε, of the heater is known to depend on the flow rate of air according to the relation, $\varepsilon \sim \dot{m}_{air}^{-0.2}$.

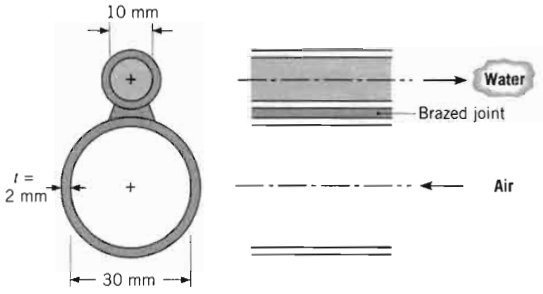
(a) If the fan is switched to high and $\dot{m}_{air}$ is doubled, determine the percentage increase in the heat added to the car, if fluid inlet temperatures remain the same.

(b) For the low-speed fan condition, the heater warms outdoor air from 0 to 30°C. When the fan is turned to medium, the airflow rate increases 50% and the heat transfer increases 20%. Find the new outlet temperature.

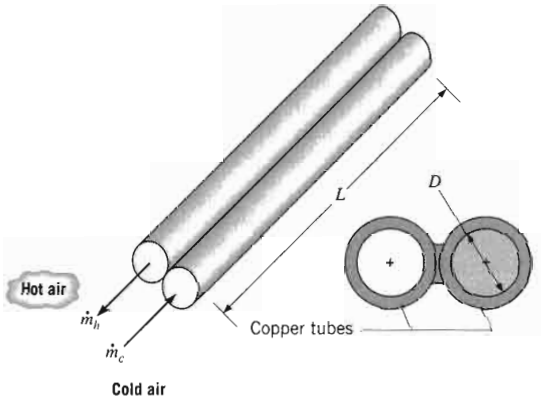
11.28 A counterflow, twin-tube heat exchanger is made by brazing two circular nickel tubes, each 40 m long, together as shown below. Hot water flows through the smaller tube of 10-mm diameter and air at atmospheric pressure flows through the larger tube of 30-mm diameter. Both tubes have a wall thickness of 2 mm. The thermal contact conductance per unit length of the brazed joint is 100 W/m · K. The mass flow rates of the water and air are 0.04 and 0.12 kg/s, respectively. The inlet temperatures of the water and air are 85 and 23°C, respectively.

Employ the ε–NTU method to determine the outlet temperature of the air. *Hint:* Account for the effects of circumferential conduction in the walls of the tubes by treating them as extended surfaces.

Patent Owner Manufacturing Resources International, Inc.
Exhibit 2017 - Page 717 of 999



11.29 A twin-tube, counterflow heat exchanger operates with balanced flow rates of 0.003 kg/s for the hot and cold airstreams. The cold stream enters at 280 K and must be heated to 340 K using hot air at 360 K. The average pressure of the airstreams is 1 atm and the maximum allowable pressure drop for the cold air is 10 kPa. The tube walls may be assumed to act as fins, each with an efficiency of 100%.



(a) Determine the tube diameter D and length L that satisfy the prescribed heat transfer and pressure drop requirements.

(b) For the diameter D and length L found in part (a), generate plots of the cold stream outlet temperature, the heat transfer rate, and pressure drop as a function of balanced flow rates in the range from 0.002 to 0.004 kg/s. Comment on your results.

11.30 A 5-m-long, twin-tube, counterflow heat exchanger, such as that illustrated in Problem 11.29, is used to heat air for a drying operation. Each tube is made from plain carbon steel ($k = 60$ W/m · K) and has an inner diameter and wall thickness of 50 mm and 4 mm, respectively. The thermal resistance per unit length of the brazed joint connecting the tubes is $R_t' = 0.01$ m · K/W. Consider conditions for which air enters one tube at a pressure of 5 atm, a temperature of 17°C, and flow rate of 0.030 kg/s, while saturated steam at 2.455 bar condenses in the other tube. The convection coefficient for condensation may be approximated as 5000 W/m^2 · K. What is the air outlet temperature? What is the mass rate at which condensate leaves the system? *Hint*: Account for the effects of circumferential conduction in the tubes by treating them as extended surfaces.

11.31 Hot water for an industrial washing operation is produced by recovering heat from the flue gases of a furnace. A cross-flow heat exchanger is used, with the gases passing over the tubes and the water making a single pass through the tubes. The steel tubes ($k = 60$ W/m · K) have inner and outer diameters of $D_i = 15$ mm and $D_o = 20$ mm, while the staggered tube array has longitudinal and transverse pitches of $S_T = S_L = 40$ mm. The plenum in which the array is installed has a width (corresponding to the tube length) of $W = 2$ m and a height (normal to the tube axis) of $H = 1.2$ m. The number of tubes in the transverse plane is therefore $N_T \approx H/S_T = 30$. The gas properties may be approximated as those of atmospheric air, and the convection coefficient associated with water flow in the tubes may be approximated as 3000 W/m^2 · K.

(a) If 50 kg/s of water are to be heated from 290 to 350 K by 40 kg/s of flue gases entering the exchanger at 700 K, what is the gas outlet temperature and how many tube rows N_L are required?

(b) The water outlet temperature may be controlled by varying the gas flow rate and/or inlet temperature. For the value of N_L determined in part (a) and the prescribed values of H, W, S_T, $\dot{m}_c$, and $T_{c,i}$, compute and plot $T_{c,o}$ as a function of $\dot{m}_h$ over the range $20 \leq \dot{m}_h \leq 40$ kg/s for values of $T_{h,i} = 500$, 600, and 700 K. Also plot the corresponding variations of $T_{h,o}$. If $T_{h,o}$ must not drop below 400 K to prevent condensation of corrosive vapors on the heat exchanger surfaces, are there any constraints on $\dot{m}_h$ and $T_{h,i}$?

11.32 A single-pass, cross-flow heat exchanger uses hot exhaust gases (mixed) to heat water (unmixed) from 30 to 80°C at a rate of 3 kg/s. The exhaust gases, having thermophysical properties similar to air, enter and exit the exchanger at 225 and 100°C, respectively. If the overall heat transfer coefficient is 200 W/m^2 · K, estimate the required surface area.

11.33 Consider the fluid conditions and overall heat transfer coefficient of Problem 11.32 for a concentric tube heat exchanger operating in parallel flow. The thin-walled separator tube has a diameter of 100 mm.

(a) Determin

(b) Assumin be fully transfer

(c) Using th atures fr rate and of the tu parallel-

(d) If the e with the atures, v length r

(e) For the tiveness tion of

11.34 A cross-flo pulmonary 5 liter/min f order to in metabolic a ice water provide an exchanger overall heat density and and 3740 J/

(a) Determ exchan

(b) Calcul

(c) What i

(d) Calcul peratu the ra meters chang chang ior an

11.35 Saturated tube heat passes con per pass o ters of 13. enters the m/s. The the outer

(a) Dete cooli cond

Patent Owner Manufacturing Resources International, Inc.
Exhibit 2017 - Page 718 of 999

(a) Determine the required length for the exchanger.

(b) Assuming water flow inside the separator tube to be fully developed, estimate the convection heat transfer coefficient.

(c) Using the overall coefficient and the inlet temperatures from Problem 11.32, plot the heat transfer rate and fluid outlet temperatures as a function of the tube length for $60 \leq L \leq 400$ m and the parallel-flow configuration.

(d) If the exchanger were operated in counterflow with the same overall coefficient and inlet temperatures, what would be the reduction in the required length relative to the value found in part (a)?

(e) For the counterflow configuration, plot the effectiveness and fluid outlet temperatures as a function of the tube length for $60 \leq L \leq 400$ m.

11.34 A cross-flow heat exchanger used in a cardiopulmonary bypass procedure cools blood flowing at 5 liter/min from a body temperature of 37°C to 25°C in order to induce body hypothermia, which reduces metabolic and oxygen requirements. The coolant is ice water at 0°C, and its flow rate is adjusted to provide an outlet temperature of 15°C. The heat exchanger operates with both fluids unmixed, and the overall heat transfer coefficient is 750 $W/m^2 \cdot K$. The density and specific heat of the blood are 1050 kg/m^3 and 3740 $J/kg \cdot K$, respectively.

(a) Determine the heat transfer rate for the exchanger.

(b) Calculate the water flow rate.

(c) What is the surface area of the heat exchanger?

(d) Calculate and plot the blood and water outlet temperatures as a function of the water flow rate for the range 2 to 4 liter/min, assuming all other parameters remain unchanged. Comment on how the changes in the outlet temperatures are affected by changes in the water flow rate. Explain this behavior and why it is an advantage for this application.

11.35 Saturated steam at 0.14 bar is condensed in a shell-and-tube heat exchanger with one shell pass and two tube passes consisting of 130 brass tubes, each with a length per pass of 2 m. The tubes have inner and outer diameters of 13.4 and 15.9 mm, respectively. Cooling water enters the tubes at 20°C with a mean velocity of 1.25 m/s. The heat transfer coefficient for condensation on the outer surfaces of the tubes is 13,500 $W/m^2 \cdot K$.

(a) Determine the overall heat transfer coefficient, the cooling water outlet temperature, and the steam condensation rate.

(b) With all other conditions remaining the same, but accounting for changes in the overall coefficient, plot the cooling water outlet temperature and the steam condensation rate as a function of the water flow rate for $10 \leq \dot{m}_c \leq 30$ kg/s.

11.36 A feedwater heater that supplies a boiler consists of a shell-and-tube heat exchanger with one shell pass and two tube passes. One hundred thin-walled tubes each have a diameter of 20 mm and a length (per pass) of 2 m. Under normal operating conditions water enters the tubes at 10 kg/s and 290 K and is heated by condensing saturated steam at 1 atm on the outer surface of the tubes. The convection coefficient of the saturated steam is 10,000 $W/m^2 \cdot K$.

(a) Determine the water outlet temperature.

(b) With all other conditions remaining the same, but accounting for changes in the overall heat transfer coefficient, plot the water outlet temperature as a function of the water flow rate for $5 \leq \dot{m}_c \leq 20$ kg/s.

(c) On the plot of part (b), generate two additional curves for the water outlet temperature as a function of flow rate for fouling factors of $R''_f = 0.0002$ and 0.0005 $m^2 \cdot K/W$.

11.37 Saturated steam at 110°C is condensed in a shell-and-tube heat exchanger (1 shell pass; 2, 4, ⋯ tube passes) with a UA value of 2.5 kW/K. Cooling water enters at 40°C.

(a) Calculate the cooling water flow rate required to maintain a heat rate of 150 kW.

(b) Assuming that UA is independent of flow rate, calculate and plot the water flow rate required to provide heat rates over the range from 130 to 160 kW. Comment on the validity of your assumption.

11.38 A shell-and-tube heat exchanger (1 shell pass, 2 tube passes) is to be used to condense 2.73 kg/s of saturated steam at 340 K. Condensation occurs on the outer tube surfaces, and the corresponding convection coefficient is 10,000 $W/m^2 \cdot K$. The temperature of the cooling water entering the tubes is 15°C, and the exit temperature is not to exceed 30°C. Thin-walled tubes of 19-mm diameter are specified, and the mean velocity of water flow through the tubes is to be maintained at 0.5 m/s.

(a) What is the minimum number of tubes that should be used, and what is the corresponding tube length per pass?

(b) To reduce the size of the heat exchanger, it is proposed to increase the water-side convection coefficient by inserting a wire mesh in the tubes. If the

Patent Owner Manufacturing Resources International, Inc.
Exhibit 2017 - Page 719 of 999

mesh increases the convection coefficient by a factor of two, what is the required tube length per pass?

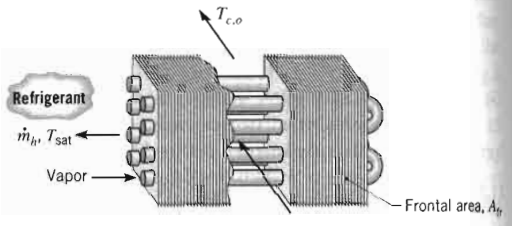
11.39 Saturated water vapor leaves a steam turbine at a flow rate of 1.5 kg/s and a pressure of 0.51 bar. The vapor is to be completely condensed to saturated liquid in a shell-and-tube heat exchanger that uses city water as the cold fluid. The water enters the thin-walled tubes at 17°C and is to leave at 57°C. Assuming an overall heat transfer coefficient of 2000 $W/m^2 \cdot K$, determine the required heat exchanger surface area and the water flow rate. After extended operation, fouling causes the overall heat transfer coefficient to decrease to 1000 $W/m^2 \cdot K$, and to completely condense the vapor, there must be an attendant reduction in the vapor flow rate. For the same water inlet temperature and flow rate, what is the new vapor flow rate required for complete condensation?

11.40 A two-fluid heat exchanger has inlet and outlet temperatures of 65 and 40°C for the hot fluid and 15 and 30°C for the cold fluid. Can you tell whether this exchanger is operating under counterflow or parallel-flow conditions? Determine the effectiveness of the heat exchanger.

11.41 The human brain is especially sensitive to elevated temperatures. The cool blood in the veins leaving the face and neck and returning to the heart may contribute to thermal regulation of the brain by cooling the arterial blood flowing to the brain. Consider a vein and artery running between the chest and the base of the skull for a distance $L = 250$ mm, with mass flow rates of 3×10^{-3} kg/s in opposite directions in the two vessels. The vessels are of diameter $D = 5$ mm and are separated by a distance $w = 7$ mm. The thermal conductivity of the surrounding tissue is $k_t = 0.5$ $W/m \cdot K$. If the arterial blood enters at 37°C and the venous blood enters at 27°C, at what temperature will the arterial blood exit? If the arterial blood becomes overheated, and the body responds by halving the blood flow rate, how much hotter can the entering arterial blood be and still maintain its exit temperature below 37°C? *Hint:* If we assume that all the heat leaving the artery enters the vein, then heat transfer between the two vessels can be modeled using a relationship found in Table 4.1. Approximate the blood properties as those of water.

11.42 Consider a *very long,* concentric tube heat exchanger having hot and cold water inlet temperatures of 85 and 15°C. The flow rate of the hot water is twice that of the cold water. Assuming equivalent hot and cold water specific heats, determine the hot water outlet temperature for the following modes of operation: (a) counterflow and (b) parallel flow.

11.43 A plate-fin heat exchanger is used to condense a saturated refrigerant vapor in an air-conditioning system. The vapor has a saturation temperature of 45°C, and a condensation rate of 0.015 kg/s is dictated by system performance requirements. The frontal area of the condenser is fixed at $A_{fr} = 0.25$ m^2 by installation requirements, and a value of $h_{fg} = 135$ kJ/kg may be assumed for the refrigerant.



(a) The condenser design is to be based on a nominal air inlet temperature of $T_{c,i} = 30$°C and nominal air inlet velocity of $V = 2$ m/s for which the manufacturer of the heat exchanger core indicates an overall coefficient of $U = 50$ $W/m^2 \cdot K$. What is the corresponding value of the heat transfer surface area required to achieve the prescribed condensation rate? What is the air outlet temperature?

(b) From the manufacturer of the heat exchanger core, it is also known that $U \propto V^{0.7}$. During daily operation the air inlet temperature is not controllable and may vary from 27 to 38°C. If the heat exchanger area is fixed by the result of part (a), what is the range of air velocities needed to maintain the prescribed condensation rate? Plot the velocity as a function of the air inlet temperature.

11.44 A shell-and-tube heat exchanger is to heat 10,000 kg/h of water from 16 to 84°C by hot engine oil flowing through the shell. The oil makes a single shell pass, entering at 160°C and leaving at 94°C, with an average heat transfer coefficient of 400 $W/m^2 \cdot K$. The water flows through 11 brass tubes of 22.9-mm inside diameter and 25.4-mm outside diameter, with each tube making four passes through the shell.

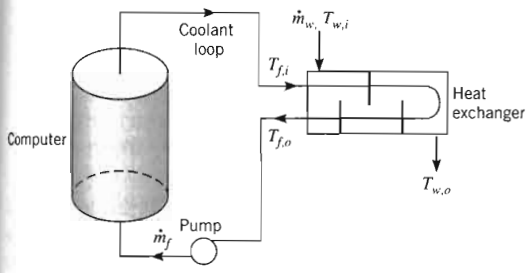
(a) Assuming fully developed flow for the water, determine the required tube length per pass.

(b) For the tube length found in part (a), plot the effectiveness, fluid outlet temperatures, and water-side convection coefficient as a function of the water

Patent Owner Manufacturing Resources International, Inc.
Exhibit 2017 - Page 720 of 999

flow rate for $5000 \leq \dot{m}_c \leq 15{,}000$ kg/h, with all other conditions remaining the same.

11.45 In a supercomputer, signal propagation delays are reduced by resorting to high-density circuit arrangements which are cooled by immersing them in a special dielectric liquid. The fluid is pumped in a closed loop through the computer and an adjoining shell-and-tube heat exchanger having one shell and two tube passes.



During normal operation, heat generated within the computer is transferred to the dielectric fluid passing through the computer at a flow rate of $\dot{m}_f = 4.81$ kg/s. In turn, the fluid passes through the tubes of the heat exchanger and the heat is transferred to water passing over the tubes. The dielectric fluid may be assumed to have constant properties of $c_p = 1040$ J/kg · K, $\mu = 7.65 \times 10^{-4}$ kg/s · m, $k = 0.058$ W/m · K, and $Pr = 14$. During normal operation, chilled water at a flow rate of $\dot{m}_w = 2.5$ kg/s and an inlet temperature of $T_{w,i} = 5°C$ passes over the tubes. The water has a specific heat of 4200 J/kg · K and provides an average convection coefficient of 10,000 W/m² · K over the outer surface of the tubes.

(a) If the heat exchanger consists of 72 thin-walled tubes, each of 10-mm diameter, and fully developed flow is assumed to exist within the tubes, what is the convection coefficient associated with flow through the tubes?

(b) If the dielectric fluid enters the heat exchanger at $T_{f,i} = 25°C$ and is to leave at $T_{f,o} = 15°C$, what is the required tube length per pass?

(c) For the exchanger with the tube length per pass determined in part (b), plot the outlet temperature of the dielectric fluid as a function of its flow rate for $4 \leq \dot{m}_f \leq 6$ kg/s. Account for corresponding changes in the overall heat transfer coefficient, but assume all other conditions to remain the same.

(d) The site specialist for the computer facilities is concerned about changes in the performance of the water chiller supplying the cold water ($\dot{m}_w$, $T_{w,i}$) and their effect on the outlet temperature $T_{f,o}$ of the dielectric fluid. With all other conditions remaining the same, determine the effect of a ±10% change in the cold water flow rate on $T_{f,o}$.

(e) Repeat the performance analysis of part (d) to determine the effect of a ±3°C change in the water inlet temperature on $T_{f,o}$, with all other conditions remaining the same.

11.46 A shell-and-tube heat exchanger consists of 135 thin-walled tubes in a double-pass arrangement, each of 12.5-mm diameter with a total surface area of 47.5 m². Water (the tube-side fluid) enters the heat exchanger at 15°C and 6.5 kg/s and is heated by exhaust gas entering at 200°C and 5 kg/s. The gas may be assumed to have the properties of atmospheric air, and the overall heat transfer coefficient is approximately 200 W/m² · K.

(a) What are the gas and water outlet temperatures?

(b) Assuming fully developed flow, what is the tube-side convection coefficient?

(c) With all other conditions remaining the same, plot the effectiveness and fluid outlet temperatures as a function of the water flow rate over the range from 6 to 12 kg/s.

(d) What gas inlet temperature is required for the exchanger to supply 10 kg/s of hot water at an outlet temperature of 42°C, all other conditions remaining the same? What is the effectiveness for this operating condition?

11.47 An ocean thermal energy conversion system is being proposed for electric power generation. Such a system is based on the standard power cycle for which the working fluid is evaporated, passed through a turbine, and subsequently condensed. The system is to be used in very special locations for which the oceanic water temperature near the surface is approximately 300 K, while the temperature at reasonable depths is approximately 280 K. The warmer water is used as a heat source to evaporate the working fluid, while the colder water is used as a heat sink for condensation of the fluid. Consider a power plant that is to generate 2 MW of electricity at an efficiency (electric power output per heat input) of 3%. The evaporator is a heat exchanger consisting of a single shell with many tubes executing two passes. If the working fluid is evaporated at its phase change temperature of 290 K, with ocean water entering at 300 K and leaving at 292 K, what is the heat exchanger area required for the evaporator? What flow rate must be maintained for the water passing through the evaporator? The overall heat transfer coefficient may be approximated as 1200 W/m² · K.

Patent Owner Manufacturing Resources International, Inc.
Exhibit 2017 - Page 721 of 999

11.48 A single-pass, cross-flow heat exchanger with both fluids unmixed is being used to heat water ($\dot{m}_c = 2$ kg/s, $c_p = 4200$ J/kg · K) from 20°C to 100°C with hot exhaust gases ($c_p = 1200$ J/kg · K) entering at 320°C. What mass flow rate of exhaust gases is required? Assume that UA is equal to its design value of 4700 W/K, independent of the gas mass flow rate.

11.49 Saturated process steam at 1 atm is condensed in a shell-and-tube heat exchanger (one shell, two tube passes). Cooling water enters the tubes at 15°C with an average velocity of 3.5 m/s. The tubes are thin-walled and made of copper with a diameter of 14 mm and length of 0.5 m. The convective heat transfer coefficient for condensation on the outer surface of the tubes is 21,800 W/m² · K.

(a) Find the number of tubes/pass required to condense 2.3 kg/s of steam.

(b) Find the outlet water temperature.

(c) Find the maximum possible condensation rate that could be achieved with this heat exchanger using the same water flow rate and inlet temperature.

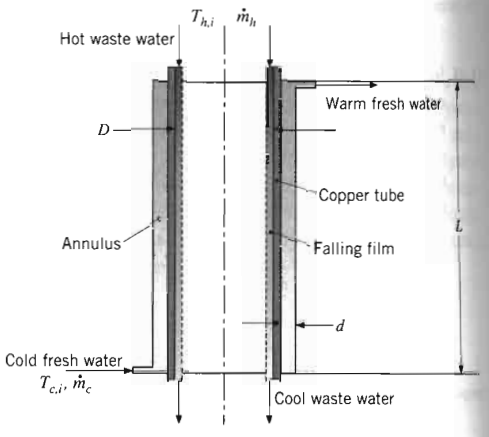
(d) Using the heat transfer surface area found in part (a), plot the water outlet temperature and steam condensation rate for water mean velocities in the range from 1 to 5 m/s. Assume that the shell-side convection coefficient remains unchanged.

11.50 The chief engineer at a university that is constructing a large number of new student dormitories decides to install a counterflow concentric tube heat exchanger on each of the dormitory shower drains. The thin-walled copper drains are of diameter $D_i = 50$ mm. Wastewater from the shower enters the heat exchanger at $T_{h,i} = 38$°C while fresh water enters the dormitory at $T_{c,i} = 10$°C. The wastewater flows down the vertical wall of the drain in a thin, *falling film*, providing $h_h = 10{,}000$ W/m² · K.

(a) If the annular gap is $d = 10$ mm, the heat exchanger length is $L = 1$ m, and the water flow rate is $\dot{m} = 10$ kg/min, determine the heat transfer rate and the outlet temperature of the warmed fresh water.

(b) If a helical spring is installed in the annular gap so the fresh water is forced to follow a spiral path from the inlet to the fresh water outlet, resulting in $h_c = 9050$ W/m² · K, determine the heat transfer rate and the outlet temperature of the fresh water.

(c) Based on the result for part (b), calculate the daily savings if 15,000 students each take a 10-minute shower per day and the cost of water heating is \$0.07/kW · h.



11.51 A shell-and-tube heat exchanger with single shell and tube passes (Figure 11.3) is used to cool the oil of a large marine engine. Lake water (the shell-side fluid) enters the heat exchanger at 2 kg/s and 15°C, while the oil enters at 1 kg/s and 140°C. The oil flows through 100 copper tubes, each 500 mm long and having inner and outer diameters of 6 and 8 mm. The shell-side convection coefficient is approximately 500 W/m² · K.

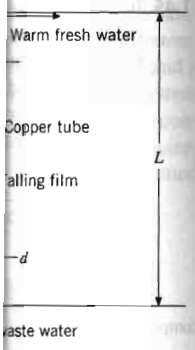
(a) What is the oil outlet temperature?

(b) Over time there is some degradation in the performance of the engine's water pump, as well as an accumulation of deposits on the outer surface of the tubes. To assess the effect of these changes on heat exchanger performance, obtain two plots of the oil outlet temperature as a function of water flow rate in the range from 1 to 2 kg/s. One should correspond to a clean outer surface ($R''_{f,c} = 0$) and the other to surface conditions for which $R''_{f,c} = 0.0003$ m² · K/W.

11.52 A shell-and-tube heat exchanger with one shell pass and 20 tube passes uses hot water on the tube side to heat oil on the shell side. The single copper tube has inner and outer diameters of 20 and 24 mm and a length per pass of 3 m. The water enters at 87°C and 0.2 kg/s and leaves at 27°C. Inlet and outlet temperatures of the oil are 7 and 37°C. What is the average convection coefficient for the tube outer surface?

11.53 The oil in an engine is cooled by air in a cross-flow heat exchanger where both fluids are unmixed. Atmospheric air enters at 30°C and 0.53 kg/s. Oil at 0.026 kg/s enters at 75°C and flows through a tube of 10-mm diameter. Assuming fully developed flow and constant wall heat flux, estimate the oil-side heat transfer coefficient. If the overall convection coefficient is 53 W/m² · K and the

Patent Owner Manufacturing Resources International, Inc.
Exhibit 2017 - Page 722 of 999



r with single shell and
ed to cool the oil of a
er (the shell-side fluid)
g/s and 15°C, while the
The oil flows through
long and having inner
8 mm. The shell-side
imately 500 W/m² · K.

erature?

gradation in the perfor-
er pump, as well as an
on the outer surface of
ect of these changes on
ce, obtain two plots of
as a function of water
rom 1 to 2 kg/s. One
clean outer surface
surface conditions for
K/W.

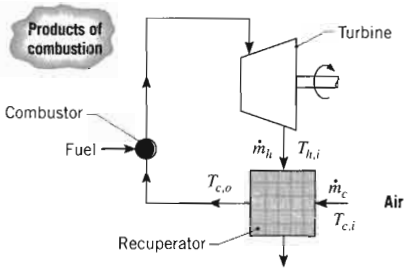
er with one shell pass
ater on the tube side to
single copper tube has
20 and 24 mm and a
ater enters at 87°C and
let and outlet tempera-
C. What is the average
be outer surface?

air in a cross-flow heat
unmixed. Atmospheric
Oil at 0.026 kg/s enters
be of 10-mm diameter.
and constant wall heat
ansfer coefficient. If the
is 53 W/m² · K and the

total heat transfer area is 1 m², determine the effectiveness. What is the exit temperature of the oil?

11.54 It is proposed that the exhaust gas from a diesel-powered electric generation plant be used to generate steam in a shell-and-tube heat exchanger with one shell and one tube pass. The steel tubes have a thermal conductivity of 40 W/m · K, an inner diameter of 50 mm, and a wall thickness of 4 mm. The exhaust gas, whose flow rate is 2 kg/s, enters the heat exchanger at 400°C and must leave at 215°C. To limit the pressure drop within the tubes, the tube gas velocity should not exceed 25 m/s. If saturated water at 11.7 bar is supplied to the shell side of the exchanger, determine the required number of tubes and their length. Assume that the properties of the exhaust gas can be approximated as those of atmospheric air and that the water-side thermal resistance is negligible. However, account for fouling on the gas-side of the tubes and use a fouling resistance of 0.0015 m² · K/W.

11.55 A recuperator is a heat exchanger that heats air used in a combustion process by extracting energy from the products of combustion. It can be used to increase the efficiency of a gas turbine by increasing the temperature of air entering the combustor.



Consider a system for which the recuperator is a cross-flow heat exchanger with both fluids unmixed and the flow rates associated with the turbine exhaust and the air are $\dot{m}_h = 6.5$ kg/s and $\dot{m}_c = 6.2$ kg/s, respectively. The corresponding value of the overall heat transfer coefficient is $U = 100$ W/m² · K.

(a) If the gas and air inlet temperatures are $T_{h,i} = 700$ K and $T_{c,i} = 300$ K, respectively, what heat transfer surface area is needed to provide an air outlet temperature of $T_{c,o} = 500$ K? Both the air and the products of combustion may be assumed to have a specific heat of 1040 J/kg · K.

(b) For the prescribed conditions, compute and plot the air outlet temperature as a function of the heat transfer surface area.

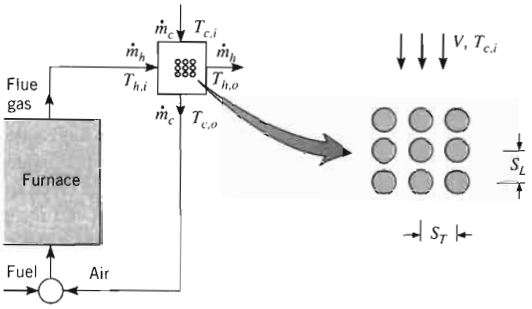
11.56 A concentric tube heat exchanger uses water, which is available at 15°C, to cool ethylene glycol from 100 to 60°C. The water and glycol flow rates are each 0.5 kg/s. What are the maximum possible heat transfer rate and effectiveness of the exchanger? Which is preferred, a parallel-flow or counterflow mode of operation?

11.57 Water is used for both fluids (unmixed) flowing through a single-pass, cross-flow heat exchanger. The hot water enters at 90°C and 10,000 kg/h, while the cold water enters at 10°C and 20,000 kg/h. If the effectiveness of the exchanger is 60%, determine the cold water exit temperature.

11.58 A cross-flow heat exchanger consists of a bundle of 32 tubes in a 0.6-m² duct. Hot water at 150°C and a mean velocity of 0.5 m/s enters the tubes having inner and outer diameters of 10.2 and 12.5 mm. Atmospheric air at 10°C enters the exchanger with a volumetric flow rate of 1.0 m³/s. The convection heat transfer coefficient on the tube outer surfaces is 400 W/m² · K. Estimate the fluid outlet temperatures.

11.59 Exhaust gas from a furnace is used to preheat the combustion air supplied to the furnace burners. The gas, which has a flow rate of 15 kg/s and an inlet temperature of 1100 K, passes through a bundle of tubes, while the air, which has a flow rate of 10 kg/s and an inlet temperature of 300 K, is in cross flow over the tubes. The tubes are unfinned, and the overall heat transfer coefficient is 100 W/m² · K. Determine the total tube surface area required to achieve an air outlet temperature of 850 K. The exhaust gas and the air may each be assumed to have a specific heat of 1075 J/kg · K.

11.60 A recuperator is a heat exchanger that heats the air used in a combustion process by extracting energy from the products of combustion (the flue gas). Consider using a single-pass, cross-flow heat exchanger as a recuperator.



Eighty (80) silicon carbide ceramic tubes ($k = 20$ W/m · K) of inner and outer diameters equal to 55 and 80 mm, respectively, and of length $L = 1.4$ m are

Patent Owner Manufacturing Resources International, Inc.
Exhibit 2017 - Page 723 of 999

arranged as an aligned tube bank of longitudinal and transverse pitches $S_L = 100$ mm and $S_T = 120$ mm, respectively. Cold air is in cross flow over the tube bank with upstream conditions of $V = 1$ m/s and $T_{c,i} = 300$ K, while hot flue gases of inlet temperature $T_{h,i} = 1400$ K pass through the tubes. The tube outer surface is clean, while the inner surface is characterized by a fouling factor of $R''_f = 2 \times 10^{-4}$ m$^2 \cdot$ K/W. The air and flue gas flow rates are $\dot{m}_c = 1.0$ kg/s and $\dot{m}_h = 1.05$ kg/s, respectively. As first approximations, (1) evaluate all required air properties at 1 atm and 300 K, (2) assume the flue gas to have the properties of air at 1 atm and 1400 K, and (3) assume the tube wall temperature to be at 800 K for the purpose of treating the effect of variable properties on convection heat transfer.

(a) If there is a 1% fuel savings associated with each 10°C increase in the temperature of the combustion air ($T_{c,o}$) above 300 K, what is the percentage fuel savings for the prescribed conditions?

(b) The performance of the recuperator is strongly influenced by the product of the overall heat transfer coefficient and the total surface area, UA. Compute and plot $T_{c,o}$ and the percentage fuel savings as a function of UA for $300 \leq UA \leq 600$ W/K. Without changing the flow rates, what measures may be taken to increase UA?

11.61 Consider operation of the furnace–recuperator combination of Problem 11.60 under conditions for which chemical energy is converted to thermal energy in the combustor at a rate of $q_{comb} = 2.0 \times 10^6$ W and energy is transferred from the combustion gases to the load in the furnace at a rate of $q_{load} = 1.4 \times 10^6$ W. Assuming equivalent flow rates ($\dot{m}_c = \dot{m}_h = 1.0$ kg/s) and specific heats ($c_{p,c} = c_{p,h} = 1200$ J/kg $\cdot$ K) for the cold air and flue gases in the recuperator, determine $T_{h,i}$, $T_{h,o}$, and $T_{c,o}$ when $T_{c,i} = 300$ K and the recuperator has an effectiveness of $\varepsilon = 0.30$. What value of the effectiveness would be needed to achieve a combustor air inlet temperature of 800 K?

11.62 A shell-and-tube heat exchanger consisting of one shell pass and two tube passes is used to transfer heat from an ethylene glycol–water solution (shell side) supplied from a rooftop solar collector to pure water (tube side) used for household purposes. The tubes are of inner and outer diameters $D_i = 3.6$ mm and $D_o = 3.8$ mm, respectively. Each of the 100 tubes is 0.8 m long (0.4 m per pass), and the heat transfer coefficient associated with the ethylene glycol–water mixture is $h_o = 11{,}000$ W/m$^2 \cdot$ K.

(a) For pure copper tubes, calculate the heat transfer rate from the ethylene glycol–water solution ($\dot{m} = 2.5$ kg/s, $T_{h,i} = 80$°C) to the pure water ($\dot{m} = 2.5$ kg/s, $T_{c,i} = 20$°C). Determine the outlet temperatures of both streams of fluid. The density and specific heat of the ethylene glycol–water mixture are 1040 kg/m^3 and 3660 J/kg $\cdot$ K, respectively.

(b) It is proposed to replace the copper tube bundle with a bundle composed of high-temperature nylon tubes of the same diameter and tube wall thickness. The nylon is characterized by a thermal conductivity of $k_n = 0.31$ W/m $\cdot$ K. Determine the tube length required to transfer the same amount of energy as in part (a).

11.63 Consider a concentric tube heat exchanger characterized by a uniform overall heat transfer coefficient and operating under the following conditions:

	$\dot{m}$ (kg/s)	c_p (J/kg $\cdot$ K)	T_i (°C)	T_o (°C)
Cold fluid	0.125	4200	40	95
Hot fluid	0.125	2100	210	—

What is the maximum possible heat transfer rate? What is the heat exchanger effectiveness? Should the heat exchanger be operated in parallel flow or in counterflow? What is the ratio of the required areas for these two flow conditions?

11.64 Consider a concentric tube heat exchanger with hot and cold water inlet temperatures of 200 and 35°C, respectively. The flow rates of the hot and cold fluids are 42 and 84 kg/h, respectively. Assume the overall heat transfer coefficient is 180 W/m$^2 \cdot$ K.

(a) What is the maximum heat transfer rate that could be achieved for the prescribed inlet conditions?

(b) If the exchanger is operated in counterflow with a heat transfer area of 0.33 m^2, determine the outlet fluid temperatures.

(c) With all other conditions remaining the same, plot the effectiveness and fluid outlet temperatures as a function of the product UA for the range from 50 to 1000 W/K. As UA becomes very large, what is the asymptotic value for $T_{h,o}$?

(d) What is the largest possible heat transfer rate that could be achieved for the prescribed inlet conditions, if the exchanger is operated in parallel flow and is very long? What is the effectiveness of the exchanger in this configuration?

(e) For operation in parallel flow, plot the effectiveness and fluid outlet temperatures as a function of the product UA for the range from 50 to 1000 W/K.

As UA l
totic val

11.65 The floor sp
tube heat exc
tube bundle
that the floor
of the tube b
removed fro
floor space is
quently clea
ated with the
room in whic
to be installe
long heat ex
shell-and-tub
above the o
facility? Eac

11.66 Consider the
Example 11.

(a) Determi
exchang
mm for
polyvin
K) shee
bottom

(b) Plot the
tion of
PVDF c

11.67 Hot exhaus
exchanger t
The gases, a
at 200°C an
coefficient i
NTU meth
exchanger.

11.68 In open hea
the patient's
rewarmed a
tube, counte
used for this
having a dia
blood is 350

(a) If water
to heat
18°C ar
of the
heat tra

(b) The sur
and the
altering

Patent Owner Manufacturing Resources International, Inc.
Exhibit 2017 - Page 724 of 999

As UA becomes very large, what are the asymptotic values for $T_{h,o}$ and $T_{c,o}$?

11.65 The floor space of any facility that houses shell-and-tube heat exchangers must be sufficiently large so the tube bundle can be serviced easily. A rule of thumb is that the floor space must be at least 2.5 times the length of the tube bundle so that the bundle can be completely removed from the shell (hence the absolute minimum floor space is twice the tube bundle length) and subsequently cleaned, repaired, or replaced easily (associated with the extra half bundle length floor space). The room in which the heat exchanger of Problem 11.22 is to be installed is 8 m long and, therefore, the 4.7-m-long heat exchanger is too large for the facility. Will a shell-and-tube heat exchanger with two shells, one above the other, be sufficiently small to fit into the facility? Each shell has 10 tubes and 8 tube passes.

11.66 Consider the influence of a finite sheet thickness in Example 11.2, when there are 40 gaps.

(a) Determine the exterior dimension, L, of the heat exchanger core for a sheet thickness of $t = 0.8$ mm for pure aluminum ($k_{al} = 237$ W/m · K) and polyvinylidene fluoride (PVDF, $k_{pv} = 0.17$ W/m · K) sheets. Neglect the thickness of the top and bottom exterior plates.

(b) Plot the heat exchanger core dimension as a function of the sheet thickness for aluminum and PVDF over the range $0 \leq t \leq 1$ mm.

11.67 Hot exhaust gases are used in a shell-and-tube exchanger to heat 2.5 kg/s of water from 35 to 85°C. The gases, assumed to have the properties of air, enter at 200°C and leave at 93°C. The overall heat transfer coefficient is 180 W/m² · K. Using the effectiveness–NTU method, calculate the area of the heat exchanger.

11.68 In open heart surgery under hypothermic conditions, the patient's blood is cooled before the surgery and rewarmed afterward. It is proposed that a concentric tube, counterflow heat exchanger of length 0.5 m be used for this purpose, with the thin-walled inner tube having a diameter of 55 mm. The specific heat of the blood is 3500 J/kg · K.

(a) If water at $T_{h,i} = 60$°C and $\dot{m}_h = 0.10$ kg/s is used to heat blood entering the exchanger at $T_{c,i} = 18$°C and $\dot{m}_c = 0.05$ kg/s, what is the temperature of the blood leaving the exchanger? The overall heat transfer coefficient is 500 W/m² · K.

(b) The surgeon may wish to control the heat rate q and the outlet temperature $T_{c,o}$ of the blood by altering the flow rate and/or inlet temperature of the water during the rewarming process. To assist in the development of an appropriate controller for the prescribed values of $\dot{m}_c$ and $T_{c,i}$, compute and plot q and $T_{c,o}$ as a function of $\dot{m}_h$ for $0.05 \leq \dot{m}_h \leq 0.20$ kg/s and values of $T_{h,i} = 50$, 60, and 70°C. Since the dominant influence on the overall heat transfer coefficient is associated with the blood flow conditions, the value of U may be assumed to remain at 500 W/m² · K. Should certain operating conditions be excluded?

11.69 Ethylene glycol and water, at 60 and 10°C, respectively, enter a shell-and-tube heat exchanger for which the total heat transfer area is 15 m². With ethylene glycol and water flow rates of 2 and 5 kg/s, respectively, the overall heat transfer coefficient is 800 W/m² · K.

(a) Determine the rate of heat transfer and the fluid outlet temperatures.

(b) Assuming all other conditions to remain the same, plot the effectiveness and fluid outlet temperatures as a function of the flow rate of ethylene glycol for $0.5 \leq \dot{m}_h \leq 5$ kg/s.

11.70 A boiler used to generate saturated steam is in the form of an unfinned, cross-flow heat exchanger, with water flowing through the tubes and a high-temperature gas in cross flow over the tubes. The gas, which has a specific heat of 1120 J/kg · K and a mass flow rate of 10 kg/s, enters the heat exchanger at 1400 K. The water, which has a flow rate of 3 kg/s, enters as saturated liquid at 450 K and leaves as saturated vapor at the same temperature. If the overall heat transfer coefficient is 50 W/m² · K and there are 500 tubes, each of 0.025-m diameter, what is the required tube length?

11.71 Waste heat from the exhaust gas of an industrial furnace is recovered by mounting a bank of unfinned tubes in the furnace stack. Pressurized water at a flow rate of 0.025 kg/s makes a single pass through *each* of the tubes, while the exhaust gas, which has an upstream velocity of 5.0 m/s, moves in cross flow over the tubes at 2.25 kg/s. The tube bank consists of a square array of 100 thin-walled tubes (10 × 10), each 25 mm in diameter and 4 m long. The tubes are aligned with a transverse pitch of 50 mm. The inlet temperatures of the water and the exhaust gas are 300 and 800 K, respectively. The water flow is fully developed, and the gas properties may be assumed to be those of atmospheric air.

(a) What is the overall heat transfer coefficient?

(b) What are the fluid outlet temperatures?

(c) Operation of the heat exchanger may vary according to the demand for hot water. For the prescribed

Patent Owner Manufacturing Resources International, Inc.
Exhibit 2017 - Page 725 of 999

heat exchanger design and inlet conditions, compute and plot the rate of heat recovery and the fluid outlet temperatures as a function of water flow rate per tube for $0.02 \leq \dot{m}_{c,1} \leq 0.20$ kg/s.

11.72 A heat exchanger consists of a bank of 1200 thin-walled tubes with air in cross flow over the tubes. The tubes are arranged in-line, with 40 longitudinal rows (along the direction of airflow) and 30 transverse rows. The tubes are 0.07 m in diameter and 2 m long, with transverse and longitudinal pitches of 0.14 m. The hot fluid flowing through the tubes consists of saturated steam condensing at 400 K. The convection coefficient of the condensing steam is much larger than that of the air.

(a) If air enters the heat exchanger at $\dot{m}_c = 12$ kg/s, 300 K, and 1 atm, what is its outlet temperature?

(b) The condensation rate may be controlled by varying the airflow rate. Compute and plot the air outlet temperature, the heat rate, and the condensation rate as a function of flow rate for $10 \leq \dot{m}_c \leq 50$ kg/s.

11.73 In analyzing thermodynamic cycles involving heat exchangers, it is useful to express the heat rate in terms of an overall thermal resistance R_t and the inlet temperatures of the hot and cold fluids,

$$q = \frac{(T_{h,i} - T_{c,i})}{R_t}$$

The heat transfer rate can also be expressed in terms of the rate equations,

$$q = UA\,\Delta T_{\text{lm}} = \frac{1}{R_{\text{lm}}}\,\Delta T_{\text{lm}}$$

(a) Derive a relation for R_{lm}/R_t for a *parallel-flow* heat exchanger in terms of a single dimensionless parameter B, which does not involve any fluid temperatures but only U, A, C_h, C_c (or $C_{\min}$, $C_{\max}$).

(b) Calculate and plot R_{lm}/R_t for values of $B = 0.1$, 1.0, and 5.0. What conclusions can be drawn from the plot?

11.74 The power needed to overcome wind and friction drag associated with an automobile traveling at a constant velocity of 25 m/s is 9 kW.

(a) Determine the required heat transfer area of the radiator if the vehicle is equipped with an internal combustion engine operating at an efficiency of 35%. (Assume 65% of the energy generated by the engine is in the form of waste heat removed by the radiator.) The inlet and outlet mean temperatures of the water with respect to the radiator are $T_{m,i} = 400$ K and $T_{m,o} = 330$ K, respectively. Cooling air is available at 3 kg/s and 300 K. The radiator may be analyzed as a cross-flow heat exchanger with both fluids unmixed with an overall heat transfer coefficient of 400 W/m$^2 \cdot$K.

(b) Determine the required water mass flow rate and heat transfer area of the radiator if the vehicle is equipped with a fuel cell operating at 50% efficiency. The fuel cell operating temperature is limited to approximately 85°C, so the inlet and outlet mean temperatures of the water with respect to the radiator are $T_{m,i} = 355$ K and $T_{m,o} = 330$ K, respectively. The air inlet temperature is as in part (a). Assume the flow rate of air is proportional to the surface area of the radiator. *Hint:* Iteration is required.

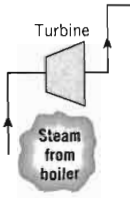
(c) Determine the required heat transfer area of the radiator and the outlet mean temperature of the water for the fuel cell–equipped vehicle if the mass flow rate of the water is the same as in part (a).

11.75 An air conditioner operating between indoor and outdoor temperatures of 23 and 43°C, respectively, removes 5 kW from a building. The air conditioner can be modeled as a reversed Carnot heat engine with refrigerant as the working fluid. The efficiency of the motor for the compressor and fan is 80%, and 0.2 kW is required to operate the fan.

(a) Assuming negligible thermal resistances (Problem 11.73) between the refrigerant in the condenser and the outside air and between the refrigerant in the evaporator and the inside air, calculate the power required by the motor.

(b) If the thermal resistances between the refrigerant and the air in the evaporator and condenser sections are the same, 3×10^{-3} K/W, determine the temperature required by the refrigerant in each section. Calculate the power required by the motor.

11.76 In a Rankine power system, 1.5 kg/s of steam leaves the turbine as saturated vapor at 0.51 bar. The steam is condensed to saturated liquid by passing it over the tubes of a shell-and-tube heat exchanger, while liquid water, having an inlet temperature of $T_{c,i} = 280$ K, is passed through the tubes. The condenser contains 100 thin-walled tubes, each of 10-mm diameter, and the total water flow rate through the tubes is 15 kg/s. The average convection coefficient associated with condensation on the outer surface of the tubes may be approximated as $\bar{h}_o = 5000$ W/m$^2 \cdot$K. Appropriate property values for the liquid water are $c_p = 4178$ J/kg$\cdot$K, $\mu = 700 \times 10^{-6}$ kg/s$\cdot$m, $k = 0.628$ W/m$\cdot$K, and $Pr = 4.6$.

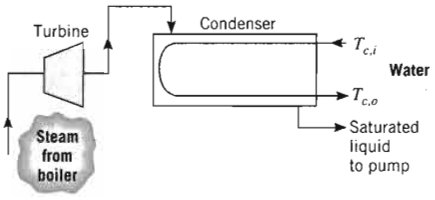


(a) What is t
(b) What is t
(c) After ex
inner an
tive foul
prescribe
tube len
condens
(d) For the
fouling
extent to
perature
ble range
Represe
appropri

11.77 Consider a R
the boiler at
sure of 10 kP
(a) Calculat
Rankine
(b) If the ne
calculate
supplied
able ten
(c) Design
shell, m
rate and
condens
ber of tu

11.78 Consider the
rejects 2.3
with a coolin
(a) Calcula
size of
conditio
(b) Conside
transfer
by 10%
tion in t
fouling,
and wat
condens

Patent Owner Manufacturing Resources International, Inc.
Exhibit 2017 - Page 726 of 999



(a) What is the water outlet temperature?

(b) What is the required tube length (per tube)?

(c) After extended use, deposits accumulating on the inner and outer tube surfaces provide a cumulative fouling factor of 0.0003 $m^2 \cdot K/W$. For the prescribed inlet conditions and the computed tube length, what mass fraction of the vapor is condensed?

(d) For the tube length computed in part (b) and the fouling factor prescribed in part (c), explore the extent to which the water flow rate and inlet temperature may be varied (within physically plausible ranges) to improve the condenser performance. Represent your results graphically, and draw appropriate conclusions.

11.77 Consider a Rankine cycle with saturated steam leaving the boiler at a pressure of 2 MPa and a condenser pressure of 10 kPa.

(a) Calculate the thermal efficiency of the ideal Rankine cycle for these operating conditions.

(b) If the net reversible work for the cycle is 0.5 MW, calculate the required flow rate of cooling water supplied to the condenser at 15°C with an allowable temperature rise of 10°C.

(c) Design a shell-and-tube heat exchanger (one-shell, multiple-tube passes) that will meet the heat rate and temperature conditions required of the condenser. Your design should specify the number of tubes and their diameter and length.

11.78 Consider the Rankine cycle of Problem 11.77, which rejects 2.3 MW to the condenser, which is supplied with a cooling water flow rate of 70 kg/s at 15°C.

(a) Calculate UA, a parameter that is indicative of the size of the condenser required for this operating condition.

(b) Consider now the situation where the overall heat transfer coefficient for the condenser, U, is reduced by 10% because of fouling. Determine the reduction in the thermal efficiency of the cycle caused by fouling, assuming that the cooling water flow rate and water temperature remain the same and that the condenser is operated at the same steam pressure.

Compact Heat Exchangers

11.79 Consider the compact heat exchanger conditions of Example 11.6. After extended use, fouling factors of 0.0005 and 0.001 $m^2 \cdot K/W$ are associated with the water- and gas-side conditions, respectively. What is the gas-side overall heat transfer coefficient?

11.80 Consider the heat exchanger core geometry and frontal area prescribed in Example 11.6. The exchanger must heat 2 kg/s of water from 300 to 350 K, using 1.25 kg/s of combustion gases entering at 700 K. Using the overall heat transfer coefficient determined in the example, find the required heat exchanger volume, assuming single-pass operation. What is the number of tube rows N_L in the longitudinal (gas-flow) direction? If the velocity of water flowing through the tubes is 100 mm/s, what is the number of tube rows N_T in the transverse direction? What is the required tube length?

11.81 Consider the conditions of Example 11.6, but with the continuous fin arrangement of Figure 11.17 used in lieu of the circular fins of Figure 11.16. The heat exchanger core is fabricated from aluminum, and the tubes have an inside diameter of 8.2 mm. An inside convection coefficient of 1500 $W/m^2 \cdot K$ may again be assumed for water flow through the tubes, with combustion gases at 1 atm and 825 K in cross flow over the tubes. For a gas flow rate of 1.25 kg/s and a frontal area of 0.20 m^2, what is the gas-side overall heat transfer coefficient? If water at a flow rate of 1 kg/s is to be heated from 290 to 370 K, what is the required heat exchanger volume? *Hint:* Estimate the fin efficiency by assuming a hypothetical circular fin of radius $r_2 = 15.8$ mm for each tube. You may use the aluminum and fluid properties provided in Example 11.6.

11.82 A cooling coil consists of a bank of aluminum (k = 237 $W/m \cdot K$) finned tubes having the core configuration of Figure 11.16 and an inner diameter of 13.8 mm. The tubes are installed in a plenum whose square cross section is 0.4 m on a side, thereby providing a frontal area of 0.16 m^2. Atmospheric air at 1.5 kg/s is in cross flow over the tubes, while saturated refrigerant-134a at 1 atm experiences evaporation in the tubes. If the air enters at 37°C and its exit temperature must not exceed 17°C, what is the minimum allowable number of tube rows in the flow direction? A convection coefficient of 5000 $W/m^2 \cdot K$ is associated with evaporation in the tubes.

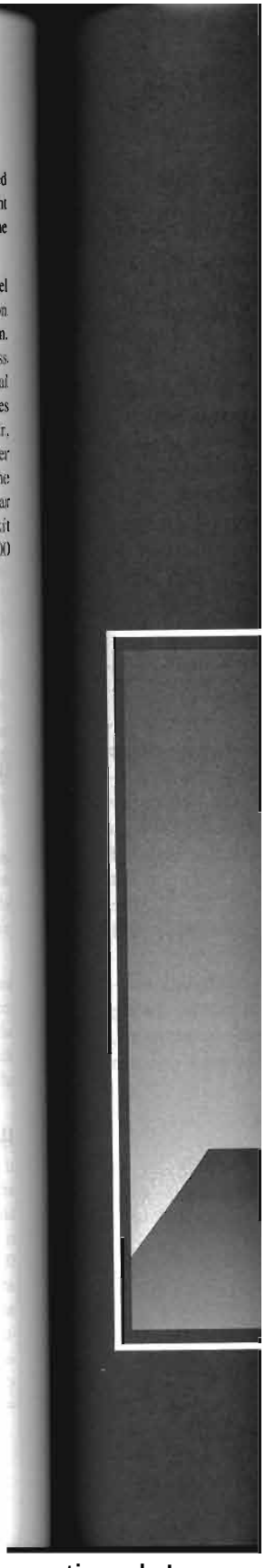
11.83 A cooling coil consists of a bank of aluminum (k = 237 $W/m \cdot K$) finned tubes having the core configuration of Figure 11.16 and an inner diameter of 13.8 mm. The tubes are installed in a plenum whose square cross section is 0.4 m on a side, thereby providing a

Patent Owner Manufacturing Resources International, Inc.
Exhibit 2017 - Page 727 of 999

frontal area of 0.16 m^2. Atmospheric air at 1.5 kg/s is in cross flow over the tubes, while saturated refrigerant-134a at 1 atm passes through the tubes. There are four rows of tubes in the airflow direction. If the air enters at 37°C, what is its exit temperature? A convection coefficient of 5000 $W/m^2 \cdot K$ is associated with evaporation in the tubes.

11.84 A steam generator consists of a bank of stainless steel ($k = 15\ W/m \cdot K$) tubes having the core configuration of Figure 11.16 and an inner diameter of 13.8 mm. The tubes are installed in a plenum whose square cross section is 0.6 m on a side, thereby providing a frontal area of 0.36 m^2. Combustion gases, whose properties may be approximated as those of atmospheric air, enter the plenum at 900 K and pass in cross flow over the tubes at 3 kg/s. If saturated water enters the tubes at a pressure of 2.455 bars and a flow rate of 0.5 kg/s, how many tube rows are required to provide saturated steam at the tube outlet? A convection coefficient of 10,000 $W/m^2 \cdot K$ is associated with boiling in the tubes.

11.85 A steam generator consists of a bank of stainless steel ($k = 15\ W/m \cdot K$) tubes having the core configuration of Figure 11.16 and an inner diameter of 13.8 mm. The tubes are installed in a plenum whose square cross section is 0.6 m on a side, thereby providing a frontal area of 0.36 m^2. Combustion gases, whose properties may be approximated as those of atmospheric air, enter the plenum at 900 K and pass in cross flow over the tubes at 3 kg/s. There are 11 rows of tubes in the gas flow direction. If saturated water at 2.455 bar experiences boiling in the tubes, what is the gas exit temperature? A convection coefficient of 10,000 $W/m^2 \cdot K$ is associated with boiling in the tubes.



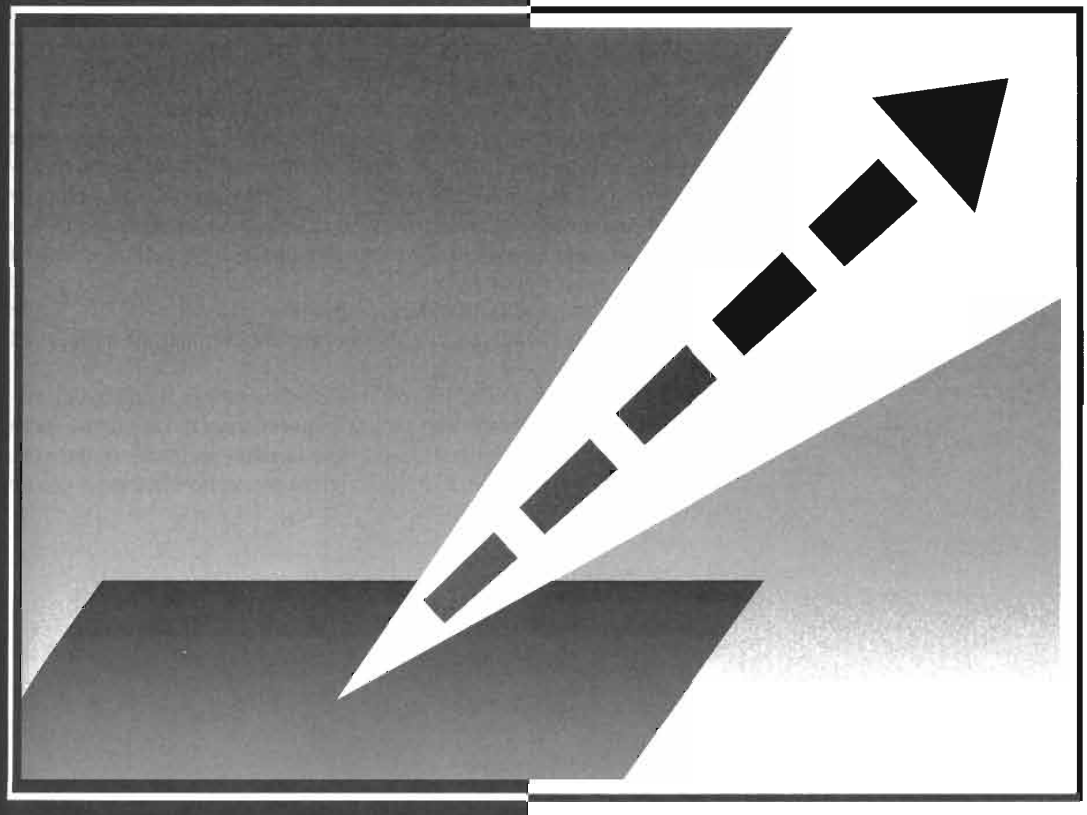
Patent Owner Manufacturing Resources International, Inc.
Exhibit 2017 - Page 728 of 999

to provide saturated
nvection coefficient
with boiling in the

ank of stainless steel
he core configuration
iameter of 13.8 mm.
n whose square cross
y providing a frontal
ses, whose properties
of atmospheric air,
ass in cross flow over
rows of tubes in the
water at 2.455 bar
, what is the gas exit
oefficient of 10,000
ng in the tubes.

CHAPTER 12

Radiation: Processes and Properties



Patent Owner Manufacturing Resources International, Inc.
Exhibit 2017 - Page 729 of 999

We have come to recognize that heat transfer by conduction and convection requires the presence of a temperature gradient in some form of matter. In contrast, heat transfer by *thermal radiation* requires no matter. It is an extremely important process, and in the physical sense it is perhaps the most interesting of the heat transfer modes. It is relevant to many industrial heating, cooling, and drying processes, as well as to energy conversion methods that involve fossil fuel combustion and solar radiation.

In this chapter our objective is to consider the means by which thermal radiation is generated, the specific nature of the radiation, and the manner in which it interacts with matter. We give particular attention to radiative interactions at a surface and to the properties that must be introduced to describe these interactions. In Chapter 13 we focus on means for computing radiative exchange between two or more surfaces.

12.1 *Fundamental Concepts*

Consider a solid that is initially at a higher temperature T_s than that of its surroundings T_{sur}, but around which there exists a vacuum (Figure 12.1). The presence of the vacuum precludes energy loss from the surface of the solid by conduction or convection. However, our intuition tells us that the solid will cool and eventually achieve thermal equilibrium with its surroundings. This cooling is associated with a reduction in the internal energy stored by the solid and is a direct consequence of the *emission* of thermal radiation from the surface. In turn, the surface will intercept and absorb radiation originating from the surroundings. However, if $T_s > T_{sur}$ the *net* heat transfer rate by radiation $q_{rad,net}$ is *from* the surface, and the surface will cool until T_s reaches T_{sur}.

We associate thermal radiation with the rate at which energy is emitted by matter as a result of its finite temperature. At this moment thermal radiation is being emitted by all the matter that surrounds you: by the furniture and walls of the room, if you are indoors, or by the ground, buildings, and the atmosphere and sun if you are

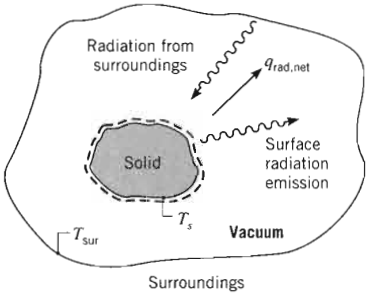


FIGURE 12.1
Radiation cooling of a heated solid.

Patent Owner Manufacturing Resources International, Inc.
Exhibit 2017 - Page 730 of 999

outdoors. The mechanism of emission is related to energy released as a result of oscillations or transitions of the many electrons that constitute matter. These oscillations are, in turn, sustained by the internal energy, and therefore the temperature, of the matter. Hence we associate the emission of thermal radiation with thermally excited conditions within the matter.

All forms of matter emit radiation. For gases and for semitransparent solids, such as glass and salt crystals at elevated temperatures, emission is a *volumetric phenomenon,* as illustrated in Figure 12.2. That is, radiation emerging from a finite volume of matter is the integrated effect of local emission throughout the volume. However, in this text we concentrate on situations for which radiation is a *surface phenomenon.* In most solids and liquids, radiation emitted from interior molecules is strongly absorbed by adjoining molecules. Accordingly, radiation that is emitted from a solid or a liquid originates from molecules that are within a distance of approximately 1 μm from the exposed surface. It is for this reason that emission from a solid or a liquid into an adjoining gas or a vacuum can be viewed as a surface phenomenon, except in situations involving nanoscale or microscale devices.

We know that radiation originates due to emission by matter and that its subsequent transport does not require the presence of any matter. But what is the nature of this transport? One theory views radiation as the propagation of a collection of particles termed *photons* or *quanta.* Alternatively, radiation may be viewed as the propagation of *electromagnetic waves.* In any case we wish to attribute to radiation the standard wave properties of frequency ν and wavelength λ. For radiation propagating in a particular medium, the two properties are related by

$$\lambda = \frac{c}{\nu} \tag{12.1}$$

where c is the speed of light in the medium. For propagation in a vacuum, $c_o = 2.998 \times 10^8$ m/s. The unit of wavelength is commonly the micrometer (μm), where 1 μm = 10^{-6} m.

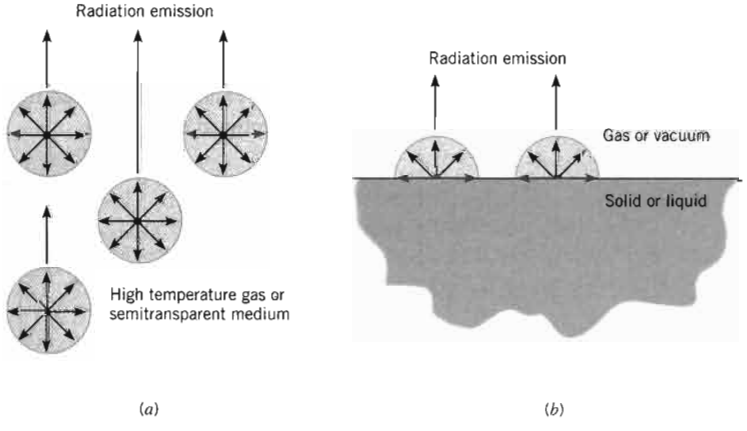


FIGURE 12.2 The emission process. (*a*) As a volumetric phenomenon. (*b*) Surface phenomenon.

Patent Owner Manufacturing Resources International, Inc.
Exhibit 2017 - Page 731 of 999

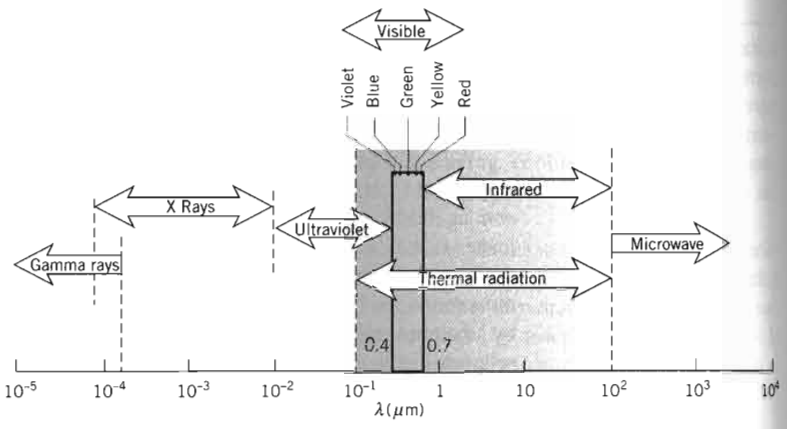


FIGURE 12.3 Spectrum of electromagnetic radiation.

The complete electromagnetic spectrum is delineated in Figure 12.3. The short wavelength gamma rays, X rays, and ultraviolet (UV) radiation are primarily of interest to the high-energy physicist and the nuclear engineer, while the long wavelength microwaves and radio waves ($\lambda > 10^5\ \mu$m) are of concern to the electrical engineer. It is the intermediate portion of the spectrum, which extends from approximately 0.1 to 100 μm and includes a portion of the UV and all of the visible and infrared (IR), that is termed *thermal radiation* because it is both caused by and affects the thermal state or temperature of matter. For this reason, thermal radiation is pertinent to heat transfer.

Thermal radiation emitted by a surface encompasses a range of wavelengths. As shown in Figure 12.4*a*, the magnitude of the radiation varies with wavelength, and the term *spectral* is used to refer to the nature of this dependence. As we will find, both the magnitude of the radiation at any wavelength and the *spectral distribution* vary with the nature and temperature of the emitting surface.

The spectral nature of thermal radiation is one of two features that complicates its description. The second feature relates to its *directionality*. As shown in Figure 12.4*b*, a surface may emit preferentially in certain directions, creating a *directional distribution* of the emitted radiation. To quantify the emission, absorption, reflection, and transmission concepts introduced in Chapter 1, we must be able to treat both spectral and directional effects.

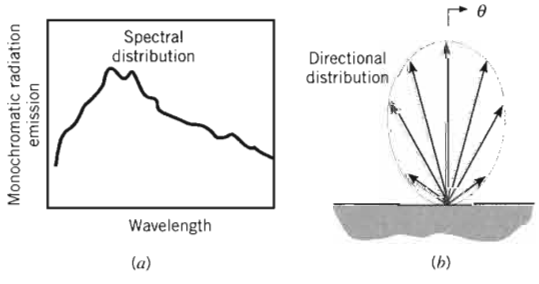


FIGURE 12.4 Radiation emitted by a surface. (*a*) Spectral distribution. (*b*) Directional distribution.

Patent Owner Manufacturing Resources International, Inc.
Exhibit 2017 - Page 732 of 999

12.2 *Radiation Intensity*

Radiation that leaves a surface can propagate in all possible directions (Figure 12.4*b*), and we are often interested in knowing its directional distribution. Also, radiation incident upon a surface may come from different directions, and the manner in which the surface responds to this radiation depends on the direction. Such directional effects can be of primary importance in determining the net radiative heat transfer rate and may be treated by introducing the concept of *radiation intensity*.

12.2.1 Mathematical Definitions

Due to its nature, mathematical treatment of radiation heat transfer involves the extensive use of the spherical coordinate system. From Figure 12.5*a*, we recall that the differential plane angle $d\alpha$ is defined by a region between the rays of a circle and is measured as the ratio of the arc length dl on the circle to the radius r of the circle. Similarly, from Figure 12.5*b*, the differential solid angle $d\omega$ is defined by a region between the rays of a sphere and is measured as the ratio of the area dA_n on the sphere to the sphere's radius squared. Accordingly,

$$d\omega \equiv \frac{dA_n}{r^2} \tag{12.2}$$

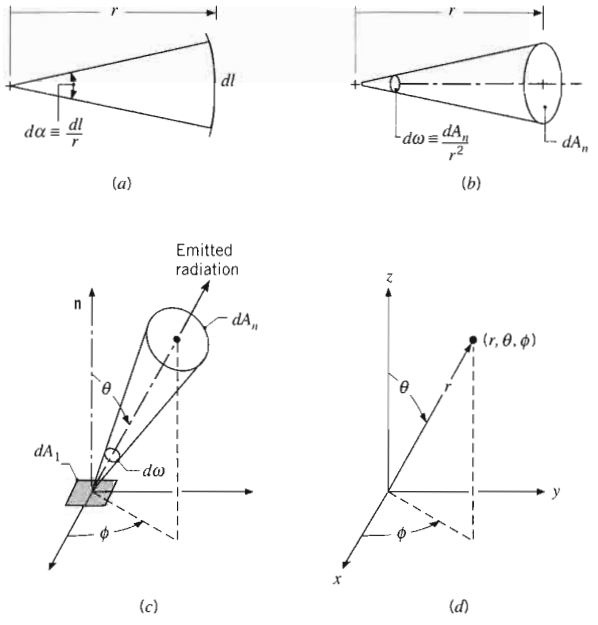


FIGURE 12.5 Mathematical definitions. (*a*) Plane angle. (*b*) Solid angle. (*c*) Emission of radiation from a differential area dA_1 into a solid angle $d\omega$ subtended by dA_n at a point on dA_1. (*d*) The spherical coordinate system.

Patent Owner Manufacturing Resources International, Inc.
Exhibit 2017 - Page 733 of 999

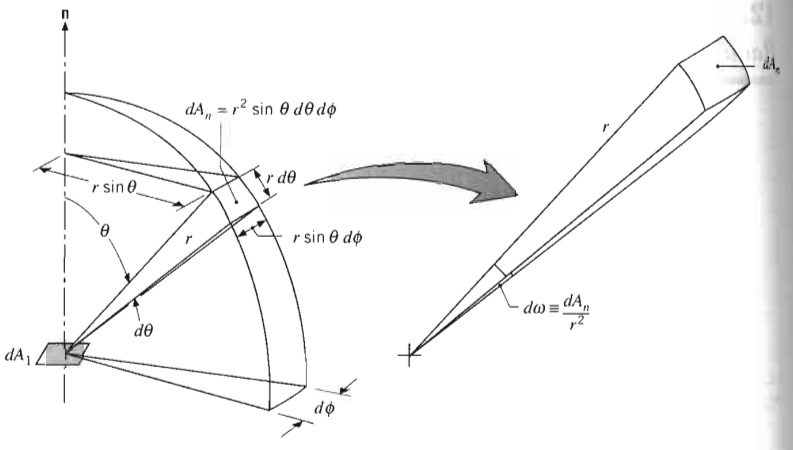


FIGURE 12.6 The solid angle subtended by dA_n at a point on dA_1 in the spherical coordinate system.

Consider emission in a particular direction from an element of surface area dA_1, as shown in Figure 12.5*c*. The direction may be specified in terms of the zenith and azimuthal angles, θ and ϕ, respectively, of a spherical coordinate system (Figure 12.5*d*). The area dA_n, through which the radiation passes, subtends a differential solid angle $d\omega$ when viewed from a point on dA_1. As shown in Figure 12.6, the area dA_n is a rectangle of dimension $r\, d\theta \times r \sin\theta\, d\phi$; thus, $dA_n = r^2 \sin\theta\, d\theta\, d\phi$. Accordingly,

$$d\omega = \sin\theta\, d\theta\, d\phi \tag{12.3}$$

When viewed from a point on an *opaque* surface area element dA_1, radiation may be emitted into any direction defined by a hypothetical hemisphere above the surface. The solid angle associated with the entire hemisphere may be obtained by integrating Equation 12.3 over the limits $\phi = 0$ to $\phi = 2\pi$ and $\theta = 0$ to $\theta = \pi/2$. Hence,

$$\int_h d\omega = \int_0^{2\pi}\int_0^{\pi/2} \sin\theta\, d\theta\, d\phi = 2\pi\int_0^{\pi/2} \sin\theta\, d\theta = 2\pi \text{ sr} \tag{12.4}$$

where the subscript h refers to integration over the hemisphere. Note that the unit of the solid angle is the steradian (sr), analogous to radians for plane angles.

12.2.2 Radiation Intensity and Its Relation to Emission

Returning to Figure 12.5*c*, we now consider the rate at which emission from dA_1 passes through dA_n. This quantity may be expressed in terms of the *spectral intensity* $I_{\lambda,e}$ of the emitted radiation. We formally define $I_{\lambda,e}$ as the *rate at which radiant energy is emitted at the wavelength* λ *in the* (θ,ϕ) *direction, per unit area of the emitting surface normal to this direction, per unit solid angle about this direction, and*

Patent Owner Manufacturing Resources International, Inc.
Exhibit 2017 - Page 734 of 999

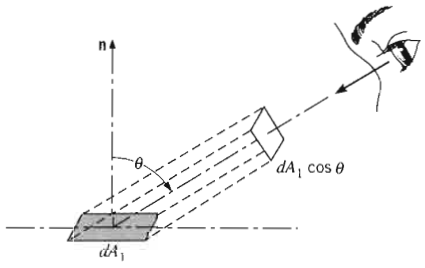


FIGURE 12.7
The projection of dA_1 normal to the direction of radiation.

per unit wavelength interval $d\lambda$ *about* λ. Note that the area used to define the intensity is the component of dA_1 perpendicular to the direction of the radiation. From Figure 12.7, we see that this projected area is equal to $dA_1 \cos\theta$. In effect it is how dA_1 would appear to an observer situated on dA_n. The spectral intensity, which has units of $W/m^2 \cdot sr \cdot \mu m$, is then

$$I_{\lambda,e}(\lambda, \theta, \phi) \equiv \frac{dq}{dA_1 \cos\theta \cdot d\omega \cdot d\lambda} \tag{12.5}$$

where $(dq/d\lambda) \equiv dq_\lambda$ is the rate at which radiation of wavelength λ leaves dA_1 and passes through dA_n. Rearranging Equation 12.5, it follows that

$$dq_\lambda = I_{\lambda,e}(\lambda, \theta, \phi) dA_1 \cos\theta \, d\omega \tag{12.6}$$

where dq_λ has the units of $W/\mu m$. This important expression allows us to compute the rate at which radiation emitted by a surface propagates into the region of space defined by the solid angle $d\omega$ about the (θ, ϕ) direction. However, to compute this rate, the spectral intensity $I_{\lambda,e}$ of the emitted radiation must be known. The manner in which this quantity may be determined is discussed later, in Sections 12.3 and 12.4. Expressing Equation 12.6 per unit area of the emitting surface and substituting from Equation 12.3, the spectral radiation *flux* associated with dA_1 is

$$dq''_\lambda = I_{\lambda,e}(\lambda, \theta, \phi) \cos\theta \sin\theta \, d\theta \, d\phi \tag{12.7}$$

If the spectral and directional distributions of $I_{\lambda,e}$ are known, that is, $I_{\lambda,e}(\lambda, \theta, \phi)$ is known, the heat flux associated with emission into any finite solid angle or over any finite wavelength interval may be determined by integrating Equation 12.7. For example, we define the *spectral, hemispherical emissive power* E_λ $(W/m^2 \cdot \mu m)$ as the rate at which radiation of wavelength λ is emitted in *all directions* from a surface per unit wavelength interval $d\lambda$ about λ and per unit surface area. Thus, E_λ is the spectral heat flux associated with emission into a hypothetical hemisphere above dA_1, as shown in Figure 12.8, or

$$E_\lambda(\lambda) = q''_\lambda(\lambda) = \int_0^{2\pi} \int_0^{\pi/2} I_{\lambda,e}(\lambda, \theta, \phi) \cos\theta \sin\theta \, d\theta \, d\phi \tag{12.8}$$

Note that E_λ is a flux based on the *actual* surface area, whereas $I_{\lambda,e}$ is based on the *projected* area. The cos θ term appearing in the integrand is a consequence of this difference.

Patent Owner Manufacturing Resources International, Inc.
Exhibit 2017 - Page 735 of 999

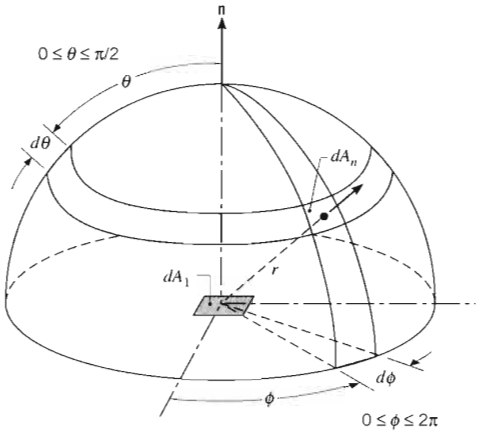


FIGURE 12.8
Emission from a differential element of area dA_1 into a hypothetical hemisphere centered at a point on dA_1.

The *total, hemispherical emissive power*, E (W/m^2), is the rate at which radiation is emitted per unit area at all possible wavelengths and in all possible directions. Accordingly,

$$E = \int_0^\infty E_\lambda(\lambda)\, d\lambda \tag{12.9}$$

or from Equation 12.8

$$E = \int_0^\infty \int_0^{2\pi} \int_0^{\pi/2} I_{\lambda,e}(\lambda, \theta, \phi) \cos\theta \sin\theta\, d\theta\, d\phi\, d\lambda \tag{12.10}$$

Since the term "emissive power" implies emission in all directions, the adjective "hemispherical" is redundant and is often dropped. One then speaks of the *spectral emissive power* E_λ, or the *total emissive power* E.

Although the directional distribution of surface emission varies according to the nature of the surface, there is a special case that provides a reasonable approximation for many surfaces. We speak of a *diffuse emitter* as a surface for which the intensity of the emitted radiation is independent of direction, in which case $I_{\lambda,e}(\lambda, \theta, \phi) = I_{\lambda,e}(\lambda)$. Removing $I_{\lambda,e}$ from the integrand of Equation 12.8 and performing the integration, it follows that

$$E_\lambda(\lambda) = \pi I_{\lambda,e}(\lambda) \tag{12.11}$$

Similarly, from Equation 12.10

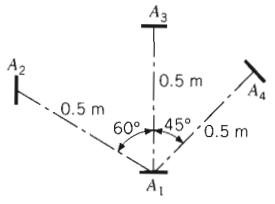
$$E = \pi I_e \tag{12.12}$$

where I_e is the *total intensity* of the emitted radiation. Note that the constant appearing in the above expressions is π, not 2π, and has the unit steradians.

Patent Owner Manufacturing Resources International, Inc.
Exhibit 2017 - Page 736 of 999

EXAMPLE 12.1

A small surface of area $A_1 = 10^{-3}$ m^2 is known to emit diffusely, and from measurements the total intensity associated with emission in the normal direction is $I_n = 7000$ W/m$^2 \cdot$ sr.



Radiation emitted from the surface is intercepted by three other surfaces of area $A_2 = A_3 = A_4 = 10^{-3}$ m^2, which are 0.5 m from A_1 and are oriented as shown. What is the intensity associated with emission in each of the three directions? What are the solid angles subtended by the three surfaces when viewed from A_1? What is the rate at which radiation emitted by A_1 is intercepted by the three surfaces?

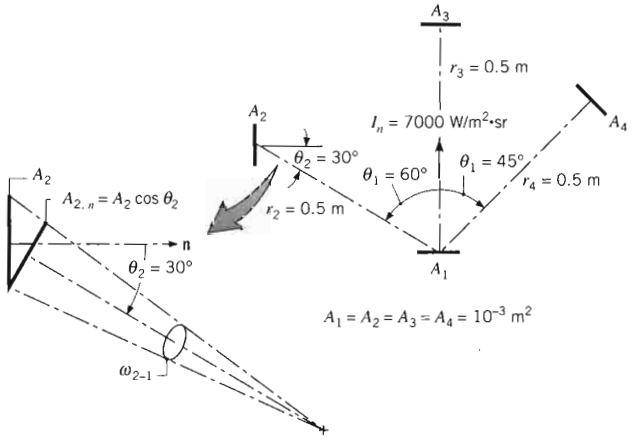
SOLUTION

Known: Normal intensity of diffuse emitter of area A_1 and orientation of three surfaces relative to A_1.

Find:

1. Intensity of emission in each of the three directions.
2. Solid angles subtended by the three surfaces.
3. Rate at which radiation is intercepted by the three surfaces.

Schematic:



Patent Owner Manufacturing Resources International, Inc.
Exhibit 2017 - Page 737 of 999

Assumptions:

1. Surface A_1 emits diffusely.
2. A_1, A_2, A_3, and A_4 may be approximated as differential surfaces, $(A_j/r_j^2) \ll 1$.

Analysis:

1. From the definition of a diffuse emitter, we know that the intensity of the emitted radiation is independent of direction. Hence

$$I = 7000 \text{ W/m}^2 \cdot \text{sr} \quad \triangleleft$$

for each of the three directions.

2. Treating A_2, A_3, and A_4 as differential surface areas, the solid angles may be computed from Equation 12.2

$$d\omega \equiv \frac{dA_n}{r^2}$$

where dA_n is the projection of the surface normal to the direction of the radiation. Since surfaces A_3 and A_4 are normal to the direction of radiation, the solid angles subtended by these surfaces can be directly found from this equation as

$$\omega_{3-1} = \omega_{4-1} = \frac{A_3}{r^2} = \frac{10^{-3} \text{ m}^2}{(0.5 \text{ m})^2} = 4.00 \times 10^{-3} \text{ sr} \quad \triangleleft$$

Since surface A_2 is not normal to the direction of radiation, we use $dA_{n,2} = dA_2 \cos \theta_2$, where θ_2 is the angle between the surface normal and the direction of the radiation. Thus

$$\omega_{2-1} = \frac{A_2 \cos \theta_2}{r^2} = \frac{10^{-3} \text{ m}^2 \times \cos 30°}{(0.5 \text{ m})^2} = 3.46 \times 10^{-3} \text{ sr} \quad \triangleleft$$

3. Approximating A_1 as a differential surface, the rate at which radiation is intercepted by each of the three surfaces may be found from Equation 12.6, which, for the total radiation, may be expressed as

$$q_{1-j} = I \times A_1 \cos \theta_1 \times \omega_{j-1}$$

where θ_1 is the angle between the normal to surface 1 and the direction of the radiation. Hence

$$\begin{aligned} q_{1-2} &= 7000 \text{ W/m}^2 \cdot \text{sr} \, (10^{-3} \text{ m}^2 \times \cos 60°) 3.46 \times 10^{-3} \text{ sr} \\ &= 12.1 \times 10^{-3} \text{ W} \quad \triangleleft \\ q_{1-3} &= 7000 \text{ W/m}^2 \cdot \text{sr} \, (10^{-3} \text{ m}^2 \times \cos 0°) 4.00 \times 10^{-3} \text{ sr} \\ &= 28.0 \times 10^{-3} \text{ W} \quad \triangleleft \\ q_{1-4} &= 7000 \text{ W/m}^2 \cdot \text{sr} \, (10^{-3} \text{ m}^2 \times \cos 45°) 4.00 \times 10^{-3} \text{ sr} \\ &= 19.8 \times 10^{-3} \text{ W} \quad \triangleleft \end{aligned}$$

Comments:

1. Note the different values of θ_1 for the emitting surface and the values of θ_2, θ_3, and θ_4 for the receiving surfaces.
2. If the surfaces were not small relative to the square of the separation distance, the solid angles and radiation heat transfer rates would have to be obtained

Patent Owner Manufacturing Resources International, Inc.
Exhibit 2017 - Page 738 of 999

by integrating Equations 12.3 and 12.6, respectively, over the appropriate surface areas.

3. Any spectral component of the radiation rate can also be obtained using these procedures, if the spectral intensity I_λ is known.
4. Even though the intensity of the emitted radiation is independent of direction, the rate at which radiation is intercepted by the three surfaces differs significantly due to differences in the solid angles and projected areas.

12.2.3 Relation to Irradiation

Although we have focused on radiation emitted by a surface, the foregoing concepts may be extended to *incident* radiation (Figure 12.9). Such radiation may originate from emission and reflection occurring at other surfaces and will have spectral and directional distributions determined by the spectral intensity $I_{\lambda,i}(\lambda, \theta, \phi)$. This quantity is defined as the rate at which radiant energy of wavelength λ is incident from the (θ, ϕ) direction, per unit area of the *intercepting surface* normal to this direction, per unit solid angle about this direction, and per unit wavelength interval $d\lambda$ about λ.

The intensity of the incident radiation may be related to an important radiative flux, termed the *irradiation,* which encompasses radiation incident *from all directions.* The *spectral irradiation* G_λ ($W/m^2 \cdot \mu m$) is defined as the rate at which radiation of wavelength λ is incident on a surface, per unit area of the surface and per unit wavelength interval $d\lambda$ about λ. Accordingly,

$$G_\lambda(\lambda) = \int_0^{2\pi} \int_0^{\pi/2} I_{\lambda,i}(\lambda, \theta, \phi) \cos\theta \sin\theta \, d\theta \, d\phi \tag{12.13}$$

where $\sin\theta \, d\theta \, d\phi$ is the unit solid angle. The $\cos\theta$ factor originates because G_λ is a flux based on the actual surface area, whereas $I_{\lambda,i}$ is defined in terms of the projected area. If the *total irradiation* G (W/m^2) represents the rate at which radiation is incident per unit area from all directions and at all wavelengths, it follows that

$$G = \int_0^\infty G_\lambda(\lambda) \, d\lambda \tag{12.14}$$

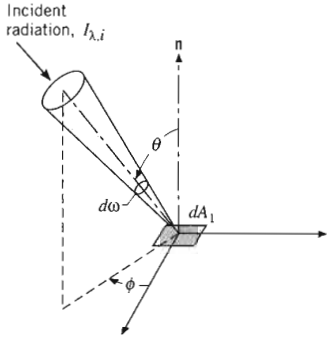


FIGURE 12.9
Directional nature of incident radiation.

Patent Owner Manufacturing Resources International, Inc.
Exhibit 2017 - Page 739 of 999

or from Equation 12.13

$$G = \int_0^{\infty} \int_0^{2\pi} \int_0^{\pi/2} I_{\lambda,i}(\lambda, \theta, \phi) \cos\theta \sin\theta \, d\theta \, d\phi \, d\lambda \tag{12.15}$$

If the incident radiation is *diffuse*, $I_{\lambda,i}$ is independent of θ and ϕ and it follows that

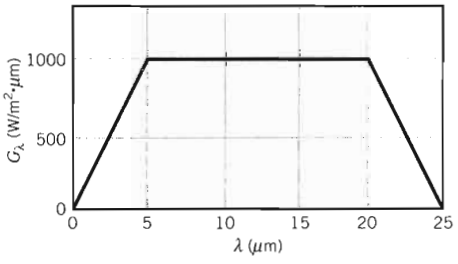
$$G_\lambda(\lambda) = \pi I_{\lambda,i}(\lambda) \tag{12.16}$$

and

$$G = \pi I_i \tag{12.17}$$

EXAMPLE 12.2

The spectral distribution of surface irradiation is as follows:



What is the total irradiation?

SOLUTION

Known: Spectral distribution of surface irradiation.

Find: Total irradiation.

Analysis: The total irradiation may be obtained from Equation 12.14

$$G = \int_0^{\infty} G_\lambda \, d\lambda$$

The integral is readily evaluated by breaking it into parts. That is,

$$G = \int_0^{5\mu m} G_\lambda \, d\lambda + \int_{5\mu m}^{20\mu m} G_\lambda \, d\lambda + \int_{20\mu m}^{25\mu m} G_\lambda \, d\lambda + \int_{25\mu m}^{\infty} G_\lambda \, d\lambda$$

Hence

$$\begin{aligned} G &= \tfrac{1}{2}(1000 \text{ W/m}^2 \cdot \mu\text{m})(5 - 0)\,\mu\text{m} + (1000 \text{ W/m}^2 \cdot \mu\text{m})(20 - 5)\,\mu\text{m} \\ &\quad + \tfrac{1}{2}(1000 \text{ W/m}^2 \cdot \mu\text{m})(25 - 20)\,\mu\text{m} + 0 \\ &= (2500 + 15{,}000 + 2500) \text{ W/m}^2 \\ G &= 20{,}000 \text{ W/m}^2 \end{aligned}$$

◁

Patent Owner Manufacturing Resources International, Inc.
Exhibit 2017 - Page 740 of 999

Comments: Generally, radiation sources do not provide such a regular spectral distribution for the irradiation. However, the procedure of computing the total irradiation from knowledge of the spectral distribution remains the same, although evaluation of the integral is likely to involve more detail.

12.2.4 Relation to Radiosity

The last radiative flux of interest, termed *radiosity,* accounts for *all* the radiant energy leaving a surface. Since this radiation includes the *reflected* portion of the irradiation, as well as direct emission (Figure 12.10), the radiosity is generally different from the emissive power. The *spectral radiosity* J_λ ($W/m^2 \cdot \mu m$) represents the rate at which radiation of wavelength λ leaves a unit area of the surface, per unit wavelength interval $d\lambda$ about λ. Since it accounts for radiation leaving in all directions, it is related to the intensity associated with emission and reflection, $I_{\lambda,e+r}(\lambda, \theta, \phi)$, by the expression

$$J_\lambda(\lambda) = \int_0^{2\pi} \int_0^{\pi/2} I_{\lambda,e+r}(\lambda, \theta, \phi) \cos\theta \sin\theta \, d\theta \, d\phi \tag{12.18}$$

Hence the *total radiosity* J (W/m^2) associated with the entire spectrum is

$$J = \int_0^\infty J_\lambda(\lambda) \, d\lambda \tag{12.19}$$

or

$$J = \int_0^\infty \int_0^{2\pi} \int_0^{\pi/2} I_{\lambda,e+r}(\lambda, \theta, \phi) \cos\theta \sin\theta \, d\theta \, d\phi \, d\lambda \tag{12.20}$$

If the surface is both a *diffuse reflector* and a *diffuse emitter,* $I_{\lambda,e+r}$ is independent of θ and ϕ, and it follows that

$$J_\lambda(\lambda) = \pi I_{\lambda,e+r} \tag{12.21}$$

and

$$J = \pi I_{e+r} \tag{12.22}$$

Again, note that the radiation flux, in this case the radiosity, is based on the actual surface area, while the intensity is based on the projected area.

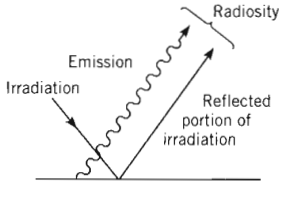


FIGURE 12.10
Surface radiosity.

Patent Owner Manufacturing Resources International, Inc.
Exhibit 2017 - Page 741 of 999

12.3 *Blackbody Radiation*

To evaluate the emissive power, irradiation, or radiosity of a real surface, we must quantify the spectral intensities used in Equations 12.8, 12.13, and 12.18. To do so, it is useful and necessary to first introduce the concept of a *blackbody*.

1. *A blackbody absorbs all incident radiation, regardless of wavelength and direction.*
2. *For a prescribed temperature and wavelength, no surface can emit more energy than a blackbody.*
3. *Although the radiation emitted by a blackbody is a function of wavelength and temperature, it is independent of direction. That is, the blackbody is a diffuse emitter.*

As the perfect absorber and emitter, the blackbody serves as a *standard* against which the radiative properties of actual surfaces may be compared.

Although closely approximated by some surfaces, it is important to note that no surface has precisely the properties of a blackbody. The closest approximation is achieved by a *cavity* whose inner surface is at a uniform temperature. If radiation enters the cavity through a small aperture (Figure 12.11*a*), it is likely to experience many reflections before reemergence. Hence it is almost entirely absorbed by the cavity, and blackbody behavior is approximated. From thermodynamic principles it may then be argued that radiation leaving the aperture depends only on the surface temperature and corresponds to blackbody emission (Figure 12.11*b*). Since blackbody emission is diffuse, the spectral intensity $I_{\lambda,b}$ of radiation leaving the cavity is independent of direction. Moreover, since the radiation field in the cavity, which is the cumulative effect of emission and reflection from the cavity surface, must be of the same form as the radiation emerging from the aperture, it also follows that a blackbody radiation field exists within the cavity. Accordingly, any small surface in

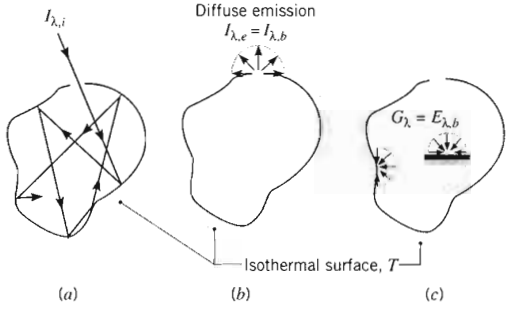


FIGURE 12.11 Characteristics of an isothermal blackbody cavity. (*a*) Complete absorption. (*b*) Diffuse emission from an aperture. (*c*) Diffuse irradiation of interior surfaces.

Patent Owner Manufacturing Resources International, Inc.
Exhibit 2017 - Page 742 of 999

the cavity (Figure 12.11*c*) experiences irradiation for which $G_\lambda = E_{\lambda,b}(\lambda, T)$. This surface is diffusely irradiated, regardless of its orientation. *Blackbody radiation exists within the cavity irrespective of whether the cavity surface is highly reflecting or absorbing.*

12.3.1 The Planck Distribution

The blackbody spectral intensity is well known, having first been determined by Planck [1]. It is

$$I_{\lambda,b}(\lambda,T) = \frac{2hc_o^2}{\lambda^5[\exp(hc_o/\lambda kT) - 1]} \tag{12.23}$$

where $h = 6.626 \times 10^{-34}$ J · s and $k = 1.381 \times 10^{-23}$ J/K are the universal Planck and Boltzmann constants, respectively, $c_o = 2.998 \times 10^8$ m/s is the speed of light in vacuum, and T is the *absolute* temperature of the blackbody (K). Since the blackbody is a diffuse emitter, it follows from Equation 12.11 that its spectral emissive power is

$$E_{\lambda,b}(\lambda, T) = \pi I_{\lambda,b}(\lambda, T) = \frac{C_1}{\lambda^5[\exp(C_2/\lambda T) - 1]} \tag{12.24}$$

where the first and second radiation constants are $C_1 = 2\pi hc_o^2 = 3.742 \times 10^8$ W · μm^4/m^2 and $C_2 = (hc_o/k) = 1.439 \times 10^4$ μm · K.

Equation 12.24, known as the *Planck distribution,* is plotted in Figure 12.12 for selected temperatures. Several important features should be noted.

1. The emitted radiation varies *continuously* with wavelength.
2. At any wavelength the magnitude of the emitted radiation increases with increasing temperature.
3. The spectral region in which the radiation is concentrated depends on temperature, with *comparatively* more radiation appearing at shorter wavelengths as the temperature increases.
4. A significant fraction of the radiation emitted by the sun, which may be approximated as a blackbody at 5800 K, is in the visible region of the spectrum. In contrast, for $T \lesssim 800$ K, emission is predominantly in the infrared region of the spectrum and is not visible to the eye.

12.3.2 Wien's Displacement Law

From Figure 12.12 we see that the blackbody spectral distribution has a maximum and that the corresponding wavelength λ_{max} depends on temperature. The nature of this dependence may be obtained by differentiating Equation 12.24 with respect to λ and setting the result equal to zero. In so doing, we obtain

$$\lambda_{max}T = C_3 \tag{12.25}$$

where the third radiation constant is $C_3 = 2898$ μm · K.

Patent Owner Manufacturing Resources International, Inc.
Exhibit 2017 - Page 743 of 999

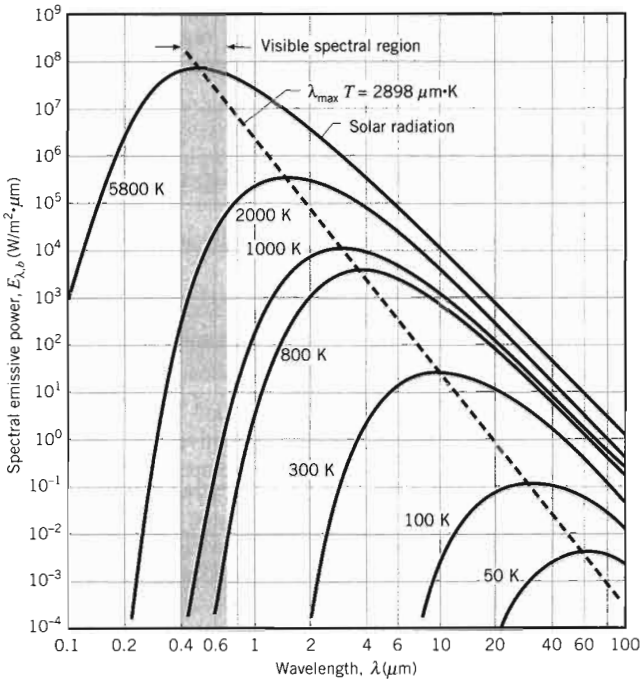


FIGURE 12.12 Spectral blackbody emissive power.

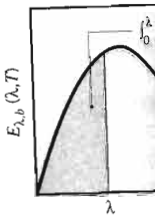


FIGURE 12.13 emission from a b the spectral band

Equation 12.25 is known as *Wien's displacement law,* and the locus of points described by the law is plotted as the dashed line of Figure 12.12. According to this result, the maximum spectral emissive power is displaced to shorter wavelengths with increasing temperature. This emission is in the middle of the visible spectrum ($\lambda \approx 0.50\ \mu$m) for solar radiation, since the sun emits approximately as a blackbody at 5800 K. For a blackbody at 1000 K, peak emission occurs at 2.90 μm, with some of the emitted radiation appearing visible as red light. With increasing temperature, shorter wavelengths become more prominent, until eventually significant emission occurs over the entire visible spectrum. For example, a tungsten filament lamp operating at 2900 K ($\lambda_{max} = 1\ \mu$m) emits white light, although most of the emission remains in the IR region.

12.3.3 The Stefan-Boltzmann Law

Substituting the Planck distribution, Equation 12.24, into Equation 12.9, the total emissive power of a blackbody E_b may be expressed as

$$E_b = \int_0^\infty \frac{C_1}{\lambda^5[\exp(C_2/\lambda T) - 1]}\, d\lambda$$

Performing the integration, it may be shown that

$$E_b = \sigma T^4 \tag{12.26}$$

Patent Owner Manufacturing Resources International, Inc.
Exhibit 2017 - Page 744 of 999

where the *Stefan–Boltzmann* constant, which depends on C_1 and C_2, has the numerical value

$$\sigma = 5.670 \times 10^{-8}\ \mathrm{W/m^2 \cdot K^4}$$

This simple, yet important, result is termed the *Stefan–Boltzmann law*. It enables calculation of the amount of radiation emitted in all directions and over all wavelengths simply from knowledge of the temperature of the blackbody. Because this emission is diffuse, it follows from Equation 12.12 that the total intensity associated with blackbody emission is

$$I_b = \frac{E_b}{\pi} \tag{12.27}$$

12.3.4 Band Emission

It is often necessary to know the fraction of the total emission from a blackbody that is in a certain wavelength interval or *band*. For a prescribed temperature and the interval from 0 to λ, this fraction is determined by the ratio of the shaded section to the total area under the curve of Figure 12.13. Hence

$$F_{(0\to\lambda)} \equiv \frac{\int_0^{\lambda} E_{\lambda,b}\, d\lambda}{\int_0^{\infty} E_{\lambda,b}\, d\lambda} = \frac{\int_0^{\lambda} E_{\lambda,b}\, d\lambda}{\sigma T^4} = \int_0^{\lambda T} \frac{E_{\lambda,b}}{\sigma T^5}\, d(\lambda T) = f(\lambda T) \tag{12.28}$$

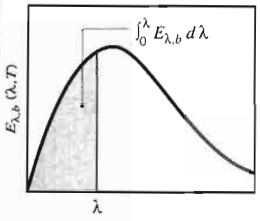


FIGURE 12.13 Radiation emission from a blackbody in the spectral band 0 to λ.

Since the integrand $(E_{\lambda,b}/\sigma T^5)$ is exclusively a function of the wavelength–temperature product λT, the integral of Equation 12.28 may be evaluated to obtain $F_{(0\to\lambda)}$ as a function of only λT. The results are presented in Table 12.1 and Figure 12.14. They may also be used to obtain the fraction of the radiation between any two wavelengths λ_1 and λ_2, since

$$F_{(\lambda_1\to\lambda_2)} = \frac{\int_0^{\lambda_2} E_{\lambda,b}\, d\lambda - \int_0^{\lambda_1} E_{\lambda,b}\, d\lambda}{\sigma T^4} = F_{(0\to\lambda_2)} - F_{(0\to\lambda_1)} \tag{12.29}$$

Additional blackbody functions are listed in the third and fourth columns of Table 12.1. The third column facilitates calculation of the spectral intensity for a prescribed wavelength and temperature. In lieu of computing this quantity from Equation 12.23, it may be obtained by simply multiplying the tabulated value of $I_{\lambda,b}/\sigma T^5$ by σT^5. The fourth column is used to obtain a quick estimate of the ratio of the spectral intensity at any wavelength to that at λ_{max}.

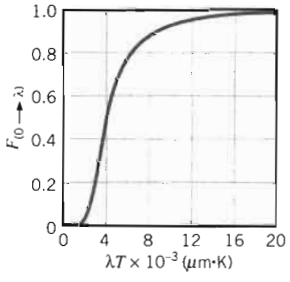


FIGURE 12.14 Fraction of the total blackbody emission in the spectral band from 0 to λ as a function of λT.

Patent Owner Manufacturing Resources International, Inc.
Exhibit 2017 - Page 745 of 999

TABLE 12.1 Blackbody Radiation Functions

λT (μm · K)	$F_{(0\to\lambda)}$	$I_{\lambda,b}(\lambda,T)/\sigma T^5$ (μm · K · sr)$^{-1}$	$\frac{I_{\lambda,b}(\lambda,T)}{I_{\lambda,b}(\lambda_{max},T)}$
200	0.000000	0.375034×10^{-27}	0.000000
400	0.000000	0.490335×10^{-13}	0.000000
600	0.000000	0.104046×10^{-8}	0.000014
800	0.000016	0.991126×10^{-7}	0.001372
1,000	0.000321	0.118505×10^{-5}	0.016406
1,200	0.002134	0.523927×10^{-5}	0.072534
1,400	0.007790	0.134411×10^{-4}	0.186082
1,600	0.019718	0.249130	0.344904
1,800	0.039341	0.375568	0.519949
2,000	0.066728	0.493432	0.683123
2,200	0.100888	0.589649×10^{-4}	0.816329
2,400	0.140256	0.658866	0.912155
2,600	0.183120	0.701292	0.970891
2,800	0.227897	0.720239	0.997123
2,898	0.250108	0.722318×10^{-4}	1.000000
3,000	0.273232	0.720254×10^{-4}	0.997143
3,200	0.318102	0.705974	0.977373
3,400	0.361735	0.681544	0.943551
3,600	0.403607	0.650396	0.900429
3,800	0.443382	0.615225×10^{-4}	0.851737
4,000	0.480877	0.578064	0.800291
4,200	0.516014	0.540394	0.748139
4,400	0.548796	0.503253	0.696720
4,600	0.579280	0.467343	0.647004
4,800	0.607559	0.433109	0.599610
5,000	0.633747	0.400813	0.554898
5,200	0.658970	0.370580×10^{-4}	0.513043
5,400	0.680360	0.342445	0.474092
5,600	0.701046	0.316376	0.438002
5,800	0.720158	0.292301	0.404671
6,000	0.737818	0.270121	0.373965
6,200	0.754140	0.249723×10^{-4}	0.345724
6,400	0.769234	0.230985	0.319783
6,600	0.783199	0.213786	0.295973
6,800	0.796129	0.198008	0.274128
7,000	0.808109	0.183534	0.254090
7,200	0.819217	0.170256×10^{-4}	0.235708
7,400	0.829527	0.158073	0.218842
7,600	0.839102	0.146891	0.203360
7,800	0.848005	0.136621	0.189143
8,000	0.856288	0.127185	0.176079
8,500	0.874608	0.106772×10^{-4}	0.147819
9,000	0.890029	0.901463×10^{-5}	0.124801

Patent Owner Manufacturing Resources International, Inc.
Exhibit 2017 - Page 746 of 999

TABLE 12.1 *Continued*

λT (μm · K)	$F_{(0\rightarrow\lambda)}$	$I_{\lambda,b}(\lambda,T)/\sigma T^5$ (μm · K · sr)$^{-1}$	$\frac{I_{\lambda,b}(\lambda,T)}{I_{\lambda,b}(\lambda_{max},T)}$
9,500	0.903085	0.765338	0.105956
10,000	0.914199	0.653279×10^{-5}	0.090442
10,500	0.923710	0.560522	0.077600
11,000	0.931890	0.483321	0.066913
11,500	0.939959	0.418725	0.057970
12,000	0.945098	0.364394×10^{-5}	0.050448
13,000	0.955139	0.279457	0.038689
14,000	0.962898	0.217641	0.030131
15,000	0.969981	0.171866×10^{-5}	0.023794
16,000	0.973814	0.137429	0.019026
18,000	0.980860	0.908240×10^{-6}	0.012574
20,000	0.985602	0.623310	0.008629
25,000	0.992215	0.276474	0.003828
30,000	0.995340	0.140469×10^{-6}	0.001945
40,000	0.997967	0.473891×10^{-7}	0.000656
50,000	0.998953	0.201605	0.000279
75,000	0.999713	0.418597×10^{-8}	0.000058
100,000	0.999905	0.135752	0.000019

EXAMPLE 12.3

Consider a large isothermal enclosure that is maintained at a uniform temperature of 2000 K. Calculate the emissive power of the radiation that emerges from a small aperture on the enclosure surface. What is the wavelength λ_1 below which 10% of the emission is concentrated? What is the wavelength λ_2 above which 10% of the emission is concentrated? Determine the maximum spectral emissive power and the wavelength at which this emission occurs. What is the irradiation incident on a small object placed inside the enclosure?

SOLUTION

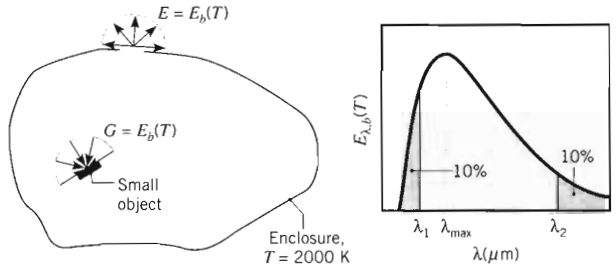
Known: Large isothermal enclosure at uniform temperature.

Find:

1. Emissive power of a small aperture on the enclosure.
2. Wavelengths below which and above which 10% of the radiation is concentrated.
3. Spectral emissive power and wavelength associated with maximum emission.
4. Irradiation on a small object inside the enclosure.

Patent Owner Manufacturing Resources International, Inc.
Exhibit 2017 - Page 747 of 999

Schematic:



Assumptions: Areas of aperture and object are very small relative to enclosure surface.

Analysis:

1. Emission from the aperture of any isothermal enclosure will have the characteristics of blackbody radiation. Hence, from Equation 12.26,

$$E = E_b(T) = \sigma T^4 = 5.670 \times 10^{-8}\ \text{W/m}^2 \cdot \text{K}^4 (2000\ \text{K})^4$$
$$E = 9.07 \times 10^5\ \text{W/m}^2 \quad \triangleleft$$

2. The wavelength λ_1 corresponds to the upper limit of the spectral band $(0 \rightarrow \lambda_1)$ containing 10% of the emitted radiation. With $F_{(0\rightarrow\lambda_1)} = 0.10$ it follows from Table 12.1 that $\lambda_1 T = 2195\ \mu\text{m} \cdot \text{K}$. Hence

$$\lambda_1 = 1.1\ \mu\text{m} \quad \triangleleft$$

The wavelength λ_2 corresponds to the lower limit of the spectral band $(\lambda_2 \rightarrow \infty)$ containing 10% of the emitted radiation. With

$$F_{(\lambda_2\rightarrow\infty)} = 1 - F_{(0\rightarrow\lambda_2)} = 0.1$$
$$F_{(0\rightarrow\lambda_2)} = 0.9$$

it follows from Table 12.1 that $\lambda_2 T = 9382\ \mu\text{m} \cdot \text{K}$. Hence

$$\lambda_2 = 4.69\ \mu\text{m} \quad \triangleleft$$

3. From Wien's law, Equation 12.25, $\lambda_{\text{max}} T = 2898\ \mu\text{m} \cdot \text{K}$. Hence

$$\lambda_{\text{max}} = 1.45\ \mu\text{m} \quad \triangleleft$$

The spectral emissive power associated with this wavelength may be computed from Equation 12.24 or from the third column of Table 12.1. For $\lambda_{\text{max}} T = 2898\ \mu\text{m} \cdot \text{K}$ it follows from Table 12.1 that

$$I_{\lambda,b}(1.45\ \mu\text{m}, T) = 0.722 \times 10^{-4} \sigma T^5$$

Hence

$$I_{\lambda,b}(1.45\ \mu\text{m}, 2000\ \text{K}) = 0.722 \times 10^{-4}\ (1/\mu\text{m} \cdot \text{K} \cdot \text{sr})\ 5.67 \times 10^{-8}\ \text{W/m}^2 \cdot \text{K}^4 (2000\ \text{K})^5$$

$$I_{\lambda,b}(1.45\ \mu\text{m}, 2000\ \text{K}) = 1.31 \times 10^5\ \text{W/m}^2 \cdot \text{sr} \cdot \mu\text{m}$$

Patent Owner Manufacturing Resources International, Inc.
Exhibit 2017 - Page 748 of 999

Since the emission is diffuse, it follows from Equation 12.11 that

$$E_{\lambda,b} = \pi I_{\lambda,b} = 4.12 \times 10^5 \text{ W/m}^2 \cdot \mu\text{m}$$

4. Irradiation of any small object inside the enclosure may be approximated as being equal to emission from a blackbody at the enclosure surface temperature. Hence $G = E_b(T)$, in which case

$$G = 9.07 \times 10^5 \text{ W/m}^2$$

EXAMPLE 12.4

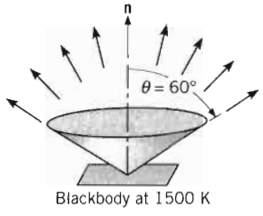
A surface emits as a blackbody at 1500 K. What is the rate per unit area (W/m^2) at which it emits radiation over all directions corresponding to $0° \leq \theta \leq 60°$ and over the wavelength interval $2\ \mu m \leq \lambda \leq 4\ \mu m$?

SOLUTION

Known: Temperature of a surface that emits as a blackbody.

Find: Rate of emission per unit area over all directions between $\theta = 0°$ and 60° and over all wavelengths between $\lambda = 2$ and 4 μm.

Schematic:



Assumptions: Surface emits as a blackbody.

Analysis: The desired emission may be inferred from Equation 12.10, with the limits of integration restricted as follows:

$$\Delta E = \int_2^4 \int_0^{2\pi} \int_0^{\pi/3} I_{\lambda,b} \cos\theta \sin\theta \, d\theta \, d\phi \, d\lambda$$

or, since a blackbody emits diffusely,

$$\Delta E = \int_2^4 I_{\lambda,b} \left(\int_0^{2\pi} \int_0^{\pi/3} \cos\theta \sin\theta \, d\theta \, d\phi \right) d\lambda$$

$$\Delta E = \int_2^4 I_{\lambda,b} \left(2\pi \frac{\sin^2\theta}{2} \Big|_0^{\pi/3} \right) d\lambda = 0.75 \int_2^4 \pi I_{\lambda,b} \, d\lambda$$

Patent Owner Manufacturing Resources International, Inc.
Exhibit 2017 - Page 749 of 999

Substituting from Equation 12.11 and multiplying and dividing by E_b, this result may be put in a form that allows for use of Table 12.1 in evaluating the spectral integration. In particular,

$$\Delta E = 0.75E_b \int_2^4 \frac{E_{\lambda,b}}{E_b}\, d\lambda = 0.75E_b\,[F_{(0\to 4)} - F_{(0\to 2)}]$$

where from Table 12.1

$$\lambda_1 T = 2\ \mu\text{m} \times 1500\ \text{K} = 3000\ \mu\text{m}\cdot\text{K}: \qquad F_{(0\to 2)} = 0.273$$

$$\lambda_2 T = 4\ \mu\text{m} \times 1500\ \text{K} = 6000\ \mu\text{m}\cdot\text{K}: \qquad F_{(0\to 4)} = 0.738$$

Hence

$$\Delta E = 0.75(0.738 - 0.273)E_b = 0.75(0.465)E_b$$

From Equation 12.26, it then follows that

$$\Delta E = 0.75(0.465)5.67 \times 10^{-8}\ \text{W/m}^2\cdot\text{K}^4\,(1500\ \text{K})^4 = 10^5\ \text{W/m}^2 \qquad \triangleleft$$

Comments: The total, hemispherical emissive power is reduced by 25% and 53.5% due to the directional and spectral restrictions, respectively.

12.4 *Emission from Real Surfaces*

Having developed the notion of a blackbody to describe *ideal* surface behavior, we may now consider the behavior of *real* surfaces. Recall that the blackbody is an ideal emitter in the sense that no surface can emit more radiation than a blackbody at the same temperature. It is therefore convenient to choose the blackbody as a reference in describing emission from a real surface. A surface radiative property known as the *emissivity*[1] may then be defined as the *ratio* of the radiation emitted by the surface to the radiation emitted by a blackbody at the same temperature.

It is important to acknowledge that, in general, the spectral radiation emitted by a real surface differs from the Planck distribution (Figure 12.15*a*). Moreover, the directional distribution (Figure 12.15*b*) may be other than diffuse. Hence the emissivity may assume different values according to whether one is interested in emission at a given wavelength or in a given direction, or in integrated averages over wavelength and direction.

We define the *spectral, directional emissivity* $\varepsilon_{\lambda,\theta}(\lambda, \theta, \phi, T)$ of a surface at the temperature T as the ratio of the intensity of the radiation emitted at the wavelength λ

[1]In this text we use the *-ivity,* rather than the *-ance,* ending for material radiative properties (e.g., "emissivity" rather than "emittance"). Although efforts are being made to reserve the -ivity ending for optically smooth, uncontaminated surfaces, no such distinction is made in much of the literature, and none is made in this text.

Patent Owner Manufacturing Resources International, Inc.
Exhibit 2017 - Page 750 of 999

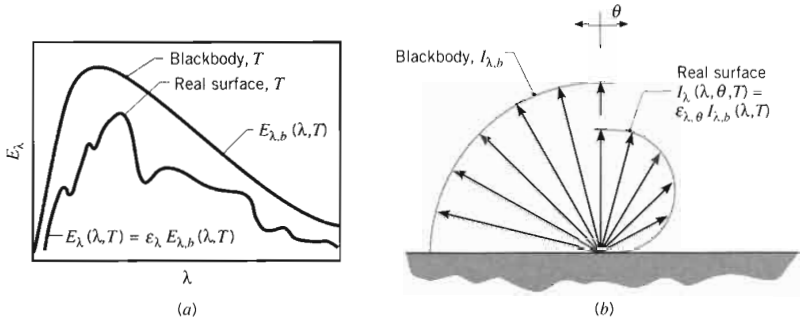


FIGURE 12.15 Comparison of blackbody and real surface emission. (*a*) Spectral distribution. (*b*) Directional distribution.

and in the direction of θ and ϕ to the intensity of the radiation emitted by a blackbody at the same values of T and λ. Hence

$$\varepsilon_{\lambda,\theta}(\lambda,\theta,\phi,T) \equiv \frac{I_{\lambda,e}(\lambda,\theta,\phi,T)}{I_{\lambda,b}(\lambda,T)} \tag{12.30}$$

Note how the subscripts λ and θ designate interest in a specific wavelength and direction for the emissivity. In contrast, terms appearing within parentheses designate functional dependence on wavelength, direction, and/or temperature. The absence of directional variables in the parentheses of the denominator in Equation 12.30 implies that the intensity is independent of direction, which is, of course, a characteristic of blackbody emission. In like manner a *total, directional emissivity* ε_θ, which represents a spectral average of $\varepsilon_{\lambda,\theta}$, may be defined as

$$\varepsilon_\theta(\theta,\phi,T) \equiv \frac{I_e(\theta,\phi,T)}{I_b(T)} \tag{12.31}$$

For most engineering calculations, it is desirable to work with surface properties that represent directional averages. A *spectral, hemispherical emissivity* is therefore defined as

$$\varepsilon_\lambda(\lambda,T) \equiv \frac{E_\lambda(\lambda,T)}{E_{\lambda,b}(\lambda,T)} \tag{12.32}$$

It may be related to the directional emissivity $\varepsilon_{\lambda,\theta}$ by substituting the expression for the spectral emissive power, Equation 12.8, to obtain

$$\varepsilon_\lambda(\lambda,T) = \frac{\int_0^{2\pi}\int_0^{\pi/2} I_{\lambda,e}(\lambda,\theta,\phi,T)\cos\theta\sin\theta\,d\theta\,d\phi}{\int_0^{2\pi}\int_0^{\pi/2} I_{\lambda,b}(\lambda,T)\cos\theta\sin\theta\,d\theta\,d\phi}$$

In contrast to Equation 12.8, the temperature dependence of emission is now acknowledged. From Equation 12.30 and the fact that $I_{\lambda,b}$ is independent of θ and ϕ,

Patent Owner Manufacturing Resources International, Inc.
Exhibit 2017 - Page 751 of 999

it follows that

$$\varepsilon_\lambda(\lambda, T) = \frac{\int_0^{2\pi}\int_0^{\pi/2} \varepsilon_{\lambda,\theta}(\lambda, \theta, \phi, T)\cos\theta \sin\theta \, d\theta \, d\phi}{\int_0^{2\pi}\int_0^{\pi/2} \cos\theta \sin\theta \, d\theta \, d\phi} \tag{12.33}$$

Assuming $\varepsilon_{\lambda,\theta}$ to be independent of ϕ, which is a reasonable assumption for most surfaces, and evaluating the denominator, we obtain

$$\varepsilon_\lambda(\lambda, T) = 2\int_0^{\pi/2} \varepsilon_{\lambda,\theta}(\lambda, \theta, T)\cos\theta \sin\theta \, d\theta \tag{12.34}$$

The *total, hemispherical emissivity,* which represents an average over all possible directions and wavelengths, is defined as

$$\varepsilon(T) \equiv \frac{E(T)}{E_b(T)} \tag{12.35}$$

Substituting from Equations 12.9 and 12.32, it follows that

$$\varepsilon(T) = \frac{\int_0^\infty \varepsilon_\lambda(\lambda, T) E_{\lambda,b}(\lambda, T)\, d\lambda}{E_b(T)} \tag{12.36}$$

If the emissivities of a surface are known, it is a simple matter to compute its emission characteristics. For example, if $\varepsilon_\lambda(\lambda, T)$ is known, it may be used with Equations 12.24 and 12.32 to compute the spectral emissive power of the surface at any wavelength and temperature. Similarly, if $\varepsilon(T)$ is known, it may be used with Equations 12.26 and 12.35 to compute the total emissive power of the surface at any temperature. Measurements have been performed to determine these properties for many different materials and surface coatings.

The directional emissivity of a *diffuse emitter* is a constant, independent of direction. However, although this condition is often a reasonable *approximation,* all surfaces exhibit some departure from diffuse behavior. Representative variations of ε_θ with θ are shown schematically in Figure 12.16 for conducting and nonconducting materials. For conductors ε_θ is approximately constant over the range $\theta \lesssim 40°$, after which it increases with increasing θ but ultimately decays to zero. In contrast, for nonconductors ε_θ is approximately constant for $\theta \lesssim 70°$, beyond which it decreases sharply with increasing θ. One implication of these variations is that, although there are preferential directions for emission, the hemispherical emissivity ε will not differ

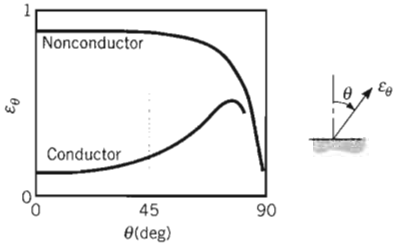


FIGURE 12.16
Representative directional distributions of the total, directional emissivity.

Patent Owner Manufacturing Resources International, Inc.
Exhibit 2017 - Page 752 of 999

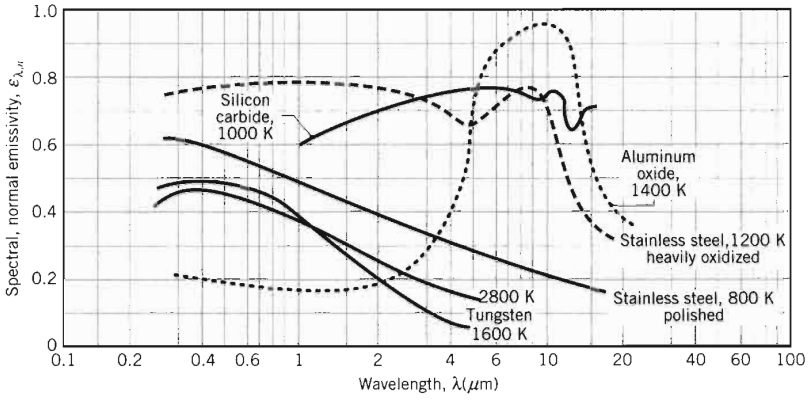


FIGURE 12.17 Spectral dependence of the spectral, normal emissivity $\varepsilon_{\lambda,n}$ of selected materials.

markedly from the normal emissivity ε_n, corresponding to $\theta = 0$. In fact the ratio rarely falls outside the range $1.0 \leq (\varepsilon/\varepsilon_n) \leq 1.3$ for conductors and the range of $0.95 \leq (\varepsilon/\varepsilon_n) \leq 1.0$ for nonconductors. Hence to a reasonable approximation,

$$\varepsilon \approx \varepsilon_n \tag{12.37}$$

Note that, although the foregoing statements were made for the total emissivity, they also apply to spectral components.

Since the spectral distribution of emission from real surfaces departs from the Planck distribution (Figure 12.15*a*), we do not expect the value of the spectral emissivity ε_λ to be independent of wavelength. Representative spectral distributions of ε_λ are shown in Figure 12.17. The manner in which ε_λ varies with λ depends on whether the solid is a conductor or nonconductor, as well as on the nature of the surface coating.

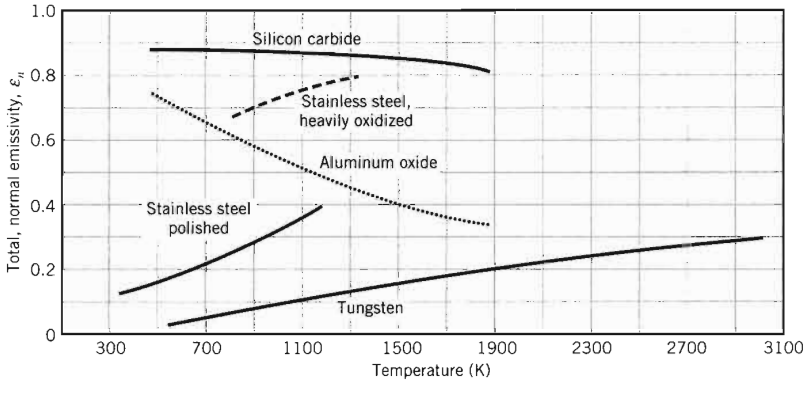


FIGURE 12.18 Temperature dependence of the total, normal emissivity ε_n of selected materials.

Patent Owner Manufacturing Resources International, Inc.
Exhibit 2017 - Page 753 of 999

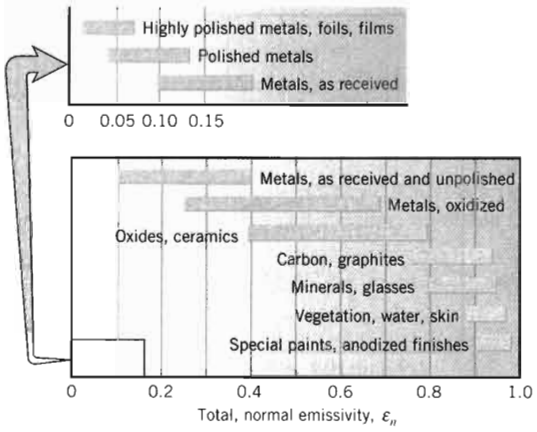


FIGURE 12.19 Representative values of the total, normal emissivity ε_n.

Representative values of the total, normal emissivity ε_n are plotted in Figures 12.18 and 12.19 and listed in Table A.11. Several generalizations may be made.

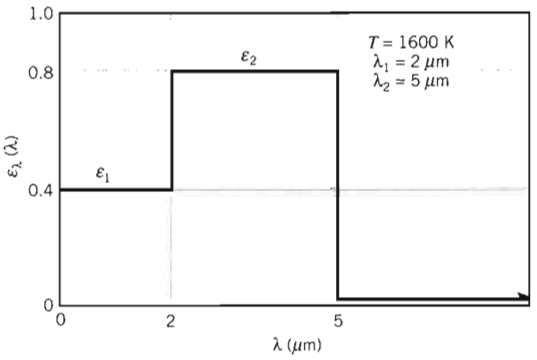
1. The emissivity of metallic surfaces is generally small, achieving values as low as 0.02 for highly polished gold and silver.
2. The presence of oxide layers may significantly increase the emissivity of metallic surfaces. From Figure 12.18, contrast the values of 0.3 and 0.7 for stainless steel at 900 K, depending on whether it is polished or heavily oxidized.
3. The emissivity of nonconductors is comparatively large, generally exceeding 0.6.
4. The emissivity of conductors increases with increasing temperature; however, depending on the specific material, the emissivity of nonconductors may either increase or decrease with increasing temperature. Note that the variations of ε_n with T shown in Figure 12.18 are consistent with the spectral distributions of $\varepsilon_{\lambda,n}$ shown in Figure 12.17. These trends follow from Equation 12.36. Although the spectral distribution of $\varepsilon_{\lambda,n}$ is approximately independent of temperature, there is proportionately more emission at lower wavelengths with increasing temperature. Hence, if $\varepsilon_{\lambda,n}$ increases with decreasing wavelength for a particular material, ε_n will increase with increasing temperature for that material.

It should be recognized that the emissivity depends strongly on the nature of the surface, which can be influenced by the method of fabrication, thermal cycling, and chemical reaction with its environment. More comprehensive surface emissivity compilations are available in the literature [2–5].

EXAMPLE 12.5

A diffuse surface at 1600 K has the spectral, hemispherical emissivity shown as follows.

Patent Owner Manufacturing Resources International, Inc.
Exhibit 2017 - Page 754 of 999



Determine the total, hemispherical emissivity and the total emissive power. At what wavelength will the spectral emissive power be a maximum?

SOLUTION

Known: Spectral, hemispherical emissivity of a diffuse surface at 1600 K.

Find:

1. Total, hemispherical emissivity.
2. Total emissive power.
3. Wavelength at which spectral emissive power will be a maximum.

Assumptions: Surface is a diffuse emitter.

Analysis:

1. The total, hemispherical emissivity is given by Equation 12.36, where the integration may be performed in parts as follows:

$$\varepsilon = \frac{\int_0^\infty \varepsilon_\lambda E_{\lambda,b}\, d\lambda}{E_b} = \frac{\varepsilon_1 \int_0^2 E_{\lambda,b}\, d\lambda}{E_b} + \frac{\varepsilon_2 \int_2^5 E_{\lambda,b}\, d\lambda}{E_b}$$

or

$$\varepsilon = \varepsilon_1 F_{(0\to 2\,\mu\text{m})} + \varepsilon_2 [F_{(0\to 5\,\mu\text{m})} - F_{(0\to 2\,\mu\text{m})}]$$

From Table 12.1 we obtain

$$\lambda_1 T = 2\ \mu\text{m} \times 1600\ \text{K} = 3200\ \mu\text{m} \cdot \text{K}: \qquad F_{(0\to 2\,\mu\text{m})} = 0.318$$
$$\lambda_2 T = 5\ \mu\text{m} \times 1600\ \text{K} = 8000\ \mu\text{m} \cdot \text{K}: \qquad F_{(0\to 5\,\mu\text{m})} = 0.856$$

Hence

$$\varepsilon = 0.4 \times 0.318 + 0.8[0.856 - 0.318] = 0.558$$ ◁

2. From Equation 12.35 the total emissive power is

$$E = \varepsilon E_b = \varepsilon \sigma T^4$$
$$E = 0.558(5.67 \times 10^{-8}\ \text{W/m}^2 \cdot \text{K}^4)(1600\ \text{K})^4 = 207\ \text{kW/m}^2$$ ◁

3. If the surface emitted as a blackbody or if its emissivity were a constant, independent of λ, the wavelength corresponding to maximum spectral emission

Patent Owner Manufacturing Resources International, Inc.
Exhibit 2017 - Page 755 of 999

could be obtained from Wien's law. However, because ε_λ varies with λ, it is not immediately obvious where peak emission occurs. From Equation 12.25 we know that

$$\lambda_{max} = \frac{2898\ \mu m \cdot K}{1600\ K} = 1.81\ \mu m$$

The spectral emissive power at this wavelength may be obtained by using Equation 12.32 with Table 12.1. That is,

$$E_\lambda(\lambda_{max}, T) = \varepsilon_\lambda(\lambda_{max}) E_{\lambda,b}(\lambda_{max}, T)$$

or, since the surface is a diffuse emitter,

$$\begin{aligned} E_\lambda(\lambda_{max}, T) &= \pi \varepsilon_\lambda(\lambda_{max}) I_{\lambda,b}(\lambda_{max}, T) \\ &= \pi \varepsilon_\lambda(\lambda_{max}) \frac{I_{\lambda,b}(\lambda_{max}, T)}{\sigma T^5} \times \sigma T^5 \\ E_\lambda(1.81\ \mu m, 1600\ K) &= \pi \times 0.4 \times 0.722 \times 10^{-4}\ (1/\mu m \cdot K \cdot sr) 5.67 \\ &\quad \times 10^{-8}\ W/m^2 \cdot K^4 \times (1600\ K)^5 = 54\ kW/m^2 \cdot \mu m \end{aligned}$$

Since $\varepsilon_\lambda = 0.4$ from $\lambda = 0$ to $\lambda = 2\ \mu m$, the foregoing result provides the maximum spectral emissive power for the region $\lambda < 2\ \mu m$. However, with the change in ε_λ that occurs at $\lambda = 2\ \mu m$, the value of E_λ at $\lambda = 2\ \mu m$ may be larger than that for $\lambda = 1.81\ \mu m$. To determine whether this is, in fact, the case, we compute

$$E_\lambda(\lambda_1, T) = \pi \varepsilon_\lambda(\lambda_1) \frac{I_{\lambda,b}(\lambda_1, T)}{\sigma T^5} \times \sigma T^5$$

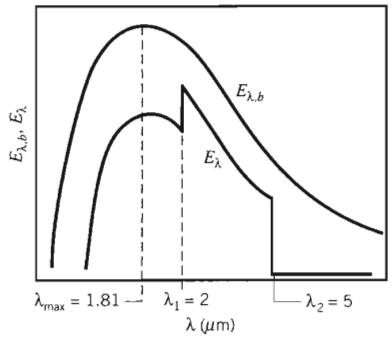
where, for $\lambda_1 T = 3200\ \mu m \cdot K$, $[I_{\lambda,b}(\lambda_1, T)/\sigma T^5] = 0.706 \times 10^{-4}\ (\mu m \cdot K \cdot sr)^{-1}$. Hence

$$\begin{aligned} E_\lambda(2\ \mu m, 1600\ K) &= \pi \times 0.80 \times 0.706 \times 10^{-4}\ (1/\mu m \cdot K \cdot sr) 5.67 \\ &\quad \times 10^{-8}\ W/m^2 \cdot K^4\ (1600\ K)^5 \\ E_\lambda(2\ \mu m, 1600\ K) &= 105.5\ kW/m^2 \cdot \mu m > E_\lambda(1.81\ \mu m, 1600\ K) \end{aligned}$$

and peak emission occurs at

$$\lambda = \lambda_1 = 2\ \mu m \quad \triangleleft$$

Comments: For the prescribed spectral distribution of ε_λ, the spectral emissive power will vary with wavelength as shown.



Patent Owner Manufacturing Resources International, Inc.
Exhibit 2017 - Page 756 of 999

varies with λ, it is
Equation 12.25 we

obtained by using

K · sr)5.67
54 kW/m² · μm
lt provides the maxi-
ever, with the change
ay be larger than that
se, we compute

10^{-4} (μm · K · sr)$^{-1}$.

· K · sr)5.67

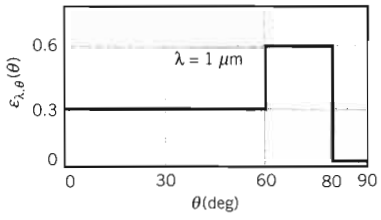
, 1600 K)

◁

the spectral emissive

EXAMPLE 12.6

Measurements of the spectral, directional emissivity of a metallic surface at $T = 2000$ K and $\lambda = 1.0$ μm yield a directional distribution that may be approximated as follows:



Determine corresponding values of the spectral, normal emissivity; the spectral, hemispherical emissivity; the spectral intensity of radiation emitted in the normal direction; and the spectral emissive power.

SOLUTION

Known: Directional distribution of $\varepsilon_{\lambda,\theta}$ at $\lambda = 1$ μm for a metallic surface at 2000 K.

Find:

1. Spectral, normal emissivity $\varepsilon_{\lambda,n}$ and spectral, hemispherical emissivity ε_λ.
2. Spectral, normal intensity $I_{\lambda,n}$ and spectral emissive power E_λ.

Analysis:

1. From the measurement of $\varepsilon_{\lambda,\theta}$ at $\lambda = 1$ μm, we see that

$$\varepsilon_{\lambda,n} = \varepsilon_{\lambda,\theta}(1\ \mu\text{m}, 0°) = 0.3 \qquad \triangleleft$$

From Equation 12.34, the spectral, hemispherical emissivity is

$$\varepsilon_\lambda(1\ \mu\text{m}) = 2\int_0^{\pi/2} \varepsilon_{\lambda,\theta} \cos\theta \sin\theta\, d\theta$$

or

$$\varepsilon_\lambda(1\ \mu\text{m}) = 2\left[0.3\int_0^{\pi/3} \cos\theta \sin\theta\, d\theta + 0.6\int_{\pi/3}^{4\pi/9} \cos\theta \sin\theta\, d\theta\right]$$

$$\varepsilon_\lambda(1\ \mu\text{m}) = 2\left[0.3\,\frac{\sin^2\theta}{2}\bigg|_0^{\pi/3} + 0.6\,\frac{\sin^2\theta}{2}\bigg|_{\pi/3}^{4\pi/9}\right]$$

$$= 2\left[\frac{0.3}{2}(0.75) + \frac{0.6}{2}(0.97 - 0.75)\right]$$

$$\varepsilon_\lambda(1\ \mu\text{m}) = 0.36 \qquad \triangleleft$$

Patent Owner Manufacturing Resources International, Inc.
Exhibit 2017 - Page 757 of 999

2. From Equation 12.30 the spectral intensity of radiation emitted at $\lambda = 1\ \mu$m in the normal direction is

$$I_{\lambda,n}(1\ \mu\text{m}, 0°, 2000\ \text{K}) = \varepsilon_{\lambda,\theta}(1\ \mu\text{m}, 0°)\, I_{\lambda,b}(1\ \mu\text{m}, 2000\ \text{K})$$

where $\varepsilon_{\lambda,\theta}(1\ \mu\text{m}, 0°) = 0.3$ and $I_{\lambda,b}(1\ \mu\text{m}, 2000\ \text{K})$ may be obtained from Table 12.1. For $\lambda T = 2000\ \mu\text{m} \cdot \text{K}$, $(I_{\lambda,b}/\sigma T^5) = 0.493 \times 10^{-4}\ (\mu\text{m} \cdot \text{K} \cdot \text{sr})^{-1}$ and

$$I_{\lambda,b} = 0.493 \times 10^{-4}\ (\mu\text{m} \cdot \text{K} \cdot \text{sr})^{-1} \times 5.67 \times 10^{-8}\ \text{W/m}^2 \cdot \text{K}^4 (2000\ \text{K})^5$$

$$I_{\lambda,b} = 8.95 \times 10^4\ \text{W/m}^2 \cdot \mu\text{m} \cdot \text{sr}$$

Hence

$$I_{\lambda,n}(1\ \mu\text{m}, 0°, 2000\ \text{K}) = 0.3 \times 8.95 \times 10^4\ \text{W/m}^2 \cdot \mu\text{m} \cdot \text{sr}$$

$$I_{\lambda,n}(1\ \mu\text{m}, 0°, 2000\ \text{K}) = 2.69 \times 10^4\ \text{W/m}^2 \cdot \mu\text{m} \cdot \text{sr} \quad \triangleleft$$

From Equation 12.32 the spectral emissive power for $\lambda = 1\ \mu$m and $T = 2000$ K is

$$E_\lambda(1\ \mu\text{m}, 2000\ \text{K}) = \varepsilon_\lambda(1\ \mu\text{m}) E_{\lambda,b}(1\ \mu\text{m}, 2000\ \text{K})$$

where

$$E_{\lambda,b}(1\ \mu\text{m}, 2000\ \text{K}) = \pi I_{\lambda,b}(1\ \mu\text{m}, 2000\ \text{K})$$

$$E_{\lambda,b}(1\ \mu\text{m}, 2000\ \text{K}) = \pi\ \text{sr} \times 8.95 \times 10^4\ \text{W/m}^2 \cdot \mu\text{m} \cdot \text{sr}$$

$$= 2.81 \times 10^5\ \text{W/m}^2 \cdot \mu\text{m}$$

Hence

$$E_\lambda(1\ \mu\text{m}, 2000\ \text{K}) = 0.36 \times 2.81 \times 10^5\ \text{W/m}^2 \cdot \mu\text{m}$$

or

$$E_\lambda(1\ \mu\text{m}, 2000\ \text{K}) = 1.01 \times 10^5\ \text{W/m}^2 \cdot \mu\text{m} \quad \triangleleft$$

12.5 *Absorption, Reflection, and Transmission by Real Surfaces*

In Section 12.2.3 we defined the *spectral irradiation* G_λ ($\text{W/m}^2 \cdot \mu\text{m}$) as the rate at which radiation of wavelength λ is incident on a surface per unit area of the surface and per unit wavelength interval $d\lambda$ about λ. It may be incident from all possible directions, and it may originate from several different sources. The *total irradiation* G (W/m^2) encompasses all spectral contributions and may be evaluated from Equation 12.14. In this section we consider the *processes* resulting from interception of this radiation by a solid (or liquid) medium.

In the most general situation the irradiation interacts with a *semitransparent medium,* such as a layer of water or a glass plate. As shown in Figure 12.20 for a spectral component of the irradiation, portions of this radiation may be

Patent Owner Manufacturing Resources International, Inc.
Exhibit 2017 - Page 758 of 999

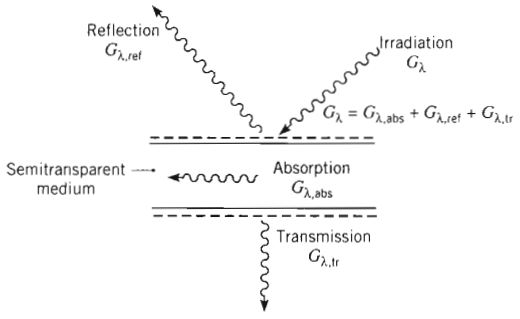


FIGURE 12.20
Absorption, reflection, and transmission processes associated with a semitransparent medium.

reflected, absorbed, and *transmitted.* From a radiation balance on the medium, it follows that

$$G_\lambda = G_{\lambda,ref} + G_{\lambda,abs} + G_{\lambda,tr} \tag{12.38}$$

In general, determination of these components is complex, depending on the upper and lower surface conditions, the wavelength of the radiation, and the composition and thickness of the medium. Moreover, conditions may be strongly influenced by *volumetric* effects occurring within the medium.

In a simpler situation, which pertains to most engineering applications, the medium is *opaque* to the incident radiation. In this case, $G_{\lambda,tr} = 0$ and the remaining absorption and reflection processes may be treated as *surface phenomena.* That is, they are controlled by processes occurring within a fraction of a micrometer from the irradiated surface. It is therefore appropriate to speak of irradiation being absorbed and reflected *by the surface,* with the relative magnitudes of $G_{\lambda,abs}$ and $G_{\lambda,ref}$ depending on λ and the nature of the surface material. There is no net effect of the reflection process on the medium, while absorption has the effect of increasing the internal thermal energy of the medium.

It is interesting to note that surface absorption and reflection are responsible for our perception of *color.* Unless the surface is at a high temperature ($T_s \gtrsim 1000$ K), such that it is *incandescent,* color is in no way due to emission, which is concentrated in the IR region, and is hence imperceptible to the eye. Color is instead due to selective reflection and absorption of the visible portion of the irradiation that is incident from the sun or an artificial source of light. A shirt is "red" because it contains a pigment that preferentially absorbs the blue, green, and yellow components of the incident light. Hence the relative contributions of these components to the reflected light, which is seen, is diminished, and the red component is dominant. Similarly, a leaf is "green" because its cells contain chlorophyll, a pigment that shows strong absorption in the blue and the red and preferential reflection in the green. A surface appears "black" if it absorbs all incident visible radiation, and it is "white" if it reflects this radiation. However, we must be careful how we interpret such *visual* effects. For a prescribed irradiation, the "color" of a surface may not indicate its overall capacity as an absorber or reflector, since much of the irradiation may be in the IR region. A "white" surface such as snow, for example, is highly reflective to visible radiation but strongly absorbs IR radiation, thereby approximating blackbody behavior at long wavelengths.

In Section 12.4 we introduced a property, which we called the emissivity, to characterize the process of surface emission. In the subsections that follow we shall

Patent Owner Manufacturing Resources International, Inc.
Exhibit 2017 - Page 759 of 999

introduce properties to characterize the absorption, reflection, and transmission processes. In general these properties depend on surface material and finish, surface temperature, and the wavelength and direction of the incident radiation.

12.5.1 Absorptivity

The absorptivity is a property that determines the fraction of the irradiation absorbed by a surface. Determination of the property is complicated by the fact that, like emission, it may be characterized by both a directional and spectral dependence. The *spectral, directional absorptivity,* $\alpha_{\lambda,\theta}(\lambda, \theta, \phi)$, of a surface is defined as the fraction of the spectral intensity incident in the direction of θ and ϕ that is absorbed by the surface. Hence

$$\alpha_{\lambda,\theta}(\lambda, \theta, \phi) \equiv \frac{I_{\lambda,i,\text{abs}}(\lambda, \theta, \phi)}{I_{\lambda,i}(\lambda, \theta, \phi)} \tag{12.39}$$

In this expression, we have neglected any dependence of the absorptivity on the surface temperature. Such a dependence is small for most spectral radiative properties.

It is implicit in the foregoing result that surfaces may exhibit selective absorption with respect to the wavelength and direction of the incident radiation. For most engineering calculations, however, it is desirable to work with surface properties that represent directional averages. We therefore define a *spectral, hemispherical absorptivity* $\alpha_\lambda(\lambda)$ as

$$\alpha_\lambda(\lambda) \equiv \frac{G_{\lambda,\text{abs}}(\lambda)}{G_\lambda(\lambda)} \tag{12.40}$$

which, from Equations 12.13 and 12.39, may be expressed as

$$\alpha_\lambda(\lambda) = \frac{\int_0^{2\pi}\int_0^{\pi/2} \alpha_{\lambda,\theta}(\lambda, \theta, \phi) I_{\lambda,i}(\lambda, \theta, \phi) \cos\theta \sin\theta \, d\theta \, d\phi}{\int_0^{2\pi}\int_0^{\pi/2} I_{\lambda,i}(\lambda, \theta, \phi) \cos\theta \sin\theta \, d\theta \, d\phi} \tag{12.41}$$

Hence α_λ depends on the directional distribution of the incident radiation, as well as on the wavelength of the radiation and the nature of the absorbing surface. Note that, if the incident radiation is diffusely distributed and $\alpha_{\lambda,\theta}$ is independent of ϕ, Equation 12.41 reduces to

$$\alpha_\lambda(\lambda) = 2\int_0^{\pi/2} \alpha_{\lambda,\theta}(\lambda, \theta) \cos\theta \sin\theta \, d\theta \tag{12.42}$$

The *total, hemispherical absorptivity,* α, represents an integrated average over both direction and wavelength. It is defined as the fraction of the total irradiation absorbed by a surface

$$\alpha \equiv \frac{G_{\text{abs}}}{G} \tag{12.43}$$

Patent Owner Manufacturing Resources International, Inc.
Exhibit 2017 - Page 760 of 999

and, from Equations 12.14 and 12.40, it may be expressed as

$$\alpha = \frac{\int_0^\infty \alpha_\lambda(\lambda) G_\lambda(\lambda)\, d\lambda}{\int_0^\infty G_\lambda(\lambda)\, d\lambda} \tag{12.44}$$

Accordingly, α depends on the spectral distribution of the incident radiation, as well as on its directional distribution and the nature of the absorbing surface. Note that, although α is approximately independent of surface temperature, the same may not be said for the total, hemispherical emissivity, ε. From Equation 12.36 it is evident that this property is strongly temperature dependent.

Because α depends on the spectral distribution of the irradiation, its value for a surface exposed to solar radiation may differ appreciably from its value for the same surface exposed to longer wavelength radiation originating from a source of lower temperature. Since the spectral distribution of solar radiation is nearly proportional to that of emission from a blackbody at 5800 K, it follows from Equation 12.44 that the total absorptivity to solar radiation α_S may be approximated as

$$\alpha_S \approx \frac{\int_0^\infty \alpha_\lambda(\lambda) E_{\lambda,b}(\lambda, 5800\ \text{K})\, d\lambda}{\int_0^\infty E_{\lambda,b}(\lambda, 5800\ \text{K})\, d\lambda} \tag{12.45}$$

The integrals appearing in this equation may be evaluated by using the blackbody radiation function $F_{(0\to\lambda)}$ of Table 12.1.

12.5.2 Reflectivity

The reflectivity is a property that determines the fraction of the incident radiation reflected by a surface. However, its specific definition may take several different forms, because the property is inherently *bidirectional* [6]. That is, in addition to depending on the direction of the incident radiation, it also depends on the direction of the reflected radiation. We shall avoid this complication by working exclusively with a reflectivity that represents an integrated average over the hemisphere associated with the reflected radiation and therefore provides no information concerning the directional distribution of this radiation. Accordingly, the *spectral, directional reflectivity*, $\rho_{\lambda,\theta}(\lambda, \theta, \phi)$, of a surface is defined as the fraction of the spectral intensity incident in the direction of θ and ϕ, which is reflected by the surface. Hence

$$\rho_{\lambda,\theta}(\lambda, \theta, \phi) \equiv \frac{I_{\lambda,i,\text{ref}}(\lambda, \theta, \phi)}{I_{\lambda,i}(\lambda, \theta, \phi)} \tag{12.46}$$

The *spectral, hemispherical reflectivity* $\rho_\lambda(\lambda)$ is then defined as the fraction of the spectral irradiation that is reflected by the surface. Accordingly,

$$\rho_\lambda(\lambda) \equiv \frac{G_{\lambda,\text{ref}}(\lambda)}{G_\lambda(\lambda)} \tag{12.47}$$

Patent Owner Manufacturing Resources International, Inc.
Exhibit 2017 - Page 761 of 999

which is equivalent to

$$\rho_\lambda(\lambda) = \frac{\int_0^{2\pi}\int_0^{\pi/2} \rho_{\lambda,\theta}(\lambda,\theta,\phi) I_{\lambda,i}(\lambda,\theta,\phi)\cos\theta\sin\theta\, d\theta\, d\phi}{\int_0^{2\pi}\int_0^{\pi/2} I_{\lambda,i}(\lambda,\theta,\phi)\cos\theta\sin\theta\, d\theta\, d\phi} \tag{12.48}$$

The *total, hemispherical reflectivity* ρ is then defined as

$$\rho \equiv \frac{G_{\text{ref}}}{G} \tag{12.49}$$

in which case

$$\rho = \frac{\int_0^\infty \rho_\lambda(\lambda) G_\lambda(\lambda)\, d\lambda}{\int_0^\infty G_\lambda(\lambda)\, d\lambda} \tag{12.50}$$

Surfaces may be idealized as *diffuse* or *specular,* according to the manner in which they reflect radiation (Figure 12.21). Diffuse reflection occurs if, regardless of the direction of the incident radiation, the intensity of the reflected radiation is independent of the reflection angle. In contrast, if all the reflection is in the direction of θ_2, which equals the incident angle θ_1, specular reflection is said to occur. Although no surface is perfectly diffuse or specular, the latter condition is more closely approximated by polished, mirror-like surfaces and the former condition by rough surfaces. The assumption of diffuse reflection is reasonable for most engineering applications.

12.5.3 Transmissivity

Although treatment of the response of a semitransparent material to incident radiation is a complicated problem [6], reasonable results may often be obtained through the use of hemispherical transmissivities defined as

$$\tau_\lambda = \frac{G_{\lambda,\text{tr}}(\lambda)}{G_\lambda(\lambda)} \tag{12.51}$$

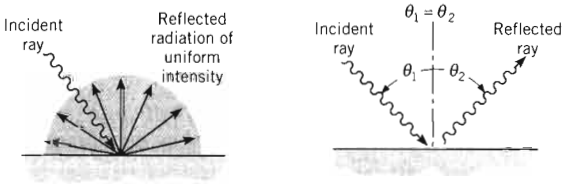


FIGURE 12.21 Diffuse and specular reflection.

Patent Owner Manufacturing Resources International, Inc.
Exhibit 2017 - Page 762 of 999

and

$$\tau = \frac{G_{tr}}{G} \tag{12.52}$$

The total transmissivity τ is related to the spectral component τ_λ by

$$\tau = \frac{\int_0^\infty G_{\lambda,tr}(\lambda)\, d\lambda}{\int_0^\infty G_\lambda(\lambda)\, d\lambda} = \frac{\int_0^\infty \tau_\lambda(\lambda) G_\lambda(\lambda)\, d\lambda}{\int_0^\infty G_\lambda(\lambda)\, d\lambda} \tag{12.53}$$

12.5.4 Special Considerations

We conclude this section by noting that, from the radiation balance of Equation 12.38 and the foregoing definitions,

$$\rho_\lambda + \alpha_\lambda + \tau_\lambda = 1 \tag{12.54}$$

for a *semitransparent* medium. For properties that are averaged over the entire spectrum, it also follows that

$$\rho + \alpha + \tau = 1 \tag{12.55}$$

Of course, if the medium is *opaque*, there is no transmission, and absorption and reflection are surface processes for which

$$\alpha_\lambda + \rho_\lambda = 1 \tag{12.56}$$

and

$$\alpha + \rho = 1 \tag{12.57}$$

Hence knowledge of one property implies knowledge of the other.

Spectral distributions of the normal reflectivity and absorptivity are plotted in Figure 12.22 for selected *opaque* surfaces. A material such as glass or water, which is semitransparent at short wavelengths, becomes opaque at longer wavelengths. This behavior is shown in Figure 12.23, which presents the spectral transmissivity of several common *semitransparent* materials. Note that the transmissivity of glass is affected by its iron content and that the transmissivity of plastics, such as Tedlar, is greater than that of glass in the IR region. These factors have an important bearing on the selection of cover plate materials for solar collector applications, design and selection of windows for energy conservation, and specification of materials for fabrication of the optical components of infrared imaging systems. Values for the total transmissivity to solar radiation of common collector cover plate materials are presented in Table A.12, along with surface solar absorptivities and low-temperature emissivities.

Patent Owner Manufacturing Resources International, Inc.
Exhibit 2017 - Page 763 of 999

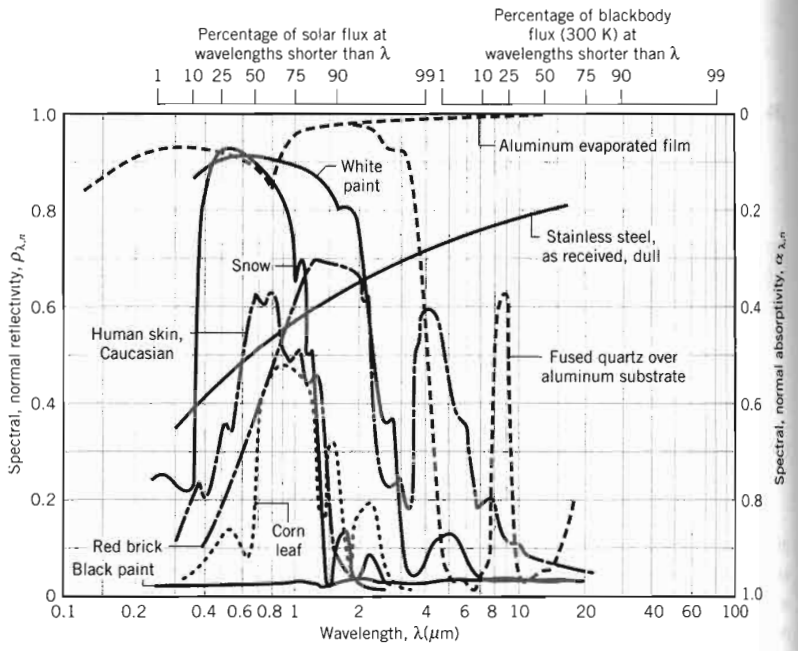


FIGURE 12.22 Spectral dependence of the spectral, normal absorptivity $\alpha_{\lambda,n}$ and reflectivity $\rho_{\lambda,n}$ of selected opaque materials.

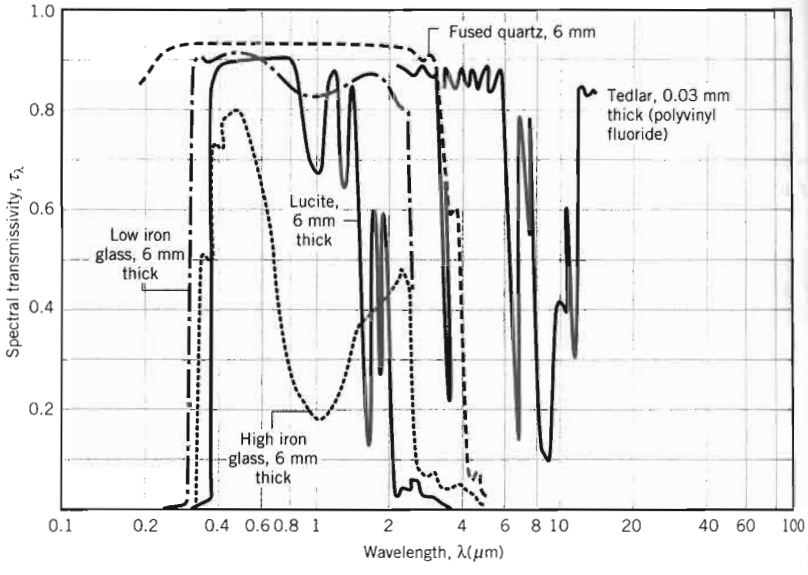
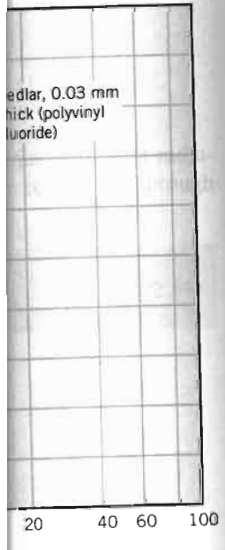


FIGURE 12.23 Spectral dependence of the spectral transmissivities τ_λ of selected semitransparent materials.

Patent Owner Manufacturing Resources International, Inc.
Exhibit 2017 - Page 764 of 999



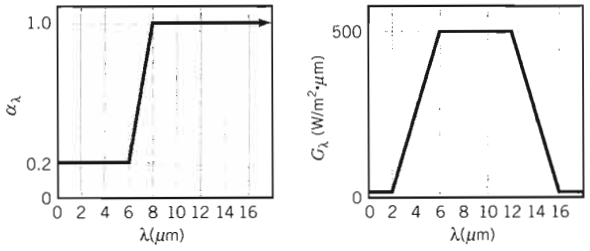
ity $\alpha_{\lambda,n}$ and



τ_λ of selected

EXAMPLE 12.7

The spectral, hemispherical absorptivity of an opaque surface and the spectral irradiation at the surface are as shown.



How does the spectral, hemispherical reflectivity vary with wavelength? What is the total, hemispherical absorptivity of the surface? If the surface is initially at 500 K and has a total, hemispherical emissivity of 0.8, how will its temperature change upon exposure to the irradiation?

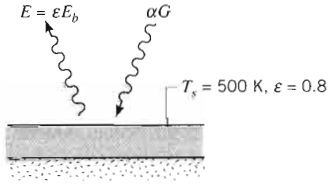
SOLUTION

Known: Spectral, hemispherical absorptivity and irradiation of a surface. Surface temperature (500 K) and total, hemispherical emissivity (0.8).

Find:

1. Spectral distribution of reflectivity.
2. Total, hemispherical absorptivity.
3. Nature of surface temperature change.

Schematic:



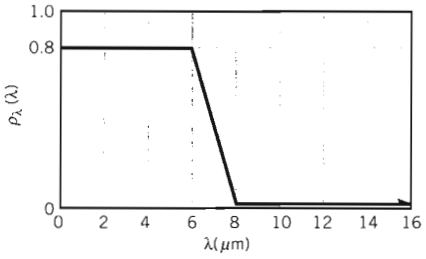
Assumptions:

1. Surface is opaque.
2. Surface convection effects are negligible.
3. Back surface is insulated.

Analysis:

1. From Equation 12.56, $\rho_\lambda = 1 - \alpha_\lambda$. Hence from knowledge of $\alpha_\lambda(\lambda)$, the spectral distribution of ρ_λ is as shown.

Patent Owner Manufacturing Resources International, Inc.
Exhibit 2017 - Page 765 of 999



2. From Equations 12.43 and 12.44,

$$\alpha = \frac{G_{abs}}{G} = \frac{\int_0^\infty \alpha_\lambda G_\lambda \, d\lambda}{\int_0^\infty G_\lambda \, d\lambda}$$

or, subdividing the integral into parts,

$$\alpha = \frac{0.2\int_2^6 G_\lambda d\lambda + 500\int_6^8 \alpha_\lambda \, d\lambda + 1.0\int_8^{16} G_\lambda \, d\lambda}{\int_2^6 G_\lambda \, d\lambda + \int_6^{12} G_\lambda \, d\lambda + \int_{12}^{16} G_\lambda \, d\lambda}$$

$$\begin{aligned}\alpha = \{&0.2(\tfrac{1}{2})500\ \text{W/m}^2\cdot\mu\text{m}\,(6-2)\,\mu\text{m}\\ &+ 500\ \text{W/m}^2\cdot\mu\text{m}\,[0.2(8-6)\,\mu\text{m} + (1-0.2)(\tfrac{1}{2})(8-6)\,\mu\text{m}]\\ &+ [1\times 500\ \text{W/m}^2\cdot\mu\text{m}\,(12-8)\,\mu\text{m}\\ &+ 1(\tfrac{1}{2})500\ \text{W/m}^2\cdot\mu\text{m}\,(16-12)\,\mu\text{m}]\}\\ &\div [(\tfrac{1}{2})500\ \text{W/m}^2\cdot\mu\text{m}\,(6-2)\,\mu\text{m} + 500\ \text{W/m}^2\cdot\mu\text{m}\,(12-6)\,\mu\text{m}\\ &+ (\tfrac{1}{2})500\ \text{W/m}^2\cdot\mu\text{m}\,(16-12)\,\mu\text{m}]\end{aligned}$$

Hence

$$\alpha = \frac{G_{abs}}{G} = \frac{(200+600+3000)\ \text{W/m}^2}{(1000+3000+1000)\ \text{W/m}^2} = \frac{3800\ \text{W/m}^2}{5000\ \text{W/m}^2} = 0.76$$ ◁

3. Neglecting convection effects, the net heat flux *to* the surface is

$$q''_{net} = \alpha G - E = \alpha G - \varepsilon\sigma T^4$$

Hence

$$q''_{net} = 0.76(5000\ \text{W/m}^2) - 0.8\times 5.67\times 10^{-8}\ \text{W/m}^2\cdot\text{K}^4(500\ \text{K})^4$$

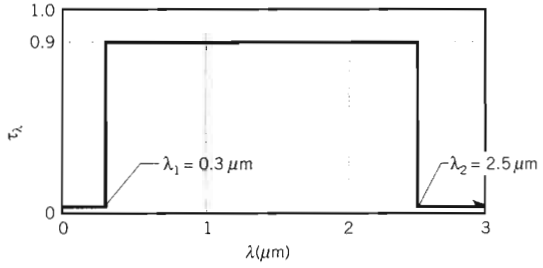
$$q''_{net} = 3800 - 2835 = 965\ \text{W/m}^2$$

Since $q''_{net} > 0$, the surface temperature will *increase* with time. ◁

Patent Owner Manufacturing Resources International, Inc.
Exhibit 2017 - Page 766 of 999

EXAMPLE 12.8

The cover glass on a flat-plate solar collector has a low iron content, and its spectral transmissivity may be approximated by the following distribution.



What is the total transmissivity of the cover glass to solar radiation?

SOLUTION

Known: Spectral transmissivity of solar collector cover glass.

Find: Total transmissivity of cover glass to solar radiation.

Assumptions: Spectral distribution of solar irradiation is proportional to that of blackbody emission at 5800 K.

Analysis: From Equation 12.53 the total transmissivity of the cover is

$$\tau = \frac{\int_0^\infty \tau_\lambda G_\lambda \, d\lambda}{\int_0^\infty G_\lambda d\lambda}$$

where the irradiation G_λ is due to solar emission. Having assumed that the sun emits as a blackbody at 5800 K, it follows that

$$G_\lambda(\lambda) \propto E_{\lambda,b}(5800\ \text{K})$$

With the proportionality constant canceling from the numerator and denominator of the expression for τ, we obtain

$$\tau = \frac{\int_0^\infty \tau_\lambda E_{\lambda,b}(5800\ \text{K})\, d\lambda}{\int_0^\infty E_{\lambda,b}(5800\ \text{K})\, d\lambda}$$

or, for the prescribed spectral distribution of $\tau_\lambda(\lambda)$,

$$\tau = 0.90 \frac{\int_{0.3}^{2.5} E_{\lambda,b}(5800\ \text{K})\, d\lambda}{E_b(5800\ \text{K})}$$

Patent Owner Manufacturing Resources International, Inc.
Exhibit 2017 - Page 767 of 999

From Table 12.1

$\lambda_1 = 0.3\ \mu\text{m}, T = 5800\ \text{K}$: $\lambda_1 T = 1740\ \mu\text{m} \cdot \text{K}, F_{(0\to\lambda_1)} = 0.0335$

$\lambda_2 = 2.5\ \mu\text{m}, T = 5800\ \text{K}$: $\lambda_2 T = 14{,}500\ \mu\text{m} \cdot \text{K}, F_{(0\to\lambda_2)} = 0.9664$

Hence from Equation 12.29

$$\tau = 0.90[F_{(0\to\lambda_2)} - F_{(0\to\lambda_1)}] = 0.90(0.9660 - 0.1245) = 0.84 \quad \triangleleft$$

Comments: It is important to recognize that the irradiation at the cover plate is not equal to the emissive power of a blackbody at 5800 K, $G_\lambda \neq E_{\lambda,b}$ (5800 K). It is simply assumed to be proportional to this emissive power, in which case it is assumed to have a spectral distribution of the same form. With G_λ appearing in both the numerator and denominator of the expression for τ, it is then possible to replace G_λ by $E_{\lambda,b}$.

12.6 *Kirchhoff's Law*

In the foregoing sections we separately considered real surface properties associated with emission and absorption. In Sections 12.6 and 12.7 we consider conditions for which these properties are equal.

Consider a *large, isothermal enclosure* of surface temperature T_s, within which several small bodies are confined (Figure 12.24). Since these bodies are small relative to the enclosure, they have a negligible influence on the radiation field, which is due to the cumulative effect of emission and reflection by the enclosure surface. Recall that, regardless of its radiative properties, such a surface forms a *blackbody cavity*. Accordingly, regardless of its orientation, the irradiation experienced by any body in the cavity is diffuse and equal to emission from a blackbody at T_s.

$$G = E_b(T_s) \tag{12.58}$$

Under steady-state conditions, *thermal equilibrium* must exist between the bodies and the enclosure. Hence $T_1 = T_2 = \cdots = T_s$, and the net rate of energy transfer

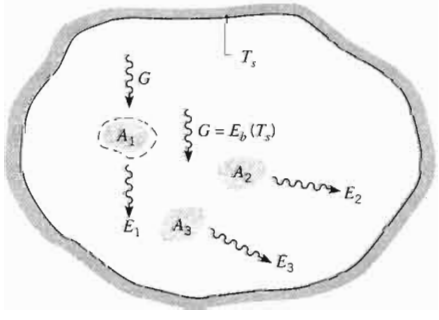


FIGURE 12.24
Radiative exchange in an isothermal enclosure.

Patent Owner Manufacturing Resources International, Inc.
Exhibit 2017 - Page 768 of 999

to each surface must be zero. Applying an energy balance to a control surface about body 1, it follows that

$$\alpha_1 G A_1 - E_1(T_s) A_1 = 0$$

or, from Equation 12.58,

$$\frac{E_1(T_s)}{\alpha_1} = E_b(T_s)$$

Since this result must apply to each of the confined bodies, we then obtain

$$\frac{E_1(T_s)}{\alpha_1} = \frac{E_2(T_s)}{\alpha_2} = \cdots = E_b(T_s) \tag{12.59}$$

This relation is known as *Kirchhoff's law.* A major implication is that, since $\alpha \leq 1$, $E(T_s) \leq E_b(T_s)$. Hence *no real surface can have an emissive power exceeding that of a black surface at the same temperature,* and the notion of the blackbody as an ideal emitter is confirmed.

From the definition of the total, hemispherical emissivity, Equation 12.35, an alternative form of Kirchhoff's law, is

$$\frac{\varepsilon_1}{\alpha_1} = \frac{\varepsilon_2}{\alpha_2} = \cdots = 1$$

Hence, for any surface in the enclosure,

$$\varepsilon = \alpha \tag{12.60}$$

That is, the total, hemispherical emissivity of the surface is equal to its total, hemispherical absorptivity.

We will later find that calculations of radiative exchange between surfaces are greatly simplified if Equation 12.60 may be applied to each of the surfaces. However, the restrictive conditions inherent in its derivation should be remembered. In particular, the surface irradiation has been assumed to correspond to emission from a blackbody at the same temperature as the surface. In Section 12.7 we consider other, less restrictive, conditions for which Equation 12.60 is applicable.

The preceding derivation may be repeated for spectral conditions, and for any surface in the enclosure it follows that

$$\varepsilon_\lambda = \alpha_\lambda \tag{12.61}$$

Conditions associated with the use of Equation 12.61 are less restrictive than those associated with Equation 12.60. In particular, it will be shown that Equation 12.61 is applicable if the irradiation is diffuse *or* if the surface is diffuse. A form of Kirchhoff's law for which there are *no restrictions* involves the spectral, directional properties.

$$\varepsilon_{\lambda,\theta} = \alpha_{\lambda,\theta} \tag{12.62}$$

This equality is always applicable because $\varepsilon_{\lambda,\theta}$ and $\alpha_{\lambda,\theta}$ are *inherent* surface properties. That is, respectively, they are independent of the spectral and directional distributions of the emitted and incident radiation.

More detailed developments of Kirchhoff's law are provided by Planck [1] and Siegel and Howell [6].

Patent Owner Manufacturing Resources International, Inc.
Exhibit 2017 - Page 769 of 999

12.7 *The Gray Surface*

In Chapter 13 we will find that the problem of predicting radiant energy exchange between surfaces is greatly simplified if Equation 12.60 may be assumed to apply for each individual surface. It is therefore important to examine whether this equality may be applied to conditions other than those for which it was derived, namely, irradiation due to emission from a blackbody at the same temperature as the surface.

Accepting the fact that the spectral, directional emissivity and absorptivity are equal under any conditions, Equation 12.62, we begin by considering the conditions associated with using Equation 12.61. According to the definitions of the spectral, hemispherical properties, Equations 12.33 and 12.41, we are really asking under what conditions, if any, the following equality will hold:

$$\varepsilon_\lambda = \frac{\int_0^{2\pi}\int_0^{\pi/2} \varepsilon_{\lambda,\theta} \cos\theta \sin\theta \, d\theta \, d\phi}{\int_0^{2\pi}\int_0^{\pi/2} \cos\theta \sin\theta \, d\theta \, d\phi} \stackrel{?}{=} \frac{\int_0^{2\pi}\int_0^{\pi/2} \alpha_{\lambda,\theta} I_{\lambda,i} \cos\theta \sin\theta \, d\theta \, d\phi}{\int_0^{2\pi}\int_0^{\pi/2} I_{\lambda,i} \cos\theta \sin\theta \, d\theta \, d\phi} = \alpha_\lambda \tag{12.63}$$

Since $\varepsilon_{\lambda,\theta} = \alpha_{\lambda,\theta}$, it follows by inspection that Equation 12.61 is applicable if *either* of the following conditions is satisfied:

1. The *irradiation* is *diffuse* ($I_{\lambda,i}$ is independent of θ and ϕ).
2. The *surface* is *diffuse* ($\varepsilon_{\lambda,\theta}$ and $\alpha_{\lambda,\theta}$ are independent of θ and ϕ).

The first condition is a reasonable approximation for many engineering calculations; the second condition is reasonable for many surfaces, particularly for electrically nonconducting materials (Figure 12.16).

Assuming the existence of either diffuse irradiation or a diffuse surface, we now consider what *additional* conditions must be satisfied for Equation 12.60 to be valid. From Equations 12.36 and 12.44, the equality applies if

$$\varepsilon = \frac{\int_0^\infty \varepsilon_\lambda E_{\lambda,b}(\lambda, T)\, d\lambda}{E_b(T)} \stackrel{?}{=} \frac{\int_0^\infty \alpha_\lambda G_\lambda(\lambda)\, d\lambda}{G} = \alpha \tag{12.64}$$

Since $\varepsilon_\lambda = \alpha_\lambda$, it follows by inspection that Equation 12.60 applies if *either* of the following conditions is satisfied:

1. The irradiation corresponds to emission from a blackbody at the surface temperature T, in which case $G_\lambda(\lambda) = E_{\lambda,b}(\lambda, T)$ and $G = E_b(T)$.
2. The *surface* is *gray* (α_λ and ε_λ are independent of λ).

Note that the first condition corresponds to the major assumption required for the derivation of Kirchhoff's law (Section 12.6).

Because the total absorptivity of a surface depends on the spectral distribution of the irradiation, it cannot be stated unequivocally that $\alpha = \varepsilon$. For example, a particular surface may be highly absorbing to radiation in one spectral region and virtually

Patent Owner Manufacturing Resources International, Inc.
Exhibit 2017 - Page 770 of 999

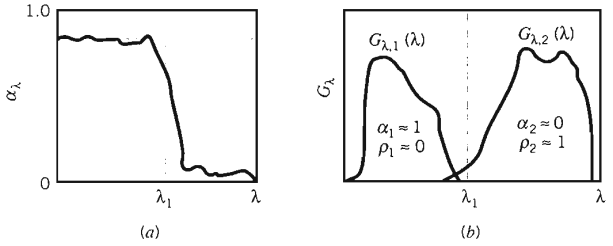


FIGURE 12.25 Spectral distribution of (*a*) the spectral absorptivity of a surface and (*b*) the spectral irradiation at the surface.

nonabsorbing in another region (Figure 12.25*a*). Accordingly, for the two possible irradiation fields $G_{\lambda,1}(\lambda)$ and $G_{\lambda,2}(\lambda)$ of Figure 12.25*b*, the values of α will differ drastically. In contrast, the value of ε is independent of the irradiation. Hence there is *no* basis for stating that α is *always* equal to ε.

To assume gray surface behavior, hence the validity of Equation 12.60, it is not necessary for α_λ and ε_λ to be independent of λ over the entire spectrum. Practically speaking, a *gray surface* may be defined as *one for which α_λ and ε_λ are independent of λ over the spectral regions of the irradiation and the surface emission.* From Equation 12.64 it is readily shown that gray surface behavior may be assumed for the conditions of Figure 12.26. That is, the irradiation and surface emission are concentrated in a region for which the spectral properties of the surface are approximately constant. Accordingly,

$$\varepsilon = \frac{\varepsilon_{\lambda,o}\int_{\lambda_1}^{\lambda_2} E_{\lambda,b}(\lambda, T)\, d\lambda}{E_b(T)} = \varepsilon_{\lambda,o} \qquad \text{and} \qquad \alpha = \frac{\alpha_{\lambda,o}\int_{\lambda_3}^{\lambda_4} G_\lambda(\lambda)\, d\lambda}{G} = \alpha_{\lambda,o}$$

in which case $\alpha = \varepsilon = \varepsilon_{\lambda,o}$. However, if the irradiation were in a spectral region corresponding to $\lambda < \lambda_1$ or $\lambda > \lambda_4$, gray surface behavior could not be assumed.

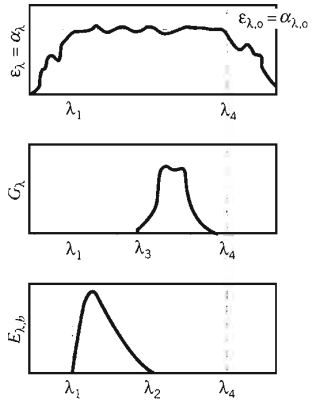


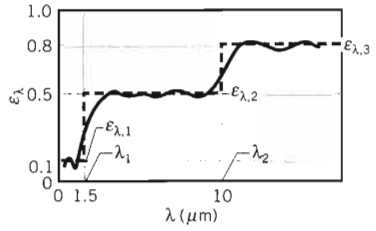
FIGURE 12.26
A set of conditions for which gray surface behavior may be assumed.

Patent Owner Manufacturing Resources International, Inc.
Exhibit 2017 - Page 771 of 999

A surface for which $\alpha_{\lambda,\theta}$ and $\varepsilon_{\lambda,\theta}$ are independent of θ and λ is termed a *diffuse, gray surface* (diffuse because of the directional independence and gray because of the wavelength independence). It is a surface for which both Equations 12.60 and 12.61 are satisfied. We assume such surface conditions in many of our subsequent considerations. However, although the assumption of a gray surface is reasonable for many practical applications, some caution should be exercised in its use, particularly if the spectral regions of the irradiation and emission are widely separated.

EXAMPLE 12.9

A diffuse, fire brick wall of temperature $T_s = 500$ K has the spectral emissivity shown and is exposed to a bed of coals at 2000 K.



Determine the total, hemispherical emissivity and emissive power of the fire brick wall. What is the total absorptivity of the wall to irradiation resulting from emission by the coals?

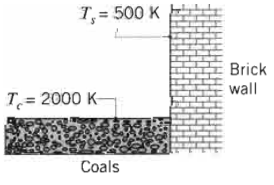
SOLUTION

Known: Brick wall of surface temperature $T_s = 500$ K and prescribed $\varepsilon_\lambda(\lambda)$ is exposed to coals at $T_c = 2000$ K.

Find:

1. Total, hemispherical emissivity of the fire brick wall.
2. Total emissive power of the brick wall.
3. Absorptivity of the wall to irradiation from the coals.

Schematic:



Patent Owner Manufacturing Resources International, Inc.
Exhibit 2017 - Page 772 of 999

Assumptions:

1. Brick wall is opaque and diffuse.
2. Spectral distribution of irradiation at the brick wall approximates that due to emission from a blackbody at 2000 K.

Analysis:

1. The total, hemispherical emissivity follows from Equation 12.36.

$$\varepsilon(T_s) = \frac{\int_0^\infty \varepsilon_\lambda(\lambda) E_{\lambda,b}(\lambda, T_s)\, d\lambda}{E_b(T_s)}$$

Breaking the integral into parts,

$$\varepsilon(T_s) = \varepsilon_{\lambda,1} \frac{\int_0^{\lambda_1} E_{\lambda,b}\, d\lambda}{E_b} + \varepsilon_{\lambda,2} \frac{\int_{\lambda_1}^{\lambda_2} E_{\lambda,b}\, d\lambda}{E_b} + \varepsilon_{\lambda,3} \frac{\int_{\lambda_2}^{\infty} E_{\lambda,b}\, d\lambda}{E_b}$$

and introducing the blackbody functions, it follows that

$$\varepsilon(T_s) = \varepsilon_{\lambda,1} F_{(0\to\lambda_1)} + \varepsilon_{\lambda,2}[F_{(0\to\lambda_2)} - F_{(0\to\lambda_1)}] + \varepsilon_{\lambda,3}[1 - F_{(0\to\lambda_2)}]$$

From Table 12.1

$$\lambda_1 T_s = 1.5\ \mu\text{m} \times 500\ \text{K} = 750\ \mu\text{m} \cdot \text{K}: \qquad F_{(0\to\lambda_1)} = 0.000$$
$$\lambda_2 T_s = 10\ \mu\text{m} \times 500\ \text{K} = 5000\ \mu\text{m} \cdot \text{K}: \qquad F_{(0\to\lambda_2)} = 0.634$$

Hence

$$\varepsilon(T_s) = 0.1 \times 0 + 0.5 \times 0.634 + 0.8\,(1 - 0.634) = 0.610 \qquad \triangleleft$$

2. From Equations 12.26 and 12.35, the total emissive power is

$$E(T_s) = \varepsilon(T_s) E_b(T_s) = \varepsilon(T_s) \sigma T_s^4$$
$$E(T_s) = 0.61 \times 5.67 \times 10^{-8}\ \text{W/m}^2 \cdot \text{K}^4 (500\ \text{K})^4 = 2162\ \text{W/m}^2 \qquad \triangleleft$$

3. From Equation 12.44, the total absorptivity of the wall to radiation from the coals is

$$\alpha = \frac{\int_0^\infty \alpha_\lambda(\lambda) G_\lambda(\lambda)\, d\lambda}{\int_0^\infty G_\lambda(\lambda)\, d\lambda}$$

Since the surface is diffuse, $\alpha_\lambda(\lambda) = \varepsilon_\lambda(\lambda)$. Moreover, since the spectral distribution of the irradiation approximates that due to emission from a blackbody at 2000 K, $G_\lambda(\lambda) \propto E_{\lambda,b}(\lambda, T_c)$. It follows that

$$\alpha = \frac{\int_0^\infty \varepsilon_\lambda(\lambda) E_{\lambda,b}(\lambda, T_c)\, d\lambda}{\int_0^\infty E_{\lambda,b}(\lambda, T_c)\, d\lambda}$$

Breaking the integral into parts and introducing the blackbody functions, we then obtain

$$\alpha = \varepsilon_{\lambda,1} F_{(0\to\lambda_1)} + \varepsilon_{\lambda,2}[F_{(0\to\lambda_2)} - F_{(0\to\lambda_1)}] + \varepsilon_{\lambda,3}[1 - F_{(0\to\lambda_2)}]$$

Patent Owner Manufacturing Resources International, Inc.
Exhibit 2017 - Page 773 of 999

From Table 12.1

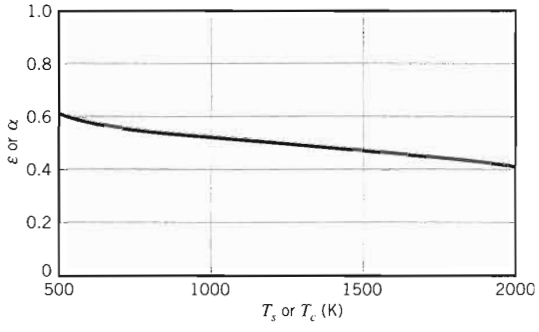
$$\lambda_1 T_c = 1.5\ \mu\text{m} \times 2000\ \text{K} = 3000\ \mu\text{m} \cdot \text{K}: \qquad F_{(0\to\lambda_1)} = 0.273$$
$$\lambda_2 T_c = 10\ \mu\text{m} \times 2000\ \text{K} = 20{,}000\ \mu\text{m} \cdot \text{K}: \qquad F_{(0\to\lambda_2)} = 0.986$$

Hence

$$\alpha = 0.1 \times 0.273 + 0.5(0.986 - 0.273) + 0.8(1 - 0.986) = 0.395 \quad \triangleleft$$

Comments:

1. The emissivity depends on the surface temperature T_s, while the absorptivity depends on the spectral distribution of the irradiation, which depends on the temperature of the source T_c.
2. The surface is not gray, $\alpha \neq \varepsilon$. This result is to be expected. Since emission is associated with $T_s = 500$ K, its spectral maximum occurs at $\lambda_{max} \approx 6\ \mu$m. In contrast, since irradiation is associated with emission from a source at $T_c = 2000$ K, its spectral maximum occurs at $\lambda_{max} \approx 1.5\ \mu$m. Even though ε_λ and α_λ are equal, because they are not constant over the spectral ranges of both emission and irradiation, $\alpha \neq \varepsilon$. For the prescribed spectral distribution of $\varepsilon_\lambda = \alpha_\lambda$, ε and α decrease with increasing T_s and T_c, respectively, and it is only for $T_s = T_c$ that $\varepsilon = \alpha$. The foregoing expressions for ε and α may be used to determine their equivalent variation with T_s and T_c, and the following result is obtained:



EXAMPLE 12.10

A *small,* solid metallic sphere has an opaque, diffuse coating for which $\alpha_\lambda = 0.8$ for $\lambda \leq 5\ \mu$m and $\alpha_\lambda = 0.1$ for $\lambda > 5\ \mu$m. The sphere, which is initially at a uniform temperature of 300 K, is inserted into a *large* furnace whose walls are at 1200 K. Determine the total, hemispherical absorptivity and emissivity of the coating for the initial condition and for the final, steady-state condition.

SOLUTION

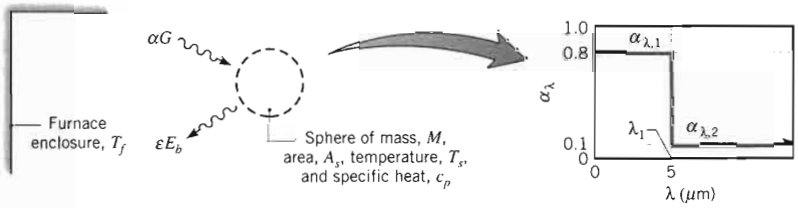
Known: Small metallic sphere with spectrally selective absorptivity, initially at $T_s = 300$ K, is inserted into a large furnace at $T_f = 1200$ K.

Patent Owner Manufacturing Resources International, Inc.
Exhibit 2017 - Page 774 of 999

Find:

1. Total, hemispherical absorptivity and emissivity of sphere coating for the initial condition.
2. Values of α and ε after sphere has been in furnace a long time.

Schematic:



Assumptions:

1. Coating is opaque and diffuse.
2. Since furnace surface is much larger than that of sphere, irradiation approximates emission from a blackbody at T_f.

Analysis:

1. From Equation 12.44 the total, hemispherical absorptivity is

$$\alpha = \frac{\int_0^\infty \alpha_\lambda(\lambda) G_\lambda(\lambda)\, d\lambda}{\int_0^\infty G_\lambda(\lambda)\, d\lambda}$$

or, with $G_\lambda = E_{\lambda,b}(T_f) = E_{\lambda,b}(\lambda, 1200\ \text{K})$,

$$\alpha = \frac{\int_0^\infty \alpha_\lambda(\lambda) E_{\lambda,b}(\lambda, 1200\ \text{K})\, d\lambda}{E_b(1200\ \text{K})}$$

Hence

$$\alpha = \alpha_{\lambda,1} \frac{\int_0^{\lambda_1} E_{\lambda,b}(\lambda, 1200\ \text{K})\, d\lambda}{E_b(1200\ \text{K})} + \alpha_{\lambda,2} \frac{\int_{\lambda_1}^\infty E_{\lambda,b}(\lambda, 1200\ \text{K})\, d\lambda}{E_b(1200\ \text{K})}$$

or

$$\alpha = \alpha_{\lambda,1} F_{(0\to\lambda_1)} + \alpha_{\lambda,2}[1 - F_{(0\to\lambda_1)}]$$

From Table 12.1,

$$\lambda_1 T_f = 5\ \mu\text{m} \times 1200\ \text{K} = 6000\ \mu\text{m} \cdot \text{K}: \qquad F_{(0\to\lambda_1)} = 0.738$$

Hence

$$\alpha = 0.8 \times 0.738 + 0.1\,(1 - 0.738) = 0.62$$

Patent Owner Manufacturing Resources International, Inc.
Exhibit 2017 - Page 775 of 999

The total, hemispherical emissivity follows from Equation 12.36.

$$\varepsilon(T_s) = \frac{\int_0^\infty \varepsilon_\lambda E_{\lambda,b}(\lambda, T_s)\, d\lambda}{E_b(T_s)}$$

Since the surface is diffuse, $\varepsilon_\lambda = \alpha_\lambda$ and it follows that

$$\varepsilon = \alpha_{\lambda,1} \frac{\int_0^{\lambda_1} E_{\lambda,b}(\lambda, 300\ \text{K})\, d\lambda}{E_b(300\ \text{K})} + \alpha_{\lambda,2} \frac{\int_{\lambda_1}^\infty E_{\lambda,b}(\lambda, 300\ \text{K})\, d\lambda}{E_b(300\ \text{K})}$$

or,

$$\varepsilon = \alpha_{\lambda,1} F_{(0\to\lambda_1)} + \alpha_{\lambda,2}[1 - F_{(0\to\lambda_1)}]$$

From Table 12.1,

$$\lambda_1 T_s = 5\ \mu\text{m} \times 300\ \text{K} = 1500\ \mu\text{m} \cdot \text{K}: \qquad F_{(0\to\lambda_1)} = 0.014$$

Hence

$$\varepsilon = 0.8 \times 0.014 + 0.1\,(1 - 0.014) = 0.11$$ ◁

2. Because the spectral characteristics of the coating and the furnace temperature remain fixed, there is no change in the value of α with increasing time. However, as T_s increases with time, the value of ε will change. After a sufficiently long time, $T_s = T_f$, and $\varepsilon = \alpha$ ($\varepsilon = 0.62$).

Comments:

1. The equilibrium condition that eventually exists ($T_s = T_f$) corresponds precisely to the condition for which Kirchhoff's law was derived. Hence α must equal ε.
2. Approximating the sphere as a lumped capacitance and neglecting convection, an energy balance for a control volume about the sphere yields

$$\dot{E}_{\text{in}} - \dot{E}_{\text{out}} = \dot{E}_{\text{st}}$$

$$(\alpha G)A_s - (\varepsilon\sigma T_s^4)A_s = Mc_p \frac{dT_s}{dt}$$

The differential equation could be solved to determine $T(t)$ for $t > 0$, and the variation in ε that occurs with increasing time would have to be included in the solution.

12.8 *Environmental Radiation*

It would be inappropriate to conclude this chapter without commenting on the radiation that comprises our natural environment. Solar radiation is, of course, essential

Patent Owner Manufacturing Resources International, Inc.
Exhibit 2017 - Page 776 of 999

to all life on earth. Through the process of photosynthesis, it satisfies our need for food, fiber, and fuel. Moreover, through thermal and photovoltaic processes, it has the potential to satisfy much of our demand for space heat, process heat, and electricity.

The sun is a nearly spherical radiation source that is 1.39×10^9 m in diameter and is located 1.50×10^{11} m from the earth. As noted previously, the sun emits approximately as a blackbody at 5800 K. As the radiation emitted by the sun travels through space, the radiation flux decreases because of the greater (spherical) area through which it passes. At the outer edge of the earth's atmosphere, the flux of solar energy has decreased by a factor of $(r_s/r_d)^2$, where r_s is the radius of the sun and r_d is the distance from the sun to the earth. The *solar constant*, S_c, is defined as the flux of solar energy incident on a surface oriented *normal* to the sun's rays, at the outer edge of the earth's atmosphere, when the earth is at its mean distance from the sun (Figure 12.27). It has a value of $S_c = 1353$ W/m^2. For a *horizontal* surface (that is, parallel to earth's surface), solar radiation appears as a beam of nearly *parallel rays* that form an angle θ, the *zenith angle*, relative to the surface normal. The *extraterrestrial solar irradiation* $G_{S,o}$, defined for a horizontal surface, depends on the geographic latitude, as well as the time of day and year. It may be determined from an expression of the form

$$G_{S,o} = S_c \cdot f \cdot \cos\theta \tag{12.65}$$

The quantity f is a small correction factor to account for the eccentricity of the earth's orbit about the sun ($0.97 \lesssim f \lesssim 1.03$).

The spectral distribution of solar radiation is significantly different from that associated with emission by engineering surfaces. As shown in Figure 12.28, the extraterrestrial distribution approximates that of a blackbody at 5800 K. The radiation is concentrated in the low wavelength region ($0.2 \lesssim \lambda \lesssim 3$ μm) of the thermal spectrum, with the peak occurring at approximately 0.50 μm. It is this short wavelength concentration that frequently precludes the assumption of graybody behavior for solar irradiated surfaces, since emission is generally in the spectral region beyond 4 μm and it is unlikely that surface spectral properties would be constant over such a wide spectral range.

As solar radiation passes through the earth's atmosphere, its magnitude and its spectral and directional distributions experience significant change. The change is due to *absorption* and *scattering* of the radiation by the atmospheric constituents. The effect of absorption by the atmospheric gases O_3 (ozone), H_2O, O_2, and CO_2 is shown by the lower curve of Figure 12.28. Absorption by ozone is strong in the UV

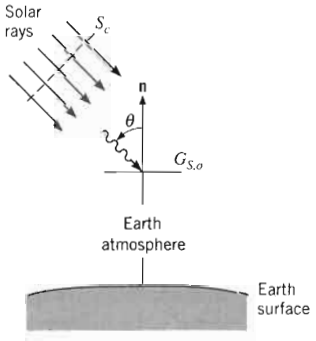


FIGURE 12.27
Directional nature of solar radiation outside the earth's atmosphere.

Patent Owner Manufacturing Resources International, Inc.
Exhibit 2017 - Page 777 of 999

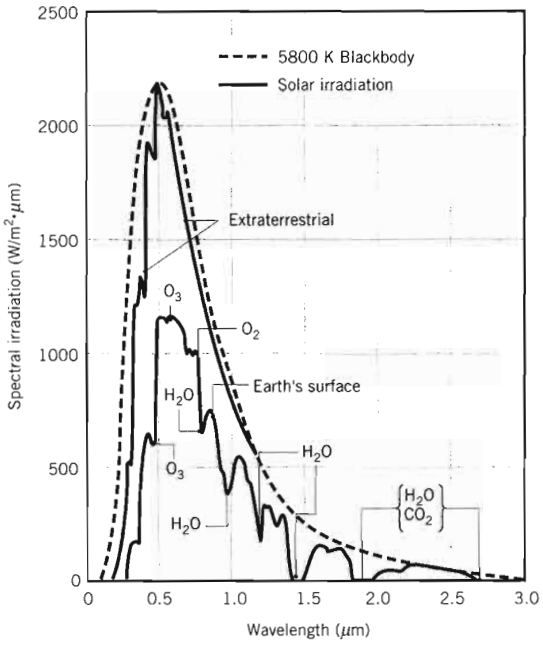


FIGURE 12.28 Spectral distribution of solar radiation.

region, providing considerable attenuation below 0.4 μm and complete attenuation below 0.3 μm. In the visible region there is some absorption by O_3 and O_2; and in the near and far IR regions, absorption is dominated by water vapor. Throughout the solar spectrum, there is also continuous absorption of radiation by the dust and aerosol content of the atmosphere.

Atmospheric scattering provides for *redirection* of the sun's rays and consists of two kinds (Figure 12.29). *Rayleigh* (or *molecular*) *scattering* by very small gas molecules occurs when the ratio of the effective molecule diameter to the wavelength of the radiation, $\pi D/\lambda$, is much less than unity and provides for nearly uniform scattering of radiation in all directions. Hence approximately half of the scattered radiation is redirected to space, while the remaining portion strikes the earth's surface. At any point on this surface, the scattered radiation is incident from all directions. In contrast, *Mie scattering* by larger dust and aerosol particles of the atmosphere occurs when $\pi D/\lambda$ is approximately unity and is concentrated in directions that are close to that of the incident rays. Hence virtually all this radiation strikes the earth's surface in directions close to that of the sun's rays.

The cumulative effect of the scattering processes on the directional distribution of solar radiation striking the earth's surface is shown in Figure 12.30*a*. That portion of the radiation that has penetrated the atmosphere without having been scattered (or absorbed) is in the direction of the zenith angle and is termed the *direct radiation.* The scattered radiation is incident from all directions, although its intensity is largest for directions close to that of the direct radiation. However, because the radiation intensity is often *assumed* to be independent of direction (Figure 12.30*b*),

Patent Owner Manufacturing Resources International, Inc.
Exhibit 2017 - Page 778 of 999

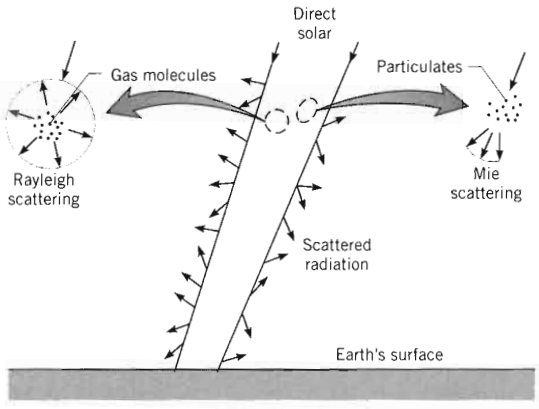


FIGURE 12.29 Scattering of solar radiation in the earth's atmosphere.

the radiation is termed *diffuse*. The total solar radiation reaching the earth's surface is therefore the sum of direct and diffuse contributions. The diffuse contribution may vary from approximately 10% of the total solar radiation on a clear day to nearly 100% on a totally overcast day.

The foregoing discussion has focused on the *nature* of solar radiation. Heat transfer analyses related to its use are considered in many of the examples and problems of the text. Detailed treatment of solar energy technologies is left to the literature [7–11].

Long wavelength forms of environmental radiation include emission from the earth's surface, as well as emission from certain atmospheric constituents. The emissive power associated with the earth's surface may be computed in the conventional manner. That is,

$$E = \varepsilon \sigma T^4 \tag{12.66}$$

where ε and T are the surface emissivity and temperature, respectively. Emissivities are generally close to unity, and that of water, for example, is approximately 0.97.

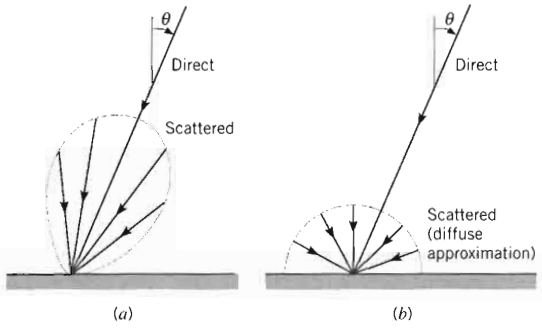


FIGURE 12.30 Directional distribution of solar radiation at the earth's surface. (*a*) Actual distribution. (*b*) Diffuse approximation.

Patent Owner Manufacturing Resources International, Inc.
Exhibit 2017 - Page 779 of 999

TABLE 12.2 Solar Absorptivity α_S and Emissivity ε of Surfaces Having Spectral Absorptivity Given in Figure 12.22

Surface	α_S	ε (300 K)	α_S/ε
Evaporated aluminum film	0.09	0.03	3.0
Fused quartz on aluminum film	0.19	0.81	0.24
White paint on metallic substrate	0.21	0.96	0.22
Black paint on metallic substrate	0.97	0.97	1.0
Stainless steel, as received, dull	0.50	0.21	2.4
Red brick	0.63	0.93	0.68
Human skin (Caucasian)	0.62	0.97	0.64
Snow	0.28	0.97	0.29
Corn leaf	0.76	0.97	0.78

Since temperatures typically range from 250 to 320 K, emission is concentrated in the spectral region from approximately 4 to 40 μm, with the peak occurring at approximately 10 μm.

Atmospheric emission is largely from the CO_2 and H_2O molecules and is concentrated in the spectral regions from 5 to 8 μm and above 13 μm. Although the spectral distribution of atmospheric emission does not correspond to that of a blackbody, its contribution to irradiation of the earth's surface can be estimated using Equation 12.26. In particular, earth irradiation due to atmospheric emission may be expressed in the form

$$G_{atm} = \sigma T_{sky}^4 \tag{12.67}$$

where T_{sky} is termed the effective sky temperature. Its value depends on atmospheric conditions, ranging from a low of 230 K under a cold, clear sky to a high of approximately 285 K under warm, cloudy conditions. At night, atmospheric emission is the only source of earth irradiation. When its value is small, as on a cool, clear night, an exposed pool of water may freeze even though the air temperature exceeds 273 K.

We close by recalling that values of the spectral properties of a surface at short wavelengths may be appreciably different from values at long wavelengths (Figures 12.17 and 12.22). Since solar radiation is concentrated in the short wavelength region of the spectrum and surface emission is at much longer wavelengths, it follows that many surfaces may not be approximated as gray in their response to solar irradiation. In other words, the solar absorptivity of a surface α_S may differ from its emissivity ε. Values of α_S and the emissivity at moderate temperatures are presented in Table 12.2 for representative surfaces. Note that the ratio α_S/ε is an important engineering parameter. Small values are desired if the surface is intended to reject heat; large values are required if the surface is intended to collect solar energy.

EXAMPLE 12.11

A flat-plate solar collector with no cover plate has a selective absorber surface of emissivity 0.1 and solar absorptivity 0.95. At a given time of day the absorber surface

Patent Owner Manufacturing Resources International, Inc.
Exhibit 2017 - Page 780 of 999

temperature T_s is 120°C when the solar irradiation is 750 W/m^2, the effective sky temperature is −10°C, and the ambient air temperature T_∞ is 30°C. Assume that the heat transfer convection coefficient for the calm day conditions can be estimated from

$$\bar{h} = 0.22(T_s - T_\infty)^{1/3}\ \text{W/m}^2 \cdot \text{K}$$

Calculate the useful heat removal rate (W/m^2) from the collector for these conditions. What is the corresponding efficiency of the collector?

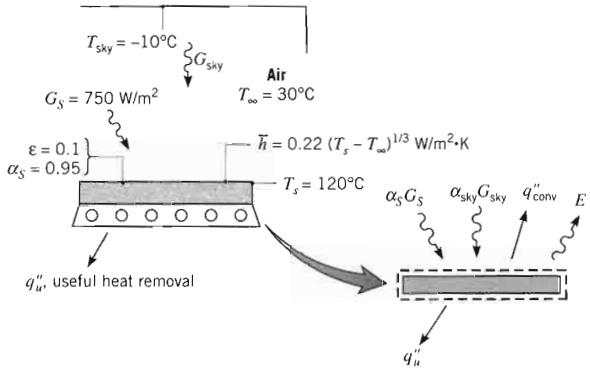
SOLUTION

Known: Operating conditions for a flat-plate solar collector.

Find:

1. Useful heat removal rate per unit area, q_u'' (W/m^2).
2. Efficiency η of the collector.

Schematic:



Assumptions:

1. Steady-state conditions.
2. Bottom of collector well insulated.
3. Absorber surface diffuse.

Analysis:

1. Performing an energy balance on the absorber,

$$\dot{E}_{in} - \dot{E}_{out} = 0$$

or, per unit surface area,

$$\alpha_S G_S + \alpha_{sky} G_{sky} - q''_{conv} - E - q_u'' = 0$$

Patent Owner Manufacturing Resources International, Inc.
Exhibit 2017 - Page 781 of 999

From Equation 12.67,

$$G_{sky} = \sigma T_{sky}^4$$

Since the sky radiation is concentrated in approximately the same spectral region as that of surface emission, it is reasonable to assume that

$$\alpha_{sky} \approx \varepsilon = 0.1$$

With

$$q''_{conv} = \bar{h}(T_s - T_\infty) = 0.22\,(T_s - T_\infty)^{4/3} \quad \text{and} \quad E = \varepsilon\sigma T_s^4$$

it follows that

$$q''_u = \alpha_S G_S + \varepsilon\sigma T_{sky}^4 - 0.22(T_s - T_\infty)^{4/3} - \varepsilon\sigma T_s^4$$

$$q''_u = \alpha_S G_S - 0.22(T_s - T_\infty)^{4/3} - \varepsilon\sigma(T_s^4 - T_{sky}^4)$$

$$q''_u = 0.95 \times 750\ \text{W/m}^2 - 0.22(120 - 30)^{4/3}\ \text{W/m}^2$$

$$-0.1 \times 5.67 \times 10^{-8}\ \text{W/m}^2 \cdot \text{K}^4(393^4 - 263^4)\ \text{K}^4$$

$$q''_u = (712.5 - 88.7 - 108.1)\ \text{W/m}^2 = 516\ \text{W/m}^2 \quad \triangleleft$$

2. The collector efficiency, defined as the fraction of the solar irradiation extracted as useful energy, is then

$$\eta = \frac{q''_u}{G_S} = \frac{516\ \text{W/m}^2}{750\ \text{W/m}^2} = 0.69 \quad \triangleleft$$

Comments:

1. Since the spectral range of G_{sky} is entirely different from that of G_S, it would be *incorrect* to assume that $\alpha_{sky} = \alpha_S$.
2. The convection heat transfer coefficient is extremely low ($\bar{h} \approx 1\ \text{W/m}^2 \cdot \text{K}$). With a modest increase to $\bar{h} = 5\ \text{W/m}^2 \cdot \text{K}$, the useful heat flux and the efficiency are reduced to $q''_u = 154\ \text{W/m}^2$ and $\eta = 0.21$. A cover plate can contribute significantly to reducing convection (and radiation) heat loss from the absorber plate.

12.9 *Summary*

Many new and important ideas have been introduced in this chapter, and at this stage you may well be confused, particularly by the terminology. However, the subject matter has been developed in a systematic fashion, and a careful rereading of the material should make you more comfortable with its application. A glossary has been provided in Table 12.3 to assist you in assimilating the terminology.

Patent Owner Manufacturing Resources International, Inc.
Exhibit 2017 - Page 782 of 999

TABLE 12.3 Glossary of Radiative Terms

Term	Definition
Absorption	The process of converting radiation intercepted by matter to internal thermal energy.
Absorptivity	Fraction of the incident radiation absorbed by matter. Equations 12.39, 12.40, and 12.43. Modifiers: *directional, hemispherical, spectral, total.*
Blackbody	The ideal emitter and absorber. Modifier referring to ideal behavior. Denoted by the subscript b.
Diffuse	Modifier referring to the directional independence of the intensity associated with emitted, reflected, or incident radiation.
Directional	Modifier referring to a particular direction. Denoted by the subscript θ.
Directional distribution	Refers to variation with direction.
Emission	The process of radiation production by matter at a finite temperature. Modifiers: *diffuse, blackbody, spectral.*
Emissive power	Rate of radiant energy emitted by a surface in all directions per unit area of the surface, E (W/m^2). Modifiers: *spectral, total, blackbody.*
Emissivity	Ratio of the radiation emitted by a surface to the radiation emitted by a blackbody at the same temperature. Equations 12.30, 12.31, 12.32, and 12.35. Modifiers: *directional, hemispherical, spectral, total.*
Gray surface	A surface for which the spectral absorptivity and the emissivity are independent of wavelength over the spectral regions of surface irradiation and emission.
Hemispherical	Modifier referring to all directions in the space above a surface.
Intensity	Rate of radiant energy propagation in a particular direction, per unit area normal to the direction, per unit solid angle about the direction, I (W/m$^2 \cdot$ sr). Modifier: *spectral.*
Irradiation	Rate at which radiation is incident on a surface from all directions per unit area of the surface, G (W/m^2). Modifiers: *spectral, total, diffuse.*
Kirchhoff's law	Relation between emission and absorption properties for surfaces irradiated by a blackbody at the same temperature. Equations 12.59, 12.60, 12.61, and 12.62.
Planck's law	Spectral distribution of emission from a blackbody. Equations 12.23 and 12.24.
Radiosity	Rate at which radiation leaves a surface due to emission and reflection in all directions per unit area of the surface, J (W/m^2). Modifiers: *spectral, total.*
Reflection	The process of redirection of radiation incident on a surface. Modifiers: *diffuse, specular.*
Reflectivity	Fraction of the incident radiation reflected by matter. Equations 12.46, 12.47, and 12.49. Modifiers: *directional, hemispherical, spectral, total.*

Patent Owner Manufacturing Resources International, Inc.
Exhibit 2017 - Page 783 of 999

TABLE 12.3 *Continued*

Term	Definition
Semitransparent	Refers to a medium in which radiation absorption is a volumetric process.
Solid angle	Region subtended by an element of area on the surface of a sphere with respect to the center of the sphere, ω (sr). Equations 12.2 and 12.3.
Spectral	Modifier referring to a single-wavelength (monochromatic) component. Denoted by the subscript λ.
Spectral distribution	Refers to variation with wavelength.
Specular	Refers to a surface for which the angle of reflected radiation is equal to the angle of incident radiation.
Stefan–Boltzmann law	Emissive power of a blackbody. Equation 12.26.
Thermal radiation	Electromagnetic energy emitted by matter at a finite temperature and concentrated in the spectral region from approximately 0.1 to 100 μm.
Total	Modifier referring to all wavelengths.
Transmission	The process of thermal radiation passing through matter.
Transmissivity	Fraction of the incident radiation transmitted by matter. Equations 12.51 and 12.52. Modifiers: *hemispherical, spectral, total.*
Wien's law	Locus of the wavelength corresponding to peak emission by a blackbody. Equation 12.25.

Test your understanding of the terms and concepts introduced in this chapter by addressing the following questions.

- What is the nature of radiation? What two important features characterize radiation?
- What is the physical origin of radiation *emission* from a surface? How does emission affect the thermal energy of a material?
- In what region of the electromagnetic spectrum is *thermal radiation* concentrated?
- What is the *spectral intensity* of radiation emitted by a surface? On what variables does it depend? How may knowledge of this dependence be used to determine the rate at which matter loses thermal energy due to emission from its surface?
- What is a *steradian*? How many steradians are associated with a hemisphere?
- What is the distinction between *spectral* and *total* radiation? Between *directional* and *hemispherical* radiation?
- What is *total emissive power*? What role does it play in a surface energy balance?
- What is a *diffuse emitter*? For such an emitter, how is the intensity related to the total emissive power?

Patent Owner Manufacturing Resources International, Inc.
Exhibit 2017 - Page 784 of 999

- What is *irradiation*? How is it related to the intensity of incident radiation, if the radiation is diffuse?
- What is *radiosity*? What role do the total radiosity and the total irradiation play in a surface energy balance?
- What are the characteristics of a *blackbody*? Does such a thing actually exist in nature? What is the principal role of blackbody behavior in radiation analysis?
- What is the *Planck distribution*? What is *Wien's displacement law*?
- From memory, sketch the spectral distribution of radiation emission from a blackbody at three temperatures, $T_1 < T_2 < T_3$. Identify salient features of the distributions.
- In what region of the electromagnetic spectrum is radiation emission from a surface at room temperature concentrated? What is the spectral region of concentration for a surface at 1000°C? For the surface of the sun?
- What is the *Stefan–Boltzmann law*? How would you determine the total intensity of radiation emitted by a blackbody at a prescribed temperature?
- How would you approximate the total irradiation of a small surface in a large isothermal enclosure?
- In the term *total*, *hemispherical emissivity*, to what do the adjectives *total* and *hemispherical* refer?
- How does the directional emissivity of a material change as the zenith angle associated with emission approaches 90°?
- If the spectral emissivity of a material increases with increasing wavelength, how does its total emissivity vary with temperature?
- What is larger, the emissivity of a polished metal or an oxidized metal? A refractory brick or ice?
- What processes accompany irradiation of a *semitransparent* material? An *opaque* material?
- Are glass and water semitransparent or opaque materials?
- How is the perceived color of a material determined by its response to irradiation in the infrared portion of the spectrum? How is its color affected by its temperature?
- Can snow be thought of as a good absorber or reflector of incident radiation?
- How is the thermal energy of a material affected by the absorption of incident radiation? By the reflection of incident radiation?
- Can the total absorptivity of an opaque surface at a fixed temperature differ according to whether irradiation is from a source at room temperature or from the sun? Can its reflectivity differ? Its emissivity?
- What is a *diffuse reflector*? A *specular reflector*? How does the roughness of a surface affect the nature of reflection for the surface?
- Under what conditions is there equivalence between the spectral, directional emissivity of a surface and the spectral, directional absorptivity? The spectral, hemispherical emissivity and the spectral, hemispherical absorptivity? The total, hemispherical emissivity and the total, hemispherical absorptivity?
- What is a *gray surface*?
- What is the directional nature of solar radiation outside the earth's atmosphere? At the surface of the earth?
- What are representative values of the total, hemispherical emissivity for constituents of the natural environment, such as vegetation, water, and ice?
- What is *sky radiation*?

Patent Owner Manufacturing Resources International, Inc.
Exhibit 2017 - Page 785 of 999

References

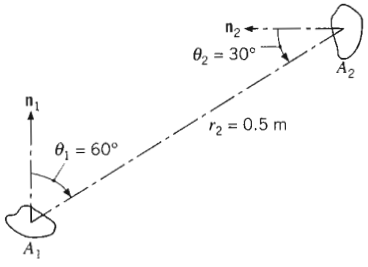
1. Planck, M., *The Theory of Heat Radiation,* Dover Publications, New York, 1959.
2. Gubareff, G. G., J. E. Janssen, and R. H. Torberg, *Thermal Radiation Properties Survey,* 2nd ed., Honeywell Research Center, Minneapolis, 1960.
3. Wood, W. D., H. W. Deem, and C. F. Lucks, *Thermal Radiative Properties,* Plenum Press, New York, 1964.
4. Touloukian, Y. S., *Thermophysical Properties of High Temperature Solid Materials,* Macmillan, New York, 1967.
5. Touloukian, Y. S., and D. P. DeWitt, *Thermal Radiative Properties,* Vols. 7, 8, and 9, from *Thermophysical Properties of Matter,* TPRC Data Series, Y. S. Touloukian and C. Y. Ho, Eds., IFI Plenum, New York, 1970–1972.
6. Siegel, R., and J. R. Howell, *Thermal Radiation Heat Transfer,* 4th ed., Taylor & Francis, New York, 2002.
7. Duffie, J.A., and W.A. Beckman, *Solar Engineering of Thermal Processes*, 2nd ed., Wiley, New York, 1991.
8. Meinel, A. B., and M. P. Meinel, *Applied Solar Energy: An Introduction,* Addison-Wesley, Reading, MA, 1976.
9. Sayigh, A. A. M., Ed., *Solar Energy Engineering,* Academic Press, New York, 1977.
10. Goswami, D.Y., F. Kreith, and J. F. Kreider, *Principles of Solar Energy*, 2nd ed., Taylor & Francis, New York, 2002.
11. Howell, J. R., R. B. Bannerot, and G. C. Vliet, *Solar-Thermal Energy Systems, Analysis and Design,* McGraw-Hill, New York, 1982.

Problems

Intensity, Emissive Power, and Irradiation

12.1 What is the irradiation at surfaces A_2, A_3, and A_4 of Example 12.1 due to emission from A_1?

12.2 Consider a small surface of area $A_1 = 10^{-4}$ m^2, which emits diffusely with a total, hemispherical emissive power of $E_1 = 5 \times 10^4$ W/m^2.

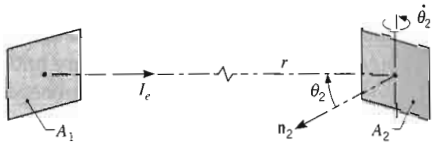


(a) At what rate is this emission intercepted by a small surface of area $A_2 = 5 \times 10^{-4}$ m^2, which is oriented as shown?

(b) What is the irradiation G_2 on A_2?

(c) For zenith angles of $\theta_2 = 0$, 30, and 60°, plot G_2 as a function of the separation distance for $0.25 \leq r_2 \leq 1.0$ m.

12.3 A small stationary surface of area $A_1 = 10^{-4}$ m^2 emits diffusely with a total intensity of $I_e = 100$ W/m$^2 \cdot$ sr. A second surface of equivalent area $A_2 = 10^{-4}$ m^2 is located at a fixed distance of $r = 0.5$ m from A_1. The connecting line between the two surfaces remains perpendicular to A_1, while A_2 rotates at an angular frequency of $\dot{\theta}_2 = d\theta_2/dt = 2$ rad/s.



What is the amount of energy intercepted by the two sides of A_2, during one complete revolution?

12.4 A furnace with an aperture of 20-mm diameter and emissive power of 3.72×10^5 W/m^2 is used to calibrate a heat flux gage having a sensitive area of 1.6×10^{-5} m^2.

(a) At what distance, measured along a normal from the aperture, should the gage be positioned to receive irradiation of 1000 W/m^2?

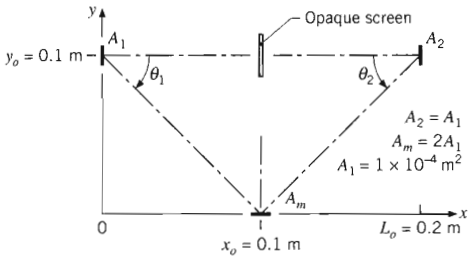
(b) If the gage is tilted off normal by 20°, what will be its irradiation?

(c) For tilt angles of 0, 20, and 60°, plot the gage irradiation as a function of the separation distance for values ranging from 100 to 300 mm.

12.5 A small radiant source A_1 emits diffusely with an intensity $I_1 = 1.2 \times 10^5$ W/m$^2 \cdot$ sr. The radiation detector A_2 is aligned normal to the source at a distance of $L_o = 0.2$ m. An opaque screen is positioned midway between A_1 and A_2 to prevent radiation from the source reaching the detector. The small surface A_m is a perfectly diffuse

Patent Owner Manufacturing Resources International, Inc.
Exhibit 2017 - Page 786 of 999

mirror that permits radiation emitted from the source to be reflected into the detector.



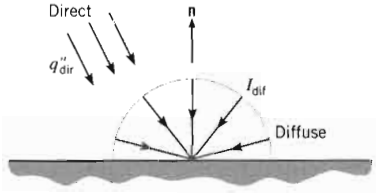
(a) Calculate the radiant power incident on A_m due to emission from the source A_1, $q_{1\to m}$(W).

(b) Assuming that the radiant power, $q_{1\to m}$, is perfectly and diffusely reflected, calculate the intensity leaving A_m, I_m (W/m^2 · sr).

(c) Calculate the radiant power incident on A_2 due to the reflected radiation leaving A_m, $q_{m\to 2}(\mu$W).

(d) Plot the radiant power $q_{m\to 2}$ as a function of the lateral separation distance y_o for the range $0 \le y_o \le 0.2$ m. Explain the features of the resulting curve.

12.6 According to its directional distribution, solar radiation incident on the earth's surface may be divided into two components. The *direct* component consists of parallel rays incident at a fixed zenith angle θ, while the *diffuse* component consists of radiation that may be approximated as being diffusely distributed with θ.



Consider clear sky conditions for which the direct radiation is incident at $\theta = 30°$, with a total flux (based on an area that is normal to the rays) of $q''_{dir} = 1000$ W/m^2, and the total intensity of the diffuse radiation is $I_{dif} = 70$ W/m^2 · sr. What is the total solar irradiation at the earth's surface?

12.7 Solar radiation incident on the earth's surface may be divided into the direct and diffuse components described in Problem 12.6. Consider conditions for a day in which the intensity of the direct solar radiation is $I_{dir} = 2.10 \times 10^7$ W/m^2 · sr in the solid angle subtended by the sun with respect to the earth, $\Delta\omega_s = 6.74 \times 10^{-5}$ sr. The intensity of the diffuse radiation is $I_{dif} = 70$ W/m^2 · sr.

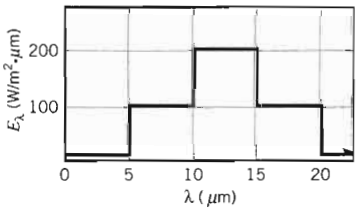
(a) What is the total solar irradiation at the earth's surface when the direct radiation is incident at $\theta = 30°$?

(b) Verify the prescribed value for $\Delta\omega_s$, recognizing that the diameter of the sun is 1.39×10^9 m and the distance between the sun and the earth is 1.496×10^{11} m (1 astronomical unit).

12.8 On an overcast day the directional distribution of the solar radiation incident on the earth's surface may be approximated by an expression of the form $I_i = I_n \cos\theta$, where $I_n = 80$ W/m^2 · sr is the total intensity of radiation directed normal to the surface and θ is the zenith angle. What is the solar irradiation at the earth's surface?

12.9 Determine the fraction of the total, hemispherical emissive power that leaves a diffuse surface in the directions $\pi/4 \le \theta \le \pi/2$ and $0 \le \phi \le \pi$.

12.10 The spectral distribution of the radiation emitted by a diffuse surface may be approximated as follows.

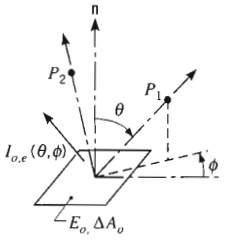


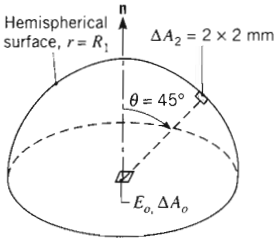
(a) What is the total emissive power?

(b) What is the total intensity of the radiation emitted in the normal direction and at an angle of 30° from the normal?

(c) Determine the fraction of the emissive power leaving the surface in the directions $\pi/4 \le \theta \le \pi/2$.

12.11 Consider a 5-mm-square, diffuse surface ΔA_o having a total emissive power of $E_o = 4000$ W/m^2. The radiation





Patent Owner Manufacturing Resources International, Inc.
Exhibit 2017 - Page 787 of 999

field due to emission into the hemispherical space above the surface is diffuse, thereby providing a uniform intensity $I(\theta, \phi)$. Moreover, if the space is a nonparticipating medium (nonabsorbing, nonscattering, and nonemitting), the intensity is independent of radius for any (θ, ϕ) direction. Hence intensities at any points P_1 and P_2 would be equal.

(a) What is the rate at which radiant energy is emitted by ΔA_o, q_{emit}?

(b) What is the intensity $I_{o,e}$ of the radiation field emitted from the surface ΔA_o?

(c) Beginning with Equation 12.8 and presuming knowledge of the intensity $I_{o,e}$, obtain an expression for q_{emit}.

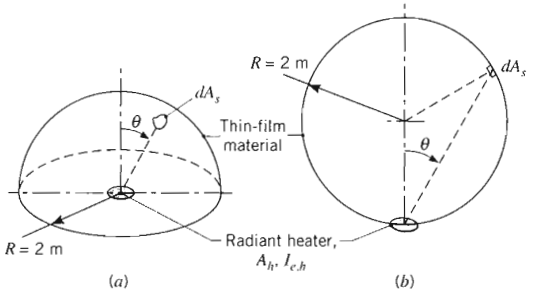
(d) Consider the hemispherical surface located at $r = R_1 = 0.5$ m. Using the conservation of energy requirement, determine the rate at which radiant energy is incident on this surface due to emission from ΔA_o.

(e) Using Equation 12.6, determine the rate at which radiant energy leaving ΔA_o is intercepted by the small area ΔA_2 located in the direction $(45°, \phi)$ on the hemispherical surface. What is the irradiation on ΔA_2?

(f) Repeat part (e) for the location $(0°, \phi)$. Are the irradiations at the two locations equal?

(g) Using Equation 12.13, determine the irradiation G_1 on the hemispherical surface at $r = R_1$.

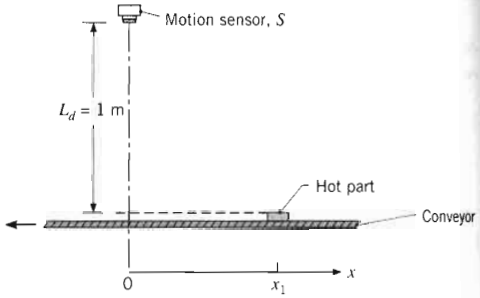
12.12 During radiant heat treatment of a thin-film material, its shape, which may be hemispherical (a) or spherical (b), is maintained by a relatively low air pressure (as in the case of a rubber balloon). Irradiation on the film is due to emission from a radiant heater of area $A_h = 0.0052$ m^2, which emits diffusely with an intensity of $I_{e,h} = 169{,}000$ W/m$^2 \cdot$ sr.



(a) Obtain an expression for the irradiation on the film as a function of the zenith angle θ.

(b) Based on the expressions derived in part (a), which shape provides the more uniform irradiation G and hence provides better quality control for the treatment process?

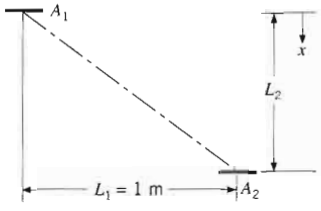
12.13 In order to initiate a process operation, an infrared motion sensor (radiation detector) is employed to determine the approach of a hot part on a conveyor system. To set the sensor's amplifier discriminator, the engineer needs a relationship between the sensor output signal, S, and the position of the part on the conveyor. The sensor output signal is proportional to the rate at which radiation is incident on the sensor.



(a) For $L_d = 1$ m, at what location x_1 will the sensor signal S_1 be 75% of the signal corresponding to the position directly beneath the sensor, S_o $(x = 0)$?

(b) For values of $L_d = 0.8$, 1.0, and 1.2 m, plot the signal ratio, S/S_o, versus part position, x, for signal ratios in the range from 1.0 to 0.2. Compare the x-locations for which $S/S_o = 0.75$.

12.14 A small radiant heat source of area $A_1 = 2 \times 10^{-4}$ m^2 emits diffusely with an intensity $I_1 = 1000$ W/m$^2 \cdot$ sr. A second small area, $A_2 = 1 \times 10^{-4}$ m^2, is located as shown in the sketch.



(a) Determine the irradiation of A_2 for $L_2 = 0.5$ m.

(b) Plot the irradiation of A_2 over the range $0 \leq L_2 \leq 10$ m.

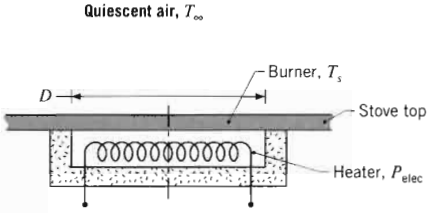
Blackbody Radiation

12.15 Assuming blackbody behavior, determine the temperature of, and the energy emitted by, areas A_1 in Example

Patent Owner Manufacturing Resources International, Inc.
Exhibit 2017 - Page 788 of 999

12.1 and Problems 12.3, 12.5, and 12.14, as well as area A_n in Problem 12.12.

12.16 The dark surface of a ceramic stove top may be approximated as a blackbody. The "burners," which are integral with the stove top, are heated from below by electric resistance heaters.



(a) Consider a burner of diameter $D = 200$ mm operating at a uniform surface temperature of $T_s = 250°C$ in ambient air at $T_\infty = 20°C$. Without a pot or pan on the burner, what are the rates of heat loss by radiation and convection from the burner? If the efficiency associated with energy transfer from the heaters to the burners is 90%, what is the electric power requirement? At what wavelength is the spectral emission a maximum?

(b) Compute and plot the effect of the burner temperature on the heat rates for $100 \leq T_s \leq 350°C$.

12.17 A spherical aluminum shell of inside diameter $D = 2$ m is evacuated and is used as a radiation test chamber. If the inner surface is coated with carbon black and maintained at 600 K, what is the irradiation on a small test surface placed in the chamber? If the inner surface were not coated and maintained at 600 K, what would the irradiation be?

12.18 An enclosure has an inside area of 100 m^2, and its inside surface is black and is maintained at a constant temperature. A small opening in the enclosure has an area of 0.02 m^2. The radiant power emitted from this opening is 70 W. What is the temperature of the interior enclosure wall? If the interior surface is maintained at this temperature, but is now polished, what will be the value of the radiant power emitted from the opening?

12.19 Assuming the earth's surface is black, estimate its temperature if the sun has an equivalent blackbody temperature of 5800 K. The diameters of the sun and earth are 1.39×10^9 and 1.29×10^7 m, respectively, and the distance between the sun and the earth is 1.5×10^{11} m.

12.20 The energy flux associated with solar radiation incident on the outer surface of the earth's atmosphere has been accurately measured and is known to be 1353 W/m^2. The diameters of the sun and earth are 1.39×10^9 and 1.29×10^7 m, respectively, and the distance between the sun and the earth is 1.5×10^{11} m.

(a) What is the emissive power of the sun?

(b) Approximating the sun's surface as black, what is its temperature?

(c) At what wavelength is the spectral emissive power of the sun a maximum?

(d) Assuming the earth's surface to be black and the sun to be the only source of energy for the earth, estimate the earth's surface temperature.

12.21 A small flat plate is positioned just beyond the earth's atmosphere and is oriented such that the normal to the plate passes through the center of the sun. Refer to Problem 12.20 for pertinent earth–sun dimensions.

(a) What is the solid angle subtended by the sun about a point on the surface of the plate?

(b) Determine the incident intensity, I_i, on the plate using the known value of the solar irradiation above the earth's atmosphere ($G_S = 1353$ W/m^2).

(c) Sketch the incident intensity I_i as a function of the zenith angle θ, where θ is measured from the normal to the plate.

12.22 Estimate the wavelength corresponding to maximum emission from each of the following surfaces: the sun, a tungsten filament at 2500 K, a heated metal at 1500 K, human skin at 305 K, and a cryogenically cooled metal surface at 60 K. Estimate the fraction of the solar emission that is in the following spectral regions: the ultraviolet, the visible, and the infrared.

12.23 The human eye, as well as the light-sensitive chemicals on color photographic film, respond differently to lighting sources with different spectral distributions. *Daylight* lighting corresponds to the spectral distribution of the solar disk, which may be approximated as a blackbody at 5800 K. *Incandescent* lighting from the usual household lamp bulb corresponds approximately to the spectral distribution of a blackbody at 2900 K.

(a) Calculate the band emission fractions for the visible region, 0.47 μm (blue) to 0.65 μm (red), for each of the two lighting sources.

(b) Calculate the wavelength corresponding to the maximum spectral intensity for each of the light sources. Comment on the results of your calculation in terms of the rendering of *true* colors under the different lighting conditions.

12.24 Thermal imagers have radiation detectors that are sensitive to a spectral region and provide white-black or color images with shading to indicate relative temperature differences in the scene. The imagers,

Patent Owner Manufacturing Resources International, Inc.
Exhibit 2017 - Page 789 of 999

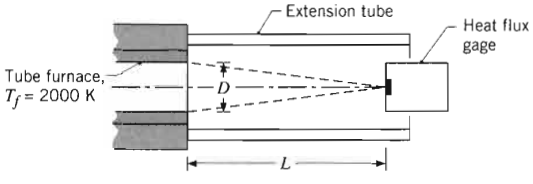
which have appearances similar to a video camcorder, have numerous applications, such as for equipment maintenance to identify overheated motors or electrical transformers and for fire-fighting service to determine the direction of fire spread and to aid search and rescue for victims. The most common operating spectral regions are 3 to 5 μm and 8 to 14 μm. The selection of a particular region typically depends on the temperature of the scene, although the atmospheric conditions (water vapor, smoke, etc.) may also be important.

(a) Determine the band emission fractions for each of the spectral regions, 3 to 5 μm and 8 to 14 μm, for temperatures of 300 and 900 K.

(b) Using the *IHT* model builder *Tools/Radiation/Band Emission Factor*, calculate and plot the band emission factors for each of the spectral regions for the temperature range 300 to 1000 K. Identify the temperatures at which the fractions are a maximum. What conclusions can you draw from this graph concerning the choice of an imager for an application?

(c) The noise-equivalent temperature (NET) is a specification of the imager that indicates the minimum temperature change that can be resolved in the image scene. Consider imagers operating at the maximum-fraction temperatures identified in part (b). For each of these conditions, determine the sensitivity (%) required of the radiation detector in order to provide a NET of 5°C. Explain the significance of your results. *Note:* The sensitivity (% units) can be defined as the difference in the band emission fractions for two temperatures differing by the NET, divided by the band emission fraction at one of the temperatures.

12.25 A furnace with a long isothermal, graphite tube of diameter $D = 12.5$ mm is maintained at $T_f = 2000$ K and is used as a blackbody source to calibrate heat flux gages. Traditional heat flux gages are constructed as blackened thin films with thermopiles to indicate the temperature change caused by absorption of the incident radiant power over the entire spectrum. The traditional gage of interest has a sensitive area of 5 mm^2 and is mounted coaxial with the furnace centerline, but positioned at a distance of $L = 60$ mm from the beginning of the heated section. The cool extension tube serves to shield the gage from extraneous radiation sources and to contain the inert gas required to prevent rapid oxidation of the graphite tube.

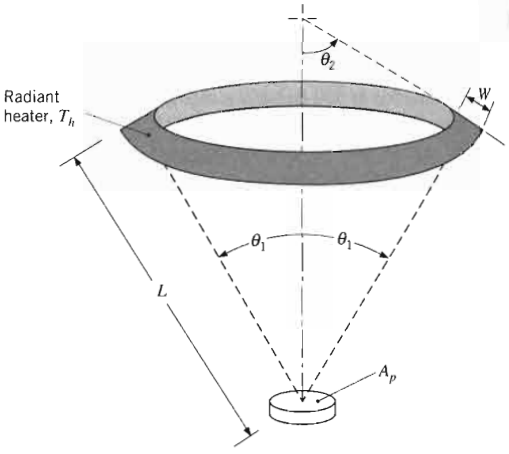


(a) Calculate the heat flux (W/m^2) on the traditional gage for this condition, assuming that the extension tube is cold relative to the furnace.

(b) The traditional gage is replaced by a solid-state (photoconductive) heat flux gage of the same area, but sensitive only to the spectral region between 0.4 and 2.5 μm. Calculate the radiant heat flux incident on the solid-state gage within the prescribed spectral region.

(c) Calculate and plot the total heat flux and the heat flux in the prescribed spectral region for the solid-state gage as a function of furnace temperature for the range $2000 \leq T_f \leq 3000$ K. Which gage will have an output signal that is more sensitive to changes in the furnace temperature?

12.26 An electrically powered, ring-shaped radiant heating element is maintained at a temperature of $T_h = 3000$ K and is used in a manufacturing process to heat a small part having a surface area of $A_p = 0.007$ m^2. The surface of the heating element may be assumed to be black.



For $\theta_1 = 30°$, $\theta_2 = 60°$, $L = 3$ m, and $W = 30$ mm, what is the rate at which radiant energy emitted by the heater is incident on the part?

12.27 Approximations to Planck's law for the spectral emissive power are the Wien and Rayleigh-Jeans spectral distributions, which are useful for the extreme low and high limits of the product λT, respectively.

Patent Owner Manufacturing Resources International, Inc.
Exhibit 2017 - Page 790 of 999

(a) Show that Planck's spectral distribution will have the form

$$E_{\lambda,b}(\lambda, T) \approx \frac{C_1}{\lambda^5} \exp\left(-\frac{C_2}{\lambda T}\right)$$

when $C_2/\lambda T \gg 1$ and determine the error (compared to Planck's law) for the condition $\lambda T = 2898\ \mu\text{m} \cdot \text{K}$. This form is known as Wien's law.

(b) Show that the Planck distribution will have the form

$$E_{\lambda,b}(\lambda, T) \approx \frac{C_1}{C_2} \frac{T}{\lambda^4}$$

when $C_2/\lambda T \ll 1$ and determine the error (compared to Planck's law) for the condition $\lambda T = 100{,}000\ \mu\text{m} \cdot \text{K}$. This form is known as the Rayleigh-Jeans law.

12.28 Isothermal furnaces with small apertures approximating a blackbody are frequently used to calibrate heat flux gages, radiation thermometers, and other radiometric devices. In such applications, it is necessary to control power to the furnace such that the variation of temperature and the spectral intensity of the aperture are within desired limits.

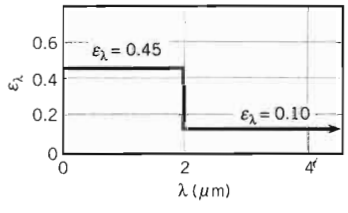
(a) By considering the Planck spectral distribution, Equation 12.24, show that the ratio of the fractional change in the spectral intensity to the fractional change in the temperature of the furnace has the form

$$\frac{dI_\lambda/I_\lambda}{dT/T} = \frac{C_2}{\lambda T} \frac{1}{1 - \exp(-C_2/\lambda T)}$$

(b) Using this relation, determine the allowable variation in temperature of the furnace operating at 2000 K to ensure that the spectral intensity at 0.65 μm will not vary by more than 0.5%. What is the allowable variation at 10 μm?

Properties: Emissivity

12.29 The spectral, hemispherical emissivity of tungsten may be approximated by the distribution depicted below. Consider a cylindrical tungsten filament that is of diameter $D = 0.8$ mm and length $L = 20$ mm. The filament is enclosed in an evacuated bulb and is heated by an electrical current to a steady-state temperature of 2900 K.



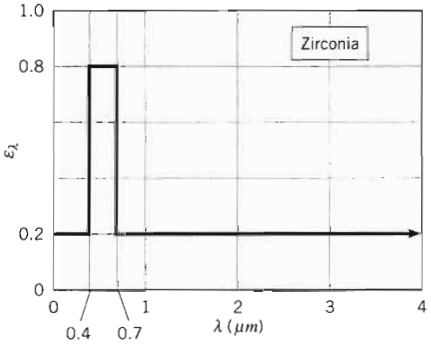
(a) What is the total hemispherical emissivity when the filament temperature is 2900 K?

(b) Assuming the surroundings are at 300 K, what is the initial rate of cooling of the filament when the current is switched off?

(c) Generate a plot of the emissivity as a function of filament temperature for $1300 \leq T \leq 2900$ K.

(d) Estimate the time required for the filament to cool from 2900 to 1300 K.

12.30 A zirconia-based ceramic has the spectral, hemispherical emissivity shown below and is being considered for use as the filament of a light bulb.

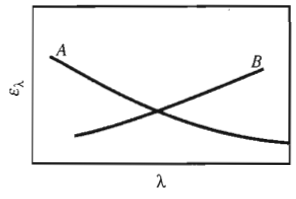


(a) What is the total, hemispherical emissivity of a zirconia filament operating at 3000 K?

(b) Using the spectral distribution provided in Problem 12.29, determine the total hemispherical emissivity of a tungsten filament at 3000 K and compare the result with that obtained for zirconia. For zirconia and tungsten operating at 3000 K in an evacuated bulb, what filament requires the larger power consumption?

(c) With respect to the production of visible radiation, which of the two filaments is the more efficient? Justify your answer quantitatively.

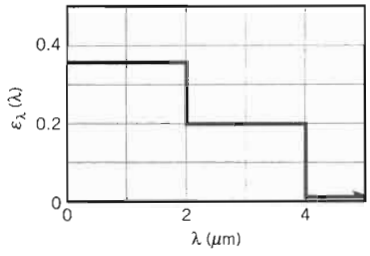
12.31 For materials A and B, whose spectral hemispherical emissivities vary with wavelength as shown below,



Patent Owner Manufacturing Resources International, Inc.
Exhibit 2017 - Page 791 of 999

how does the total, hemispherical emissivity vary with temperature? Explain briefly.

12.32 Consider the metallic surface of Example 12.6. Additional measurements of the spectral, hemispherical emissivity yield a spectral distribution which may be approximated as follows:



(a) Determine corresponding values of the total, hemispherical emissivity ε and the total emissive power E at 2000 K.

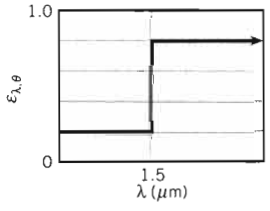
(b) Plot the emissivity as a function of temperature for $500 \leq T \leq 3000$ K. Explain the variation.

12.33 The spectral emissivity of unoxidized titanium at room temperature is well described by the expression $\varepsilon_\lambda = 0.52\lambda^{-0.5}$ for $0.3\ \mu\text{m} \leq \lambda \leq 30\ \mu\text{m}$.

(a) Determine the emissive power associated with an unoxidized titanium surface at $T = 300$ K. Assume the spectral emissivity is $\varepsilon_\lambda = 0.1$ for $\lambda > 30\ \mu$m.

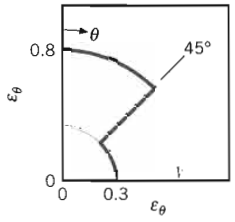
(b) Determine the value of λ_{max} for the emissive power of the surface in part (a).

12.34 The spectral, directional emissivity of a diffuse material at 2000 K has the following distribution:



Determine the total, hemispherical emissivity at 2000 K. Determine the emissive power over the spectral range 0.8 to 2.5 μm *and* for the directions $0 \leq \theta \leq 30°$.

12.35 Consider the directionally selective surface having the directional emissivity ε_θ, as shown. Assuming that the surface is isotropic in the ϕ direction, calculate the ratio of the normal emissivity ε_n to the hemispherical emissivity ε_h.



12.36 The directional total emissivity of nonmetallic materials may be approximated as $\varepsilon_\theta = \varepsilon_n \cos\theta$, where ε_n is the normal emissivity. Show that the total hemispherical emissivity for such materials is 2/3 of the normal emissivity.

12.37 A sphere is suspended in air in a dark room and maintained at a uniform incandescent temperature. When first viewed with the naked eye, the sphere appears to be brighter around the rim. After several hours, however, it appears to be brighter in the center. Of what type material would you reason the sphere is made? Give plausible reasons for the nonuniformity of brightness of the sphere and for the changing appearance with time.

12.38 A proposed *proximity meter* is based on the physical arrangement of Problem 12.14. The sensing area of a meter that is installed on a vehicle, A_2, is irradiated by a stationary warm object, A_1. The sensor's electrical output signal is proportional to its irradiation.

(a) The object temperature and emissivity are 200°C and $\varepsilon = 0.85$, respectively. Determine the distance, $L_{2,crit}$, associated with the maximum sensor output signal. Assume the object is a diffuse emitter.

(b) If the object emits as a nonmetallic material, the total directional emissivity may be approximated as $\varepsilon_\theta = \varepsilon_n \cos\theta$, where ε_n is the normal emissivity (Problem 12.36). Determine the distance $L_{2,crit}$ associated with the maximum sensor output signal.

(c) Calculate and plot the irradiation of A_2 over the range $0 \leq L_2 \leq 10$ m.

12.39 A radiation thermometer is a device that responds to a radiant flux within a prescribed spectral interval and is calibrated to indicate the temperature of a blackbody that produces the same flux.

(a) When viewing a surface at an elevated temperature T_s and emissivity less than unity, the thermometer will indicate an apparent temperature referred to as the brightness or spectral radiance temperature T_λ. Will T_λ be greater than, less than, or equal to T_s?

(b) Write a
power o
distribut
emissivi
expressi
of the su

where λ
thermo

(c) Conside
a spect
0.65 μm
meter i
(0.65 μ
Wien's
proxim

12.40 For a presc
spectral int
ted by a dif
surface ten
known, or t
known.

(a) Definir
minatic
this un
sity me
the int
the un
For T =

(b) Defini
minati
this ur
sity m
in the
tainty

12.41 Sheet stee
steel mill
$\delta = 3$ mm
tral, hemis

1.0
0.6
ε_λ 0.4
0.2
(

Patent Owner Manufacturing Resources International, Inc.
Exhibit 2017 - Page 792 of 999

(b) Write an expression for the spectral emissive power of the surface in terms of Wien's spectral distribution (see Problem 12.27) and the spectral emissivity of the surface. Write the equivalent expression using the spectral radiance temperature of the surface and show that

$$\frac{1}{T_s} = \frac{1}{T_\lambda} + \frac{\lambda}{C_2} \ln \varepsilon_\lambda$$

where λ represents the wavelength at which the thermometer operates.

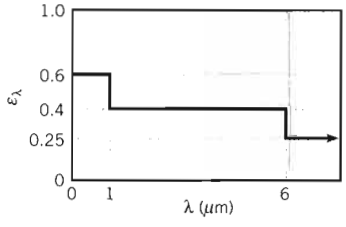
(c) Consider a radiation thermometer that responds to a spectral flux centered about the wavelength 0.65 μm. What temperature will the thermometer indicate when viewing a surface with ε_λ (0.65 μm) = 0.9 and T_s = 1000 K? Verify that Wien's spectral distribution is a reasonable approximation to Planck's law for this situation.

12.40 For a prescribed wavelength λ, measurement of the spectral intensity $I_{\lambda,e}(\lambda, T) = \varepsilon_\lambda I_{\lambda,b}$ of radiation emitted by a diffuse surface may be used to determine the surface temperature, if the spectral emissivity ε_λ is known, or the spectral emissivity, if the temperature is known.

(a) Defining the uncertainty of the temperature determination as dT/T, obtain an expression relating this uncertainty to that associated with the intensity measurement, dI_λ/I_λ. For a 10% uncertainty in the intensity measurement at λ = 10 μm, what is the uncertainty in the temperature for T = 500 K? For T = 1000 K?

(b) Defining the uncertainty of the emissivity determination as $d\varepsilon_\lambda/\varepsilon_\lambda$, obtain an expression relating this uncertainty to that associated with the intensity measurement, dI_λ/I_λ. For a 10% uncertainity in the intensity measurement, what is the uncertainty in the emissivity?

12.41 Sheet steel emerging from the hot roll section of a steel mill has a temperature of 1200 K, a thickness of δ = 3 mm, and the following distribution for the spectral, hemispherical emissivity.

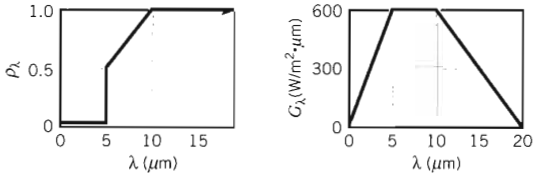


The density and specific heat of the steel are 7900 kg/m^3 and 640 J/kg · K, respectively. What is the total, hemispherical emissivity? Accounting for emission from both sides of the sheet and neglecting conduction, convection, and radiation from the surroundings, determine the initial time rate of change of the sheet temperature $(dT/dt)_i$. As the steel cools, it oxidizes and its total, hemispherical emissivity increases. If this increase may be correlated by an expression of the form $\varepsilon = \varepsilon_{1200}[1200\ \text{K}/T\ (\text{K})]$, how long will it take for the steel to cool from 1200 to 600 K?

12.42 A large body of nonluminous gas at a temperature of 1200 K has emission bands between 2.5 and 3.5 μm and between 5 and 8 μm. The effective emissivity in the first band is 0.8 and in the second 0.6. Determine the emissive power of this gas.

Absorptivity, Reflectivity, and Transmissivity

12.43 An opaque surface with the prescribed spectral, hemispherical reflectivity distribution is subjected to the spectral irradiation shown.



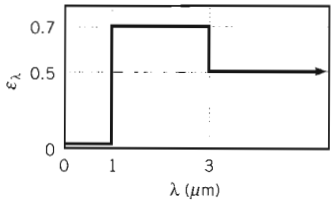
(a) Sketch the spectral, hemispherical absorptivity distribution.

(b) Determine the total irradiation on the surface.

(c) Determine the radiant flux that is absorbed by the surface.

(d) What is the total, hemispherical absorptivity of this surface?

12.44 A small, opaque, diffuse object at T_s = 400 K is suspended in a large furnace whose interior walls are at T_f = 2000 K. The walls are diffuse and gray and have an emissivity of 0.20. The spectral, hemispherical emissivity for the surface of the small object is given below.



Patent Owner Manufacturing Resources International, Inc.
Exhibit 2017 - Page 793 of 999

(a) Determine the total emissivity and absorptivity of the surface.

(b) Evaluate the reflected radiant flux and the net radiative flux *to* the surface.

(c) What is the spectral emissive power at $\lambda = 2\ \mu$m?

(d) What is the wavelength $\lambda_{1/2}$ for which one-half of the total radiation emitted by the surface is in the spectral region $\lambda \geq \lambda_{1/2}$?

12.45 The spectral reflectivity distribution for white paint (Figure 12.22) can be approximated by the following stair-step function:

α_λ	0.75	0.15	0.96
λ (μm)	<0.4	0.4–3.0	>3.0

A small flat plate coated with this paint is suspended inside a large enclosure, and its temperature is maintained at 400 K. The surface of the enclosure is maintained at 3000 K and the spectral distribution of its emissivity has the following characteristics:

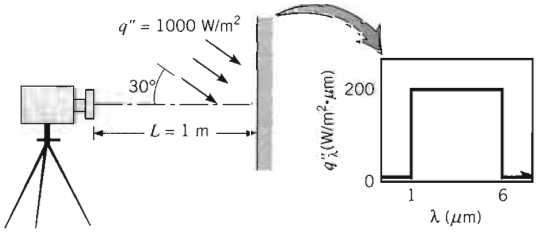
ε_λ	0.2	0.9
λ (μm)	<2.0	>2.0

(a) Determine the total emissivity, ε, of the enclosure surface.

(b) Determine the total emissivity, ε, and absorptivity, α, of the plate.

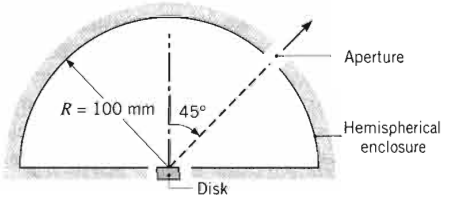
12.46 An opaque surface, 2 m by 2 m, is maintained at 400 K and is simultaneously exposed to solar irradiation with $G = 1200$ W/m^2. The surface is diffuse and its spectral absorptivity is $\alpha_\lambda = 0$, 0.8, 0, and 0.9 for $0 \leq \lambda \leq 0.5\ \mu$m, $0.5\ \mu\text{m} < \lambda \leq 1\ \mu$m, $1\ \mu\text{m} < \lambda \leq 2\ \mu$m, and $\lambda > 2\ \mu$m, respectively. Determine the absorbed irradiation, emissive power, radiosity, and net radiation heat transfer from the surface.

12.47 A diffuse, opaque surface at 700 K has spectral emissivities of $\varepsilon_\lambda = 0$ for $0 \leq \lambda \leq 3\ \mu$m, $\varepsilon_\lambda = 0.5$ for $3\ \mu\text{m} < \lambda \leq 10\ \mu$m, and $\varepsilon_\lambda = 0.9$ for $10\ \mu\text{m} < \lambda < \infty$. A radiant flux of 1000 W/m^2, which is uniformly distributed between 1 and 6 μm, is incident on the surface at an angle of 30° relative to the surface normal.



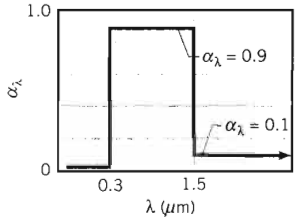
Calculate the total radiant power from a 10^{-4} m^2 area of the surface that reaches a radiation detector positioned along the normal to the area. The aperture of the detector is 10^{-5} m^2, and its distance from the surface is 1 m.

12.48 A small disk 5 mm in diameter is positioned at the center of an isothermal, hemispherical enclosure. The disk is diffuse and gray with an emissivity of 0.7 and is maintained at 900 K. The hemispherical enclosure, maintained at 300 K, has a radius of 100 mm and an emissivity of 0.85.



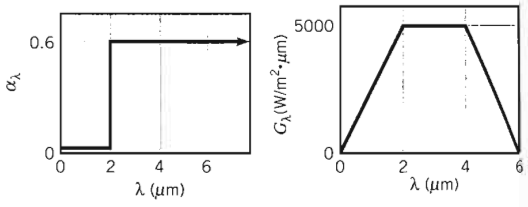
Calculate the radiant power leaving an aperture of diameter 2 mm located on the enclosure as shown.

12.49 The spectral, hemispherical absorptivity of an opaque surface is as shown.



What is the solar absorptivity, α_S? If it is assumed that $\varepsilon_\lambda = \alpha_\lambda$ and that the surface is at a temperature of 340 K, what is its total, hemispherical emissivity?

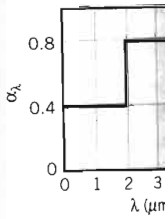
12.50 The spectral, hemispherical absorptivity of an opaque surface and the spectral distribution of radiation incident on the surface are depicted below.



What is the total, hemispherical absorptivity of the surface? If it is assumed that $\varepsilon_\lambda = \alpha_\lambda$ and that the surface is at 1000 K, what is its total, hemispherical

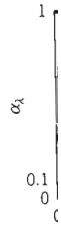
emissivity? surface?

12.51 Consider an spectral abso



What is the prescribed i ture of 125(the surface scribed con

12.52 The tungste sipates 75 75-mm diar surrounding of the glass ity is charac



What is th for a tungs

12.53 The spectr is as shown

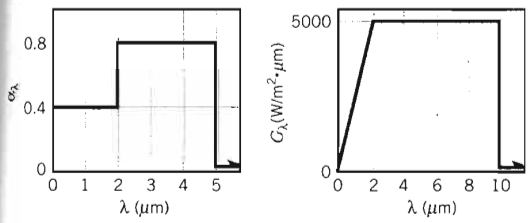


(a) If the total,

Patent Owner Manufacturing Resources International, Inc.
Exhibit 2017 - Page 794 of 999

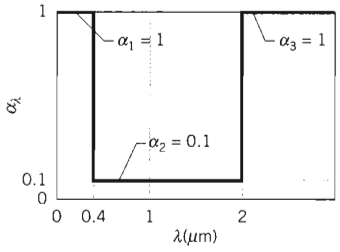
emissivity? What is the net radiant heat flux to the surface?

12.51 Consider an opaque, diffuse surface for which the spectral absorptivity and irradiation are as follows:



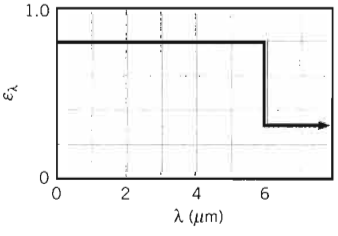
What is the total absorptivity of the surface for the prescribed irradiation? If the surface is at a temperature of 1250 K, what is its emissive power? How will the surface temperature vary with time, for the prescribed conditions?

12.52 The tungsten filament described in Problem 12.29 dissipates 75 W in an evacuated spherical light bulb of 75-mm diameter. The bulb is in quiescent air and large surroundings at a temperature of 25°C. The reflectivity of the glass is negligible, while the spectral absorptivity is characterized by the following distribution.



What is the steady-state temperature of the glass bulb for a tungsten filament operating at 3000 K?

12.53 The spectral emissivity of an opaque, diffuse surface is as shown.



(a) If the surface is maintained at 1000 K, what is the total, hemispherical emissivity?

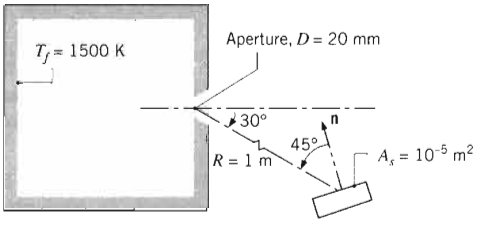
(b) What is the total, hemispherical absorptivity of the surface when irradiated by large surroundings of emissivity 0.8 and temperature 1500 K?

(c) What is the radiosity of the surface when it is maintained at 1000 K and subjected to the irradiation prescribed in part (b)?

(d) Determine the net radiation flux into the surface for the conditions of part (c).

(e) Plot each of the parameters featured in parts (a)–(d) as a function of the surface temperature for $750 \leq T \leq 2000$ K.

12.54 Radiation leaves a furnace of inside surface temperature 1500 K through an aperture 20 mm in diameter. A portion of the radiation is intercepted by a detector that is 1 m from the aperture, has a surface area of 10^{-5} m², and is oriented as shown.



If the aperture is open, what is the rate at which radiation leaving the furnace is intercepted by the detector? If the aperture is covered with a diffuse, semitransparent material of spectral transmissivity $\tau_\lambda = 0.8$ for $\lambda \leq 2\ \mu$m and $\tau_\lambda = 0$ for $\lambda > 2\ \mu$m, what is the rate at which radiation leaving the furnace is intercepted by the detector?

12.55 The spectral transmissivity of a 1-mm-thick layer of liquid water can be approximated as follows:

$$\tau_{\lambda 1} = 0.99 \quad 0 \leq \lambda \leq 1.2\ \mu\text{m}$$
$$\tau_{\lambda 2} = 0.54 \quad 1.2\ \mu\text{m} < \lambda \leq 1.8\ \mu\text{m}$$
$$\tau_{\lambda 3} = 0 \quad 1.8\ \mu\text{m} < \lambda$$

(a) Liquid water can exist only below its critical temperature, $T_c = 647.3$ K. Determine the maximum possible total transmissivity of a 1-mm-thick layer of liquid water when the water is housed in an opaque container and boiling does not occur. Assume the irradiation is that of a blackbody.

(b) Determine the transmissivity of a 1-mm-thick layer of liquid water associated with melting the platinum wire used in Nukiyama's boiling experiment, as described in Section 10.3.1.

(c) Determine the total transmissivity of a 1-mm-thick layer of liquid water exposed to solar

Patent Owner Manufacturing Resources International, Inc.
Exhibit 2017 - Page 795 of 999

irradiation. Assume the sun emits as a blackbody at $T_s = 5800$ K.

12.56 The spectral transmissivity of plain and tinted glass can be approximated as follows:

Plain glass:	$\tau_\lambda = 0.9$	$0.3 \leq \lambda \leq 2.5\ \mu$m
Tinted glass:	$\tau_\lambda = 0.9$	$0.5 \leq \lambda \leq 1.5\ \mu$m

Outside the specified wavelength ranges, the spectral transmissivity is zero for both glasses. Compare the solar energy that could be transmitted through the glasses. With solar irradiation on the glasses, compare the visible radiant energy that could be transmitted.

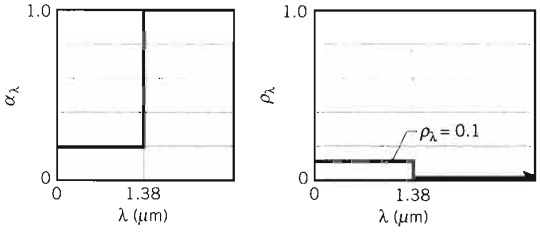
12.57 The research group of a glass manufacturer is working on development of a coating that would render glass highly transparent to radiation at wavelengths below 0.7 μm and highly reflective to radiation above 0.7 μm. An application of special interest is to the inner surface of glass light bulbs.

(a) Explain the advantages of having a light bulb whose inner surface is perfectly transparent ($\tau_\lambda = 1$) to radiation for $\lambda \leq 0.7\ \mu$m and perfectly reflecting ($\rho_\lambda = 1$) for $\lambda > 0.7\ \mu$m.

(b) Consider such a light bulb with a tungsten filament whose spectral emissivity is characterized by the distribution of Problem 12.29. What is the electric power required to maintain a filament temperature of 3000 K if the filament diameter and length are $D = 0.8$ mm and $L = 20$ mm? What is the power requirement if the coating can only provide complete reflection for $\lambda > 2.0\ \mu$m, with complete transmission maintained at lower wavelengths?

12.58 Referring to the distribution of the spectral transmissivity of low iron glass (Figure 12.23), describe briefly what is meant by the "greenhouse effect." That is, how does the glass influence energy transfer to and from the contents of a greenhouse?

12.59 The spectral absorptivity α_λ and spectral reflectivity ρ_λ for a spectrally selective, diffuse material are as shown.



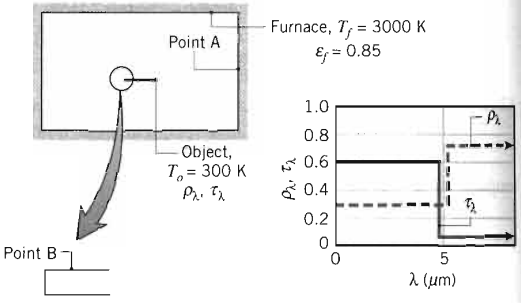
(a) Sketch the spectral transmissivity τ_λ.

(b) If solar irradiation with $G_S = 750$ W/m^2 and the spectral distribution of a blackbody at 5800 K is incident on this material, determine the fractions of the irradiation that are transmitted, reflected, and absorbed by the material.

(c) If the temperature of this material is 350 K, determine the emissivity ε.

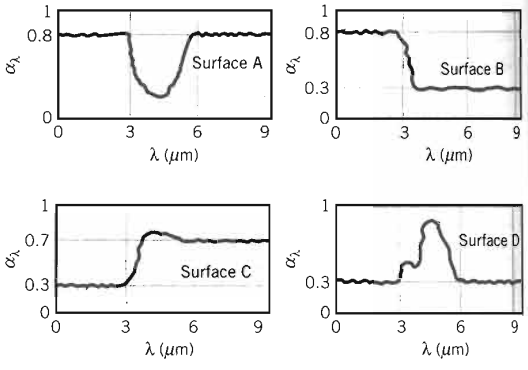
(d) Determine the net heat flux by radiation to the material.

12.60 Consider a large furnace with opaque, diffuse, gray walls at 3000 K having an emissivity of 0.85. A small, diffuse, spectrally selective object in the furnace is maintained at 300 K.



For the specified points on the furnace wall (A) and the object (B), indicate values for ε, α, E, G, and J.

12.61 Four diffuse surfaces having the spectral characteristics shown are at 300 K and are exposed to solar radiation.



Which of the surfaces may be approximated as being gray?

12.62 Consider a material that is gray, but directionally selective with $\alpha_\theta(\theta, \phi) = 0.5(1 - \cos\phi)$. Determine the hemispherical absorptivity α when collimated solar

flux irradia
tion $\theta = 4$
emissivity

12.63 The spectr
film is mea
$\lambda \leq 15\ \mu$r
mated as τ
for 7 μm
$\lambda \leq 15\ \mu$n
not be acq
instrument
total transı

(a) Estim
ity of
blackb

(b) Estim
ity of
blackb

(c) Repea
600°C

Energy Balai

12.64 An opaque
mm and th
flows adja
temperatu
at $T_{\infty,a} = 2$
plate is dil
of which
and bottor
35°C, res
reflectivity
the plate
the top of
fer coeffic

12.65 Two smal
isothermal
enclosure
each of the
dent radia
tively. Cc
elapsed.

(a) What
What

(b) Deter

(c) What

(d) Deter

12.66 Consider
lated on it

Patent Owner Manufacturing Resources International, Inc.
Exhibit 2017 - Page 796 of 999

flux irradiates the surface of the material in the direction $\theta = 45°$ and $\phi = 0°$. Determine the hemispherical emissivity ε of the material.

12.63 The spectral transmissivity of a 50-μm-thick polymer film is measured over the wavelength range 2.5 μm $\leq \lambda \leq$ 15 μm. The spectral distribution may be approximated as $\tau_\lambda = 0.80$ for 2.5 μm $\leq \lambda \leq 7$ μm, $\tau_\lambda = 0.05$ for 7 μm $< \lambda \leq 13$ μm, and $\tau_\lambda = 0.55$ for 13 μm $< \lambda \leq 15$ μm. Transmissivity data outside the range cannot be acquired due to limitations associated with the instrumentation. An engineer wishes to determine the total transmissivity of the film.

(a) Estimate the *maximum possible* total transmissivity of the film associated with irradiation from a blackbody at $T = 30°C$.

(b) Estimate the *minimum possible* total transmissivity of the film associated with irradiation from a blackbody at $T = 30°C$.

(c) Repeat parts (a) and (b) for a blackbody at $T = 600°C$.

Energy Balances and Properties

12.64 An opaque, horizontal plate has a thickness of $L = 21$ mm and thermal conductivity $k = 25$ W/m · K. Water flows adjacent to the bottom of the plate and is at a temperature of $T_{\infty,w} = 25°C$. Air flows above the plate at $T_{\infty,a} = 260°C$ with $h_a = 40$ W/m^2 · K. The top of the plate is diffuse and is irradiated with $G = 1450$ W/m^2, of which 435 W/m^2 is reflected. The steady-state top and bottom plate temperatures are $T_t = 43°C$ and $T_b = 35°C$, respectively. Determine the transmissivity, reflectivity, absorptivity, and emissivity of the plate. Is the plate gray? What is the radiosity associated with the top of the plate? What is the convective heat transfer coefficient associated with the water flow?

12.65 Two small surfaces, A and B, are placed inside an isothermal enclosure at a uniform temperature. The enclosure provides an irradiation of 6300 W/m^2 to each of the surfaces, and surfaces A and B absorb incident radiation at rates of 5600 and 630 W/m^2, respectively. Consider conditions after a long time has elapsed.

(a) What are the net heat fluxes for each surface? What are their temperatures?

(b) Determine the absorptivity of each surface.

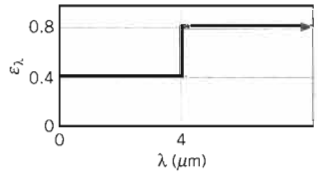
(c) What are the emissive powers of each surface?

(d) Determine the emissivity of each surface.

12.66 Consider an opaque horizontal plate that is well insulated on its back side. The irradiation on the plate is 2500 W/m^2, of which 500 W/m^2 is reflected. The plate is at 227°C and has an emissive power of 1200 W/m^2. Air at 127°C flows over the plate with a heat transfer convection coefficient of 15 W/m^2 · K. Determine the emissivity, absorptivity, and radiosity of the plate. What is the net heat transfer rate per unit area?

12.67 A horizontal, opaque surface at a steady-state temperature of 77°C is exposed to an airflow having a free stream temperature of 27°C with a convection heat transfer coefficient of 28 W/m^2 · K. The emissive power of the surface is 628 W/m^2, the irradiation is 1380 W/m^2, and the reflectivity is 0.40. Determine the absorptivity of the surface. Determine the net radiation heat transfer rate for this surface. Is this heat transfer to the surface or from the surface? Determine the combined heat transfer rate for the surface. Is this heat transfer to the surface or from the surface?

12.68 A diffuse surface having the following spectral characteristics is maintained at 500 K when situated in a large furnace enclosure whose walls are maintained at 1500 K:



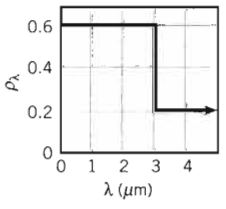
(a) Sketch the spectral distribution of the surface emissive power E_λ and the emissive power $E_{\lambda,b}$ that the surface would have if it were a blackbody.

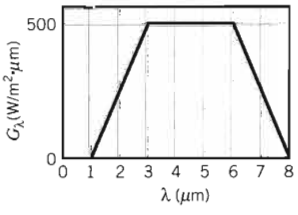
(b) Neglecting convection effects, what is the net heat flux to the surface for the prescribed conditions?

(c) Plot the net heat flux as a function of the surface temperature for $500 \leq T \leq 1000$ K. On the same coordinates, plot the heat flux for a diffuse, gray surface with total emissivities of 0.4 and 0.8.

(d) For the prescribed spectral distribution of ε_λ, how do the total emissivity and absorptivity of the surface vary with temperature in the range $500 \leq T \leq 1000$ K?

12.69 Consider an opaque, diffuse surface whose spectral reflectivity varies with wavelength as shown. The





Patent Owner Manufacturing Resources International, Inc.
Exhibit 2017 - Page 797 of 999

surface is at 750 K, and irradiation on one side varies with wavelength as shown. The other side of the surface is insulated.

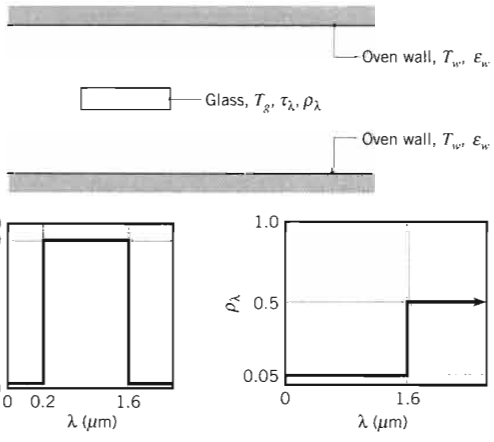
What are the total absorptivity and emissivity of the surface? What is the net radiative heat flux to the surface?

12.70 A special diffuse glass with prescribed spectral radiative properties is heated in a large oven. The walls of the oven are lined with a diffuse, gray refractory brick having an emissivity of 0.75 and are maintained at $T_w = 1800$ K. Consider conditions for which the glass temperature is $T_g = 750$ K.

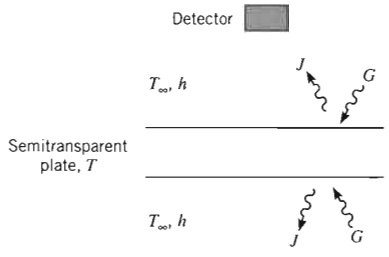
(a) What are the total transmissivity τ, the total reflectivity ρ, and the total emissivity ε of the glass?

(b) What is the net radiative heat flux, $q''_{\text{net,in}}$ (W/m^2), to the glass?

(c) For oven wall temperatures of 1500, 1800, and 2000 K, plot $q''_{\text{net,in}}$ as a function of glass temperature for $500 \leq T_g \leq 800$ K.



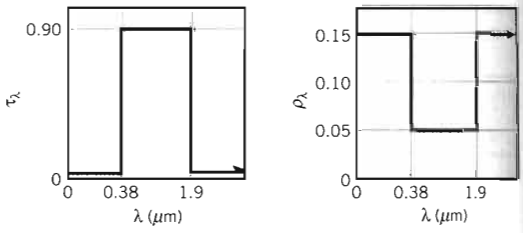
12.71 A horizontal semitransparent plate is uniformly irradiated from above and below, while air at $T_\infty = 300$ K flows over the top and bottom surfaces, providing a uniform convection heat transfer coefficient of $h = 40$ W/m$^2 \cdot$K. The total, hemispherical absorptivity of the plate to the irradiation is 0.40. Under steady-state conditions measurements made with a radiation detector above the top surface indicate a radiosity (which includes transmission, as well as reflection and emission) of $J = 5000$ W/m^2, while the plate is at a uniform temperature of $T = 350$ K.



Determine the irradiation G and the total hemispherical emissivity of the plate. Is the plate gray for the prescribed conditions?

12.72 The 50-mm peephole of a large furnace operating at 450°C is covered with a material having $\tau = 0.8$ and $\rho = 0$ for irradiation originating from the furnace. The material has an emissivity of 0.8 and is opaque to irradiation from a source at room temperature. The outer surface of the cover is exposed to surroundings and ambient air at 27°C with a convection heat transfer coefficient of 50 W/m$^2 \cdot$K. Assuming that convection effects on the inner surface of the cover are negligible, calculate the heat loss by the furnace and the temperature of the cover.

12.73 The window of a large vacuum chamber is fabricated from a material of prescribed spectral characteristics. A collimated beam of radiant energy from a solar simulator is incident on the window and has a flux of 3000 W/m^2. The inside walls of the chamber, which are large compared to the window area, are maintained at 77 K. The outer surface of the window is subjected to surroundings and room air at 25°C, with a convection heat transfer coefficient of 15 W/m$^2 \cdot$K.



(a) Determine the transmissivity of the window material to radiation from the solar simulator, which approximates the solar spectral distribution.

(b) Assuming that the window is insulated from its chamber mounting arrangement, what steady-state temperature does the window reach?

(c) Calculate the net radiation transfer per unit area of the window to the vacuum chamber wall, excluding the transmitted simulated solar flux.

12.74 A thermocouple whose surface is diffuse and gray with an emissivity of 0.6 indicates a temperature of 180°C when used to measure the temperature of a gas

flowing th
emissivity
(a) If the
the th
125 W
losses
peratu
(b) Consi
and pl
a func
$\bar{h} \leq 1$
your r

12.75 A thermoc
steel tube
sivity of 0
conditione
30 and 20
(a) What
if the
(b) Comp
error
$0.1 \leq$

12.76 A tempera
tube havin
0.8 is cent
room wh
20°C, resp
(a) What
conve
and th
(b) What
airflo
as a
$2 \leq h$
and 0

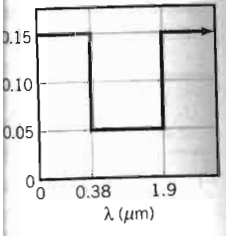
12.77 A sphere
30-mm di
an emissi
walls are
ature of th
heat trans
oven air is
(a) Deter
its ter
(b) What
spher
(c) How
300 K
tempe
(d) For
elaps
vecti

Patent Owner Manufacturing Resources International, Inc.
Exhibit 2017 - Page 798 of 999

ispherical absorptiv-
0.40. Under steady-
ade with a radiation
indicate a radiosity
well as reflection and
hile the plate is at a
K.
and the total hemi-
Is the plate gray for

furnace operating at
l having $\tau = 0.8$ and
from the furnace. The
and is opaque to irra-
mperature. The outer
to surroundings and
nvection heat transfer
uming that convection
e cover are negligible,
nace and the tempera-

chamber is fabricated
pectral characteristics.
ergy from a solar sim-
and has a flux of 3000
e chamber, which are
area, are maintained at
window is subjected to
5°C, with a convection
$W/m^2 \cdot K$.



ity of the window mater-
solar simulator, which
ctral distribution.
ow is insulated from its
ngement, what steady-
window reach?
n transfer per unit area of
m chamber wall, exclud-
ated solar flux.
face is diffuse and gray
dicates a temperature of
the temperature of a gas

flowing through a large duct whose walls have an emissivity of 0.85 and a uniform temperature of 450°C.

(a) If the convection heat transfer coefficient between the thermocouple and the gas stream is $\bar{h} = 125\ W/m^2 \cdot K$ and there are negligible conduction losses from the thermocouple, determine the temperature of the gas.

(b) Consider a gas temperature of 125°C. Compute and plot the thermocouple *measurement error* as a function of the convection coefficient for $10 \leq \bar{h} \leq 1000\ W/m^2 \cdot K$. What are the implications of your results?

12.75 A thermocouple inserted in a 4-mm-diameter stainless steel tube having a diffuse, gray surface with an emissivity of 0.4 is positioned horizontally in a large air-conditioned room whose walls and air temperature are 30 and 20°C, respectively.

(a) What temperature will the thermocouple indicate if the air is quiescent?

(b) Compute and plot the thermocouple *measurement error* as a function of the surface emissivity for $0.1 \leq \varepsilon \leq 1.0$.

12.76 A temperature sensor imbedded in the tip of a small tube having a diffuse, gray surface with an emissivity of 0.8 is centrally positioned within a large air-conditioned room whose walls and air temperature are 30 and 20°C, respectively.

(a) What temperature will the sensor indicate if the convection coefficient between the sensor tube and the air is $5\ W/m^2 \cdot K$?

(b) What would be the effect of using a fan to induce airflow over the tube? Plot the sensor temperature as a function of the convection coefficient for $2 \leq h \leq 25\ W/m^2 \cdot K$ and values of $\varepsilon = 0.2$, 0.5, and 0.8.

12.77 A sphere ($k = 185\ W/m \cdot K$, $\alpha = 7.25 \times 10^{-5}\ m^2/s$) of 30-mm diameter whose surface is diffuse and gray with an emissivity of 0.8 is placed in a large oven whose walls are of uniform temperature at 600 K. The temperature of the air in the oven is 400 K, and the convection heat transfer coefficient between the sphere and the oven air is $15\ W/m^2 \cdot K$.

(a) Determine the net heat transfer to the sphere when its temperature is 300 K.

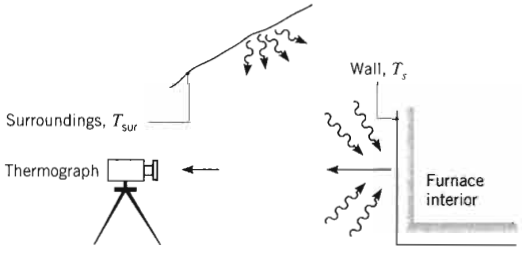
(b) What will be the steady-state temperature of the sphere?

(c) How long will it take for the sphere, initially at 300 K, to come within 20 K of the steady-state temperature?

(d) For emissivities of 0.2, 0.4, and 0.8, plot the elapsed time of part (c) as a function of the convection coefficient for $10 \leq h \leq 25\ W/m^2 \cdot K$.

Radiation Detection

12.78 A thermograph is a device responding to the radiant power from the scene, which reaches its radiation detector within the spectral region 9–12 μm. The thermograph provides an image of the scene, such as the side of a furnace, from which the surface temperature can be determined.



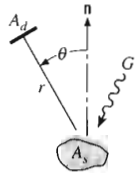
(a) For a black surface at 60°C, determine the emissive power for the spectral region 9–12 μm.

(b) Calculate the radiant power (W) received by the thermograph in the same range (9–12 μm) when viewing, in a normal direction, a small black wall area, 200 mm^2, at $T_s = 60$°C. The solid angle ω subtended by the aperture of the thermograph when viewed from the target is 0.001 sr.

(c) Determine the radiant power (W) received by the thermograph for the same wall area (200 mm^2) and solid angle (0.001 sr) when the wall is a gray, opaque, diffuse material at $T_s = 60$°C with emissivity 0.7 and the surroundings are black at $T_{sur} = 23$°C.

12.79 A radiation thermometer is a radiometer calibrated to indicate the temperature of a blackbody. A steel billet having a diffuse, gray surface of emissivity 0.8 is heated in a furnace whose walls are at 1500 K. Estimate the temperature of the billet when the radiation thermometer viewing the billet through a small hole in the furnace indicates 1160 K.

12.80 A radiation detector has an aperture of area $A_d = 10^{-6}$ m^2 and is positioned at a distance of $r = 1$ m from a surface of area $A_s = 10^{-4}$ m^2. The angle formed by the normal to the detector and the surface normal is $\theta = 30°$.



Patent Owner Manufacturing Resources International, Inc.
Exhibit 2017 - Page 799 of 999

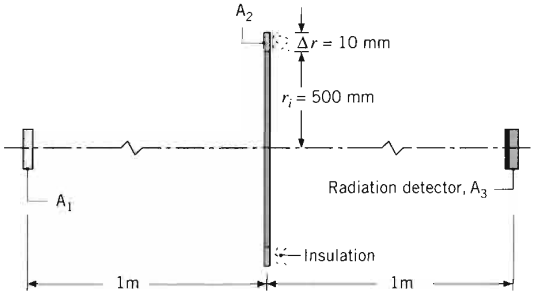
The surface is at 500 K and is opaque, diffuse, and gray with an emissivity of 0.7. If the surface irradiation is 1500 W/m^2, what is the rate at which the detector intercepts radiation from the surface?

12.81 A small anodized aluminum block at 35°C is heated in a large oven whose walls are diffuse and gray with $\varepsilon = 0.85$ and maintained at a uniform temperature of 175°C. The anodized coating is also diffuse and gray with $\varepsilon = 0.92$. A radiation detector views the block through a small opening in the oven and receives the radiant energy from a small area, referred to as the target, A_t, on the block. The target has a diameter of 3 mm, and the detector receives radiation within a solid angle 0.001 sr centered about the normal from the block.

(a) If the radiation detector views a small, but deep, hole drilled into the block, what is the total power (W) received by the detector?

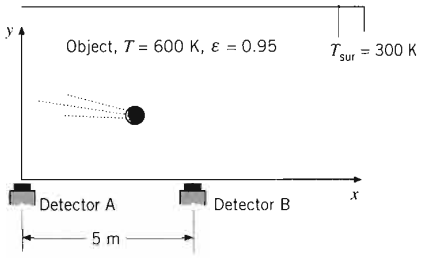
(b) If the radiation detector now views an area on the block surface, what is the total power (W) received by the detector?

12.82 Consider the diffuse, gray opaque disk A_1, which has a diameter of 10 mm, an emissivity of 0.3, and is at a temperature of 400 K. Coaxial to the disk A_1, there is a black, ring-shaped disk A_2 at 1000 K having the dimensions shown in the sketch. The backside of A_2 is insulated and does not directly irradiate the cryogenically cooled detector disk A_3, which is of diameter 10 mm and is located 2 m from A_1.

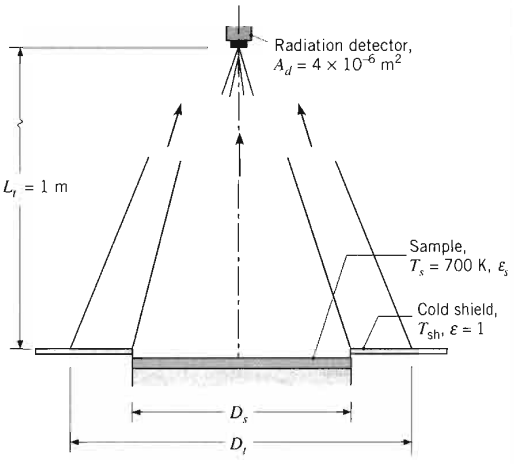


Calculate the rate at which radiation is incident on A_3 due to emission and reflection from A_1.

12.83 A diffuse, spherical object of diameter and temperature 9 mm and 600 K, respectively, has an emissivity of 0.95. Two very sensitive radiation detectors, each with an aperture area of 300×10^{-6} m^2, detect the object as it passes over at high velocity from left to right as shown in the schematic. The detectors capture hemispherical irradiation and are equipped with filters characterized by $\tau_\lambda = 0.9$ for $\lambda < 2.5$ μm and $\tau_\lambda = 0$ for $\lambda \geq 2.5$ μm. At time $t_1 = 0$, detectors A and B indicate irradiations of $G_{A,1} = 5.060$ mW/m^2 and $G_{B,1} = 5.000$ mW/m^2, respectively. At time $t_2 = 4$ ms, detectors A and B indicate irradiations of $G_{A,2} = 5.010$ mW/m^2 and $G_{B,2} = 5.050$ mW/m^2, respectively. The environment is at 300 K. Determine the velocity components of the particle, v_x and v_y. Determine when and where the particle will strike a horizontal plane located at $y = 0$. *Hint:* The object is located at an elevation above $y = 2$ m when it is detected. Assume the object's trajectory is a straight line in the plane of the page. Recall that the projected area of a sphere is a circle.



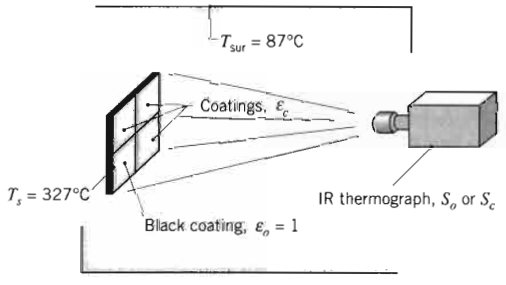
12.84 A radiation detector having a sensitive area of $A_d = 4 \times 10^{-6}$ m^2 is configured to receive radiation from a target area of diameter $D_t = 40$ mm when located a distance of $L_t = 1$ m from the target. For the experimental apparatus shown in the sketch, we wish to determine the emitted radiation from a hot sample of diameter $D_s = 20$ mm. The temperature of the aluminum sample is $T_s = 700$ K and its emissivity is $\varepsilon_s = 0.1$. A ring-shaped cold shield is provided to minimize the effect of radiation from outside the sample area, but within the target area. The sample and the shield are diffuse emitters.



(a) Assuming the shield is black, at what temperature, T_{sh}, should the shield be maintained so that its emitted radiation is 1% of the total radiant power received by the detector?

(b) Subject to the parametric constraint that radiation emitted from the cold shield is 0.05, 1, or 1.5% of the total radiation received by the detector, plot the required cold shield temperature, T_{sh}, as a function of the sample emissivity for $0.05 \leq \varepsilon_s \leq 0.35$.

12.85 An infrared (IR) thermograph is a radiometer that provides an image of the target scene, indicating the apparent temperature of elements in the scene by a black–white brightness or blue–red color scale. Radiation originating from an element in the target scene is incident on the radiation detector, which provides a signal proportional to the incident radiant power. The signal sets the image brightness or color scale for the image pixel associated with that element. A scheme is proposed for field calibration of an infrared thermograph having a radiation detector with a 3- to 5-μm spectral bandpass. A heated metal plate, which is maintained at 327°C and has four diffuse, gray coatings with different emissivities, is viewed by the IR thermograph in surroundings for which $T_{sur} = 87$°C.



(a) Consider the thermograph output when viewing the black coating, $\varepsilon_o = 1$. The radiation reaching the detector is proportional to the product of the blackbody emissive power (or emitted intensity) at the temperature of the surface and the band emission fraction corresponding to the IR thermograph spectral bandpass. The proportionality constant is referred to as the responsivity, $R(\mu\text{V} \cdot \text{m}^2/\text{W})$. Write an expression for the thermograph output signal, S_o, in terms of R, the coating blackbody emissive power, and the appropriate band emission fraction. Assuming $R = 1\ \mu\text{V} \cdot \text{m}^2/\text{W}$, evaluate S_o (μV).

(b) Consider the thermograph output when viewing one of the coatings for which the emissivity ε_c is less than unity. Radiation from the coating reaches the detector due to emission and the reflection of irradiation from the surroundings. Write an expression for the signal, S_c, in terms of R, the coating blackbody emissive power, the blackbody emissive power of the surroundings, the coating emissivity, and the appropriate band emission fractions. For the diffuse, gray coatings, the reflectivity is $\rho_c = 1 - \varepsilon_c$.

(c) Assuming $R = 1\ \mu\text{V} \cdot \text{m}^2/\text{W}$, evaluate the thermograph signals, S_c (μV), when viewing panels with emissivities of 0.8, 0.5, and 0.2.

(d) The thermograph is calibrated so that the signal S_o (with the black coating) will give a correct scale indication of $T_s = 327$°C. The signals from the other three coatings, S_c, are less than S_o. Hence the thermograph will indicate an apparent (blackbody) temperature less than T_s. Estimate the temperatures indicated by the thermograph for the three panels of part (c).

12.86 A charge-coupled device (CCD) infrared imaging system (see Problem 12.85) operates in a manner similar to a digital video camera. Instead of being sensitive to irradiation in the visible part of the spectrum, however, each small sensor in the infrared system's CCD array is sensitive in the spectral region 9–12 μm. Note that the system is designed to only view radiation coming from directly in front of it. An experimenter wishes to use the infrared imaging system to map the surface temperature distribution of a heated object in a wind tunnel experiment. The air temperature in the wind tunnel, as well as the surroundings temperature in the laboratory, is 23°C.

(a) In a preliminary test of the concept, the experimenter views a small aluminum billet located in the wind tunnel that is at a billet temperature of 50°C. The aluminum is coated with a high-emissivity paint, $\varepsilon = 0.96$. If the infrared imaging system is calibrated to indicate the temperature of a blackbody, what temperature will be indicated by the infrared imaging system as it is used to view the aluminum billet through a 6-mm-thick fused quartz window?

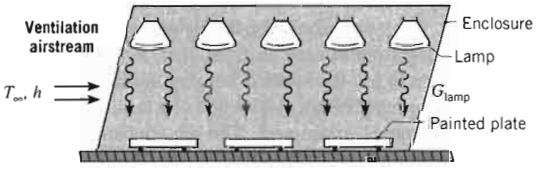
(b) In a subsequent experiment, the experimenter replaces the quartz window with a thin (130-μm-thick) household polyethylene film with $\tau \approx 0.78$ within the spectral range of the imaging system. What temperature will be indicated by the infrared imaging system when it is used to view the aluminum billet through the polyethylene film?

Patent Owner Manufacturing Resources International, Inc.
Exhibit 2017 - Page 801 of 999

12.87 A *two-color pyrometer* is a device that is used to measure the temperature of a diffuse surface, T_s. The device measures the spectral, directional intensity emitted by the surface at two distinct wavelengths separated by $\Delta\lambda$. Calculate and plot the ratio of the intensities $I_{\lambda+\Delta\lambda,e}(\lambda + \Delta\lambda, \theta, \phi, T_s)$ and $I_{\lambda,e}(\lambda, \theta, \phi, T_s)$ as a function of the surface temperature over the range $500\ \text{K} \le T_s \le 1000\ \text{K}$ for $\lambda = 5\ \mu\text{m}$ and $\Delta\lambda = 0.1, 0.5$, and $1\ \mu\text{m}$. Comment on the sensitivity to temperature and on whether the ratio depends on the emissivity of the surface. Discuss the tradeoffs associated with specification of the various values of $\Delta\lambda$. *Hint*: The change in the emissivity over small wavelength intervals is modest for most solids, as evident in Figure 12.17.

Applications

12.88 Square plates freshly sprayed with an epoxy paint must be cured at 140°C for an extended period of time. The plates are located in a large enclosure and heated by a bank of infrared lamps. The top surface of each plate has an emissivity of $\varepsilon = 0.8$ and experiences convection with a ventilation airstream that is at $T_\infty = 27°\text{C}$ and provides a convection coefficient of $h = 20\ \text{W/m}^2 \cdot \text{K}$. The irradiation from the enclosure walls is estimated to be $G_{\text{wall}} = 450\ \text{W/m}^2$, for which the plate absorptivity is $\alpha_{\text{wall}} = 0.7$.



(a) Determine the irradiation that must be provided by the lamps, G_{lamp}. The absorptivity of the plate surface for this irradiation is $\alpha_{\text{lamp}} = 0.6$.

(b) For convection coefficients of $h = 15$, 20, and $30\ \text{W/m}^2 \cdot \text{K}$, plot the lamp irradiation, G_{lamp}, as a function of the plate temperature, T_s, for $100 \le T_s \le 300°\text{C}$.

(c) For convection coefficients in the range from 10 to $30\ \text{W/m}^2 \cdot \text{K}$ and a lamp irradiation of $G_{\text{lamp}} = 3000\ \text{W/m}^2$, plot the airstream temperature T_∞ required to maintain the plate at $T_s = 140°\text{C}$.

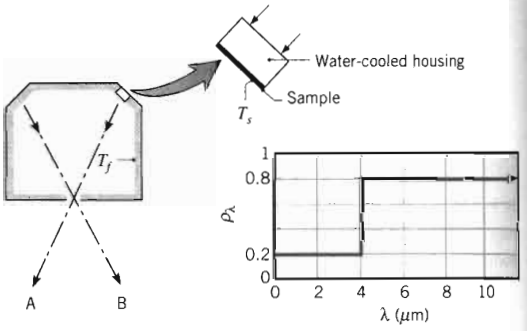
12.89 An apparatus commonly used for measuring the reflectivity of materials is shown below. A water-cooled sample, of 30-mm diameter and temperature $T_s = 300$ K, is mounted flush with the inner surface of a large enclosure. The walls of the enclosure are gray and diffuse with an emissivity of 0.8 and a uniform temperature $T_f = 1000$ K. A small aperture is located at the bottom of the enclosure to permit sighting of the sample or the enclosure wall. The spectral reflectivity ρ_λ of an opaque, diffuse sample material is as shown. The heat transfer coefficient for convection between the sample and the air within the cavity, which is also at 1000 K, is $h = 10\ \text{W/m}^2 \cdot \text{K}$.

(a) Calculate the absorptivity of the sample.

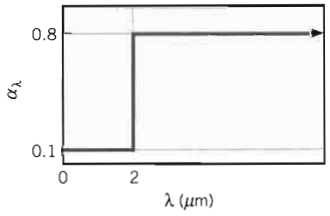
(b) Calculate the emissivity of the sample.

(c) Determine the heat removal rate (W) by the coolant.

(d) The ratio of the radiation in the A direction to that in the B direction will give the reflectivity of the sample. Briefly explain why this is so.



12.90 A very small sample of an opaque surface is initially at 1200 K and has the spectral, hemispherical absorptivity shown.



The sample is placed inside a very large enclosure whose walls have an emissivity of 0.2 and are maintained at 2400 K.

(a) What is the total, hemispherical absorptivity of the sample surface?

(b) What is its total, hemispherical emissivity?

(c) What are the values of the absorptivity and emissivity after the sample has been in the enclosure a long time?

(d) For a evacu tion o heate

12.91 A manufac rods, whic nace whos perature T gas at 1-a The film i of $\varepsilon_\lambda = 0.$

(a) Consi and in such t the lu equati chang tion. variab

(b) If T 10 m rod lump

(c) Com ature

12.92 A proced solids at a sample is of thick width W walls of t tom surfa lower ter the samp and gray measured

Patent Owner Manufacturing Resources International, Inc.
Exhibit 2017 - Page 802 of 999

(d) For a 10-mm-diameter spherical sample in an evacuated enclosure, compute and plot the variation of the sample temperature with time, as it is heated from its initial temperature of 1200 K.

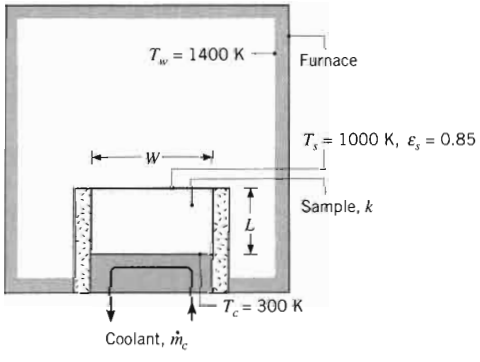
12.91 A manufacturing process involves heating long copper rods, which are coated with a thin film, in a large furnace whose walls are maintained at an elevated temperature T_w. The furnace contains quiescent nitrogen gas at 1-atm pressure and a temperature of $T_\infty = T_w$. The film is a diffuse surface with a spectral emissivity of $\varepsilon_\lambda = 0.9$ for $\lambda \leq 2\ \mu$m and $\varepsilon_\lambda = 0.4$ for $\lambda > 2\ \mu$m.

(a) Consider conditions for which a rod of diameter D and initial temperature T_i is inserted in the furnace, such that its axis is horizontal. Assuming validity of the lumped capacitance approximation, derive an equation that could be used to determine the rate of change of the rod temperature at the time of insertion. Express your result in terms of appropriate variables.

(b) If $T_w = T_\infty = 1500$ K, $T_i = 300$ K, and $D = 10$ mm, what is the initial rate of change of the rod temperature? Confirm the validity of the lumped capacitance approximation.

(c) Compute and plot the variation of the rod temperature with time during the heating process.

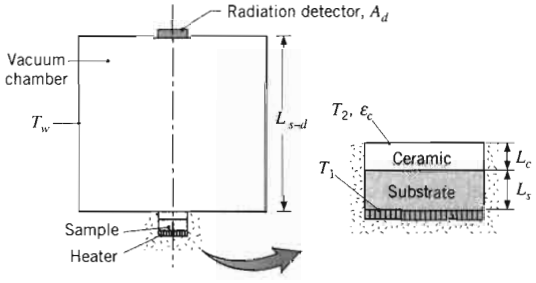
12.92 A procedure for measuring the thermal conductivity of solids at elevated temperatures involves placement of a sample at the bottom of a large furnace. The sample is of thickness L and is placed in a square container of width W on a side. The sides are well insulated. The walls of the cavity are maintained at T_w, while the bottom surface of the sample is maintained at a much lower temperature T_c by circulating coolant through the sample container. The sample surface is diffuse and gray with an emissivity ε_s. Its temperature T_s is measured optically.



(a) Neglecting convection effects, obtain an expression from which the sample thermal conductivity may be evaluated in terms of measured and known quantities (T_w, T_s, T_c, ε_s, L). The measurements are made under steady-state conditions. If $T_w = 1400$ K, $T_s = 1000$ K, $\varepsilon_s = 0.85$, $L = 0.015$ m, and $T_c = 300$ K, what is the sample thermal conductivity?

(b) If $W = 0.10$ m and the coolant is water with a flow rate of $\dot{m}_c = 0.1$ kg/s, is it reasonable to assume a uniform bottom surface temperature T_c?

12.93 One scheme for extending the operation of gas turbine blades to higher temperatures involves applying a ceramic coating to the surfaces of blades fabricated from a superalloy such as inconel. To assess the reliability of such coatings, an apparatus has been developed for testing samples under laboratory conditions. The sample is placed at the bottom of a large vacuum chamber whose walls are cryogenically cooled and which is equipped with a radiation detector at the top surface. The detector has a surface area of $A_d = 10^{-5}$ m^2, is located at a distance of $L_{s\text{-}d} = 1$ m from the sample, and views radiation originating from a portion of the ceramic surface having an area of $\Delta A_c = 10^{-4}$ m^2. An electric heater attached to the bottom of the sample dissipates a uniform heat flux, q''_h, which is transferred upward through the sample. The bottom of the heater and sides of the sample are well insulated.



Consider conditions for which a ceramic coating of thickness $L_c = 0.5$ mm and thermal conductivity $k_c = 6$ W/m · K has been sprayed on a metal substrate of thickness $L_s = 8$ mm and thermal conductivity $k_s = 25$ W/m · K. The opaque surface of the ceramic may be approximated as diffuse and gray, with a total, hemispherical emissivity of $\varepsilon_c = 0.8$.

(a) Consider steady-state conditions for which the bottom surface of the substrate is maintained at $T_1 = 1500$ K, while the chamber walls (including the surface of the radiation detector) are maintained at $T_w = 90$ K. Assuming negligible

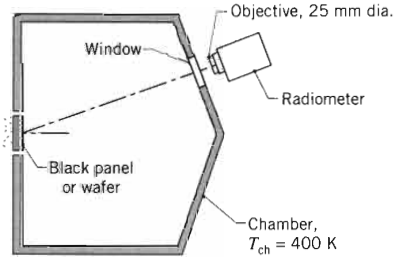
Patent Owner Manufacturing Resources International, Inc.
Exhibit 2017 - Page 803 of 999

thermal contact resistance at the ceramic–substrate interface, determine the ceramic top surface temperature T_2 and the heat flux q''_h.

(b) For the prescribed conditions, what is the rate at which radiation emitted by the ceramic is intercepted by the detector?

(c) After repeated experiments, numerous cracks develop at the ceramic–substrate interface, creating an interfacial thermal contact resistance. If T_w and q''_h are maintained at the conditions associated with part (a), will T_1 increase, decrease, or remain the same? Similarly, will T_2 increase, decrease, or remain the same? In each case, justify your answer.

12.94 The equipment for heating a wafer during a semiconductor manufacturing process is shown schematically. The wafer is heated by an ion beam source (not shown) to a uniform, steady-state temperature. The large chamber contains the process gas, and its walls are at a uniform temperature of $T_{ch} = 400$ K. A 5 × 5 mm target area on the wafer is viewed by a radiometer, whose objective lens has a diameter of 25 mm and is located 500 mm from the wafer. The line-of-sight of the radiometer is 30° off the wafer normal.

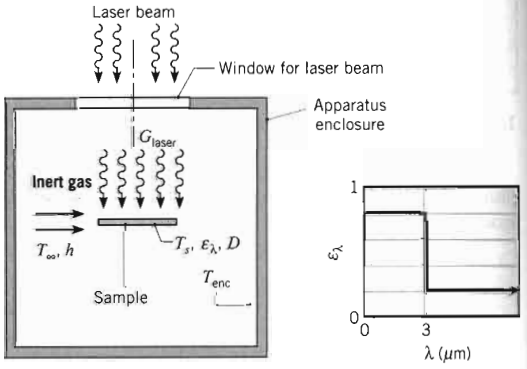


(a) In a preproduction test of the equipment, a black panel ($\varepsilon \approx 1.0$) is mounted in place of the wafer. Calculate the radiant power (W) received by the radiometer if the temperature of the panel is 800 K.

(b) The wafer, which is opaque, diffuse-gray with an emissivity of 0.7, is now placed in the equipment, and the ion beam is adjusted so that the power received by the radiometer is the same as that found for part (a). Calculate the temperature of the wafer for this heating condition.

12.95 The fire brick of Example 12.9 is used to construct the walls of a brick oven. The irradiation on the interior surface of the wall is $G = 50{,}000$ W/m^2 and has a spectral distribution proportional to that of a blackbody at 2000 K. The temperature of the gases adjacent to the inner wall of the oven is 500 K, and the convection heat transfer coefficient is 25 W/m^2. Find the wall surface temperature if the heat loss through the wall is negligible. If the brick wall is 0.1 m thick and of thermal conductivity $k_b = 1.0$ W/m · K, and is insulated with a 0.1-m-thick layer of thermal conductivity $k_i = 0.05$ W/m · K, what is the steady-state interior wall surface temperature if the temperature of the external surface of the insulation is 300 K?

12.96 A laser-materials-processing apparatus encloses a sample in the form of a disk of diameter $D = 25$ mm and thickness $w = 1$ mm. The sample has a diffuse surface for which the spectral distribution of the emissivity, $\varepsilon_\lambda(\lambda)$, is prescribed. To reduce oxidation, an inert gas stream of temperature $T_\infty = 500$ K and convection coefficient $h = 50$ W/m^2 · K flows over the sample upper and lower surfaces. The apparatus enclosure is large, with isothermal walls at $T_{enc} = 300$ K. To maintain the sample at a suitable operating temperature of $T_s = 2000$ K, a collimated laser beam with an operating wavelength of $\lambda = 0.5$ μm irradiates its upper surface.



(a) Determine the total emissivity ε of the sample.

(b) Determine the total absorptivity α of the sample for irradiation from the enclosure walls.

(c) Perform an energy balance on the sample and determine the laser irradiation, G_{laser}, required to maintain the sample at $T_s = 2000$ K.

(d) Consider a *cool-down* process, when the laser and the inert gas flow are deactivated. Sketch the total emissivity as a function of the sample temperature, $T_s(t)$, during the process. Identify key features, including the emissivity for the final condition ($t \to \infty$).

(e) Estimate the time to cool a sample from its operating condition at $T_s(0) = 2000$ K to a *safe-to-touch*

Patent Owner Manufacturing Resources International, Inc.
Exhibit 2017 - Page 804 of 999

temperature of $T_s(t) = 40°C$. Use the lumped capacitance method and include the effect of convection to the inert gas with $h = 50$ W/m$^2 \cdot$ K and $T_\infty = T_{enc} = 300$ K. The thermophysical properties of the sample material are $\rho = 3900$ kg/m^3, $c_p = 760$ J/kg $\cdot$ K, and $k = 45$ W/m $\cdot$ K.

12.97 A cylinder of 30-mm diameter and 150-mm length is heated in a large furnace having walls at 1000 K, while air at 400 K is circulating at 3 m/s. Estimate the steady-state cylinder temperature under the following specified conditions.

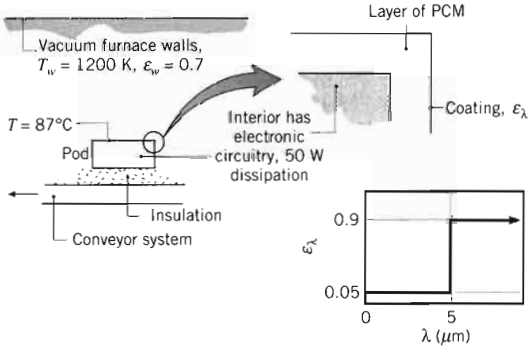
(a) The cylinder is in cross flow, and its surface is diffuse and gray with an emissivity of 0.5.

(b) The cylinder is in cross flow, but its surface is spectrally selective with $\alpha_\lambda = 0.1$ for $\lambda \leq 3$ μm and $\alpha_\lambda = 0.5$ for $\lambda > 3$ μm.

(c) The cylinder surface is positioned such that the airflow is longitudinal and its surface is diffuse and gray.

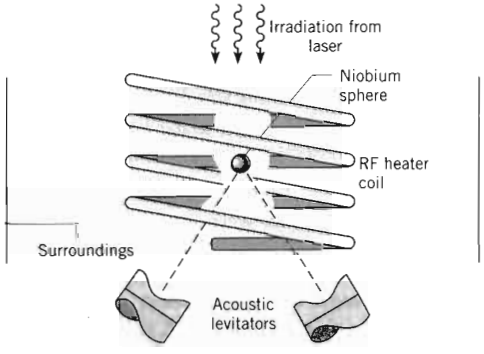
(d) For the conditions of part (a), compute and plot the cylinder temperature as a function of the air velocity for $1 \leq V \leq 20$ m/s.

12.98 An instrumentation transmitter pod is a box containing electronic circuitry and a power supply for sending sensor signals to a base receiver for recording. Such a pod is placed on a conveyor system, which passes through a large vacuum brazing furnace as shown in the sketch. The exposed surfaces of the pod have a special diffuse, opaque coating with spectral emissivity as shown.



To stabilize the temperature of the pod and prevent overheating of the electronics, the inner surface of the pod is surrounded by a layer of a phase-change material (PCM) having a fusion temperature of 87°C and a heat of fusion of 25 kJ/kg. The pod has an exposed surface area of 0.040 m^2 and the mass of the PCM is 1.6 kg. Furthermore, it is known that the power dissipated by the electronics is 50 W. Consider the situation when the pod enters the furnace at a uniform temperature of 87°C and all the PCM is in the solid state. How long will it take before all the PCM changes to the liquid state?

12.99 To simulate materials processing under the microgravity conditions of space, a niobium sphere of diameter 3 mm is levitated by an acoustical technique in a vacuum chamber. Initially the sphere is at 300 K and is suddenly irradiated with a laser providing an irradiation of 10 W/mm^2 to raise its temperature as quickly as possible to its melting point (2741 K). When the melting point is reached, the laser is switched off and a radio frequency (RF) heater is energized, causing uniform internal volumetric generation $\dot{q}$ to occur within the sphere. Assume that the niobium sphere is isothermal and diffuse and gray with an emissivity of 0.6, and that the chamber walls are at 300 K.



(a) How much time is required to reach the melting point? *Hint:* See Section 5.3 and modify the lumped capacitance analysis accordingly.

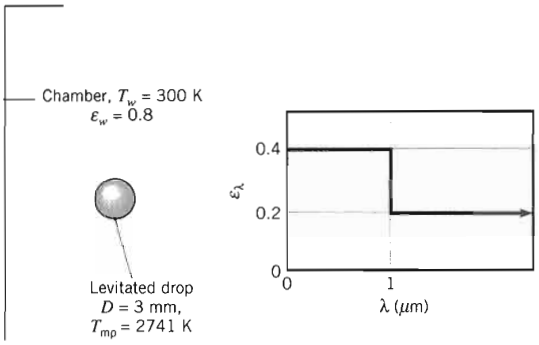
(b) How much power must be provided by the RF heater to maintain the sphere at its melting point?

(c) Is the spacewise isothermal assumption realistic for the conditions of parts (a) and (b)?

12.100 A spherical niobium droplet of diameter $D = 3$ mm is levitated by an acoustical technique in a vacuum chamber having walls that are diffuse and gray with an emissivity of $\varepsilon_w = 0.8$ and a temperature of $T_w = 300$ K. The niobium surface is diffuse and has the prescribed spectral emissivity distribution.

Two heating methods for maintaining the drop at its melting temperature, $T_{mp} = 2741$ K, are to be investigated.

Patent Owner Manufacturing Resources International, Inc.
Exhibit 2017 - Page 805 of 999

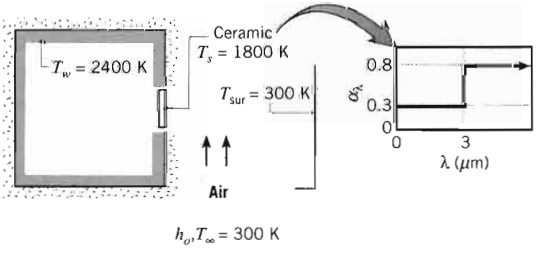


(a) The effect of applying a radio frequency (RF) field to the drop is to create a uniform internal generation rate, $\dot{q}$ (W/m^3), within the drop. Calculate the value of $\dot{q}$ required to maintain the drop at its melting temperature.

(b) A laser beam, having a diameter larger than that of the drop and operating at 10.6 μm, irradiates the drop. Determine the irradiation, G_{laser} (W/mm^2), required to maintain the drop at its melting temperature. What irradiation would be required if the laser operating wavelength were 0.632 μm?

(c) Estimate the time it would take for the drop to cool to 400 K if the RF field or laser heating were terminated.

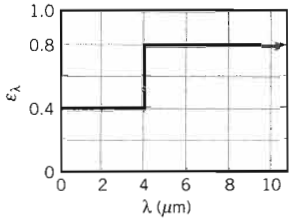
12.101 A thin-walled plate separates the interior of a large furnace from surroundings at 300 K. The plate is fabricated from a ceramic material for which diffuse surface behavior may be assumed and the exterior surface is air cooled. With the furnace operating at 2400 K, convection at the interior surface may be neglected.



(a) If the temperature of the ceramic plate is not to exceed 1800 K, what is the minimum value of the outside convection coefficient, h_o, that must be maintained by the air-cooling system?

(b) Compute and plot the plate temperature as a function of h_o for $50 \le h_o \le 250$ W/m$^2 \cdot$ K.

12.102 A thin coating, which is applied to long, cylindrical copper rods of 10-mm diameter, is cured by placing the rods horizontally in a large furnace whose walls are maintained at 1300 K. The furnace is filled with nitrogen gas, which is also at 1300 K and at a pressure of 1 atm. The coating is diffuse, and its spectral emissivity has the distribution shown.



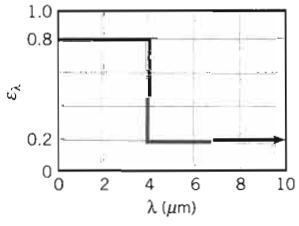
(a) What are the emissivity and absorptivity of the coated rods when their temperature is 300 K?

(b) What is the initial rate of change of their temperature?

(c) What are the emissivity and absorptivity of the coated rods when they reach a steady-state temperature?

(d) Estimate the time required for the rods to reach 1000 K.

12.103 A large combination convection–radiation oven is used to heat-treat a small cylindrical product of diameter 25 mm and length 0.2 m. The oven walls are at a uniform temperature of 1000 K, and hot air at 750 K is in cross flow over the cylinder with a velocity of 5 m/s. The cylinder surface is opaque and diffuse with the spectral emissivity shown.



(a) Determine the rate of heat transfer to the cylinder when it is first placed in the oven at 300 K.

(b) What is the steady-state temperature of the cylinder?

(c) How long will it take for the cylinder to reach a temperature that is within 50°C of its steady-state value?

12.104 A 10-mm-th
annealed at
of at least 5
is opaque a
of its emis
is effected i
ing air at
100 W/m^2 ·
workpiece
k = 165 W

1
0.8
ε_λ
0.3

(a) Calcu
the w
its ini

(b) Deter
for th
ing ra
work

(c) Using
IHT,
work
range

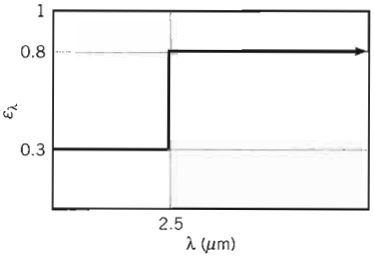
(d) Assu
tance
work
tion
deriv
IHT
as a

(e) Calc
from
40°C
pera
is 1(

(f) Assu
incre
5 mi
is ir
the
end
proc

Patent Owner Manufacturing Resources International, Inc.
Exhibit 2017 - Page 806 of 999

12.104 A 10-mm-thick workpiece, initially at 25°C, is to be annealed at a temperature above 725°C for a period of at least 5 minutes and then cooled. The workpiece is opaque and diffuse, and the spectral distribution of its emissivity is shown schematically. Heating is effected in a large furnace with walls and circulating air at 750°C and a convection coefficient of 100 W/m^2 · K. The thermophysical properties of the workpiece are $\rho = 2700$ kg/m^3, $c = 885$ J/kg · K, and $k = 165$ W/m · K.



(a) Calculate the emissivity and the absorptivity of the workpiece when it is placed in the furnace at its initial temperature of 25°C.

(b) Determine the net heat flux into the workpiece for this initial condition. What is the corresponding rate of change in temperature, dT/dt, for the workpiece?

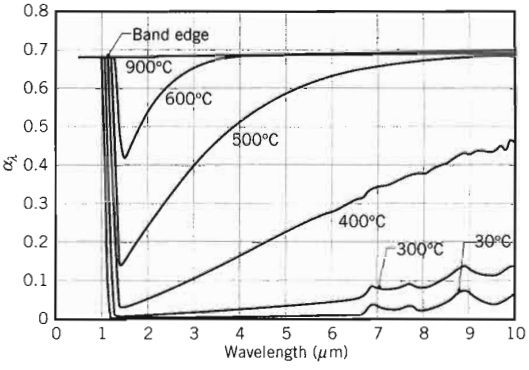
(c) Using the *Tools/Radiation/Band Emission* model of *IHT*, calculate and plot the emissivity of the workpiece as a function of temperature for the range from 25 to 750°C.

(d) Assuming applicability of the lumped capacitance method, calculate the time required for the workpiece to reach 725°C. Use the DER function in *IHT* to represent the temperature-time derivative in your energy balance. Also use the *IHT* code of part (c) to represent the emissivity as a function of workpiece temperature.

(e) Calculate the time for the workpiece to cool from 750°C to a safe-to-touch temperature of 40°C, if the surroundings and cooling air temperature are 25°C and the convection coefficient is 100 W/m^2 · K.

(f) Assuming that the workpiece temperature increases from 725°C to 750°C during a 5 minute annealing period, after which cooling is initiated, sketch the temperature history of the workpiece from the start of heating to the end of cooling. Identify key features of the process and determine the total time requirement. Is the lumped-capacitance method of analysis justified?

12.105 After being cut from a large single-crystal boule and polished, silicon wafers undergo a high-temperature annealing process. One technique for heating the wafer is to irradiate its top surface using high-intensity, tungsten-halogen lamps having a spectral distribution approximating that of a blackbody at 2800 K. To determine the lamp power and the rate at which radiation is absorbed by the wafer, the equipment designer needs to know its absorptivity as a function of temperature. Silicon is a semiconductor material that exhibits a characteristic *band edge*, and its spectral absorptivity may be idealized as shown schematically. At low and moderate temperatures, silicon is semitransparent at wavelengths larger than that of the band edge, but becomes nearly opaque above 600°C.



(a) What are the 1% limits of the spectral band that includes 98% of the blackbody radiation corresponding to the spectral distribution of the lamps? Over what spectral region do you need to know the spectral absorptivity?

(b) How do you expect the total absorptivity of silicon to vary as a function of its temperature? Sketch the variation and explain its key features.

(c) Calculate the total absorptivity of the silicon wafer for the lamp irradiation and each of the five temperatures shown schematically. From the data, calculate the emissivity of the wafer at 600 and 900°C. Explain your results and why the emissivity changes with temperature. *Hint*: Within *IHT*, create a *look-up* table to specify values of the spectral properties and the LOOKUPVAL and INTEGRAL functions to perform the necessary integrations.

Patent Owner Manufacturing Resources International, Inc.
Exhibit 2017 - Page 807 of 999

(d) If the wafer is in a vacuum and radiation exchange only occurs at one face, what is the irradiation needed to maintain a wafer temperature of 600°C?

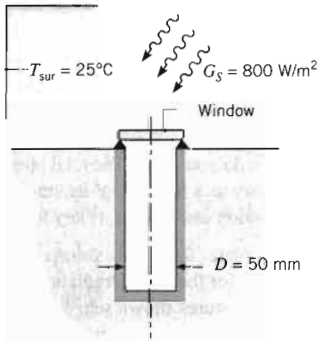
Environmental Radiation

12.106 Solar irradiation of 1100 W/m^2 is incident on a large, flat, horizontal metal roof on a day when the wind blowing over the roof causes a convection heat transfer coefficient of 25 W/m^2 · K. The outside air temperature is 27°C, the metal surface absorptivity for incident solar radiation is 0.60, the metal surface emissivity is 0.20, and the roof is well insulated from below.

(a) Estimate the roof temperature under steady-state conditions.

(b) Explore the effect of changes in the absorptivity, emissivity, and convection coefficient on the steady-state temperature.

12.107 A deep cavity of 50-mm diameter approximates a blackbody and is maintained at 250°C while exposed to solar irradiation of 800 W/m^2 and surroundings and ambient air at 25°C. A thin window of spectral transmissivity and reflectivity 0.9 and 0, respectively, for the spectral range 0.2 to 4 μm is placed over the cavity opening. In the spectral range beyond 4 μm, the window behaves as an opaque, diffuse, gray body of emissivity 0.95. Assuming that the convection coefficient on the upper surface of the window is 10 W/m^2 · K, determine the temperature of the window and the power required to maintain the cavity at 250°C.



12.108 Consider the evacuated tube solar collector described in part (d) of Problem 1.73 of Chapter 1. In the interest of maximizing collector efficiency, what spectral radiative characteristics are desired for the outer tube and for the inner tube?

12.109 Solar flux of 900 W/m^2 is incident on the top side of a plate whose surface has a solar absorptivity of 0.9 and an emissivity of 0.1. The air and surroundings are at 17°C and the convection heat transfer coefficient between the plate and air is 20 W/m^2 · K. Assuming that the bottom side of the plate is insulated, determine the steady-state temperature of the plate.

12.110 Consider an opaque, gray surface whose directional absorptivity is 0.8 for $0 \leq \theta \leq 60°$ and 0.1 for $\theta > 60°$. The surface is horizontal and exposed to solar irradiation comprised of direct and diffuse components.

(a) What is the surface absorptivity to direct solar radiation that is incident at an angle of 45° from the normal? What is the absorptivity to diffuse irradiation?

(b) Neglecting convection heat transfer between the surface and the surrounding air, what would be the equilibrium temperature of the surface if the direct and diffuse components of the irradiation were 600 and 100 W/m^2, respectively? The back side of the surface is insulated.

12.111 The absorber plate of a solar collector may be coated with an opaque material for which the spectral, directional absorptivity is characterized by relations of the form

$$\alpha_{\lambda,\theta}(\lambda, \theta) = \alpha_1 \cos\theta \qquad \lambda < \lambda_c$$
$$\alpha_{\lambda,\theta}(\lambda, \theta) = \alpha_2 \qquad \lambda > \lambda_c$$

The zenith angle θ is formed by the sun's rays and the plate normal, and α_1 and α_2 are constants.

(a) Obtain an expression for the total, hemispherical absorptivity, α_S, of the plate to solar radiation incident at $\theta = 45°$. Evaluate α_S for $\alpha_1 = 0.93$, $\alpha_2 = 0.25$, and a cut-off wavelength of $\lambda_c = 2\ \mu$m.

(b) Obtain an expression for the total, hemispherical emissivity ε of the plate. Evaluate ε for a plate temperature of $T_p = 60°C$ and the prescribed values of α_1, α_2, and λ_c.

(c) For a solar flux of $q''_S = 1000$ W/m^2 incident at $\theta = 45°$ and the prescribed values of $\alpha_1, \alpha_2, \lambda_c$, and T_p, what is the net radiant heat flux, q''_{net}, to the plate?

(d) Using the prescribed conditions and the *Radiation/Band Emission Factor* option in the *Tools* section of *IHT* to evaluate $F_{(0\rightarrow\lambda_c)}$, explore the effect of λ_c on α_S, ε, and q''_{net} for the wavelength range $0.7 \leq \lambda_c \leq 5\ \mu$m.

12.112 A contra
from the
shown. W
lower roo
mer use?
tion of α
winter us

1.0
0.8
0.6
α_λ 0.4
0.2

12.113 It is not
desert re
temperat
for still
can a sha

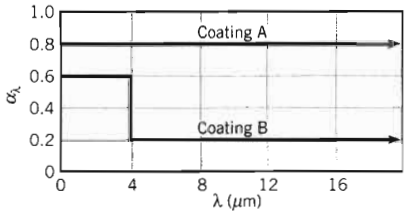
12.114 Radiatio
mated as
sponding
That is,
$G_{sky} = \varepsilon$
sivity is
$\varepsilon_{sky} = 0.$
temperat
night sk
humidity
is insula
the fron
$\overline{h}$(W/m^2
value of
dew for
metallic

12.115 A thin s
house a

The irr
flux G_s

Patent Owner Manufacturing Resources International, Inc.
Exhibit 2017 - Page 808 of 999

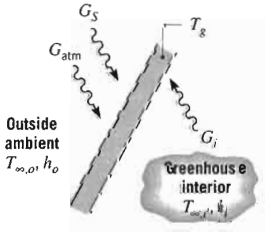
12.112 A contractor must select a roof covering material from the two diffuse, opaque coatings with $\alpha_\lambda(\lambda)$ as shown. Which of the two coatings would result in a lower roof temperature? Which is preferred for summer use? For winter use? Sketch the spectral distribution of α_λ that would be ideal for summer use. For winter use.



12.113 It is not uncommon for the night sky temperature in desert regions to drop to $-40°C$. If the ambient air temperature is 20°C and the convection coefficient for still air conditions is approximately 5 $W/m^2 \cdot K$, can a shallow pan of water freeze?

12.114 Radiation from the atmosphere or sky can be estimated as a fraction of the blackbody radiation corresponding to the air temperature near the ground, T_{air}. That is, irradiation from the sky can be expressed as $G_{sky} = \varepsilon_{sky}\sigma T_{air}^4$ and for a clear night sky, the emissivity is correlated by an expression of the form $\varepsilon_{sky} = 0.741 + 0.0062T_{dp}$, where T_{dp} is the dew point temperature (°C). Consider a flat plate exposed to the night sky and in ambient air at 15°C with a relative humidity of 70%. Assume the back side of the plate is insulated, and that the convection coefficient on the front side can be estimated by the correlation $\bar{h}(W/m^2 \cdot K) = 1.25\Delta T^{1/3}$, where ΔT is the absolute value of the plate-to-air temperature difference. Will dew form on the plate if the surface is (a) clean and metallic with $\varepsilon = 0.23$, and (b) painted with $\varepsilon = 0.85$?

12.115 A thin sheet of glass is used on the roof of a greenhouse and is irradiated as shown.

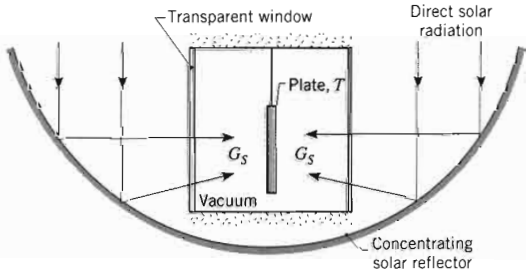


The irradiation comprises the total solar flux G_S, the flux G_{atm} due to atmospheric emission (sky radiation), and the flux G_i due to emission from interior surfaces. The fluxes G_{atm} and G_i are concentrated in the far IR region ($\lambda \gtrsim 8\ \mu m$). The glass may also exchange energy by convection with the outside and inside atmospheres. The glass may be assumed to be totally transparent for $\lambda < 1\ \mu m$ ($\tau_\lambda = 1.0$ for $\lambda < 1\ \mu m$) and opaque, with $\alpha_\lambda = 1.0$ for $\lambda \geq 1\ \mu m$.

(a) Assuming steady-state conditions, with all radiative fluxes uniformly distributed over the surfaces and the glass characterized by a uniform temperature T_g, write an appropriate energy balance for a unit area of the glass.

(b) For $T_g = 27°C$, $h_i = 10\ W/m^2 \cdot K$, $G_S = 1100\ W/m^2$, $T_{\infty,o} = 24°C$, $h_o = 55\ W/m^2 \cdot K$, $G_{atm} = 250\ W/m^2$, and $G_i = 440\ W/m^2$, calculate the temperature of the greenhouse ambient air, $T_{\infty,i}$.

12.116 A solar furnace consists of an evacuated chamber with transparent windows, through which concentrated solar radiation is passed. Concentration may be achieved by mounting the furnace at the focal point of a large curved reflector that tracks radiation incident directly from the sun. The furnace may be used to evaluate the behavior of materials at elevated temperatures, and we wish to design an experiment to assess the durability of a diffuse, spectrally selective coating for which $\alpha_\lambda = 0.95$ in the range $\lambda \leq 4.5\ \mu m$ and $\alpha_\lambda = 0.03$ for $\lambda > 4.5\ \mu m$. The coating is applied to a plate that is suspended in the furnace.

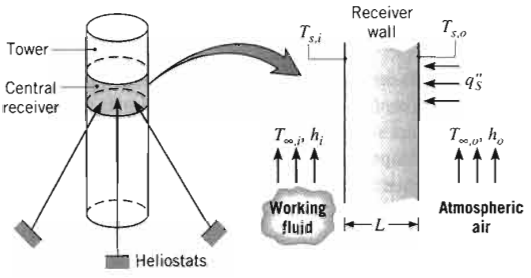


(a) If the experiment is to be operated at a steady-state plate temperature of $T = 2000$ K, how much solar irradiation G_S must be provided? The irradiation may be assumed to be uniformly distributed over the plate surface, and other sources of incident radiation may be neglected.

(b) The solar irradiation may be *tuned* to allow operation over a range of plate temperatures. Compute and plot G_S as a function of temperature for $500 \leq T \leq 3000$ K. Plot the corresponding values of α and ε as a function of T for the designated range.

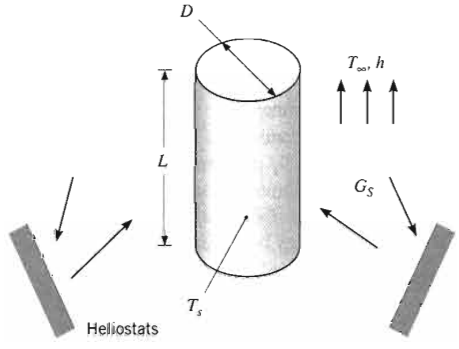
Patent Owner Manufacturing Resources International, Inc.
Exhibit 2017 - Page 809 of 999

12.117 In the central receiver concept of solar energy collection, a large number of heliostats (reflectors) provide a concentrated solar flux of $q''_S = 80{,}000$ W/m^2 to the receiver, which is positioned at the top of a tower.



The receiver wall is exposed to the solar flux at its outer surface and to atmospheric air for which $T_{\infty,o} = 300$ K and $h_o = 25$ W/m$^2 \cdot$ K. The outer surface is opaque and diffuse, with a spectral absorptivity of $\alpha_\lambda = 0.9$ for $\lambda < 3$ μm and $\alpha_\lambda = 0.2$ for $\lambda > 3$ μm. The inner surface is exposed to a working fluid (a pressurized liquid) for which $T_{\infty,i} = 700$ K and $h_i = 1000$ W/m$^2 \cdot$ K. The outer surface is also exposed to surroundings for which $T_{sur} = 300$ K. If the wall is fabricated from a high-temperature material for which $k = 15$ W/m $\cdot$ K, what is the minimum thickness L needed to ensure that the outer surface temperature does not exceed $T_{s,o} = 1000$ K? What is the collection efficiency associated with this thickness?

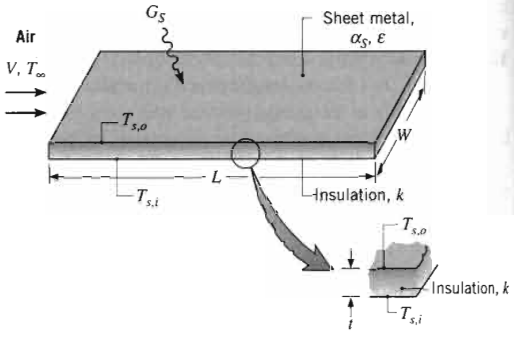
12.118 Consider the central receiver of Problem 12.117 to be a cylindrical shell of outer diameter $D = 7$ m and length $L = 12$ m. The outer surface is opaque and diffuse, with a spectral absorptivity of $\alpha_\lambda = 0.9$ for $\lambda < 3$ μm and $\alpha_\lambda = 0.2$ for $\lambda > 3$ μm. The surface is exposed to *quiescent* ambient air for which $T_\infty = 300$ K.



(a) Consider representative operating conditions for which solar irradiation at $G_S = 80{,}000$ W/m^2 is uniformly distributed over the receiver surface and the surface temperature is $T_s = 800$ K. Determine the rate at which energy is collected by the receiver and the corresponding collector efficiency.

(b) The surface temperature is affected by conditions internal to the receiver. For $G_S = 80{,}000$ W/m^2, compute and plot the rate of energy collection and the collector efficiency for $600 \leq T_s \leq 1000$ K.

12.119 The flat roof on the refrigeration compartment of a food delivery truck is of length $L = 5$ m and width $W = 2$ m. It is fabricated from thin sheet metal to which a fiberboard insulating material of thickness $t = 25$ mm and thermal conductivity $k = 0.05$ W/m $\cdot$ K is bonded. During normal operation, the truck moves at a velocity of $V = 30$ m/s in air at $T_\infty = 27$°C, with a rooftop solar irradiation of $G_S = 900$ W/m^2 and with the interior surface temperature maintained at $T_{s,i} = -13$°C.



(a) The owner has the option of selecting a roof coating from one of the three paints listed in Table A.12 (Parsons Black, Acrylic White, or Zinc Oxide White). Which should be chosen and why?

(b) For the preferred paint of part (a), determine the steady-state value of the outer surface temperature $T_{s,o}$. The boundary layer is tripped at the leading edge of the roof, and turbulent flow may be assumed to exist over the entire roof. Properties of the air may be taken to be $\nu = 15 \times 10^{-6}$ m^2/s, $k = 0.026$ W/m $\cdot$ K, and $Pr = 0.71$.

(c) What is the load (W) imposed on the refrigeration system by heat transfer through the roof?

(d) Explore the effect of the truck velocity on the outer surface temperature and the heat load.

12.120 Growers use giant fans to prevent grapes from freezing when the effective sky temperature is low. The

Patent Owner Manufacturing Resources International, Inc.
Exhibit 2017 - Page 810 of 999

receiver surface and
= 800 K. Determine
lected by the receiver
r efficiency.

affected by condi-
r. For $G_S = 80{,}000$
rate of energy col-
fficiency for $600 \leq$

n compartment of a
$L = 5$ m and width
thin sheet metal to
aterial of thickness
vity $k = 0.05$ W/m ·
peration, the truck
in air at $T_\infty = 27°C$,
of $G_S = 900$ W/m^2
perature maintained

et metal,
α_S, ε
W
lation, k
$T_{s,o}$
Insulation, k
$T_{s,i}$

selecting a roof coat-
aints listed in Table
lic White, or Zinc
be chosen and why?

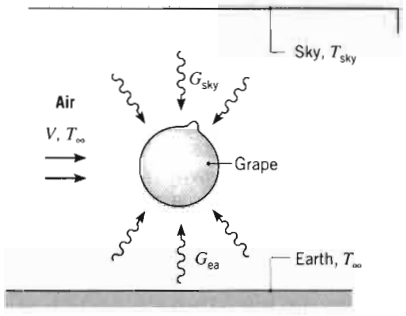
rt (a), determine the
ter surface tempera-
er is tripped at the
d turbulent flow may
entire roof. Proper-
to be $\nu = 15 \times 10^{-6}$
d $Pr = 0.71$.

sed on the refrigera-
through the roof?

uck velocity on the
d the heat load.

t grapes from freez-
perature is low. The

grape, which may be viewed as a thin skin of negligible thermal resistance enclosing a volume of sugar water, is exposed to ambient air and is irradiated from the sky above and ground below. Assume the grape to be an isothermal sphere of 15-mm diameter, and assume uniform blackbody irradiation over its top and bottom hemispheres due to emission from the sky and the earth, respectively.



(a) Derive an expression for the rate of change of the grape temperature. Express your result in terms of a convection coefficient and appropriate temperatures and radiative quantities.

(b) Under conditions for which $T_{sky} = 235$ K, $T_\infty = 273$ K, and the fan is off ($V = 0$), determine whether the grapes will freeze. To a good approximation, the skin emissivity is 1 and the grape thermophysical properties are those of sugarless water. However, because of the sugar content, the grape freezes at $-5°C$.

(c) With all conditions remaining the same, except that the fans are now operating with $V = 1$ m/s, will the grapes freeze?

12.121 A circular metal disk having a diameter of 0.4 m is placed firmly against the ground in a barren horizontal region where the earth is at a temperature of 280 K. The effective sky temperature is also 280 K. The disk is exposed to quiescent ambient air at 300 K and direct solar irradiation of 745 W/m^2. The surface of the disk is diffuse with $\varepsilon_\lambda = 0.9$ for $0 < \lambda < 1$ μm and $\varepsilon_\lambda = 0.2$ for $\lambda > 1$ μm. After some time has elapsed, the disk achieves a uniform, steady-state temperature. The thermal conductivity of the soil is 0.52 W/m · K.

(a) Determine the fraction of the incident solar irradiation that is absorbed.

(b) What is the emissivity of the disk surface?

(c) For a steady-state disk temperature of 340 K, employ a suitable correlation to determine the average free convection heat transfer coefficient at the upper surface of the disk.

(d) Show that a disk temperature of 340 K does indeed yield a steady-state condition for the disk.

12.122 The neighborhood cat likes to sleep on the roof of our shed in the backyard. The roofing surface is weathered galvanized sheet metal ($\varepsilon = 0.65$, $\alpha_S = 0.8$). Consider a cool spring day when the ambient air temperature is 10°C and the convection coefficient can be estimated from an empirical correlation of the form $\bar{h} = 1.0\Delta T^{1/3}$, where ΔT is the difference between the surface and ambient temperatures. Assume the sky temperature is $-40°C$.

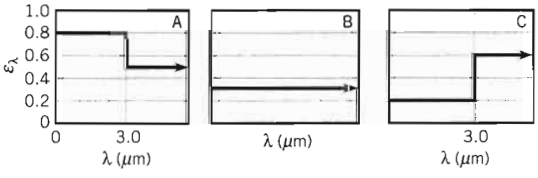
(a) Assuming the backside of the roof is well insulated, calculate the roof temperature when the solar irradiation is 600 W/m^2. Will the cat enjoy sleeping under these conditions?

(b) Consider the case when the backside of the roof is not insulated, but is exposed to ambient air with the same convection coefficient relation and experiences radiation exchange with the ground, also at the ambient air temperature. Calculate the roof temperature and comment on whether the roof will be a comfortable place for the cat to snooze.

12.123 The exposed surface of a power amplifier for an earth satellite receiver of area 130 mm by 130 mm has a diffuse, gray, opaque coating with an emissivity of 0.5. For typical amplifier operating conditions, the surface temperature is 58°C under the following environmental conditions: air temperature, $T_\infty = 27°C$; sky temperature, $T_{sky} = -20°C$; convection coefficient, $h = 15$ W/m^2 · K; and solar irradiation, $G_S = 800$ W/m^2.

(a) For the above conditions, determine the electrical power being generated within the amplifier.

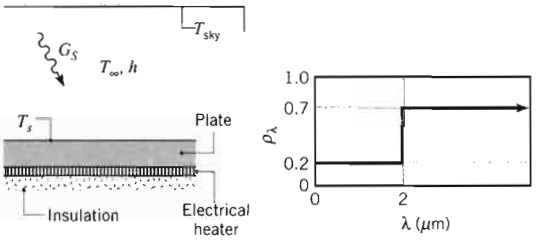
(b) It is desired to reduce the surface temperature by applying one of the diffuse coatings (A, B, C) shown as follows.



Which coating will result in the coolest surface temperature for the same amplifier operating and environmental conditions?

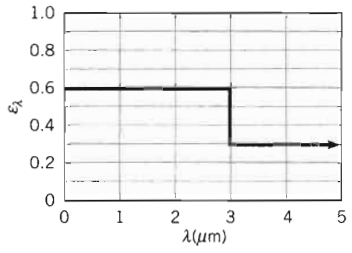
Patent Owner Manufacturing Resources International, Inc.
Exhibit 2017 - Page 811 of 999

12.124 Consider a thin opaque, horizontal plate with an electrical heater on its backside. The front side is exposed to ambient air that is at 20°C and provides a convection heat transfer coefficient of 10 W/m^2 · K, solar irradiation of 600 W/m^2, and an effective sky temperature of −40°C.



What is the electrical power (W/m^2) required to maintain the plate surface temperature at $T_s = 60$°C if the plate is diffuse and has the designated spectral, hemispherical reflectivity?

12.125 The oxidized-aluminum wing of an aircraft has a chord length of $L_c = 4$ m and a spectral, hemispherical emissivity characterized by the following distribution.



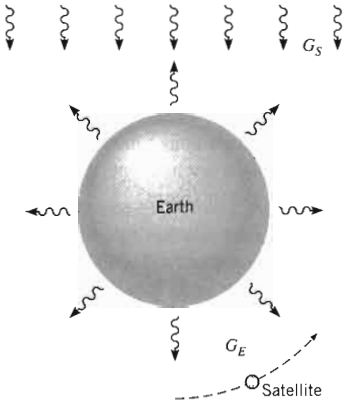
(a) Consider conditions for which the plane is on the ground where the air temperature is 27°C, the solar irradiation is 800 W/m^2, and the effective sky temperature is 270 K. If the air is quiescent, what is the temperature of the top surface of the wing? The wing may be approximated as a horizontal, flat plate.

(b) When the aircraft is flying at an elevation of approximately 9000 m and a speed of 200 m/s, the air temperature, solar irradiation, and effective sky temperature are −40°C, 1100 W/m^2, and 235 K, respectively. What is the temperature of the wing's top surface? The properties of the air may be approximated as $\rho = 0.470$ kg/m^3, $\mu = 1.50 \times 10^{-5}$ N · s/m^2, $k = 0.021$ W/m · K, and Pr = 0.72.

Space Radiation

12.126 Two plates, one with a black painted surface and the other with a special coating (chemically oxidized copper) are in earth orbit and are exposed to solar radiation. The solar rays make an angle of 30° with the normal to the plate. Estimate the equilibrium temperature of each plate assuming they are diffuse and that the solar flux is 1353 W/m^2. The spectral absorptivity of the black painted surface can be approximated by $\alpha_\lambda = 0.95$ for $0 \le \lambda \le \infty$ and that of the special coating by $\alpha_\lambda = 0.95$ for $0 \le \lambda < 3\ \mu$m and $\alpha_\lambda = 0.05$ for $\lambda \ge 3\ \mu$m.

12.127 A spherical satellite of diameter D is in orbit about the earth and is coated with a diffuse material for which the spectral absorptivity is $\alpha_\lambda = 0.6$ for $\lambda \le 3\ \mu$m and $\alpha_\lambda = 0.3$ for $\lambda > 3\ \mu$m. When it is on the "dark" side of the earth, the satellite sees irradiation from the earth's surface only. The irradiation may be assumed to be incident as parallel rays, and its magnitude is $G_E = 340$ W/m^2. On the "bright" side of the earth the satellite sees the earth irradiation G_E plus the solar irradiation $G_S = 1353$ W/m^2. The spectral distribution of radiation from the earth may be approximated as that of a blackbody at 280 K, and the temperature of the satellite may be assumed to remain below 500 K.



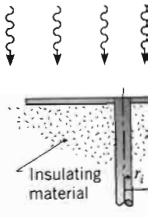
What is the steady-state temperature of the satellite when it is on the dark side of the earth and when it is on the bright side?

12.128 A radiator on a proposed satellite solar power station must dissipate heat being generated within the satellite by radiating it into space. The radiator surface has a solar absorptivity of 0.5 and an emissivity of 0.95. What is the equilibrium surface temperature when the

solar irrac
dissipatio

12.129 A spheric
solar irrac
operating
intends tc
F of the s
aluminur
tion (1-F
($\varepsilon = 0.85$
mal and
the fracti
tain the sa

12.130 An annul
dissipate
insulated
irradiatio
trally sel
specified



Heat is
radius r_i
radiates
zero tem

(a) If c
base
fin
diss
side
exp
oth

(b) In
100
incr
ate
tior
tem
app

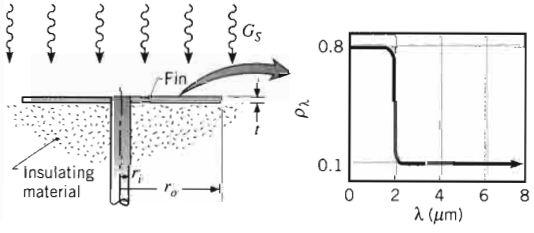
12.131 A rectar
W is pr
applicat
tivity o

Patent Owner Manufacturing Resources International, Inc.
Exhibit 2017 - Page 812 of 999

solar irradiation is 1000 W/m^2 and the required heat dissipation is 1500 W/m^2?

12.129 A spherical satellite in near-earth orbit is exposed to solar irradiation of 1353 W/m^2. To maintain a desired operating temperature, the thermal control engineer intends to use a checker pattern for which a fraction F of the satellite surface is coated with an evaporated aluminum film ($\varepsilon = 0.03$, $\alpha_S = 0.09$) and the fraction (1-F) is coated with a white, zinc-oxide paint ($\varepsilon = 0.85, \alpha_S = 0.22$). Assume the satellite is isothermal and has no internal power dissipation. Determine the fraction F of the checker pattern required to maintain the satellite at 300 K.

12.130 An annular fin of thickness t is used as a radiator to dissipate heat for a space power system. The fin is insulated on the bottom and may be exposed to solar irradiation G_S. The fin is coated with a diffuse, spectrally selective material whose spectral reflectivity is specified.

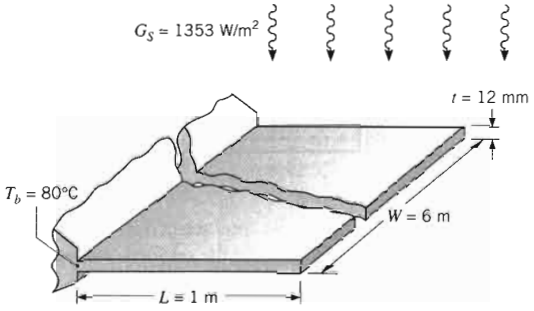


Heat is conducted to the fin through a solid rod of radius r_i, and the exposed upper surface of the fin radiates to free space, which is essentially at absolute zero temperature.

(a) If conduction through the rod maintains a fin base temperature of $T(r_i) = T_b = 400$ K and the fin efficiency is 100%, what is the rate of heat dissipation for a fin of radius $r_o = 0.5$ m? Consider two cases, one for which the radiator is exposed to the sun with $G_S = 1000$ W/m^2 and the other with no exposure ($G_S = 0$).

(b) In practice, the fin efficiency will be less than 100% and its temperature will decrease with increasing radius. Beginning with an appropriate control volume, derive the differential equation that determines the steady-state, radial temperature distribution in the fin. Specify appropriate boundary conditions.

12.131 A rectangular plate of thickness t, length L, and width W is proposed for use as a radiator in a spacecraft application. The plate material has a thermal conductivity of 300 W/m · K, a solar absorptivity of 0.45, and an emissivity of 0.9. The radiator is exposed to solar radiation only on its top surface, while both surfaces are exposed to deep space at a temperature of 4 K.

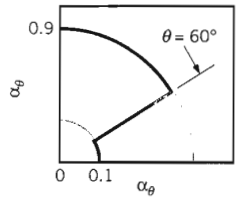


(a) If the base of the radiator is maintained at $T_b = 80$°C, what is its tip temperature and the rate of heat rejection? Use a computer-based, finite-difference method with a space increment of 0.1 m to obtain your solution.

(b) Repeat the calculation of part (a) for the case when the space ship is on the dark side of the earth and is not exposed to the sun.

(c) Use your computer code to calculate the heat rate and tip temperature for $G_S = 0$ and an extremely large value of the thermal conductivity. Compare your results to those obtained from a hand calculation that assumes the radiator to be at a uniform temperature T_b. What other approach might you use to validate your code?

12.132 The directional absorptivity of a gray surface varies with θ as follows.

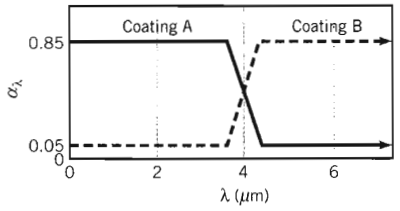


(a) What is the ratio of the normal absorptivity α_n to the hemispherical emissivity of the surface?

(b) Consider a plate with these surface characteristics on both sides in earth orbit. If the solar flux incident on one side of the plate is q''_S = 1353 W/m^2, what equilibrium temperature will the plate assume if it is oriented normal to the sun's rays? What temperature will it assume if it is oriented at 75° to the sun's rays?

Patent Owner Manufacturing Resources International, Inc.
Exhibit 2017 - Page 813 of 999

12.133 Two special coatings are available for application to an absorber plate installed below the cover glass described in Example 12.8. Each coating is diffuse and is characterized by the spectral distributions shown.



Which coating would you select for the absorber plate? Explain briefly. For the selected coating, what is the rate at which radiation is absorbed per unit area of the absorber plate if the total solar irradiation at the cover glass is $G_S = 1000$ W/m^2?

12.134 Consider the spherical satellite of Problem 12.127. Instead of the entire satellite being coated with a material that is spectrally selective, half of the satellite is covered with a diffuse gray coating characterized by $\alpha_1 = 0.6$. The other half of the satellite is coated with a diffuse gray material with $\alpha_2 = 0.3$.

(a) Determine the steady-state satellite temperature when the satellite is on the bright side of the earth with the high-absorptivity coating facing the sun. Determine the steady-state satellite temperature when the low-absorptivity coating faces the sun. *Hint*: Assume one hemisphere of the satellite is irradiated by the sun and the opposite hemisphere is irradiated by the earth.

(b) Determine the steady-state satellite temperature when the satellite is on the dark side of the earth with the high-absorptivity coating facing the earth. Determine the steady-state satellite temperature when the low-absorptivity coating faces the earth.

(c) Identify a scheme to minimize the temperature variations of the satellite as it travels between the bright and dark sides of the earth.

12.135 A spherical capsule of 3-m radius is fired from a space platform in earth orbit, such that it travels toward the center of the sun at 16,000 km/s. Assume that the capsule is a lumped capacitance body with a density–specific heat product of 4×10^6 J/m$^3 \cdot$ K and that its surface is black.

(a) Derive a differential equation for predicting the capsule temperature as a function of time. Solve this equation to obtain the temperature as a function of time in terms of capsule parameters and its initial temperature T_i.

(b) If the capsule begins its journey at 20°C, predict the position of the capsule relative to the sun at which its destruction temperature, 150°C, is reached.

12.136 Consider the spherical satellite of Problem 12.127. By changing the chemistry of the diffuse material used for the coating, engineers can control the *cutoff wavelength* that marks the boundary between $\alpha_\lambda = 0.6$ and $\alpha_\lambda = 0.3$.

(a) What cutoff wavelength will minimize the steady-state temperature of the satellite when it is on the bright side of the earth? Using this coating, what will the steady-state temperature on the dark side of the earth be?

(b) What cutoff wavelength will maximize the steady-state temperature of the satellite when it is on the dark side of the earth? What will the corresponding steady-state temperature be on the bright side?

12.137 A solar panel mounted on a spacecraft has an area of 1 m^2 and a solar-to-electrical power conversion efficiency of 12%. The side of the panel with the photovoltaic array has an emissivity of 0.8 and a solar absorptivity of 0.8. The back side of the panel has an emissivity of 0.7. The array is oriented normal to solar irradiation of 1500 W/m^2.

(a) Determine the steady-state temperature of the panel and the electrical power (W) produced for the prescribed conditions.

(b) If the panel were a thin plate without the solar cells, but with the same radiative properties, determine the temperature of the plate for the prescribed conditions. Compare this result with that from part (a). Are they the same or different? Explain why.

(c) Determine the temperature of the solar panel 1500 s after the spacecraft is eclipsed by the earth. The thermal capacity of the panel per unit area is 9000 J/m$^2 \cdot$ K.

Heat and Mass Transfer

12.138 It is known that on clear nights a thin layer of water on the ground will freeze before the air temperature drops below 0°C. Consider such a layer of water on a clear night for which the effective sky temperature is −30°C and the convection heat transfer coefficient due to wind motion is $h = 25$ W/m$^2 \cdot$ K. The water may be assumed to have an emissivity of 1.0 and to be insulated from the ground as far as conduction is concerned. Neglecting evaporation, determine the lowest temperature that the air can have without the water freezing. Accounting now for the effect of

evapor
air can
air to b

12.139 A shal
enviro

Consi
pheric
300 W
relativ
respec
the sc
and ρ
ity is
cient a
the wa
decrea

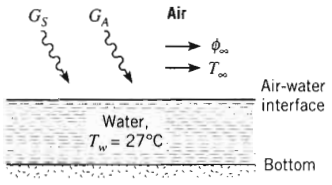
12.140 A roof
a thin l
reduce
enviro
mine t
sheet r
0.50 a
sentati
tion co
of 700
pheric
65%.
from b
withou
surface
temper
the her
binatio

12.141 A wet
for wl
$G_S =$
atmos
200 W
moder
ture of
a conv
at botl

Patent Owner Manufacturing Resources International, Inc.
Exhibit 2017 - Page 814 of 999

evaporation, what is the lowest temperature that the air can have without the water freezing? Assume the air to be dry.

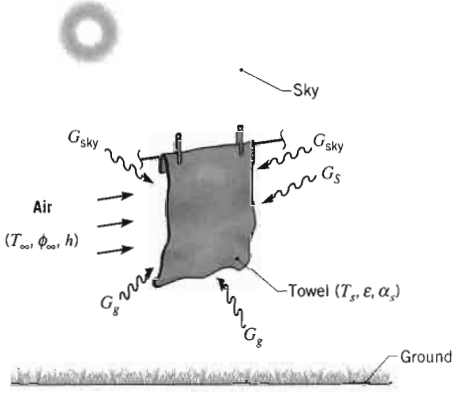
12.139 A shallow layer of water is exposed to the natural environment as shown.



Consider conditions for which the solar and atmospheric irradiations are $G_S = 600$ W/m^2 and $G_A = 300$ W/m^2, respectively, and the air temperature and relative humidity are $T_\infty = 27°C$ and $\phi_\infty = 0.50$, respectively. The reflectivities of the water surface to the solar and atmospheric irradiation are $\rho_S = 0.3$ and $\rho_A = 0$, respectively, while the surface emissivity is $\varepsilon = 0.97$. The convection heat transfer coefficient at the air–water interface is $h = 25$ W/m$^2 \cdot$ K. If the water is at 27°C, will this temperature increase or decrease with time?

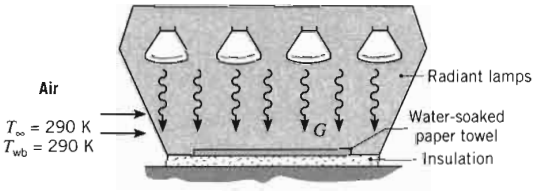
12.140 A roof-cooling system, which operates by maintaining a thin film of water on the roof surface, may be used to reduce air-conditioning costs or to maintain a cooler environment in nonconditioned buildings. To determine the effectiveness of such a system, consider a sheet metal roof for which the solar absorptivity α_S is 0.50 and the hemispherical emissivity ε is 0.3. Representative conditions correspond to a surface convection coefficient h of 20 W/m$^2 \cdot$ K, a solar irradiation G_S of 700 W/m^2, a sky temperature of $-10°C$, an atmospheric temperature of 30°C, and a relative humidity of 65%. The roof may be assumed to be well insulated from below. Determine the roof surface temperature without the water film. Assuming the film and roof surface temperatures to be equal, determine the surface temperature with the film. The solar absorptivity and the hemispherical emissivity of the film–surface combination are $\alpha_S = 0.8$ and $\varepsilon = 0.9$, respectively.

12.141 A wet towel hangs on a clothes line under conditions for which one surface receives solar irradiation of $G_S = 900$ W/m^2 and both surfaces are exposed to atmospheric (sky) and ground radiation of $G_{sky} = 200$ W/m^2 and $G_g = 250$ W/m^2, respectively. Under moderately windy conditions, air flow at a temperature of 27°C and a relative humidity of 60% maintains a convection heat transfer coefficient of 20 W/m$^2 \cdot$ K at both surfaces. The wet towel has an emissivity of 0.96 and a solar absorptivity of 0.65. As a first approximation the properties of the atmospheric air may be evaluated at a temperature of 300 K.



Determine the temperature T_s of the towel. What is the corresponding evaporation rate for a towel that is 0.75 m wide by 1.50 m long?

12.142 Our students perform a laboratory experiment to determine mass transfer from a wet paper towel experiencing forced convection and irradiation from radiant lamps. For the values of T_∞ and T_{wb} prescribed on the sketch, the towel temperature was found to be $T_s = 310$ K. In addition, flat-plate correlations yielded average heat and mass transfer convection coefficients of $\bar{h} = 28.7$ W/m$^2 \cdot$ K and $\bar{h}_m = 0.027$ m/s, respectively. The towel has dimensions of 92.5 mm $\times$ 92.5 mm and is diffuse and gray with an emissivity of 0.96.



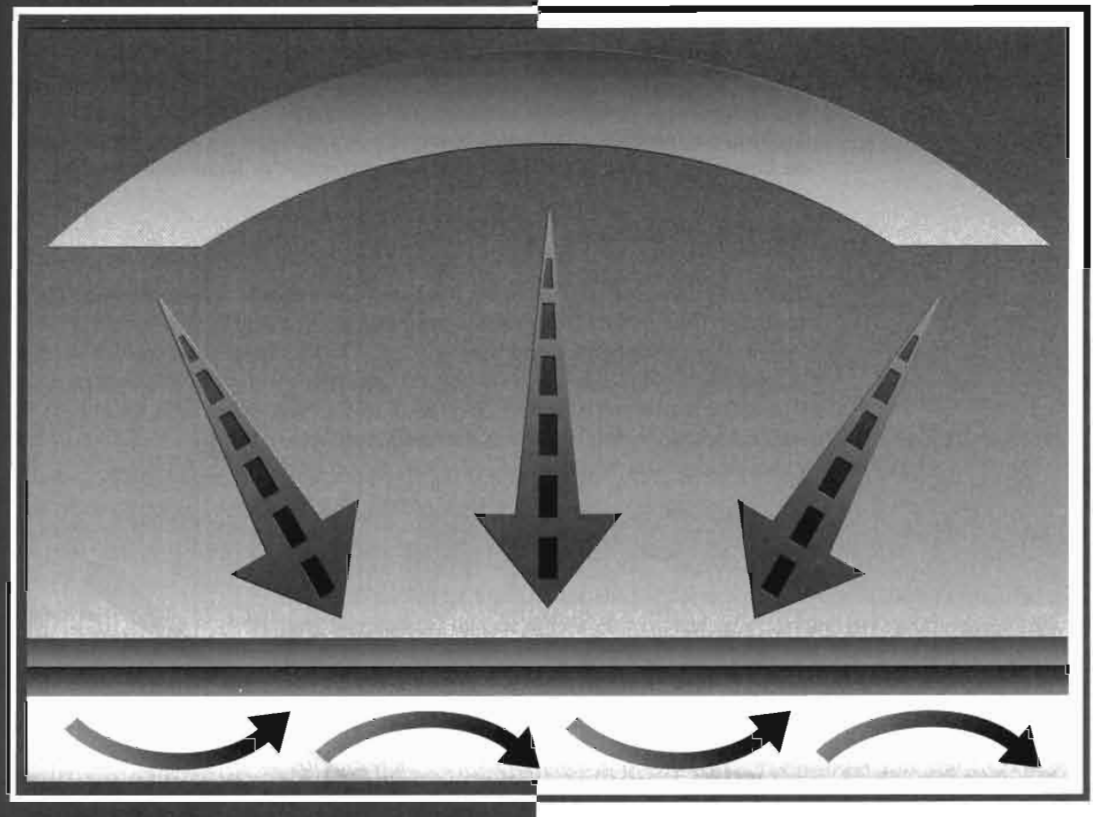
(a) From the foregoing results, determine the vapor densities, $\rho_{A,s}$ and $\rho_{A,\infty}$, the evaporation rate, n_A (kg/s), and the net rate of radiation transfer to the towel, q_{rad} (W).

(b) Using results from part (a) and assuming that the irradiation G is uniform over the towel, determine the emissive power E, the irradiation G, and the radiosity J.

Patent Owner Manufacturing Resources International, Inc.
Exhibit 2017 - Page 815 of 999

CHAPTER 13

Radiation Exchange Between Surfaces



Patent Owner Manufacturing Resources International, Inc.
Exhibit 2017 - Page 816 of 999

Having thus far restricted our attention to radiative processes that occur at a *single surface*, we now consider the problem of radiative exchange between two or more surfaces. This exchange depends strongly on the surface geometries and orientations, as well as on their radiative properties and temperatures. Initially, we assume that the surfaces are separated by a *nonparticipating medium.* Since such a medium neither emits, absorbs, nor scatters, it has no effect on the transfer of radiation between surfaces. A vacuum meets these requirements exactly, and most gases meet them to an excellent approximation.

Our first objective is to establish geometrical features of the radiation exchange problem by developing the notion of a *view factor.* Our second objective is to develop procedures for predicting radiative exchange between surfaces that form an *enclosure.* We conclude our consideration of radiation exchange between surfaces by considering the effects of a *participating medium*, namely, an intervening gas that emits and absorbs radiation.

13.1 The View Factor

To compute radiation exchange between any two surfaces, we must first introduce the concept of a *view factor* (also called a *configuration* or *shape factor*).

13.1.1 The View Factor Integral

The view factor F_{ij} is defined as the *fraction of the radiation leaving surface i that is intercepted by surface j.* To develop a general expression for F_{ij}, we consider the arbitrarily oriented surfaces A_i and A_j of Figure 13.1. Elemental areas on each surface, dA_i and dA_j, are connected by a line of length R, which forms the polar angles θ_i and θ_j, respectively, with the surface normals $\mathbf{n}_i$ and $\mathbf{n}_j$. The values of R, θ_i, and θ_j vary with the position of the elemental areas on A_i and A_j.

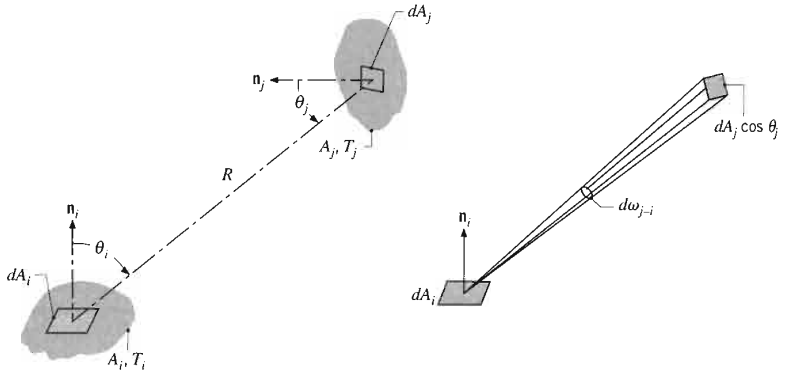


FIGURE 13.1 View factor associated with radiation exchange between elemental surfaces of area dA_i and dA_j.

Patent Owner Manufacturing Resources International, Inc.
Exhibit 2017 - Page 817 of 999

From the definition of the radiation intensity, Section 12.2.2, and Equation 12.6, the rate at which radiation *leaves* dA_i and is *intercepted* by dA_j may be expressed as

$$dq_{i\to j} = I_{e+r,i} \cos\theta_i \, dA_i \, d\omega_{j-i}$$

where $I_{e+r,i}$ is the intensity of radiation leaving surface i by emission and reflection and $d\omega_{j-i}$ is the solid angle subtended by dA_j when viewed from dA_i. With $d\omega_{j-i} = (\cos\theta_j \, dA_j)/R^2$ from Equation 12.2, it follows that

$$dq_{i\to j} = I_{e+r,i} \frac{\cos\theta_i \cos\theta_j}{R^2} dA_i \, dA_j$$

Assuming that surface i *emits* and *reflects diffusely* and substituting from Equation 12.22, we then obtain

$$dq_{i\to j} = J_i \frac{\cos\theta_i \cos\theta_j}{\pi R^2} dA_i \, dA_j$$

The total rate at which radiation leaves surface i and is intercepted by j may then be obtained by integrating over the two surfaces. That is,

$$q_{i\to j} = J_i \int_{A_i} \int_{A_j} \frac{\cos\theta_i \cos\theta_j}{\pi R^2} dA_i \, dA_j$$

where it is assumed that the radiosity J_i is uniform over the surface A_i. From the definition of the view factor as the fraction of the radiation that leaves A_i and is intercepted by A_j,

$$F_{ij} = \frac{q_{i\to j}}{A_i J_i}$$

it follows that

$$F_{ij} = \frac{1}{A_i} \int_{A_i} \int_{A_j} \frac{\cos\theta_i \cos\theta_j}{\pi R^2} dA_i \, dA_j \tag{13.1}$$

Similarly, the view factor F_{ji} is defined as the fraction of the radiation that leaves A_j and is intercepted by A_i. The same development then yields

$$F_{ji} = \frac{1}{A_j} \int_{A_i} \int_{A_j} \frac{\cos\theta_i \cos\theta_j}{\pi R^2} dA_i \, dA_j \tag{13.2}$$

Either Equation 13.1 or 13.2 may be used to determine the view factor associated with any two surfaces that are *diffuse emitters* and *reflectors* and have *uniform radiosity*.

13.1.2 View Factor Relations

An important view factor relation is suggested by Equations 13.1 and 13.2. In particular, equating the integrals appearing in these equations, it follows that

$$A_i F_{ij} = A_j F_{ji} \tag{13.3}$$

This expression, termed the *reciprocity relation*, is useful in determining one view factor from knowledge of the other.

Patent Owner Manufacturing Resources International, Inc.
Exhibit 2017 - Page 818 of 999

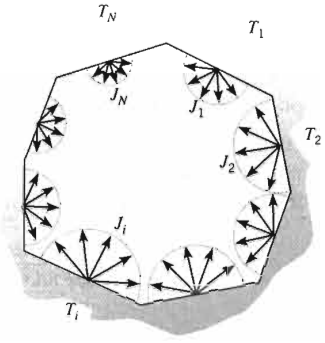


FIGURE 13.2
Radiation exchange in an enclosure.

Another important view factor relation pertains to the surfaces of an *enclosure* (Figure 13.2). From the definition of the view factor, the *summation rule*

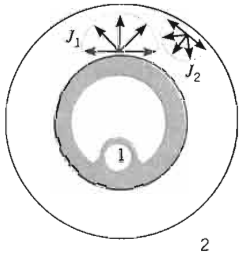
$$\sum_{j=1}^{N} F_{ij} = 1 \tag{13.4}$$

may be applied to each of the N surfaces in the enclosure. This rule follows from the conservation requirement that all radiation leaving surface i must be intercepted by the enclosure surfaces. The term F_{ii} appearing in this summation represents the fraction of the radiation that leaves surface i and is directly intercepted by i. If the surface is concave, it *sees itself* and F_{ii} is nonzero. However, for a plane or convex surface, $F_{ii} = 0$.

To calculate radiation exchange in an enclosure of N surfaces, a total of N^2 view factors is needed. This requirement becomes evident when the view factors are arranged in the matrix form:

$$\begin{bmatrix} F_{11} & F_{12} & \cdots & F_{1N} \\ F_{21} & F_{22} & \cdots & F_{2N} \\ \vdots & \vdots & & \vdots \\ F_{N1} & F_{N2} & \cdots & F_{NN} \end{bmatrix}$$

However, all the view factors need not be calculated *directly*. A total of N view factors may be obtained from the N equations associated with application of the



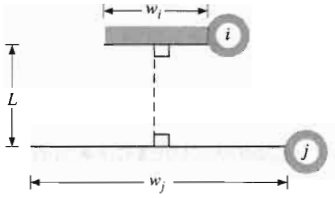
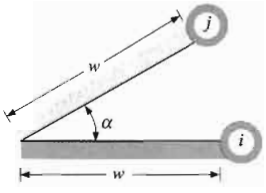
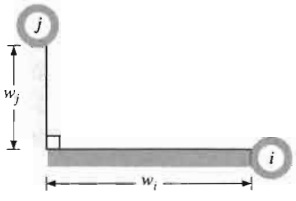
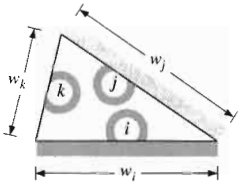
$$F_{12} = 1 \qquad F_{11} = 0$$
$$F_{21} = \frac{A_1}{A_2} \qquad F_{22} = 1 - \frac{A_1}{A_2}$$

FIGURE 13.3
View factors for the enclosure formed by two spheres.

Patent Owner Manufacturing Resources International, Inc.
Exhibit 2017 - Page 819 of 999

summation rule, Equation 13.4, to each of the surfaces in the enclosure. In addition, $N(N-1)/2$ view factors may be obtained from the $N(N-1)/2$ applications of the reciprocity relation, Equation 13.3, which are possible for the enclosure. Accordingly, only $[N^2 - N - N(N-1)/2] = N(N-1)/2$ view factors need be determined directly. For example, in a three-surface enclosure this requirement corresponds to

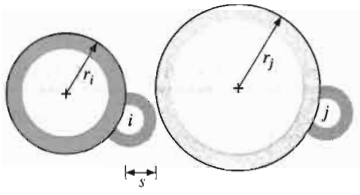
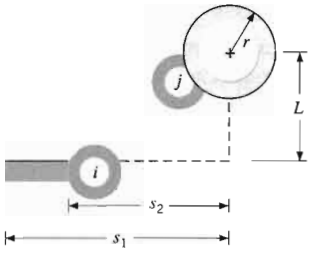
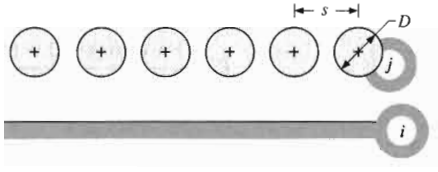
TABLE 13.1 View Factors for Two-Dimensional Geometries [4]

Geometry	Relation
Parallel Plates with Midlines Connected by Perpendicular 	$F_{ij} = \dfrac{[(W_i + W_j)^2 + 4]^{1/2} - [(W_j - W_i)^2 + 4]^{1/2}}{2W_i}$ $W_i = w_i/L,\ W_j = w_j/L$
Inclined Parallel Plates of Equal Width and a Common Edge 	$F_{ij} = 1 - \sin\left(\dfrac{\alpha}{2}\right)$
Perpendicular Plates with a Common Edge 	$F_{ij} = \dfrac{1 + (w_j/w_i) - [1 + (w_j/w_i)^2]^{1/2}}{2}$
Three-Sided Enclosure 	$F_{ij} = \dfrac{w_i + w_j - w_k}{2w_i}$

(continues)

Patent Owner Manufacturing Resources International, Inc.
Exhibit 2017 - Page 820 of 999

TABLE 13.1 *Continued*

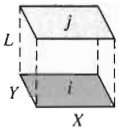
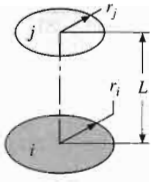
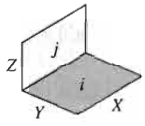
Geometry	Relation
Parallel Cylinders of Different Radii 	$F_{ij} = \frac{1}{2\pi}\left\{\pi + [C^2 - (R+1)^2]^{1/2} - [C^2 - (R-1)^2]^{1/2} + (R-1)\cos^{-1}\left[\left(\frac{R}{C}\right) - \left(\frac{1}{C}\right)\right] - (R+1)\cos^{-1}\left[\left(\frac{R}{C}\right) + \left(\frac{1}{C}\right)\right]\right\}$ $R = r_j/r_i,\ S = s/r_i$ $C = 1 + R + S$
Cylinder and Parallel Rectangle 	$F_{ij} = \frac{r}{s_1 - s_2}\left[\tan^{-1}\frac{s_1}{L} - \tan^{-1}\frac{s_2}{L}\right]$
Infinite Plane and Row of Cylinders 	$F_{ij} = 1 - \left[1 - \left(\frac{D}{s}\right)^2\right]^{1/2} + \left(\frac{D}{s}\right)\tan^{-1}\left[\left(\frac{s^2 - D^2}{D^2}\right)^{1/2}\right]$

only $3(3-1)/2 = 3$ view factors. The remaining six view factors may be obtained by solving the six equations that result from use of Equations 13.3 and 13.4.

To illustrate the foregoing procedure, consider a simple, two-surface enclosure involving the spherical surfaces of Figure 13.3. Although the enclosure is characterized by $N^2 = 4$ view factors (F_{11}, F_{12}, F_{21}, F_{22}), only $N(N-1)/2 = 1$ view factor need be determined directly. In this case such a determination may be made by *inspection*. In particular, since all radiation leaving the inner surface must reach the outer surface, it follows that $F_{12} = 1$. The same may not be said of radiation leaving

Patent Owner Manufacturing Resources International, Inc.
Exhibit 2017 - Page 821 of 999

TABLE 13.2 View Factors for Three-Dimensional Geometries [4]

Geometry	Relation
Aligned Parallel Rectangles (Figure 13.4) 	$\bar{X} = X/L,\ \bar{Y} = Y/L$ $F_{ij} = \frac{2}{\pi \bar{X}\bar{Y}}\left\{\ln\left[\frac{(1+\bar{X}^2)(1+\bar{Y}^2)}{1+\bar{X}^2+\bar{Y}^2}\right]^{1/2} + \bar{X}(1+\bar{Y}^2)^{1/2}\tan^{-1}\frac{\bar{X}}{(1+\bar{Y}^2)^{1/2}} + \bar{Y}(1+\bar{X}^2)^{1/2}\tan^{-1}\frac{\bar{Y}}{(1+\bar{X}^2)^{1/2}} - \bar{X}\tan^{-1}\bar{X} - \bar{Y}\tan^{-1}\bar{Y}\right\}$
Coaxial Parallel Disks (Figure 13.5) 	$R_i = r_i/L,\ R_j = r_j/L$ $S = 1 + \frac{1+R_j^2}{R_i^2}$ $F_{ij} = \frac{1}{2}\{S - [S^2 - 4(r_j/r_i)^2]^{1/2}\}$
Perpendicular Rectangles with a Common Edge (Figure 13.6) 	$H = Z/X,\ W = Y/X$ $F_{ij} = \frac{1}{\pi W}\left(W\tan^{-1}\frac{1}{W} + H\tan^{-1}\frac{1}{H} - (H^2+W^2)^{1/2}\tan^{-1}\frac{1}{(H^2+W^2)^{1/2}} + \frac{1}{4}\ln\left\{\frac{(1+W^2)(1+H^2)}{1+W^2+H^2}\left[\frac{W^2(1+W^2+H^2)}{(1+W^2)(W^2+H^2)}\right]^{W^2} \times \left[\frac{H^2(1+H^2+W^2)}{(1+H^2)(H^2+W^2)}\right]^{H^2}\right\}\right)$

the outer surface, since this surface sees itself. However, from the reciprocity relation, Equation 13.3, we obtain

$$F_{21} = \left(\frac{A_1}{A_2}\right)F_{12} = \left(\frac{A_1}{A_2}\right)$$

From the summation rule, we also obtain

$$F_{11} + F_{12} = 1$$

in which case $F_{11} = 0$, and

$$F_{21} + F_{22} = 1$$

in which case

$$F_{22} = 1 - \left(\frac{A_1}{A_2}\right)$$

Patent Owner Manufacturing Resources International, Inc.
Exhibit 2017 - Page 822 of 999

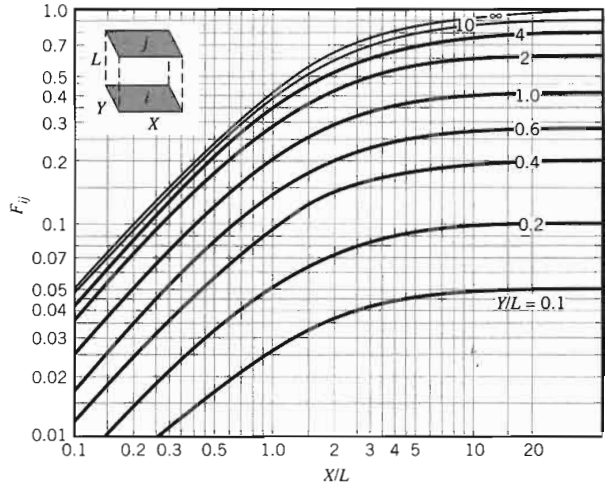


FIGURE 13.4 View factor for aligned parallel rectangles.

For more complicated geometries, the view factor may be determined by solving the double integral of Equation 13.1. Such solutions have been obtained for many different surface arrangements and are available in equation, graphical, and tabular form [1–4]. Results for several common geometries are presented in Tables 13.1 and 13.2 and Figures 13.4 through 13.6. The configurations of Table 13.1 are assumed to be infinitely long (in a direction perpendicular to the page) and are hence two-dimensional. The configurations of Table 13.2 and Figures 13.4 through 13.6 are three-dimensional.

It is useful to note that the results of Figures 13.4 through 13.6 may be used to determine other view factors. For example, the view factor for an end surface of a

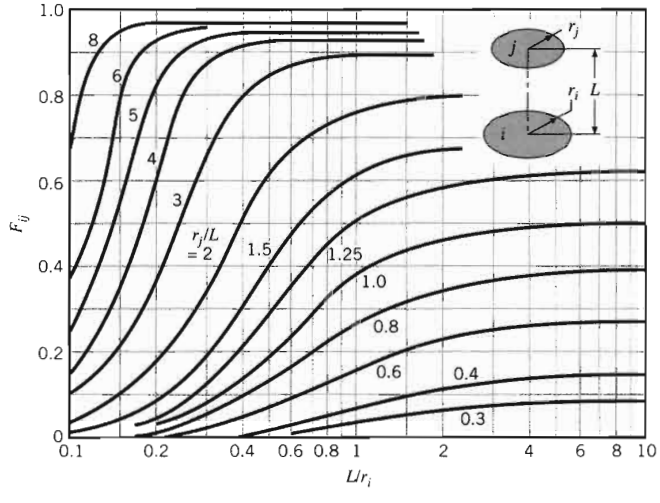


FIGURE 13.5 View factor for coaxial parallel disks.

Patent Owner Manufacturing Resources International, Inc.
Exhibit 2017 - Page 823 of 999

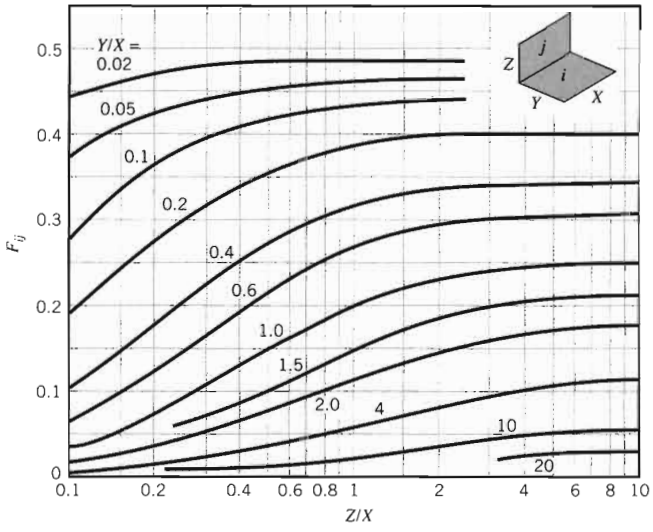


FIGURE 13.6 View factor for perpendicular rectangles with a common edge.

cylinder (or a truncated cone) relative to the lateral surface may be obtained by using the results of Figure 13.5 with the summation rule, Equation 13.4. Moreover, Figures 13.4 and 13.6 may be used to obtain other useful results if two additional view factor relations are developed.

The first relation concerns the additive nature of the view factor for a subdivided surface and may be inferred from Figure 13.7. Considering radiation from surface i to surface j, which is divided into n components, it is evident that

$$F_{i(j)} = \sum_{k=1}^{n} F_{ik} \tag{13.5}$$

where the parentheses around a subscript indicate that it is a composite surface, in which case (j) is equivalent to $(1, 2, \ldots, k, \ldots, n)$. This expression simply states that radiation reaching a composite surface is the sum of the radiation reaching its parts. Although it pertains to subdivision of the receiving surface, it may also be used to obtain the second view factor relation, which pertains to subdivision of the originating

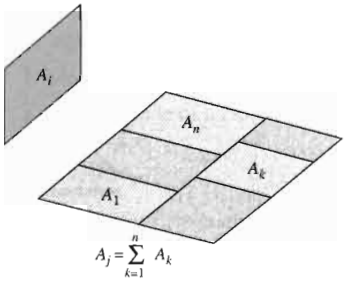


FIGURE 13.7
Areas used to illustrate view factor relations.

Patent Owner Manufacturing Resources International, Inc.
Exhibit 2017 - Page 824 of 999

surface. Multiplying Equation 13.5 by A_i and applying the reciprocity relation, Equation 13.3, to each of the resulting terms, it follows that

$$A_j F_{(j)i} = \sum_{k=1}^{n} A_k F_{ki} \tag{13.6}$$

or

$$F_{(j)i} = \frac{\sum_{k=1}^{n} A_k F_{ki}}{\sum_{k=1}^{n} A_k} \tag{13.7}$$

Equations 13.6 and 13.7 may be applied when the originating surface is composed of several parts.

For problems involving complicated geometries, analytical solutions to Equation 13.1 may not be obtainable, in which case values of the view factors must be estimated using numerical methods. In situations involving extremely complex structures that may have hundreds or thousands of radiative surfaces, considerable error may be associated with the numerically calculated view factors. In such situations, Equation 13.3 should be used to check the accuracy of individual view factors, and Equation 13.4 should be used to determine whether the conservation of energy principle is satisfied [5].

EXAMPLE 13.1

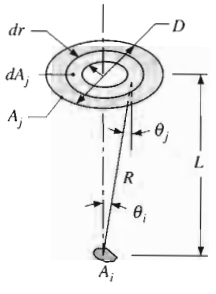
Consider a diffuse circular disk of diameter D and area A_j and a plane diffuse surface of area $A_i \ll A_j$. The surfaces are parallel, and A_i is located at a distance L from the center of A_j. Obtain an expression for the view factor F_{ij}.

SOLUTION

Known: Orientation of small surface relative to large circular disk.

Find: View factor of small surface with respect to disk, F_{ij}.

Schematic:



Assumptions:

1. Diffuse surfaces.
2. $A_i \ll A_j$.

Patent Owner Manufacturing Resources International, Inc.
Exhibit 2017 - Page 825 of 999

Analysis: The desired view factor may be obtained from Equation 13.1.

$$F_{ij} = \frac{1}{A_i}\int_{A_i}\int_{A_j} \frac{\cos\theta_i \cos\theta_j}{\pi R^2}\, dA_i\, dA_j$$

Recognizing that θ_i, θ_j, and R are approximately independent of position on A_i, this expression reduces to

$$F_{ij} = \int_{A_j} \frac{\cos\theta_i \cos\theta_j}{\pi R^2}\, dA_j$$

or, with $\theta_i = \theta_j \equiv \theta$,

$$F_{ij} = \int_{A_j} \frac{\cos^2\theta}{\pi R^2}\, dA_j$$

With $R^2 = r^2 + L^2$, $\cos\theta = (L/R)$, and $dA_j = 2\pi r\, dr$, it follows that

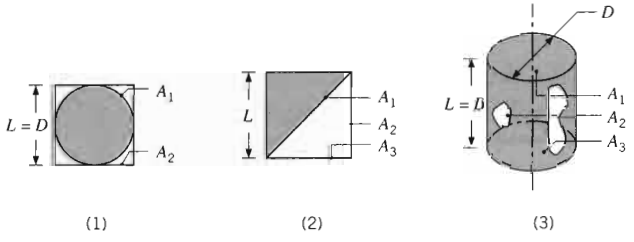
$$F_{ij} = 2L^2 \int_0^{D/2} \frac{r\, dr}{(r^2 + L^2)^2} = \frac{D^2}{D^2 + 4L^2} \qquad \triangleleft \quad (13.8)$$

Comments:

1. Equation 13.8 may be used to quantify the asymptotic behavior of the curves in Figure 13.5 as the radius of the lower circle, r_i, approaches zero.
2. The preceding geometry is one of the simplest cases for which the view factor may be obtained from Equation 13.1. Geometries involving more detailed integrations are considered in the literature [1, 3].

EXAMPLE 13.2

Determine the view factors F_{12} and F_{21} for the following geometries:



(1) (2) (3)

1. Sphere of diameter D inside a cubical box of length $L = D$.
2. One side of a diagonal partition within a long square duct.
3. End and side of a circular tube of equal length and diameter.

SOLUTION

Known: Surface geometries.

Find: View factors.

Patent Owner Manufacturing Resources International, Inc.
Exhibit 2017 - Page 826 of 999

Assumptions: Diffuse surfaces with uniform radiosities.

Analysis: The desired view factors may be obtained from inspection, the reciprocity rule, the summation rule, and/or use of the charts.

1. Sphere within a cube:

By inspection, $F_{12} = 1$ ◁

By reciprocity, $F_{21} = \frac{A_1}{A_2} F_{12} = \frac{\pi D^2}{6L^2} \times 1 = \frac{\pi}{6}$ ◁

2. Partition within a square duct:

From summation rule, $F_{11} + F_{12} + F_{13} = 1$

where $F_{11} = 0$

By symmetry, $F_{12} = F_{13}$

Hence $F_{12} = 0.50$ ◁

By reciprocity, $F_{21} = \frac{A_1}{A_2} F_{12} = \frac{\sqrt{2}L}{L} \times 0.5 = 0.71$ ◁

3. Circular tube:

From Table 13.2 or Figure 13.5, with $(r_3/L) = 0.5$ and $(L/r_1) = 2$, $F_{13} = 0.172$

From summation rule, $F_{11} + F_{12} + F_{13} = 1$

or, with $F_{11} = 0$, $F_{12} = 1 - F_{13} = 0.828$ ◁

From reciprocity, $F_{21} = \frac{A_1}{A_2} F_{12} = \frac{\pi D^2/4}{\pi DL} \times 0.828 = 0.207$ ◁

13.2 *Radiation Exchange Between Opaque, Diffuse, Gray Surfaces in an Enclosure*

In general, radiation may leave an opaque surface due to both reflection and emission, and on reaching a second opaque surface, experience reflection as well as absorption. In an enclosure, such as that of Figure 13.8*a*, radiation may experience multiple reflections off all surfaces, with partial absorption occurring at each.

Analyzing radiation exchange in an enclosure may be simplified by making certain assumptions. Each surface of the enclosure is assumed to be *isothermal* and to be characterized by a *uniform radiosity* and a *uniform irradiation*. *Opaque, diffuse, gray* surface behavior is also assumed, and the medium within the enclosure is taken to be *nonparticipating*. The problem is generally one in which either the temperature T_i or the net radiative heat flux q_i'' associated with each of the surfaces is known. The objective is to use this information to determine the unknown radiative heat fluxes and temperatures associated with each of the surfaces.

Patent Owner Manufacturing Resources International, Inc.
Exhibit 2017 - Page 827 of 999

13.2.1 Net Radiation Exchange at a Surface

The term q_i, which is the *net* rate at which radiation *leaves* surface i, represents the net effect of radiative interactions occurring at the surface (Figure 13.8*b*). It is the rate at which energy would have to be transferred to the surface by other means to maintain it at a constant temperature. It is equal to the difference between the surface radiosity and irradiation and may be expressed as

$$q_i = A_i(J_i - G_i) \tag{13.9}$$

From Equation 13.9 and the definition of the radiosity J_i,

$$J_i \equiv E_i + \rho_i G_i \tag{13.10}$$

The net radiative transfer from the surface may also be expressed in terms of the surface emissive power and the absorbed irradiation:

$$q_i = A_i(E_i - \alpha_i G_i) \tag{13.11}$$

where use has been made of the relationship $\alpha_i = 1 - \rho_i$ for an opaque surface. This relationship is illustrated in Figure 13.8*c*. Substituting from Equation 12.35 and recognizing that $\rho_i = 1 - \alpha_i = 1 - \varepsilon_i$ for an opaque, diffuse, gray surface, the radiosity may also be expressed as

$$J_i = \varepsilon_i E_{bi} + (1 - \varepsilon_i)G_i \tag{13.12}$$

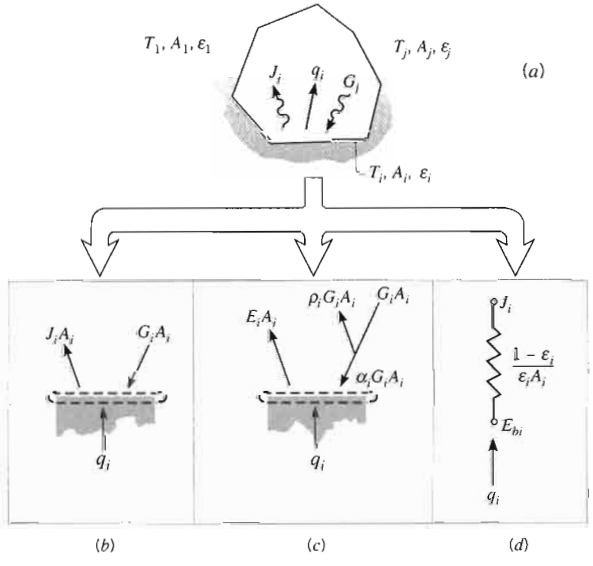


FIGURE 13.8 Radiation exchange in an enclosure of diffuse, gray surfaces with a nonparticipating medium. (*a*) Schematic of the enclosure. (*b*) Radiative balance according to Equation 13.9. (*c*) Radiative balance according to Equation 13.11. (*d*) Network element representing the net radiation transfer from a surface.

Patent Owner Manufacturing Resources International, Inc.
Exhibit 2017 - Page 828 of 999

Solving for G_i and substituting into Equation 13.9, it follows that

$$q_i = A_i\left(J_i - \frac{J_i - \varepsilon_i E_{bi}}{1 - \varepsilon_i}\right)$$

or

$$q_i = \frac{E_{bi} - J_i}{(1 - \varepsilon_i)/\varepsilon_i A_i} \tag{13.13}$$

Equation 13.13 provides a convenient representation for the net radiative heat transfer rate from a surface. This transfer, which may be represented by the network element of Figure 13.8*d*, is associated with the driving potential $(E_{bi} - J_i)$ and a *surface radiative resistance* of the form $(1 - \varepsilon_i)/\varepsilon_i A_i$. Hence, if the emissive power that the surface would have if it were black exceeds its radiosity, there is net radiation heat transfer from the surface; if the inverse is true, the net transfer is to the surface.

It is sometimes the case that one of the surfaces is very large relative to the other surfaces under consideration. For example, the system might consist of multiple small surfaces in a large room. In this case, the area of the large surface is effectively infinite ($A_i \to \infty$), and we see that its surface radiative resistance, $(1 - \varepsilon_i)/\varepsilon_i A_i$, is effectively zero, just as it would be for a black surface ($\varepsilon_i = 1$). Hence, $J_i = E_{bi}$, and *a surface which is large relative to all other surfaces under consideration can be treated as if it were a blackbody*. This important conclusion was reached in Section 12.6 based on a physical argument and has now been confirmed from our treatment of gray surface radiation exchange. Again, the physical explanation is that, even though the large surface may reflect some of the irradiation incident upon it, it is so big that there is a high probability that the reflected radiation reaches another point on the same large surface. After many such reflections, all the radiation that was originally incident on the large surface is absorbed by the large surface, and none ever reaches any of the smaller surfaces.

13.2.2 Radiation Exchange Between Surfaces

To use Equation 13.13, the surface radiosity J_i must be known. To determine this quantity, it is necessary to consider radiation exchange between the surfaces of the enclosure.

The irradiation of surface i can be evaluated from the radiosities of all the surfaces in the enclosure. In particular, from the definition of the view factor, it follows that the total rate at which radiation reaches surface i from all surfaces, including i, is

$$A_i G_i = \sum_{j=1}^{N} F_{ji} A_j J_j$$

or from the reciprocity relation, Equation 13.3,

$$A_i G_i = \sum_{j=1}^{N} A_i F_{ij} J_j$$

Canceling the area A_i and substituting into Equation 13.9 for G_i,

$$q_i = A_i\left(J_i - \sum_{j=1}^{N} F_{ij} J_j\right)$$

Patent Owner Manufacturing Resources International, Inc.
Exhibit 2017 - Page 829 of 999

or, from the summation rule, Equation 13.4,

$$q_i = A_i\left(\sum_{j=1}^{N} F_{ij}J_i - \sum_{j=1}^{N} F_{ij}J_j\right)$$

Hence

$$q_i = \sum_{j=1}^{N} A_iF_{ij}(J_i - J_j) = \sum_{j=1}^{N} q_{ij} \tag{13.14}$$

This result equates the net rate of radiation transfer from surface i, q_i, to the sum of components q_{ij} related to radiative exchange with the other surfaces. Each component may be represented by a network element for which $(J_i - J_j)$ is the driving potential and $(A_iF_{ij})^{-1}$ is a *space* or *geometrical resistance* (Figure 13.9).

Combining Equations 13.13 and 13.14, we then obtain

$$\frac{E_{bi} - J_i}{(1-\varepsilon_i)/\varepsilon_iA_i} = \sum_{j=1}^{N} \frac{J_i - J_j}{(A_iF_{ij})^{-1}} \tag{13.15}$$

As shown in Figure 13.9, this expression represents a radiation balance for the radiosity *node* associated with surface i. The rate of radiation transfer (current flow) to i through its surface resistance must equal the net rate of radiation transfer (current flows) from i to all other surfaces through the corresponding geometrical resistances.

Note that Equation 13.15 is especially useful when the surface temperature T_i (hence E_{bi}) is known. Although this situation is typical, it does not always apply. In particular, situations may arise for which the net radiation transfer rate at the surface q_i, rather than the temperature T_i, is known. In such cases the preferred form of the radiation balance is Equation 13.14, rearranged as

$$q_i = \sum_{j=1}^{N} \frac{J_i - J_j}{(A_iF_{ij})^{-1}} \tag{13.16}$$

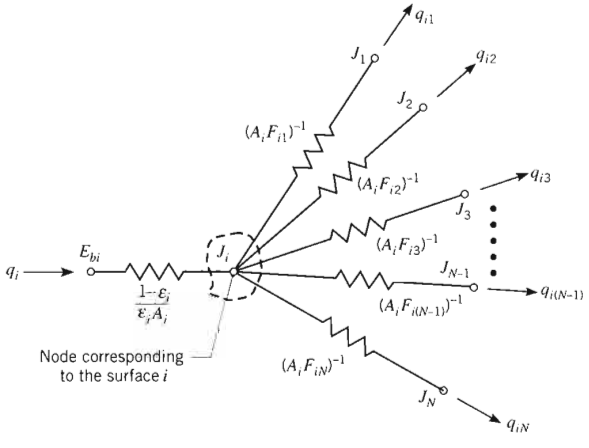


FIGURE 13.9 Network representation of radiative exchange between surface i and the remaining surfaces of an enclosure.

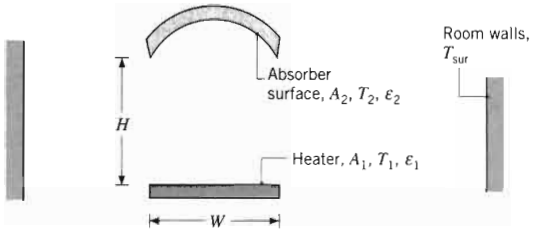
Patent Owner Manufacturing Resources International, Inc.
Exhibit 2017 - Page 830 of 999

Use of network representations was first suggested by Oppenheim [6]. The network is built by first identifying nodes associated with the radiosities of each of the N surfaces of the enclosure. The method provides a useful tool for visualizing radiation exchange in the enclosure and, at least for simple enclosures, may be used as the basis for predicting this exchange.

An alternative *direct approach* to solving radiation enclosure problems involves writing Equation 13.15 for each surface at which T_i is known, and writing Equation 13.16 for each surface at which q_i is known. The resulting set of N linear, algebraic equations is solved for $J_1, J_2, \ldots, J_N$. With knowledge of the J_i, Equation 13.13 may then be used to determine the net radiation heat transfer rate q_i at each surface of known T_i or the value of T_i at each surface of known q_i. For any number N of surfaces in the enclosure, the foregoing problem may readily be solved by the iteration or matrix inversion methods of Chapter 4.

EXAMPLE 13.3

In manufacturing, the special coating on a curved solar absorber surface of area $A_2 = 15\ \text{m}^2$ is cured by exposing it to an infrared heater of width $W = 1$ m. The absorber and heater are each of length $L = 10$ m and are separated by a distance of $H = 1$ m. The upper surface of the absorber and the lower surface of the heater are insulated.



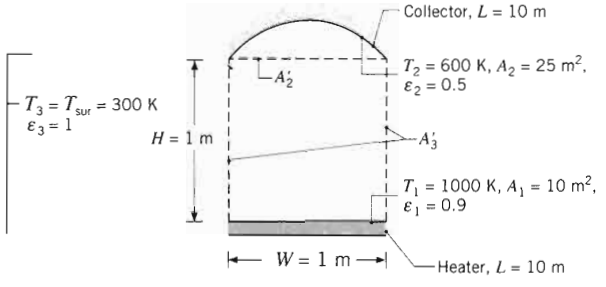
The heater is at $T_1 = 1000$ K and has an emissivity of $\varepsilon_1 = 0.9$, while the absorber is at $T_2 = 600$ K and has an emissivity of $\varepsilon_2 = 0.5$. The system is in a large room whose walls are at 300 K. What is the net rate of heat transfer to the absorber surface?

SOLUTION

Known: A curved, solar absorber surface with a special coating is being cured by use of an infrared heater in a large room.

Find: Net rate of heat transfer to the absorber surface.

Schematic:



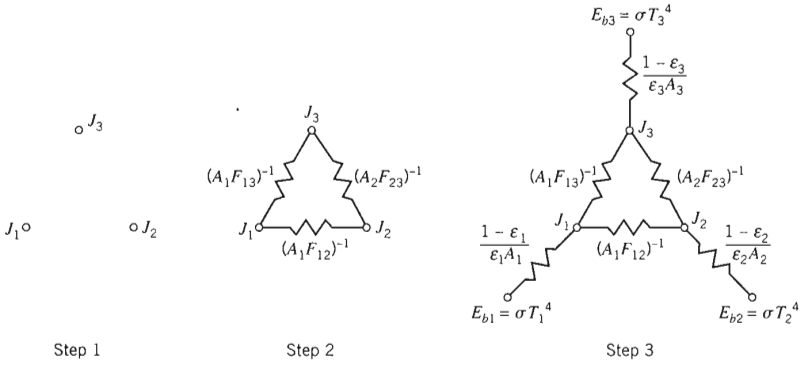
Patent Owner Manufacturing Resources International, Inc.
Exhibit 2017 - Page 831 of 999

Assumptions:

1. Steady-state conditions exist.
2. Convection effects are negligible.
3. Absorber and heater surfaces are diffuse and gray.
4. The surrounding room is large and therefore behaves as a blackbody.

Analysis: The system may be viewed as a three-surface enclosure, with the third surface being the large surrounding room, which behaves as a blackbody. We are interested in obtaining the net rate of radiation transfer to surface 2. We solve the problem using both the radiation network and direct approaches.

Radiation Network Approach The radiation network is constructed by first identifying nodes associated with the radiosities of each surface, as shown in step 1 in the schematic below. Then each radiosity node is connected to each of the other radiosity nodes through the appropriate space resistance, as shown in step 2. We will treat the surroundings as having a large but unspecified area, which introduces difficulty in expressing the space resistances $(A_3F_{31})^{-1}$ and $(A_3F_{32})^{-1}$. Fortunately, from the reciprocity relation (Equation 13.3), we can replace A_3F_{31} with A_1F_{13} and A_3F_{32} with A_2F_{23}, which are more readily obtained. The final step is to connect the blackbody emissive powers associated with the temperature of each surface to the radiosity nodes, using the appropriate form of the surface resistance.



In this problem, the surface resistance associated with surface 3 is zero according to assumption 4; therefore, $J_3 = E_{b3} = \sigma T_3^4 = 459\ \text{W/m}^2$.

Summing currents at the J_1 node yields

$$\frac{\sigma T_1^4 - J_1}{(1-\varepsilon_1)/\varepsilon_1 A_1} = \frac{J_1 - J_2}{1/A_1F_{12}} + \frac{J_1 - \sigma T_3^4}{1/A_1F_{13}} \tag{1}$$

while summing the currents at the J_2 node results in

$$\frac{\sigma T_2^4 - J_2}{(1-\varepsilon_2)/\varepsilon_2 A_2} = \frac{J_2 - J_1}{1/A_1F_{12}} + \frac{J_2 - \sigma T_3^4}{1/A_2F_{23}} \tag{2}$$

The view factor F_{12} may be obtained by recognizing that $F_{12} = F_{12'}$, where A_2' is shown in the schematic as the rectangular base of the absorber surface. Then, from

Patent Owner Manufacturing Resources International, Inc.
Exhibit 2017 - Page 832 of 999

Figure 13.4 or Table 13.2, with $Y/L = 10/1 = 10$ and $X/L = 1/1 = 1$,

$$F_{12} = 0.39$$

From the summation rule, and recognizing that $F_{11} = 0$, it also follows that

$$F_{13} = 1 - F_{12} = 1 - 0.39 = 0.61$$

The last needed view factor is F_{23}. We recognize that, since radiation propagating from surface 2 to surface 3 must pass through the hypothetical surface A_2',

$$A_2 F_{23} = A_2' F_{2'3}$$

and from symmetry $F_{2'3} = F_{13}$. Thus

$$F_{23} = \frac{A_2'}{A_2} F_{13} = \frac{10\ \text{m}^2}{15\ \text{m}^2} \times 0.61 = 0.41$$

We may now solve Equations 1 and 2 for J_1 and J_2. Recognizing that $E_{b1} = \sigma T_1^4 = 56{,}700\ \text{W/m}^2$ and canceling the area A_1, we can express Equation 1 as

$$\frac{56{,}700 - J_1}{(1 - 0.9)/0.9} = \frac{J_1 - J_2}{1/0.39} + \frac{J_1 - 459}{1/0.61}$$

or

$$-10J_1 + 0.39J_2 = -510{,}582 \tag{3}$$

Noting that $E_{b2} = \sigma T_2^4 = 7348\ \text{W/m}^2$ and dividing by the area A_2, we can express Equation 2 as

$$\frac{7348 - J_2}{(1 - 0.5)/0.5} = \frac{J_2 - J_1}{15\ \text{m}^2/(10\ \text{m}^2 \times 0.39)} + \frac{J_2 - 459}{1/0.41}$$

or

$$0.26J_1 - 1.67J_2 = -7536 \tag{4}$$

Solving Equations 3 and 4 simultaneously yields $J_2 = 12{,}487\ \text{W/m}^2$.

An expression for the net rate of heat transfer *from* the absorber surface, q_2, may be written upon inspection of the radiation network and is

$$q_2 = \frac{\sigma T_2^4 - J_2}{(1 - \varepsilon_2)/\varepsilon_2 A_2}$$

resulting in

$$q_2 = \frac{(7348 - 12{,}487)\text{W/m}^2}{(1 - 0.5)/(0.5 \times 15\ \text{m}^2)} = -77.1\ \text{kW}$$

Hence, the net heat transfer rate *to* the absorber is $q_{\text{net}} = -q_2 = 77.1\ \text{kW}$. ◁

Direct Approach Using the direct approach, we write Equation 13.15 for each of the three surfaces. We use reciprocity to rewrite the space resistances in terms of the known view factors from above and to eliminate A_3.

Surface 1

$$\frac{\sigma T_1^4 - J_1}{(1 - \varepsilon_1)/\varepsilon_1 A_1} = \frac{J_1 - J_2}{1/A_1 F_{12}} + \frac{J_1 - J_3}{1/A_1 F_{13}} \tag{5}$$

Patent Owner Manufacturing Resources International, Inc.
Exhibit 2017 - Page 833 of 999

Surface 2

$$\frac{\sigma T_2^4 - J_2}{(1-\varepsilon_2)/\varepsilon_2 A_2} = \frac{J_2 - J_1}{1/A_2 F_{21}} + \frac{J_2 - J_3}{1/A_2 F_{23}} = \frac{J_2 - J_1}{1/A_1 F_{12}} + \frac{J_2 - J_3}{1/A_2 F_{23}} \tag{6}$$

Surface 3

$$\frac{\sigma T_3^4 - J_3}{(1-\varepsilon_3)/\varepsilon_3 A_3} = \frac{J_3 - J_1}{1/A_3 F_{31}} + \frac{J_3 - J_2}{1/A_3 F_{32}} = \frac{J_3 - J_1}{1/A_1 F_{13}} + \frac{J_3 - J_2}{1/A_2 F_{23}} \tag{7}$$

Substituting values of the areas, temperatures, emissivities, and view factors into Equations 5 through 7 and solving them simultaneously, we obtain $J_1 = 51{,}541$ W/m^2, $J_2 = 12{,}487$ W/m^2, and $J_3 = 459$ W/m^2. Equation 13.13 may then be written for surface 2 as

$$q_2 = \frac{\sigma T_2^4 - J_2}{(1-\varepsilon_2)/\varepsilon_2 A_2}$$

This expression is identical to the expression that was developed using the radiation network. Hence, $q_2 = -77.1$ kW.

Comments:

1. In order to solve Equations 5 through 7 simultaneously, we must first multiply both sides of Equation 7 by $(1 - \varepsilon_3)/\varepsilon_3 A_3 = 0$ to avoid division by zero, resulting in the simplified form of Equation 7, which is $J_3 = \sigma T_3^4$.
2. If we substitute $J_3 = \sigma T_3^4$ into Equations 5 and 6, it is evident that Equations 5 and 6 are identical to Equations 1 and 2, respectively.
3. The direct approach is recommended for problems involving $N \geq 4$ surfaces, since radiation networks become quite complex as the number of surfaces increases.
4. As will be seen in Section 13.3, the radiation network approach is particularly useful when thermal energy is transferred to or from surfaces by additional means, that is, by conduction and/or convection. In these *multimode* heat transfer situations, the additional energy delivered to or taken from the surface can be represented by additional current into or out of a node.
5. Recognize the utility of using a hypothetical surface (A_2') to simplify the evaluation of view factors.
6. We could have approached the solution in a slightly different manner. Radiation leaving surface 1 must pass through the openings (hypothetical surface 3′) in order to reach the surroundings. Thus, we can write.

$$F_{13} = F_{13'}$$
$$A_1 F_{13} = A_1 F_{13'} = A_3' F_{3'1}$$

A similar relationship can be written for exchange between surface 2 and the surroundings, that is, $A_2 F_{23} = A_3' F_{3'2}$. Thus, the space resistances which connect to radiosity node 3 in the radiation network above can be replaced by space resistances pertaining to surface 3′. The resistance network would be unchanged, and the space resistances would have the same values as those determined in the foregoing solution. However, it may be more convenient to calculate the view factors by utilizing the hypothetical surfaces 3′. With the surface resistance for surface 3 equal to zero, we see that *openings of enclosures that exchange radiation with large surroundings may be treated as hypothetical, nonreflecting black surfaces* ($\varepsilon_3 = 1$) *whose temperature is equal to that of the surroundings* ($T_3 = T_{sur}$).

Patent Owner Manufacturing Resources International, Inc.
Exhibit 2017 - Page 834 of 999

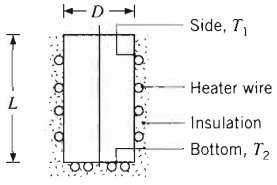
13.2.3 Blackbody Radiation Exchange

In Example 13.3, we saw that large surroundings may be treated as hypothetical black surfaces. Real surfaces, such as those that are charred or coated with high-emissivity finishes, also exhibit near-black behavior. Matters are simplified significantly when all the surfaces of the enclosure are black. Since the absorptivity of a black surface is unity, there is no reflection and the radiosity is composed solely of the emitted energy. Hence, Equation 13.14 reduces to

$$q_i = \sum_{j=1}^{N} A_i F_{ij} \sigma (T_i^4 - T_j^4) \tag{13.17}$$

EXAMPLE 13.4

A furnace cavity, which is in the form of a cylinder of 75-mm diameter and 150-mm length, is open at one end to large surroundings that are at 27°C. The sides and bottom may be approximated as blackbodies, are heated electrically, are well insulated, and are maintained at temperatures of 1350 and 1650°C, respectively.



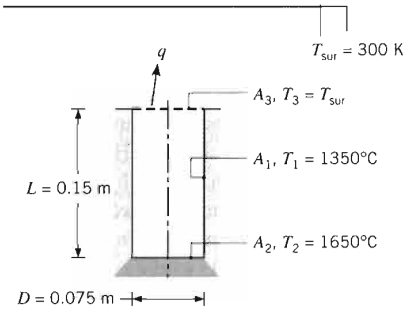
How much power is required to maintain the furnace conditions?

SOLUTION

Known: Surface temperatures of cylindrical furnace and surroundings.

Find: Power required to maintain prescribed temperatures.

Schematic:



Patent Owner Manufacturing Resources International, Inc.
Exhibit 2017 - Page 835 of 999

Assumptions:

1. Interior surfaces behave as blackbodies.
2. Heat transfer by convection is negligible.
3. Outer surface of furnace is adiabatic.
4. Treat opening as a hypothetical black surface at T_{sur}.

Analysis: The power needed to operate the furnace at the prescribed conditions must balance heat losses from the furnace. The heat loss may then be expressed as

$$q = q_{13} + q_{23}$$

or, from Equation 13.17,

$$q = A_1 F_{13}\sigma(T_1^4 - T_3^4) + A_2 F_{23}\sigma(T_2^4 - T_3^4)$$

From Table 13.2 (or Figure 13.5), with $(r_i/L) = (r_j/L) = (0.0375\ \text{m}/0.15\ \text{m}) = 0.25$, $F_{23} = 0.056$. From the summation rule

$$F_{21} = 1 - F_{23} = 1 - 0.056 = 0.944$$

and from reciprocity

$$F_{12} = \frac{A_2}{A_1}F_{21} = \frac{\pi(0.075\ \text{m})^2/4}{\pi(0.075\ \text{m})(0.15\ \text{m})} \times 0.944 = 0.118$$

Hence, since $F_{13} = F_{12}$ from symmetry,

$$q = (\pi \times 0.075\ \text{m} \times 0.15\ \text{m})\, 0.118 \times 5.67 \times 10^{-8}\ \text{W/m}^2 \cdot \text{K}^4$$
$$\times [(1623\ \text{K})^4 - (300\ \text{K})^4] + \left(\frac{\pi}{4}\right)(0.075\ \text{m})^2 \times 0.056$$
$$\times 5.67 \times 10^{-8}\ \text{W/m}^2 \cdot \text{K}^4\, [(1923\ \text{K})^4 - (300\ \text{K})^4]$$
$$q = 1639\ \text{W} + 191\ \text{W} = 1830\ \text{W}$$

13.2.4 The Two-Surface Enclosure

The simplest example of an enclosure is one involving two surfaces that exchange radiation only with each other. Such a two-surface enclosure is shown schematically in Figure 13.10*a*. Since there are only two surfaces, the net rate of radiation transfer *from* surface 1, q_1, must equal the net rate of radiation transfer *to* surface 2, $-q_2$, and both quantities must equal the net rate at which radiation is exchanged between 1 and 2. Accordingly,

$$q_1 = -q_2 = q_{12}$$

The radiation transfer rate may be determined by applying Equation 13.15 to surfaces 1 and 2 and solving the resulting two equations for J_1 and J_2. The results could then be used with Equation 13.13 to determine q_1 (or q_2). However, in this case the desired result is more readily obtained by working with the network representation of the enclosure shown in Figure 13.10*b*.

Patent Owner Manufacturing Resources International, Inc.
Exhibit 2017 - Page 836 of 999

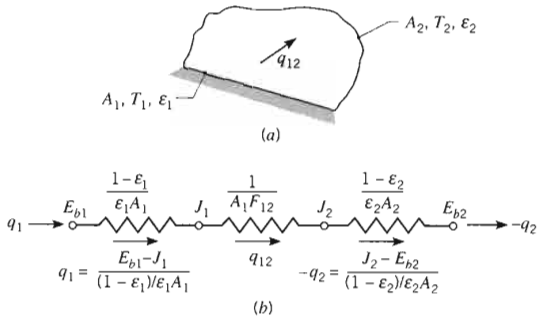


FIGURE 13.10 The two-surface enclosure. (*a*) Schematic. (*b*) Network representation.

From Figure 13.10*b* we see that the total resistance to radiation exchange between surfaces 1 and 2 is comprised of the two surface resistances and the geometrical resistance. Hence, substituting from Equation 12.26, the net radiation exchange between surfaces may be expressed as

$$q_{12} = q_1 = -q_2 = \frac{\sigma(T_1^4 - T_2^4)}{\dfrac{1-\varepsilon_1}{\varepsilon_1 A_1} + \dfrac{1}{A_1 F_{12}} + \dfrac{1-\varepsilon_2}{\varepsilon_2 A_2}} \tag{13.18}$$

The foregoing result may be used for any two diffuse, gray surfaces *that form an enclosure.* Important special cases are summarized in Table 13.3.

13.2.5 Radiation Shields

Radiation shields constructed from low emissivity (high reflectivity) materials can be used to reduce the net radiation transfer between two surfaces. Consider placing a radiation shield, surface 3, between the two large, parallel planes of Figure 13.11*a*. Without the radiation shield, the net rate of radiation transfer between surfaces 1 and 2 is given by Equation 13.19. However, with the radiation shield, additional resistances are present, as shown in Figure 13.11*b*, and the heat transfer rate is reduced. Note that the emissivity associated with one side of the shield ($\varepsilon_{3,1}$) may differ from that associated with the opposite side ($\varepsilon_{3,2}$) and the radiosities will always differ. Summing the resistances and recognizing that $F_{13} = F_{32} = 1$, it follows that

$$q_{12} = \frac{A_1\sigma(T_1^4 - T_2^4)}{\dfrac{1}{\varepsilon_1} + \dfrac{1}{\varepsilon_2} + \dfrac{1-\varepsilon_{3,1}}{\varepsilon_{3,1}} + \dfrac{1-\varepsilon_{3,2}}{\varepsilon_{3,2}}} \tag{13.23}$$

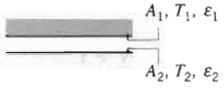
Note that the resistances associated with the radiation shield become very large when the emissivities $\varepsilon_{3,1}$ and $\varepsilon_{3,2}$ are very small.

Equation 13.23 may be used to determine the net heat transfer rate if T_1 and T_2 are known. From knowledge of q_{12} and the fact that $q_{12} = q_{13} = q_{32}$, the value of T_3 may then be determined by expressing Equation 13.19 for q_{13} or q_{32}.

Patent Owner Manufacturing Resources International, Inc.
Exhibit 2017 - Page 837 of 999

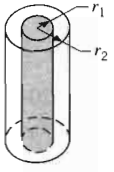
TABLE 13.3 Special Diffuse, Gray, Two-Surface Enclosures

Large (Infinite) Parallel Planes



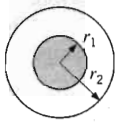
$$A_1 = A_2 = A \qquad F_{12} = 1 \qquad q_{12} = \frac{A\sigma(T_1^4 - T_2^4)}{\dfrac{1}{\varepsilon_1} + \dfrac{1}{\varepsilon_2} - 1} \tag{13.19}$$

Long (Infinite) Concentric Cylinders



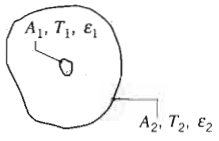
$$\frac{A_1}{A_2} = \frac{r_1}{r_2} \qquad F_{12} = 1 \qquad q_{12} = \frac{\sigma A_1(T_1^4 - T_2^4)}{\dfrac{1}{\varepsilon_1} + \dfrac{1 - \varepsilon_2}{\varepsilon_2}\left(\dfrac{r_1}{r_2}\right)} \tag{13.20}$$

Concentric Spheres



$$\frac{A_1}{A_2} = \frac{r_1^2}{r_2^2} \qquad F_{12} = 1 \qquad q_{12} = \frac{\sigma A_1(T_1^4 - T_2^4)}{\dfrac{1}{\varepsilon_1} + \dfrac{1 - \varepsilon_2}{\varepsilon_2}\left(\dfrac{r_1}{r_2}\right)^2} \tag{13.21}$$

Small Convex Object in a Large Cavity



$$\frac{A_1}{A_2} \approx 0 \qquad F_{12} = 1 \qquad q_{12} = \sigma A_1 \varepsilon_1 (T_1^4 - T_2^4) \tag{13.22}$$

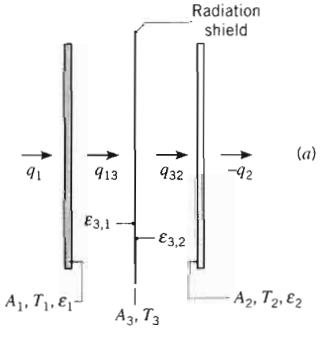


FIGURE 13.11 Radiation exchange between large parallel planes with a radiation shield. (*a*) Schematic. (*b*) Network representation.

Patent Owner Manufacturing Resources International, Inc.
Exhibit 2017 - Page 838 of 999

The foregoing procedure may readily be extended to problems involving multiple radiation shields. In the special case for which all the emissivities are equal, it may be shown that, with N shields,

$$(q_{12})_N = \frac{1}{N+1}(q_{12})_0 \tag{13.24}$$

where $(q_{12})_0$ is the radiation transfer rate with no shields ($N = 0$).

EXAMPLE 13.5

A cryogenic fluid flows through a long tube of 20-mm diameter, the outer surface of which is diffuse and gray with $\varepsilon_1 = 0.02$ and $T_1 = 77$ K. This tube is concentric with a larger tube of 50-mm diameter, the inner surface of which is diffuse and gray with $\varepsilon_2 = 0.05$ and $T_2 = 300$ K. The space between the surfaces is evacuated. Calculate the heat gain by the cryogenic fluid per unit length of tubes. If a thin radiation shield of 35-mm diameter and $\varepsilon_3 = 0.02$ (both sides) is inserted midway between the inner and outer surfaces, calculate the change (percentage) in heat gain per unit length of the tubes.

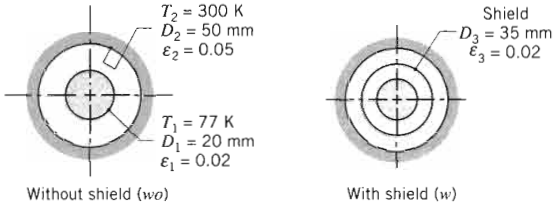
SOLUTION

Known: Concentric tube arrangement with diffuse, gray surfaces of different emissivities and temperatures.

Find:

1. Heat gain by the cryogenic fluid passing through the inner tube.
2. Percentage change in heat gain with radiation shield inserted midway between inner and outer tubes.

Schematic:



Assumptions:

1. Surfaces are diffuse and gray.
2. Space between tubes is evacuated.
3. Conduction resistance for radiation shield is negligible.
4. Concentric tubes form a two-surface enclosure (end effects are negligible).

Patent Owner Manufacturing Resources International, Inc.
Exhibit 2017 - Page 839 of 999

Analysis:

1. The network representation of the system without the shield is shown in Figure 13.10, and the desired heat rate may be obtained from Equation 13.20, where

$$q = \frac{\sigma(\pi D_1 L)(T_1^4 - T_2^4)}{\frac{1}{\varepsilon_1} + \frac{1-\varepsilon_2}{\varepsilon_2}\left(\frac{D_1}{D_2}\right)}$$

Hence

$$q' = \frac{q}{L} = \frac{5.67 \times 10^{-8}\,\text{W/m}^2 \cdot \text{K}^4\,(\pi \times 0.02\,\text{m})[(77\,\text{K})^4 - (300\,\text{K})^4]}{\frac{1}{0.02} + \frac{1-0.05}{0.05}\left(\frac{0.02\,\text{m}}{0.05\,\text{m}}\right)}$$

$$q' = -0.50\,\text{W/m} \quad \triangleleft$$

2. The network representation of the system with the shield is shown in Figure 13.11, and the desired heat rate is now

$$q = \frac{E_{b1} - E_{b2}}{R_{\text{tot}}} = \frac{\sigma(T_1^4 - T_2^4)}{R_{\text{tot}}}$$

where

$$R_{\text{tot}} = \frac{1-\varepsilon_1}{\varepsilon_1(\pi D_1 L)} + \frac{1}{(\pi D_1 L)F_{13}} + 2\left[\frac{1-\varepsilon_3}{\varepsilon_3(\pi D_3 L)}\right] + \frac{1}{(\pi D_3 L)F_{32}} + \frac{1-\varepsilon_2}{\varepsilon_2(\pi D_2 L)}$$

or

$$R_{\text{tot}} = \frac{1}{L}\left\{\frac{1-0.02}{0.02(\pi \times 0.02\,\text{m})} + \frac{1}{(\pi \times 0.02\,\text{m})1} + 2\left[\frac{1-0.02}{0.02(\pi \times 0.035\,\text{m})}\right] + \frac{1}{(\pi \times 0.035\,\text{m})1} + \frac{1-0.05}{0.05(\pi \times 0.05\,\text{m})}\right\}$$

$$R_{\text{tot}} = \frac{1}{L}(779.9 + 15.9 + 891.3 + 9.1 + 121.0) = \frac{1817}{L}\left(\frac{1}{\text{m}^2}\right)$$

Hence

$$q' = \frac{q}{L} = \frac{5.67 \times 10^{-8}\,\text{W/m}^2 \cdot \text{K}^4\,[(77\,\text{K})^4 - (300\,\text{K})^4]}{1817\,(1/\text{m})} = -0.25\,\text{W/m} \quad \triangleleft$$

The percentage change in the heat gain is then

$$\frac{q'_w - q'_{wo}}{q'_{wo}} \times 100 = \frac{(-0.25\,\text{W/m}) - (-0.50\,\text{W/m})}{-0.50\,\text{W/m}} \times 100 = -50\%$$

13.2.6 The Reradiating Surface

The assumption of a *reradiating surface* is common to many industrial applications. This idealized surface is characterized by *zero* net radiation transfer ($q_i = 0$). It is closely approached by real surfaces that are well insulated on one side *and* for

Patent Owner Manufacturing Resources International, Inc.
Exhibit 2017 - Page 840 of 999

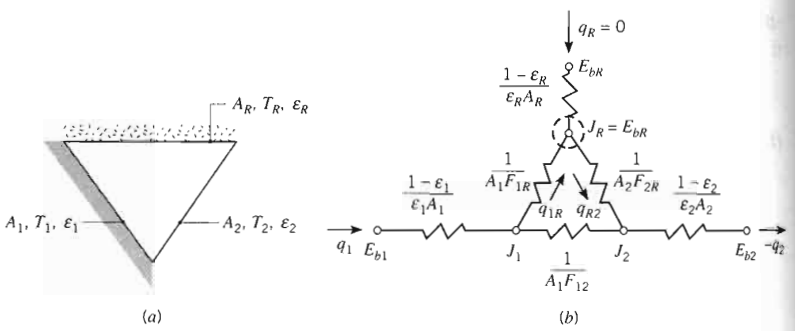


FIGURE 13.12 A three-surface enclosure with one surface reradiating. (*a*) Schematic. (*b*) Network representation.

which convection effects may be neglected on the opposite (radiating) side. With $q_i = 0$, it follows from Equations 13.9 and 13.13 that $G_i = J_i = E_{bi}$. Hence, if the radiosity of a reradiating surface is known, its temperature is readily determined. In an enclosure, the equilibrium temperature of a reradiating surface is determined by its interaction with the other surfaces, and it is *independent of the emissivity of the reradiating surface.*

A three-surface enclosure, for which the third surface, surface R, is reradiating, is shown in Figure 13.12*a*, and the corresponding network is shown in Figure 13.12*b*. Surface R is presumed to be well insulated, and convection effects are assumed to be negligible. Hence, with $q_R = 0$, the net radiation *transfer* from surface 1 must equal the net radiation transfer to surface 2. The network is a simple series–parallel arrangement, and from its analysis it is readily shown that

$$q_1 = -q_2 = \frac{E_{b1} - E_{b2}}{\dfrac{1-\varepsilon_1}{\varepsilon_1 A_1} + \dfrac{1}{A_1 F_{12} + [(1/A_1 F_{1R}) + (1/A_2 F_{2R})]^{-1}} + \dfrac{1-\varepsilon_2}{\varepsilon_2 A_2}} \tag{13.25}$$

Knowing $q_1 = -q_2$, Equation 13.13 may be applied to surfaces 1 and 2 to determine their radiosities J_1 and J_2. Knowing J_1, J_2, and the geometrical resistances, the radiosity of the reradiating surface J_R may be determined from the radiation balance

$$\frac{J_1 - J_R}{(1/A_1 F_{1R})} - \frac{J_R - J_2}{(1/A_2 F_{2R})} = 0 \tag{13.26}$$

The temperature of the reradiating surface may then be determined from the requirement that $\sigma T_R^4 = J_R$.

Note that the general procedure described in Section 13.2.2 may be applied to enclosures with reradiating surfaces. For each such surface, it is appropriate to use Equation 13.16 with $q_i = 0$.

EXAMPLE 13.6

A paint baking oven consists of a long, triangular duct in which a heated surface is maintained at 1200 K and another surface is insulated. Painted panels, which are maintained at 500 K, occupy the third surface. The triangle is of width $W = 1$ m on a side,

Patent Owner Manufacturing Resources International, Inc.
Exhibit 2017 - Page 841 of 999

and the heated and insulated surfaces have an emissivity of 0.8. The emissivity of the panels is 0.4. During steady-state operation, at what rate must energy be supplied to the heated side per unit length of the duct to maintain its temperature at 1200 K? What is the temperature of the insulated surface?

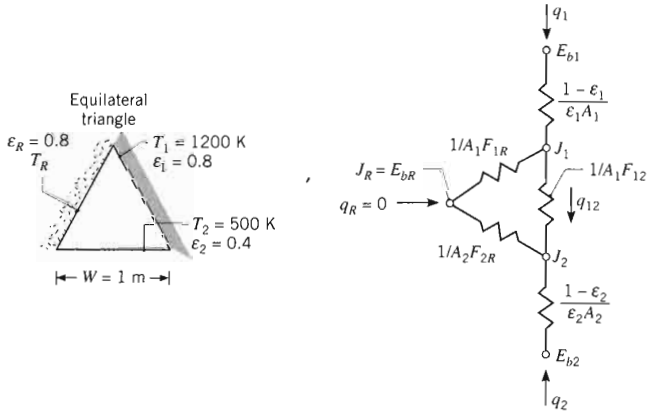
SOLUTION

Known: Surface properties of a long triangular duct that is insulated on one side and heated and cooled on the other sides.

Find:

1. Rate at which heat must be supplied per unit length of duct.
2. Temperature of the insulated surface.

Schematic:



Assumptions:

1. Steady-state conditions exist.
2. All surfaces are opaque, diffuse, gray, and of uniform radiosity.
3. Convection effects are negligible.
4. Surface R is reradiating.
5. End effects are negligible.

Analysis:

1. The system may be modeled as a three-surface enclosure with one surface reradiating. The rate at which energy must be supplied to the heated surface may then be obtained from Equation 13.25:

$$q_1 = \frac{E_{b1} - E_{b2}}{\dfrac{1-\varepsilon_1}{\varepsilon_1 A_1} + \dfrac{1}{A_1 F_{12} + [(1/A_1 F_{1R}) + (1/A_2 F_{2R})]^{-1}} + \dfrac{1-\varepsilon_2}{\varepsilon_2 A_2}}$$

Patent Owner Manufacturing Resources International, Inc.
Exhibit 2017 - Page 842 of 999

From symmetry, $F_{12} = F_{1R} = F_{2R} = 0.5$. Also, $A_1 = A_2 = W \cdot L$, where L is the duct length. Hence

$$q_1' = \frac{q_1}{L} = \frac{5.67 \times 10^{-8}\ \text{W/m}^2 \cdot \text{K}^4\,(1200^4 - 500^4)\ \text{K}^4}{\dfrac{1-0.8}{0.8 \times 1\ \text{m}} + \dfrac{1}{1\ \text{m} \times 0.5 + (2+2)^{-1}\ \text{m}} + \dfrac{1-0.4}{0.4 \times 1\ \text{m}}}$$

or

$$q_1' = 37\ \text{kW/m} = -q_2' \quad \triangleleft$$

2. The temperature of the insulated surface may be obtained from the requirement that $J_R = E_{bR}$, where J_R may be obtained from Equation 13.26. However, to use this expression J_1 and J_2 must be known. Applying the surface energy balance, Equation 13.13, to surfaces 1 and 2, it follows that

$$J_1 = E_{b1} - \frac{1-\varepsilon_1}{\varepsilon_1 W} q_1' = 5.67 \times 10^{-8}\ \text{W/m}^2 \cdot \text{K}^4\,(1200\ \text{K})^4 - \frac{1-0.8}{0.8 \times 1\ \text{m}} \times 37{,}000\ \text{W/m} = 108{,}323\ \text{W/m}^2$$

$$J_2 = E_{b2} - \frac{1-\varepsilon_2}{\varepsilon_2 W} q_2' = 5.67 \times 10^{-8}\ \text{W/m}^2 \cdot \text{K}^4\,(500\ \text{K})^4 - \frac{1-0.4}{0.4 \times 1\ \text{m}} (-37{,}000\ \text{W/m}) = 59{,}043\ \text{W/m}^2$$

From the energy balance for the reradiating surface, Equation 13.26, it follows that

$$\frac{108{,}323 - J_R}{\dfrac{1}{W \times L \times 0.5}} - \frac{J_R - 59{,}043}{\dfrac{1}{W \times L \times 0.5}} = 0$$

Hence

$$J_R = 83{,}683\ \text{W/m}^2 = E_{bR} = \sigma T_R^4$$

$$T_R = \left(\frac{83{,}683\ \text{W/m}^2}{5.67 \times 10^{-8}\ \text{W/m}^2 \cdot \text{K}^4}\right)^{1/4} = 1102\ \text{K} \quad \triangleleft$$

Comments:

1. Note that temperature and radiosity discontinuities cannot exist at the corners, and the assumptions of uniform temperature and radiosity are weakest in these regions.
2. The results are independent of the value of ε_R.
3. This problem may also be solved using the direct approach. The solution involves first determining the three unknown radiosities J_1, J_2, and J_R. The governing equations are obtained by writing Equation 13.15 for the two surfaces of known temperature, 1 and 2, and Equation 13.16 for surface R. The three equations are

$$\frac{E_{b1} - J_1}{(1-\varepsilon_1)/\varepsilon_1 A_1} = \frac{J_1 - J_2}{(A_1 F_{12})^{-1}} + \frac{J_1 - J_R}{(A_1 F_{1R})^{-1}}$$

$$\frac{E_{b2} - J_2}{(1-\varepsilon_2)/\varepsilon_2 A_2} = \frac{J_2 - J_1}{(A_2 F_{21})^{-1}} + \frac{J_2 - J_R}{(A_2 F_{2R})^{-1}}$$

$$0 = \frac{J_R - J_1}{(A_R F_{R1})^{-1}} + \frac{J_R - J_2}{(A_R F_{R2})^{-1}}$$

13.3 Multimod

Patent Owner Manufacturing Resources International, Inc.
Exhibit 2017 - Page 843 of 999

Canceling the area A_1, the first equation reduces to

$$\frac{117{,}573 - J_1}{0.25} = \frac{J_1 - J_2}{2} + \frac{J_1 - J_R}{2}$$

or

$$10J_1 - J_2 - J_R = 940{,}584 \tag{1}$$

Similarly, for surface 2,

$$\frac{3544 - J_2}{1.50} = \frac{J_2 - J_1}{2} + \frac{J_2 - J_R}{2}$$

or

$$-J_1 + 3.33J_2 - J_R = 4725 \tag{2}$$

and for the reradiating surface

$$0 = \frac{J_R - J_1}{2} + \frac{J_R - J_2}{2}$$

or

$$-J_1 - J_2 + 2J_R = 0 \tag{3}$$

Solving Equations 1, 2, and 3 simultaneously yields

$J_1 = 108{,}328\ \text{W/m}^2$ $\quad J_2 = 59{,}018\ \text{W/m}^2$ $\quad$ and $\quad J_R = 83{,}673\ \text{W/m}^2$

Recognizing that $J_R = \sigma T_R^4$, it follows that

$$T_R = \left(\frac{J_R}{\sigma}\right)^{1/4} = \left(\frac{83{,}673\ \text{W/m}^2}{5.67 \times 10^{-8}\ \text{W/m}^2 \cdot \text{K}^4}\right)^{1/4} = 1102\ \text{K}$$

13.3 *Multimode Heat Transfer*

Thus far, radiation exchange in an enclosure has been considered under conditions for which conduction and convection could be neglected. However, in many applications, convection and/or conduction are comparable to radiation and must be considered in the heat transfer analysis.

Consider the general surface condition of Figure 13.13*a*. In addition to exchanging energy by radiation with other surfaces of the enclosure, there may be external heat addition to the surface, as, for example, by electric heating, and heat transfer from the surface by convection and conduction. From a surface energy balance, it follows that

$$q_{i,\text{ext}} = q_{i,\text{rad}} + q_{i,\text{conv}} + q_{i,\text{cond}} \tag{13.27}$$

where $q_{i,\text{rad}}$, the net rate of radiation transfer from the surface, is determined by standard procedures for an enclosure. Hence, in general, $q_{i,\text{rad}}$ may be determined from Equation 13.13 or 13.14, while for special cases such as a two-surface enclosure and a three-surface enclosure with one reradiating surface, it may be determined from Equations 13.18 and 13.25, respectively. The surface network element of the

Patent Owner Manufacturing Resources International, Inc.
Exhibit 2017 - Page 844 of 999

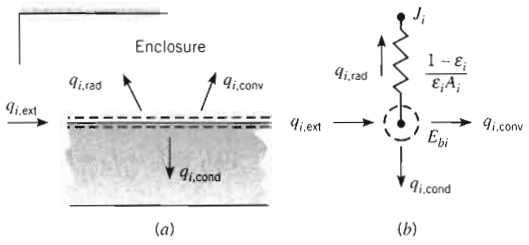


FIGURE 13.13 Multimode heat transfer from a surface in an enclosure. (*a*) Surface energy balance. (*b*) Circuit representation.

radiation circuit is modified according to Figure 13.13*b*, where $q_{i,\text{ext}}$, $q_{i,\text{cond}}$, and $q_{i,\text{conv}}$ represent current flows to or from the surface node. Note, however, that while $q_{i,\text{cond}}$ and $q_{i,\text{conv}}$ are proportional to temperature differences, $q_{i,\text{rad}}$ is proportional to the difference between temperatures raised to the fourth power. Conditions are simplified if the back of the surface is insulated, in which case $q_{i,\text{cond}} = 0$. Moreover, if there is no external heating and convection is negligible, the surface is reradiating.

EXAMPLE 13.7

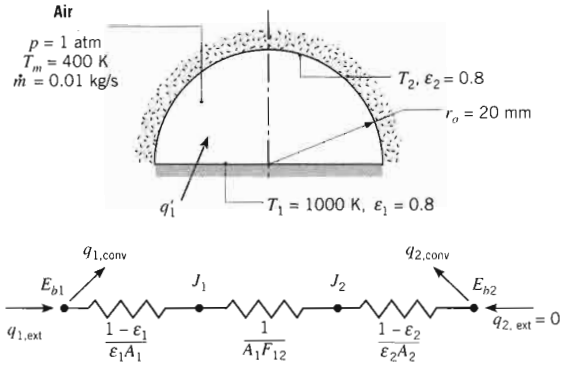
Consider an air heater consisting of a semicircular tube for which the plane surface is maintained at 1000 K and the other surface is well insulated. The tube radius is 20 mm, and both surfaces have an emissivity of 0.8. If atmospheric air flows through the tube at 0.01 kg/s and $T_m = 400$ K, what is the rate at which heat must be supplied per unit length to maintain the plane surface at 1000 K? What is the temperature of the insulated surface?

SOLUTION

Known: Airflow conditions in tubular heater and heater surface conditions.

Find: Rate at which heat must be supplied and temperature of insulated surface.

Schematic:



Patent Owner Manufacturing Resources International, Inc.
Exhibit 2017 - Page 845 of 999

Assumptions:

1. Steady-state conditions.
2. Diffuse, gray surfaces.
3. Negligible tube end effects and axial variations in gas temperature.
4. Fully developed flow.

Properties: Table A.4, air (1 atm, 400 K): $k = 0.0338$ W/m · K, $\mu = 230 \times 10^{-7}$ kg/s · m, $c_p = 1014$ J/kg · K, $Pr = 0.69$.

Analysis: Since the semicircular surface is well insulated and there is no external heat addition, a surface energy balance yields

$$-q_{2,\text{rad}} = q_{2,\text{conv}}$$

Since the tube constitutes a two-surface enclosure, the net radiation transfer to surface 2 may be evaluated from Equation 13.18. Hence

$$\frac{\sigma(T_1^4 - T_2^4)}{\dfrac{1-\varepsilon_1}{\varepsilon_1 A_1} + \dfrac{1}{A_1 F_{12}} + \dfrac{1-\varepsilon_2}{\varepsilon_2 A_2}} = hA_2(T_2 - T_m)$$

where the view factor is $F_{12} = 1$ and, per unit length, the surface areas are $A_1 = 2r_o$ and $A_2 = \pi r_o$. With

$$Re_D = \frac{\rho u_m D_h}{\mu} = \frac{\dot{m} D_h}{A_c \mu} = \frac{\dot{m} D_h}{(\pi r_o^2/2)\mu}$$

the hydraulic diameter is

$$D_h = \frac{4A_c}{P} = \frac{2\pi r_o}{\pi + 2} = \frac{0.04\pi \text{ m}}{\pi + 2} = 0.0244 \text{ m}$$

Hence

$$Re_D = \frac{0.01 \text{ kg/s} \times 0.0244 \text{ m}}{(\pi/2)\,(0.02 \text{ m})^2 \times 230 \times 10^{-7} \text{ kg/s} \cdot \text{m}} = 16{,}900$$

From the Dittus–Boelter equation,

$$Nu_D = 0.023 Re_D^{4/5} Pr^{0.4}$$

$$Nu_D = 0.023(16{,}900)^{4/5}(0.69)^{0.4} = 47.8$$

$$h = \frac{k}{D_h} Nu_D = \frac{0.0338 \text{ W/m} \cdot \text{K}}{0.0244 \text{ m}} 47.8 = 66.2 \text{ W/m}^2 \cdot \text{K}$$

Dividing both sides of the energy balance by A_1, it follows that

$$\frac{5.67 \times 10^{-8} \text{ W/m}^2 \cdot \text{K}^4 \,[(1000)^4 - T_2^4]\,\text{K}^4}{\dfrac{1-0.8}{0.8} + 1 + \dfrac{1-0.8}{0.8}\dfrac{2}{\pi}} = 66.2 \frac{\pi}{2}(T_2 - 400) \text{ W/m}^2$$

or

$$5.67 \times 10^{-8} T_2^4 + 146.5 T_2 - 115{,}313 = 0$$

A trial-and-error solution yields

$$T_2 = 696 \text{ K} \quad \triangleleft$$

Patent Owner Manufacturing Resources International, Inc.
Exhibit 2017 - Page 846 of 999

From an energy balance at the heated surface,

$$q_{1,\text{ext}} = q_{1,\text{rad}} + q_{1,\text{conv}} = q_{2,\text{conv}} + q_{1,\text{conv}}$$

Hence, on a unit length basis,

$$q'_{1,\text{ext}} = h\pi r_o(T_2 - T_m) + h2r_o(T_1 - T_m)$$

$$q'_{1,\text{ext}} = 66.2 \times 0.02[\pi\,(696 - 400) + 2(1000 - 400)]\ \text{W/m}$$

$$q'_{1,\text{ext}} = (1231 + 1589)\ \text{W/m} = 2820\ \text{W/m}$$ ◁

Comments: Applying an energy balance to a differential control volume about the air, it follows that

$$\frac{dT_m}{dx} = \frac{q'_1}{\dot{m}c_p} = \frac{2820\ \text{W/m}}{0.01\ \text{kg/s}\,(1014\ \text{J/kg} \cdot \text{K})} = 278\ \text{K/m}$$

Hence the air temperature change is significant, and a more representative analysis would subdivide the tube into axial zones and would allow for variations in air and insulated surface temperatures between zones. Moreover, a two-surface analysis of radiation exchange would no longer be appropriate.

13.4 *Radiation Exchange with Participating Media*

Although we have developed means for predicting radiation exchange between surfaces, it is important to be cognizant of the inherent limitations. Recall that we have considered *isothermal*, *opaque*, *gray* surfaces that *emit* and *reflect diffusely* and that are characterized by *uniform* surface *radiosity* and *irradiation*. For enclosures we have also considered the medium that separates the surfaces to be *nonparticipating*; that is, it neither absorbs nor scatters the surface radiation, and it emits no radiation.

The foregoing conditions and the related equations may often be used to obtain reliable first estimates and, in most cases, highly accurate results for radiation transfer in an enclosure. Sometimes, however, the assumptions are grossly inappropriate and more refined prediction methods are needed. Although beyond the scope of this text, the methods are discussed in more advanced treatments of radiation transfer [3, 7–12].

We have said little about gaseous radiation, having confined our attention to radiation exchange at the surface of an opaque solid or liquid. For *nonpolar* gases, such as O_2 or N_2, such neglect is justified, since the gases do not emit radiation and are essentially transparent to incident thermal radiation. However, the same may not be said for polar molecules, such as CO_2, H_2O (vapor), NH_3, and hydrocarbon gases, which emit and absorb over a wide temperature range. For such gases matters are complicated by the fact that, unlike radiation from a solid or a liquid, which is distributed continuously with wavelength, gaseous radiation is concentrated in specific *wavelength intervals* (called bands). Moreover, gaseous radiation is not a surface phenomenon, but is instead a *volumetric* phenomenon.

Patent Owner Manufacturing Resources International, Inc.
Exhibit 2017 - Page 847 of 999

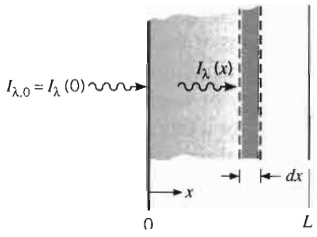


FIGURE 13.14
Absorption in a gas or liquid layer.

13.4.1 Volumetric Absorption

Spectral radiation absorption in a gas (or in a semitransparent liquid or solid) is a function of the absorption coefficient κ_λ (1/m) and the thickness L of the medium (Figure 13.14). If a monochromatic beam of intensity $I_{\lambda,0}$ is incident on the medium, the intensity is reduced due to absorption, and the reduction occurring in an infinitesimal layer of thickness dx may be expressed as

$$dI_\lambda(x) = -\kappa_\lambda I_\lambda(x)\,dx \tag{13.28}$$

Separating variables and integrating over the entire layer, we obtain

$$\int_{I_{\lambda,0}}^{I_{\lambda,L}} \frac{dI_\lambda(x)}{I_\lambda(x)} = -\kappa_\lambda \int_0^L dx$$

where κ_λ is assumed to be independent of x. It follows that

$$\frac{I_{\lambda,L}}{I_{\lambda,0}} = e^{-\kappa_\lambda L} \tag{13.29}$$

This exponential decay, termed *Beer's law*, is a useful tool in approximate radiation analysis. It may, for example, be used to infer the overall spectral absorptivity of the medium. In particular, with the transmissivity defined as

$$\tau_\lambda = \frac{I_{\lambda,L}}{I_{\lambda,0}} = e^{-\kappa_\lambda L} \tag{13.30}$$

the absorptivity is

$$\alpha_\lambda = 1 - \tau_\lambda = 1 - e^{-\kappa_\lambda L} \tag{13.31}$$

If Kirchhoff's law is assumed to be valid, $\alpha_\lambda = \varepsilon_\lambda$, Equation 13.31 also provides the spectral emissivity of the medium.

13.4.2 Gaseous Emission and Absorption

A common engineering calculation is one that requires determination of the radiant heat flux from a gas to an adjoining surface. Despite the complicated spectral and directional effects inherent in such calculations, a simplified procedure may be used. The method was developed by Hottel [13] and involves determining radiation emission from a hemispherical gas mass of temperature T_g to a surface element dA_1, which is located at the center of the hemisphere's base. Emission from the gas per unit area of the surface is expressed as

$$E_g = \varepsilon_g \sigma T_g^4 \tag{13.32}$$

Patent Owner Manufacturing Resources International, Inc.
Exhibit 2017 - Page 848 of 999

where the gas emissivity ε_g was determined by correlating available data. In particular, ε_g was correlated in terms of the temperature T_g and total pressure p of the gas, the partial pressure p_g of the radiating species, and the radius L of the hemisphere.

Results for the emissivity of water vapor are plotted in Figure 13.15 as a function of the gas temperature, for a total pressure of 1 atm, and for different values of the product of the vapor partial pressure and the hemisphere radius. To evaluate the emissivity for total pressures other than 1 atm, the emissivity from Figure 13.15 must be multiplied by the correction factor C_w from Figure 13.16. Similar results were obtained for carbon dioxide and are presented in Figures 13.17 and 13.18.

The foregoing results apply when water vapor or carbon dioxide appear *separately* in a mixture with other species that are nonradiating. However, the results may readily be extended to situations in which water vapor and carbon dioxide appear *together* in a mixture with other nonradiating gases. In particular, the total gas emissivity may be expressed as

$$\varepsilon_g = \varepsilon_w + \varepsilon_c - \Delta\varepsilon \tag{13.33}$$

where the correction factor $\Delta\varepsilon$ is presented in Figure 13.19 for different values of the gas temperature. This factor accounts for the reduction in emission associated with the mutual absorption of radiation between the two species.

Recall that the foregoing results provide the emissivity of a hemispherical gas mass of radius L radiating to an element of area at the center of its base. However,

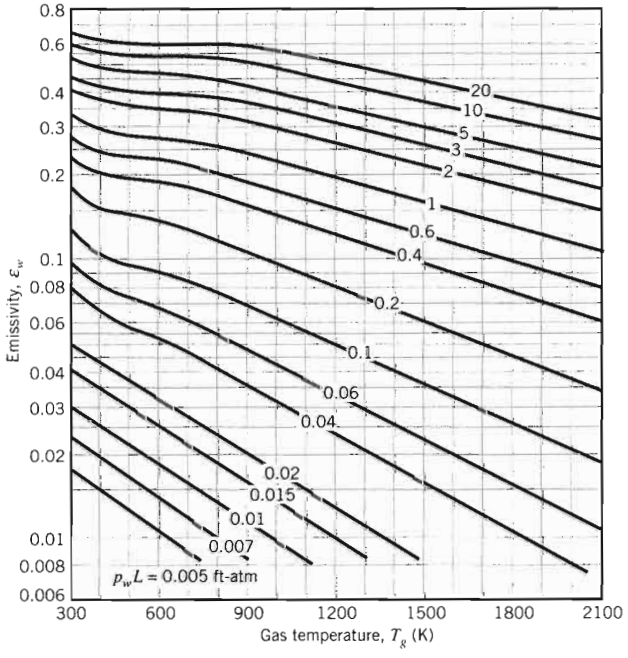


FIGURE 13.15 Emissivity of water vapor in a mixture with nonradiating gases at 1-atm total pressure and of hemispherical shape [13]. Used with permission.

Patent Owner Manufacturing Resources International, Inc.
Exhibit 2017 - Page 849 of 999

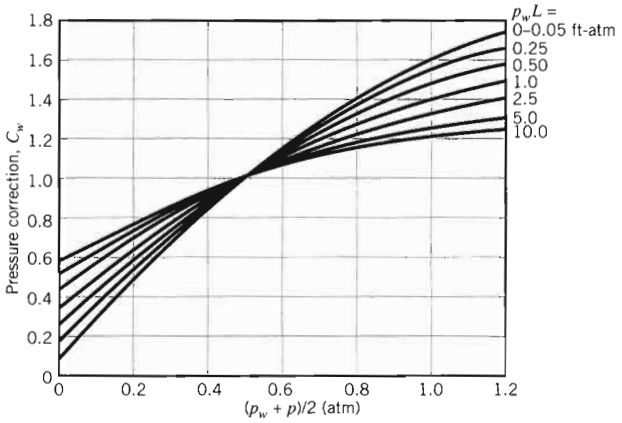


FIGURE 13.16 Correction factor for obtaining water vapor emissivities at pressures other than 1 atm ($\varepsilon_{w,p\neq 1\text{atm}} = C_w\varepsilon_{w,p=1\text{atm}}$) [13]. Used with permission.

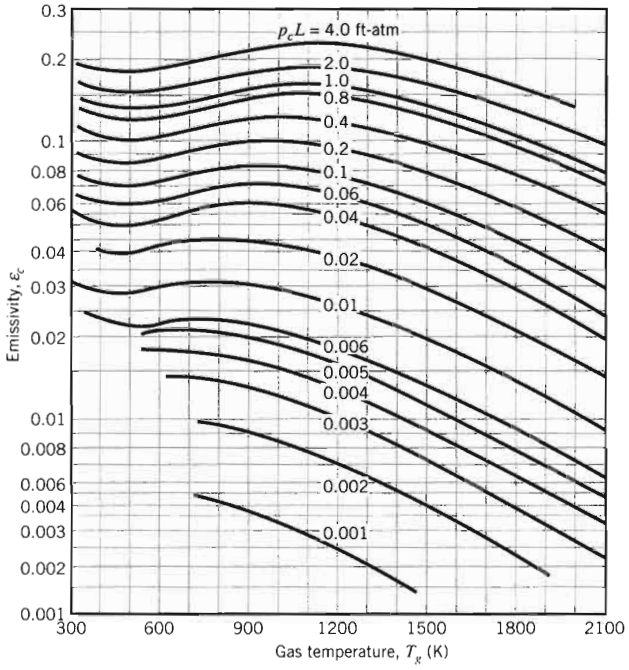


FIGURE 13.17 Emissivity of carbon dioxide in a mixture with nonradiating gases at 1-atm total pressure and of hemispherical shape [13]. Used with permission.

Patent Owner Manufacturing Resources International, Inc.
Exhibit 2017 - Page 850 of 999

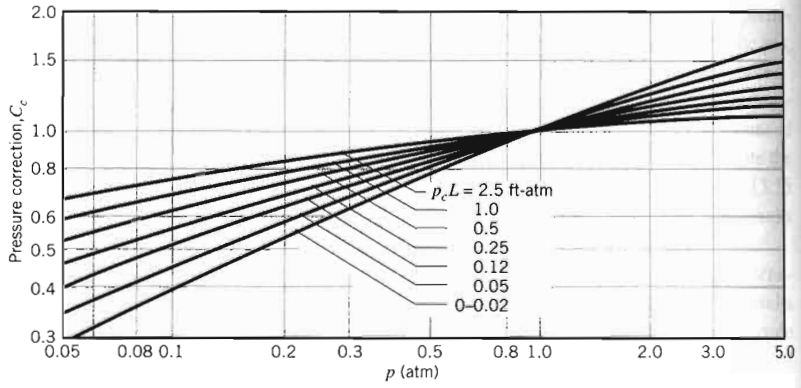


FIGURE 13.18 Correction factor for obtaining carbon dioxide emissivities at pressures other than 1 atm ($\varepsilon_{c,p\neq 1\text{atm}} = C_c\varepsilon_{c,p=1\text{atm}}$) [13]. Used with permission.

the results may be extended to other gas geometries by introducing the concept of a *mean beam length*, L_e. The quantity was introduced to correlate, in terms of a single parameter, the dependence of gas emissivity on both the size and the shape of the gas geometry. It may be interpreted as the radius of a hemispherical gas mass whose emissivity is equivalent to that for the geometry of interest. Its value has been determined for numerous gas shapes [13], and representative results are listed in Table 13.4. Replacing L by L_e in Figures 13.15 through 13.19, the emissivity associated with the geometry of interest may then be determined.

Using the results of Table 13.4 with Figures 13.15 through 13.19, it is possible to determine the rate of radiant heat transfer to a surface due to emission from an adjoining gas. This heat rate may be expressed as

$$q = \varepsilon_g A_s \sigma T_g^4 \tag{13.34}$$

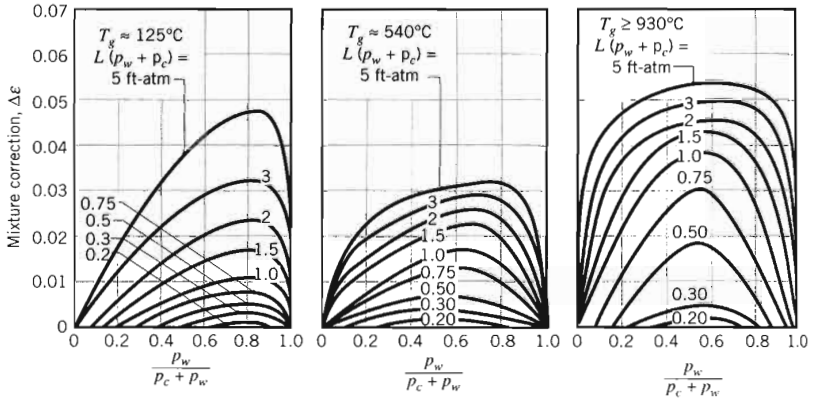


FIGURE 13.19 Correction factor associated with mixtures of water vapor and carbon dioxide [13]. Used with permission.

13.5 *Summary*

Patent Owner Manufacturing Resources International, Inc.
Exhibit 2017 - Page 851 of 999

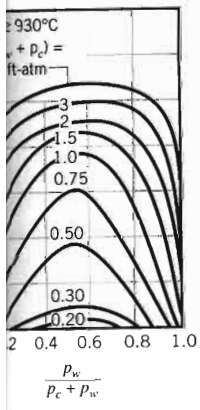


es at pressures other

ng the concept of a
n terms of a single
d the shape of the
al gas mass whose
lue has been deter-
listed in Table 13.4.
ity associated with

13.19, it is possible
emission from an

(13.34)



or and carbon dioxide

TABLE 13.4 Mean Beam Lengths L_e for Various Gas Geometries

Geometry	Characteristic Length	L_e
Sphere (radiation to surface)	Diameter (D)	$0.65D$
Infinite circular cylinder (radiation to curved surface)	Diameter (D)	$0.95D$
Semi-infinite circular cylinder (radiation to base)	Diameter (D)	$0.65D$
Circular cylinder of equal height and diameter (radiation to entire surface)	Diameter (D)	$0.60D$
Infinite parallel planes (radiation to planes)	Spacing between planes (L)	$1.80L$
Cube (radiation to any surface)	Side (L)	$0.66L$
Arbitrary shape of volume V (radiation to surface of area A)	Volume to area ratio (V/A)	$3.6V/A$

where A_s is the surface area. If the surface is black, it will, of course, absorb all this radiation. A black surface will also emit radiation, and the net rate at which radiation is exchanged between the surface at T_s and the gas at T_g is

$$q_{\text{net}} = A_s\sigma(\varepsilon_g T_g^4 - \alpha_g T_s^4) \tag{13.35}$$

For water vapor and carbon dioxide the required gas absorptivity α_g may be evaluated from the emissivity by expressions of the form [13]

Water:

$$\alpha_w = C_w\left(\frac{T_g}{T_s}\right)^{0.45} \times \varepsilon_w\left(T_s, p_w L_e \frac{T_s}{T_g}\right) \tag{13.36}$$

Carbon dioxide:

$$\alpha_c = C_c\left(\frac{T_g}{T_s}\right)^{0.65} \times \varepsilon_c\left(T_s, p_c L_e \frac{T_s}{T_g}\right) \tag{13.37}$$

where ε_w and ε_c are evaluated from Figures 13.15 and 13.17, respectively, and C_w and C_c are evaluated from Figures 13.16 and 13.18, respectively. Note, however, that in using Figures 13.15 and 13.17, T_g is replaced by T_s and $p_w L_e$ or $p_c L_e$ is replaced by $p_w L_e(T_s/T_g)$ or $p_c L_e(T_s/T_g)$, respectively. Note also that, in the presence of both water vapor and carbon dioxide, the total gas absorptivity may be expressed as

$$\alpha_g = \alpha_w + \alpha_c - \Delta\alpha \tag{13.38}$$

where $\Delta\alpha = \Delta\varepsilon$ is obtained from Figure 13.19.

13.5 *Summary*

In this chapter we focused on the analysis of radiation exchange between the surfaces of an enclosure, and in treating this exchange we introduced the concept of a *view factor*. Because knowledge of this geometrical quantity is essential to determining radiation exchange between any two diffuse surfaces, you should be familiar

Patent Owner Manufacturing Resources International, Inc.
Exhibit 2017 - Page 852 of 999

with the means by which it may be determined. You should also be adept at performing radiation calculations for an enclosure of *isothermal*, *opaque*, *diffuse*, and *gray* surfaces of *uniform radiosity* and *irradiation*. Moreover, you should be familiar with the results that apply to simple cases such as an enclosure of black surfaces, a two-surface enclosure, or a three-surface enclosure with a reradiating surface.

Test your understanding of pertinent concepts by addressing the following questions.

- What is a *view factor*? What assumptions are typically associated with computing the view factor between two surfaces?
- What is the *reciprocity relation* for view factors? What is the *summation rule*?
- Can the view factor of a surface with respect to itself be nonzero? If so, what kind of surface exhibits such behavior?
- What is a *nonparticipating medium*?
- What assumptions are inherent in treating radiation exchange between surfaces of an enclosure that may not be approximated as blackbodies? Comment on the validity of the assumptions and when or where they are most likely to break down.
- How is the radiative resistance of a surface in an enclosure defined? What is the driving potential that relates this resistance to the net rate of radiation transfer from the surface? What is the resistance if the surface may be approximated as a blackbody?
- How is the geometrical resistance associated with radiative exchange between two surfaces of an enclosure defined? What is the driving potential that relates this resistance to the net rate of radiation transfer between the surfaces?
- What is a *radiation shield* and how is net radiation transfer between two surfaces affected by an intervening shield? Is it advantageous for a shield to have a large surface absorptivity or reflectivity?
- What is a *reradiating surface*? Under what conditions may a surface be approximated as reradiating? What is the relation between radiosity, blackbody emissive power, and irradiation for a reradiating surface? Does the temperature of such a surface depend on its radiative properties?
- What can be said about a surface of an enclosure for which net radiation heat transfer to the surface is balanced by convection heat transfer from the surface to a gas in the enclosure? Is the surface reradiating? Is the back side of the surface adiabatic?
- Consider a surface in an enclosure for which net radiation transfer from the surface exceeds convection heat transfer from a gas in the enclosure. What other process or processes must occur at the surface, either independently or collectively?
- What molecular features render a gas nonemitting and nonabsorbing? What features allow for emission and absorption of radiation by a gas?
- What features distinguish emission and absorption of radiation by a gas from that of an opaque solid?
- How does the intensity of radiation propagating through a semitransparent medium vary with distance in the medium? What can be said about this variation if the absorption coefficient is very large? If the coefficient is very small?

References

1. Hamilton, D
change Conf
mittee for Ae
2. Eckert, E. R.
W. M. Rohs
Heat Transfe
3. Siegel, R., a
Transfer, 4th
4. Howell, J. R
Factors, Mc
5. Emery, A. F
J. Heat Tran
6. Oppenheim,
7. Hottel, H. C
McGraw-Hil
8. Tien, C. L., '
J. P. Hartnet
Transfer, Vo

Problems

View Factors

13.1 Determine
using the re
tor relations

(a) Lo

(b) Sm
hen

Patent Owner Manufacturing Resources International, Inc.
Exhibit 2017 - Page 853 of 999

References

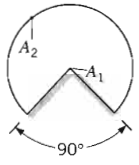
1. Hamilton, D. C., and W. R. Morgan, "Radiant Interchange Configuration Factors," National Advisory Committee for Aeronautics, Technical Note 2836, 1952.
2. Eckert, E. R. G., "Radiation: Relations and Properties," in W. M. Rohsenow and J. P. Hartnett, Eds., *Handbook of Heat Transfer*, 2nd ed., McGraw-Hill, New York, 1973.
3. Siegel, R., and J. R. Howell, *Thermal Radiation Heat Transfer*, 4th ed., Taylor & Francis, New York, 2002.
4. Howell, J. R., *A Catalog of Radiation Configuration Factors*, McGraw-Hill, New York, 1982.
5. Emery, A. F., O. Johansson, M. Lobo, and A. Abrous, *J. Heat Transfer*, **113**, 413, 1991.
6. Oppenheim, A. K., *Trans. ASME*, **65**, 725, 1956.
7. Hottel, H. C., and A. F. Sarofim, *Radiative Transfer*, McGraw-Hill, New York, 1967.
8. Tien, C. L., "Thermal Radiation Properties of Gases," in J. P. Hartnett and T. F. Irvine, Eds., *Advances in Heat Transfer*, Vol. 5, Academic Press, New York, 1968.
9. Sparrow, E. M., "Radiant Interchange Between Surfaces Separated by Nonabsorbing and Nonemitting Media," in W. M. Rohsenow and J. P. Hartnett, Eds., *Handbook of Heat Transfer*, McGraw-Hill, New York, 1973.
10. Dunkle, R. V., "Radiation Exchange in an Enclosure with a Participating Gas," in W. M. Rohsenow and J. P. Hartnett, Eds., *Handbook of Heat Transfer*, McGraw-Hill, New York, 1973.
11. Sparrow, E. M., and R. D. Cess, *Radiation Heat Transfer*, Hemisphere Publishing, New York, 1978.
12. Edwards, D. K., *Radiation Heat Transfer Notes*, Hemisphere Publishing, New York, 1981.
13. Hottel, H. C., "Radiant-Heat Transmission," in W. H. McAdams, Ed., *Heat Transmission*, 3rd ed., McGraw-Hill, New York, 1954.

Problems

View Factors

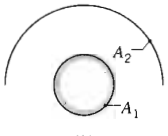
13.1 Determine F_{12} and F_{21} for the following configurations using the reciprocity theorem and other basic shape factor relations. Do not use tables or charts.

(a) Long duct



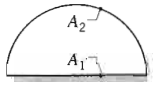
(*a*)

(b) Small sphere of area A_1 under a concentric hemisphere of area $A_2 = 2A_1$



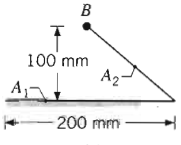
(*b*)

(c) Long duct. What is F_{22} for this case?



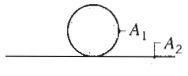
(*c*)

(d) Long inclined plates (point B is directly above the center of A_1)



(*d*)

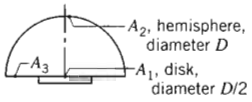
(e) Sphere lying on infinite plane



(*e*)

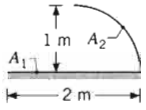
Patent Owner Manufacturing Resources International, Inc.
Exhibit 2017 - Page 854 of 999

(f) Hemisphere–disk arrangement



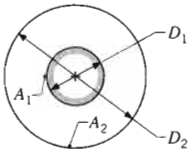
(*f*)

(g) Long, open channel



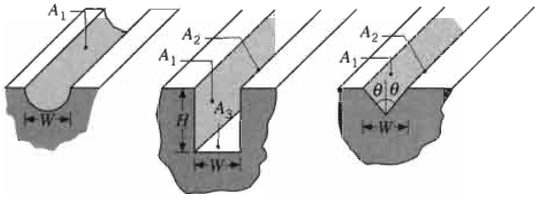
(*g*)

(h) Long concentric cylinders



(*h*)

13.2 Consider the following grooves, each of width W, that have been machined from a solid block of material.

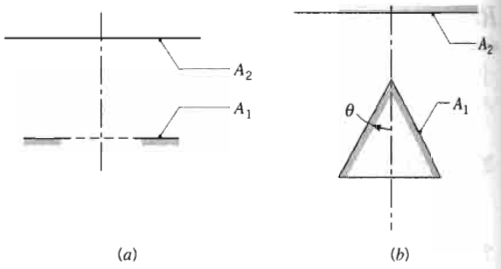


(a) For each case obtain an expression for the view factor of the groove with respect to the surroundings outside the groove.

(b) For the V groove, obtain an expression for the view factor F_{12}, where A_1 and A_2 are opposite surfaces.

(c) If $H = 2W$ in the rectangular groove, what is the view factor F_{12}?

13.3 Derive expressions for the view factor F_{12} associated with the following arrangements. Express your results in terms of A_1, A_2 and any appropriate hypothetical surface area, as well as the view factor for coaxial parallel disks (Table 13.2, Figure 13.5).

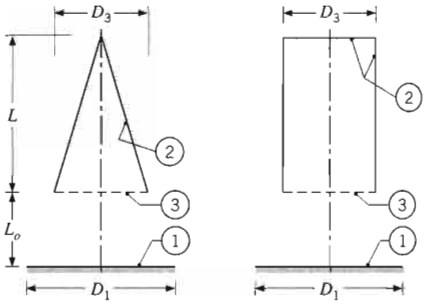


(*a*) (*b*)

(a) A circular disk and a coaxial, ring-shaped disk.

(b) A circular disk and a coaxial, right-circular cone. Sketch the variation of F_{12} with θ for $0 \leq \theta \leq \pi/2$, and explain the key features.

13.4 A right-circular cone and a right-circular cylinder of the same diameter and length (A_2) are positioned coaxially at a distance L_o from the circular disk (A_1) shown schematically. The inner base and lateral surfaces of the cylinder may be treated as a single surface, A_2. The hypothetical area corresponding to the opening of the cone and cylinder is identified as A_3.



(*a*) Right-circular cone (*b*) Right-circular cylinder

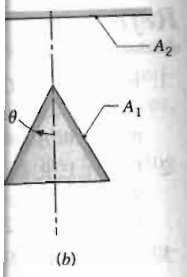
(a) Show that, for both arrangements, $F_{21} = (A_1/A_2)F_{13}$ and $F_{22} = 1 - (A_3/A_2)$, where F_{13} is the view factor between two coaxial, parallel disks (Table 13.2).

(b) For $L = L_o = 50$ mm and $D_1 = D_3 = 50$ mm, calculate F_{21} and F_{22} for the conical and cylindrical configurations and compare their relative magnitudes. Explain any similarities and differences.

(c) Do the relative magnitudes of F_{21} and F_{22} change for the conical and cylindrical configurations as L increases and all other parameters remain fixed? In the limit of very large L, what do you expect will happen? Sketch the variations of F_{21} and F_{22} with L, and explain the key features.

13.5 Consider the two parallel, coaxial, ring-shaped disks shown schematically.

Patent Owner Manufacturing Resources International, Inc.
Exhibit 2017 - Page 855 of 999

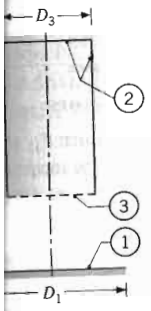


(b)

ring-shaped disk.

, right-circular cone.
ith θ for $0 \le \theta \le \pi/2$,

ircular cylinder of the
positioned coaxially
ilar disk (A_1) shown
nd lateral surfaces of
ingle surface, A_2. The
to the opening of the
A_3.



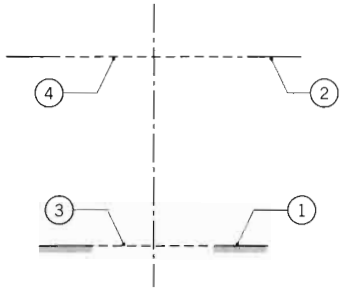
ight-circular cylinder

ments, $F_{21} = (A_1/A_2)F_{13}$
re F_{13} is the view factor
el disks (Table 13.2).

$D_1 = D_3 = 50$ mm, cal-
conical and cylindrical
re their relative magni-
ties and differences.

s of F_{21} and F_{22} change
rical configurations as L
ameters remain fixed? In
what do you expect will
ions of F_{21} and F_{22} with
tures.

axial, ring-shaped disks



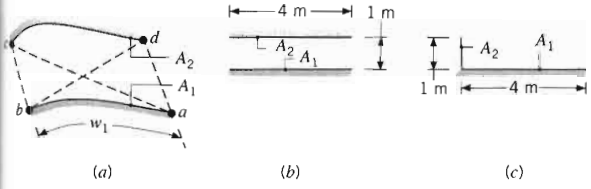
Show that F_{12} can be expressed as

$$F_{12} = \frac{1}{A_1}\{A_{(1,3)}F_{(1,3)(2,4)} - A_3F_{3(2,4)} - A_4(F_{4(1,3)} - F_{43})\}$$

where all view factors on the right-hand side of the equation can be evaluated from Figure 13.5 or Table 13.2 for coaxial parallel disks.

13.6 The "crossed-strings" method of Hottel [13] provides a simple means to calculate view factors between surfaces that are of infinite extent in one direction. For two such surfaces (a) with unobstructed views of one another, the view factor is of the form

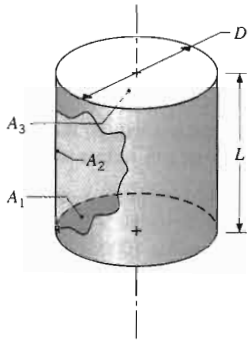
$$F_{12} = \frac{1}{2w_1}[(ac + bd) - (ad + bc)]$$



(a) (b) (c)

Use this method to evaluate the view factors F_{12} for sketches (b) and (c). Compare your results with those from the appropriate graphs and analytical expressions.

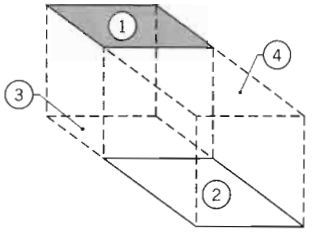
13.7 Consider the right-circular cylinder of diameter D, length L, and the areas A_1, A_2, and A_3 representing the base, inner, and top surfaces, respectively.



(a) Show that the view factor between the base of the cylinder and the inner surface has the form $F_{12} = 2H[(1 + H^2)^{1/2} - H]$, where $H = L/D$.

(b) Show that the view factor for the inner surface to itself has the form $F_{22} = 1 + H - (1 + H^2)^{1/2}$.

13.8 Consider the parallel rectangles shown schematically.

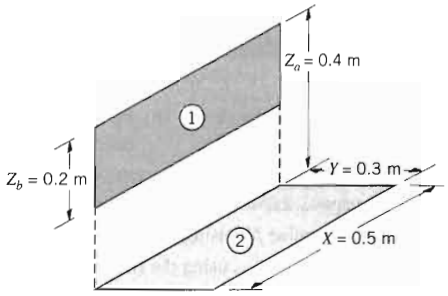


Show that the view factor F_{12} can be expressed as

$$F_{12} = \frac{1}{2A_1}[A_{(1,4)}F_{(1,4)(2,3)} - A_1F_{13} - A_4F_{42}]$$

where all view factors on the right-hand side of the equation can be evaluated from Figure 13.4 (see Table 13.2) for aligned parallel rectangles.

13.9 Consider the perpendicular rectangles shown schematically.

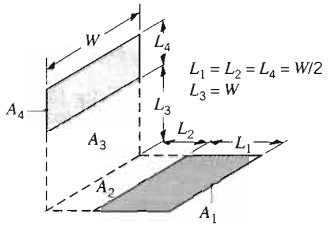


(a) Determine the shape factor F_{12}.

(b) For rectangle widths of $X = 0.5$, 1.5, and 5 m, plot F_{12} as a function of Z_b for $0.05 \le Z_b \le 0.4$ m. Compare your results with the view factor obtained from the two-dimensional relation for perpendicular plates with a common edge (Table 13.1).

13.10 The reciprocity relation, the summation rule, and Equations 13.5 to 13.7 can be used to develop view factor relations that allow for applications of Figure 13.4 and/or 13.6 to more complex configurations. Consider the view factor F_{14} for surfaces 1 and 4 of the following geometry. These surfaces are perpendicular but do not share a common edge.

Patent Owner Manufacturing Resources International, Inc.
Exhibit 2017 - Page 856 of 999

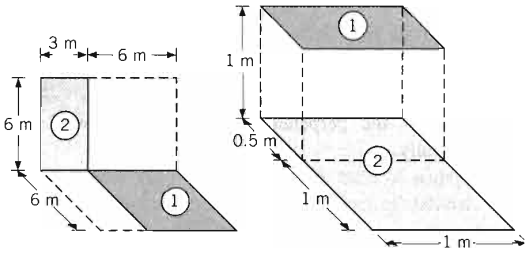


(a) Obtain the following expression for the view factor F_{14}:

$$F_{14} = \frac{1}{A_1}[(A_1 + A_2)F_{(1,2)(3,4)} + A_2F_{23} - (A_1 + A_2)F_{(1,2)3} - A_2F_{2(3,4)}]$$

(b) If $L_1 = L_2 = L_4 = (W/2)$ and $L_3 = W$, what is the value of F_{14}?

13.11 Determine the shape factor, F_{12}, for the rectangles shown.



(a) Perpendicular rectangles without a common edge.

(b) Parallel rectangles of unequal areas.

13.12 Consider parallel planes of infinite extent normal to the page as shown in the sketch.

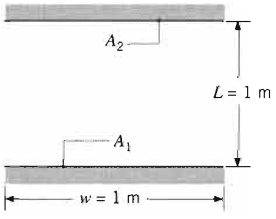
(a) Determine F_{12} using the results of Figure 13.4.

(b) Determine F_{12} using the first case of Table 13.1.

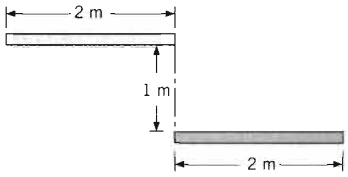
(c) Determine F_{12} using Hottel's crossed-string method described in Problem 13.6.

(d) Determine F_{12} using the second case of Table 13.1.

(e) Determine F_{12} using the results of Figure 13.4 if the dimensions are increased to $w = L = 2$ m.



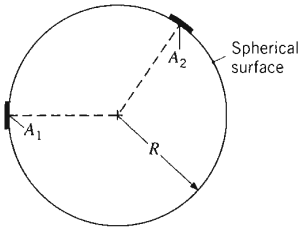
13.13 Consider the parallel planes of infinite extent normal to the page having opposite edges aligned as shown in the sketch.



(a) Using appropriate view factor relations and the results for opposing parallel planes, develop an expression for the view factor F_{12}.

(b) Use Hottel's crossed-string method described in Problem 13.6 to determine the view factor.

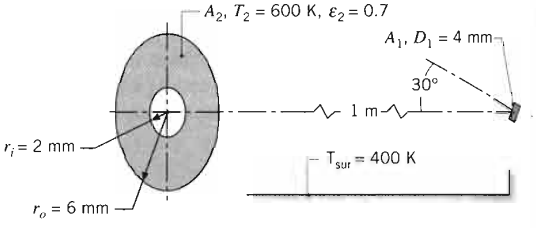
13.14 Consider two diffuse surfaces A_1 and A_2 on the inside of a spherical enclosure of radius R. Using the following methods, derive an expression for the view factor F_{12} in terms of A_2 and R.



(a) Find F_{12} by beginning with the expression $F_{ij} = q_{i\to j}/A_iJ_i$.

(b) Find F_{12} using the view factor integral, Equation 13.1.

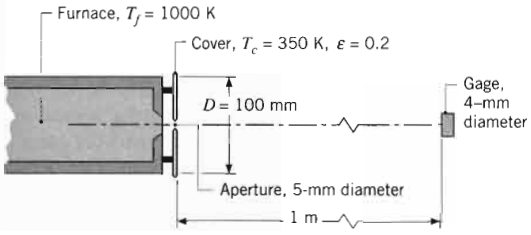
13.15 As shown in the sketch, consider the disk A_1 located coaxially 1 m distant, but tilted 30° off the normal, from the ring-shaped disk A_2.



What is the irradiation on A_1 due to radiation from A_2, which is a diffuse, gray surface with an emissivity of 0.7?

13.16 A heat flux gage of 4-mm diameter is positioned normal to and 1 m from the 5-mm-diameter aperture of a blackbody furnace at 1000 K. The diffuse, gray cover shield ($\varepsilon = 0.2$) of the furnace has an outer diameter of 100 mm and its temperature is 350 K. The furnace and gage are located in a large room whose walls have an emissivity of 0.8 and are at 300 K.

Patent Owner Manufacturing Resources International, Inc.
Exhibit 2017 - Page 857 of 999

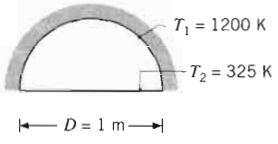


(a) What is the irradiation on the gage, G_g (W/m^2), considering only emission from the aperture of the furnace?
(b) What is the irradiation on the gage due to radiation from the cover and aperture?

Blackbody Radiation Exchange

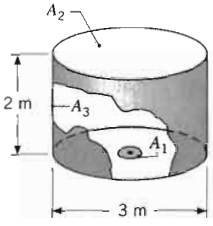
13.17 A circular ice rink 25 m in diameter is enclosed by a hemispherical dome 35 m in diameter. If the ice and dome surfaces may be approximated as blackbodies and are at 0 and 15° C, respectively, what is the net rate of radiative transfer from the dome to the rink?

13.18 A drying oven consists of a long semicircular duct of diameter D = 1 m.



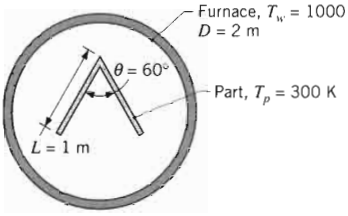
Materials to be dried cover the base of the oven while the wall is maintained at 1200 K. What is the drying rate per unit length of the oven (kg/s · m) if a water-coated layer of material is maintained at 325 K during the drying process? Blackbody behavior may be assumed for the water surface and the oven wall.

13.19 Consider the arrangement of the three black surfaces shown, where A_1 is small compared to A_2 or A_3.



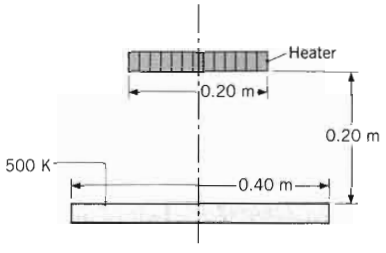
Determine the value of F_{13}. Calculate the net radiation heat transfer from A_1 to A_3 if A_1 = 0.05 m^2, T_1 = 1000 K, and T_3 = 500 K.

13.20 A long, V-shaped part is heat treated by suspending it in a tubular furnace with a diameter of 2 m and a wall temperature of 1000 K. The "vee" is 1-m long on a side and has an angle of 60°.

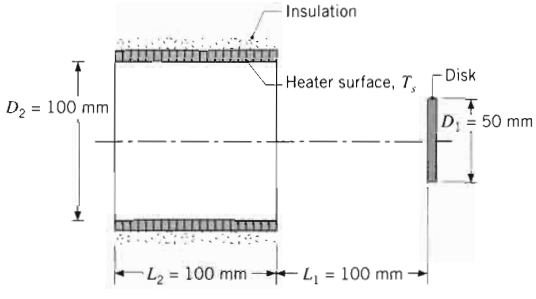


If the wall of the furnace and the surfaces of the part may be approximated as blackbodies and the part is at an initial temperature of 300 K, what is the net rate of radiation heat transfer per unit length to the part?

13.21 Consider coaxial, parallel, black disks separated a distance of 0.20 m. The lower disk of diameter 0.40 m is maintained at 500 K and the surroundings are at 300 K. What temperature will the upper disk of diameter 0.20 m achieve if electrical power of 17.5 W is supplied to the heater on the back side of the disk?



13.22 A tubular heater with a black inner surface of uniform temperature T_s = 1000 K irradiates a coaxial disk.



(a) Determine the radiant power from the heater, which is incident on the disk, $q_{s\to 1}$. What is the irradiation on the disk, G_1?

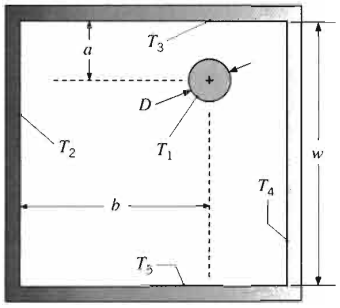
Patent Owner Manufacturing Resources International, Inc.
Exhibit 2017 - Page 858 of 999

(b) For disk diameters of $D_1 = 25$, 50, and 100 mm, plot $q_{s\to 1}$ and G_1 as a function of the separation distance L_1 for $0 \le L_1 \le 200$ mm.

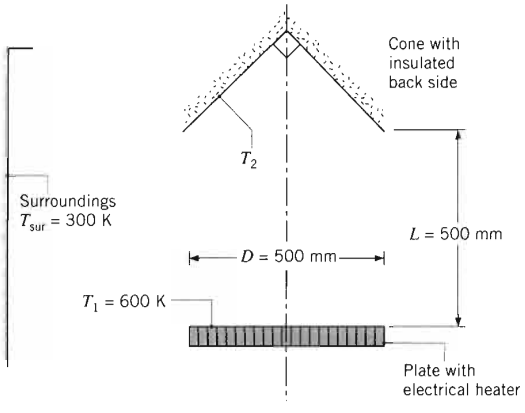
13.23 A long cylindrical rod of very high emissivity is heat treated within a long, evacuated oven of square cross section as shown in the sketch. The oven walls exhibit blackbody behavior. Due to nonuniform heat losses, the temperatures of the oven walls are slightly different and are $T_2 = 600$ K, $T_3 = 575$ K, $T_4 = 555$ K, and $T_5 = 585$ K, respectively.

(a) Determine the steady-state temperature of the $D = 0.2$-m-diameter rod if each wall of the oven is $w = 1$ m wide and $a = b = 0.5$ m.

(b) Determine the steady-state temperature of the rod when $a = 0.5$ m and $b = 0.25$ m.



13.24 A circular plate of 500-mm diameter is maintained at $T_1 = 600$ K and is positioned coaxial to a conical shape. The back side of the cone is well insulated. The plate and the cone, whose surfaces are black, are located in a large, evacuated enclosure whose walls are at 300 K.

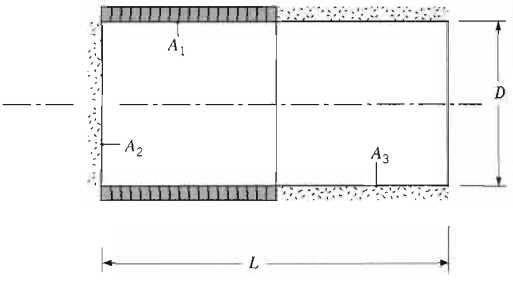


(a) What is the temperature of the conical surface, T_2?

(b) What is the electrical power that would be required to maintain the circular plate at 600 K?

13.25 Two furnace designs, as illustrated and dimensioned in Problem 13.4, are used to heat a disk-shaped work piece (A_1). The power supplied to the conical and cylindrical furnaces (A_2) is 50 W. The work piece is located in a large room at a temperature of 300 K, and its back side is well insulated. Assuming all surfaces are black, determine the temperature of the work piece, T_1, and the temperature of the furnace inner surface, T_2, for each of the designs. In your analysis, use the expressions provided in Problem 13.4 for the view factors, F_{21} and F_{22}.

13.26 A furnace is constructed in three sections, which include insulated circular (2) and cylindrical (3) sections, as well as an intermediate cylindrical section (1) with imbedded electrical resistance heaters. The overall length and diameter are 200 mm and 100 mm, respectively, and the cylindrical sections are of equal length. The surroundings are at 0 K.



(a) If all the surfaces are black, determine the electrical power, q_1, required to maintain the heated section at 1000 K.

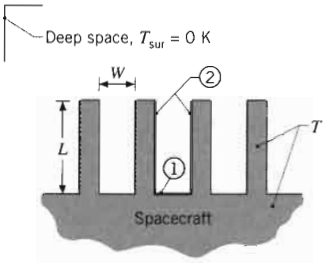
(b) What are the temperatures of the insulated sections, T_2 and T_3?

(c) For $D = 100$ mm, generate a plot of q_1, T_2, and T_3 as functions of the length-to-diameter ratio, with $1 \le L/D \le 5$.

13.27 To enhance heat rejection from a spacecraft, an engineer proposes to attach an array of rectangular fins to the outer surface of the spacecraft and to coat all surfaces with a material that approximates blackbody behavior.

Consider the U-shaped region between adjoining fins and subdivide the surface into components associated with the base (1) and the side (2). Obtain an expression for the rate per unit length at which radiation is transferred from the surfaces to deep space, which may be approximated as a blackbody at

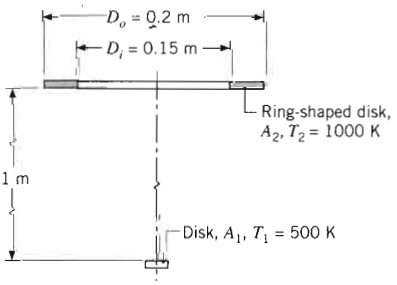
Patent Owner Manufacturing Resources International, Inc.
Exhibit 2017 - Page 859 of 999



absolute zero temperature. The fins and the base may be assumed to be isothermal at a temperature T. Comment on your result. Does the engineer's proposal have merit?

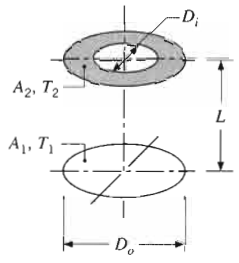
13.28 A cylindrical cavity of diameter D and depth L is machined in a metal block, and conditions are such that the base and side surfaces of the cavity are maintained at $T_1 = 1000$ K and $T_2 = 700$ K, respectively. Approximating the surfaces as black, determine the emissive power of the cavity if $L = 20$ mm and $D = 10$ mm.

13.29 In the arrangement shown, the lower disk has a diameter of 30 mm and a temperature of 500 K. The upper surface, which is at 1000 K, is a ring-shaped disk with inner and outer diameters of 0.15 m and 0.2 m. This upper surface is aligned with and parallel to the lower disk and is separated by a distance of 1 m.

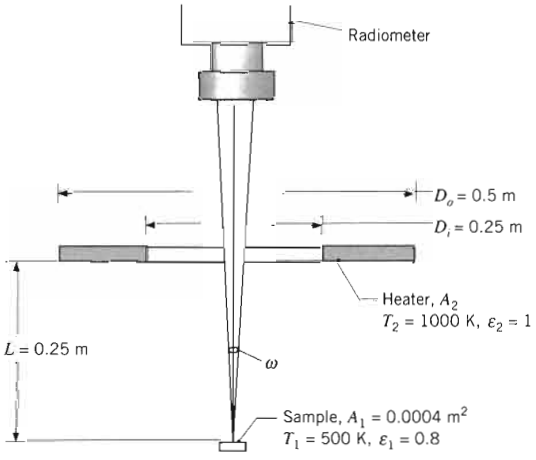


Assuming both surfaces to be blackbodies, calculate their net radiative heat exchange.

13.30 Two plane coaxial disks are separated by a distance $L = 0.20$ m. The lower disk (A_1) is solid with a diameter $D_o = 0.80$ m and a temperature $T_1 = 300$ K. The upper disk (A_2), at temperature $T_2 = 1000$ K, has the same outer diameter but is ring-shaped with an inner diameter $D_i = 0.40$ m. Assuming the disks to be blackbodies, calculate the net radiative heat exchange between them.



13.31 A radiometer views a small target (1) that is being heated by a ring-shaped disk heater (2). The target has an area of $A_1 = 0.0004$ m^2, a temperature of $T_1 = 500$ K, and a diffuse, gray emissivity of $\varepsilon_1 = 0.8$. The heater operates at $T_2 = 1000$ K and has a black surface. The radiometer views the entire sample area with a solid angle of $\omega = 0.0008$ sr.



(a) Write an expression for the radiant power leaving the target, which is collected by the radiometer, in terms of the target radiosity J_1 and relevant geometric parameters. Leave in symbolic form.

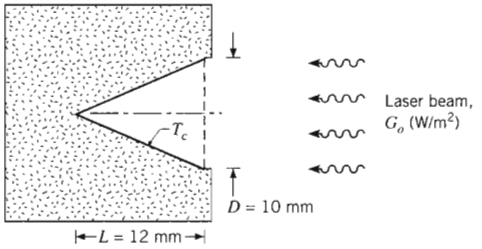
(b) Write an expression for the target radiosity J_1 in terms of its irradiation, emissive power, and appropriate radiative properties. Leave in symbolic form.

(c) Write an expression for the irradiation on the target, G_1, due to emission from the heater in terms of the heater emissive power, the heater area, and an appropriate view factor. Use this expression to numerically evaluate G_1.

(d) Use the foregoing expressions and results to determine the radiant power collected by the radiometer.

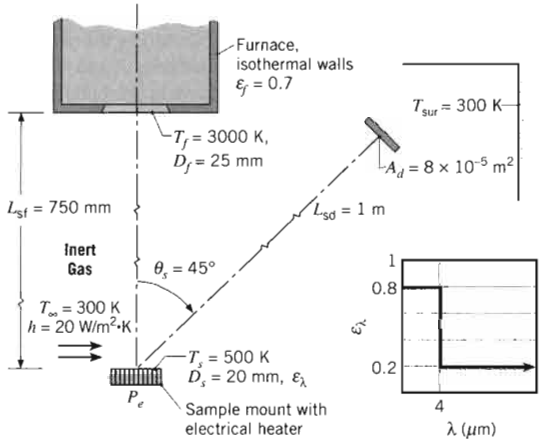
Patent Owner Manufacturing Resources International, Inc.
Exhibit 2017 - Page 860 of 999

13.32 A meter to measure the optical power of a laser beam is constructed with a thin-walled, black conical cavity that is well insulated from its housing. The cavity has an opening of $D = 10$ mm and a depth of $L = 12$ mm. The meter housing and surroundings are at a temperature of 25.0°C.



A fine-wire thermocouple attached to the surface indicates a temperature rise of 10.1°C when a laser beam is incident upon the meter. What is the optical (radiant) flux of the laser beam, G_o (W/m^2)?

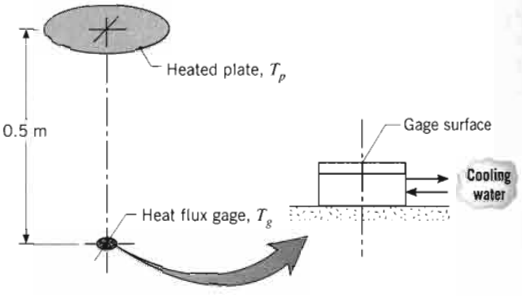
13.33 An electrically heated sample is maintained at a surface temperature of $T_s = 500$ K. The sample coating is diffuse but spectrally selective, with the spectral emissivity distribution shown schematically. The sample is irradiated by a furnace located coaxially at a distance of $L_{sf} = 750$ mm. The furnace has isothermal walls with an emissivity of $\varepsilon_f = 0.7$ and a uniform temperature of $T_f = 3000$ K. A radiation detector of area $A_d = 8 \times 10^{-5}$ m^2 is positioned at a distance of $L_{sd} = 1.0$ m from the sample along a direction that is 45° from the sample normal. The detector is sensitive to spectral radiant power only in the spectral region from 3 to 5 μm. The sample surface experiences convection with a gas for which $T_\infty = 300$ K and $h = 20$ W/m$^2 \cdot$ K. The surroundings of the sample mount are large and at a uniform temperature of $T_{sur} = 300$ K.



(a) Determine the electrical power, P_e, required to maintain the sample at $T_s = 500$ K.

(b) Considering both emission and reflected irradiation from the sample, determine the radiant power that is incident on the detector within the spectral region from 3 to 5 μm.

13.34 The arrangement shown is to be used to calibrate a heat flux gage. The gage has a black surface that is 10 mm in diameter and is maintained at 17°C by means of a water-cooled backing plate. The heater, 200 mm in diameter, has a black surface that is maintained at 800 K and is located 0.5 m from the gage. The surroundings and the air are at 27°C and the convection heat transfer coefficient between the gage and the air is 15 W/m$^2 \cdot$ K.



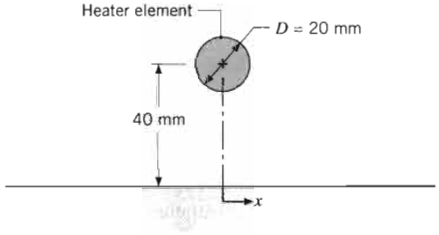
(a) Determine the net radiation exchange between the heater and the gage.

(b) Determine the net transfer of radiation to the gage per unit area of the gage.

(c) What is the net heat transfer rate to the gage per unit area of the gage?

(d) If the gage is constructed according to the description of Problem 3.98, what heat flux will it indicate?

13.35 A long, cylindrical heating element of 20-mm diameter operating at 700 K in vacuum is located 40 mm from an insulated wall of low thermal conductivity.

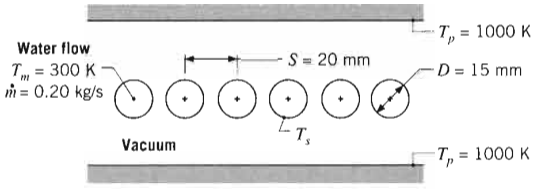


(a) Assuming both the element and the wall are black, estimate the maximum temperature reached by the wall when the surroundings are at 300 K.

Patent Owner Manufacturing Resources International, Inc.
Exhibit 2017 - Page 861 of 999

(b) Calculate and plot the steady-state wall temperature distribution over the range $-100 \text{ mm} \leq x \leq 100 \text{ mm}$.

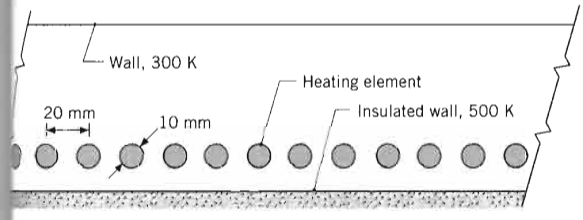
13.36 Water flowing through a large number of long, circular, thin-walled tubes is heated by means of hot parallel plates above and below the tube array. The space between the plates is evacuated, and the plate and tube surfaces may be approximated as blackbodies.



(a) Neglecting axial variations, determine the tube surface temperature, T_s, if water flows through each tube at a mass rate of $\dot{m} = 0.20$ kg/s and a mean temperature of $T_m = 300$ K.

(b) Compute and plot the surface temperature as a function of flow rate for $0.05 \leq \dot{m} \leq 0.25$ kg/s.

13.37 A row of regularly spaced, cylindrical heating elements is used to maintain an insulated furnace wall at 500 K. The opposite wall is at a uniform temperature of 300 K.



The insulated wall experiences convection with air at 450 K and a convection coefficient of 200 W/m$^2 \cdot$ K. Assuming the walls and elements are black, estimate the required operating temperature for the elements.

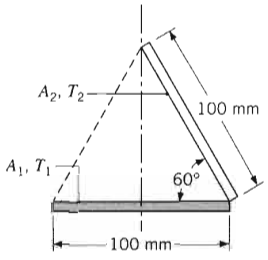
13.38 A manufacturing process calls for heating long copper rods, which are coated with a thin film having $\varepsilon = 1$, by placing them in a large evacuated oven whose surface is maintained at 1650 K. The rods are of 10-mm diameter and are placed in the oven with an initial temperature of 300 K.

(a) What is the initial rate of change of the rod temperature?

(b) How long must the rods remain in the oven to achieve a temperature of 1000 K?

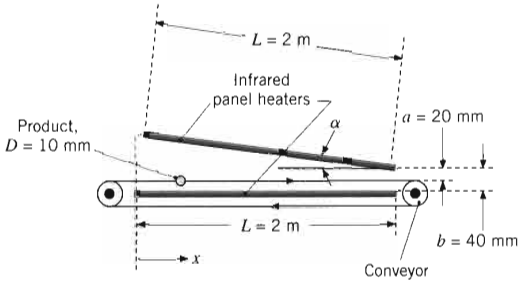
(c) The heating process may be accelerated by routing combustion gases, also at 1650 K, through the oven. For convection coefficients of 10, 100, and 500 W/m$^2 \cdot$ K, determine the time required for the rods to reach 1000 K.

13.39 Consider the very long, inclined black surfaces (A_1, A_2) maintained at uniform temperatures of $T_1 = 1000$ K and $T_2 = 800$ K.



Determine the net radiation exchange between the surfaces per unit length of the surfaces. Consider the configuration when a black surface (A_3), whose back side is insulated, is positioned along the dashed line shown. Calculate the net radiation transfer to surface A_2 per unit length of the surface and determine the temperature of the insulated surface A_3.

13.40 Many products are processed in a manner that requires a specified product temperature as a function of time. Consider a product in the shape of long, 10-mm-diameter cylinders that are conveyed slowly through a processing oven as shown in the schematic. The product exhibits near-black behavior and is attached to the conveying apparatus at the product's ends. The surroundings are at 300 K, while the radiation panel heaters are each isothermal at 500 K and have surfaces that exhibit near-black behavior. An engineer proposes a novel oven design with a tilting top surface so as to be able to quickly change the thermal response of the product.



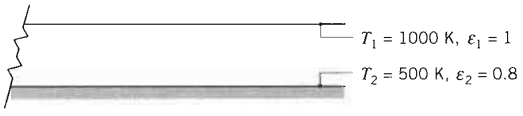
Patent Owner Manufacturing Resources International, Inc.
Exhibit 2017 - Page 862 of 999

(a) Determine the radiation per unit length incident upon the product at $x = 0.5$ m and $x = 1$ m for $\alpha = 0$.

(b) Determine the radiation per unit length incident upon the product at $x = 0.5$ m and $x = 1$ m for $\alpha = \pi/15$. *Hint:* The view factor from the cylinder to the left-hand side surroundings can be found by summing the view factors from the cylinder to the two surfaces shown as red dashed lines in the schematic.

Two-Surface Enclosures

13.41 Consider two very large parallel plates with diffuse, gray surfaces.



Determine the irradiation and radiosity for the upper plate. What is the radiosity for the lower plate? What is the net radiation exchange between the plates per unit area of the plates?

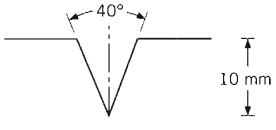
13.42 A flat-bottomed hole 6 mm in diameter is bored to a depth of 24 mm in a diffuse, gray material having an emissivity of 0.8 and a uniform temperature of 1000 K.

(a) Determine the radiant power leaving the opening of the cavity.

(b) The effective emissivity ε_e of a cavity is defined as the ratio of the radiant power leaving the cavity to that from a blackbody having the area of the cavity opening and a temperature of the inner surfaces of the cavity. Calculate the effective emissivity of the cavity described above.

(c) If the depth of the hole were increased, would ε_e increase or decrease? What is the limit of ε_e as the depth increases?

13.43 Consider a long V groove 10 mm deep machined on a block that is maintained at 1000 K.

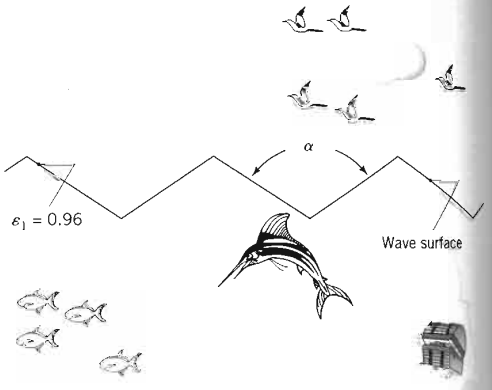


If the groove surfaces are diffuse and gray with an emissivity of 0.6, determine the radiant flux leaving the groove to its surroundings. Also determine the effective emissivity of the cavity, as defined in Problem 13.42.

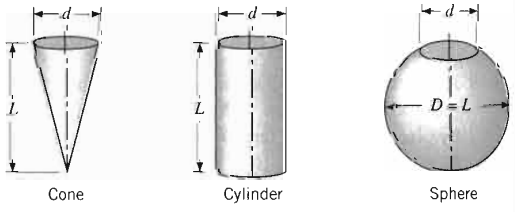
13.44 In Problems 12.19 and 12.20, we estimated the earth's surface temperature, assuming the earth is black. Most of the earth's surface is water, which has a hemispherical emissivity of $\varepsilon = 0.96$. In reality, the water surface is not flat but has waves and ripples.

(a) Assuming the wave geometry can be closely approximated as two-dimensional and as shown in the schematic, determine the effective emissivity of the water surface, as defined in Problem 13.42, for $\alpha = 3\pi/4$.

(b) Calculate and plot the effective emissivity of the water surface, normalized by the hemispherical emissivity of water ($\varepsilon_{eff}/\varepsilon$) over the range $\pi/2 \leq \alpha \leq \pi$.



13.45 Consider the cavities formed by a cone, cylinder, and sphere having the same opening size (d) and major dimension (L), as shown in the diagram.



(a) Find the view factor between the inner surface of each cavity and the opening of the cavity.

(b) Find the effective emissivity of each cavity, ε_e, as defined in Problem 13.42, assuming the

Patent Owner Manufacturing Resources International, Inc.
Exhibit 2017 - Page 863 of 999

inner walls are diffuse and gray with an emissivity of ε_w.

(c) For each cavity and wall emissivities of ε_w = 0.5, 0.7, and 0.9, plot ε_e as a function of the major dimension-to-opening size ratio, L/d, over a range from 1 to 10.

13.46 A t = 5 mm thick sheet of anodized aluminum is used to reject heat in a space power application. The edge of the sheet is attached to a hot source, and the sheet is maintained at nearly isothermal conditions at T = 300 K. The sheet is not subjected to irradiation.

(a) Determine the net radiation heat transfer from both sides of the 200 mm × 200 mm sheet to deep space.

(b) An engineer suggests boring 3-mm-diameter holes through the sheet. The holes are spaced 5 mm apart. The interior surfaces of the holes are anodized after they are bored. Determine the net radiation heat transfer from both sides of the sheet to deep space.

(c) As an alternative design, the 3-mm-diameter flat-bottomed holes are not bored completely through the sheet but are bored to depths of 2 mm on each side, leaving a 1-mm-thick web of aluminum separating the bottoms of the holes located on opposite sides of the sheet. Determine the net radiation heat transfer from both sides of the sheet to deep space.

(d) Compare the ratio of the net radiation heat transfer to the mass of the sheet for the three designs.

13.47 Consider the spacecraft heat rejection scheme of Problem 13.27, but under conditions for which surfaces 1 and 2 may not be approximated as blackbodies.

(a) For isothermal surfaces of temperature T = 325 K and emissivity ε = 0.7 and a U-section of width W = 25 mm and length L = 125 mm, determine the rate per unit length (normal to the page) at which radiation is transferred from a section to deep space.

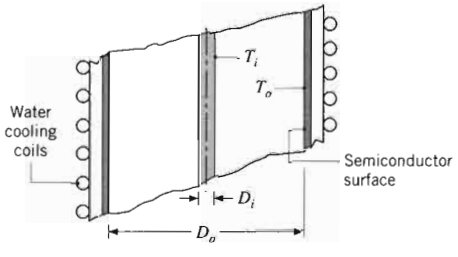
(b) Explore the effect of the emissivity on the rate of heat rejection, and contrast your results with those for emission exclusively from the base of the section.

13.48 An electronic device dissipating 50 W is attached to the inner surface of an isothermal cubical container that is 120 mm on a side. The container is located in the much larger service bay of the space shuttle, which is evacuated and whose walls are at 150 K. If the outer surface of the container has an emissivity of 0.8 and the thermal resistance between the surface and the device is 0.1 K/W, what are the temperatures of the surface and the device? All surfaces of the container may be assumed to exchange radiation with the service bay, and heat transfer through the container restraint may be neglected.

13.49 A long, thin-walled horizontal tube 100 mm in diameter is maintained at 120°C by the passage of steam through its interior. A radiation shield is installed around the tube, providing an air gap of 10 mm between the tube and the shield, and reaches a surface temperature of 35°C. The tube and shield are diffuse, gray surfaces with emissivities of 0.80 and 0.10, respectively. What is the radiant heat transfer from the tube per unit length?

13.50 A very long electrical conductor 10 mm in diameter is concentric with a cooled cylindrical tube 50 mm in diameter whose surface is diffuse and gray with an emissivity of 0.9 and temperature of 27°C. The electrical conductor has a diffuse, gray surface with an emissivity of 0.6 and is dissipating 6.0 W per meter of length. Assuming that the space between the two surfaces is evacuated, calculate the surface temperature of the conductor.

13.51 An arrangement for direct conversion of thermal energy to electrical power is shown. The inner cylinder of diameter D_i = 25 mm is heated internally by a combustion process that brings the ceramic cylinder (ε_i = 0.9) to a surface temperature of T_i = 1675°C. The outer cylinder of diameter D_o = 0.38 m consists of a semiconductor material (ε_o = 0.5) that converts absorbed incident irradiation to electrical current; the backing material for the semiconductor is a highly conducting metal that is water cooled to 20°C. The converter is assumed to be very long compared to the outer diameter. The space between the two concentric cylinders is evacuated.



Assuming diffuse, gray surfaces, determine the heat transfer rate per unit area of the outer cylinder. The electrical output of the semiconductor surface is 10% of the absorbed irradiation in the wavelength region 0.6 to 2.0 μm. For the prescribed conditions,

Patent Owner Manufacturing Resources International, Inc.
Exhibit 2017 - Page 864 of 999

determine the power generation in watts per unit of outer surface area.

13.52 Liquid oxygen is stored in a thin-walled, spherical container 0.8 m in diameter, which is enclosed within a second thin-walled, spherical container 1.2 m in diameter. The opaque, diffuse, gray container surfaces have an emissivity of 0.05 and are separated by an evacuated space. If the outer surface is at 280 K and the inner surface is at 95 K, what is the mass rate of oxygen lost due to evaporation? (The latent heat of vaporization of oxygen is 2.13×10^5 J/kg.)

13.53 Two concentric spheres of diameter $D_1 = 0.8$ m and $D_2 = 1.2$ m are separated by an air space and have surface temperatures of $T_1 = 400$ K and $T_2 = 300$ K.

(a) If the surfaces are black, what is the net rate of radiation exchange between the spheres?

(b) What is the net rate of radiation exchange between the surfaces if they are diffuse and gray with $\varepsilon_1 = 0.5$ and $\varepsilon_2 = 0.05$?

(c) What is the net rate of radiation exchange if D_2 is increased to 20 m, with $\varepsilon_2 = 0.05$, $\varepsilon_1 = 0.5$, and $D_1 = 0.8$ m? What error would be introduced by assuming blackbody behavior for the outer surface ($\varepsilon_2 = 1$), with all other conditions remaining the same?

(d) For $D_2 = 1.2$ m and emissivities of $\varepsilon_1 = 0.1$, 0.5, and 1.0, compute and plot the net rate of radiation exchange as a function of ε_2 for $0.05 \le \varepsilon_2 \le 1.0$.

13.54 Determine the steady-state temperatures of two radiation shields placed in the evacuated space between two infinite planes at temperatures of 600 and 325 K. All the surfaces are diffuse and gray with emissivities of 0.7.

13.55 Consider two large (infinite) parallel planes that are diffuse-gray with temperatures and emissivities of T_1, ε_1 and T_2, ε_2. Show that the ratio of the radiation transfer rate with multiple shields, N, of emissivity ε_s to that with no shields, $N = 0$, is

$$\frac{q_{12,N}}{q_{12,0}} = \frac{[1/\varepsilon_1 + 1/\varepsilon_2 - 1]}{[1/\varepsilon_1 + 1/\varepsilon_2 - 1] + N[2/\varepsilon_s - 1]}$$

where $q_{12,N}$ and $q_{12,0}$ represent the radiation heat transfer rates for N shields and no shields, respectively.

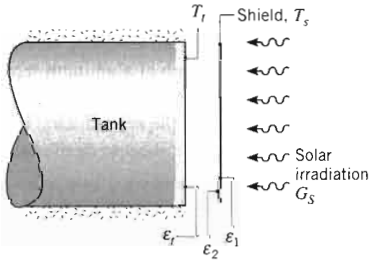
13.56 Consider two large, diffuse, gray, parallel surfaces separated by a small distance. If the surface emissivities are 0.8, what emissivity should a thin radiation shield have to reduce the radiation heat transfer rate between the two surfaces by a factor of 10?

13.57 Heat transfer by radiation occurs between two large parallel plates, which are maintained at temperatures T_1 and T_2, with $T_1 > T_2$. To reduce the rate of heat transfer between the plates, it is proposed that they be separated by a thin shield that has different emissivities on opposite surfaces. In particular, one surface has the emissivity $\varepsilon_s < 0.5$, while the opposite surface has an emissivity of $2\varepsilon_s$.

(a) How should the shield be oriented to provide the larger reduction in heat transfer between the plates? That is, should the surface of emissivity ε_s or that of emissivity $2\varepsilon_s$ be oriented toward the plate at T_1?

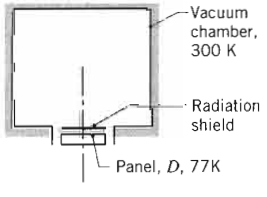
(b) What orientation will result in the larger value of the shield temperature T_s?

13.58 The end of a cylindrical liquid cryogenic propellant tank in free space is to be protected from external (solar) radiation by placing a thin metallic shield in front of the tank. Assume the view factor F_{ts} between the tank and the shield is unity; all surfaces are diffuse and gray, and the surroundings are at 0 K.



Find the temperature of the shield T_s and the heat flux (W/m²) to the end of the tank.

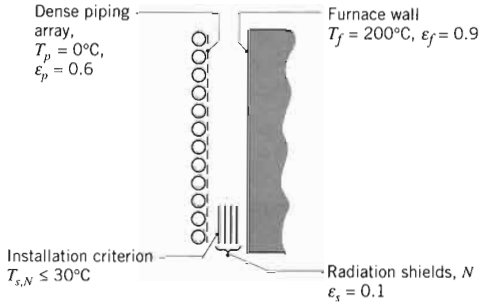
13.59 At the bottom of a very large vacuum chamber whose walls are at 300 K, a black panel 0.1 m in diameter is maintained at 77 K. To reduce the heat gain to this panel, a radiation shield of the same diameter D and an emissivity of 0.05 is placed very close to the panel. Calculate the net heat gain to the panel.



13.60 A furnace is located next to a dense array of cryogenic fluid piping. The ice-covered piping approximates a

Patent Owner Manufacturing Resources International, Inc.
Exhibit 2017 - Page 865 of 999

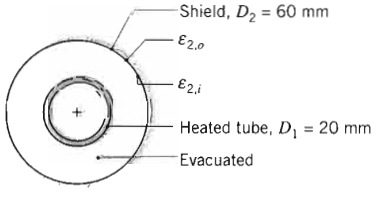
plane surface with an average temperature of $T_p = 0°C$ and an emissivity of $\varepsilon_p = 0.6$. The furnace wall has a temperature of $T_f = 200°C$ and an emissivity of $\varepsilon_f = 0.9$. To protect the refrigeration equipment and piping from excessive heat loading, reflective aluminum radiation shielding with an emissivity of $\varepsilon_s = 0.1$ is placed between the piping and the furnace wall, as shown in the schematic. Assume all surfaces are diffuse-gray.



If the temperature of the shield closest to the piping $T_{s,N}$ must be less than 30°C, how many radiation shields, N, must be installed between the piping and the furnace wall?

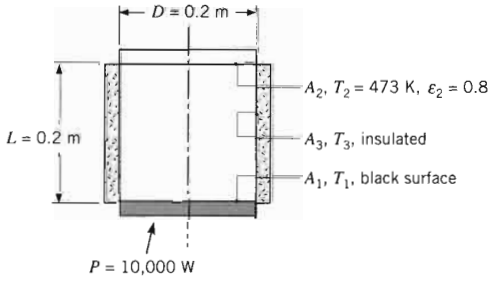
13.61 A cryogenic fluid flows through a tube 20 mm in diameter, the outer surface of which is diffuse and gray with an emissivity of 0.02 and temperature of 77 K. This tube is concentric with a larger tube of 50-mm diameter, the inner surface of which is diffuse and gray with an emissivity of 0.05 and temperature of 300 K. The space between the surfaces is evacuated. Determine the heat gain by the cryogenic fluid per unit length of the inner tube. If a thin-walled radiation shield that is diffuse and gray with an emissivity of 0.02 (both sides) is inserted midway between the inner and outer surfaces, calculate the change (percentage) in heat gain per unit length of the inner tube.

13.62 A diffuse, gray radiation shield of 60-mm diameter and emissivities of $\varepsilon_{2,i} = 0.01$ and $\varepsilon_{2,o} = 0.1$ on the inner and outer surfaces, respectively, is concentric with a long tube transporting a hot process fluid. The tube surface is black with a diameter of 20 mm. The region interior to the shield is evacuated. The exterior surface of the shield is exposed to a large room whose walls are at 17°C and experiences convection with air at 27°C and a convection heat transfer coefficient of 10 W/m² · K. Determine the operating temperature for the inner tube if the shield temperature is maintained at 42°C.



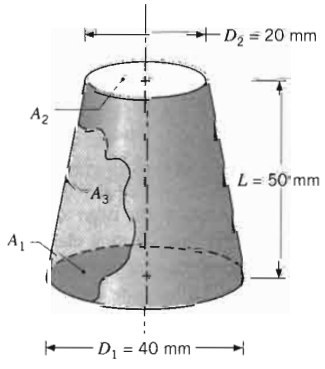
Enclosures with a Reradiating Surface

13.63 Consider the three-surface enclosure shown. The lower plate (A_1) is a black disk of 200-mm diameter and is supplied with a heat rate of 10,000 W. The upper plate (A_2), a disk coaxial to A_1, is a diffuse, gray surface with $\varepsilon_2 = 0.8$ and is maintained at $T_2 = 473$ K. The diffuse, gray sides between the plates are perfectly insulated. Assume convection heat transfer is negligible.



Determine the operating temperature of the lower plate T_1 and the temperature of the insulated side T_3.

13.64 A furnace has the form of a truncated conical section, as shown in the schematic. The floor of the furnace has an emissivity of $\varepsilon_1 = 0.7$ and is maintained at 1000 K with a heat flux of 2200 W/m². The lateral wall is perfectly insulated with an emissivity of $\varepsilon_3 = 0.3$. Assume that all the surfaces are diffuse-gray.



Patent Owner Manufacturing Resources International, Inc.
Exhibit 2017 - Page 866 of 999

(a) Determine the temperature of the upper surface, T_2 if its emissivity is $\varepsilon_2 = 0.5$. What is the temperature of the lateral wall, T_3?

(b) If conditions for the furnace floor remain unchanged, but all surfaces are black instead of diffuse-gray, determine T_2 and T_3. From the diffuse and blackbody enclosure analyses, what can you say about the influence of ε_2 on your results?

13.65 Consider two aligned, parallel, square planes (0.4 m × 0.4 m) spaced 0.8 m apart and maintained at $T_1 = 500$ K and $T_2 = 800$ K. Calculate the net radiative heat transfer *from surface 1* for the following special conditions:

(a) Both planes are black and the surroundings are at 0 K.

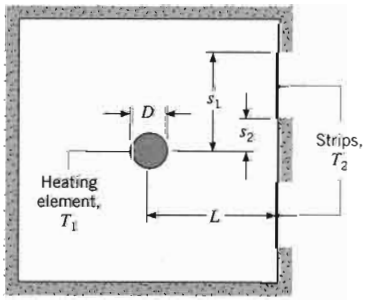
(b) Both planes are black with connecting, reradiating walls.

(c) Both planes are diffuse and gray with $\varepsilon_1 = 0.6$, $\varepsilon_2 = 0.8$, and the surroundings at 0 K.

(d) Both planes are diffuse and gray ($\varepsilon_1 = 0.6$ and $\varepsilon_2 = 0.8$) with connecting, reradiating walls.

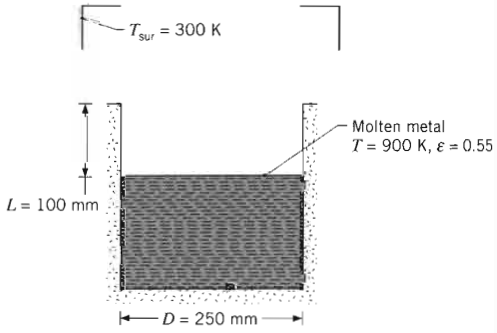
13.66 Two parallel, aligned disks, 0.4 m in diameter and separated by 0.1 m, are located in a large room whose walls are maintained at 300 K. One of the disks is maintained at a uniform temperature of 500 K with an emissivity of 0.6, while the backside of the second disk is well insulated. If the disks are diffuse, gray surfaces, determine the temperature of the insulated disk.

13.67 Coatings applied to long metallic strips are cured by installing the strips along the walls of a long oven of square cross section.



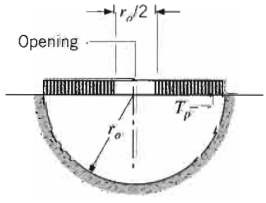
Thermal conditions in the oven are maintained by a long silicon carbide rod (heating element), which is of diameter $D = 20$ mm and is operated at $T_1 = 1700$ K. Each of two strips on one side wall has the same orientation relative to the rod ($s_1 = 60$ mm, $s_2 = 20$ mm, $L = 80$ mm) and is operated at $T_2 = 600$ K. All surfaces are diffuse and gray with $\varepsilon_1 = 0.9$ and $\varepsilon_2 = 0.4$. Assuming the oven to be well insulated at all but the strip surfaces and neglecting convection effects, determine the heater power requirement per unit length (W/m).

13.68 A molten aluminum alloy at 900 K is poured into a cylindrical container that is well insulated from large surroundings at 300 K. The inner diameter of the container is 250 mm, and the distance from the surface of the melt to the top of the container is 100 mm.



If the oxidized aluminum at the surface of the melt has an emissivity of 0.55, what is the net rate of radiation heat transfer from the melt?

13.69 The proposed design for a blackbody simulator consists of a diffuse, gray, circular plate with an emissivity of 0.9 maintained at $T_p = 600$ K and mounted over a well-insulated hemispherical cavity of radius $r_o = 100$ mm. The opening in the circular plate is $r_o/2$.



(a) Calculate the radiant power leaving the opening when the surroundings are at 300 K.

(b) Calculate the effective emissivity of the cavity, ε_c, which is defined as the ratio of the radiant power leaving the cavity to the rate at which the heated circular plate would emit radiation if it were black.

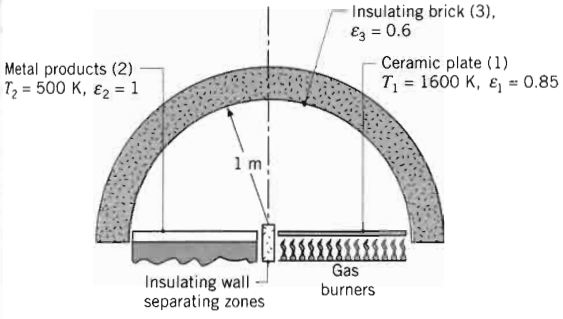
(c) Determine the surface temperature of the hemispherical cavity, T_{hc}.

(d) For plate emissivities of $\varepsilon_p = 0.5$, 0.7, and 0.9, plot ε_c and T_{hc} as a function of the opening in

Patent Owner Manufacturing Resources International, Inc.
Exhibit 2017 - Page 867 of 999

the circular plate over a range from $r_o/8$ to $r_o/2$. All other conditions remain the same.

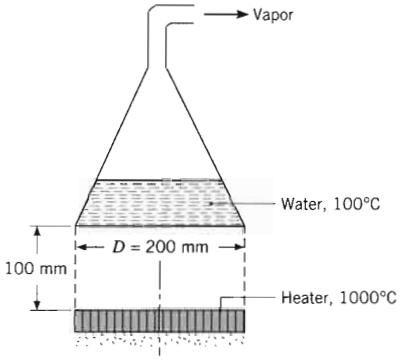
13.70 A long, hemicylindrical (1-m radius) shaped furnace used to heat treat sheet metal products is comprised of three zones. The heating zone (1) is constructed from a ceramic plate of emissivity 0.85 and is operated at 1600 K by gas burners. The load zone (2) consists of sheet metal products, assumed to be black surfaces, that are to be maintained at 500 K. The refractory zone (3) is fabricated from insulating bricks having an emissivity of 0.6. Assume steady-state conditions, diffuse, gray surfaces, and negligible convection.



(a) What is the heat rate per unit length of the furnace (normal to the page) that must be supplied by the gas burners for the prescribed conditions?

(b) What is the temperature of the insulating brick surface for the prescribed conditions?

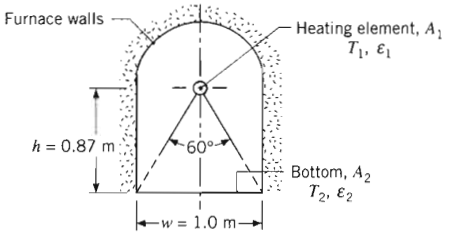
13.71 The bottom of a steam-producing still of 200-mm diameter is heated by radiation. The heater, maintained at 1000°C and separated 100 mm from the still, has the same diameter as the still bottom. The still bottom and heater surfaces are black.



(a) By what factor could the vapor production rate be increased if the cylindrical sides (dashed surface) were insulated rather than open to the surroundings maintained at 27°C?

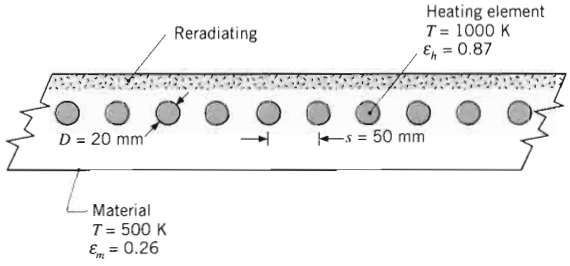
(b) For heater temperatures of 600, 800, and 1000°C, plot the net rate of radiation heat transfer to the still as a function of the separation distance over the range from 25 to 100 mm. Consider the cylindrical sides to be insulated and all other conditions to remain the same.

13.72 A long cylindrical heater element of diameter $D = 10$ mm, temperature $T_1 = 1500$ K, and emissivity $\varepsilon_1 = 1$ is used in a furnace. The bottom area A_2 is a diffuse, gray surface with $\varepsilon_2 = 0.6$ and is maintained at $T_2 = 500$ K. The side and top walls are fabricated from an insulating, refractory brick that is diffuse and gray with $\varepsilon = 0.9$. The length of the furnace normal to the page is very large compared to the width w and height h.



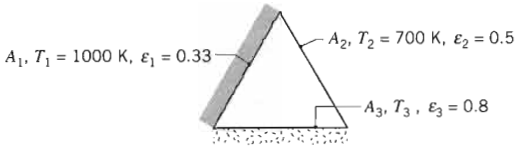
Neglecting convection and treating the furnace walls as isothermal, determine the power per unit length that must be provided to the heating element to maintain steady-state conditions. Calculate the temperature of the furnace wall.

13.73 A radiative heater consists of a bank of ceramic tubes with internal heating elements. The tubes are of diameter $D = 20$ mm and are separated by a distance $s = 50$ mm. A reradiating surface is positioned behind the heating tubes as shown in the schematic. Determine the net radiative heat flux to the heated material when the heating tubes ($\varepsilon_h = 0.87$) are maintained at 1000 K. The heated material ($\varepsilon_m = 0.26$) is at a temperature of 500 K.



Patent Owner Manufacturing Resources International, Inc.
Exhibit 2017 - Page 868 of 999

13.74 Consider a long duct constructed with diffuse, gray walls 1 m wide.

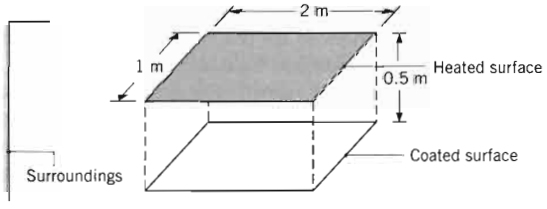


(a) Determine the net radiation transfer from surface A_1 per unit length of the duct.

(b) Determine the temperature of the insulated surface A_3.

(c) What effect would changing the value of ε_3 have on your result? After considering your assumptions, comment on whether you expect your results to be exact.

13.75 The coating on a 1 m by 2 m metallic surface is cured by placing it 0.5 m below an electrically heated surface of equivalent dimensions, and the assembly is exposed to large surroundings at 300 K. The heater is well insulated on its top side and is aligned with the coated surface. Both the heater and coated surfaces may be approximated as blackbodies. During the curing procedure, the heater and coated surfaces are maintained at 700 and 400 K, respectively. Convection effects may be neglected.



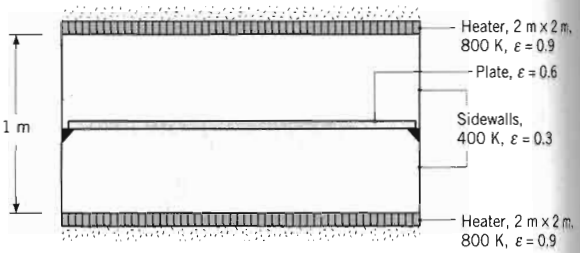
(a) What is the electric power, q_{elec}, required to operate the heater?

(b) What is q_{elec} if the surfaces are connected with reradiating sidewalls?

(c) The facility may be used to cure different surface coatings. With the heater still approximated as a blackbody, compute and plot q_{elec} as a function of the coating's emissivity for values ranging from 0.1 to 1.0. Perform the calculations for both open and reradiating sides.

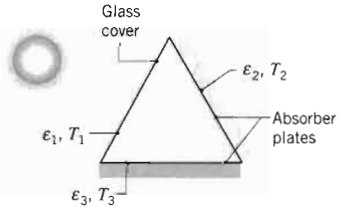
13.76 A cubical furnace 2 m on a side is used for heat treating steel plate. The top surface of the furnace consists of electrical radiant heaters that have an emissivity of 0.8 and a power input of 1.5×10^5 W. The sidewalls consist of a well-insulated refractory material, while the bottom consists of the steel plate, which has an emissivity of 0.4. Assume diffuse, gray surface behavior for the heater and the plate, and consider conditions for which the plate is at 300 K. What are the corresponding temperatures of the heater surface and the sidewalls?

13.77 An electric furnace consisting of two heater sections, top and bottom, is used to heat treat a coating that is applied to both surfaces of a thin metal plate inserted midway between the heaters.



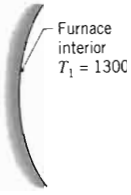
The heaters and the plate are 2 m by 2 m on a side, and each heater is separated from the plate by a distance of 0.5 m. Each heater is well insulated on its back side and has an emissivity of 0.9 at its exposed surface. The plate and the sidewalls have emissivities of 0.6 and 0.3, respectively. Sketch the equivalent radiation network for the system and label all pertinent resistances and potentials. For the prescribed conditions, obtain the required electrical power and the plate temperature.

13.78 A solar collector consists of a long duct through which air is blown; its cross section forms an equilateral triangle 1 m on a side. One side consists of a glass cover of emissivity $\varepsilon_1 = 0.9$, while the other two sides are absorber plates with $\varepsilon_2 = \varepsilon_3 = 1.0$.



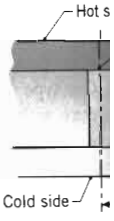
During operation the surface temperatures are known to be $T_1 = 25°C$, $T_2 = 60°C$, and $T_3 = 70°C$. What is the net rate at which radiation is transferred to the cover due to exchange with the absorber plates?

13.79 The cyli
$L = 250$
furnace
surrounc
of 300 K



Determ
peepho

13.80 A comp
separate
in the s
of thicl
$k = 0.0$
gaps of
have te
$\varepsilon_1 = 0.$
Assume
surface



(a) De
ga
to

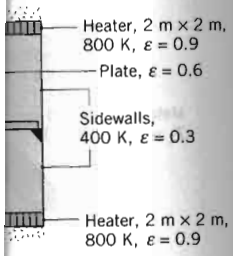
(b) Re
sp
los
by

13.81 A sma
$\varepsilon_1 = 0.$
The di
shield
$\varepsilon_2 = 0$
the bo
($\varepsilon_4 = ($
emissi

Patent Owner Manufacturing Resources International, Inc.
Exhibit 2017 - Page 869 of 999

y material, while
te, which has an
ay surface behav-
d consider condi-
K. What are the
eater surface and

o heater sections,
t a coating that is
etal plate inserted



by 2 m on a side,
the plate by a dis-
ell insulated on its
f 0.9 at its exposed
alls have emissivi-
Sketch the equiva-
stem and label all
ials. For the pre-
required electrical

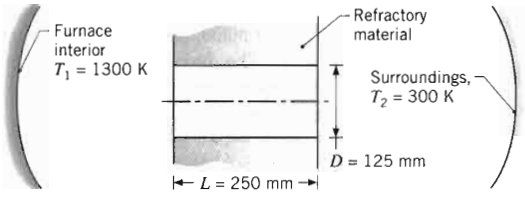
duct through which
s an equilateral tri-
ists of a glass cover
other two sides are

T_2

Absorber
plates

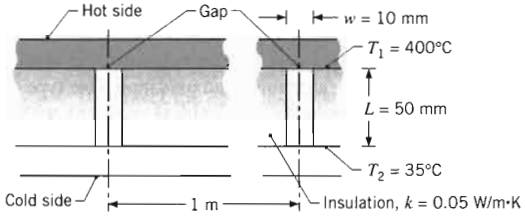
peratures are known
d $T_3 = 70°C$. What
is transferred to the
bsorber plates?

13.79 The cylindrical peephole in a furnace wall of thickness $L = 250$ mm has a diameter of $D = 125$ mm. The furnace interior has a temperature of 1300 K, and the surroundings outside the furnace have a temperature of 300 K.



Determine the heat loss by radiation through the peephole.

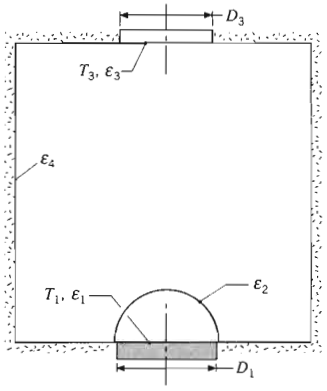
13.80 A composite wall is comprised of two large plates separated by sheets of refractory insulation, as shown in the schematic. In the installation process, the sheets of thickness $L = 50$ mm and thermal conductivity $k = 0.05$ W/m · K are separated at 1-m intervals by gaps of width $w = 10$ mm. The hot and cold plates have temperatures and emissivities of $T_1 = 400°C$, $\varepsilon_1 = 0.85$ and $T_2 = 35°C$, $\varepsilon_2 = 0.5$, respectively. Assume that the plates and insulation are diffuse-gray surfaces.



(a) Determine the heat loss by radiation through the gap per unit length of the composite wall (normal to the page).

(b) Recognizing that the gaps are located on a 1-m spacing, determine what fraction of the total heat loss through the composite wall is due to transfer by radiation through the insulation gap.

13.81 A small disk of diameter $D_1 = 50$ mm and emissivity $\varepsilon_1 = 0.6$ is maintained at a temperature of $T_1 = 900$ K. The disk is covered with a hemispherical radiation shield of the same diameter and an emissivity of $\varepsilon_2 = 0.02$ (both sides). The disk and cap are located at the bottom of a large evacuated refractory container ($\varepsilon_4 = 0.85$), facing another disk of diameter $D_3 = D_1$, emissivity $\varepsilon_3 = 0.4$, and temperature $T_3 = 400$ K. The view factor F_{23} of the shield with respect to the upper disk is 0.3.



(a) Construct an equivalent thermal circuit for the above system. Label all nodes, resistances, and currents.

(b) Find the net rate of heat transfer between the hot disk and the rest of the system.

Enclosures: Three or More Surfaces

13.82 Consider a cylindrical cavity of diameter $D = 100$ mm and depth $L = 50$ mm whose sidewall and bottom are diffuse and gray with an emissivity of 0.6 and are at a uniform temperature of 1500 K. The top of the cavity is open and exposed to surroundings that are large and at 300 K.

(a) Calculate the net radiation heat transfer from the cavity, treating the bottom and sidewall of the cavity as one surface (q_A).

(b) Calculate the net radiation heat transfer from the cavity, treating the bottom and sidewall of the cavity as two separate surfaces (q_B).

(c) Plot the percentage difference between q_A and q_B as a function of L over the range 5 mm $\leq L \leq$ 100 mm.

13.83 Consider a circular furnace that is 0.3 m long and 0.3 m in diameter. The two ends have diffuse, gray surfaces that are maintained at 400 and 500 K with emissivities of 0.4 and 0.5, respectively. The lateral surface is also diffuse and gray with an emissivity of 0.8 and a temperature of 800 K. Determine the net radiative heat transfer from each of the surfaces.

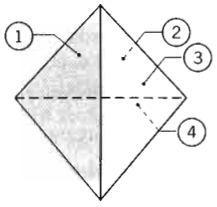
13.84 Consider two very large metal parallel plates. The top plate is at a temperature $T_t = 400$ K while the bottom plate is at $T_b = 300$ K. The desired net radiation heat flux between the two plates is $q'' = 330$ W/m^2.

Patent Owner Manufacturing Resources International, Inc.
Exhibit 2017 - Page 870 of 999

(a) If the two surfaces have the same radiative properties, show that the required surface emissivity is $\varepsilon = 0.5$.

(b) Metal surfaces at relatively low temperatures tend to have emissivities much less than 0.5 (see Table A.11). An engineer proposes to apply a checker pattern, similar to that of Problem 12.129, onto each of the metal surfaces so that half of each surface is characterized by the low emissivity of the bare metal and the other half is covered with the high-emissivity paint. If the average of the high and low emissivities is 0.5, will the net radiative heat flux between the surfaces be the desired value?

13.85 Consider the diffuse, gray, four-surface enclosure with all sides equal as shown. The temperatures of three surfaces are specified, while the fourth surface is well insulated and can be treated as a reradiating surface. Determine the temperature of the reradiating surface (4).

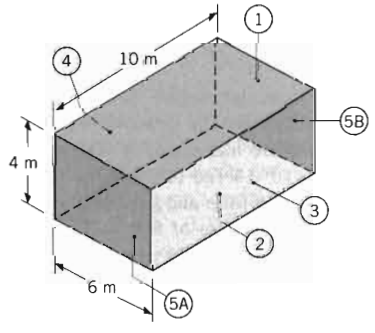


$T_1 = 700$ K, $\varepsilon_1 = 0.7$

$T_2 = 500$ K, $\varepsilon_2 = 0.5$

$T_3 = 300$ K, $\varepsilon_3 = 0.3$

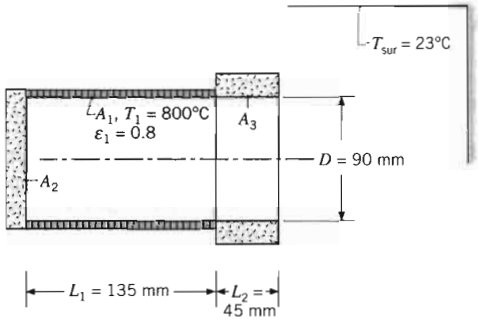
13.86 A room is represented by the following enclosure, where the ceiling (1) has an emissivity of 0.8 and is maintained at 40°C by embedded electrical heating elements. Heaters are also used to maintain the floor (2) of emissivity 0.9 at 50°C. The right wall (3) of emissivity 0.7 reaches a temperature of 15°C on a cold winter day. The left wall (4) and end walls (5A) and (5B) are very well insulated. To simplify the analysis, treat the two end walls as a single surface (5).



Assuming the surfaces are diffuse and gray, find the net radiation heat transfer from each surface.

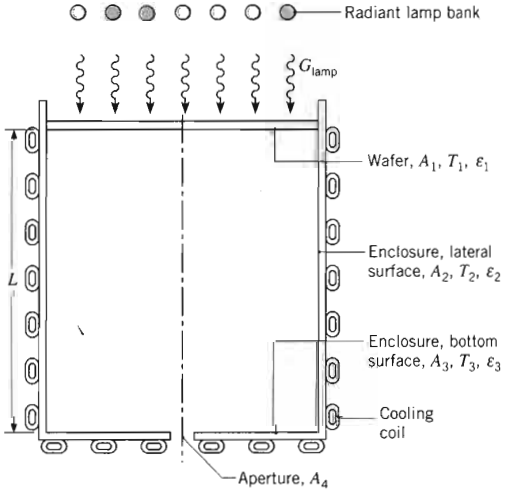
13.87 Work Problem 13.23, part (b), except with wall and cylinder emissivities of $\varepsilon_w = 0.95$ and $\varepsilon_c = 0.12$, respectively.

13.88 A cylindrical furnace for heat-treating materials in a spacecraft environment has a 90-mm diameter and an overall length of 180 mm. Heating elements in the 135-mm-long section (1) maintain a refractory lining of $\varepsilon_1 = 0.8$ at 800°C. The linings for the bottom (2) and upper (3) sections are made of the same refractory material, but are insulated.



Determine the power required to maintain the furnace operating conditions with the surroundings at 23°C.

13.89 In manufacturing semiconductors, rapid thermal processing (RTP) is used to rapidly heat a silicon wafer to an elevated temperature in order to induce effects such as ion diffusion, annealing, and oxidation. One type of RTP device consists of a cylindrical enclosure with a coaxially positioned wafer. The top side of the wafer



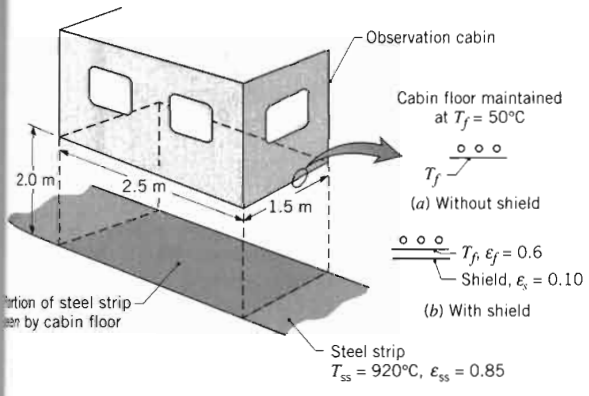
Patent Owner Manufacturing Resources International, Inc.
Exhibit 2017 - Page 871 of 999

experiences uniform irradiation from a lamp bank, G_{lamp}. The enclosure lateral (A_2) and bottom (A_3) surfaces have a low emissivity $\varepsilon_2 = \varepsilon_3 = 0.07$ and are maintained at 300 K by coolant passages. The wafer (A_1) diameter is $D = 300$ mm and the height of the enclosure is $L = 300$ mm. The aperture (A_4) diameter is $D_a = 30$ mm and provides for optical access to the wafer.

(a) What lamp irradiation, G_{lamp}, is required to maintain the wafer at 1300 K if the wafer emissivity is $\varepsilon_1 = 0.8$? What is the heat removal rate by the cooling coil? Assume there are no heat losses from the top side of the wafer.

(b) If the enclosure were perfectly reflecting, the radiosity of the wafer, J_1, would be equal to its blackbody emissive power, E_{b1}. As such, the radiosity would be independent of the wafer emissivity, thereby minimizing effects due to variation of that property from wafer-to-wafer. For wafer emissivities of $\varepsilon_1 = 0.75$, 0.8, and 0.85, plot the fractional difference, $(E_{b1} - J_1)/E_{b1}$, as a function of the aspect ratio for $0.5 \leq L/D \leq 2.5$. How sensitive is this parameter to the enclosure surface emissivity, ε_2?

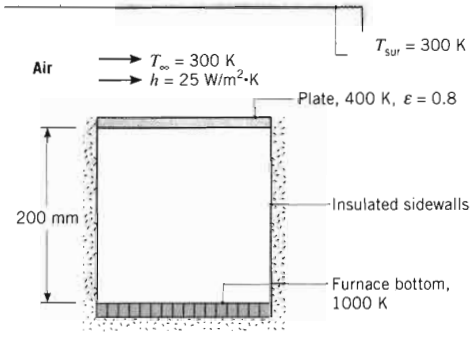
13.90 An observation cabin is located in a hot-strip mill directly over the line, as shown in the schematic. The cabin floor is exposed to a portion of the hot strip that is at a temperature of $T_{ss} = 920°C$ and has an emissivity of $\varepsilon_{ss} = 0.85$, as well as to *surroundings* within the mill (not shown) at a temperature of $T_{sur} = 80°C$. To protect the operating personnel in the cabin, the floor must be maintained at $T_f = 50°C$.



Determine the coolant system heat removal rate required to maintain the cabin floor at 50°C for the following conditions: (a) when the floor, with an emissivity of $\varepsilon_f = 0.6$, is directly exposed to the strip; and (b) when a radiation shield of emissivity $\varepsilon_s = 0.1$ is installed between the floor and the strip.

Multimode Heat Transfer: Introductory

13.91 An opaque, diffuse, gray (200 mm by 200 mm) plate with an emissivity of 0.8 is placed over the opening of a furnace and is known to be at 400 K at a certain instant. The bottom of the furnace, having the same dimensions as the plate, is black and operates at 1000 K. The sidewalls of the furnace are well insulated. The top of the plate is exposed to ambient air with a convection coefficient of 25 W/m$^2 \cdot$ K and to large surroundings. The air and surroundings are each at 300 K.



(a) Evaluate the net radiative heat transfer to the bottom surface of the plate.

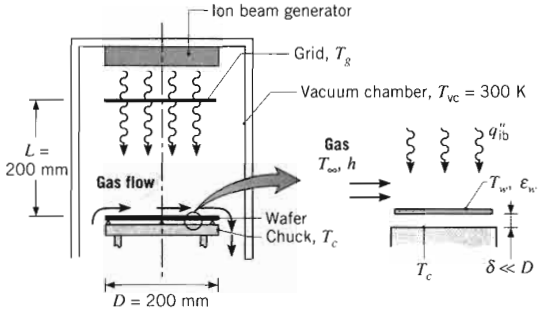
(b) If the plate has mass and specific heat of 2 kg and 900 J/kg $\cdot$ K, respectively, what will be the change in temperature of the plate with time, dT_p/dt? Assume convection to the bottom surface of the plate to be negligible.

(c) Extending the analysis of part (b), generate a plot of the change in temperature of the plate with time, dT_p/dt, as a function of the plate temperature for $350 \leq T_p \leq 900$ K and all other conditions remaining the same. What is the steady-state temperature of the plate?

13.92 A tool for processing silicon wafers is housed within a vacuum chamber whose walls are black and maintained by a coolant at $T_{vc} = 300$ K. The thin silicon wafer is mounted close to, but not touching, a chuck, which is electrically heated and maintained at the temperature T_c. The surface of the chuck facing the wafer is black. The wafer temperature is $T_w = 700$ K, and its surface is diffuse and gray with an emissivity of $\varepsilon_w = 0.6$. The function of the grid, a thin metallic foil positioned coaxial with the wafer and of the same diameter, is to control the power of the ion beam reaching the

Patent Owner Manufacturing Resources International, Inc.
Exhibit 2017 - Page 872 of 999

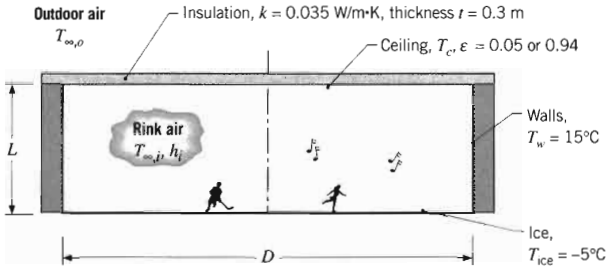
wafer. The grid surface is black with a temperature of $T_g = 500$ K. The effect of the ion beam striking the wafer is to apply a uniform heat flux of $q''_{ib} = 600$ W/m^2. The top surface of the wafer is subjected to the flow of a process gas for which $T_\infty = 500$ K and $h = 10$ W/m$^2 \cdot$K. Since the gap between the wafer and chuck, δ, is very small, flow of the process gas in this region may be neglected.



(a) Represent the wafer schematically, showing a control surface and all relevant thermal processes.

(b) Perform an energy balance on the wafer and determine the chuck temperature T_c.

13.93 Most architects know that the ceiling of an ice-skating rink must have a high reflectivity. Otherwise, condensation may occur on the ceiling, and water may drip onto the ice, causing bumps on the skating surface. Condensation will occur on the ceiling when its surface temperature drops below the dew point of the rink air. Your assignment is to perform an analysis to determine the effect of the ceiling emissivity on the ceiling temperature, and hence the propensity for condensation.

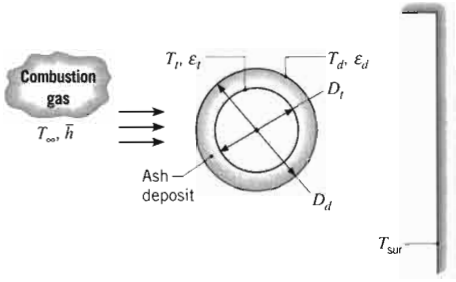


The rink has a diameter of $D = 50$ m and a height of $L = 10$ m, and the temperatures of the ice and walls are -5°C and 15°C, respectively. The rink air temperature is 15°C, and a convection coefficient of 5 W/m$^2 \cdot$K characterizes conditions on the ceiling surface. The thickness and thermal conductivity of the ceiling insulation are 0.3 m and 0.035 W/m $\cdot$ K, respectively, and the temperature of the outdoor air is -5°C. Assume that the ceiling is a diffuse-gray surface and that the walls and ice may be approximated as blackbodies.

(a) Consider a flat ceiling having an emissivity of 0.05 (highly reflective panels) or 0.94 (painted panels). Perform an energy balance on the ceiling to calculate the corresponding values of the ceiling temperature. If the relative humidity of the rink air is 70%, will condensation occur for either or both of the emissivities?

(b) For each of the emissivities, calculate and plot the ceiling temperature as a function of the insulation thickness for $0.1 \leq t \leq 1$ m. Identify conditions for which condensation will occur on the ceiling.

13.94 Boiler tubes exposed to the products of coal combustion in a power plant are subject to fouling by the ash (mineral) content of the combustion gas. The ash forms a solid deposit on the tube outer surface, which reduces heat transfer to a pressurized water/steam mixture flowing through the tubes. Consider a thin-walled boiler tube ($D_t = 0.05$ m) whose surface is maintained at $T_t = 600$ K by the boiling process. Combustion gases flowing over the tube at $T_\infty = 1800$ K provide a convection coefficient of $\bar{h} = 100$ W/m$^2 \cdot$K, while radiation from the gas and boiler walls to the tube may be approximated as that originating from large surroundings at $T_{sur} = 1500$ K.



(a) If the tube surface is diffuse and gray, with $\varepsilon_t = 0.8$, and there is *no* ash deposit layer, what is the rate of heat transfer per unit length, q', to the boiler tube?

(b) If a deposit layer of diameter $D_d = 0.06$ m and thermal conductivity $k = 1$ W/m $\cdot$ K forms on the tube, what is the deposit surface temperature, T_d? The deposit is diffuse and gray, with $\varepsilon_d = 0.9$, and T_t, T_∞, $\bar{h}$, and T_{sur} remain unchanged. What is the net rate of heat transfer per unit length, q', to the boiler tube?

Patent Owner Manufacturing Resources International, Inc.
Exhibit 2017 - Page 873 of 999

(c) Explore the effect of variations in D_d and $\bar{h}$ on q', as well as on relative contributions of convection and radiation to the net heat transfer rate. Represent your results graphically.

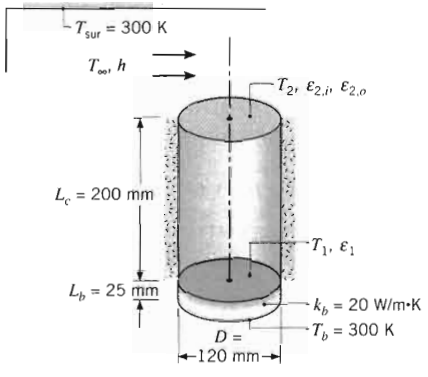
13.95 Consider two very large parallel plates. The bottom plate is warmer than the top plate, which is held at a constant temperature of $T_1 = 330$ K. The plates are separated by $L = 0.1$ m, and the gap between the two surfaces is filled with air at atmospheric pressure. The heat flux from the bottom plate is $q'' = 250$ W/m^2.

(a) Determine the temperature of the bottom plate and the ratio of the convective to radiative heat fluxes for $\varepsilon_1 = \varepsilon_2 = 0.5$. Evaluate air properties at $T = 350$ K.

(b) Repeat part (a) for $\varepsilon_1 = \varepsilon_2 = 0.25$ and 0.75.

13.96 Coated metallic disks are cured by placing them at the top of a cylindrical furnace whose bottom surface is electrically heated and whose sidewall may be approximated as a reradiating surface. Curing is accomplished by maintaining a disk at $T_2 = 400$ K for an extended period. The electrically heated surface is maintained at $T_1 = 800$ K and is mounted on a ceramic base material of thermal conductivity $k = 20$ W/m · K. The bottom of the base material, as well as the ambient air and large surroundings above the disk, are maintained at a temperature of 300 K. Emissivities of the heater and the disk inner and outer surfaces are $\varepsilon_1 = 0.9$, $\varepsilon_{2,i} = 0.5$, and $\varepsilon_{2,o} = 0.9$, respectively.

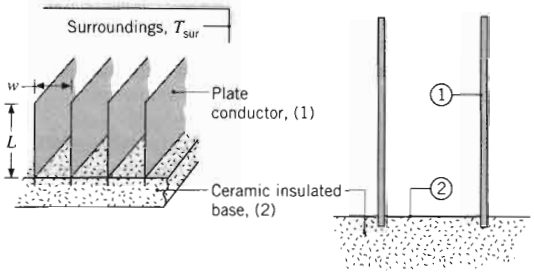
Assuming steady-state operation and neglecting convection within the cylindrical cavity, determine the electric power that must be supplied to the heater and the convection coefficient h that must be maintained at the outer surface of the disk in order to satisfy the prescribed conditions.



13.97 Electrical conductors, in the form of parallel plates of length $L = 40$ mm, have one edge mounted to a ceramic insulated base and are spaced a distance $w = 10$ mm apart. The plates are exposed to large isothermal surroundings at $T_{sur} = 300$ K. The conductor (1) and ceramic (2) surfaces are diffuse and gray with emissivities of $\varepsilon_1 = 0.8$ and $\varepsilon_2 = 0.6$, respectively. For a prescribed operating current in the conductors, their temperature is $T_1 = 500$ K.

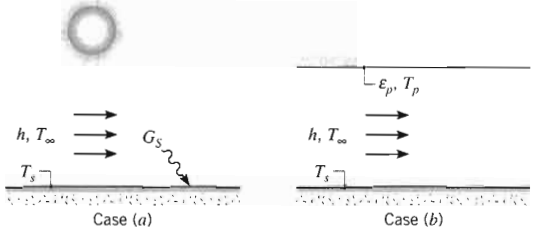
(a) Determine the electrical power dissipated in a conductor plate per unit length, q'_1, considering only radiation exchange. What is the temperature of the insulated base, T_2?

(b) Determine q'_1 and T_2 when the surfaces experience convection with an airstream at 300 K and a convection coefficient of $h = 25$ W/m^2 · K.



13.98 The spectral absorptivity of a *large* diffuse surface is $\alpha_\lambda = 0.9$ for $\lambda < 1$ μm and $\alpha_\lambda = 0.3$ for $\lambda \geq 1$ μm. The bottom of the surface is well insulated, while the top may be exposed to one of two different conditions.

(a) In case (*a*) the surface is exposed to the sun, which provides an irradiation of $G_S = 1200$ W/m^2, and to an airflow for which $T_\infty = 300$ K. If the surface temperature is $T_s = 320$ K, what is the convection coefficient associated with the airflow?



(b) In case (*b*) the surface is shielded from the sun by a large plate and an airflow is maintained between the plate and the surface. The plate is diffuse and gray with an emissivity of $\varepsilon_p = 0.8$. If $T_\infty = 300$ K and the convection coefficient is equivalent to the result obtained in part (a), what is the plate temperature T_p that is needed to maintain the surface at $T_s = 320$ K?

Patent Owner Manufacturing Resources International, Inc.
Exhibit 2017 - Page 874 of 999

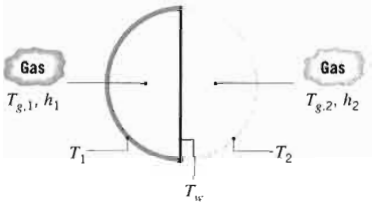
13.99 A long uniform rod of 50-mm diameter with a thermal conductivity of 15 W/m · K is heated internally by volumetric energy generation of 20 kW/m^3. The rod is positioned coaxially within a larger circular tube of 60-mm diameter whose surface is maintained at 500°C. The annular region between the rod and the tube is evacuated, and their surfaces are diffuse and gray with an emissivity of 0.2.

(a) Determine the center and surface temperatures of the rod.

(b) Determine the center and surface temperatures of the rod if atmospheric air occupies the annular space.

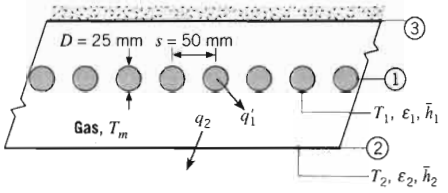
(c) For tube diameter of 60, 100, and 1000 mm and for both the evacuated and atmospheric conditions, compute and plot the center and surface temperatures as a function of equivalent surface emissivities in the range from 0.1 to 1.0.

13.100 The cross section of a long circular tube, which is divided into two semicylindrical ducts by a thin wall, is shown below.



Sides 1 and 2 are maintained at temperatures of T_1 = 600 K and T_2 = 400 K, respectively, while the mean temperatures of gas flows through ducts 1 and 2 are $T_{g,1}$ = 571 K and $T_{g,2}$ = 449 K, respectively. The foregoing temperatures are invariant in the axial direction. The gases provide surface convection coefficients of $h_1 = h_2 = 5$ W/m^2 · K, while all duct surfaces may be approximated as blackbodies ($\varepsilon_1 = \varepsilon_2 = \varepsilon_w = 1$). What is the duct wall temperature, T_w? By performing an energy balance on the gas in side 1, verify that $T_{g,1}$ is, in fact, equal to 571 K.

13.101 A row of regularly spaced, cylindrical heating elements (1) is used to cure a surface coating that is applied to a large panel (2) positioned below the elements. A second large panel (3), whose top surface is well insulated, is positioned above the elements. The elements are black and maintained at T_1 = 600 K, while the panel has an emissivity of $\varepsilon_2 = 0.5$ and is maintained at T_2 = 400 K. The cavity is filled with a nonparticipating gas and convection heat transfer occurs at surfaces 1 and 2, with $\bar{h}_1 = 10$ W/m^2 · K and $\bar{h}_2 = 2$ W/m^2 · K. (Convection at the insulated panel may be neglected.)



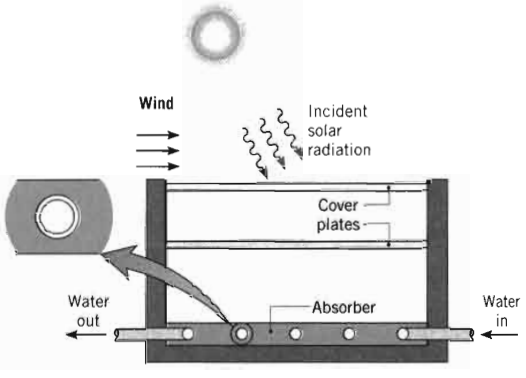
(a) Evaluate the mean gas temperature, T_m.

(b) What is the rate per unit axial length at which electrical energy must be supplied to each element to maintain its prescribed temperature?

(c) What is the rate of heat transfer to a portion of the coated panel that is 1 m wide by 1 m long?

13.102 In recent years there has been considerable interest in developing flat-plate solar collectors for home heating needs. The typical collector configuration consists of an absorbing surface that is thermally insulated on the edges and on the back side. Solar radiation is transmitted through one or more glass *cover plates* before reaching the absorber. The collected energy is removed by circulating water through tubes that are in good thermal contact with the absorber.

Identify all the energy exchange processes that influence the performance of the collector. Suggest design features that would increase collection efficiency.



13.103 Applying high-emissivity paints to radiating surfaces is a common technique used to enhance heat transfer by radiation.

(a) For large parallel plates, determine the radiation heat flux across the gap when the surfaces are at T_1 = 350 K, T_2 = 300 K, $\varepsilon_1 = \varepsilon_2 = \varepsilon_s = 0.85$.

Patent Owner Manufacturing Resources International, Inc.
Exhibit 2017 - Page 875 of 999

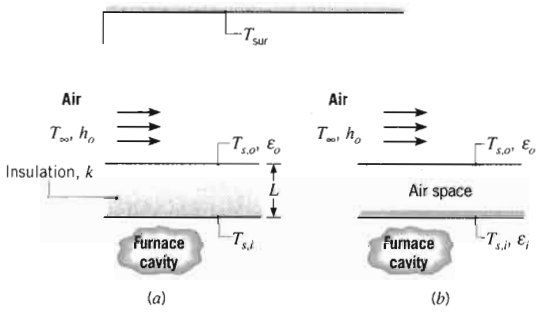
(b) Determine the radiation heat flux when a very thin layer of high-emissivity paint, $\varepsilon_p = 0.98$, is applied to both surfaces.

(c) Determine the radiation heat flux when the paint layers are each $L = 2$ mm thick and the thermal conductivity of the paint is $k = 0.21$ W/m · K.

(d) Plot the heat flux across the gap for the bare surface as a function of ε_s, with $0.05 \leq \varepsilon_s \leq 0.95$. Show on the same plot the heat flux for the painted surface with very thin paint layers and the painted surface with $L = 2$-mm thick paint layers.

Multimode Heat Transfer: Advanced

13.104 Options for thermally shielding the top ceiling of a large furnace include the use of an insulating material of thickness L and thermal conductivity k, case (*a*), or an air space of equivalent thickness formed by installing a steel sheet above the ceiling, case (*b*).

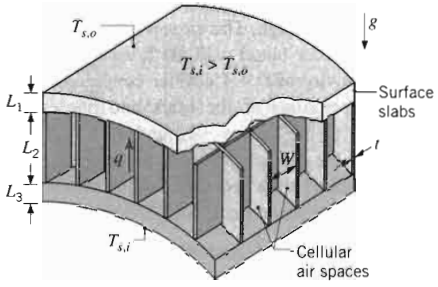


(a) Develop mathematical models that could be used to assess which of the two approaches is better. In both cases the interior surface is maintained at the same temperature, $T_{s,i}$, and the ambient air and surroundings are at equivalent temperatures ($T_\infty = T_{sur}$).

(b) If $k = 0.090$ W/m · K, $L = 25$ mm, $h_o = 25$ W/m^2 · K, the surfaces are diffuse and gray with $\varepsilon_i = \varepsilon_o = 0.50$, $T_{s,i} = 900$ K, and $T_\infty = T_{sur} = 300$ K, what is the outer surface temperature $T_{s,o}$ and the heat loss per unit surface area associated with each option?

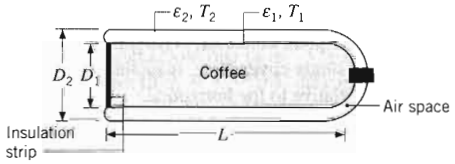
(c) For each case, assess the effect of surface radiative properties on the outer surface temperature and the heat loss per unit area for values of $\varepsilon_i = \varepsilon_o$ ranging from 0.1 to 0.9. Plot your results.

13.105 The composite insulation shown, which was described in Chapter 1 (Problem 1.72e), is being considered as a ceiling material.



It is proposed that the outer and inner slabs be made from low-density particle board of thicknesses $L_1 = L_3 = 12.5$ mm and that the honeycomb core be constructed from a high-density particle board. The square cells of the core are to have length $L_2 = 50$ mm, width $W = 10$ mm, and wall thickness $t = 2$ mm. The emissivity of both particle boards is approximately 0.85, and the honeycomb cells are filled with air at 1-atm pressure. To assess the effectiveness of the insulation, its total thermal resistance must be evaluated under representative operating conditions for which the bottom (inner) surface temperature is $T_{s,i} = 25$°C and the top (outer) surface temperature is $T_{s,o} = -10$°C. To assess the effect of free convection in the air space, assume a cell temperature difference of 20°C and evaluate air properties at 7.5°C. To assess the effect of radiation across the air space, assume inner surface temperatures of the outer and inner slabs to be −5 and 15°C, respectively.

13.106 Hot coffee is contained in a cylindrical thermos bottle that is of length $L = 0.3$ m and is lying on its side (horizontally).



The coffee container consists of a glass flask of diameter $D_1 = 0.07$ m, separated from an aluminum housing of diameter $D_2 = 0.08$ m by air at atmospheric pressure. The outer surface of the flask and the inner surface of the housing are silver coated to provide emissivities of $\varepsilon_1 = \varepsilon_2 = 0.25$. If these surface temperatures are $T_1 = 75$°C and $T_2 = 35$°C, what is the heat loss from the coffee?

Patent Owner Manufacturing Resources International, Inc.
Exhibit 2017 - Page 876 of 999

13.107 A vertical air space in the wall of a home is 0.1 m thick and 3 m high. The air separates a brick exterior from a plaster board wall, with each surface having an emissivity of 0.9. Consider conditions for which the temperatures of the brick and plaster surfaces exposed to the air are −10 and 18°C, respectively. What is the rate of heat loss per unit surface area? What would be the heat loss per unit area if the space were filled with urethane foam?

13.108 Consider a vertical, double-pane window for the conditions prescribed in Problem 9.96. That is, vertical panes at temperatures of $T_1 = 22°$ and $T_2 = -20°C$ are separated by atmospheric air, and the critical Rayleigh number for the onset of convection is $Ra_{L,c} = 2000$.

(a) What is the conduction heat flux across the air gap for the optimal spacing L_{op} between the panes?

(b) If the glass has an emissivity of $\varepsilon_g = 0.90$, what is the total heat flux across the gap?

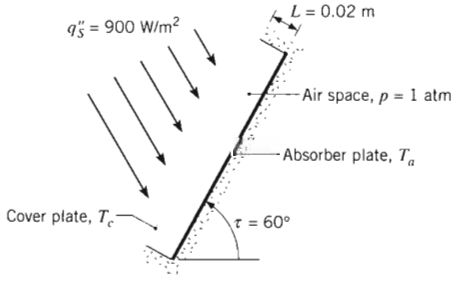
(c) What is the total heat flux if a special, low-emissivity coating ($\varepsilon_c = 0.10$) is applied to one of the panes at its air–glass interface? What is the total heat flux if both panes are coated?

13.109 Consider the double-pane window of Problem 9.97, for which 1 m × 1 m panes are separated by a 25-mm gap of atmospheric air. The window panes are approximately isothermal and separate quiescent room air at $T_{\infty,i} = 20°C$ from quiescent ambient air at $T_{\infty,o} = -20°C$.

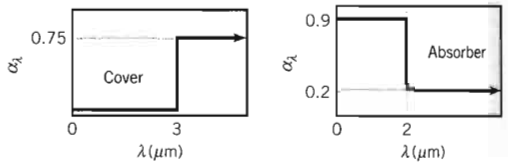
(a) For glass panes of emissivity $\varepsilon_g = 0.90$, determine the temperature of each pane and the rate of heat transfer through the window.

(b) Quantify the improvements in energy conservation that may be effected if the space between the panes is evacuated and/or a low emissivity coating ($\varepsilon_c = 0.1$) is applied to the surface of each pane adjoining the gap.

13.110 A flat-plate solar collector, consisting of an absorber plate and single cover plate, is inclined at an angle of $\tau = 60°$ relative to the horizontal.



Consider conditions for which the incident solar radiation is collimated at an angle of 60° relative to the horizontal and the solar flux is 900 W/m². The cover plate is perfectly transparent to solar radiation ($\lambda \leq 3\ \mu m$) and is opaque to radiation of larger wavelengths. The cover and absorber plates are diffuse surfaces having the spectral absorptivities shown.



The length and width of the absorber and cover plates are much larger than the plate spacing L. What is the rate at which solar radiation is absorbed per unit area of the absorber plate? With the absorber plate well insulated from below and absorber and cover plate temperatures T_a and T_c of 70 and 27°C, respectively, what is the heat loss per unit area of the absorber plate?

13.111 Consider the tube and radiation shield of Problem 13.49, but now account for free convection in the gap between the tube and the shield.

(a) What is the total rate of heat transfer per unit length between the tube and the shield?

(b) Explore the effect of variations in the shield diameter on the total heat rate, as well as on the contributions due to convection and radiation.

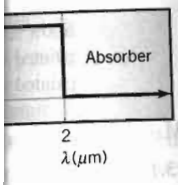
13.112 Consider the tube and radiation shield of Problem 13.49, but now account for free convection in the gap between the tube and the shield, as well as for the fact that the temperature of the shield may not be arbitrarily prescribed but, in fact, depends on the nature of the surroundings. If the radiation shield is exposed to quiescent ambient air and large surroundings, each at a temperature of 20°C, what is the temperature of the shield? What is the rate of heat loss from the tube per unit length?

13.113 Consider the flat-plate solar collector of Problem 9.100. The absorber plate has a coating for which $\varepsilon_1 = 0.96$, and the cover plate has an emissivity of $\varepsilon_2 = 0.92$. With respect to radiation exchange, both plates may be approximated as diffuse, gray surfaces.

(a) For the conditions of Problem 9.100, what is the rate of heat transfer by free convection from the absorber plate and the net rate of radiation exchange between the plates?

Patent Owner Manufacturing Resources International, Inc.
Exhibit 2017 - Page 877 of 999

the incident solar
e of 60° relative to
is 900 W/m². The
nt to solar radiation
radiation of larger
orber plates are dif-
bsorptivities shown.



absorber and cover
plate spacing L. What
tion is absorbed per
? With the absorber
w and absorber and
d T_c of 70 and 27°C,
ss per unit area of the

n shield of Problem
convection in the gap

heat transfer per unit
d the shield?

riations in the shield
rate, as well as on the
ction and radiation.

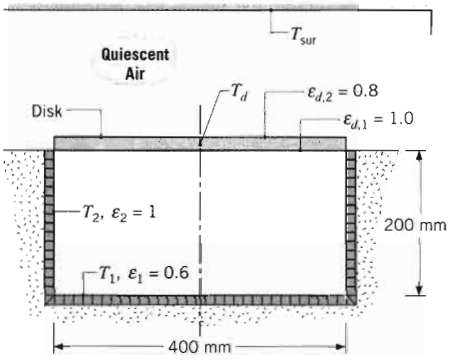
ion shield of Problem
e convection in the gap
, as well as for the fact
ld may not be arbitrar-
nds on the nature of the
hield is exposed to qui-
surroundings, each at a
the temperature of the
t loss from the tube per

llector of Problem 9.100.
ng for which $\varepsilon_1 = 0.96$,
missivity of $\varepsilon_2 = 0.92$.
change, both plates may
ray surfaces.

oblem 9.100, what is the
free convection from the
e net rate of radiation
lates?

(b) The temperature of the absorber plate varies according to the flow rate of the working fluid routed through the coiled tube. With all other parameters remaining as prescribed, compute and plot the free convection and radiant heat rates as a function of the absorber plate temperature for $50 \leq T_1 \leq 100$°C.

13.114 The lower side of a 400-mm-diameter disk is heated by an electric furnace, while the upper side is exposed to quiescent, ambient air and surroundings at 300 K. The radiant furnace (negligible convection) is of circular construction with the bottom surface ($\varepsilon_1 = 0.6$) and cylindrical side surface ($\varepsilon_2 = 1.0$) maintained at $T_1 = T_2 = 500$ K. The surface of the disk facing the radiant furnace is black ($\varepsilon_{d,1} = 1.0$), while the upper surface has an emissivity of $\varepsilon_{d,2} = 0.8$. Assume the plate and furnace surfaces to be diffuse and gray.



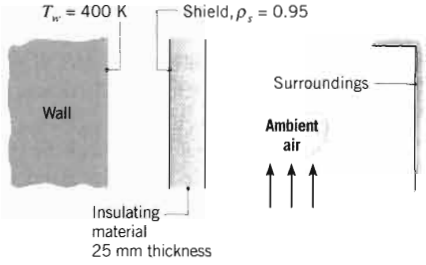
(a) Determine the net heat transfer rate to the disk, $q_{net,d}$, when $T_d = 400$ K.

(b) Plot $q_{net,d}$ as a function of the disk temperature for $300 \leq T_d \leq 500$ K, with all other conditions remaining the same. What is the steady-state temperature of the disk?

13.115 The surface of a radiation shield facing a black hot wall at 400 K has a reflectivity of 0.95. Attached to the back side of the shield is a 25-mm-thick sheet of insulating material having a thermal conductivity of 0.016 W/m · K. The overall heat transfer coefficient (convection and radiation) at the surface exposed to the ambient air and surroundings at 300 K is 10 W/m² · K.

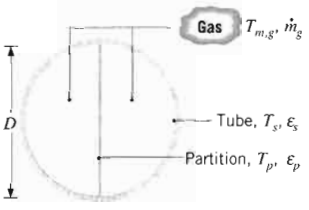
(a) Assuming negligible convection in the region between the wall and the shield, estimate the heat loss per unit area from the hot wall.

(b) Perform a parameter sensitivity analysis on the insulation system, considering the effects of



shield reflectivity, ρ_s, and insulation thermal conductivity, k. What influence do these parameters have on the heat loss from the hot wall? What is the effect of an increased overall coefficient on the heat loss? Show the results of your analysis in a graphical format.

13.116 The fire tube of a hot water heater consists of a long circular duct of diameter $D = 0.07$ m and temperature $T_s = 385$ K, through which combustion gases flow at a temperature of $T_{m,g} = 900$ K. To enhance heat transfer from the gas to the tube, a thin partition is inserted along the midplane of the tube. The gases may be assumed to have the thermophysical properties of air and to be radiatively nonparticipating.



(a) With no partition and a gas flow rate of $\dot{m}_g = 0.05$ kg/s, what is the rate of heat transfer per unit length, q', to the tube?

(b) For a gas flow rate of $\dot{m}_g = 0.05$ kg/s and emissivities of $\varepsilon_s = \varepsilon_p = 0.5$, determine the partition temperature T_p and the total rate of heat transfer q' to the tube.

(c) For $\dot{m}_g = 0.02$, 0.05, and 0.08 kg/s and equivalent emissivities $\varepsilon_p = \varepsilon_s \equiv \varepsilon$, compute and plot T_p and q' as a function of ε for $0.1 \leq \varepsilon \leq 1.0$. For $\dot{m}_g = 0.05$ kg/s and equivalent emissivities, plot the convective and radiative contributions to q' as a function of ε.

13.117 Consider Problem 9.95 with $N = 4$ sheets of thin aluminum foil ($\varepsilon_f = 0.07$), equally spaced throughout the 50-mm gap so as to form five individual air gaps

Patent Owner Manufacturing Resources International, Inc.
Exhibit 2017 - Page 878 of 999

each 10 mm thick. The hot and cold surfaces of the enclosure are characterized by $\varepsilon = 0.85$.

(a) Neglecting conduction or convection in the air, determine the heat flux through the system.

(b) Accounting for conduction but neglecting radiation, determine the heat flux through the system. The effect of variable properties is important. Calculate the air properties for each gap independently, based on the average gap temperature.

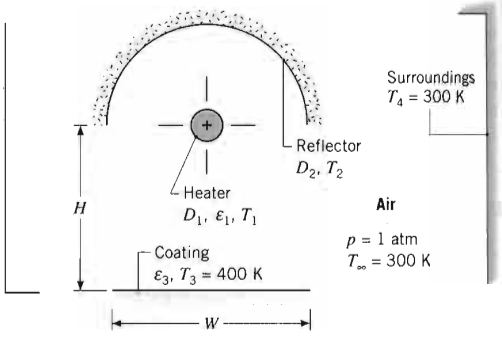
(c) Accounting for both conduction and radiation, determine the heat flux through the system. Calculate the air properties for each gap independently.

(d) Is natural convection negligible in part (c)? Explain why or why not.

13.118 Consider the conditions of Problem 9.105. Accounting for radiation, as well as convection, across the helium-filled cavity, determine the mass rate at which gaseous nitrogen is vented from the system. The cavity surfaces are diffuse and gray with emissivities of $\varepsilon_i = \varepsilon_o = 0.3$. If the cavity is evacuated, how may surface conditions be altered to further reduce the evaporation? Support your recommendation with appropriate calculations.

13.119 A special surface coating on a square panel that is 5 m by 5 m on a side is cured by placing the panel directly under a radiant heat source having the same dimensions. The heat source is diffuse and gray and operates with a power input of 75 kW. The top surface of the heater, as well as the bottom surface of the panel, may be assumed to be well insulated, and the arrangement exists in a large room with air and wall temperatures of 25°C. The surface coating is diffuse and gray, with an emissivity of 0.30 and an upper temperature limit of 400 K. Neglecting convection effects, what is the minimum spacing that may be maintained between the heater and the panel to ensure that the panel temperature will not exceed 400 K? Allowing for convection effects at the coated surface of the panel, what is the minimum spacing?

13.120 A long rod heater of diameter $D_1 = 10$ mm and emissivity $\varepsilon_1 = 1.0$ is coaxial with a well-insulated, semicylindrical reflector of diameter $D_2 = 1$ m. A long panel of width $W = 1$ m is aligned with the reflector and is separated from the heater by a distance of $H = 1$ m. The panel is coated with a special paint ($\varepsilon_3 = 0.7$), which is cured by maintaining it at 400 K. The panel is well insulated on its back side, and the entire system is located in a large room where the walls and the atmospheric, quiescent air are at 300 K. Heat transfer by convection may be neglected for the reflector surface.

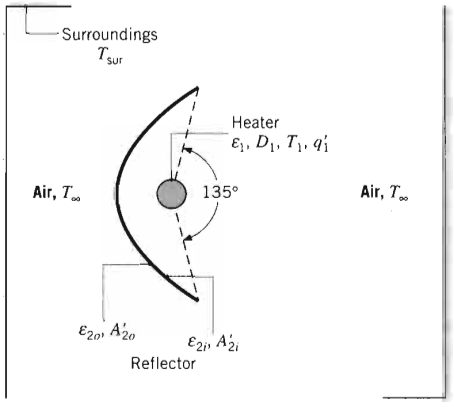


(a) Sketch the equivalent thermal circuit for the system and label all pertinent resistances and potentials.

(b) Expressing your results in terms of appropriate variables, write the system of equations needed to determine the heater and reflector temperatures, T_1 and T_2, respectively. Determine these temperatures for the prescribed conditions.

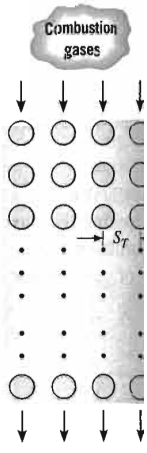
(c) Determine the rate at which electrical power must be supplied per unit length of the rod heater.

13.121 A radiant heater, which is used for surface treatment processes, consists of a long cylindrical heating element of diameter $D_1 = 0.005$ m and emissivity $\varepsilon_1 = 0.80$. The heater is partially enveloped by a long, thin parabolic reflector whose inner and outer surface emissivities are $\varepsilon_{2i} = 0.10$ and $\varepsilon_{2o} = 0.80$, respectively. Inner and outer surface areas per unit length of the reflector are each $A'_{2i} = A'_{2o} = 0.20$ m, and the average convection coefficient for the combined inner and outer surfaces is $\bar{h}_{2(i,o)} = 2$ W/m$^2 \cdot$ K. The system may be assumed to be in an infinite, quiescent



medium
exposed
(a) Sket
expr
(b) If,
pow
W/r
120
ener
(c) Wh
tran
(d) Wh

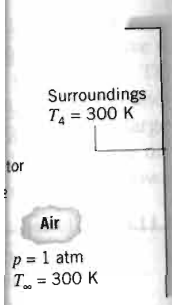
13.122 A steam
tubes, ea
$L = 1$ m
each S_L
tudinal a
Saturate
of 2.5 ba
it leaves
occurs i
temperat



(a)

(a) Con
tion
ature
resp
conv
ture,
Prop
thos
ture

Patent Owner Manufacturing Resources International, Inc.
Exhibit 2017 - Page 879 of 999



medium of atmospheric air at $T_\infty = 300$ K and to be exposed to large surroundings at $T_{sur} = 300$ K.

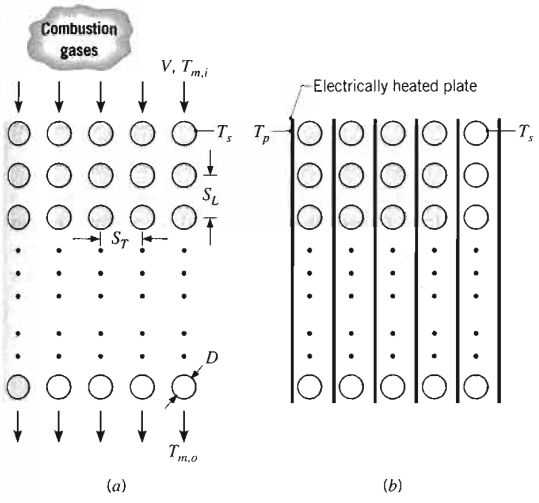
(a) Sketch the appropriate radiation circuit, and write expressions for each of the network resistances.

(b) If, under steady-state conditions, electrical power is dissipated in the heater at $P_1' = 1500$ W/m and the heater surface temperature is $T_1 = 1200$ K, what is the *net* rate at which *radiant* energy is transferred from the heater?

(c) What is the net rate at which radiant energy is transferred from the heater to the surroundings?

(d) What is the temperature, T_2, of the reflector?

13.122 A steam generator consists of an in-line array of tubes, each of outer diameter $D = 10$ mm and length $L = 1$ m. The longitudinal and transverse pitches are each $S_L = S_T = 20$ mm, while the numbers of longitudinal and transverse rows are $N_L = 20$ and $N_T = 5$. Saturated water (liquid) enters the tubes at a pressure of 2.5 bars, and its flow rate is adjusted to ensure that it leaves the tubes as saturated vapor. Boiling that occurs in the tubes maintains a uniform tube wall temperature of 400 K.

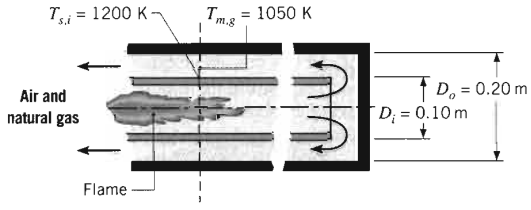


(a) Consider case (*a*) for which products of combustion *enter* the tube bank with velocity and temperature of $V = 10$ m/s and $T_{m,i} = 1200$ K, respectively. Determine the average gas-side convection coefficient, the gas outlet temperature, and the rate of steam production in kg/s. Properties of the gas may be approximated to be those of atmospheric air at an average temperature of 900 K.

(b) An alternative steam generator design, case (*b*), consists of the same tube arrangement, but the gas flow is replaced by an evacuated space with electrically heated plates inserted between each line of tubes. If the plates are maintained at a uniform temperature of $T_p = 1200$ K, what is the rate of steam production? The plate and tube surfaces may be approximated as blackbodies.

(c) Consider conditions for which the plates are installed, as in case (*b*), and the high-temperature products of combustion flow over the tubes, as in case (*a*). The plates are no longer electrically heated, but their thermal conductivity is sufficiently large to ensure a uniform plate temperature. Comment on factors that influence the plate temperature and the gas temperature distribution. Contrast (qualitatively) the gas outlet temperature and the steam generation rate with the results of case (*a*).

13.123 The sketch shows a gas-fired radiant tube of the single-ended recuperative (SER) type. A mixture of air and natural gas is injected at the left end of the central tube, and combustion is essentially complete while the gases are still in the inner tube. The products of combustion are exhausted through the annulus. Thermocouple measurements at a particular axial location indicate an inner tube wall temperature of 1200 K and a gas temperature of 1050 K in the annulus. The radiant tube is located in a furnace, the walls of which are 950 K, and the furnace atmosphere is quiescent and also at 950 K. The thin-walled tubes are made of silicon carbide with an emissivity of 0.6. The gas mass flow rate is 0.13 kg/s, and the gas pressure is 101.5 kPa.

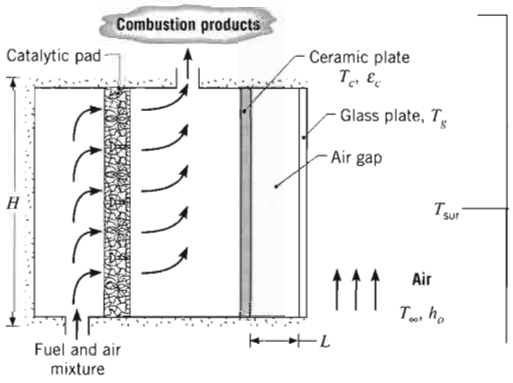


Calculate the temperature of the outer tube at the axial location where thermocouple measurements are being made. Assume the gas to be radiatively nonparticipating and to have the following thermophysical properties: $\rho = 0.32$ kg/m^3, $\nu = 130 \times 10^{-6}$ m^2/s, $k = 70 \times 10^{-3}$ W/m · K, and $Pr = 0.72$.

13.124 A wall-mounted natural gas heater uses combustion on a porous catalytic pad to maintain a ceramic plate of emissivity $\varepsilon_c = 0.95$ at a uniform temperature of $T_c = 1000$ K. The ceramic plate is separated from a

Patent Owner Manufacturing Resources International, Inc.
Exhibit 2017 - Page 880 of 999

glass plate by an air gap of thickness $L = 50$ mm. The surface of the glass is diffuse, and its spectral transmissivity and absorptivity may be approximated as $\tau_\lambda = 0$ and $\alpha_\lambda = 1$ for $0 \leq \lambda \leq 0.4$ μm, $\tau_\lambda = 1$ and $\alpha_\lambda = 0$ for $0.4 < \lambda \leq 1.6$ μm, and $\tau_\lambda = 0$ and $\alpha_\lambda = 0.9$ for $\lambda > 1.6$ μm. The exterior surface of the glass is exposed to quiescent ambient air and large surroundings for which $T_\infty = T_{sur} = 300$ K. The height and width of the heater are $H = W = 2$ m.



(a) What is the total transmissivity of the glass to irradiation from the ceramic plate? Can the glass be approximated as opaque and gray?

(b) For the prescribed conditions, evaluate the glass temperature, T_g, and the rate of heat transfer from the heater, q_h.

(c) A fan may be used to control the convection coefficient h_o at the exterior surface of the glass. Compute and plot T_g and q_h as a function of h_o for $10 \leq h_o \leq 100$ W/m$^2 \cdot$ K.

Gaseous Radiation

13.125 A furnace having a spherical cavity of 0.5-m diameter contains a gas mixture at 1 atm and 1400 K. The mixture consists of CO_2 with a partial pressure of 0.25 atm and nitrogen with a partial pressure of 0.75 atm. If the cavity wall is black, what is the cooling rate needed to maintain its temperature at 500 K?

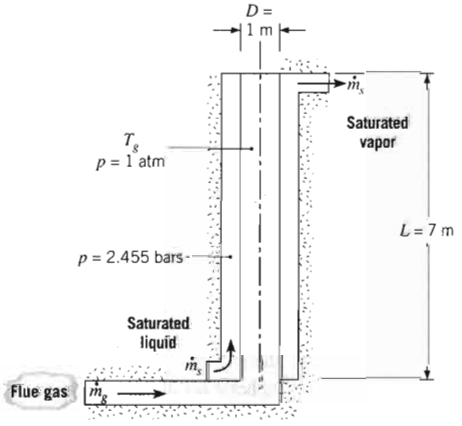
13.126 A gas turbine combustion chamber may be approximated as a long tube of 0.4-m diameter. The combustion gas is at a pressure and temperature of 1 atm and 1000°C, respectively, while the chamber surface temperature is 500°C. If the combustion gas contains CO_2 and water vapor, each with a mole fraction of 0.15, what is the net radiative heat flux between the gas and the chamber surface, which may be approximated as a blackbody?

13.127 A flue gas at 1-atm total pressure and a temperature of 1400 K contains CO_2 and water vapor at partial pressures of 0.05 and 0.10 atm, respectively. If the gas flows through a long flue of 1-m diameter and 400 K surface temperature, determine the net radiative heat flux from the gas to the surface. Blackbody behavior may be assumed for the surface.

13.128 A furnace consists of two large parallel plates separated by 0.75 m. A gas mixture comprised of O_2, N_2, CO_2, and water vapor, with mole fractions of 0.20, 0.50, 0.15, and 0.15, respectively, flows between the plates at a total pressure of 2 atm and a temperature of 1300 K. If the plates may be approximated as blackbodies and are maintained at 500 K, what is the net radiative heat flux to the plates?

13.129 In an industrial process, products of combustion at a temperature and pressure of 2000 K and 1 atm, respectively, flow through a long, 0.25-m-diameter pipe whose inner surface is black. The combustion gas contains CO_2 and water vapor, each at a partial pressure of 0.10 atm. The gas may be assumed to have the thermophysical properties of atmospheric air and to be in fully developed flow with $\dot{m} = 0.25$ kg/s. The pipe is cooled by passing water in cross flow over its outer surface. The upstream velocity and temperature of the water are 0.30 m/s and 300 K, respectively. Determine the pipe wall temperature and heat flux. *Hint:* Emission from the pipe wall may be neglected.

13.130 Waste heat recovery from the exhaust (flue) gas of a melting furnace is accomplished by passing the gas through a vertical metallic tube and introducing saturated water (liquid) at the bottom of an annular region around the tube.

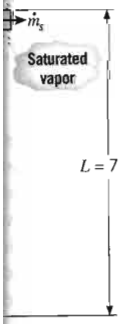


and a temperature
er vapor at partial
respectively. If the
1-m diameter and
nine the net radia-
surface. Blackbody
urface.

arallel plates sepa-
mprised of O_2, N_2,
fractions of 0.20,
flows between the
and a temperature
e approximated as
500 K, what is the
?

of combustion at a
00 K and 1 atm,
g, 0.25-m-diameter
k. The combustion
r, each at a partial
nay be assumed to
ies of atmospheric
low with $\dot{m} = 0.25$
sing water in cross
upstream velocity
0.30 m/s and 300 K,
e wall temperature
n the pipe wall may

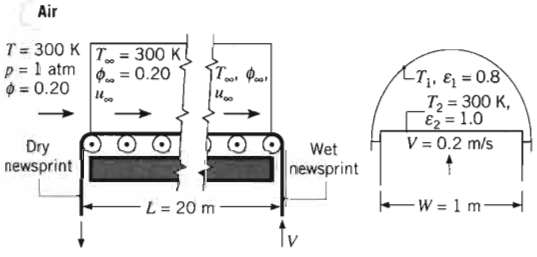
haust (flue) gas of a
by passing the gas
nd introducing satu-
tom of an annular



The tube length and inside diameter are 7 and 1 m, respectively, and the tube inner surface is black. The gas in the tube is at atmospheric pressure, with CO_2 and $H_2O(v)$ partial pressures of 0.1 and 0.2 atm, respectively, and its mean temperature may be approximated as $T_g = 1400$ K. The gas flow rate is $\dot{m}_g = 2$ kg/s. If saturated water is introduced at a pressure of 2.455 bars, estimate the water flow rate $\dot{m}_s$ for which there is complete conversion from saturated liquid at the inlet to saturated vapor at the outlet. Thermophysical properties of the gas may be approximated as $\mu = 530 \times 10^{-7}$ kg/s · m, $k = 0.091$ W/m · K, and $Pr = 0.70$.

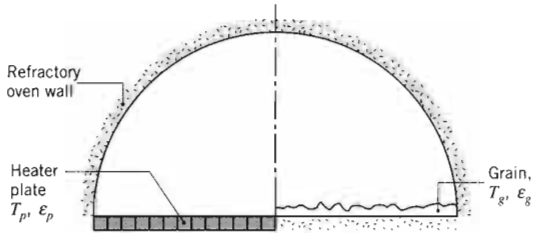
Heat and Mass Transfer

13.131 A radiant oven for drying newsprint consists of a long duct ($L = 20$ m) of semicircular cross section. The newsprint moves through the oven on a conveyor belt at a velocity of $V = 0.2$ m/s. The newsprint has a water content of 0.02 kg/m^2 as it enters the oven and is completely dry as it exits. To assure quality, the newsprint must be maintained at room temperature (300 K) during drying. To aid in maintaining this condition, all system components and the air flowing through the oven have a temperature of 300 K. The inner surface of the semicircular duct, which is of emissivity 0.8 and temperature T_1, provides the radiant heat required to accomplish the drying. The wet surface of the newsprint can be considered to be black. Air entering the oven has a temperature of 300 K and a relative humidity of 20%.



Since the velocity of the air is large, its temperature and relative humidity can be assumed to be constant over the entire duct length. Calculate the required evaporation rate, air velocity u_∞, and temperature T_1 that will ensure steady-state conditions for the process.

13.132 A grain dryer consists of a long semicircular duct of radius $R = 1$ m. One-half of the base surface consists of an electrically heated plate of emissivity $\varepsilon_p = 0.8$, while the other half supports the grain to be dried, which has an emissivity of $\varepsilon_g = 0.9$. In a batch drying process for which the temperature of the grain is $T_g = 330$ K, 2.50 kg of water are to be removed per meter of duct length over a 1-hour period.

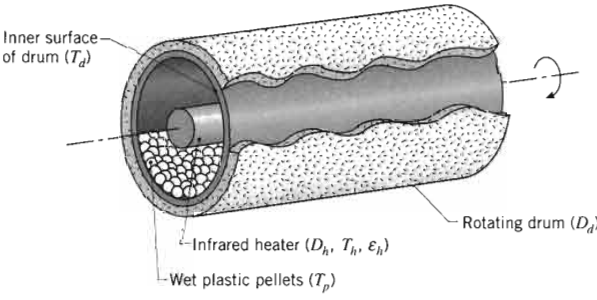


(a) Neglecting convection heat transfer, determine the required temperature T_p of the heater plate.

(b) If the water vapor is swept from the duct by the flow of dry air, what convection mass transfer coefficient h_m must be maintained by the flow?

(c) If the air is at 300 K, is the assumption of negligible convection justified?

13.133 A novel *infrared recycler* has been proposed for reclaiming the millions of kilograms of waste plastics produced by the dismantling and shredding of automotive vehicles following their retirement. To address the problem of sorting mixed plastics into components such as polypropylene and polycarbonate, a washed stream of the mixed plastics is routed to an infrared heating system, where it is dried and subsequently heated to a temperature for which one of the components begins to soften, while the others remain rigid. The mixed stream is then routed through steel rollers, to which the softened plastic sticks and is removed from the stream. Heating of the stream is then continued to facilitate removal of a second component, and the heating/removal process is repeated until all of the components are separated.



Consider the initial drying stage for a system comprised of a cylindrical heater aligned coaxially with a rotating drum of diameter $D_d = 1$ m. Shortly after

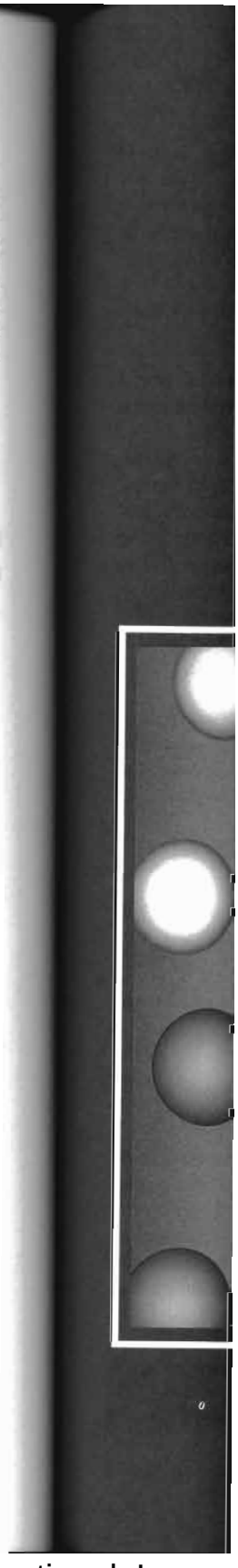
Patent Owner Manufacturing Resources International, Inc.
Exhibit 2017 - Page 882 of 999

entering the drum, wet plastic pellets may be assumed to fully cover the bottom semicylindrical section and to remain at a temperature of $T_p = 325$ K during the drying process. The surface area of the pellets may be assumed to correspond to that of the semicylinder and to have an emissivity of $\varepsilon_p = 0.95$.

(a) If the flow of dry air through the drum maintains a convection mass transfer coefficient of 0.024 m/s on the surface of the pellets, what is the evaporation rate per unit length of the drum?

(b) Neglecting convection heat transfer, determine the temperature T_h that must be maintained by a heater of diameter $D_h = 0.10$ m and emissivity $\varepsilon_h = 0.8$ to sustain the foregoing evaporation rate. What is the corresponding value of the temperature T_d for the top surface of the drum? The outer surface of the drum is well insulated, and its length-to-diameter ratio is large. As applied to the top *(d)* or bottom *(p)* surface of the drum, the view factor of an infinitely long semicylinder to itself, in the presence of a concentric, coaxial cylinder, may be expressed as

$$F_{ii} = 1 - \frac{2}{\pi}\left\{\left[1 - (D_h/D_d)^2\right]^{1/2} + (D_h/D_d)\sin^{-1}(D_h/D_d)\right\}$$



Patent Owner Manufacturing Resources International, Inc.
Exhibit 2017 - Page 883 of 999

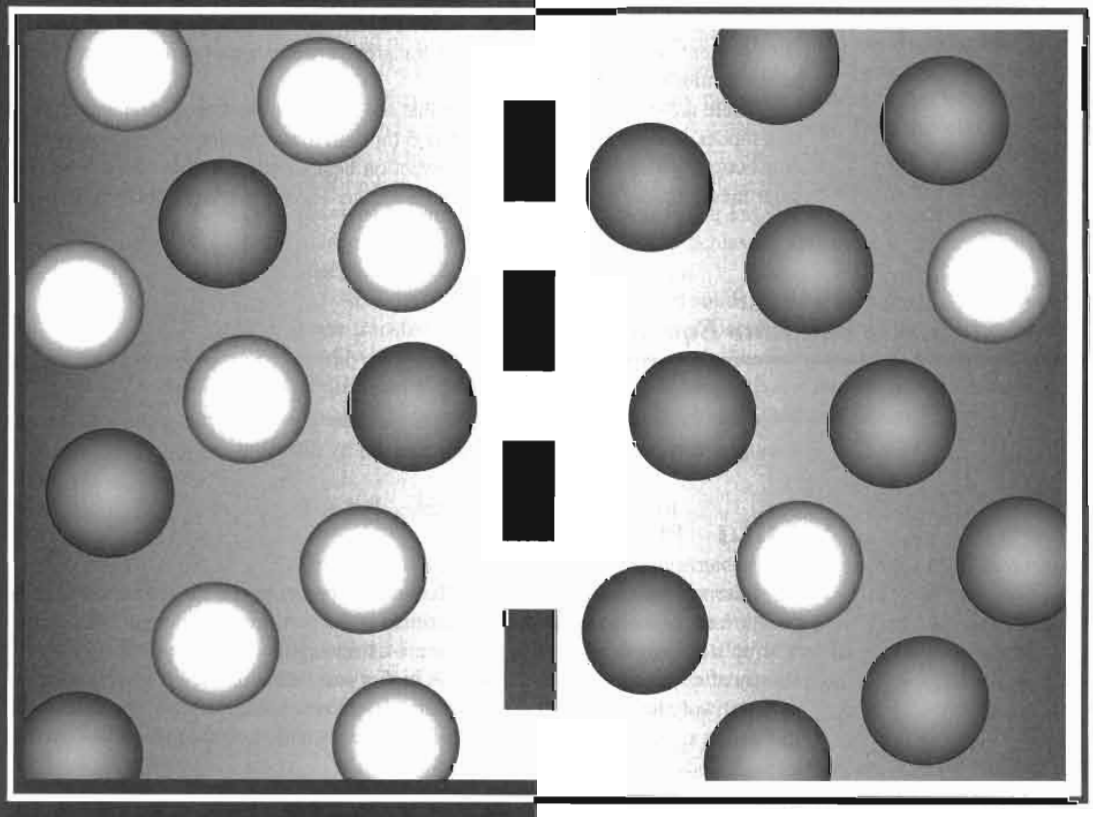
going evaporation
g value of the tem-
e of the drum? The
well insulated, and
large. As applied to
ace of the drum, the
ong semicylinder to
concentric, coaxial

$/D_d)^2]^{1/2}$

$^{-1}(D_h/D_d)\}$

CHAPTER 14

Diffusion Mass Transfer



Patent Owner Manufacturing Resources International, Inc.
Exhibit 2017 - Page 884 of 999

We have learned that heat is transferred if there is a temperature difference in a medium. Similarly, if there is a difference in the concentration of some chemical species in a mixture, mass transfer *must* occur.[1]

Mass transfer is mass in transit as the result of a species concentration difference in a mixture.

Just as a *temperature gradient* constitutes the *driving potential* for heat transfer, a species *concentration gradient* in a mixture provides the *driving potential* for transport of that species.

It is important to clearly understand the context in which the term *mass transfer* is used. Although mass is certainly transferred whenever there is bulk fluid motion, this is not what we have in mind. For example, we do *not* use the term *mass transfer* to describe the motion of air that is induced by a fan or the motion of water being forced through a pipe. In both cases, there is gross or bulk fluid motion due to mechanical work. We do, however, use the term to describe the relative motion of species in a mixture due to the presence of concentration gradients. One example is the dispersion of oxides of sulfur released from a power plant smoke stack into the environment. Another example is the transfer of water vapor into dry air, as in a home humidifier.

There are *modes* of *mass transfer* that are similar to the conduction and convection modes of heat transfer. In Chapters 6 through 8 we considered mass transfer by convection, which is *analogous* to convection heat transfer; in this chapter we consider mass transfer by diffusion, which can be *analogous* to conduction heat transfer.

14.1 *Physical Origins and Rate Equations*

From the standpoint of physical origins and the governing rate equations, strong analogies exist between heat and mass transfer by diffusion.

14.1.1 Physical Origins

Consider a chamber in which two different gas species at the same temperature and pressure are initially separated by a partition. If the partition is removed, both species will be transported by diffusion. Figure 14.1 shows the situation as it might exist shortly after removal of the partition. A higher concentration means more molecules per unit volume, and the concentration of species A (light dots) decreases with increasing x, while the concentration of B increases with x. Since mass diffusion is in

[1] A *species* is an identifiable molecule, such as carbon dioxide, CO_2, that can be transported by diffusion and advection and/or converted to some other form by a chemical reaction. A species may be a single atom or a complex polyatomic molecule. It can also be appropriate to identify a mixture (such as air) as a species.

Patent Owner Manufacturing Resources International, Inc.
Exhibit 2017 - Page 885 of 999

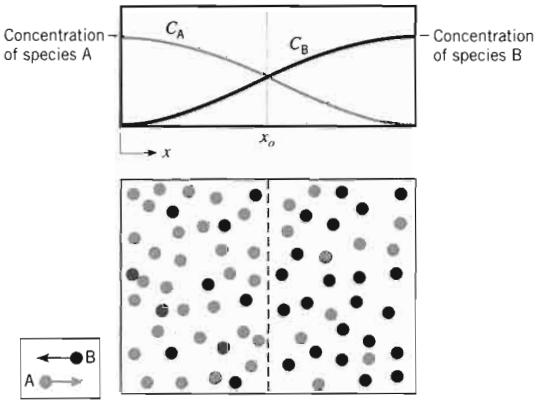


FIGURE 14.1 Mass transfer by diffusion in a binary gas mixture.

the direction of decreasing concentration, there is net transport of species A to the right and of species B to the left. The physical mechanism may be explained by considering the imaginary plane shown as a dashed line at x_o. Since molecular motion is random, there is equal probability of any molecule moving to the left or the right. Accordingly, more molecules of species A cross the plane from the left (since this is the side of higher A concentration) than from the right. Similarly, the concentration of B molecules is higher to the right of the plane than to the left, and random motion provides for *net* transfer of species B to the left. Of course, after a sufficient time, uniform concentrations of A and B are achieved, and there is no *net* transport of species A or B across the imaginary plane.

Mass diffusion occurs in liquids and solids, as well as in gases. However, since mass transfer is strongly influenced by molecular spacing, diffusion occurs more readily in gases than in liquids and more readily in liquids than in solids. Examples of diffusion in gases, liquids, and solids, respectively, include nitrous oxide from an automobile exhaust in air, dissolved oxygen in water, and helium in Pyrex.

14.1.2 Mixture Composition

Throughout this chapter we will be concerned with the transfer of mass in mixtures. We first review various concepts from thermodynamics. A mixture consists of two or more chemical constituents (*species*), and the amount of any species i may be quantified in terms of its *mass density* ρ_i (kg/m^3) or its *molar concentration* C_i (kmol/m^3). The mass density and molar concentration are related through the species molecular weight, $\mathcal{M}_i$ (kg/kmol), such that

$$\rho_i = \mathcal{M}_i C_i \tag{14.1}$$

With ρ_i representing the mass of species i per unit volume of the mixture, the mixture mass density is

$$\rho = \sum_i \rho_i \tag{14.2}$$

Patent Owner Manufacturing Resources International, Inc.
Exhibit 2017 - Page 886 of 999

Similarly, the total number of moles per unit volume of the mixture is

$$C = \sum_i C_i \tag{14.3}$$

The amount of species i in a mixture may also be quantified in terms of its *mass fraction*

$$m_i = \frac{\rho_i}{\rho} \tag{14.4}$$

or its *mole fraction*

$$x_i = \frac{C_i}{C} \tag{14.5}$$[2]

From Equations 14.2 and 14.3, it follows that

$$\sum_i m_i = 1 \tag{14.6}$$

and

$$\sum_i x_i = 1 \tag{14.7}$$

For a mixture of ideal gases, the mass density and molar concentration of any constituent are related to the partial pressure of the constituent through the ideal gas law. That is,

$$\rho_i = \frac{p_i}{R_i T} \tag{14.8}$$

and

$$C_i = \frac{p_i}{\mathcal{R} T} \tag{14.9}$$

where R_i is the gas constant for species i and $\mathcal{R}$ is the universal gas constant. Using Equations 14.5 and 14.9 with *Dalton's law* of partial pressures,

$$p = \sum_i p_i \tag{14.10}$$

it follows that

$$x_i = \frac{C_i}{C} = \frac{p_i}{p} \tag{14.11}$$

14.1.3 Fick's Law of Diffusion

Since similar physical mechanisms are associated with heat and mass transfer by diffusion, it is not surprising that the corresponding rate equations are of the same form. The rate equation for mass diffusion is known as *Fick's law,* and for the

[2]Do not confuse x_i, the mole fraction of species i, with the spatial coordinate x. The former variable will always be subscripted with the species designation.

Patent Owner Manufacturing Resources International, Inc.
Exhibit 2017 - Page 887 of 999

transfer of species A in a *binary mixture* of A and B, it may be expressed in vector form as

$$\mathbf{j}_A = -\rho D_{AB} \nabla m_A \tag{14.12}^3$$

or

$$\mathbf{J}_A^* = -CD_{AB} \nabla x_A \tag{14.13}^3$$

The form of these expressions is similar to that of Fourier's law, Equation 2.3. Moreover, just as Fourier's law serves to define one important transport property, the thermal conductivity, Fick's law defines a second important transport property, namely, the *binary diffusion coefficient* or *mass diffusivity*, D_{AB}.

The quantity $\mathbf{j}_A$ (kg/s · m^2) is defined as the diffusive mass flux of species A. It is the amount of A that is transferred by diffusion per unit time and per unit area perpendicular to the direction of transfer, and it is proportional to the mixture mass density, $\rho = \rho_A + \rho_B$ (kg/m^3), and to the gradient in the species mass fraction, $m_A = \rho_A/\rho$. The species flux may also be evaluated on a molar basis, where $\mathbf{J}_A^*$ (kmol/s · m^2) is the diffusive molar flux of species A. It is proportional to the total molar concentration of the mixture, $C = C_A + C_B$ (kmol/m^3), and to the gradient in the species mole fraction, $x_A = C_A/C$. The foregoing forms of Fick's law may be simplified when the total mass density ρ or the total molar concentration C is a constant.

14.1.4 Mass Diffusivity

Considerable attention has been given to predicting the mass diffusivity D_{AB} for the binary mixture of two gases, A and B. Assuming ideal gas behavior, kinetic theory may be used to show that

$$D_{AB} \sim p^{-1} T^{3/2} \tag{14.14}$$

where T is expressed in kelvins. This relation applies for restricted pressure and temperature ranges and is useful for estimating values of the mass diffusivity at conditions other than those for which data are available. Bird et al. [1–3] provide detailed discussions of available theoretical treatments and comparisons with experiment.

For binary liquid solutions, it is necessary to rely exclusively on experimental measurements. For small concentrations of A (the solute) in B (the solvent), D_{AB} is known to increase with increasing temperature. The mechanism of diffusion of gases, liquids, and solids in solids is extremely complicated and generalized theories are not available. Furthermore, only limited experimental results are available in the literature.

Data for binary diffusion in selected mixtures are presented in Table A.8. Skelland [4] and Poling et al. [5] provide more detailed treatments of this subject.

---

[3]Inherent in Equations 14.12 and 14.13 is the assumption that mass diffusion results only from a concentration gradient. In fact, mass diffusion may also result from a temperature gradient, a pressure gradient, or an external force. In most problems, these effects are negligible and the dominant driving potential is the species concentration gradient. This condition is referred to as *ordinary diffusion*. Treatment of the other (higher-order) effects is presented by Bird et al. [1–3].

Patent Owner Manufacturing Resources International, Inc.
Exhibit 2017 - Page 888 of 999

EXAMPLE 14.1

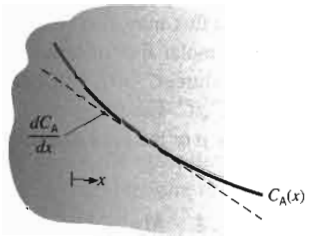
Consider the diffusion of hydrogen (species A) in air, liquid water, or iron (species B) at $T = 293$ K. Calculate the species flux on both molar and mass bases if the concentration gradient at a particular location is $dC_A/dx = 1$ kmol/m$^3 \cdot$ m. Compare the value of the mass diffusivity to the thermal diffusivity. The mole fraction of the hydrogen, x_A, is much less than unity.

SOLUTION

Known: Concentration gradient of hydrogen in air, liquid water, or iron at $T = 293$ K.

Find: Molar and mass fluxes of hydrogen and the relative values of the mass and thermal diffusivities for the three cases.

Schematic:



Assumptions: Steady-state conditions.

Properties: Table A.8, hydrogen–air (298 K): $D_{AB} = 0.41 \times 10^{-4}$ m^2/s, hydrogen–water (298 K): $D_{AB} = 0.63 \times 10^{-8}$ m^2/s, hydrogen–iron (293 K): $D_{AB} = 0.26 \times 10^{-12}$ m^2/s. Table A.4, air (293 K): $\alpha = 21.6 \times 10^{-6}$ m^2/s; Table A.6, water (293 K): $k = 0.603$ W/m $\cdot$ K, $\rho = 998$ kg/m^3, $c_p = 4182$ J/kg $\cdot$ K. Table A.1, iron (300 K): $\alpha = 23.1 \times 10^{-6}$ m^2/s.

Analysis: Using Equation 14.14, we find that the mass diffusivity of hydrogen in air at $T = 293$ K is

$$D_{AB,T} = D_{AB,298\,K} \times \left(\frac{T}{298\ K}\right)^{3/2} = 0.41 \times 10^{-4}\ \text{m}^2/\text{s} \times \left(\frac{293\ K}{298\ K}\right)^{3/2} = 0.40 \times 10^{-4}\ \text{m}^2/\text{s}$$

For the case where hydrogen is a *dilute species*, that is, $x_A \ll 1$, the thermal properties of the medium can be taken to be those of the host medium consisting of species B. The thermal diffusivity of water is

$$\alpha = \frac{k}{\rho c_p} = \frac{0.603\ \text{W/m} \cdot \text{K}}{998\ \text{kg/m}^3 \cdot 4182\ \text{J/kg} \cdot \text{K}} = 0.144 \times 10^{-6}\ \text{m}^2/\text{s}$$

The ratio of the thermal diffusivity to the mass diffusivity is the Lewis number, *Le*, defined in Equation 6.50.

The molar flux of hydrogen is described by Fick's law, Equation 14.13,

$$J_A^* = -CD_{AB}\frac{dx_A}{dx}$$

14.2 Mass Tran

Patent Owner Manufacturing Resources International, Inc.
Exhibit 2017 - Page 889 of 999

The total molar concentration, C, is approximately constant since A is a dilute species; therefore

$$\mathbf{J}_A^* = -D_{AB}\frac{dC_A}{dx}$$

Hence, for the hydrogen–air mixture,

$$\mathbf{J}_A^* = -0.40 \times 10^{-4}\,\text{m}^2/\text{s} \times 1\,\frac{\text{kmol}}{\text{m}^3 \cdot \text{m}} = -4 \times 10^{-5}\,\frac{\text{kmol}}{\text{s} \cdot \text{m}^2}$$

The mass flux of hydrogen in air is found from the expression

$$\mathbf{j}_A = \mathcal{M}_A \mathbf{J}_A^* = 2\,\frac{\text{kg}}{\text{kmol}} \times \left(-4 \times 10^{-5}\,\frac{\text{kmol}}{\text{s} \cdot \text{m}^2}\right) = -8 \times 10^{-5}\,\frac{\text{kg}}{\text{s} \cdot \text{m}^2}$$

The results for the three different mixtures are summarized in the following table.

Species B	$\alpha \times 10^6$ (m²/s)	$D_{AB} \times 10^6$ (m²/s)	*Le*	$\mathbf{j}_A \times 10^6$ (kg/s · m²)
Air	21.6	40	0.54	80
Water	0.14	6.3×10^{-3}	23	13×10^{-3}
Iron	23.1	260×10^{-9}	89×10^6	0.52×10^{-6}

Comments:

1. The thermal diffusivities of the three media vary by two orders of magnitude. We saw in Chapter 5 that this relatively broad range of thermal diffusivities is responsible for the different rates at which objects respond thermally during transient conduction processes. In mass transfer, mass diffusivities can vary by 8 or more orders of magnitude, with the highest diffusivities associated with diffusion of gases in gases and the lowest diffusivities associated with diffusion in solids. Different materials respond to mass transfer at very different rates, depending on whether the host medium is a gas, liquid, or solid.
2. The ratio of the thermal diffusivity to the mass diffusivity, the Lewis number, is typically of order unity for gases. This implies that changes in the thermal and species distributions progress at approximately the same rates in gases that undergo simultaneous transient heat conduction and species diffusion processes. In solids or liquids, thermal energy is conducted much more readily than chemical species can be transferred by diffusion.

14.2 *Mass Transfer in Nonstationary Media*[4]

14.2.1 Absolute and Diffusive Species Fluxes

We have seen that diffusion mass transfer is similar to conduction heat transfer and that the diffusive fluxes, as given by Equations 14.12 and 14.13, are analogous to the heat flux as expressed by Fourier's law. If there is bulk motion, then, like heat

[4]If only problems involving stationary media are of interest, the reader may proceed directly to Section 14.3.

Patent Owner Manufacturing Resources International, Inc.
Exhibit 2017 - Page 890 of 999

transfer, mass transfer can also occur by advection. Unlike conduction heat transfer, however, the diffusion of a species always involves the movement of molecules or atoms from one location to another. In many cases, this molecular scale motion results in bulk motion. In this section we define the total or *absolute flux* of a species, which includes both diffusive and advective components.

The absolute mass (or molar) flux of a species is defined as the total flux relative to a fixed coordinate system. To obtain an expression for the absolute mass flux, consider species A in a binary mixture of A and B. The absolute mass flux $\mathbf{n}''_A$ is related to the species absolute velocity $\mathbf{v}_A$ by

$$\mathbf{n}''_A \equiv \rho_A \mathbf{v}_A \tag{14.15}$$

A value of $\mathbf{v}_A$ may be associated with any point in the mixture, and it is interpreted as the average velocity of all the A particles in a small volume element about the point. An average, or aggregate, velocity may also be associated with the particles of species B, in which case

$$\mathbf{n}''_B \equiv \rho_B \mathbf{v}_B \tag{14.16}$$

A *mass-average velocity for the mixture* may then be obtained from the requirement that

$$\rho \mathbf{v} = \mathbf{n}'' = \mathbf{n}''_A + \mathbf{n}''_B = \rho_A \mathbf{v}_A + \rho_B \mathbf{v}_B \tag{14.17}$$

giving

$$\mathbf{v} = m_A \mathbf{v}_A + m_B \mathbf{v}_B \tag{14.18}$$

It is important to note that we have defined the velocities ($\mathbf{v}_A$, $\mathbf{v}_B$, $\mathbf{v}$) and the fluxes ($\mathbf{n}''_A$, $\mathbf{n}''_B$, $\mathbf{n}''$) as *absolute* quantities. That is, they are referred to axes that are fixed in space. The mass-average velocity $\mathbf{v}$ is a useful parameter of the binary mixture, for two reasons. First, it need only be multiplied by the total mass density to obtain the total mass flux with respect to fixed axes. Second, it is the mass-average velocity which is required in the equations expressing conservation of mass, momentum, and energy such as those presented and discussed in Chapter 6.

We may now define the *mass flux of species* A *relative to the mixture mass-average velocity* as

$$\mathbf{j}_A \equiv \rho_A(\mathbf{v}_A - \mathbf{v}) \tag{14.19}$$

Whereas $\mathbf{n}''_A$ is the *absolute flux* of species A, $\mathbf{j}_A$ is the *relative* or *diffusive flux* of the species and is the quantity previously given by Fick's law, Equation 14.12. It represents the motion of the species relative to the average motion of the mixture. It follows from Equations 14.15 and 14.19 that

$$\mathbf{n}''_A = \mathbf{j}_A + \rho_A \mathbf{v} \tag{14.20}$$

This expression delineates the two contributions to the absolute flux of species A: a contribution due to *diffusion* (i.e., due to the motion of A *relative* to the mass-average motion of the mixture) and a contribution due to *advection* (i.e., due to motion of A *with* the mass-average motion of the mixture). Substituting from Equations 14.12 and 14.17, we obtain

$$\mathbf{n}''_A = -\rho D_{AB} \nabla m_A + m_A(\mathbf{n}''_A + \mathbf{n}''_B) \tag{14.21}$$

Patent Owner Manufacturing Resources International, Inc.
Exhibit 2017 - Page 891 of 999

If the second term on the right-hand side of Equation 14.21 is zero, mass transfer of species A occurs purely by diffusion, and the situation is analogous to heat transfer purely by conduction. We will later identify special situations for which this occurs.

The foregoing considerations may be extended to species B. The *mass flux of* B *relative to the mixture mass-average velocity* (the *diffusive flux*) is

$$\mathbf{j}_B \equiv \rho_B(\mathbf{v}_B - \mathbf{v}) \tag{14.22}$$

where

$$\mathbf{j}_B = -\rho D_{BA} \nabla m_B \tag{14.23}$$

It follows from Equations 14.17, 14.19, and 14.22 that the diffusive fluxes in a binary mixture are related by

$$\mathbf{j}_A + \mathbf{j}_B = 0 \tag{14.24}$$

If Equations 14.12 and 14.23 are substituted into Equation 14.24, and it is recognized that $\nabla m_A = -\nabla m_B$, since $m_A + m_B = 1$ for a binary mixture, it follows that

$$D_{BA} = D_{AB} \tag{14.25}$$

Hence, as in Equation 14.21, the *absolute* flux of species B may be expressed as

$$\mathbf{n}''_B = -\rho D_{AB} \nabla m_B + m_B(\mathbf{n}''_A + \mathbf{n}''_B) \tag{14.26}$$

Although the foregoing expressions pertain to *mass* fluxes, the same procedures can be used to obtain results on a *molar* basis. The absolute molar fluxes of species A and B may be expressed as

$$\mathbf{N}''_A \equiv C_A \mathbf{v}_A \qquad \text{and} \qquad \mathbf{N}''_B \equiv C_B \mathbf{v}_B \tag{14.27}$$

and a *molar-average velocity for the mixture,* $\mathbf{v}^*$, is obtained from the requirement that

$$\mathbf{N}'' = \mathbf{N}''_A + \mathbf{N}''_B = C\mathbf{v}^* = C_A \mathbf{v}_A + C_B \mathbf{v}_B \tag{14.28}$$

giving

$$\mathbf{v}^* = x_A \mathbf{v}_A + x_B \mathbf{v}_B \tag{14.29}$$

Note that the molar-average velocity is not the same as the mass-average velocity and is therefore not appropriate for use in the conservation equations of Chapter 6.

The significance of the molar-average velocity is that, when multiplied by the total molar concentration C, it provides the total molar flux $\mathbf{N}''$ with respect to a fixed coordinate system. Equation 14.27 provides the *absolute molar flux* of species A and B. In contrast, the molar flux of A relative to the mixture molar average velocity $\mathbf{J}^*_A$, termed the *diffusive flux,* may be obtained from Equation 14.13 or from the expression

$$\mathbf{J}^*_A \equiv C_A(\mathbf{v}_A - \mathbf{v}^*) \tag{14.30}$$

To determine an expression similar in form to Equation 14.21, we combine Equations 14.27 and 14.30 to obtain

$$\mathbf{N}''_A = \mathbf{J}^*_A + C_A \mathbf{v}^* \tag{14.31}$$

or, from Equations 14.13 and 14.28,

$$\mathbf{N}''_A = -CD_{AB} \nabla x_A + x_A(\mathbf{N}''_A + \mathbf{N}''_B) \tag{14.32}$$

Patent Owner Manufacturing Resources International, Inc.
Exhibit 2017 - Page 892 of 999

Note that Equation 14.32 represents the absolute molar flux as the sum of a diffusive flux and an advective flux. Again, if the second term on the right-hand side is zero, mass transfer is purely by diffusion and is analogous to heat conduction, when formulated in molar quantities instead of mass quantities. For the binary mixture, it also follows that

$$\mathbf{J}_A^* + \mathbf{J}_B^* = 0 \tag{14.33}$$

14.2.2 Evaporation in a Column

Let us now consider diffusion in the binary gas mixture of Figure 14.2. Fixed species concentrations $x_{A,L}$ and $x_{B,L}$ are maintained at the top of a tube containing a liquid layer of species A, and the system is at constant pressure and temperature. Since equilibrium exists between the vapor and liquid phases at the liquid interface, the vapor concentration corresponds to saturated conditions. With $x_{A,0} > x_{A,L}$, species A *evaporates* from the liquid interface and is transferred upward by diffusion. For steady, one-dimensional conditions with no chemical reactions, species A cannot accumulate in the control volume of Figure 14.2, and the absolute molar flux of A must be constant throughout the column. Hence

$$\frac{dN''_{A,x}}{dx} = 0 \tag{14.34}$$

From the definition of the total molar concentration, $C = C_A + C_B$, $x_A + x_B = 1$ throughout the column. Knowing that $x_{A,0} > x_{A,L}$, we immediately conclude that $x_{B,L} > x_{B,0}$. Therefore, dx_B/dx is positive, and gas B must diffuse from the top of the column to the liquid interface. However, if species B cannot be absorbed into liquid A,

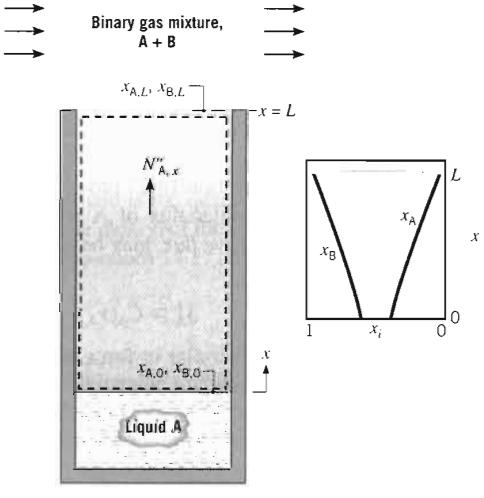


FIGURE 14.2 Evaporation of liquid A into a binary gas mixture, A + B.

Patent Owner Manufacturing Resources International, Inc.
Exhibit 2017 - Page 893 of 999

steady-state conditions can be maintained only if $N''_{B,x} = 0$ everywhere within the control volume of Figure 14.2. The only way this can be possible is if the downward diffusion of gas B is exactly balanced by upward advection of gas B. The implication of this important conclusion is that we must account for the advection of the gases in the column in order to successfully predict the species distributions $x_A(x)$ and $x_B(x)$, as well as the evaporation rate of liquid A. An appropriate expression for $N''_{A,x}$ may be obtained by substituting the requirement that $N''_{B,x} = 0$ into Equation 14.32, giving

$$N''_{A,x} = -CD_{AB}\frac{dx_A}{dx} + x_A N''_{A,x} \tag{14.35}$$

or, from Equation 14.28,

$$N''_{A,x} = -CD_{AB}\frac{dx_A}{dx} + C_A v_x^* \tag{14.36}$$

From this equation it is evident that the diffusive transport of species A $[-CD_{AB}(dx_A/dx)]$ is augmented by bulk motion $(C_A v_x^*)$. Rearranging Equation 14.35, we obtain

$$N''_{A,x} = -\frac{CD_{AB}}{1 - x_A}\frac{dx_A}{dx} \tag{14.37}$$

For constant p and T, C and D_{AB} are also constant. Substituting Equation 14.37 into Equation 14.34, we then obtain

$$\frac{d}{dx}\left(\frac{1}{1 - x_A}\frac{dx_A}{dx}\right) = 0$$

Integrating twice, we have

$$-\ln(1 - x_A) = C_1 x + C_2$$

Applying the conditions $x_A(0) = x_{A,0}$ and $x_A(L) = x_{A,L}$, the constants of integration may be evaluated and the concentration distribution becomes

$$\frac{1 - x_A}{1 - x_{A,0}} = \left(\frac{1 - x_{A,L}}{1 - x_{A,0}}\right)^{x/L} \tag{14.38}$$

Since $1 - x_A = x_B$, we also obtain

$$\frac{x_B}{x_{B,0}} = \left(\frac{x_{B,L}}{x_{B,0}}\right)^{x/L} \tag{14.39}$$

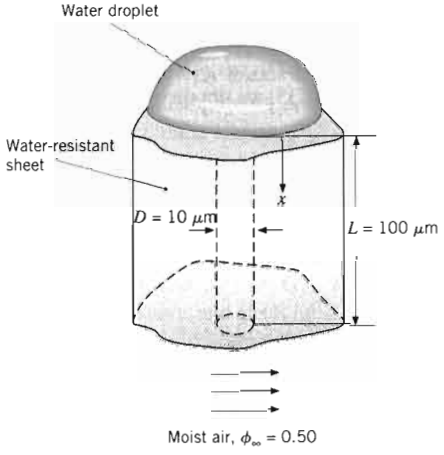
To determine the evaporation rate of species A, Equation 14.38 is first used to evaluate the concentration gradient (dx_A/dx). Substituting the result into Equation 14.37, it follows that

$$N''_{A,x} = \frac{CD_{AB}}{L}\ln\left(\frac{1 - x_{A,L}}{1 - x_{A,0}}\right) \tag{14.40}$$

Patent Owner Manufacturing Resources International, Inc.
Exhibit 2017 - Page 894 of 999

EXAMPLE 14.2

A water-resistant sheet used for water-proofing applications is formed from an impermeable polymeric material. The *microstructure* of the sheet is engineered to provide open pores of diameter $D = 10$ μm that extend through the entire thickness of the $L = 100$-μm-thick sheet. The pore diameter is large enough to allow water vapor to be transferred through the pore but is sufficiently small to prohibit liquid water from penetrating through the sheet. Determine the rate at which water vapor is transmitted through a single pore when saturated liquid exists on the top of the sheet and moist air at $\phi_\infty = 50\%$ relative humidity exists on the bottom side of the sheet. Evaluate the transfer rate at a temperature of $T = 298$ K and a pressure of $p = 1$ atm. Investigate the sensitivity of the transfer rate to the temperature, and compare the transfer rates to rates that are predicted by neglecting the molar-average motion of the mixture in the pore.



SOLUTION

Known: Thickness and pore diameter of a porous sheet, thermal conditions, and humidity.

Find: Evaporation rate through a single pore.

Assumptions:

1. Steady-state, isothermal, one-dimensional conditions.
2. No chemical reactions.
3. Pore penetrates the thickness of the sheet in a perpendicular manner and is of circular cross section.
4. Binary system consisting of water vapor (A) and air (B).

Properties: Table A.6, saturated water, vapor (298 K): $p_{sat} = 0.03165$ bar. Table A.8, water vapor–air (298 K): $D_{AB} = 0.26 \times 10^{-4}$ m^2/s.

Patent Owner Manufacturing Resources International, Inc.
Exhibit 2017 - Page 895 of 999

Analysis:

1. Equation 14.40 may be used to determine the water vapor transferred through a single pore, accounting for the effects of the nonzero molar-averaged velocity. Hence,

$$N_{A,x} = A_{pore} N''_{A,x} = \frac{\pi D^2 C D_{AB}}{4L} \ln\left(\frac{1 - x_{A,L}}{1 - x_{A,0}}\right) \tag{1}$$

where the total concentration is

$$C = \frac{p}{\mathcal{R}T} = \frac{1.0133 \text{ bar}}{8.314 \times 10^{-2} \dfrac{\text{m}^3 \cdot \text{bar}}{\text{kmol} \cdot \text{K}} \times 298 \text{ K}} = 40.9 \times 10^{-3} \text{ kmol/m}^3$$

From Section 6.7.2, the mole fraction at $x = 0$ is

$$x_{A,0} = \frac{p_{A,sat}}{p} = \frac{0.03165 \text{ bar}}{1.0133 \text{ bar}} = 31.23 \times 10^{-3}$$

while at $x = L$ the mole fraction is

$$x_{A,L} = \frac{\phi_\infty p_{A,sat}}{p} = \frac{0.5 \times 0.03165 \text{ bar}}{1.0133 \text{ bar}} = 15.62 \times 10^{-3}$$

Therefore, the evaporation rate per pore may be evaluated using Equation 1 as

$$N_{A,x} = \frac{\pi \times (10 \times 10^{-6} \text{ m})^2 \times 40.9 \times 10^{-3} \text{ kmol/m}^3 \times 0.26 \times 10^{-4} \text{ m}^2/\text{s}}{4 \times 100 \times 10^{-6} \text{ m}} \times \ln\left(\frac{1 - 15.62 \times 10^{-3}}{1 - 31.23 \times 10^{-3}}\right)$$
$$= 13.4 \times 10^{-15} \text{ kmol/s} \quad \triangleleft$$

2. Neglecting the effects of the molar-averaged velocity, we see that Equation 14.32 reduces to

$$N''_{A,x} = -C D_{AB} \frac{dx_A}{dx}$$

where the total concentration, C, is constant, and the flux of water vapor is independent of x. Hence, the species transfer rate per pore may be expressed as

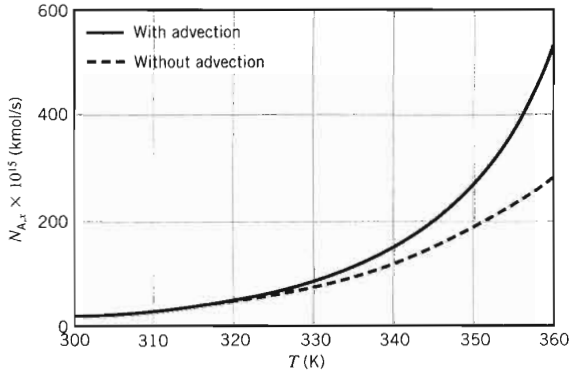
$$N_{A,x} = A_{pore} N''_{A,x} = \frac{\pi D^2 C D_{AB}}{4L} (x_{A,0} - x_{A,L}) \tag{2}$$
$$= \frac{\pi \times (10 \times 10^{-6} \text{ m})^2 \times 40.9 \times 10^{-3} \text{ kmol/m}^3 \times 0.26 \times 10^{-4} \text{ m}^2/\text{s}}{4 \times 100 \times 10^{-6} \text{ m}} \times (31.23 \times 10^{-3} - 15.62 \times 10^{-3})$$
$$= 13.0 \times 10^{-15} \text{ kmol/s} \quad \triangleleft$$

Advection effects associated with the nonzero molar-average velocity augment the diffusive flux, and a slightly increased evaporation rate is predicted to occur when advection is considered.

3. The temperature dependence of the evaporation rate is determined by accounting for the sensitivity of the binary diffusion coefficient to temperature (Equation 14.14), $D_{AB} \propto T^{3/2}$, and repeating the calculations over the range $300 < T < 360$ K. The results, shown below in graphical form, indicate a significant dependence of the evaporation rate on the temperature. This strong dependence is due

Patent Owner Manufacturing Resources International, Inc.
Exhibit 2017 - Page 896 of 999

primarily to the significant variation of the saturation pressure of water vapor with temperature, as evident in Table A.6.



Comments:

1. As the temperature and, in turn, the saturation pressure and mole fraction of the water vapor increase, the molar-average velocity becomes large, and advection effects become important. Alternatively, the molar-average velocity may be neglected when the concentration of water vapor is small. It is the existence of the two conditions $N''_{B,x} \approx 0$ and $x_A \ll 1$ that will be implied in future use of the *stationary medium approximation.*
2. The total evaporation rate per area of the packaging material could be determined by multiplying the number of pores per unit area by the evaporation rate per pore.
3. The pressure was assumed constant in developing this solution. Since the molar-average velocity is nonzero, there must be a pressure gradient to overcome friction at the pore walls. If the pore is oriented vertically, there is also a static pressure gradient. The pressure gradient to overcome friction can be estimated by first determining the mass-average velocity. From Equation 14.17

$$v_x = \frac{n''_{A,x} + n''_{B,x}}{\rho} = \frac{n''_{A,x}}{\rho} = \frac{N''_{A,x}\mathcal{M}_A}{\rho} = \frac{N_{A,x}\mathcal{M}_A}{A_{pore}\rho}$$

Then the pressure gradient can be estimated by treating the flow as if it were a fully developed flow in a circular pipe. From Equation 8.14

$$\left|\frac{dp}{dx}\right| = \frac{32\mu v_x}{D^2} = \frac{32\nu N_{A,x}\mathcal{M}_A}{A_{pore}D^2}$$

Since the mixture is mostly air, we use the kinematic viscosity of air. Then taking the worst case of $T = 360$ K, $N_{A,x} = 530 \times 10^{-15}$ kmol/s,

$$\left|\frac{dp}{dx}\right| = \frac{32 \times 22.0 \times 10^{-6}\ \text{m}^2/\text{s} \times 530 \times 10^{-15}\ \text{kmol/s} \times 18\ \text{kg/kmol}}{\pi(10 \times 10^{-6}\ \text{m})^4/4}$$

$$= 860 \times 10^3\ \text{Pa/m}$$

14.3
The Stati

Patent Owner Manufacturing Resources International, Inc.
Exhibit 2017 - Page 897 of 999

Thus the pressure drop to overcome friction is

$$\Delta p_{\text{friction}} = 860 \times 10^3 \text{ Pa/m} \times 100 \times 10^{-6} \text{ m} = 86 \text{ Pa}$$

If the pore is vertical, the static pressure drop is

$$\Delta p_{\text{static}} = \rho_{\text{air}} g L = 0.970 \text{ kg/m}^3 \times 9.8 \text{ m/s}^2 \times 100 \times 10^{-6} \text{ m} = 0.001 \text{ Pa}$$

Both of these pressure drops are negligible relative to atmospheric pressure, so the assumption of constant pressure was appropriate.

14.3 *The Stationary Medium Approximation*

Fick's law for the diffusive flux of a species was introduced in Equations 14.12 and 14.13. In Section 14.2, we saw that the molecular motion associated with mass transfer can induce bulk motion within an otherwise stagnant fluid. In this case the total or absolute species flux (given by Equation 14.21 or 14.32) includes both a diffusive component (given by Equation 14.12 or 14.13) and an advective component associated with the bulk motion. In this section we consider a scenario for which it is appropriate to neglect the advective contribution to mass transfer.

When the diffusion of a very small amount of species A occurs within a stagnant species B, the molecular motion associated with the mass transfer will not induce significant bulk motion of the medium. This situation is common when one considers the diffusion of a *dilute* gas or liquid within a stagnant liquid or a solid *host medium*, such as when water vapor is transferred through the solid wall of a room. In these cases, the medium can be assumed to be *stationary*, and advection can be neglected. For situations where this *stationary medium approximation* is appropriate, the diffusive mass and molar fluxes of Equations 14.12 and 14.13 are identical to the absolute mass and molar fluxes.[5] That is,

$$\mathbf{n}''_A = \mathbf{j}_A = -\rho D_{AB} \nabla m_A \tag{14.41}$$

$$\mathbf{N}''_A = \mathbf{J}^*_A = -C D_{AB} \nabla x_A \tag{14.42}$$

Furthermore, since the concentration of species A is small, the total density (ρ) or concentration (C) is approximately that of the host medium, species B. The important conclusion is that the stationary medium approximation allows one to utilize the results of Chapters 2 through 5 by employing an *analogy* between conduction heat transfer and diffusion mass transfer.

[5]For readers who skipped Section 14.2 on mass transfer in *nonstationary* media, the absolute flux of species A measured relative to fixed coordinates is denoted by $\mathbf{n}''_A$ (mass flux) or $\mathbf{N}''_A$ (molar flux). For those who read Section 14.2, note that the stationary medium approximation is equivalent to saying that the host medium (B) is stationary, $\mathbf{n}''_B = 0$ and $\mathbf{N}''_B = 0$, and species A is dilute, $m_A \ll 1$ and $x_A \ll 1$. Thus, in Equations 14.21 and 14.32, the advective component is negligible, resulting in Equations 14.41 and 14.42.

Patent Owner Manufacturing Resources International, Inc.
Exhibit 2017 - Page 898 of 999

14.4 *Conservation of Species for a Stationary Medium*

Just as the first law of thermodynamics (the law of *conservation of energy*) plays an important role in heat transfer analyses, the law of *conservation of species* plays an important role in the analysis of mass transfer problems. In this section we consider a general statement of this law, as well as application of the law to species diffusion in a stationary medium.

14.4.1 Conservation of Species for a Control Volume

A general formulation of the energy conservation requirement, Equation 1.11c, was expressed for the control volume of Figure 1.7*b*. We may now express an analogous species mass conservation requirement for the control volume of Figure 14.3.

> *The rate at which the mass of some species enters a control volume, plus the rate at which the species mass is generated within the control volume, minus the rate at which this species mass leaves the control volume must equal the rate of increase of the species mass stored within the control volume.*

For example, any species A may enter and leave the control volume due to both fluid motion and diffusion across the control surface; these processes are *surface* phenomena represented by $\dot{M}_{A,in}$ and $\dot{M}_{A,out}$. The same species A may also be generated, $\dot{M}_{A,g}$, and accumulated or stored, $\dot{M}_{A,st}$, *within* the control volume. The conservation equation may then be expressed on a rate basis as

$$\dot{M}_{A,in} + \dot{M}_{A,g} - \dot{M}_{A,out} = \frac{dM_A}{dt} \equiv \dot{M}_{A,st} \tag{14.43}$$

Species generation exists when chemical reactions occur in the system. For example, for a dissociation reaction of the form AB → A + B, there would be net production of species A and B, as well as net reduction of the species AB.

14.4.2 The Mass Diffusion Equation

The foregoing result may be used to obtain a mass, or species, diffusion equation that is analogous to the heat equation of Chapter 2. We will consider a medium that is a binary mixture of species A and B for which the *stationary medium approximation* holds. That is, mass transfer may be approximated as occurring only by diffusion

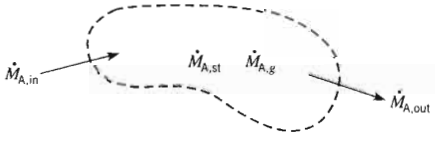


FIGURE 14.3
Conservation of species for a control volume.

Patent Owner Manufacturing Resources International, Inc.
Exhibit 2017 - Page 899 of 999

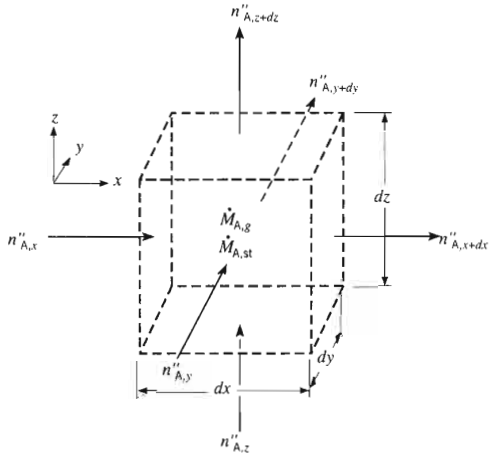


FIGURE 14.4
Differential control volume, $dx\ dy\ dz$, for species diffusion analysis in Cartesian coordinates.

because advection is negligible. The resulting equation could be solved for the species concentration distribution, which could, in turn, be used with Fick's law to determine the species diffusion rate at any point in the medium.

Allowing for concentration gradients in each of the x, y, and z coordinate directions, we first define a differential control volume, $dx\ dy\ dz$, within the medium (Figure 14.4) and consider the processes that influence the distribution of species A. With the concentration gradients, diffusion must result in the transport of species A through the control surfaces. Moreover, relative to stationary coordinates, the species transport rates at opposite surfaces must be related by

$$n''_{A,x+dx}\,dy\,dz = n''_{A,x}\,dy\,dz + \frac{\partial[n''_{A,x}\,dy\,dz]}{\partial x}\,dx \tag{14.44a}$$

$$n''_{A,y+dy}\,dx\,dz = n''_{A,y}\,dx\,dz + \frac{\partial[n''_{A,y}\,dx\,dz]}{\partial y}\,dy \tag{14.44b}$$

$$n''_{A,z+dz}\,dx\,dy = n''_{A,z}\,dx\,dy + \frac{\partial[n''_{A,z}\,dx\,dy]}{\partial z}\,dz \tag{14.44c}$$

In addition, there may be volumetric (also referred to as *homogeneous*) chemical reactions occurring throughout the medium, perhaps nonuniformly. The rate at which species A is generated within the control volume due to such reactions may be expressed as

$$\dot{M}_{A,g} = \dot{n}_A\,dx\,dy\,dz \tag{14.45}$$

where $\dot{n}_A$ is the rate of increase of the mass of species A per unit volume of the mixture (kg/s · m^3). Finally, these processes may change the mass of species A stored within the control volume, and the rate of change is

$$\dot{M}_{A,st} = \frac{\partial \rho_A}{\partial t}\,dx\,dy\,dz \tag{14.46}$$

Patent Owner Manufacturing Resources International, Inc.
Exhibit 2017 - Page 900 of 999

With mass inflow rates determined by $n''_{A,x}$, $n''_{A,y}$, and $n''_{A,z}$ and the outflow rates determined by Equations 14.44, Equations 14.44 through 14.46 may be substituted into Equation 14.43 to obtain

$$-\frac{\partial n''_A}{\partial x} - \frac{\partial n''_A}{\partial y} - \frac{\partial n''_A}{\partial z} + \dot{n}_A = \frac{\partial \rho_A}{\partial t}$$

In the remainder of the chapter we restrict our attention to cases where the stationary medium approximation is appropriate. Then, substituting the x, y, and z components of Equation 14.41, we obtain

$$\frac{\partial}{\partial x}\left(\rho D_{AB}\frac{\partial m_A}{\partial x}\right) + \frac{\partial}{\partial y}\left(\rho D_{AB}\frac{\partial m_A}{\partial y}\right) + \frac{\partial}{\partial z}\left(\rho D_{AB}\frac{\partial m_A}{\partial z}\right) + \dot{n}_A = \frac{\partial \rho_A}{\partial t} \qquad (14.47a)$$

In terms of the molar concentration, a similar derivation yields

$$\frac{\partial}{\partial x}\left(CD_{AB}\frac{\partial x_A}{\partial x}\right) + \frac{\partial}{\partial y}\left(CD_{AB}\frac{\partial x_A}{\partial y}\right) + \frac{\partial}{\partial z}\left(CD_{AB}\frac{\partial x_A}{\partial z}\right) + \dot{N}_A = \frac{\partial C_A}{\partial t} \qquad (14.48a)$$

In subsequent treatments of species diffusion phenomena, we shall work with simplified versions of the foregoing equations. In particular, if D_{AB} and ρ are constant, Equation 14.47a may be expressed as

$$\frac{\partial^2 \rho_A}{\partial x^2} + \frac{\partial^2 \rho_A}{\partial y^2} + \frac{\partial^2 \rho_A}{\partial z^2} + \frac{\dot{n}_A}{D_{AB}} = \frac{1}{D_{AB}}\frac{\partial \rho_A}{\partial t} \qquad (14.47b)$$

Similarly, if D_{AB} and C are constant, Equation 14.48a may be expressed as

$$\frac{\partial^2 C_A}{\partial x^2} + \frac{\partial^2 C_A}{\partial y^2} + \frac{\partial^2 C_A}{\partial z^2} + \frac{\dot{N}_A}{D_{AB}} = \frac{1}{D_{AB}}\frac{\partial C_A}{\partial t} \qquad (14.48b)$$

Equations 14.47b and 14.48b are analogous to the heat equation, Equation 2.19. As for the heat equation, two boundary conditions must be specified for each coordinate needed to describe the system. Conditions are also needed at an *initial time* if the problem of interest is transient. Hence it follows that, for analogous boundary and initial conditions, the solution to Equation 14.47b for $\rho_A(x, y, z, t)$ or to Equation 14.48b for $C_A(x, y, z, t)$ is of the same form as the solution to Equation 2.19 for $T(x, y, z, t)$.

The species diffusion equations may also be expressed in cylindrical and spherical coordinates. These alternative forms can be inferred from the analogous expressions for heat transfer, Equations 2.24 and 2.27, and in terms of the molar concentration have the following forms:

Cylindrical Coordinates:

$$\frac{1}{r}\frac{\partial}{\partial r}\left(CD_{AB}r\frac{\partial x_A}{\partial r}\right) + \frac{1}{r^2}\frac{\partial}{\partial \phi}\left(CD_{AB}\frac{\partial x_A}{\partial \phi}\right) + \frac{\partial}{\partial z}\left(CD_{AB}\frac{\partial x_A}{\partial z}\right) + \dot{N}_A = \frac{\partial C_A}{\partial t} \qquad (14.49)$$

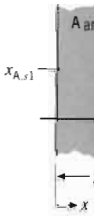


FIGURE 14
transfer in a
planar medi

Patent Owner Manufacturing Resources International, Inc.
Exhibit 2017 - Page 901 of 999

Spherical Coordinates:

$$\frac{1}{r^2}\frac{\partial}{\partial r}\left(CD_{AB}r^2\frac{\partial x_A}{\partial r}\right)+\frac{1}{r^2\sin^2\theta}\frac{\partial}{\partial\phi}\left(CD_{AB}\frac{\partial x_A}{\partial\phi}\right)$$
$$+\frac{1}{r^2\sin\theta}\frac{\partial}{\partial\theta}\left(CD_{AB}\sin\theta\frac{\partial x_A}{\partial\theta}\right)+\dot{N}_A=\frac{\partial C_A}{\partial t} \quad (14.50)$$

Simpler forms are, of course, associated with the absence of chemical reactions ($\dot{n}_A = \dot{N}_A = 0$) and with one-dimensional, steady-state conditions.

14.4.3 Stationary Media with Specified Surface Concentrations

Consider, for example, one-dimensional diffusion of species A through a planar medium of A and B, as shown in Figure 14.5. For steady-state conditions with no homogeneous chemical reactions, the molar form of the species diffusion equation (14.48a) reduces to

$$\frac{d}{dx}\left(CD_{AB}\frac{dx_A}{dx}\right)=0 \quad (14.51)$$

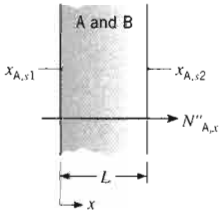


FIGURE 14.5 Mass transfer in a stationary planar medium.

Assuming the total molar concentration and the diffusion coefficient to be constant, Equation 14.51 may be solved and the boundary conditions illustrated in Figure 14.5 may be applied to yield

$$x_A(x)=(x_{A,s2}-x_{A,s1})\frac{x}{L}+x_{A,s1} \quad (14.52)$$

From Equation 14.42, it follows that

$$N''_{A,x}=-CD_{AB}\frac{x_{A,s2}-x_{A,s1}}{L} \quad (14.53)$$

Multiplying by the surface area A and substituting for $x_A \equiv C_A/C$, the molar rate is then

$$N_{A,x}=\frac{D_{AB}A}{L}(C_{A,s1}-C_{A,s2}) \quad (14.54)$$

From this expression we can define a resistance to species transfer by diffusion in a planar medium as

$$R_{m,dif}=\frac{C_{A,s1}-C_{A,s2}}{N_{A,x}}=\frac{L}{D_{AB}A} \quad (14.55)$$

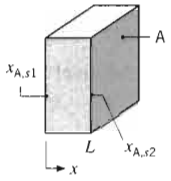
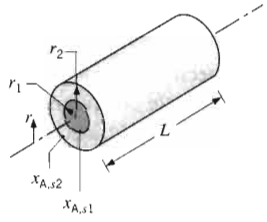
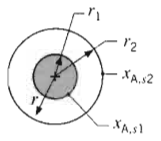
Comparing the foregoing results with those obtained for one-dimensional, steady-state conduction in a plane wall with no generation (Section 3.1), it is evident that a direct analogy exists between heat and mass transfer by diffusion.

The analogy also applies to cylindrical and spherical systems. For one-dimensional, steady diffusion in a cylindrical, nonreacting medium, Equation 14.49 reduces to

$$\frac{d}{dr}\left(rCD_{AB}\frac{dx_A}{dr}\right)=0 \quad (14.56)$$

Patent Owner Manufacturing Resources International, Inc.
Exhibit 2017 - Page 902 of 999

TABLE 14.1 Summary of Species Diffusion Solutions for Stationary Media with Specified Surface Concentrations[a]

Geometry	Species Concentration Distribution, $x_A(x)$ or $x_A(r)$	Species Diffusion Resistance, $R_{m,dif}$
	$x_A(x) = (x_{A,s2} - x_{A,s1})\dfrac{x}{L} + x_{A,s1}$	$R_{m,dif} = \dfrac{L}{D_{AB}A}$[b]
	$x_A(r) = \dfrac{x_{A,s1} - x_{A,s2}}{\ln(r_1/r_2)} \ln\left(\dfrac{r}{r_2}\right) + x_{A,s2}$	$R_{m,dif} = \dfrac{\ln(r_2/r_1)}{2\pi L D_{AB}}$[c]
	$x_A(r) = \dfrac{x_{A,s1} - x_{A,s2}}{1/r_1 - 1/r_2}\left(\dfrac{1}{r} - \dfrac{1}{r_2}\right) + x_{A,s2}$	$R_{m,dif} = \dfrac{1}{4\pi D_{AB}}\left(\dfrac{1}{r_1} - \dfrac{1}{r_2}\right)$[c]

[a] Assuming C and D_{AB} are constant.
[b] $N_{A,x} = (C_{A,s1} - C_{A,s2})/R_{m,dif}$.
[c] $N_{A,r} = (C_{A,s1} - C_{A,s2})/R_{m,dif}$.

Similarly, for a spherical medium,

$$\frac{d}{dr}\left(r^2 C D_{AB}\frac{dx_A}{dr}\right) = 0 \tag{14.57}$$

Equations 14.56 and 14.57, as well as Equation 14.51, dictate that the molar transfer rate, $N_{A,r}$ or $N_{A,x}$, is constant in the direction of transfer (r or x). Assuming C and D_{AB} to be constant, it is a simple matter to obtain general solutions to Equations 14.56 and 14.57. For prescribed surface species concentrations, the corresponding solutions and diffusion resistances are summarized in Table 14.1.

EXAMPLE 14.3

The efficacy of pharmaceutical products is reduced by prolonged exposure to high temperature, light, and humidity. For water vapor–sensitive consumer products that are in tablet or capsule form, and might be stored in humid environments such as bathroom medicine cabinets, *blister packaging* is used to limit the direct exposure of the medicine to humid conditions until immediately before their use.

Patent Owner Manufacturing Resources International, Inc.
Exhibit 2017 - Page 903 of 999

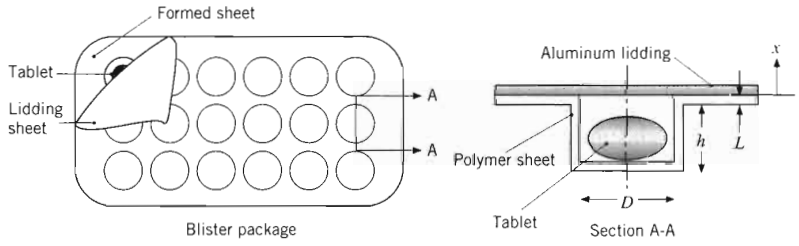
Consider tablets that are contained in a blister package composed of a flat *lidding sheet* and a second, *formed sheet* that includes troughs to hold each tablet. The formed sheet is $L = 50\ \mu$m thick and is fabricated of a polymer material. Each trough is of diameter $D = 5$ mm and depth $h = 3$ mm. The lidding sheet is fabricated of aluminum foil. The binary diffusion coefficient for water vapor in the polymer is $D_{AB} = 6 \times 10^{-14}$ m^2/s while the aluminum may be assumed to be impermeable to water vapor. For molar concentrations of water vapor in the polymer at the outer and inner surfaces of $C_{A,s1} = 4.5 \times 10^{-3}$ kmol/m^3 and $C_{A,s2} = 0.5 \times 10^{-3}$ kmol/m^3, respectively, determine the rate at which water vapor is transferred through the trough wall to the tablet.

SOLUTION

Known: Molar concentrations of water vapor at the inner and outer surfaces of a polymer sheet and trough geometry.

Find: Rate of water vapor molar diffusive transfer through the trough wall.

Schematic:



Assumptions:

1. Steady-state, one-dimensional conditions.
2. Stationary medium.
3. No chemical reactions.
4. Polymer sheet is thin relative to the dimensions of the trough, and diffusion may be analyzed as though it occurs through a plane wall.

Analysis:
The total water vapor transfer rate is the summation of the transfer rate through the cylindrical walls of the trough and the bottom, circular surface of the trough. From Equation 14.54 we may write

$$N_{A,x} = \frac{D_{AB}A}{L}(C_{A,s1} - C_{A,s2}) = \frac{D_{AB}}{L}\left(\frac{\pi D^2}{4} + \pi Dh\right)(C_{A,s1} - C_{A,s2})$$

Hence

$$N_{A,x} = \frac{6 \times 10^{-14}\ \text{m}^2/\text{s}}{50 \times 10^{-6}\ \text{m}}\left(\frac{\pi(5 \times 10^{-3}\ \text{m})^2}{4} + \pi(5 \times 10^{-3}\ \text{m})(3 \times 10^{-3}\ \text{m})\right) \times (4.5 \times 10^{-3} - 0.5 \times 10^{-3})\ \text{kmol/m}^3$$

$$= 0.32 \times 10^{-15}\ \text{kmol/s}$$

Patent Owner Manufacturing Resources International, Inc.
Exhibit 2017 - Page 904 of 999

Comments:

1. The mass diffusion rate of water vapor is $n_{A,x} = \mathcal{M}_A N_{A,x} = 18$ kg/kmol $\times$ 0.32 $\times$ 10^{-15} kmol/s $= 5.8 \times 10^{-15}$ kg/s.
2. The *shelf life* of the medicine is inversely proportional to the rate at which water vapor is transferred through the polymer sheet. Shelf life may be extended by increasing the thickness of the sheet, resulting in increased cost of the package. Specification of materials for use in blister packaging involves tradeoffs between shelf life, cost, formability, and recyclability of the polymer material.

14.5 *Boundary Conditions and Discontinuous Concentrations at Interfaces*

In the previous section, expressions for mass transfer resistances were developed by applying *constant surface concentration* boundary conditions. For a surface at $x = 0$, the constant surface species concentration boundary condition is expressed as

$$x_A(0,t) = x_{A,s} \tag{14.58}$$

We have already used Equation 14.58 in Examples 14.2 and 14.3. A constant surface concentration boundary condition can equivalently be expressed in terms of a mass or molar fraction or density. While the form of Equation 14.58 is simple, determination of the appropriate value of $x_{A,s}$ can be complicated, as discussed below.

The second boundary condition that is analogous to the conduction heat transfer conditions of Table 2.2 is that of a constant species flux, $J^*_{A,s}$, at a surface. Using Fick's law, Equation 14.13, the condition is expressed for a surface at $x = 0$ as

$$-CD_{AB}\left.\frac{\partial x_A}{\partial x}\right|_{x=0} = J^*_{A,s} \tag{14.59}$$

A special case of this condition corresponds to the *impermeable surface* for which $\partial x_A/\partial x|_{x=0} = 0$ when a stationary medium is considered. A constant species flux boundary condition can also be expressed on a mass basis.

One phenomenon that makes mass transfer more complex than heat transfer is that species concentrations are typically *discontinuous* at the interface between two materials, whereas temperature is continuous. To take a familiar example, consider a pool of water that is exposed to air. If we are interested in determining the rate at which water vapor is transferred into the air, we would need to specify the water vapor concentration in the air at the air–water interface. We know that the mole fraction of water in the pool is essentially unity (neglecting the small amount of dissolved oxygen or nitrogen in the water). But it would be incorrect to specify $x_{A,s} = 1$ for the water vapor mole fraction *in the air* at the interface. Clearly, the concentration of water is discontinuous across the interface. In general, concentration boundary conditions at the interface that separates two materials describe a *relationship* between the concentrations on either side of the interface. The relationships are either based on theory or are deduced from experiments. They can be expressed in a variety of forms, a few of which are now introduced.

Patent Owner Manufacturing Resources International, Inc.
Exhibit 2017 - Page 905 of 999

14.5.1 Evaporation and Sublimation

A common mass transfer scenario is the transfer of a species A into a gas stream due to evaporation or sublimation from a liquid or solid surface, respectively (Figure 14.6*a*). Conditions *within the gas phase* are of interest, and the concentration (or partial pressure) of species A in the gas phase at the interface (located at $x = 0$) may readily be determined from *Raoult's law*,

$$p_A(0) = x_A(0)p_{A,sat} \tag{14.60}$$

where p_A is the partial pressure of A *in the gas phase*, x_A is the mole fraction of species A *in the liquid or solid*, and $p_{A,sat}$ is the saturation pressure of species A at the surface temperature. Raoult's law applies if the gas phase can be approximated as ideal and the liquid or solid phase has a high concentration of species A. If the liquid or solid is a pure species A, that is, $x_A = 1$, Equation 14.60 simplifies to $p_A(0) = p_{A,sat}$. That is, the partial pressure of the vapor at the interface corresponds to saturated conditions at the temperature of the interface and may be determined from standard thermodynamic tables. This boundary condition was utilized in the solution of Example 14.2 and in Section 6.7.2.

14.5.2 Solubility of Gases in Liquids and Solids

Another common mass transfer problem is similar to the evaporation or sublimation problem, except mass transfer *within the liquid or solid phase* is of interest. We consider the transfer of species A *from* a gas stream *into* a liquid or solid, species B (Figure 14.6*b*).

If species A is only weakly soluble (x_A is small) in a *liquid, Henry's law* may be used to relate the mole fraction of A in the liquid to the partial pressure of A in the gas phase outside the liquid:

$$x_A(0) = \frac{p_A(0)}{H} \tag{14.61}$$

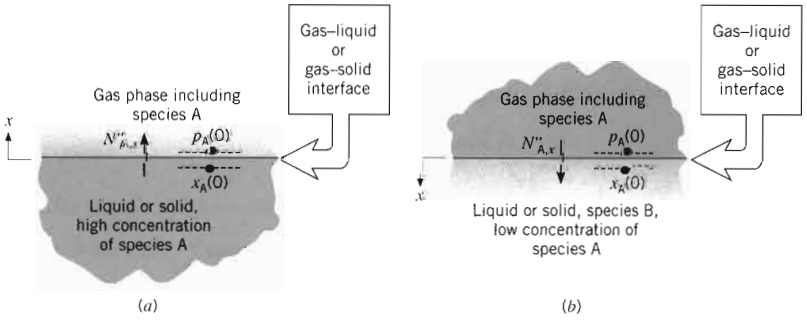


FIGURE 14.6 Species concentration at a gas–liquid or gas–solid interface. (*a*) Evaporation or sublimation of species A from a liquid or solid into a gas. (*b*) Transfer of weakly soluble species A from the gas to a liquid or solid.

Patent Owner Manufacturing Resources International, Inc.
Exhibit 2017 - Page 906 of 999

The coefficient H is known as *Henry's constant*, and values for selected aqueous solutions are listed in Table A.9. Although H depends on temperature, its pressure dependence may generally be neglected for values of p up to 5 bars.

Conditions at a *gas–solid* interface may also be determined if the gas, species A, dissolves in a solid, species B, and a solution is formed. In such cases mass transfer in the solid is independent of the structure of the solid and may be treated as a diffusion process. In contrast, there are many situations for which the porosity of the solid strongly influences gas transport through the solid. Treatment of such cases is left to more advanced texts [2, 4].

Treating the gas and solid as a solution, we can obtain the concentration of the gas in the solid at the interface through use of a property known as the *solubility, S*. It is defined by the expression

$$C_A(0) = Sp_A(0) \tag{14.62}$$

where $p_A(0)$ is once again the partial pressure (bars) of the gas adjoining the interface. The molar concentration of A in the solid at the interface, $C_A(0)$, is in units of kilomoles of A per cubic meter of solid, in which case the units of S must be *kilomoles of* A *per cubic meter of solid per bar (or atm) partial pressure of* A. Values of S for several gas–solid combinations are given in Table A.10. Values of solubility are often presented in units of cubic meters of species A (at STP, Standard Temperature and Pressure, of 0°C and 1 atm) per cubic meter of solid per atm partial pressure of A. Denoting this solubility value as $\tilde{S}$, and recognizing that at STP one kilomole occupies 22.414 m^3, we find that the unit conversion is given by $S = \tilde{S}/(22.414\ m^3/kmol)$. (Additional conversion between bar and atm may be needed.)

EXAMPLE 14.4

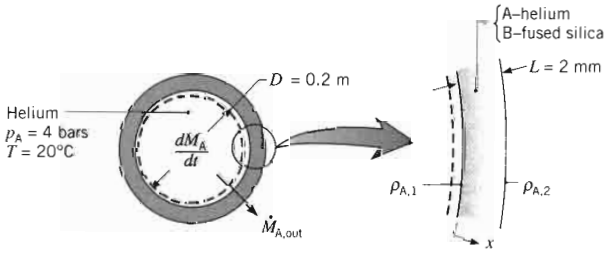
Helium gas is stored at 20°C in a spherical container of fused silica (SiO_2), which has a diameter of 0.20 m and a wall thickness of 2 mm. If the container is charged to an initial pressure of 4 bars, what is the rate at which this pressure decreases with time?

SOLUTION

Known: Initial pressure of helium in a spherical, fused silica container of prescribed diameter D and wall thickness L.

Find: The rate of change of the helium pressure, dp_A/dt.

Schematic:



Patent Owner Manufacturing Resources International, Inc.
Exhibit 2017 - Page 907 of 999

selected aqueous
ature, its pressure
s.
he gas, species A,
ases mass transfer
treated as a diffu-
orosity of the solid
uch cases is left to

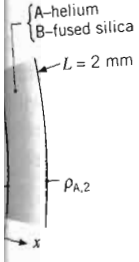
oncentration of the
as the *solubility, S*.

(14.62)

adjoining the inter-
$C_A(0)$, is in units of
s of S must be *kilo-*
sure of A. Values of
Values of solubility
, Standard Tempera-
r atm partial pressure
at STP one kilomole
by $S = \bar{S}/(22.414\ m^3/$
ded.)

ilica (SiO_2), which has
ntainer is charged to an
e decreases with time?

silica container of pre-



Assumptions:

1. Since $D \gg L$, diffusion may be approximated as being one-dimensional through a plane wall.
2. Quasisteady diffusion (pressure variation is sufficiently slow to permit assuming steady-state conditions for diffusion through the fused silica at any instant).
3. Stationary medium has uniform density ρ.
4. Pressure of helium in outside air is negligible.
5. Helium exhibits ideal gas behavior.

Properties: Table A.8, helium-fused silica (293 K): $D_{AB} = 0.4 \times 10^{-13}$ m^2/s. Table A.10, helium-fused silica (293 K): $S = 0.45 \times 10^{-3}$ kmol/m$^3 \cdot$ bar.

Analysis: The rate of change of the helium pressure may be obtained by applying the species conservation requirement, Equation 14.43, to a control volume about the helium. It follows that

$$-\dot{M}_{A,out} = \dot{M}_{A,st}$$

or, since the helium outflow is due to diffusion through the fused silica,

$$\dot{M}_{A,out} = n''_{A,x} A$$

and the change in mass storage is

$$\dot{M}_{A,st} = \frac{dM_A}{dt} = \frac{d(\rho_A V)}{dt}$$

the species balance reduces to

$$-n''_{A,x} A = \frac{d(\rho_A V)}{dt}$$

Recognizing that $\rho_A = \mathcal{M}_A C_A$ and applying the ideal gas law

$$C_A = \frac{p_A}{\mathcal{R}T}$$

the species balance becomes

$$\frac{dp_A}{dt} = -\frac{\mathcal{R}T}{\mathcal{M}_A V} A n''_{A,x}$$

For a stationary medium the absolute flux of species A through the fused silica is equal to the diffusion flux, $n''_{A,x} = j_{A,x}$, in which case, from Fick's law, Equation 14.12,

$$n''_{A,x} = -\rho D_{AB} \frac{dm_A}{dx} = -D_{AB} \frac{d\rho_A}{dx}$$

or, for the assumed conditions,

$$n''_{A,x} = D_{AB} \frac{\rho_{A,1} - \rho_{A,2}}{L}$$

The species densities $\rho_{A,1}$ and $\rho_{A,2}$ pertain to conditions *within* the fused silica at its inner and outer surfaces, respectively, and may be evaluated from knowledge of the solubility through Equation 14.62. Hence with $\rho_A = \mathcal{M}_A C_A$,

$$\rho_{A,1} = \mathcal{M}_A S p_{A,i} = \mathcal{M}_A S p_A \qquad \text{and} \qquad \rho_{A,2} = \mathcal{M}_A S p_{A,o} = 0$$

Patent Owner Manufacturing Resources International, Inc.
Exhibit 2017 - Page 908 of 999

where $p_{A,i}$ and $p_{A,o}$ are helium pressures at the inner and outer surfaces, respectively. Hence

$$n''_{A,x} = \frac{D_{AB}\mathcal{M}_A S p_A}{L}$$

and substituting into the species balance it follows that

$$\frac{dp_A}{dt} = -\frac{\mathcal{R}TAD_{AB}S}{LV}p_A$$

or with $A = \pi D^2$ and $V = \pi D^3/6$

$$\frac{dp_A}{dt} = -\frac{6\mathcal{R}TD_{AB}S}{LD}p_A$$

Substituting numerical values, the rate of change of the pressure is

$$\frac{dp_A}{dt} = [-6(0.08314\ \text{m}^3 \cdot \text{bar/kmol} \cdot \text{K})\ 293\ \text{K}\ (0.4 \times 10^{-13}\ \text{m}^2/\text{s}) \times 0.45 \times 10^{-3}\ \text{kmol/m}^3 \cdot \text{bar} \times 4\ \text{bar}] \div [0.002\ \text{m}\ (0.2\ \text{m})]$$

$$\frac{dp_A}{dt} = -2.63 \times 10^{-8}\ \text{bar/s} \quad \triangleleft$$

Comments: The foregoing result provides the initial (maximum) leakage rate for the system. The leakage rate decreases as the inside pressure decreases.

EXAMPLE 14.5

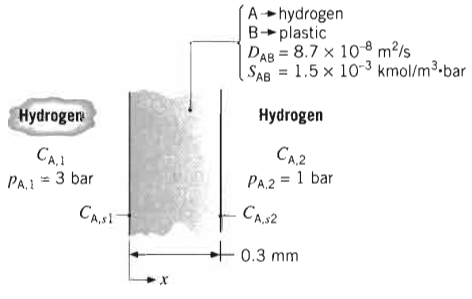
Hydrogen gas is maintained at 3 bars and 1 bar on opposite sides of a plastic membrane, which is 0.3 mm thick. The temperature is 25°C, and the binary diffusion coefficient of hydrogen in the plastic is 8.7×10^{-8} m^2/s. The solubility of hydrogen in the membrane is 1.5×10^{-3} kmol/m^3 · bar. What is the mass diffusive flux of hydrogen through the membrane?

SOLUTION

Known: Pressure of hydrogen on opposite sides of a membrane.

Find: The hydrogen mass diffusive flux $n''_{A,x}$ (kg/s · m^2).

Schematic:



Patent Owner Manufacturing Resources International, Inc.
Exhibit 2017 - Page 909 of 999

Assumptions:

1. Steady-state, one-dimensional conditions exist.
2. Membrane is a stationary, nonreacting medium of uniform total molar concentration.

Analysis: For the prescribed conditions, Equation 14.42 reduces to Equation 14.53, which may be expressed as

$$N''_{A,x} = CD_{AB}\frac{x_{A,s1} - x_{A,s2}}{L} = \frac{D_{AB}}{L}(C_{A,s1} - C_{A,s2})$$

The surface molar concentrations of hydrogen may be obtained from Equation 14.62, where

$$C_{A,s1} = 1.5 \times 10^{-3}\,\text{kmol/m}^3 \cdot \text{bar} \times 3\,\text{bars} = 4.5 \times 10^{-3}\,\text{kmol/m}^3$$
$$C_{A,s2} = 1.5 \times 10^{-3}\,\text{kmol/m}^3 \cdot \text{bar} \times 1\,\text{bar} = 1.5 \times 10^{-3}\,\text{kmol/m}^3$$

Hence

$$N''_{A,x} = \frac{8.7 \times 10^{-8}\,\text{m}^2/\text{s}}{0.3 \times 10^{-3}\,\text{m}}(4.5 \times 10^{-3} - 1.5 \times 10^{-3})\,\text{kmol/m}^3$$
$$N''_{A,x} = 8.7 \times 10^{-7}\,\text{kmol/s} \cdot \text{m}^2$$

On a mass basis,

$$n''_{A,x} = N''_{A,x}\mathcal{M}_A$$

where the molecular weight of hydrogen is 2 kg/kmol. Hence

$$n''_{A,x} = 8.7 \times 10^{-7}\,\text{kmol/s} \cdot \text{m}^2 \times 2\,\text{kg/kmol} = 1.74 \times 10^{-6}\,\text{kg/s} \cdot \text{m}^2 \quad \triangleleft$$

Comments: The molar concentrations of hydrogen in the gas phase, $C_{A,1}$ and $C_{A,2}$, differ from the surface concentrations in the membrane and may be calculated from the ideal gas equation of state

$$C_A = \frac{p_A}{\mathcal{R}T}$$

where $\mathcal{R} = 8.314 \times 10^{-2}\,\text{m}^3 \cdot \text{bar/kmol} \cdot \text{K}$. It follows that $C_{A,1} = 0.121\,\text{kmol/m}^3$ and $C_{A,2} = 0.040\,\text{kmol/m}^3$. Even though $C_{A,s2} < C_{A,2}$, hydrogen transport will occur from the membrane to the gas at $p_{A,2} = 1$ bar. This seemingly anomalous result may be explained by recognizing that the two concentrations are based on *different* volumes; in one case the concentration is per unit volume of the membrane and in the other case it is per unit volume of the adjoining gas phase. For this reason it is not possible to infer the direction of hydrogen transport from a simple comparison of the numerical values of $C_{A,s2}$ and $C_{A,2}$.

14.5.3 Catalytic Surface Reactions

Many mass transfer problems involve specification of the species flux, rather than the species concentration, at a surface. One such problem relates to the process of catalysis, which involves the use of special surfaces to promote *heterogeneous*

Patent Owner Manufacturing Resources International, Inc.
Exhibit 2017 - Page 910 of 999

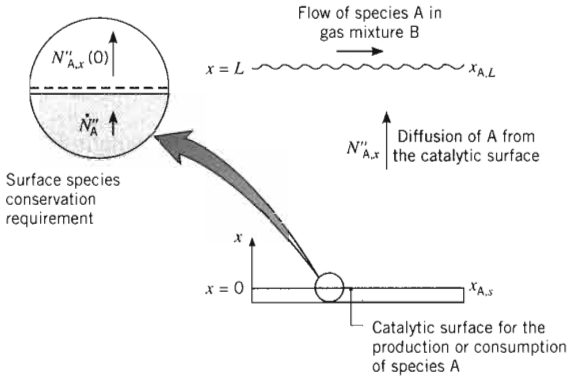


FIGURE 14.7 One-dimensional diffusion with heterogeneous catalysis.

chemical reactions. A heterogeneous chemical reaction occurs at the surface of a material, can be viewed as a *surface phenomenon*, and can be treated as a boundary condition.[6] Often a one-dimensional diffusion analysis may be used to *approximate* the performance of a catalytic reactor.

Consider the system of Figure 14.7. A catalytic surface is placed in a gas stream to promote a heterogeneous chemical reaction involving species A. Assume that the reaction produces species A at a rate $\dot{N}''_A$, which is defined as the molar rate of production per unit surface area of the catalyst. Once steady-state conditions are reached, the rate of species transfer from the surface, $N''_{A,x}$, must equal the surface reaction rate:

$$N''_{A,x}(0) = \dot{N}''_A \tag{14.63}$$

It is also assumed that species A leaves the surface as a result of one-dimensional transfer through a thin film of thickness L and that no reactions occur within the film itself. Although bulk motion influences transfer of A through the film, it is reasonable to assume, as a first estimate, that the effect is negligible and that transfer occurs exclusively by diffusion. The mole fraction of A at $x = L$, $x_{A,L}$, corresponds to conditions in the mainstream of the mixture and is presumed to be known. Representing the remaining species of the mixture as a single species B and assuming the medium to be stationary, Equation 14.48a reduces to

$$\frac{d}{dx}\left(CD_{AB}\frac{dx_A}{dx}\right) = 0 \tag{14.64}$$

where D_{AB} is the binary diffusion coefficient for A in B and B may be a multicomponent mixture. Assuming C and D_{AB} to be constant, Equation 14.64 may be solved subject to the conditions that

$$x_A(L) = x_{A,L}$$

[6]The generation terms that appear in Equations 14.47 through 14.50 are due to chemical reactions that occur *volumetrically*. These volumetric reactions are referred to as *homogeneous chemical reactions* and will be treated in Section 14.6.

Patent Owner Manufacturing Resources International, Inc.
Exhibit 2017 - Page 911 of 999

and

$$N''_{A,x}(0) = -CD_{AB}\frac{dx_A}{dx}\bigg|_{x=0} = \dot{N}''_A \tag{14.65}$$

This expression follows from Equation 14.63 and the substitution of Fick's law, Equation 14.42.

For a catalytic surface, the surface reaction rate $\dot{N}''_A$ generally depends on the surface concentration $C_A(0)$. For a *first-order reaction* that results in species consumption at the surface, the reaction rate is of the form

$$\dot{N}''_A = -k''_1 C_A(0) \tag{14.66}$$

where k''_1 (m/s) is the reaction rate constant. Accordingly, the surface boundary condition, Equation 14.65, reduces to

$$-D_{AB}\frac{dx_A}{dx}\bigg|_{x=0} = -k''_1 x_A(0) \tag{14.67}$$

Solving Equation 14.64 subject to the above conditions, it is readily verified that the concentration distribution is linear and of the form

$$\frac{x_A(x)}{x_{A,L}} = \frac{1 + (xk''_1/D_{AB})}{1 + (Lk''_1/D_{AB})} \tag{14.68}$$

At the catalytic surface this result reduces to

$$\frac{x_A(0)}{x_{A,L}} = \frac{1}{1 + (Lk''_1/D_{AB})} \tag{14.69}$$

and the molar flux is

$$N''_A(0) = -CD_{AB}\frac{dx_A}{dx}\bigg|_{x=0} = -k''_1 C x_A(0)$$

or

$$N''_A(0) = -\frac{k''_1 C x_{A,L}}{1 + (Lk''_1/D_{AB})} \tag{14.70}$$

The negative sign implies mass transfer *to* the surface.

Two limiting cases of the foregoing results are of special interest. For the limit $k''_1 \to 0$, $(Lk''_1/D_{AB}) \ll 1$ and Equations 14.69 and 14.70 reduce to

$$\frac{x_{A,s}}{x_{A,L}} \approx 1 \qquad \text{and} \qquad N''_A(0) \approx -k''_1 C x_{A,L}$$

In such cases the rate of reaction is controlled by the reaction rate constant, and the limitation due to diffusion is negligible. The process is said to be *reaction limited.* Conversely, for the limit $k''_1 \to \infty$, $(Lk''_1/D_{AB}) \gg 1$ and Equations 14.69 and 14.70 reduce to

$$x_{A,s} \approx 0 \qquad \text{and} \qquad N''_A(0) \approx -\frac{CD_{AB}x_{A,L}}{L}$$

In this case the reaction is controlled by the rate of diffusion to the surface, and the process is said to be *diffusion limited.*

Patent Owner Manufacturing Resources International, Inc.
Exhibit 2017 - Page 912 of 999

14.6 *Mass Diffusion with Homogeneous Chemical Reactions*

Just as heat diffusion may be influenced by internal sources of energy, species transfer by diffusion may be influenced by homogeneous chemical reactions. We restrict our attention to stationary media, in which case Equation 14.41 or 14.42 determines the absolute species flux. If we also assume steady, one-dimensional transfer in the x direction and that D_{AB} and C are constant, Equation 14.48b reduces to

$$D_{AB}\frac{d^2C_A}{dx^2} + \dot{N}_A = 0 \tag{14.71}$$

The volumetric production rate, $\dot{N}_A$, is often described using one of the following forms.

Zero-Order Reaction:

$$\dot{N}_A = k_0$$

First-Order Reaction:

$$\dot{N}_A = k_1 C_A$$

That is, the reaction may occur at a constant rate (zero order) or at a rate that is proportional to the local concentration (first order). The units of k_0 and k_1 are kmol/s · m^3 and s^{-1}, respectively. If $\dot{N}_A$ is positive, the reaction results in the generation of species A; if it is negative, it results in the consumption of A.

In many applications the species of interest is converted to another form through a first-order chemical reaction, and Equation 14.71 becomes

$$D_{AB}\frac{d^2C_A}{dx^2} - k_1 C_A = 0 \tag{14.72}$$

This linear, homogeneous differential equation has the general solution

$$C_A(x) = C_1 e^{mx} + C_2 e^{-mx} \tag{14.73}$$

where $m = (k_1/D_{AB})^{1/2}$ and the constants C_1 and C_2 depend on the prescribed boundary conditions. The form of this equation is identical to that characterizing heat conduction in an extended surface, Equation 3.66.

Consider the situation illustrated in Figure 14.8. Gas A is soluble in liquid B, where it is transferred by diffusion and experiences a first-order chemical reaction. The solution is dilute, and the concentration of A in the liquid at the interface is a known constant $C_{A,0}$. If the bottom of the container is impermeable to A, the boundary conditions are

$$C_A(0) = C_{A,0} \qquad \text{and} \qquad \left.\frac{dC_A}{dx}\right|_{x=L} = 0$$

These species boundary conditions are analogous to the thermal boundary conditions of case B in Table 3.4. Since Equation 14.73 is of the same form as Equation 3.66, it follows that

Patent Owner Manufacturing Resources International, Inc.
Exhibit 2017 - Page 913 of 999

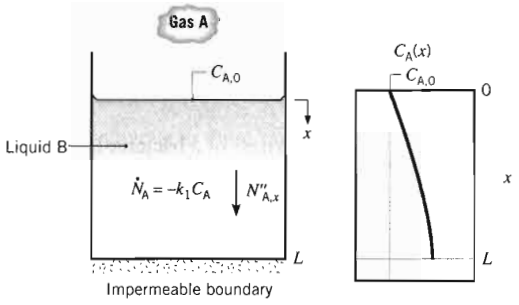


FIGURE 14.8
Diffusion and homogeneous reaction of gas A in liquid B.

$$C_A(x) = C_{A,0}\frac{\cosh m(L-x)}{\cosh mL} \tag{14.74}$$

Quantities of special interest are the concentration of A at the bottom and the flux of A across the gas–liquid interface. Applying Equation 14.74 at $x = L$, we obtain

$$C_A(L) = \frac{C_{A,0}}{\cosh mL} \tag{14.75}$$

Moreover,

$$N''_{A,x}(0) = -D_{AB}\left.\frac{dC_A}{dx}\right|_{x=0}$$

$$= D_{AB}C_{A,0}m\left.\frac{\sinh m(L-x)}{\cosh mL}\right|_{x=0}$$

or

$$N''_{A,x}(0) = D_{AB}C_{A,0}\,m\tanh mL \tag{14.76}$$

Results for a container with its bottom held at a fixed concentration or an infinitely deep container may be obtained by analogy to cases C and D, respectively, of Table 3.4.

EXAMPLE 14.6

Biofilms, which are colonies of bacteria that can cling to living or inert surfaces, can cause a wide array of human infections. Infections caused by bacteria living within biofilms are often chronic because antibiotics that are applied to the surface of a biofilm have difficulty penetrating through the film thickness. Consider a biofilm that is associated with a skin infection. An antibiotic (species A) is applied to the top layer of a biofilm (species B) so that a fixed concentration of medication, $C_{A,0} = 4 \times 10^{-3}$ kmol/m^3, exists at the upper surface of the biofilm. The diffusion coefficient of the medication within the biofilm is $D_{AB} = 2 \times 10^{-12}$ m^2/s. The antibiotic is consumed by biochemical reactions within the film, and the consumption rate depends on the local concentration of medication expressed as $\dot{N}_A = -k_1 C_A$ where $k_1 = 0.1$ s^{-1}. To eradicate the bacteria, the antibiotic must be consumed at a rate of at least 0.2×10^{-3} kmol/s · m^3 ($\dot{N}_A \leq -0.2 \times 10^{-3}$ kmol/s · m^3) since, at smaller absolute consumption rates, the bacteria will be able to grow back faster than it is destroyed. Determine the maximum thickness of a biofilm, L, that may be treated successfully by the antibiotic.

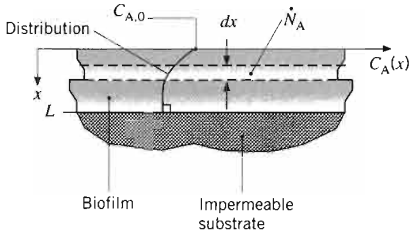
Patent Owner Manufacturing Resources International, Inc.
Exhibit 2017 - Page 914 of 999

SOLUTION

Known: Topical antibiotic and biofilm properties, surface concentration of the medication, and required minimum consumption rate of antibiotic.

Find: Maximum thickness of a bacteria-laden biofilm, L, that may be successfully treated.

Schematic:



Assumptions:

1. Steady-state, one-dimensional conditions.
2. Stationary, homogeneous medium.
3. Constant properties.
4. Impermeable bottom of the biofilm.

Analysis: The absolute antibiotic consumption rate will be smallest at $x = L$, where the antibiotic concentration is smallest. Thus, we require $\dot{N}_A(L) = -0.2 \times 10^{-3}$ kmol/s · m^3. The expression for the first-order reaction may be combined with Equation 14.74 to write

$$\dot{N}_A(L) = -k_1 C_A(L) = -k_1 \frac{C_{A,0}}{\cosh mL} \tag{1}$$

where

$$m = (k_1/D_{AB})^{1/2} = \left(\frac{0.1\ \text{s}^{-1}}{2 \times 10^{-12}\ \text{m}^2/\text{s}}\right)^{1/2} = 2.24 \times 10^5\ \text{m}^{-1}$$

Equation 1 may be solved for the maximum allowable thickness:

$$L = m^{-1} \cosh^{-1}[-k_1 C_{A,0}/\dot{N}_A(L)] \tag{2}$$

Substituting values into Equation 2 yields

$$L = (2.24 \times 10^5\ \text{m}^{-1})^{-1} \cosh^{-1}[-0.1\ \text{s}^{-1} \times 4 \times 10^{-3}\ \text{kmol/m}^3/(-0.2 \times 10^{-3}\ \text{kmol/s} \cdot \text{m}^3)]$$
$$= 5.9 \times 10^{-6}\ \text{m} = 5.9\ \mu\text{m} \quad \triangleleft$$

Comment: The ability of the antibiotic agent to kill bacteria in thicker biofilms is hampered by the high rate at which the agent is consumed and the slow rate at which it can be diffused through the complex, polymeric matrix of the biofilm [6].

14.7 Transien

Patent Owner Manufacturing Resources International, Inc.
Exhibit 2017 - Page 915 of 999

14.7 *Transient Diffusion*

Results analogous to those of Chapter 5 may be obtained for the transient diffusion of a dilute species A in a stationary medium. Assuming no homogeneous reactions, constant D_{AB} and C, and one-dimensional transfer in the x direction, Equation 14.48b reduces to

$$D_{AB}\frac{\partial^2 C_A}{\partial x^2} = \frac{\partial C_A}{\partial t} \tag{14.77}$$

Assuming an initial uniform concentration,

$$C_A(x, 0) = C_{A,i} \tag{14.78}$$

Equation 14.77 may be solved for boundary conditions that depend on the particular geometry and surface conditions. If, for example, the geometry is a plane wall of thickness $2L$ with surface convection, the boundary conditions are

$$\left.\frac{\partial C_A}{\partial x}\right|_{x=0} = 0 \tag{14.79}$$

$$C_A(L, t) = C_{A,s} \tag{14.80}$$

Equation 14.79 describes the symmetry requirement at the midplane. Equation 14.80 represents the surface convection condition if the *mass transfer Biot number*, $Bi_m = h_m L/D_{AB}$, is much larger than unity. In this case the resistance to species transfer by diffusion in the medium is much larger than the resistance to species transfer by convection at the surface. If this situation is taken to the limit of $Bi_m \to \infty$, or $Bi_m^{-1} \to 0$, it follows that the species concentration in the fluid is essentially uniform, equal to the free stream species concentration. Then $C_{A,s}$, the species concentration in the medium at its surface, can be found from Equation 14.60 or 14.61, where p_A is the free stream partial pressure of species A.

The analogy between heat and mass transfer may conveniently be applied if we nondimensionalize the above equations. Introducing a dimensionless concentration and time, as follows,

$$\gamma^* \equiv \frac{\gamma}{\gamma_i} = \frac{C_A - C_{A,s}}{C_{A,i} - C_{A,s}} \tag{14.81}$$

$$t_m^* \equiv \frac{D_{AB}t}{L^2} \equiv Fo_m \tag{14.82}$$

and substituting into Equation 14.77, we obtain

$$\frac{\partial^2 \gamma^*}{\partial x^{*2}} = \frac{\partial \gamma^*}{\partial Fo_m} \tag{14.83}$$

where $x^* = x/L$. Similarly, the initial and boundary conditions are

$$\gamma^*(x^*, 0) = 1 \tag{14.84}$$

$$\left.\frac{\partial \gamma^*}{\partial x^*}\right|_{x^*=0} = 0 \tag{14.85}$$

Patent Owner Manufacturing Resources International, Inc.
Exhibit 2017 - Page 916 of 999

and

$$\gamma^*(1, t_m^*) = 0 \tag{14.86}$$

One need only compare Equations 14.83 through 14.86 with Equations 5.34 through 5.36 and Equation 5.37 for the case of $Bi \rightarrow \infty$ to confirm the existence of the analogy. Note that for $Bi \rightarrow \infty$, Equation 5.37 reduces to $\theta^*(1, t^*) = 0$, which is analogous to Equation 14.86. Hence the two systems of equations must have equivalent solutions.

The correspondence between variables for transient heat and mass diffusion is summarized in Table 14.2. From this correspondence it is possible to use many of the previous heat transfer results to solve transient mass diffusion problems. For example, replacing θ_o^* and Fo by γ_o^* and Fo_m, Equation 5.41 could be used, with $Bi \rightarrow \infty$ ($\zeta_1 = 1.5707$; $C_1 = 1.2733$), to determine the midplane concentration $C_{A,o}$. The remaining equations may be applied in a similar fashion, along with results obtained for the semi-infinite solid.

The results of Sections 5.5 and 5.6 should be used with care because, as illustrated in Example 14.1 and in Table A.8, the mass diffusivities associated with many liquid and solid host media are extremely small relative to their thermal diffusivities. Therefore, values of the mass transfer Fourier number, Fo_m, are usually many orders of magnitude smaller than the values of the heat transfer Fourier number, Fo. Hence, the *approximate solutions* of Sections 5.5.2 and 5.6.2 are often of little value in analyzing mass transfer within stationary media, since the approximate solutions are valid only for $Fo_m > 0.2$. Recourse to solution of the *exact expressions* of Sections 5.5.1 and 5.6.1 may be required. The infinite series solutions of Equations 5.39, 5.47, and 5.48 may necessitate evaluation of many terms before convergence is obtained. The semi-infinite solid solutions of Section 5.7, on the other hand, are often applicable in mass transfer problems because of the slow diffusion rates of boundary condition information into the host medium. The approximate results of Section 5.8 are also applicable, since results are presented over the entire Fourier number range.

TABLE 14.2 Correspondence Between Heat and Mass Transfer Variables for Transient Diffusion

Heat Transfer	Mass Transfer
$\theta^* = \dfrac{T - T_\infty}{T_i - T_\infty}$	$\gamma^* = \dfrac{C_A - C_{A,s}}{C_{A,i} - C_{A,s}}$
$1 - \theta^* = \dfrac{T - T_i}{T_\infty - T_i}$	$1 - \gamma^* = \dfrac{C_A - C_{A,i}}{C_{A,s} - C_{A,i}}$
$Fo = \dfrac{\alpha t}{L^2}$	$Fo_m = \dfrac{D_{AB} t}{L^2}$
$Bi = \dfrac{hL}{k}$	$Bi_m = \dfrac{h_m L}{D_{AB}}$
$\dfrac{x}{2\sqrt{\alpha t}}$	$\dfrac{x}{2\sqrt{D_{AB} t}}$

Patent Owner Manufacturing Resources International, Inc.
Exhibit 2017 - Page 917 of 999

(14.86)

Equations 5.34
the existence of
$f^*) = 0$, which is
must have equiv-

mass diffusion is
o use many of the
ems. For example,
with $Bi \rightarrow \infty$ ($\zeta_1 =$
$_{A,o}$. The remaining
s obtained for the

because, as illus-
ociated with many
ermal diffusivities.
sually many orders
umber, *Fo*. Hence,
little value in ana-
mate solutions are
essions of Sections
quations 5.39, 5.47,
rgence is obtained.
are often applicable
boundary condition
Section 5.8 are also
ber range.

EXAMPLE 14.7

Transdermal drug delivery involves the controlled time-release of medication through the skin to the bloodstream, usually from a *patch* that is adhered to the body. Advantages include steady and mild drug delivery rates that reduce shock to the system as might occur with intravenous infusions, the ability to deliver medication to nauseated or unconscious patients that would be otherwise delivered in oral form, and ease of use.

Consider a square patch of length and width $L = 50$ mm that consists of a host medium containing an initial, uniform density of medication, $\rho_{A,p,i} = 100$ kg/m^3. The patch is applied to the skin, which contains an initial drug concentration of $\rho_{A,s,i} = 0$. At the patch–skin interface located at $x = 0$, the ratio of the medication density on the patch side to the medication density on the patient side is described by a *partition coefficient* of $K = 0.5$.

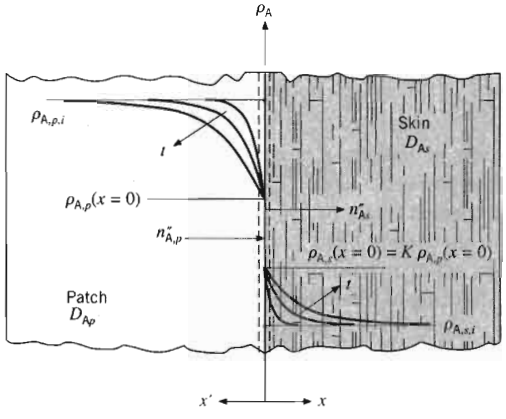
1. Determine the total amount of medication (dosage) delivered to the patient over a treatment period of one week. Nominal values of the diffusion coefficients of the medication within the patch and skin are $D_{Ap} = 0.1 \times 10^{-12}$ m^2/s and $D_{As} = 0.2 \times 10^{-12}$ m^2/s, respectively.
2. Investigate the sensitivity of the total dosage delivered to the patient to the mass diffusivity of the patch, D_{Ap}, and the mass diffusivity of the patient's skin, D_{As}.

SOLUTION

Known: Initial densities of a drug within a transdermal patch, size of the patch, partition coefficient, and mass diffusivities.

Find: Total dosage of medicine delivered to the patient over a one-week time period, sensitivity of the dosage to the mass diffusivity of the patch and skin.

Schematic:



Assumptions:

1. One-dimensional conditions with constant properties.
2. Semi-infinite patch and skin.
3. No chemical reactions.
4. Stationary media.

Patent Owner Manufacturing Resources International, Inc.
Exhibit 2017 - Page 918 of 999

Analysis:

1. The conservation of species equation applies to both the patch and skin. With the foregoing assumptions, Equation 14.47b becomes

$$\frac{\partial^2 \rho_A}{\partial x^2} = \frac{1}{D_{AB}} \frac{\partial \rho_A}{\partial t}$$

which is analogous to Equation 5.26. Moreover, the initial conditions

$$\rho_A(x < 0,\ t = 0) = \rho_{A,p,i}; \quad \rho_A(x > 0,\ t = 0) = \rho_{A,s,i}$$

boundary conditions

$$\rho_{A,p}(x \to -\infty) = \rho_{A,p,i}; \quad \rho_{A,s}(x \to +\infty) = \rho_{A,s,i} \tag{1a}$$

and interface condition

$$n''_{A,x,p}(x = 0) = n''_{A,x,s}(x = 0) \tag{1b}$$

are analogous to the situation in Figure 5.9 and Equation 5.61 where two semi-infinite solids are brought into thermal contact. In this problem, the partitioning of the species must also be accounted for. That is,

$$\rho_{A,s}(x = 0) = K \cdot \rho_{A,p}(x = 0) \tag{1c}$$

By analogy to Equation 5.62, we have

$$\frac{-D_{Ap}(\rho_{A,p}(x = 0) - \rho_{A,p,i})}{\sqrt{\pi D_{Ap} t}} = \frac{D_{As}(\rho_{A,s}(x = 0) - \rho_{A,s,i})}{\sqrt{\pi D_{As} t}}$$

which, after noting that $\rho_{A,s,i} = 0$, may be solved to yield

$$\rho_{A,s}(x = 0) = \rho_{A,p,i}\left(\frac{\sqrt{D_{Ap}}}{\sqrt{D_{As}} + \sqrt{D_{Ap}}/K}\right) \tag{2}$$

The instantaneous flux of medication to the patient may be determined by noting the analogy with Equation 5.58:

$$n''_A(x = 0,t) = \frac{D_{As}\rho_{A,s}(x = 0)}{\sqrt{\pi D_{As} t}} \tag{3}$$

Substituting Equation 2 into Equation 3 yields

$$n''_A(x = 0,t) = \frac{\rho_{A,p,i}}{\sqrt{\pi t}} \cdot \frac{\sqrt{D_{As} D_{Ap}}}{\sqrt{D_{As}} + \sqrt{D_{Ap}}/K}$$

The dosage, D, delivered to the patient from $t = 0$ to a treatment time of t_t may be expressed as

$$D = L^2 \int_{t=0}^{t_t} n''_A(x = 0,t)dt$$

$$D = \frac{\rho_{A,p,i} L^2}{\sqrt{\pi}} \cdot \frac{\sqrt{D_{As} D_{Ap}}}{\sqrt{D_{As}} + \sqrt{D_{Ap}}/K} \int_{t=0}^{t_t} t^{-1/2} dt$$

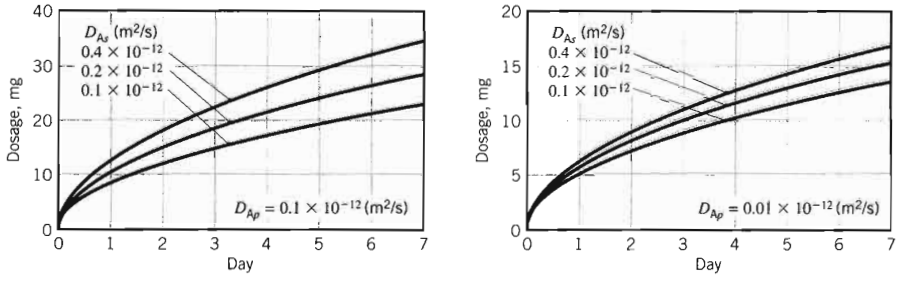
$$= \frac{2\rho_{A,p,i} L^2}{\sqrt{\pi}} \cdot \frac{\sqrt{D_{As} D_{Ap}}}{\sqrt{D_{As}} + \sqrt{D_{Ap}}/K} \sqrt{t_t} \tag{4}$$

Patent Owner Manufacturing Resources International, Inc.
Exhibit 2017 - Page 919 of 999

For a total treatment time of $t_t = 7$ days $\times$ 24 h/day $\times$ 3600 s/h $= 605 \times 10^3$ s, the dosage is

$$D = \frac{2 \times 100 \text{ kg/m}^3 \times (50 \times 10^{-3} \text{ m})^2}{\sqrt{\pi}} \times \frac{\sqrt{0.2 \times 10^{-12} \text{ m}^2/\text{s} \times 0.1 \times 10^{-12} \text{ m}^2/\text{s}}}{\sqrt{0.2 \times 10^{-12} \text{ m}^2/\text{s}} + \sqrt{0.1 \times 10^{-12} \text{ m}^2/\text{s}}/0.5} \sqrt{605 \times 10^3 \text{ s}}$$
$$= 29 \times 10^{-6} \text{ kg} = 29 \text{ mg} \quad \triangleleft$$

2. The sensitivity of the dosage to the patch and skin mass diffusivities may be evaluated by solving Equation 4 for different combinations of D_{Ap} and D_{As}. Results are shown in the following graphs for $D_{Ap} = 0.1 \times 10^{-12}$ m^2/s and 0.01×10^{-12} m^2/s and for $D_{As} = 0.1 \times 10^{-12}$ m^2/s, 0.2×10^{-12} m^2/s, and 0.4×10^{-12} m^2/s. Note that as either mass diffusivity is increased, the dosage increases.



Comments:

1. The function of the outer layer of the skin, the *epidermis,* is to protect the body from external contamination. Transdermal drug delivery is feasible only for medications characterized by extremely small molecules that can diffuse through the relatively impenetrable epidermis. Mass transfer considerations restrict the number of drugs that can be delivered transdermally. The skin diffusivity is variable from location to location on the body, and the patient is instructed where to apply the patch.
2. It is desirable to desensitize the dosage to variations in the skin diffusivity, since this parameter varies from patient to patient. Therefore, the host medium of the patch (called the *vehicle*) is designed so that it is the rate-limiting factor in controlling the dosage. The sensitivity of the dosage to the patient's skin diffusivity is reduced by decreasing the mass diffusivity in the vehicle, as evident by comparing the results of part 2 of the problem. In general, it is desirable to design the vehicle so that $D_{Ap}/D_{As} \ll 1$.
3. The patch is designed to deliver medication as though it is a semi-infinite medium. The required patch thickness for this assumption to be valid may be estimated by calculating the location where the density of the medication in the vehicle is reduced to 95% of the difference between $\rho_{A,p,i}$ and $\rho_{A,p}(x = 0)$ over the treatment time. By analogy to Equation 5.57, the *species penetration depth*, x_S, associated with 5% depletion of the drug may be determined from

$$\frac{\rho_{A,p}(x') - \rho_{A,p}(x' = 0)}{\rho_{A,p,i} - \rho_{A,p}(x' = 0)} = 0.95 = \text{erf} \frac{x_S}{\sqrt{4 D_{Ap} t_t}}$$

Patent Owner Manufacturing Resources International, Inc.
Exhibit 2017 - Page 920 of 999

Evaluating this expression yields a species penetration depth of 690×10^{-6} m = 0.69 mm. The assumption of a semi-infinite patch is valid for a vehicle thickness greater than 0.69 mm.

4. If the vehicle is much thinner than the species penetration depth calculated in Comment 3, the actual dosage will fall below the desired dosage prior to the end of the one-week treatment period. Therefore, a tradeoff in the design of the patch involves (a) loading enough medication to assure semi-infinite behavior and (b) minimizing the cost of the patch. In practice, more than 95% of the medication remains in the vehicle after the treatment period, necessitating careful disposal of the patch after its use.

14.8 Summary

In this chapter we focused on the analysis of species transfer by diffusion. Although transfer rates are generally small, particularly in liquids and solids, the process is germane to many technologies, as well as to the environmental and life sciences. You should test your understanding of fundamental issues by addressing the following questions.

- If a cube of sugar is placed in a cup of coffee, what is the driving potential for dispersion of the sugar in the coffee? What is the physical mechanism responsible for dispersion if the coffee is stagnant? What is the physical mechanism if the coffee is stirred?
- What is the relationship between the molar concentration and the mass density of a species in a mixture?
- How is the mass density of a mixture defined? The molar concentration of the mixture?
- In using *Fick's law* to determine the mass or molar flux of a species in a mixture, what specifically is being determined?
- Under what conditions does the species diffusion flux equal the absolute flux associated with transport of the species?
- What is the stationary medium approximation?
- Is the species flux N''_A independent of location for a stationary medium within which there is species transfer by diffusion and production (or consumption) by a homogeneous chemical reaction?
- Under what conditions may a diffusion resistance be used to determine the species flux from knowledge of the species concentrations at the inner and outer surfaces of a medium?
- In heat transfer, equilibrium dictates equivalent temperatures on the gas and liquid (or solid) sides of an interface between the two phases. Can the same be said about the concentration of a chemical species present in the gas and liquid (or solid) phases?

Referen

1. Bird, R. E
2. Bird, R. E *Phenome*
3. Hirschfelc *Theory of*
4. Skelland, Malabar,

Problem

Mixture C

14.1 Assur N_2, w what

14.2 A mix each s late th fractic

14.3 A He helium applic spheri and th ular capac

14.4 Consi

(a) D ti ti s n

Patent Owner Manufacturing Resources International, Inc.
Exhibit 2017 - Page 921 of 999

- What is *Henry's constant*? How does the concentration of a chemical species in a liquid vary with the partial pressure of the species in an adjoining gas? How does the concentration vary with the temperature of the liquid?
- What is the difference between a *homogeneous* and a *heterogeneous chemical reaction*?
- In heterogeneous catalysis, what is implied if the process is said to be *reaction limited*? What is implied if the process is said to be *diffusion limited?*
- What is a *zero-order reaction*? A *first-order reaction*?
- If convection mass transfer is associated with gas flow over a liquid or solid in which the gas is transferred by diffusion, what can be said about the ratio of convection to diffusion resistances? How is the *mass transfer Biot number* defined?
- In a transient diffusion process, what can be said about the mass transfer Biot number?

References

1. Bird, R. B., *Adv. Chem. Eng.*, **1,** 170, 1956.
2. Bird, R. B., W. E. Stewart, and E. N. Lightfoot, *Transport Phenomena,* 2nd ed. Wiley, New York, 2002.
3. Hirschfelder, J. O., C. F. Curtiss, and R. B. Bird, *Molecular Theory of Gases and Liquids,* Wiley, New York, 1964.
4. Skelland, A. H. P., *Diffusional Mass Transfer,* Krieger, Malabar, FL, 1985.
5. Poling, B. E., J. M. Prausnitz, and J. O'Connell, *The Properties of Gases and Liquids*, 5th ed., McGraw-Hill, New York, 2001.
6. Costerton, J. W., P. S. Stewart, and E. P. Greenberg, *Science*, **284**, 1318, 1999.

Problems

Mixture Composition

14.1 Assuming air to be composed exclusively of O_2 and N_2, with their partial pressures in the ratio 0.21:0.79, what are their mass fractions?

14.2 A mixture of CO_2 and N_2 is in a container at 25°C, with each species having a partial pressure of 1 bar. Calculate the molar concentration, the mass density, the mole fraction, and the mass fraction of each species.

14.3 A He-Xe mixture containing 0.75 mole fraction of helium is used for cooling of electronics in an avionics application. At a temperature of 300 K and atmospheric pressure, calculate the mass fraction of helium and the mass density, molar concentration, and molecular weight of the mixture. If the cooling system capacity is 10 liters, what is the mass of the coolant?

14.4 Consider an ideal gas mixture of n species.

(a) Derive an equation for determining the mass fraction of species i from knowledge of the mole fraction and the molecular weight of each of the n species. Derive an equation for determining the mole fraction of species i from knowledge of the mass fraction and the molecular weight of each of the n species.

(b) In a mixture containing equal mole fractions of O_2, N_2, and CO_2, what is the mass fraction of each species? In a mixture containing equal mass fractions of O_2, N_2, and CO_2, what is the mole fraction of each species?

Fick's Law and Mass Diffusivity

14.5 Consider air in a closed, cylindrical container with its axis vertical and with opposite ends maintained at different temperatures. Assume that the total pressure of the air is uniform throughout the container.

(a) If the bottom surface is colder than the top surface, what is the nature of conditions within the container? For example, will there be vertical gradients of the species (O_2 and N_2) concentrations? Is there any motion of the air? Does mass transfer occur?

(b) What is the nature of conditions within the container if it is inverted (i.e., the warm surface is now at the bottom)?

Patent Owner Manufacturing Resources International, Inc.
Exhibit 2017 - Page 922 of 999

14.6 Estimate values of the mass diffusivity D_{AB} for binary mixtures of the following gases at 350 K and 1 atm: ammonia–air and hydrogen–air.

14.7 A 100-mm-long, hollow iron cylinder is exposed to a 1000°C carburizing gas (a mixture of CO and CO_2) at its inner and outer surfaces of radii 4.30 and 5.70 mm, respectively. Consider steady-state conditions for which carbon diffuses from the inner surface of the iron wall to the outer surface and the total transport amounts to 3.6×10^{-3} kg of carbon over 100 hours. The variation of the carbon composition (weight % carbon) with radius is tabulated for selected radii.

r (mm)	4.49	4.66	4.79	4.91	5.16	5.27	5.40	5.53
Wt.C (%)	1.42	1.32	1.20	1.09	0.82	0.65	0.46	0.28

(a) Beginning with Fick's law and the assumption of a constant diffusion coefficient, D_{C-Fe}, show that $d\rho_C/d\,(\ln r)$ is a constant. Sketch the carbon mass density, $\rho_C(r)$, as a function of $\ln r$ for such a diffusion process.

(b) The foregoing table corresponds to measured distributions of the carbon mass density. Is D_{C-Fe} a constant for this diffusion process? If not, does D_{C-Fe} increase or decrease with an increasing carbon concentration?

(c) Using the experimental data, calculate and tabulate D_{C-Fe} for selected carbon compositions.

14.8 An old-fashioned glass apothecary jar contains a patent medicine. The neck is closed with a rubber stopper that is 20 mm tall, with a diameter of 10 mm at the bottom end, widening to 20 mm at the top end. The molar concentration of medicine vapor in the stopper is 2×10^{-3} kmol/m^3 at the bottom surface and is negligible at the top surface. If the mass diffusivity of medicine vapor in rubber is 0.2×10^{-9} m^2/s, find the rate (kmol/s) at which vapor exits through the stopper.

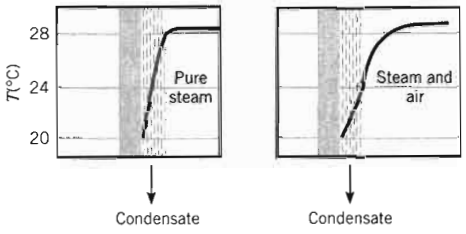
Nonstationary Media: Column Evaporation

14.9 Consider the evaporation of liquid A into a column containing a binary gas mixture of A and B. Species B cannot be absorbed in liquid A and the boundary conditions are the same as in Section 14.2.2. Show how the ratio of the molar-average velocity to the species velocity of A, $v_x^*/v_{A,x}$, varies with the mole fraction of species A.

14.10 An open pan of diameter 0.2 m and height 80 mm (above water at 27°C) is exposed to ambient air at 27°C and 25% relative humidity. Determine the evaporation rate, assuming that only mass diffusion occurs. Determine the evaporation rate, considering bulk motion.

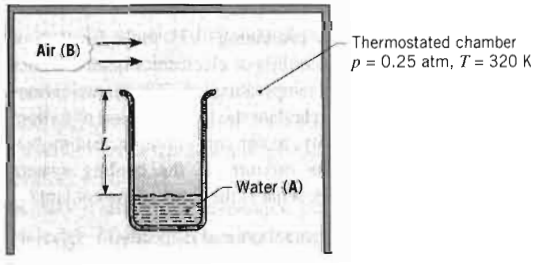
14.11 A spherical droplet of liquid A and radius r_o evaporates into a stagnant layer of gas B. Derive an expression for the evaporation rate of species A in terms of the saturation pressure of species A, $p_A(r_o) = p_{A,sat}$, the partial pressure of species A at an arbitrary radius r, $p_A(r)$, the total pressure p, and other pertinent quantities. Assume the droplet and the mixture are at a uniform pressure p and temperature T.

14.12 The presence of a small amount of air may cause a significant reduction in the heat rate to a water-cooled steam condenser surface. For a clean surface with pure steam and the prescribed conditions, the condensate rate is 0.020 kg/m$^2 \cdot$ s. With the presence of stagnant air in the steam, the condensate surface temperature drops from 28 to 24°C and the condensate rate is reduced by a factor of 2.



For the air–steam mixture, determine the partial pressure of air as a function of distance from the condensate film.

14.13 A laboratory apparatus to measure the diffusion coefficient of vapor–gas mixtures consists of a vertical, small-diameter column containing the liquid phase that evaporates into the gas flowing over the mouth of the column. The gas flow rate is sufficient to maintain a negligible vapor concentration at the exit plane. The column is 150 mm high, and the pressure and temperature in the chamber are maintained at 0.25 atm and 320 K, respectively.



For calibration purposes, you've been asked to calculate the expected evaporation rate (kg/h $\cdot$ m^2) for a test with water and air under the foregoing conditions, using the known value of D_{AB} for the vapor–air mixture.

Patent Owner Manufacturing Resources International, Inc.
Exhibit 2017 - Page 923 of 999

Stationary Media: Conservation of Species and Mass Diffusion Equation

14.14 Beginning with a differential control volume, derive the diffusion equation, on a molar basis, for species A in a three-dimensional (Cartesian coordinates), stationary medium, considering species generation with constant properties. Compare your result with Equation 14.48b.

14.15 Consider the radial diffusion of a gaseous species (A) through the wall of a plastic tube (B), and allow for chemical reactions that provide for the depletion of A at a rate $\dot{N}_A$ (kmol/s · m^3). Derive a differential equation that governs the molar concentration of species A in the plastic.

14.16 Beginning with a differential control volume, derive the diffusion equation, on a molar basis, for species A in a one-dimensional, spherical, stationary medium, considering species generation. Compare your result with Equation 14.50.

14.17 Gaseous hydrogen at 10 bars and 27°C is stored in a 100-mm-diameter spherical tank having a steel wall 2 mm thick. The molar concentration of hydrogen in the steel is 1.50 kmol/m^3 at the inner surface and negligible at the outer surface, while the diffusion coefficient of hydrogen in steel is approximately 0.3×10^{-12} m^2/s. What is the initial rate of mass loss of hydrogen by diffusion through the tank wall? What is the initial rate of pressure drop within the tank?

14.18 A thin plastic membrane is used to separate helium from a gas stream. Under steady-state conditions the concentration of helium in the membrane is known to be 0.02 and 0.005 kmol/m^3 at the inner and outer surfaces, respectively. If the membrane is 1 mm thick and the binary diffusion coefficient of helium with respect to the plastic is 10^{-9} m^2/s, what is the diffusive flux?

Discontinuous Concentrations at Interfaces

14.19 Consider the interface between atmospheric air and a body of water, both at 17°C.

(a) What are the mole and mass fractions of water at the air side of the interface? At the water side of the interface?

(b) What are the mole and mass fractions of oxygen at the air side of the interface? At the water side of the interface? The atmospheric air may be assumed to contain 20.5% oxygen by volume.

14.20 Oxygen gas is maintained at pressures of 2 bars and 1 bar on opposite sides of a rubber membrane that is 0.5 mm thick, and the entire system is at 25°C. What is the molar diffusive flux of O_2 through the membrane? What are the molar concentrations of O_2 on both sides of the membrane (outside the rubber)?

14.21 Insulation degrades (experiences an increase in thermal conductivity) if it is subjected to water vapor condensation. The problem may occur in home insulation during cold periods, when vapor in a humidified room diffuses through the dry wall (plaster board) and condenses in the adjoining insulation. Estimate the mass diffusion rate for a 3 m by 5 m wall, under conditions for which the vapor pressure is 0.03 bar in the room air and 0.0 bar in the insulation. The dry wall is 10 mm thick, and the solubility of water vapor in the wall material is approximately 5×10^{-3} kmol/m^3 · bar. The binary diffusion coefficient for water vapor in the dry wall is approximately 10^{-9} m^2/s.

14.22 Helium gas at 25°C and 4 bars is contained in a glass cylinder of 100-mm inside diameter and 5-mm thickness. What is the rate of mass loss per unit length of the cylinder?

14.23 Helium gas at 25°C and 4 bars is stored in a spherical Pyrex container of 200-mm inside diameter and 10-mm thickness. What is the rate of mass loss from the container?

14.24 Hydrogen at a pressure of 2 atm flows within a tube of diameter 40 mm and wall thickness 0.5 mm. The outer surface is exposed to a gas stream for which the hydrogen partial pressure is 0.1 atm. The mass diffusivity and solubility of hydrogen in the tube material are 1.8×10^{-11} m^2/s and 160 kmol/m^3 · atm, respectively. When the system is at 500 K, what is the rate of hydrogen transfer through the tube per unit length (kg/s · m)?

14.25 Consider the blister packaging material of Example 14.3.

(a) Under the same conditions as in the example, determine the solubility of the polymer material (kmol/m^3 · bar) if the temperature is 295 K and the relative humidity inside and outside the package is $\phi_2 = 0.1$ and $\phi_1 = 0.9$, respectively.

(b) By selecting a different packaging material, the diffusivity of the film may be changed. Determine the total water vapor transfer rate associated with reducing the diffusivity to 10% of its original value.

(c) The solubility of the material adjacent to its exposed surface may be modified by coating it with various thin films. Determine the water vapor transfer rate after coating both sides of the original polymer sheet and, in turn, reducing the solubility near both surfaces to 10% of the original value.

Patent Owner Manufacturing Resources International, Inc.
Exhibit 2017 - Page 924 of 999

(d) Determine the water vapor transfer rate after coating the exterior of the original polymer sheet and reducing its solubility by a factor of 9, while leaving the interior surface untreated.

14.26 An experiment is designed to measure the *partition coefficient, K,* associated with the transfer of a pharmaceutical product through a polymer material. The partition coefficient is defined as the ratio of the densities of the species of interest (the pharmaceutical) on either side of an interface. In the experiment, liquid pharmaceutical ($\rho_p = 1250$ kg/m^3) is injected into a hollow polymer sphere of inner and outer diameters $D_i = 5$ mm and $D_o = 5.1$ mm, respectively. The sphere is exposed to convective conditions for which the density of the pharmaceutical at the outer surface is zero. After one week, the sphere's mass is reduced by $\Delta M = 8.2$ mg. What is the value of the partition coefficient if the mass diffusivity is $D_{AB} = 0.2 \times 10^{-11}$ m^2/s?

14.27 Ultra-pure hydrogen is required in applications ranging from the manufacturing of semiconductors to powering fuel cells. The crystalline structure of palladium allows only the transfer of atomic hydrogen (H) through its thickness, and therefore palladium membranes are used to filter hydrogen from contaminated streams containing mixtures of hydrogen and other gases. Hydrogen molecules (H_2) are first adsorbed onto the palladium's surface and are then dissociated into atoms (H), which subsequently diffuse through the metal. The H atoms recombine on the opposite side of the membrane, forming pure H_2. The surface concentration of H takes the form $C_H = K_s p_{H_2}^{0.5}$, where $K_s \approx 1.4$ kmol/m$^3 \cdot$ bar$^{0.5}$ is known as *Sievert's constant.* Consider an industrial hydrogen purifier consisting of an array of palladium tubes with one tube end connected to a collector plenum and the other end closed. The tube bank is inserted into a shell. Impure H_2 at $T = 600$ K, $p = 15$ bars, $x_{H_2} = 0.85$ is introduced into the shell while pure H_2 at $p = 6$ bars, $T = 600$ K is extracted through the tubes. Determine the production rate of pure hydrogen (kg/h) for $N = 100$ tubes which are of inside diameter $D_i = 1.6$ mm, wall thickness $t = 75$ μm, and length $L = 80$ mm. The mass diffusivity of hydrogen (H) in palladium at 600 K is approximately $D_{AB} = 7 \times 10^{-9}$ m^2/s.

Catalytic Surface Reactions

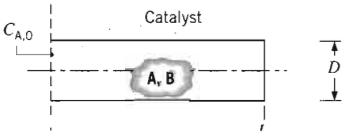
14.28 Nitric oxide (NO) emissions from automobile exhaust can be reduced by using a catalytic converter, and the following reaction occurs at the catalytic surface:

$$NO + CO \rightarrow \tfrac{1}{2}N_2 + CO_2$$

The concentration of NO is reduced by passing the exhaust gases over the surface, and the rate of reduction at the catalyst is governed by a first-order reaction of the form given by Equation 14.66. As a first approximation it may be assumed that NO reaches the surface by one-dimensional diffusion through a thin gas film of thickness L that adjoins the surface. Referring to Figure 14.7, consider a situation for which the exhaust gas is at 500°C and 1.2 bars and the mole fraction of NO is $x_{A,L} = 0.15$. If $D_{AB} = 10^{-4}$ m^2/s, $k_1'' = 0.05$ m/s, and the film thickness is $L = 1$ mm, what is the mole fraction of NO at the catalytic surface and what is the NO removal rate for a surface of area $A = 200$ cm^2?

14.29 Pulverized coal pellets, which may be approximated as carbon spheres of radius $r_o = 1$ mm, are burned in a pure oxygen atmosphere at 1450 K and 1 atm. Oxygen is transferred to the particle surface by diffusion, where it is consumed in the reaction $C + O_2 \rightarrow CO_2$. The reaction rate is first order and of the form $N''_{O_2} = -k_1'' C_{O_2}(r_o)$, where $k_1'' = 0.1$ m/s. Neglecting changes in r_o, determine the steady-state O_2 molar consumption rate in kmol/s. At 1450 K, the binary diffusion coefficient for O_2 and CO_2 is 1.71×10^{-4} m^2/s.

14.30 To enhance the effective surface, and hence the chemical reaction rate, catalytic surfaces often take the form of porous solids. One such solid may be visualized as consisting of a large number of cylindrical pores, each of diameter D and length L.



Consider conditions involving a gaseous mixture of A and B for which species A is chemically consumed at the catalytic surface. The reaction is known to be first order, and the rate at which it occurs per unit area of the surface may be expressed as $k_1'' C_A$, where k_1'' (m/s) is the reaction rate constant and C_A (kmol/m^3) is the local molar concentration of species A. Under steady-state conditions, flow over the porous solid is known to maintain a fixed value of the molar concentration $C_{A,0}$ at the pore mouth. Beginning from fundamentals, obtain the differential equation that governs the variation of C_A with distance x along the pore. Applying appropriate boundary conditions, solve the equation to obtain an expression for $C_A(x)$.

14.31 A platinum catalytic reactor in an automobile is used to convert carbon monoxide to carbon dioxide in an

Patent Owner Manufacturing Resources International, Inc.
Exhibit 2017 - Page 925 of 999

oxidation reaction of the form $2CO + O_2 \rightarrow 2CO_2$. Species transfer between the catalytic surface and the exhaust gases may be assumed to occur by diffusion in a film of thickness $L = 10$ mm. Consider an exhaust gas that has a pressure of 1.2 bars, a temperature of 500°C, and a CO mole fraction of 0.0012. If the reaction rate constant of the catalyst is $k_1'' = 0.005$ m/s and the diffusion coefficient of CO in the mixture is 10^{-4} m^2/s, what is the molar concentration of CO at the catalytic surface? What is the rate of removal of CO per unit area of the catalyst? What is the removal rate if k_1'' is adjusted to render the process diffusion limited?

14.32 A novel process has been proposed to create a composite palladium tube for use as a hydrogen separation membrane in order to produce high-purity hydrogen. To fabricate the composite palladium tube, a gas containing palladium (species A) flows through a porous-walled tube, and the palladium deposits into the pores of the tube wall. The gas mass flow rate is $\dot{m}$ and the inlet mass concentration of palladium is $\rho_{A,m,i}$. The mass transfer coefficient for transfer of palladium between the gas and the surface is h_m, and the deposition rate is proportional to the mass concentration of palladium at the tube surface, that is, $-n''_{A,s} = k_1\rho_{A,s}$. The palladium is a dilute species, so the total mass flow rate is approximately constant down the length of the tube.

(a) Building upon the convection mass transfer analysis presented in Section 8.9, derive an expression for the variation of the mean species density of palladium with distance from the tube entrance, and determine an expression for the local deposition rate (kg/m^2 · s) for a tube of diameter D. Neglect any leakage of gas through the porous tube walls.

(b) If the tube is too long, the variation in deposit thickness will be unacceptably large. What is the ratio of the deposition rates at $x = L$ and $x = 0$?

Homogeneous Chemical Reactions: Steady State

14.33 Consider combustion of hydrogen gas in a mixture of hydrogen and oxygen adjacent to the metal wall of a combustion chamber. Combustion occurs at constant temperature and pressure according to the chemical reaction $2H_2 + O_2 \rightarrow 2H_2O$. Measurements under steady-state conditions at a distance of 10 mm from the wall indicate that the molar concentrations of hydrogen, oxygen, and water vapor are 0.10, 0.10, and 0.20 kmol/m^3, respectively. The generation rate of water vapor is 0.96×10^{-2} kmol/m^3 · s throughout the region of interest. The binary diffusion coefficient for each of the species (H_2, O_2, and H_2O) in the remaining species is 0.6×10^{-5} m^2/s.

(a) Determine an expression for and make a qualitative plot of C_{H_2} as a function of distance from the wall.

(b) Determine the value of C_{H_2} at the wall.

(c) On the same coordinates used in part (a), sketch curves for the concentrations of oxygen and water vapor.

(d) What is the molar flux of water vapor at $x = 10$ mm?

14.34 Consider a spherical organism of radius r_o within which respiration occurs at a uniform volumetric rate of $\dot{N}_A = -k_0$. That is, oxygen (species A) consumption is governed by a zero-order, homogeneous chemical reaction.

(a) If a molar concentration of $C_A(r_o) = C_{A,o}$ is maintained at the surface of the organism, obtain an expression for the radial distribution of oxygen, $C_A(r)$, within the organism. From your solution, can you discern any limits on applicability of the result?

(b) Obtain an expression for the rate of oxygen consumption within the organism.

(c) Consider an organism of radius $r_o = 0.10$ mm and a diffusion coefficient for oxygen transfer of $D_{AB} = 10^{-8}$ m^2/s. If $C_{A,o} = 5 \times 10^{-5}$ kmol/m^3 and $k_0 = 1.2 \times 10^{-4}$ kmol/s · m^3, what is the molar concentration of O_2 at the center of the organism?

14.35 Referring to Problem 14.34, a more representative model of respiration in a spherical organism is one for which oxygen consumption is governed by a first-order reaction of the form $\dot{N}_A = -k_1C_A$.

(a) If a molar concentration of $C_A(r_o) = C_{A,o}$ is maintained at the surface of the organism, obtain an expression for the radial distribution of oxygen, $C_A(r)$, within the organism. *Hint*: To simplify solution of the species diffusion equation, invoke the tranformation $y \equiv rC_A$.

(b) Obtain an expression for the rate of oxygen consumption within the organism.

(c) Consider an organism of radius $r_o = 0.10$ mm and a diffusion coefficient of $D_{AB} = 10^{-8}$ m^2/s. If $C_{A,o} = 5 \times 10^{-5}$ kmol/m^3 and $k_1 = 20$ s^{-1}, estimate the corresponding value of the molar concentration at the center of the organism. What is the rate of oxygen consumption by the organism?

Patent Owner Manufacturing Resources International, Inc.
Exhibit 2017 - Page 926 of 999

14.36 Consider the problem of oxygen transfer from the interior lung cavity, across the lung tissue, to the network of blood vessels on the opposite side. The lung tissue (species B) may be approximated as a plane wall of thickness L. The inhalation process may be assumed to maintain a constant molar concentration $C_A(0)$ of oxygen (species A) in the tissue at its inner surface ($x = 0$), and assimilation of oxygen by the blood may be assumed to maintain a constant molar concentration $C_A(L)$ of oxygen in the tissue at its outer surface ($x = L$). There is oxygen consumption in the tissue due to metabolic processes, and the reaction is zero order, with $\dot{N}_A = -k_0$. Obtain expressions for the distribution of the oxygen concentration in the tissue and for the rate of assimilation of oxygen by the blood per unit tissue surface area.

14.37 As an employee of the Los Angeles Air Quality Commission, you have been asked to develop a model for computing the distribution of NO_2 in the atmosphere. The molar flux of NO_2 at ground level, $N''_{A,0}$, is presumed known. This flux is attributed to automobile and smoke stack emissions. It is also known that the concentration of NO_2 at a distance well above ground level is zero and that NO_2 reacts chemically in the atmosphere. In particular, NO_2 reacts with unburned hydrocarbons (in a process that is activated by sunlight) to produce PAN (peroxyacetylnitrate), the final product of photochemical smog. The reaction is first order, and the local rate at which it occurs may be expressed as $\dot{N}_A = -k_1 C_A$.

(a) Assuming steady-state conditions and a stagnant atmosphere, obtain an expression for the vertical distribution $C_A(x)$ of the molar concentration of NO_2 in the atmosphere.

(b) If an NO_2 partial pressure of $p_A = 2 \times 10^{-6}$ bar is sufficient to cause pulmonary damage, what is the value of the ground level molar flux for which you would issue a smog alert? You may assume an isothermal atmosphere at $T = 300$ K, a reaction coefficient of $k_1 = 0.03\ s^{-1}$, and an NO_2–air diffusion coefficient of $D_{AB} = 0.15 \times 10^{-4}\ m^2/s$.

Transient Diffusion: Introductory

14.38 In Problem 14.37, NO_2 transport by diffusion in a stagnant atmosphere was considered for steady-state conditions. However, the problem is actually time dependent, and a more realistic approach would account for transient effects. Consider the ground level emission of NO_2 to begin in the early morning (at $t = 0$), when the NO_2 concentration in the atmosphere is everywhere zero. Emission occurs throughout the day at a constant flux $N''_{A,0}$, and the NO_2 again experiences a first-order photochemical reaction in the atmosphere ($\dot{N}_A = -k_1 C_A$).

(a) For a differential element in the atmosphere, derive a differential equation that could be used to determine the molar concentration $C_A(x, t)$. State appropriate initial and boundary conditions.

(b) Obtain an expression for $C_A(x, t)$ under the special condition for which photochemical reactions may be neglected. For this condition what are the molar concentrations of NO_2 at ground level and at 100-m elevation 3 h after the start of the emissions, if $N''_{A,0} = 3 \times 10^{-11}$ kmol/s · m^2 and $D_{AB} = 0.15 \times 10^{-4}\ m^2/s$?

14.39 A large sheet of material 40 mm thick contains dissolved hydrogen (H_2) having a uniform concentration of 3 kmol/m^3. The sheet is exposed to a fluid stream that causes the concentration of the dissolved hydrogen to be reduced suddenly to zero at both surfaces. This surface condition is maintained constant thereafter. If the mass diffusivity of hydrogen is $9 \times 10^{-7}\ m^2/s$, how much time is required to bring the density of dissolved hydrogen to a value of 1.2 kg/m^3 at the center of the sheet?

14.40 A common procedure for increasing the moisture content of air is to bubble it through a column of water. Assume the air bubbles to be spheres of radius $r_o = 1$ mm and to be in thermal equilibrium with the water at 25°C. How long should the bubbles remain in the water to achieve a vapor concentration at the center that is 99% of the maximum possible (saturated) concentration? The air is dry when it enters the water.

14.41 Steel is carburized in a high-temperature process that depends on the transfer of carbon by diffusion. The value of the diffusion coefficient is strongly temperature dependent and may be approximated as $D_{C-S}\ (m^2/s) \approx 2 \times 10^{-5} \exp[-17{,}000/T\ (K)]$. If the process is effected at 1000°C and a carbon mole fraction of 0.02 is maintained at the surface of the steel, how much time is required to elevate the carbon content of the steel from an initial value of 0.1% to a value of 1.0% at a depth of 1 mm?

14.42 A thick plate of pure iron at 1000°C is subjected to a carburization process in which the surface of the plate is suddenly exposed to a gas that induces a carbon concentration $C_{C,s}$ at one surface. The average diffusion coefficient for carbon and iron at this temperature is $D_{C-Fe} = 3 \times 10^{-11}\ m^2/s$. Use the correspondence between heat and mass transfer variables in addressing the following questions.

(a) Consider the heat transfer analog to the carburization problem. Sketch the mass and heat transfer

Patent Owner Manufacturing Resources International, Inc.
Exhibit 2017 - Page 927 of 999

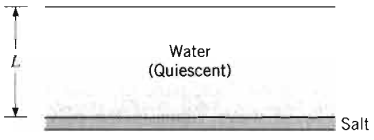
systems. Show and explain the correspondence between variables. Provide the analytical solutions to the heat and mass transfer problems.

(b) Determine the carbon concentration ratio, $C_C(x, t)/C_{C,s}$, at a depth of 10 mm after 1 hour of carburization.

(c) From the analogy, show that the time dependence of the mass flux of carbon into the plate may be expressed as $n''_C = \rho_{C,s}(D_{C-Fe}/\pi t)^{1/2}$. Also, obtain an expression for the mass of carbon per unit area entering the iron plate over the time period t.

(d) Consider conditions for which the plate has a uniform carbon concentration of $C_{C,o}$ and the surface concentration is suddenly reduced to a smaller value, $C_{C,s}$. Write an expression for the subsequent variation of the concentration with distance and time, $C_C(x, t)$.

14.43 A solar pond operates on the principle that heat losses from a shallow layer of water, which acts as a solar absorber, may be minimized by establishing a stable vertical salinity gradient in the water. In practice such a condition may be achieved by applying a layer of pure salt to the bottom and adding an overlying layer of pure water. The salt enters into solution at the bottom and is transferred through the water layer by diffusion, thereby establishing salt-stratified conditions.



As a first approximation, the total mass density ρ and the diffusion coefficient for salt in water (D_{AB}) may be assumed to be constant, with $D_{AB} = 1.2 \times 10^{-9}$ m^2/s.

(a) If a saturated density of $\rho_{A,s}$ is maintained for salt in solution at the bottom of the water layer of thickness $L = 1$ m, how long will it take for the mass density of salt at the top of the layer to reach 25% of saturation?

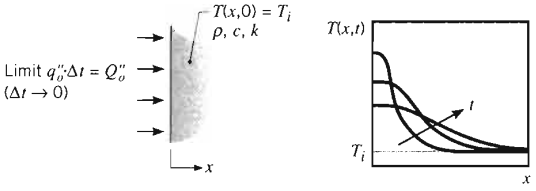
(b) In the time required to achieve 25% of saturation at the top of the layer, how much salt is transferred from the bottom into the water per unit surface area (kg/m^2)? The saturation density of salt in solution is $\rho_{A,s} = 380$ kg/m^3.

(c) If the bottom is depleted of salt at the time that the salt density reaches 25% of saturation at the top, what is the final (steady-state) density of the salt at the bottom? What is the final density of the salt at the top?

14.44 If an amount of energy Q''_o (J/m^2) is released instantaneously, as, for example, from a pulsed laser, and it is absorbed by the surface of a semi-infinite medium, with no attendant losses to the surroundings, the subsequent temperature distribution in the medium is

$$T(x, t) - T_i = \frac{Q''_o}{\rho c(\pi\alpha t)^{1/2}} \exp(-x^2/4\alpha t)$$

where T_i is the initial, uniform temperature of the medium. Consider an analogous mass transfer process involving deposition of a thin layer of phosphorous (P) on a silicon (Si) wafer at room temperature. If the wafer is placed in a furnace, the diffusion of P into Si is significantly enhanced by the high-temperature environment.



A Si wafer with 1-μm-thick P film is suddenly placed in a furnace at 1000°C, and the resulting distribution of P is characterized by an expression of the form

$$C_P(x, t) = \frac{M''_{P,o}}{(\pi D_{P-Si} t)^{1/2}} \exp(-x^2/4D_{P-Si} t)$$

where $M''_{P,o}$ is the molar area density (kmol/m^2) of P associated with the film of concentration C_P and thickness d_o.

(a) Explain the correspondence between variables in the analogous temperature and concentration distributions.

(b) Determine the mole fraction of P at a depth of 0.1 μm in the Si after 30 s. The diffusion coefficient is $D_{P-Si} = 1.2 \times 10^{-17}$ m^2/s. The mass densities of P and Si are 2000 and 2300 kg/m^3, respectively, and their molecular weights are 30.97 and 28.09 kg/kmol.

Transient Diffusion: Advanced

14.45 The presence of CO_2 in solution is essential to the growth of aquatic plant life, with CO_2 used as a reactant in the photosynthesis. Consider a stagnant body of water in which the concentration of CO_2 (ρ_A) is everywhere zero. At time $t = 0$, the water is exposed to a source of CO_2, which maintains the surface ($x = 0$) concentration

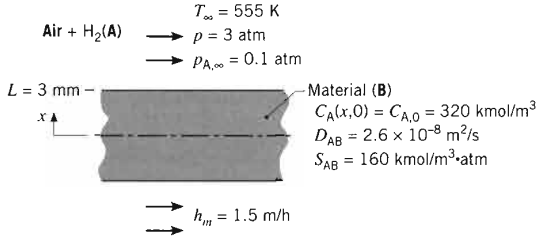
Patent Owner Manufacturing Resources International, Inc.
Exhibit 2017 - Page 928 of 999

at a fixed value $\rho_{A,0}$. For time $t > 0$, CO_2 will begin to accumulate in the water, but the accumulation is inhibited by CO_2 consumption due to photosynthesis. The time rate at which this consumption occurs per unit volume is equal to the product of a reaction rate constant k_1 and the local CO_2 concentration $\rho_A(x, t)$.

(a) Write (do not derive) a differential equation that could be used to determine $\rho_A(x, t)$ in the water. What does each term in the equation represent physically?

(b) Write appropriate boundary conditions that could be used to obtain a particular solution, assuming a "deep" body of water. What would be the form of this solution for the special case of negligible CO_2 consumption ($k_1 \approx 0$)?

14.46 Hydrogen gas is used in a process to manufacture a sheet material of 6-mm thickness. At the end of the process, H_2 remains in solution in the material with a uniform concentration of 320 kmol/m^3. To remove H_2 from the material, both surfaces of the sheet are exposed to an air stream at 500 K and a total pressure of 3 atm. Due to contamination, the hydrogen partial pressure is 0.1 atm in the air stream, which provides a convection mass transfer coefficient of 1.5 m/h. The mass diffusivity and solubility of hydrogen (A) in the sheet material (B) are $D_{AB} = 2.6 \times 10^{-8}$ m^2/s and $S_{AB} = 160$ kmol/m^3·atm, respectively.



(a) If the sheet material is left exposed to the air stream for a long time, determine the final content of hydrogen in the material (kg/m^3).

(b) Identify and evaluate the parameter that can be used to determine whether the transient mass diffusion process in the sheet can be assumed to be characterized by a uniform concentration at any time during the process. *Hint*: This situation is analogous to that used to determine the validity of the lumped-capacitance method for a transient heat transfer analysis.

(c) Determine the time required to reduce the hydrogen mass density at the center of the sheet to twice the limiting value calculated in part (a).

14.47 Consider the hydrogen-removal process described in Problem 14.46, but under conditions for which the mass diffusivity of the hydrogen gas (A) in the sheet material (B) is $D_{AB} = 1.8 \times 10^{-11}$ m^2/s (instead of 2.6×10^{-8} m^2/s). With the smaller value of D_{AB}, a *uniform concentration* may no longer be assumed to exist in the material during the removal process.

(a) If the sheet material is left exposed to the air stream for a very long time, what is the final content of hydrogen in the material (kg/m^3)?

(b) Identify and evaluate the parameters that describe the transient mass diffusion process in the sheet. *Hint*: The situation is analogous to that of transient heat conduction in a plane wall.

(c) Determine the time required to reduce the hydrogen mass density at the center of the sheet to twice the limiting value calculated in part (a).

(d) Assuming a uniform concentration at any time during the removal process, calculate the time required to reach twice the limiting density calculated in part (a). Compare the result with that obtained from part (c), and explain the differences.

14.48 A 1-mm-thick square (100 mm × 100 mm) sheet of polymer is suspended from a precision scale in a chamber characterized by a temperature and relative humidity of $T = 300$ K and $\phi = 0$, respectively. Suddenly, at time $t = 0$, the chamber's relative humidity is raised to $\phi = 0.95$. The measured mass of the sheet increases by 0.012 mg over 24 hours and by 0.016 mg over 48 hours. Determine the solubility and mass diffusivity of water vapor in the polymer. Preliminary experiments have indicated that the mass diffusivity is greater than 7×10^{-13} m^2/s.

14.49 Consider a DVD similar to that of Problem 5.86. To protect sensitive information within the storage medium, a *very thin* film of reactive polymer is embedded within the polycarbonate at a distance $d = 0.5$ mm from the surface. The thin film can undergo a chemical reaction with oxygen during which it is converted from a transparent material to an opaque material, rendering the information unreadable. The chemical reaction begins when the oxygen concentration at the reactive polymer reaches $C_{crit} = 5 \times 10^{-5}$ kmol/m^3. The DVD is shipped in an oxygen-proof pouch; determine the elapsed time after removal from the pouch before the DVD self-destructs. The solubility and diffusivity of oxygen in polycarbonate are $S = 8.9 \times 10^{-3}$ kmol/m^3 · bar and $D_{AB} = 6.5 \times 10^{-12}$ m^2/s, respectively.

14.50 Consider the DVD of Problem 14.49, except now the reacting polymer is blended uniformly with the

Patent Owner Manufacturing Resources International, Inc.
Exhibit 2017 - Page 929 of 999

polycarbonate to reduce manufacturing costs. Assume that a first-order homogeneous chemical reaction takes place between the polymer and oxygen; the reaction rate is proportional to the oxygen molar concentration.

(a) Write the governing equation, boundary conditions, and initial condition for the oxygen molar concentration after the DVD is removed from the oxygen-proof pouch, for a DVD of thickness $2L$. Do not solve.

(b) The DVD will gradually become more opaque over time as the reaction proceeds. The ability to read the DVD will depend on how well the laser light can penetrate through the thickness of the DVD. Therefore, it is important to know the volume-averaged molar concentration of product, $\overline{C}_{\text{prod}}$, as a function of time. Write an expression for $\overline{C}_{\text{prod}}$ in terms of the oxygen molar concentration, assuming that every mole of oxygen that reacts with the polymer results in p moles of product.

14.51 A vitreous silica optical fiber of diameter 100 μm is used to send optical signals from a sensor placed deep inside a hydrogen chamber. The hydrogen is at a pressure of 20 bars. The mass diffusivity and solubility of the hydrogen in the glass fiber are $D_{AB} = 2.88 \times 10^{-15}$ m^2/s and $S = 4.15 \times 10^{-3}$ kmol/m^3 · bar, respectively. Hydrogen diffusion into the fiber is undesirable, since it changes the spectral transmissivity and refractive index of the glass and can lead to failure of the detection system.

(a) Determine the average hydrogen concentration in an uncoated optical fiber, $\overline{C}$, after 100 hours of operation in the hydrogen environment. Determine the corresponding change in the refractive index, Δn, of the fiber. For vitreous silica, $\Delta n = (1.6 \times 10^{-3}\ \text{m}^3/\text{kmol}) \times \overline{C}$.

(b) Determine the average hydrogen concentration and change in refractive index after 1 hour and 10 hours of operation in the hydrogen environment.

14.52 The surface of glass *quickly* develops very small *microcracks* when exposed to high humidity. Although microcracks can be safely ignored in most applications, they can significantly decrease the mechanical strength of very small glass structures such as optical fibers. Consider a glass optical fiber of diameter $D_i = 125$ μm that is coated with an acrylate polymer to form a coated fiber of outer diameter $D_o = 250$ μm. A telecommunications engineer insists that the optical fiber be stored in a low-humidity environment prior to installation so that it is sufficiently strong to withstand rough treatment by technicians in the field. If installation of a roll of fiber requires several hot and humid days to complete, will careful storage beforehand prevent microcracking? The mass diffusivity of water vapor in the acrylate is $D_{AB} = 5.5 \times 10^{-13}$ m^2/s while the glass can be considered impermeable.

14.53 A person applies an insect repellent onto an exposed area of $A = 0.5$ m^2 of their body. The mass of spray used is $M = 10$ grams, and the spray contains 25% (by mass) active ingredient. The inactive ingredient quickly evaporates from the skin surface.

(a) If the spray is applied uniformly and the density of the dried active ingredient is $\rho = 2000$ kg/m^3, determine the initial thickness of the film of active ingredient on the skin surface. The temperature, molecular weight, and saturation pressure of the active ingredient are 32°C, 152 kg/kmol, and 1.2×10^{-5} bars, respectively.

(b) If the convective mass transfer coefficient associated with sublimation of the active ingredient to the air is $\overline{h}_m = 5 \times 10^{-3}$ m/s, the partition coefficient associated with the ingredient–skin interface is $K = 0.05$, and the mass diffusivity of the active ingredient in the skin is $D_{AB} = 1 \times 10^{-13}$ m^2/s, determine how long the insect repellent remains effective. The partition coefficient is the ratio of the ingredient density in the skin to the ingredient density outside the skin.

(c) If the spray is reformulated so that the partition coefficient becomes very small, how long does the insect repellent remain effective?

Patent Owner Manufacturing Resources International, Inc.
Exhibit 2017 - Page 930 of 999

APPENDIX A

Thermophysical Properties of Matter[1]

Table		*Page*
A.1	Thermophysical Properties of Selected Metallic Solids	929
A.2	Thermophysical Properties of Selected Nonmetallic Solids	933
A.3	Thermophysical Properties of Common Materials	935
	Structural Building Materials	935
	Insulating Materials and Systems	936
	Industrial Insulation	937
	Other Materials	939
A.4	Thermophysical Properties of Gases at Atmospheric Pressure	941
A.5	Thermophysical Properties of Saturated Fluids	946
	Saturated Liquids	946
	Saturated Liquid–Vapor, 1 atm	948
A.6	Thermophysical Properties of Saturated Water	949
A.7	Thermophysical Properties of Liquid Metals	951
A.8	Binary Diffusion Coefficients at One Atmosphere	952
A.9	Henry's Constant for Selected Gases in Water at Moderate Pressure	953
A.10	The Solubility of Selected Gases and Solids	953

[1] The convention used to present numerical values of the properties is illustrated by this example:

T (K)	$\nu \cdot 10^7$ (m^2/s)	$k \cdot 10^3$ (W/m · K)
300	0.349	521

where $\nu = 0.349 \times 10^{-7}$ m^2/s and $k = 521 \times 10^{-3} = 0.521$ W/m · K at 300 K.

Patent Owner Manufacturing Resources International, Inc.
Exhibit 2017 - Page 931 of 999

A.11	Total, Normal (n) or Hemispherical (h) Emissivity of Selected Surfaces	954
	Metallic Solids and Their Oxides	954
	Nonmetallic Substances	955
A.12	Solar Radiative Properties for Selected Materials	956
	References	957

TABLE A.1 Thermophysical Properties of Selected Metallic Solids[a]

	Melting	Properties at 300 K			Properties at Various Temperatures (K)					
					k (W/m · K)/c_p (J/kg · K)					
		ρ	k	c_p						
		kg/m³	W/m · K	J/kg · K	100 K	200 K	400 K	600 K	800 K	1000 K
Aluminum	933	2702	237	903	302/482	237/798	240/949	231/1033	218/1146	188/1STS
Beryllium	1550	1850	200	1825	990/1114	301/1622	161/2191	126/2604	106/2823	90/3018
Bismuth	545	9780	7.86	122	9.69/104	8.54/113	7.04/122	6.08/127	5.26/130	4.60/132
Cadmium	594	8650	96.8	231	203/198	99.3/216	94.6/242	89.9/267	87.5/291	85.2/315
Chromium	2118	7160	93.7	449	159/276	111/390	90.9/484	80.7/542	71.4/581	63.2/616
Cobalt	1769	8862	100	421	165/275	122/362	87/456	73/515	66/562	61/604
Copper	1358	8933	401	385	482/252	413/356	393/393	379/417	366/433	352/451
Gallium	303	5907	40.6	371	29.3/264	33.2/324	37.4/367	36.6/385	34.6/397	32.4/409
Gold	1337	19300	317	129	327/109	323/122	312/131	304/135	298/138	292/140
Hafnium	2495	13300	23.0	144	25.0/108	23.5/126	22.3/138	22.3/146	22.7/151	23.1/155
Indium	430	7310	81.8	233	93.2/191	85.9/216	78.2/240	73.6/257	71.1/272	69.4/287
Iridium	2720	22500	147	131	153/100	150/122	147/133	144/138	141/142	138/145
Iron	1810	7870	80.2	447	134/236	94.0/384	69.5/490	54.7/574	43.3/680	33.3/975
Lead	601	11340	35.3	129	38.6/118	35.9/126	33.4/134	31.4/142	29.8/151	28.4/160
Lithium	454	534	71.8	3570	86.6/2262	76.5/3110	65.6/3847	58.2/4247	53.2/4491	49.7/4685
Magnesium	924	1740	156	1024	169/629	159/870	153/1088	149/1229	146/1341	142/1443
Manganese	1519	7470	7.81	486	3.92/276	5.81/389	7.85/469	9.74/502	11.6/519	13.4/536
Mercury	234	13534	8.54	139	4.61/124	7.25/131	9.24/135	10.4/137	11.3/139	12.1/141
Molybdenum	2894	10240	138	251	179/138	146/200	133/238	123/257	113/270	104/282
Nickel	1728	8900	90.7	444	164/261	106/383	80.2/485	67.4/562	59.5/627	52.6/695
Niobium	2741	8578	53.7	265	55.2/191	52.3/238	54.4/273	57.5/292	60.5/305	63.3/314
Osmium	3306	22610	61.2	130	87.6/94.1	81.2/108	71.2/117	64.6/122	59.2/126	54.7/129
Palladium	1825	12020	71.8	244	77.5/164	73.2/211	73.2/236	75.6/248	78.0/257	80.4/265
Platinum	2045	21450	71.6	133	73.5/100	72.4/117	72.6/126	73.5/131	74.5/135	75.5/138
Rhodium	2236	12450	150	243	278/162	200/210	154/249	132/269	117/283	105/295
Rubidium	312	1532	58.2	363	62.9/329	58.9/347	54.1/360	50.5/368	48.0/374	46.1/380
Ruthenium	2607	12370	117	238	134/147	122/185	109/214	100/230	93.0/242	86.9/253
Silver	1235	10500	429	235	483/210	430/225	419/239	412/250	407/262	404/277
Tantalum	3269	16600	57.5	140	63.2/111	59.2/129	57.8/137	58.2/142	58.9/146	59.8/150
Thorium	2023	11720	54.0	118	57.5/101	55.4/111	52.9/122	51.1/131	49.8/141	48.8/151
Tin	505	7310	66.8	227	85.2/167	73.3/202	62.2/222	56.6/233	52.9/241	50.2/249
Titanium	1953	4500	21.9	522	29.5/300	24.5/425	20.4/511	18.4/555	17.4/585	16.8/612
Tungsten	3683	19300	174	132	208/100	185/120	159/132	142/138	130/142	120/145
Uranium	1406	19070	27.6	116	21.7/97.6	24.0/108	27.4/118	30.0/126	32.3/135	34.7/144
Vanadium	2192	6090	30.7	489	26.8/337	28.0/420	31.5/481	34.7/515	37.8/536	40.8/556
Zinc	693	7140	116	389	135/237	121/328	106/378	97.6/402	91.5/417	87.0/428
Zirconium	2125	6570	22.7	278	25.2/183	23.2/226	21.6/262	21.6/281	22.1/293	22.8/301

Patent Owner Manufacturing Resources International, Inc.
Exhibit 2017 - Page 932 of 999

TABLE A.1 Thermophysical Properties of Selected Metallic Solids[a]

Composition	Melting Point (K)	Properties at 300 K				Properties at Various Temperatures (K)									
						k (W/m · K)/c_p (J/kg · K)									
		ρ (kg/m^3)	c_p (J/kg · K)	k (W/m · K)	$\alpha \cdot 10^6$ (m^2/s)	100	200	400	600	800	1000	1200	1500	2000	2500
Aluminum															
Pure	933	2702	903	237	97.1	302	237	240	231	218					
						482	798	949	1033	1146					
Alloy 2024-T6 (4.5% Cu, 1.5% Mg, 0.6% Mn)	775	2770	875	177	73.0	65	163	186	186						
						473	787	925	1042						
Alloy 195, Cast (4.5% Cu)		2790	883	168	68.2			174	185						
								—	—						
Beryllium	1550	1850	1825	200	59.2	990	301	161	126	106	90.8	78.7			
						203	1114	2191	2604	2823	3018	3227	3519		
Bismuth	545	9780	122	7.86	6.59	16.5	9.69	7.04							
						112	120	127							
Boron	2573	2500	1107	27.0	9.76	190	55.5	16.8	10.6	9.60	9.85				
						128	600	1463	1892	2160	2338				
Cadmium	594	8650	231	96.8	48.4	203	99.3	94.7							
						198	222	242							
Chromium	2118	7160	449	93.7	29.1	159	111	90.9	80.7	71.3	65.4	61.9	57.2	49.4	
						192	384	484	542	581	616	682	779	937	
Cobalt	1769	8862	421	99.2	26.6	167	122	85.4	67.4	58.2	52.1	49.3	42.5		
						236	379	450	503	550	628	733	674		
Copper															
Pure	1358	8933	385	401	117	482	413	393	379	366	352	339			
						252	356	397	417	433	451	480			
Commercial bronze (90% Cu, 10% Al)	1293	8800	420	52	14		42	52	59						
							785	460	545						
Phosphor gear bronze (89% Cu, 11% Sn)	1104	8780	355	54	17		41	65	74						
							—	—	—						
Cartridge brass (70% Cu, 30% Zn)	1188	8530	380	110	33.9	75	95	137	149						
							360	395	425						
Constantan (55% Cu, 45% Ni)	1493	8920	384	23	6.71	17	19								
						237	362								
Germanium	1211	5360	322	59.9	34.7	232	96.8	43.2	27.3	19.8	17.4	17.4			
						190	290	337	348	357	375	395			

Patent Owner Manufacturing Resources International, Inc.
Exhibit 2017 - Page 933 of 999

TABLE A.1 *Continued*

Composition	Melting Point (K)	Properties at 300 K				Properties at Various Temperatures (K)									
						k (W/m · K)/c_p (J/kg · K)									
		ρ (kg/m^3)	c_p (J/kg · K)	k (W/m · K)	$\alpha \cdot 10^6$ (m^2/s)	100	200	400	600	800	1000	1200	1500	2000	2500
Gold	1336	19300	129	317	127	327 109	323 124	311 131	298 135	284 140	270 145	255 155			
Iridium	2720	22500	130	147	50.3	172 90	153 122	144 133	138 138	132 144	126 153	120 161	111 172		
Iron															
Pure	1810	7870	447	80.2	23.1	134 216	94.0 384	69.5 490	54.7 574	43.3 680	32.8 975	28.3 609	32.1 654		
Armco (99.75% pure)		7870	447	72.7	20.7	95.6 215	80.6 384	65.7 490	53.1 574	42.2 680	32.3 975	28.7 609	31.4 654		
Carbon steels															
Plain carbon (Mn ≤ 1%, Si ≤ 0.1%)		7854	434	60.5	17.7			56.7 487	48.0 559	39.2 685	30.0 1169				
AISI 1010		7832	434	63.9	18.8			58.7 487	48.8 559	39.2 685	31.3 1168				
Carbon–silicon (Mn ≤ 1%, 0.1% < Si ≤ 0.6%)		7817	446	51.9	14.9			49.8 501	44.0 582	37.4 699	29.3 971				
Carbon–manganese–silicon (1% < Mn ≤ 1.65%, 0.1% < Si ≤ 0.6%)		8131	434	41.0	11.6			42.2 487	39.7 559	35.0 685	27.6 1090				
Chromium (low) steels															
½Cr–¼Mo–Si (0.18% C, 0.65% Cr, 0.23% Mo, 0.6% Si)		7822	444	37.7	10.9			38.2 492	36.7 575	33.3 688	26.9 969				
1 Cr–½Mo (0.16% C, 1% Cr, 0.54% Mo, 0.39% Si)		7858	442	42.3	12.2			42.0 492	39.1 575	34.5 688	27.4 969				
1 Cr–V (0.2% C, 1.02% Cr, 0.15% V)		7836	443	48.9	14.1			46.8 492	42.1 575	36.3 688	28.2 969				
Stainless steels															
AISI 302		8055	480	15.1	3.91			17.3 512	20.0 559	22.8 585	25.4 606				
AISI 304	1670	7900	477	14.9	3.95	9.2 272	12.6 402	16.6 515	19.8 557	22.6 582	25.4 611	28.0 640	31.7 682		
AISI 316		8238	468	13.4											

Patent Owner Manufacturing Resources International, Inc.
Exhibit 2017 - Page 934 of 999

1 Cr–½Mo (0.16% C, 1% Cr, 0.54% Mo, 0.39% Si)		7858 7836	442 443	48.9	14.1			492 46.8 492	575 42.1 575	688 36.3 688	28.2 969				
1 Cr–V (0.2% C, 1.02% Cr, 0.15% V)															
Stainless steels															
AISI 302		8055	480	15.1	3.91			17.3 512	20.0 559	22.8 585	25.4 606				
AISI 304	1670	7900	477	14.9	3.95	9.2 272	12.6 402	16.6 515	19.8 557	22.6 582	25.4 611	28.0 640	31.7 682		
AISI 316		8238	468	13.4	3.48			15.2 504	18.3 550	21.3 576	24.2 602				
AISI 347		7978	480	14.2	3.71			15.8 513	18.9 559	21.9 585	24.7 606				
Lead	601	11340	129	35.3	24.1	39.7 118	36.7 125	34.0 132	31.4 142						
Magnesium	923	1740	1024	156	87.6	169 649	159 934	153 1074	149 1170	146 1267					
Molybdenum	2894	10240	251	138	53.7	179 141	143 224	134 261	126 275	118 285	112 295	105 308	98 330	90 380	86 459
Nickel															
Pure	1728	8900	444	90.7	23.0	164 232	107 383	80.2 485	65.6 592	67.6 530	71.8 562	76.2 594	82.6 616		
Nichrome (80% Ni, 20% Cr)	1672	8400	420	12	3.4			14 480	16 525	21 545					
Inconel X-750 (73% Ni, 15% Cr, 6.7% Fe)	1665	8510	439	11.7	3.1	8.7 —	10.3 372	13.5 473	17.0 510	20.5 546	24.0 626	27.6 —	33.0 —		
Niobium	2741	8570	265	53.7	23.6	55.2 188	52.6 249	55.2 274	58.2 283	61.3 292	64.4 301	67.5 310	72.1 324	79.1 347	
Palladium	1827	12020	244	71.8	24.5	76.5 168	71.6 227	73.6 251	79.7 261	86.9 271	94.2 281	102 291	110 307		
Platinum															
Pure	2045	21450	133	71.6	25.1	77.5 100	72.6 125	71.8 136	73.2 141	75.6 146	78.7 152	82.6 157	89.5 165	99.4 179	
Alloy 60Pt–40Rh (60% Pt, 40% Rh)	1800	16630	162	47	17.4			52 —	59 —	65 —	69 —	73 —	76 —		
Rhenium	3453	21100	136	47.9	16.7	58.9 97	51.0 127	46.1 139	44.2 145	44.1 151	44.6 156	45.7 162	47.8 171	51.9 186	
Rhodium	2236	12450	243	150	49.6	186 147	154 220	146 253	136 274	127 293	121 311	116 327	110 349	112 376	
Silicon	1685	2330	712	148	89.2	884 259	264 556	98.9 790	61.9 867	42.2 913	31.2 946	25.7 967	22.7 992		
Silver	1235	10500	235	429	174	444 187	430 225	425 239	412 250	396 262	379 277	361 292			
Tantalum	3269	16600	140	57.5	24.7	59.2 110	57.5 133	57.8 144	58.6 146	59.4 149	60.2 152	61.0 155	62.2 160	64.1 172	65.6 189
Thorium	2023	11700	118	54.0	39.1	59.8 99	54.6 112	54.5 124	55.8 134	56.9 145	56.9 156	58.7 167			
Tin	505	7310	227	66.6	40.1	85.2 188	73.3 215	62.2 243							

Patent Owner Manufacturing Resources International, Inc.
Exhibit 2017 - Page 935 of 999

TABLE A.1 *Continued*

Composition	Melting Point (K)	Properties at 300 K				Properties at Various Temperatures (K)									
						k (W/m · K)/c_p (J/kg · K)									
		ρ (kg/m^3)	c_p (J/kg · K)	k (W/m · K)	$\alpha \cdot 10^6$ (m^2/s)	100	200	400	600	800	1000	1200	1500	2000	2500
Titanium	1953	4500	522	21.9	9.32	30.5 300	24.5 465	20.4 551	19.4 591	19.7 633	20.7 675	22.0 620	24.5 686		
Tungsten	3660	19300	132	174	68.3	208 87	186 122	159 137	137 142	125 145	118 148	113 152	107 157	100 167	95 176
Uranium	1406	19070	116	27.6	12.5	21.7 94	25.1 108	29.6 125	34.0 146	38.8 176	43.9 180	49.0 161			
Vanadium	2192	6100	489	30.7	10.3	35.8 258	31.3 430	31.3 515	33.3 540	35.7 563	38.2 597	40.8 645	44.6 714	50.9 867	
Zinc	693	7140	389	116	41.8	117 297	118 367	111 402	103 436						
Zirconium	2125	6570	278	22.7	12.4	33.2 205	25.2 264	21.6 300	20.7 322	21.6 342	23.7 362	26.0 344	28.8 344	33.0 344	

[a]Adapted from References 1–7.

TABLE A.2 Thermophysical Properties of Selected Nonmetallic Solids[a]

	Melting	Properties at 300 K				Properties at Various Temperatures (K)									
						k (W/m · K)/c_p (J/kg · K)									

Patent Owner Manufacturing Resources International, Inc.
Exhibit 2017 - Page 936 of 999

TABLE A.2 Thermophysical Properties of Selected Nonmetallic Solids[a]

Composition	Melting Point (K)	Properties at 300 K				Properties at Various Temperatures (K)									
						k (W/m · K)/c_p (J/kg · K)									
		ρ (kg/m^3)	c_p (J/kg · K)	k (W/m · K)	$\alpha \cdot 10^6$ (m^2/s)	100	200	400	600	800	1000	1200	1500	2000	2500
Aluminum oxide, sapphire	2323	3970	765	46	15.1	450 —	82 —	32.4 940	18.9 1110	13.0 1180	10.5 1225				
Aluminum oxide, polycrystalline	2323	3970	765	36.0	11.9	133 —	55 —	26.4 940	15.8 1110	10.4 1180	7.85 1225	6.55 —	5.66 —	6.00 —	
Beryllium oxide	2725	3000	1030	272	88.0			196 1350	111 1690	70 1865	47 1975	33 2055	21.5 2145	15 2750	
Boron	2573	2500	1105	27.6	9.99	190 —	52.5 —	18.7 1490	11.3 1880	8.1 2135	6.3 2350	5.2 2555			
Boron fiber epoxy (30% vol) composite	590	2080													
k, ∥ to fibers				2.29		2.10	2.23	2.28							
k, ⊥ to fibers				0.59		0.37	0.49	0.60							
c_p			1122			364	757	1431							
Carbon															
Amorphous	1500	1950	—	1.60	—	0.67 —	1.18 —	1.89 —	2.19 —	2.37 —	2.53 —	2.84 —	3.48 —		
Diamond, type IIa	—	3500	509	2300	—	10,000	4000	1540							
insulator						21	194	853							
Graphite, pyrolytic	2273	2210													
k, ∥ to layers				1950		4970	3230	1390	892	667	534	448	357	262	
k, ⊥ to layers				5.70		16.8	9.23	4.09	2.68	2.01	1.60	1.34	1.08	0.81	
c_p			709			136	411	992	1406	1650	1793	1890	1974	2043	
Graphite fiber epoxy (25% vol) composite	450	1400													
k, heat flow ∥ to fibers				11.1		5.7	8.7	13.0							
k, heat flow ⊥ to fibers				0.87		0.46	0.68	1.1							
c_p			935			337	642	1216							
Pyroceram, Corning 9606	1623	2600	808	3.98	1.89	5.25 —	4.78 —	3.64 908	3.28 1038	3.08 1122	2.96 1197	2.87 1264	2.79 1498		

Patent Owner Manufacturing Resources International, Inc.
Exhibit 2017 - Page 937 of 999

TABLE A.2 *Continued*

Composition	Melting Point (K)	Properties at 300 K				Properties at Various Temperatures (K)									
						k (W/m · K)/c_p (J/kg · K)									
		ρ (kg/m^3)	c_p (J/kg · K)	k (W/m · K)	$\alpha \cdot 10^6$ (m^2/s)	100	200	400	600	800	1000	1200	1500	2000	2500
Silicon carbide	3100	3160	675	490	230			— 880	— 1050	— 1135	87 1195	58 1243	30 1310		
Silicon dioxide, crystalline (quartz)	1883	2650													
k, ∥ to c axis				10.4		39	16.4	7.6	5.0	4.2					
k, ⊥ to c axis				6.21		20.8	9.5	4.70	3.4	3.1					
c_p			745			—	—	885	1075	1250					
Silicon dioxide, polycrystalline (fused silica)	1883	2220	745	1.38	0.834	0.69 —	1.14 —	1.51 905	1.75 1040	2.17 1105	2.87 1155	4.00 1195			
Silicon nitride	2173	2400	691	16.0	9.65	— —	— 578	13.9 778	11.3 937	9.88 1063	8.76 1155	8.00 1226	7.16 1306	6.20 1377	
Sulfur	392	2070	708	0.206	0.141	0.165 403	0.185 606								
Thorium dioxide	3573	9110	235	13	6.1			10.2 255	6.6 274	4.7 285	3.68 295	3.12 303	2.73 315	2.5 330	
Titanium dioxide, polycrystalline	2133	4157	710	8.4	2.8			7.01 805	5.02 880	3.94 910	3.46 930	3.28 945			

[a]Adapted from References 1, 2, 3, and 6.

Patent Owner Manufacturing Resources International, Inc.
Exhibit 2017 - Page 938 of 999

TABLE A.3 Thermophysical Properties of Common Materials[a]

Structural Building Materials

Description/Composition	Typical Properties at 300 K: Density, ρ (kg/m^3)	Thermal Conductivity, k (W/m · K)	Specific Heat, c_p (J/kg · K)
Building Boards			
Asbestos–cement board	1920	0.58	—
Gypsum or plaster board	800	0.17	—
Plywood	545	0.12	1215
Sheathing, regular density	290	0.055	1300
Acoustic tile	290	0.058	1340
Hardboard, siding	640	0.094	1170
Hardboard, high density	1010	0.15	1380
Particle board, low density	590	0.078	1300
Particle board, high density	1000	0.170	1300
Woods			
Hardwoods (oak, maple)	720	0.16	1255
Softwoods (fir, pine)	510	0.12	1380
Masonry Materials			
Cement mortar	1860	0.72	780
Brick, common	1920	0.72	835
Brick, face	2083	1.3	—
Clay tile, hollow			
1 cell deep, 10 cm thick	—	0.52	—
3 cells deep, 30 cm thick	—	0.69	—
Concrete block, 3 oval cores			
Sand/gravel, 20 cm thick	—	1.0	—
Cinder aggregate, 20 cm thick	—	0.67	—
Concrete block, rectangular core			
2 cores, 20 cm thick, 16 kg	—	1.1	—
Same with filled cores	—	0.60	—
Plastering Materials			
Cement plaster, sand aggregate	1860	0.72	—
Gypsum plaster, sand aggregate	1680	0.22	1085
Gypsum plaster, vermiculite aggregate	720	0.25	—

Patent Owner Manufacturing Resources International, Inc.
Exhibit 2017 - Page 939 of 999

TABLE A.3 *Continued*

Insulating Materials and Systems

Description/Composition	Typical Properties at 300 K		
	Density, ρ (kg/m^3)	Thermal Conductivity, k (W/m · K)	Specific Heat, c_p (J/kg · K)
Blanket and Batt			
Glass fiber, paper faced	16	0.046	—
	28	0.038	—
	40	0.035	—
Glass fiber, coated; duct liner	32	0.038	835
Board and Slab			
Cellular glass	145	0.058	1000
Glass fiber, organic bonded	105	0.036	795
Polystyrene, expanded			
Extruded (R-12)	55	0.027	1210
Molded beads	16	0.040	1210
Mineral fiberboard; roofing material	265	0.049	—
Wood, shredded/cemented	350	0.087	1590
Cork	120	0.039	1800
Loose Fill			
Cork, granulated	160	0.045	—
Diatomaceous silica, coarse	350	0.069	—
Powder	400	0.091	—
Diatomaceous silica, fine powder	200	0.052	—
	275	0.061	—
Glass fiber, poured or blown	16	0.043	835
Vermiculite, flakes	80	0.068	835
	160	0.063	1000
Formed/Foamed-in-Place			
Mineral wool granules with asbestos/inorganic binders, sprayed	190	0.046	—
Polyvinyl acetate cork mastic; sprayed or troweled	—	0.100	—
Urethane, two-part mixture; rigid foam	70	0.026	1045
Reflective			
Aluminum foil separating fluffy glass mats; 10–12 layers, evacuated; for cryogenic applications (150 K)	40	0.00016	—
Aluminum foil and glass paper laminate; 75–150 layers; evacuated; for cryogenic application (150 K)	120	0.000017	—
Typical silica powder, evacuated	160	0.0017	—

TABLE A.3 *Continued*

Industrial Insulation

Description/	Maximum Service	Typical	Typical Thermal Conductivity, k (W/m · K), at Various Temperatures (K)

Patent Owner Manufacturing Resources International, Inc.
Exhibit 2017 - Page 940 of 999

TABLE A.3 *Continued*

Industrial Insulation

Description/ Composition	Maximum Service Temperature (K)	Typical Density (kg/m³)	Typical Thermal Conductivity, k (W/m · K), at Various Temperatures (K)												
			200	215	230	240	255	270	285	300	310	365	420	530	645	750
Blankets																
Blanket, mineral fiber, metal reinforced	920	96–192									0.038	0.046	0.056	0.078		
Blanket, mineral fiber, glass; fine fiber, organic bonded	815	40–96									0.035	0.045	0.058	0.088		
	450	10				0.036	0.038	0.040	0.043	0.048	0.052	0.076				
		12				0.035	0.036	0.039	0.042	0.046	0.049	0.069				
		16				0.033	0.035	0.036	0.039	0.042	0.046	0.062				
		24				0.030	0.032	0.033	0.036	0.039	0.040	0.053				
		32				0.029	0.030	0.032	0.033	0.036	0.038	0.048				
		48				0.027	0.029	0.030	0.032	0.033	0.035	0.045				
Blanket, alumina–silica fiber	1530	48												0.071	0.105	0.150
		64												0.059	0.087	0.125
		96												0.052	0.076	0.100
		128												0.049	0.068	0.091
Felt, semirigid; organic bonded	480	50–125						0.035	0.036	0.038	0.039	0.051	0.063			
	730	50	0.023	0.025	0.026	0.027	0.029	0.030	0.032	0.033	0.035	0.051	0.079			
Felt, laminated; no binder	920	120											0.051	0.065	0.087	
Blocks, Boards, and Pipe Insulations																
Asbestos paper, laminated and corrugated																
4-ply	420	190								0.078	0.082	0.098				
6-ply	420	255								0.071	0.074	0.085				
8-ply	420	300								0.068	0.071	0.082				
Magnesia, 85%	590	185									0.051	0.055	0.061			
Calcium silicate	920	190									0.055	0.059	0.063	0.075	0.089	0.104

Patent Owner Manufacturing Resources International, Inc.
Exhibit 2017 - Page 941 of 999

TABLE A.3 *Continued*

Industrial Insulation (Continued)

Description/ Composition	Maximum Service Temperature (K)	Typical Density (kg/m^3)	Typical Thermal Conductivity, k (W/m · K), at Various Temperatures (K)												
			200	215	230	240	255	270	285	300	310	365	420	530	645	750
Cellular glass	700	145			0.046	0.048	0.051	0.052	0.055	0.058	0.062	0.069	0.079			
Diatomaceous	1145	345												0.092	0.098	0.104
silica	1310	385												0.101	0.100	0.115
Polystyrene, rigid																
Extruded (R-12)	350	56	0.023	0.023	0.022	0.023	0.023	0.025	0.026	0.027	0.029					
Extruded (R-12)	350	35	0.023	0.023	0.023	0.025	0.025	0.026	0.027	0.029						
Molded beads	350	16	0.026	0.029	0.030	0.033	0.035	0.036	0.038	0.040						
Rubber, rigid																
foamed	340	70						0.029	0.030	0.032	0.033					
Insulating Cement																
Mineral fiber																
(rock, slag or glass)																
With clay binder	1255	430									0.071	0.079	0.088	0.105	0.123	
With hydraulic																
setting binder	922	560									0.108	0.115	0.123	0.137		
Loose Fill																
Cellulose, wood																
or paper pulp	—	45							0.038	0.039	0.042					
Perlite, expanded	—	105	0.036	0.039	0.042	0.043	0.046	0.049	0.051	0.053	0.056					
Vermiculite,																
expanded	—	122			0.056	0.058	0.061	0.063	0.065	0.068	0.071					
		80			0.049	0.051	0.055	0.058	0.061	0.063	0.066					

Patent Owner Manufacturing Resources International, Inc.
Exhibit 2017 - Page 942 of 999

TABLE A.3 *Continued*

Other Materials

Description/ Composition	Temperature (K)	Density, ρ (kg/m^3)	Thermal Conductivity, k (W/m · K)	Specific Heat, c_p (J/kg · K)
Asphalt	300	2115	0.062	920
Bakelite	300	1300	1.4	1465
Brick, refractory				
Carborundum	872	—	18.5	—
	1672	—	11.0	—
Chrome brick	473	3010	2.3	835
	823		2.5	
	1173		2.0	
Diatomaceous	478	—	0.25	—
silica, fired	1145	—	0.30	
Fireclay, burnt 1600 K	773	2050	1.0	960
	1073	—	1.1	
	1373	—	1.1	
Fireclay, burnt 1725 K	773	2325	1.3	960
	1073		1.4	
	1373		1.4	
Fireclay brick	478	2645	1.0	960
	922		1.5	
	1478		1.8	
Magnesite	478	—	3.8	1130
	922	—	2.8	
	1478		1.9	
Clay	300	1460	1.3	880
Coal, anthracite	300	1350	0.26	1260
Concrete (stone mix)	300	2300	1.4	880
Cotton	300	80	0.06	1300
Foodstuffs				
Banana (75.7% water content)	300	980	0.481	3350
Apple, red (75% water content)	300	840	0.513	3600
Cake, batter	300	720	0.223	—
Cake, fully baked	300	280	0.121	—
Chicken meat, white	198	—	1.60	—
(74.4% water content)	233	—	1.49	
	253		1.35	
	263		1.20	
	273		0.476	
	283		0.480	
	293		0.489	
Glass				
Plate (soda lime)	300	2500	1.4	750
Pyrex	300	2225	1.4	835

Patent Owner Manufacturing Resources International, Inc.
Exhibit 2017 - Page 943 of 999

TABLE A.3 *Continued*

Other Materials (Continued)

Description/ Composition	Temperature (K)	Density, ρ (kg/m^3)	Thermal Conductivity, k (W/m · K)	Specific Heat, c_p (J/kg · K)
Ice	273	920	1.88	2040
	253	—	2.03	1945
Leather (sole)	300	998	0.159	—
Paper	300	930	0.180	1340
Paraffin	300	900	0.240	2890
Rock				
Granite, Barre	300	2630	2.79	775
Limestone, Salem	300	2320	2.15	810
Marble, Halston	300	2680	2.80	830
Quartzite, Sioux	300	2640	5.38	1105
Sandstone, Berea	300	2150	2.90	745
Rubber, vulcanized				
Soft	300	1100	0.13	2010
Hard	300	1190	0.16	—
Sand	300	1515	0.27	800
Soil	300	2050	0.52	1840
Snow	273	110	0.049	—
		500	0.190	—
Teflon	300	2200	0.35	—
	400		0.45	—
Tissue, human				
Skin	300	—	0.37	—
Fat layer (adipose)	300	—	0.2	—
Muscle	300	—	0.5	—
Wood, cross grain				
Balsa	300	140	0.055	—
Cypress	300	465	0.097	—
Fir	300	415	0.11	2720
Oak	300	545	0.17	2385
Yellow pine	300	640	0.15	2805
White pine	300	435	0.11	—
Wood, radial				
Oak	300	545	0.19	2385
Fir	300	420	0.14	2720

[a]Adapted from References 1 and 8–13.

Patent Owner Manufacturing Resources International, Inc.
Exhibit 2017 - Page 944 of 999

TABLE A.4 Thermophysical Properties of Gases at Atmospheric Pressure[a]

T (K)	ρ (kg/m^3)	c_p (kJ/kg · K)	$\mu \cdot 10^7$ (N · s/m^2)	$\nu \cdot 10^6$ (m^2/s)	$k \cdot 10^3$ (W/m · K)	$\alpha \cdot 10^6$ (m^2/s)	Pr
Air							
100	3.5562	1.032	71.1	2.00	9.34	2.54	0.786
150	2.3364	1.012	103.4	4.426	13.8	5.84	0.758
200	1.7458	1.007	132.5	7.590	18.1	10.3	0.737
250	1.3947	1.006	159.6	11.44	22.3	15.9	0.720
300	1.1614	1.007	184.6	15.89	26.3	22.5	0.707
350	0.9950	1.009	208.2	20.92	30.0	29.9	0.700
400	0.8711	1.014	230.1	26.41	33.8	38.3	0.690
450	0.7740	1.021	250.7	32.39	37.3	47.2	0.686
500	0.6964	1.030	270.1	38.79	40.7	56.7	0.684
550	0.6329	1.040	288.4	45.57	43.9	66.7	0.683
600	0.5804	1.051	305.8	52.69	46.9	76.9	0.685
650	0.5356	1.063	322.5	60.21	49.7	87.3	0.690
700	0.4975	1.075	338.8	68.10	52.4	98.0	0.695
750	0.4643	1.087	354.6	76.37	54.9	109	0.702
800	0.4354	1.099	369.8	84.93	57.3	120	0.709
850	0.4097	1.110	384.3	93.80	59.6	131	0.716
900	0.3868	1.121	398.1	102.9	62.0	143	0.720
950	0.3666	1.131	411.3	112.2	64.3	155	0.723
1000	0.3482	1.141	424.4	121.9	66.7	168	0.726
1100	0.3166	1.159	449.0	141.8	71.5	195	0.728
1200	0.2902	1.175	473.0	162.9	76.3	224	0.728
1300	0.2679	1.189	496.0	185.1	82	238	0.719
1400	0.2488	1.207	530	213	91	303	0.703
1500	0.2322	1.230	557	240	100	350	0.685
1600	0.2177	1.248	584	268	106	390	0.688
1700	0.2049	1.267	611	298	113	435	0.685
1800	0.1935	1.286	637	329	120	482	0.683
1900	0.1833	1.307	663	362	128	534	0.677
2000	0.1741	1.337	689	396	137	589	0.672
2100	0.1658	1.372	715	431	147	646	0.667
2200	0.1582	1.417	740	468	160	714	0.655
2300	0.1513	1.478	766	506	175	783	0.647
2400	0.1448	1.558	792	547	196	869	0.630
2500	0.1389	1.665	818	589	222	960	0.613
3000	0.1135	2.726	955	841	486	1570	0.536
Ammonia (NH_3)							
300	0.6894	2.158	101.5	14.7	24.7	16.6	0.887
320	0.6448	2.170	109	16.9	27.2	19.4	0.870
340	0.6059	2.192	116.5	19.2	29.3	22.1	0.872
360	0.5716	2.221	124	21.7	31.6	24.9	0.872
380	0.5410	2.254	131	24.2	34.0	27.9	0.869

Patent Owner Manufacturing Resources International, Inc.
Exhibit 2017 - Page 945 of 999

TABLE A.4 *Continued*

T (K)	ρ (kg/m^3)	c_p (kJ/kg · K)	$\mu \cdot 10^7$ (N · s/m^2)	$\nu \cdot 10^6$ (m^2/s)	$k \cdot 10^3$ (W/m · K)	$\alpha \cdot 10^6$ (m^2/s)	Pr
Ammonia (NH_3) *(continued)*							
400	0.5136	2.287	138	26.9	37.0	31.5	0.853
420	0.4888	2.322	145	29.7	40.4	35.6	0.833
440	0.4664	2.357	152.5	32.7	43.5	39.6	0.826
460	0.4460	2.393	159	35.7	46.3	43.4	0.822
480	0.4273	2.430	166.5	39.0	49.2	47.4	0.822
500	0.4101	2.467	173	42.2	52.5	51.9	0.813
520	0.3942	2.504	180	45.7	54.5	55.2	0.827
540	0.3795	2.540	186.5	49.1	57.5	59.7	0.824
560	0.3708	2.577	193	52.0	60.6	63.4	0.827
580	0.3533	2.613	199.5	56.5	63.8	69.1	0.817
Carbon Dioxide (CO_2)							
280	1.9022	0.830	140	7.36	15.20	9.63	0.765
300	1.7730	0.851	149	8.40	16.55	11.0	0.766
320	1.6609	0.872	156	9.39	18.05	12.5	0.754
340	1.5618	0.891	165	10.6	19.70	14.2	0.746
360	1.4743	0.908	173	11.7	21.2	15.8	0.741
380	1.3961	0.926	181	13.0	22.75	17.6	0.737
400	1.3257	0.942	190	14.3	24.3	19.5	0.737
450	1.1782	0.981	210	17.8	28.3	24.5	0.728
500	1.0594	1.02	231	21.8	32.5	30.1	0.725
550	0.9625	1.05	251	26.1	36.6	36.2	0.721
600	0.8826	1.08	270	30.6	40.7	42.7	0.717
650	0.8143	1.10	288	35.4	44.5	49.7	0.712
700	0.7564	1.13	305	40.3	48.1	56.3	0.717
750	0.7057	1.15	321	45.5	51.7	63.7	0.714
800	0.6614	1.17	337	51.0	55.1	71.2	0.716
Carbon Monoxide (CO)							
200	1.6888	1.045	127	7.52	17.0	9.63	0.781
220	1.5341	1.044	137	8.93	19.0	11.9	0.753
240	1.4055	1.043	147	10.5	20.6	14.1	0.744
260	1.2967	1.043	157	12.1	22.1	16.3	0.741
280	1.2038	1.042	166	13.8	23.6	18.8	0.733
300	1.1233	1.043	175	15.6	25.0	21.3	0.730
320	1.0529	1.043	184	17.5	26.3	23.9	0.730
340	0.9909	1.044	193	19.5	27.8	26.9	0.725
360	0.9357	1.045	202	21.6	29.1	29.8	0.725
380	0.8864	1.047	210	23.7	30.5	32.9	0.729
400	0.8421	1.049	218	25.9	31.8	36.0	0.719
450	0.7483	1.055	237	31.7	35.0	44.3	0.714
500	0.67352	1.065	254	37.7	38.1	53.1	0.710
550	0.61226	1.076	271	44.3	41.1	62.4	0.710
600	0.56126	1.088	286	51.0	44.0	72.1	0.707

Patent Owner Manufacturing Resources International, Inc.
Exhibit 2017 - Page 946 of 999

TABLE A.4 *Continued*

T (K)	ρ (kg/m^3)	c_p (kJ/kg · K)	$\mu \cdot 10^7$ (N · s/m^2)	$\nu \cdot 10^6$ (m^2/s)	$k \cdot 10^3$ (W/m · K)	$\alpha \cdot 10^6$ (m^2/s)	Pr
Carbon Monoxide (CO) *(continued)*							
650	0.51806	1.101	301	58.1	47.0	82.4	0.705
700	0.48102	1.114	315	65.5	50.0	93.3	0.702
750	0.44899	1.127	329	73.3	52.8	104	0.702
800	0.42095	1.140	343	81.5	55.5	116	0.705
Helium (He)							
100	0.4871	5.193	96.3	19.8	73.0	28.9	0.686
120	0.4060	5.193	107	26.4	81.9	38.8	0.679
140	0.3481	5.193	118	33.9	90.7	50.2	0.676
160	—	5.193	129	—	99.2	—	—
180	0.2708	5.193	139	51.3	107.2	76.2	0.673
200	—	5.193	150	—	115.1	—	—
220	0.2216	5.193	160	72.2	123.1	107	0.675
240	—	5.193	170	—	130	—	—
260	0.1875	5.193	180	96.0	137	141	0.682
280	—	5.193	190	—	145	—	—
300	0.1625	5.193	199	122	152	180	0.680
350	—	5.193	221	—	170	—	—
400	0.1219	5.193	243	199	187	295	0.675
450	—	5.193	263	—	204	—	—
500	0.09754	5.193	283	290	220	434	0.668
550	—	5.193	—	—	—	—	—
600	—	5.193	320	—	252	—	—
650	—	5.193	332	—	264	—	—
700	0.06969	5.193	350	502	278	768	0.654
750	—	5.193	364	—	291	—	—
800	—	5.193	382	—	304	—	—
900	—	5.193	414	—	330	—	—
1000	0.04879	5.193	446	914	354	1400	0.654
Hydrogen (H_2)							
100	0.24255	11.23	42.1	17.4	67.0	24.6	0.707
150	0.16156	12.60	56.0	34.7	101	49.6	0.699
200	0.12115	13.54	68.1	56.2	131	79.9	0.704
250	0.09693	14.06	78.9	81.4	157	115	0.707
300	0.08078	14.31	89.6	111	183	158	0.701
350	0.06924	14.43	98.8	143	204	204	0.700
400	0.06059	14.48	108.2	179	226	258	0.695
450	0.05386	14.50	117.2	218	247	316	0.689
500	0.04848	14.52	126.4	261	266	378	0.691
550	0.04407	14.53	134.3	305	285	445	0.685

Patent Owner Manufacturing Resources International, Inc.
Exhibit 2017 - Page 947 of 999

TABLE A.4 *Continued*

T (K)	ρ (kg/m^3)	c_p (kJ/kg · K)	$\mu \cdot 10^7$ (N · s/m^2)	$\nu \cdot 10^6$ (m^2/s)	$k \cdot 10^3$ (W/m · K)	$\alpha \cdot 10^6$ (m^2/s)	Pr
Hydrogen (H_2) *(continued)*							
600	0.04040	14.55	142.4	352	305	519	0.678
700	0.03463	14.61	157.8	456	342	676	0.675
800	0.03030	14.70	172.4	569	378	849	0.670
900	0.02694	14.83	186.5	692	412	1030	0.671
1000	0.02424	14.99	201.3	830	448	1230	0.673
1100	0.02204	15.17	213.0	966	488	1460	0.662
1200	0.02020	15.37	226.2	1120	528	1700	0.659
1300	0.01865	15.59	238.5	1279	568	1955	0.655
1400	0.01732	15.81	250.7	1447	610	2230	0.650
1500	0.01616	16.02	262.7	1626	655	2530	0.643
1600	0.0152	16.28	273.7	1801	697	2815	0.639
1700	0.0143	16.58	284.9	1992	742	3130	0.637
1800	0.0135	16.96	296.1	2193	786	3435	0.639
1900	0.0128	17.49	307.2	2400	835	3730	0.643
2000	0.0121	18.25	318.2	2630	878	3975	0.661
Nitrogen (N_2)							
100	3.4388	1.070	68.8	2.00	9.58	2.60	0.768
150	2.2594	1.050	100.6	4.45	13.9	5.86	0.759
200	1.6883	1.043	129.2	7.65	18.3	10.4	0.736
250	1.3488	1.042	154.9	11.48	22.2	15.8	0.727
300	1.1233	1.041	178.2	15.86	25.9	22.1	0.716
350	0.9625	1.042	200.0	20.78	29.3	29.2	0.711
400	0.8425	1.045	220.4	26.16	32.7	37.1	0.704
450	0.7485	1.050	239.6	32.01	35.8	45.6	0.703
500	0.6739	1.056	257.7	38.24	38.9	54.7	0.700
550	0.6124	1.065	274.7	44.86	41.7	63.9	0.702
600	0.5615	1.075	290.8	51.79	44.6	73.9	0.701
700	0.4812	1.098	321.0	66.71	49.9	94.4	0.706
800	0.4211	1.22	349.1	82.90	54.8	116	0.715
900	0.3743	1.146	375.3	100.3	59.7	139	0.721
1000	0.3368	1.167	399.9	118.7	64.7	165	0.721
1100	0.3062	1.187	423.2	138.2	70.0	193	0.718
1200	0.2807	1.204	445.3	158.6	75.8	224	0.707
1300	0.2591	1.219	466.2	179.9	81.0	256	0.701
Oxygen (O_2)							
100	3.945	0.962	76.4	1.94	9.25	2.44	0.796
150	2.585	0.921	114.8	4.44	13.8	5.80	0.766
200	1.930	0.915	147.5	7.64	18.3	10.4	0.737
250	1.542	0.915	178.6	11.58	22.6	16.0	0.723
300	1.284	0.920	207.2	16.14	26.8	22.7	0.711

Patent Owner Manufacturing Resources International, Inc.
Exhibit 2017 - Page 948 of 999

TABLE A.4 *Continued*

T (K)	ρ (kg/m^3)	c_p (kJ/kg · K)	$\mu \cdot 10^7$ (N · s/m^2)	$\nu \cdot 10^6$ (m^2/s)	$k \cdot 10^3$ (W/m · K)	$\alpha \cdot 10^6$ (m^2/s)	Pr
Oxygen (O_2) *(continued)*							
350	1.100	0.929	233.5	21.23	29.6	29.0	0.733
400	0.9620	0.942	258.2	26.84	33.0	36.4	0.737
450	0.8554	0.956	281.4	32.90	36.3	44.4	0.741
500	0.7698	0.972	303.3	39.40	41.2	55.1	0.716
550	0.6998	0.988	324.0	46.30	44.1	63.8	0.726
600	0.6414	1.003	343.7	53.59	47.3	73.5	0.729
700	0.5498	1.031	380.8	69.26	52.8	93.1	0.744
800	0.4810	1.054	415.2	86.32	58.9	116	0.743
900	0.4275	1.074	447.2	104.6	64.9	141	0.740
1000	0.3848	1.090	477.0	124.0	71.0	169	0.733
1100	0.3498	1.103	505.5	144.5	75.8	196	0.736
1200	0.3206	1.115	532.5	166.1	81.9	229	0.725
1300	0.2960	1.125	588.4	188.6	87.1	262	0.721
Water Vapor (Steam)							
380	0.5863	2.060	127.1	21.68	24.6	20.4	1.06
400	0.5542	2.014	134.4	24.25	26.1	23.4	1.04
450	0.4902	1.980	152.5	31.11	29.9	30.8	1.01
500	0.4405	1.985	170.4	38.68	33.9	38.8	0.998
550	0.4005	1.997	188.4	47.04	37.9	47.4	0.993
600	0.3652	2.026	206.7	56.60	42.2	57.0	0.993
650	0.3380	2.056	224.7	66.48	46.4	66.8	0.996
700	0.3140	2.085	242.6	77.26	50.5	77.1	1.00
750	0.2931	2.119	260.4	88.84	54.9	88.4	1.00
800	0.2739	2.152	278.6	101.7	59.2	100	1.01
850	0.2579	2.186	296.9	115.1	63.7	113	1.02

[a]Adapted from References 8, 14, and 15.

Patent Owner Manufacturing Resources International, Inc.
Exhibit 2017 - Page 949 of 999

TABLE A.5 Thermophysical Properties of Saturated Fluids[a]

Saturated Liquids

T (K)	ρ (kg/m^3)	c_p (kJ/kg · K)	$\mu \cdot 10^2$ (N · s/m^2)	$\nu \cdot 10^6$ (m^2/s)	$k \cdot 10^3$ (W/m · K)	$\alpha \cdot 10^7$ (m^2/s)	Pr	$\beta \cdot 10^3$ (K^{-1})
Engine Oil (Unused)								
273	899.1	1.796	385	4280	147	0.910	47,000	0.70
280	895.3	1.827	217	2430	144	0.880	27,500	0.70
290	890.0	1.868	99.9	1120	145	0.872	12,900	0.70
300	884.1	1.909	48.6	550	145	0.859	6400	0.70
310	877.9	1.951	25.3	288	145	0.847	3400	0.70
320	871.8	1.993	14.1	161	143	0.823	1965	0.70
330	865.8	2.035	8.36	96.6	141	0.800	1205	0.70
340	859.9	2.076	5.31	61.7	139	0.779	793	0.70
350	853.9	2.118	3.56	41.7	138	0.763	546	0.70
360	847.8	2.161	2.52	29.7	138	0.753	395	0.70
370	841.8	2.206	1.86	22.0	137	0.738	300	0.70
380	836.0	2.250	1.41	16.9	136	0.723	233	0.70
390	830.6	2.294	1.10	13.3	135	0.709	187	0.70
400	825.1	2.337	0.874	10.6	134	0.695	152	0.70
410	818.9	2.381	0.698	8.52	133	0.682	125	0.70
420	812.1	2.427	0.564	6.94	133	0.675	103	0.70
430	806.5	2.471	0.470	5.83	132	0.662	88	0.70
Ethylene Glycol [$C_2H_4(OH)_2$]								
273	1130.8	2.294	6.51	57.6	242	0.933	617	0.65
280	1125.8	2.323	4.20	37.3	244	0.933	400	0.65
290	1118.8	2.368	2.47	22.1	248	0.936	236	0.65
300	1114.4	2.415	1.57	14.1	252	0.939	151	0.65
310	1103.7	2.460	1.07	9.65	255	0.939	103	0.65
320	1096.2	2.505	0.757	6.91	258	0.940	73.5	0.65
330	1089.5	2.549	0.561	5.15	260	0.936	55.0	0.65
340	1083.8	2.592	0.431	3.98	261	0.929	42.8	0.65
350	1079.0	2.637	0.342	3.17	261	0.917	34.6	0.65
360	1074.0	2.682	0.278	2.59	261	0.906	28.6	0.65
370	1066.7	2.728	0.228	2.14	262	0.900	23.7	0.65
373	1058.5	2.742	0.215	2.03	263	0.906	22.4	0.65
Glycerin [$C_3H_5(OH)_3$]								
273	1276.0	2.261	1060	8310	282	0.977	85,000	0.47
280	1271.9	2.298	534	4200	284	0.972	43,200	0.47
290	1265.8	2.367	185	1460	286	0.955	15,300	0.48
300	1259.9	2.427	79.9	634	286	0.935	6780	0.48
310	1253.9	2.490	35.2	281	286	0.916	3060	0.49
320	1247.2	2.564	21.0	168	287	0.897	1870	0.50

TABLE A.

Saturate

T (K)	(kg
Refrigerant	
230	1·
240	1:
250	1:
260	1:
270	1:
280	1:
290	1:
300	1:
310	1:
320	1:
330	1(
340	1(
350	9
360	8
370	7
Refrigerant	
230	14
240	13
250	13
260	13
270	12
280	12
290	12
300	11
310	11
320	1(
330	1(
340	9
350	9
360	8
Mercury (H	
273	13,5
300	13,5
350	13,4
400	13,2
450	13,1
500	13,0
550	12,9
600	12,8

Patent Owner Manufacturing Resources International, Inc.
Exhibit 2017 - Page 950 of 999

TABLE A.5 *Continued*

Saturated Liquids (Continued)

T (K)	ρ (kg/m^3)	c_p (kJ/kg · K)	$\mu \cdot 10^2$ (N · s/m^2)	$\nu \cdot 10^6$ (m^2/s)	$k \cdot 10^3$ (W/m · K)	$\alpha \cdot 10^7$ (m^2/s)	Pr	$\beta \cdot 10^3$ (K^{-1})
Refrigerant-134a ($C_2H_2F_4$)								
230	1426.8	1.249	0.04912	0.3443	112.1	0.629	5.5	2.02
240	1397.7	1.267	0.04202	0.3006	107.3	0.606	5.0	2.11
250	1367.9	1.287	0.03633	0.2656	102.5	0.583	4.6	2.23
260	1337.1	1.308	0.03166	0.2368	97.9	0.560	4.2	2.36
270	1305.1	1.333	0.02775	0.2127	93.4	0.537	4.0	2.53
280	1271.8	1.361	0.02443	0.1921	89.0	0.514	3.7	2.73
290	1236.8	1.393	0.02156	0.1744	84.6	0.491	3.5	2.98
300	1199.7	1.432	0.01905	0.1588	80.3	0.468	3.4	3.30
310	1159.9	1.481	0.01680	0.1449	76.1	0.443	3.3	3.73
320	1116.8	1.543	0.01478	0.1323	71.8	0.417	3.2	4.33
330	1069.1	1.627	0.01292	0.1209	67.5	0.388	3.1	5.19
340	1015.0	1.751	0.01118	0.1102	63.1	0.355	3.1	6.57
350	951.3	1.961	0.00951	0.1000	58.6	0.314	3.2	9.10
360	870.1	2.437	0.00781	0.0898	54.1	0.255	3.5	15.39
370	740.3	5.105	0.00580	0.0783	51.8	0.137	5.7	55.24
Refrigerant-22 ($CHClF_2$)								
230	1416.0	1.087	0.03558	0.2513	114.5	0.744	3.4	2.05
240	1386.6	1.100	0.03145	0.2268	109.8	0.720	3.2	2.16
250	1356.3	1.117	0.02796	0.2062	105.2	0.695	3.0	2.29
260	1324.9	1.137	0.02497	0.1884	100.7	0.668	2.8	2.45
270	1292.1	1.161	0.02235	0.1730	96.2	0.641	2.7	2.63
280	1257.9	1.189	0.02005	0.1594	91.7	0.613	2.6	2.86
290	1221.7	1.223	0.01798	0.1472	87.2	0.583	2.5	3.15
300	1183.4	1.265	0.01610	0.1361	82.6	0.552	2.5	3.51
310	1142.2	1.319	0.01438	0.1259	78.1	0.518	2.4	4.00
320	1097.4	1.391	0.01278	0.1165	73.4	0.481	2.4	4.69
330	1047.5	1.495	0.01127	0.1075	68.6	0.438	2.5	5.75
340	990.1	1.665	0.00980	0.0989	63.6	0.386	2.6	7.56
350	920.1	1.997	0.00831	0.0904	58.3	0.317	2.8	11.35
360	823.4	3.001	0.00668	0.0811	53.1	0.215	3.8	23.88
Mercury (Hg)								
273	13,595	0.1404	0.1688	0.1240	8180	42.85	0.0290	0.181
300	13,529	0.1393	0.1523	0.1125	8540	45.30	0.0248	0.181
350	13,407	0.1377	0.1309	0.0976	9180	49.75	0.0196	0.181
400	13,287	0.1365	0.1171	0.0882	9800	54.05	0.0163	0.181
450	13,167	0.1357	0.1075	0.0816	10,400	58.10	0.0140	0.181
500	13,048	0.1353	0.1007	0.0771	10,950	61.90	0.0125	0.182
550	12,929	0.1352	0.0953	0.0737	11,450	65.55	0.0112	0.184
600	12,809	0.1355	0.0911	0.0711	11,950	68.80	0.0103	0.187

Patent Owner Manufacturing Resources International, Inc.
Exhibit 2017 - Page 951 of 999

TABLE A.5 *Continued*

Saturated Liquid–Vapor, 1 atm[b]

Fluid	T_{sat} (K)	h_{fg} (kJ/kg)	ρ_f (kg/m^3)	ρ_g (kg/m^3)	$\sigma \cdot 10^3$ (N/m)
Ethanol	351	846	757	1.44	17.7
Ethylene glycol	470	812	1111[c]	—	32.7
Glycerin	563	974	1260[c]	—	63.0[c]
Mercury	630	301	12,740	3.90	417
Refrigerant R-134a	247	217	1377	5.26	15.4
Refrigerant R-22	232	234	1409	4.70	18.1

[a]Adapted from References 15–19.
[b]Adapted from References 8, 20, and 21.
[c]Property value corresponding to 300 K.

TABLE A.6 Thermophysical Properties of Saturated Water[a]

Temperature	Specific Volume	Heat of Vapor-	Specific Heat	Viscosity	Thermal Conductivity	Prandtl	Surface	Expansion Coeffi-

Patent Owner Manufacturing Resources International, Inc.
Exhibit 2017 - Page 952 of 999

TABLE A.6 Thermophysical Properties of Saturated Water[a]

Temperature, T (K)	Pressure, p (bars)[b]	Specific Volume (m^3/kg) $v_f \cdot 10^3$	Specific Volume (m^3/kg) v_g	Heat of Vaporization, h_{fg} (kJ/kg)	Specific Heat (kJ/kg · K) $c_{p,f}$	Specific Heat (kJ/kg · K) $c_{p,g}$	Viscosity ($N \cdot s/m^2$) $\mu_f \cdot 10^6$	Viscosity ($N \cdot s/m^2$) $\mu_g \cdot 10^6$	Thermal Conductivity (W/m · K) $k_f \cdot 10^3$	Thermal Conductivity (W/m · K) $k_g \cdot 10^3$	Prandtl Number Pr_f	Prandtl Number Pr_g	Surface Tension, $\sigma_f \cdot 10^3$ (N/m)	Expansion Coefficient, $\beta_f \cdot 10^6$ (K^{-1})	Temperature, T (K)
273.15	0.00611	1.000	206.3	2502	4.217	1.854	1750	8.02	569	18.2	12.99	0.815	75.5	−68.05	273.15
275	0.00697	1.000	181.7	2497	4.211	1.855	1652	8.09	574	18.3	12.22	0.817	75.3	−32.74	275
280	0.00990	1.000	130.4	2485	4.198	1.858	1422	8.29	582	18.6	10.26	0.825	74.8	46.04	280
285	0.01387	1.000	99.4	2473	4.189	1.861	1225	8.49	590	18.9	8.81	0.833	74.3	114.1	285
290	0.01917	1.001	69.7	2461	4.184	1.864	1080	8.69	598	19.3	7.56	0.841	73.7	174.0	290
295	0.02617	1.002	51.94	2449	4.181	1.868	959	8.89	606	19.5	6.62	0.849	72.7	227.5	295
300	0.03531	1.003	39.13	2438	4.179	1.872	855	9.09	613	19.6	5.83	0.857	71.7	276.1	300
305	0.04712	1.005	29.74	2426	4.178	1.877	769	9.29	620	20.1	5.20	0.865	70.9	320.6	305
310	0.06221	1.007	22.93	2414	4.178	1.882	695	9.49	628	20.4	4.62	0.873	70.0	361.9	310
315	0.08132	1.009	17.82	2402	4.179	1.888	631	9.69	634	20.7	4.16	0.883	69.2	400.4	315
320	0.1053	1.011	13.98	2390	4.180	1.895	577	9.89	640	21.0	3.77	0.894	68.3	436.7	320
325	0.1351	1.013	11.06	2378	4.182	1.903	528	10.09	645	21.3	3.42	0.901	67.5	471.2	325
330	0.1719	1.016	8.82	2366	4.184	1.911	489	10.29	650	21.7	3.15	0.908	66.6	504.0	330
335	0.2167	1.018	7.09	2354	4.186	1.920	453	10.49	656	22.0	2.88	0.916	65.8	535.5	335
340	0.2713	1.021	5.74	2342	4.188	1.930	420	10.69	660	22.3	2.66	0.925	64.9	566.0	340
345	0.3372	1.024	4.683	2329	4.191	1.941	389	10.89	668	22.6	2.45	0.933	64.1	595.4	345
350	0.4163	1.027	3.846	2317	4.195	1.954	365	11.09	668	23.0	2.29	0.942	63.2	624.2	350
355	0.5100	1.030	3.180	2304	4.199	1.968	343	11.29	671	23.3	2.14	0.951	62.3	652.3	355
360	0.6209	1.034	2.645	2291	4.203	1.983	324	11.49	674	23.7	2.02	0.960	61.4	697.9	360
365	0.7514	1.038	2.212	2278	4.209	1.999	306	11.69	677	24.1	1.91	0.969	60.5	707.1	365
370	0.9040	1.041	1.861	2265	4.214	2.017	289	11.89	679	24.5	1.80	0.978	59.5	728.7	370
373.15	1.0133	1.044	1.679	2257	4.217	2.029	279	12.02	680	24.8	1.76	0.984	58.9	750.1	373.15
375	1.0815	1.045	1.574	2252	4.220	2.036	274	12.09	681	24.9	1.70	0.987	58.6	761	375
380	1.2869	1.049	1.337	2239	4.226	2.057	260	12.29	683	25.4	1.61	0.999	57.6	788	380
385	1.5233	1.053	1.142	2225	4.232	2.080	248	12.49	685	25.8	1.53	1.004	56.6	814	385
390	1.794	1.058	0.980	2212	4.239	2.104	237	12.69	686	26.3	1.47	1.013	55.6	841	390
400	2.455	1.067	0.731	2183	4.256	2.158	217	13.05	688	27.2	1.34	1.033	53.6	896	400
410	3.302	1.077	0.553	2153	4.278	2.221	200	13.42	688	28.2	1.24	1.054	51.5	952	410
420	4.370	1.088	0.425	2123	4.302	2.291	185	13.79	688	29.8	1.16	1.075	49.4	1010	420
430	5.699	1.099	0.331	2091	4.331	2.369	173	14.14	685	30.4	1.09	1.10	47.2		430

Patent Owner Manufacturing Resources International, Inc.
Exhibit 2017 - Page 953 of 999

TABLE A.6 *Continued*

Temperature, T (K)	Pressure, p (bars)[b]	Specific Volume (m^3/kg)		Heat of Vaporization, h_{fg} (kJ/kg)	Specific Heat (kJ/kg · K)		Viscosity ($N \cdot s/m^2$)		Thermal Conductivity (W/m · K)		Prandtl Number		Surface Tension, $\sigma_f \cdot 10^3$ (N/m)	Expansion Coefficient, $\beta_f \cdot 10^6$ (K^{-1})	Temperature, T (K)
		$v_f \cdot 10^3$	v_g		c_{pf}	c_{pg}	$\mu_f \cdot 10^6$	$\mu_g \cdot 10^6$	$k_f \cdot 10^3$	$k_g \cdot 10^3$	Pr_f	Pr_g			
440	7.333	1.110	0.261	2059	4.36	2.46	162	14.50	682	31.7	1.04	1.12	45.1		440
450	9.319	1.123	0.208	2024	4.40	2.56	152	14.85	678	33.1	0.99	1.14	42.9		450
460	11.71	1.137	0.167	1989	4.44	2.68	143	15.19	673	34.6	0.95	1.17	40.7		460
470	14.55	1.152	0.136	1951	4.48	2.79	136	15.54	667	36.3	0.92	1.20	38.5		470
480	17.90	1.167	0.111	1912	4.53	2.94	129	15.88	660	38.1	0.89	1.23	36.2		480
490	21.83	1.184	0.0922	1870	4.59	3.10	124	16.23	651	40.1	0.87	1.25	33.9	—	490
500	26.40	1.203	0.0766	1825	4.66	3.27	118	16.59	642	42.3	0.86	1.28	31.6	—	500
510	31.66	1.222	0.0631	1779	4.74	3.47	113	16.95	631	44.7	0.85	1.31	29.3	—	510
520	37.70	1.244	0.0525	1730	4.84	3.70	108	17.33	621	47.5	0.84	1.35	26.9	—	520
530	44.58	1.268	0.0445	1679	4.95	3.96	104	17.72	608	50.6	0.85	1.39	24.5	—	530
540	52.38	1.294	0.0375	1622	5.08	4.27	101	18.1	594	54.0	0.86	1.43	22.1	—	540
550	61.19	1.323	0.0317	1564	5.24	4.64	97	18.6	580	58.3	0.87	1.47	19.7	—	550
560	71.08	1.355	0.0269	1499	5.43	5.09	94	19.1	563	63.7	0.90	1.52	17.3	—	560
570	82.16	1.392	0.0228	1429	5.68	5.67	91	19.7	548	76.7	0.94	1.59	15.0	—	570
580	94.51	1.433	0.0193	1353	6.00	6.40	88	20.4	528	76.7	0.99	1.68	12.8	—	580
590	108.3	1.482	0.0163	1274	6.41	7.35	84	21.5	513	84.1	1.05	1.84	10.5	—	590
600	123.5	1.541	0.0137	1176	7.00	8.75	81	22.7	497	92.9	1.14	2.15	8.4	—	600
610	137.3	1.612	0.0115	1068	7.85	11.1	77	24.1	467	103	1.30	2.60	6.3	—	610
620	159.1	1.705	0.0094	941	9.35	15.4	72	25.9	444	114	1.52	3.46	4.5	—	620
625	169.1	1.778	0.0085	858	10.6	18.3	70	27.0	430	121	1.65	4.20	3.5	—	625
630	179.7	1.856	0.0075	781	12.6	22.1	67	28.0	412	130	2.0	4.8	2.6	—	630
635	190.9	1.935	0.0066	683	16.4	27.6	64	30.0	392	141	2.7	6.0	1.5	—	635
640	202.7	2.075	0.0057	560	26	42	59	32.0	367	155	4.2	9.6	0.8	—	640
645	215.2	2.351	0.0045	361	90	—	54	37.0	331	178	12	26	0.1	—	645
647.3[c]	221.2	3.170	0.0032	0	∞	∞	45	45.0	238	238	∞	∞	0.0	—	647.3[c]

[a]Adapted from Reference 22.
[b]1 bar = 10^5 N/m^2.
[c]Critical temperature.

TABLE A

Compositi
Bismuth
Lead
Potassium
Sodium
NaK, (45%/55%)
NaK, (22%/78%)
PbBi, (44.5%/55.5
Mercury

[a]Adapted fro

Patent Owner Manufacturing Resources International, Inc.
Exhibit 2017 - Page 954 of 999

TABLE A.7 Thermophysical Properties of Liquid Metals[a]

Composition	Melting Point (K)	T (K)	ρ (kg/m^3)	c_p (kJ/kg · K)	$\nu \cdot 10^7$ (m^2/s)	k (W/m · K)	$\alpha \cdot 10^5$ (m^2/s)	Pr
Bismuth	544	589	10,011	0.1444	1.617	16.4	0.138	0.0142
		811	9739	0.1545	1.133	15.6	1.035	0.0110
		1033	9467	0.1645	0.8343	15.6	1.001	0.0083
Lead	600	644	10,540	0.159	2.276	16.1	1.084	0.024
		755	10,412	0.155	1.849	15.6	1.223	0.017
		977	10,140	—	1.347	14.9	—	—
Potassium	337	422	807.3	0.80	4.608	45.0	6.99	0.0066
		700	741.7	0.75	2.397	39.5	7.07	0.0034
		977	674.4	0.75	1.905	33.1	6.55	0.0029
Sodium	371	366	929.1	1.38	7.516	86.2	6.71	0.011
		644	860.2	1.30	3.270	72.3	6.48	0.0051
		977	778.5	1.26	2.285	59.7	6.12	0.0037
NaK, (45%/55%)	292	366	887.4	1.130	6.522	25.6	2.552	0.026
		644	821.7	1.055	2.871	27.5	3.17	0.0091
		977	740.1	1.043	2.174	28.9	3.74	0.0058
NaK, (22%/78%)	262	366	849.0	0.946	5.797	24.4	3.05	0.019
		672	775.3	0.879	2.666	26.7	3.92	0.0068
		1033	690.4	0.883	2.118	—	—	—
PbBi, (44.5%/55.5%)	398	422	10,524	0.147	—	9.05	0.586	—
		644	10,236	0.147	1.496	11.86	0.790	0.189
		922	9835	—	1.171	—	—	—
Mercury	234			See Table A.5				

[a]Adapted from Reference 23.

647.3[c] 221.2 3.170 0.0032 0 8 8 45 45.0 238 238 8 8 0.0 — 647.3[c]

[a]Adapted from Reference 22.
[b]1 bar = 10^5 N/m^2.
[c]Critical temperature.

Patent Owner Manufacturing Resources International, Inc.
Exhibit 2017 - Page 955 of 999

TABLE A.8 Binary Diffusion Coefficients at One Atmosphere[a,b]

Substance A	Substance B	T (K)	D_{AB} (m^2/s)
Gases			
NH_3	Air	298	0.28×10^{-4}
H_2O	Air	298	0.26×10^{-4}
CO_2	Air	298	0.16×10^{-4}
H_2	Air	298	0.41×10^{-4}
O_2	Air	298	0.21×10^{-4}
Acetone	Air	273	0.11×10^{-4}
Benzene	Air	298	0.88×10^{-5}
Naphthalene	Air	300	0.62×10^{-5}
Ar	N_2	293	0.19×10^{-4}
H_2	O_2	273	0.70×10^{-4}
H_2	N_2	273	0.68×10^{-4}
H_2	CO_2	273	0.55×10^{-4}
CO_2	N_2	293	0.16×10^{-4}
CO_2	O_2	273	0.14×10^{-4}
O_2	N_2	273	0.18×10^{-4}
Dilute Solutions			
Caffeine	H_2O	298	0.63×10^{-9}
Ethanol	H_2O	298	0.12×10^{-8}
Glucose	H_2O	298	0.69×10^{-9}
Glycerol	H_2O	298	0.94×10^{-9}
Acetone	H_2O	298	0.13×10^{-8}
CO_2	H_2O	298	0.20×10^{-8}
O_2	H_2O	298	0.24×10^{-8}
H_2	H_2O	298	0.63×10^{-8}
N_2	H_2O	298	0.26×10^{-8}
Solids			
O_2	Rubber	298	0.21×10^{-9}
N_2	Rubber	298	0.15×10^{-9}
CO_2	Rubber	298	0.11×10^{-9}
He	SiO_2	293	0.4×10^{-13}
H_2	Fe	293	0.26×10^{-12}
Cd	Cu	293	0.27×10^{-18}
Al	Cu	293	0.13×10^{-33}

[a]Adapted with permission from References 24, 25, and 26.

[b]Assuming ideal gas behavior, the pressure and temperature dependence of the diffusion coefficient for a binary mixture of gases may be estimated from the relation

$$D_{AB} \propto p^{-1} T^{3/2}$$

TABLE A.

T (K)
273
280
290
300
310
320
323

[a]Adapted wit

Patent Owner Manufacturing Resources International, Inc.
Exhibit 2017 - Page 956 of 999

here[a,b]

D_{AB} (m^2/s)
0.28×10^{-4}
0.26×10^{-4}
0.16×10^{-4}
0.41×10^{-4}
0.21×10^{-4}
0.11×10^{-4}
0.88×10^{-5}
0.62×10^{-5}
0.19×10^{-4}
0.70×10^{-4}
0.68×10^{-4}
0.55×10^{-4}
0.16×10^{-4}
0.14×10^{-4}
0.18×10^{-4}
0.63×10^{-9}
0.12×10^{-8}
0.69×10^{-9}
0.94×10^{-9}
0.13×10^{-8}
0.20×10^{-8}
0.24×10^{-8}
0.63×10^{-8}
0.26×10^{-8}
0.21×10^{-9}
0.15×10^{-9}
0.11×10^{-9}
0.4×10^{-13}
0.26×10^{-12}
0.27×10^{-18}
0.13×10^{-33}

n coefficient for a

TABLE A.9 Henry's Constant for Selected Gases in Water at Moderate Pressure[a]

	$H = p_{A,i}/x_{A,i}$ (bars)							
T (K)	NH_3	Cl_2	H_2S	SO_2	CO_2	CH_4	O_2	H_2
273	21	265	260	165	710	22,880	25,500	58,000
280	23	365	335	210	960	27,800	30,500	61,500
290	26	480	450	315	1300	35,200	37,600	66,500
300	30	615	570	440	1730	42,800	45,700	71,600
310	—	755	700	600	2175	50,000	52,500	76,000
320	—	860	835	800	2650	56,300	56,800	78,600
323	—	890	870	850	2870	58,000	58,000	79,000

[a]Adapted with permission from Reference 27.

TABLE A.10 The Solubility of Selected Gases and Solids[a]

Gas	Solid	T (K)	$S = C_{A,i}/p_{A,i}$ (kmol/m³ · bar)
O_2	Rubber	298	3.12×10^{-3}
N_2	Rubber	298	1.56×10^{-3}
CO_2	Rubber	298	40.15×10^{-3}
He	SiO_2	293	0.45×10^{-3}
H_2	Ni	358	9.01×10^{-3}

[a]Adapted with permission from Reference 26.

Patent Owner Manufacturing Resources International, Inc.
Exhibit 2017 - Page 957 of 999

TABLE A.11 Total, Normal (n) or Hemispherical (h) Emissivity of Selected Surfaces

Metallic Solids and Their Oxides[a]

Description/Composition		Emissivity, ε_n or ε_h, at Various Temperatures (K)										
		100	200	300	400	600	800	1000	1200	1500	2000	2500
Aluminum												
Highly polished, film	(h)	0.02	0.03	0.04	0.05	0.06						
Foil, bright	(h)	0.06	0.06	0.07								
Anodized	(h)			0.82	0.76							
Chromium												
Polished or plated	(n)	0.05	0.07	0.10	0.12	0.14						
Copper												
Highly polished	(h)			0.03	0.03	0.04	0.04	0.04				
Stably oxidized	(h)					0.50	0.58	0.80				
Gold												
Highly polished or film	(h)	0.01	0.02	0.03	0.03	0.04	0.05	0.06				
Foil, bright	(h)	0.06	0.07	0.07								
Molybdenum												
Polished	(h)					0.06	0.08	0.10	0.12	0.15	0.21	0.26
Shot-blasted, rough	(h)					0.25	0.28	0.31	0.35	0.42		
Stably oxidized	(h)					0.80	0.82					
Nickel												
Polished	(h)					0.09	0.11	0.14	0.17			
Stably oxidized	(h)					0.40	0.49	0.57				
Platinum												
Polished	(h)						0.10	0.13	0.15	0.18		
Silver												
Polished	(h)			0.02	0.02	0.03	0.05	0.08				
Stainless steels												
Typical, polished	(n)			0.17	0.17	0.19	0.23	0.30				
Typical, cleaned	(n)			0.22	0.22	0.24	0.28	0.35				
Typical, lightly oxidized	(n)						0.33	0.40				
Typical, highly oxidized	(n)						0.67	0.70	0.76			
AISI 347, stably oxidized	(n)					0.87	0.88	0.89	0.90			
Tantalum												
Polished	(h)								0.11	0.17	0.23	0.28
Tungsten												
Polished	(h)							0.10	0.13	0.18	0.25	0.29

Patent Owner Manufacturing Resources International, Inc.
Exhibit 2017 - Page 958 of 999

TABLE A.11 *Continued*

Nonmetallic Substances[b]

Description/Composition		Temperature (K)	Emissivity ε
Aluminum oxide	(*n*)	600	0.69
		1000	0.55
		1500	0.41
Asphalt pavement	(*h*)	300	0.85–0.93
Building materials			
Asbestos sheet	(*h*)	300	0.93–0.96
Brick, red	(*h*)	300	0.93–0.96
Gypsum or plaster board	(*h*)	300	0.90–0.92
Wood	(*h*)	300	0.82–0.92
Cloth	(*h*)	300	0.75–0.90
Concrete	(*h*)	300	0.88–0.93
Glass, window	(*h*)	300	0.90–0.95
Ice	(*h*)	273	0.95–0.98
Paints			
Black (Parsons)	(*h*)	300	0.98
White, acrylic	(*h*)	300	0.90
White, zinc oxide	(*h*)	300	0.92
Paper, white	(*h*)	300	0.92–0.97
Pyrex	(*n*)	300	0.82
		600	0.80
		1000	0.71
		1200	0.62
Pyroceram	(*n*)	300	0.85
		600	0.78
		1000	0.69
		1500	0.57
Refractories (furnace liners)			
Alumina brick	(*n*)	800	0.40
		1000	0.33
		1400	0.28
		1600	0.33
Magnesia brick	(*n*)	800	0.45
		1000	0.36
		1400	0.31
		1600	0.40
Kaolin insulating brick	(*n*)	800	0.70
		1200	0.57
		1400	0.47
		1600	0.53
Sand	(*h*)	300	0.90
Silicon carbide	(*n*)	600	0.87
		1000	0.87
		1500	0.85
Skin	(*h*)	300	0.95
Snow	(*h*)	273	0.82–0.90

			0.11	0.17	0.23	0.28		
Tantalum	(*h*)							
Polished			0.13	0.18	0.25	0.29		
		0.10						
Tungsten	(*h*)							
Polished								

Patent Owner Manufacturing Resources International, Inc.
Exhibit 2017 - Page 959 of 999

TABLE A.11 *Continued*

Nonmetallic Substances[b]

Description/Composition		Temperature (K)	Emissivity ε
Soil	(*h*)	300	0.93–0.96
Rocks	(*h*)	300	0.88–0.95
Teflon	(*h*)	300	0.85
		400	0.87
		500	0.92
Vegetation	(*h*)	300	0.92–0.96
Water	(*h*)	300	0.96

[a]Adapted from Reference 1.
[b]Adapted from References 1, 9, 28, and 29.

TABLE A.12 Solar Radiative Properties for Selected Materials[a]

Description/Composition	α_S	ε^b	α_S/ε	τ_S
Aluminum				
Polished	0.09	0.03	3.0	
Anodized	0.14	0.84	0.17	
Quartz overcoated	0.11	0.37	0.30	
Foil	0.15	0.05	3.0	
Brick, red (Purdue)	0.63	0.93	0.68	
Concrete	0.60	0.88	0.68	
Galvanized sheet metal				
Clean, new	0.65	0.13	5.0	
Oxidized, weathered	0.80	0.28	2.9	
Glass, 3.2-mm thickness				
Float or tempered				0.79
Low iron oxide type				0.88
Metal, plated				
Black sulfide	0.92	0.10	9.2	
Black cobalt oxide	0.93	0.30	3.1	
Black nickel oxide	0.92	0.08	11	
Black chrome	0.87	0.09	9.7	
Mylar, 0.13-mm thickness				0.87
Paints				
Black (Parsons)	0.98	0.98	1.0	
White, acrylic	0.26	0.90	0.29	
White, zinc oxide	0.16	0.93	0.17	
Plexiglas, 3.2-mm thickness				0.90
Snow				
Fine particles, fresh	0.13	0.82	0.16	
Ice granules	0.33	0.89	0.37	
Tedlar, 0.10-mm thickness				0.92
Teflon, 0.13-mm thickness				0.92

[a]Adapted with permission from Reference 29.
[b]The emissivity values in this table correspond to a surface temperature of approximately 300 K.

Referen

1. Toulouk
Propert
Metallic
metallic
Vol. 5,
mal Rac
mal Ra
Therma
New Yc
2. Toulouk
Propert
mal Rac
ties of
Properti
Univers
3. Ho, C.
Ref. Da
4. Desai,
mann,
of Carb
Low Cl
ties of
of Stai
Univers
5. Americ
Proper
Park, O
6. Hultgre
K. K. K
Therma
Society
7. Hultgre
and K.
Proper
Metals
8. Americ
Conditi
mental
9. Mallor
hold, N
10. Hanley
mal Tr
peratur
the Se
Americ
1977.
11. Sweat,
for Fo
Paper

Patent Owner Manufacturing Resources International, Inc.
Exhibit 2017 - Page 960 of 999

	Emissivity ε
	0.93–0.96
	0.88–0.95
	0.85
	0.87
	0.92
	0.92–0.96
	0.96

terials[a]

/ε	τ_S
0	
17	
30	
0	
68	
68	
0	
9	
	0.79
	0.88
2	
1	
7	
	0.87
0	
29	
17	
	0.90
16	
37	
	0.92
	0.92

ately 300 K.

References

1. Touloukian, Y. S., and C. Y. Ho, Eds., *Thermophysical Properties of Matter,* Vol. 1, *Thermal Conductivity of Metallic Solids;* Vol. 2, *Thermal Conductivity of Nonmetallic Solids;* Vol. 4, *Specific Heat of Metallic Solids;* Vol. 5, *Specific Heat of Nonmetallic Solids;* Vol. 7, *Thermal Radiative Properties of Metallic Solids;* Vol. 8, *Thermal Radiative Properties of Nonmetallic Solids;* Vol. 9, *Thermal Radiative Properties of Coatings,* Plenum Press, New York, 1972.
2. Touloukian, Y. S., and C. Y. Ho, Eds., *Thermophysical Properties of Selected Aerospace Materials,* Part I: Thermal Radiative Properties; Part II: Thermophysical Properties of Seven Materials. Thermophysical and Electronic Properties Information Analysis Center, CINDAS, Purdue University, West Lafayette, IN, 1976.
3. Ho, C. Y., R. W. Powell, and P. E. Liley, *J. Phys. Chem. Ref. Data,* **3,** Supplement 1, 1974.
4. Desai, P. D., T. K. Chu, R. H. Bogaard, M. W. Ackermann, and C. Y. Ho, Part I: Thermophysical Properties of Carbon Steels; Part II: Thermophysical Properties of Low Chromium Steels; Part III: Thermophysical Properties of Nickel Steels; Part IV: Thermophysical Properties of Stainless Steels. CINDAS Special Report, Purdue University, West Lafayette, IN, September 1976.
5. American Society for Metals, *Metals Handbook,* Vol. 1, *Properties and Selection of Metals,* 8th ed., ASM, Metals Park, OH, 1961.
6. Hultgren, R., P. D. Desai, D. T. Hawkins, M. Gleiser, K. K. Kelley, and D. D. Wagman, *Selected Values of the Thermodynamic Properties of the Elements,* American Society of Metals, Metals Park, OH, 1973.
7. Hultgren, R., P. D. Desai, D. T. Hawkins, M. Gleiser, and K. K. Kelley, *Selected Values of the Thermodynamic Properties of Binary Alloys,* American Society of Metals, Metals Park, OH, 1973.
8. American Society of Heating, Refrigerating and Air Conditioning Engineers, *ASHRAE Handbook of Fundamentals,* ASHRAE, New York, 1981.
9. Mallory, J. F., *Thermal Insulation,* Van Nostrand Reinhold, New York, 1969.
10. Hanley, E. J., D. P. DeWitt, and R. E. Taylor, "The Thermal Transport Properties at Normal and Elevated Temperature of Eight Representative Rocks," *Proceedings of the Seventh Symposium on Thermophysical Properties,* American Society of Mechanical Engineers, New York, 1977.
11. Sweat, V. E., "A Miniature Thermal Conductivity Probe for Foods," American Society of Mechanical Engineers, Paper 76-HT-60, August 1976.
12. Kothandaraman, C. P., and S. Subramanyan, *Heat and Mass Transfer Data Book,* Halsted Press/Wiley, New York, 1975.
13. Chapman, A. J., *Heat Transfer,* 4th ed., Macmillan, New York, 1984.
14. Vargaftik, N. B., *Tables of Thermophysical Properties of Liquids and Gases,* 2nd ed., Hemisphere Publishing, New York, 1975.
15. Eckert, E. R. G., and R. M. Drake, *Analysis of Heat and Mass Transfer,* McGraw-Hill, New York, 1972.
16. Vukalovich, M. P., A. I. Ivanov, L. R. Fokin, and A. T. Yakovelev, *Thermophysical Properties of Mercury,* State Committee on Standards, State Service for Standards and Handbook Data, Monograph Series No. 9, Izd. Standartov, Moscow, 1971.
17. Tillner-Roth, R., and H. D. Baehr, *J. Phys. Chem. Ref. Data,* **23,** 657, 1994.
18. Kamei, A., S. W. Beyerlein, and R. T. Jacobsen, *Int. J. Thermophysics,* **16,** 1155, 1995.
19. Lemmon, E. W., M. O. McLinden, and M. L. Huber, *NIST Standard Reference Database* 23: Reference Fluid Thermodynamic and Transport Properties-REFPROP, Version 7.0 National Institute of Standards and Technology, Standard Reference Data Program, Gaithersburg, 2002.
20. Bolz, R. E., and G. L. Tuve, Eds., CRC Handbook of Tables for Applied Engineering Science, 2nd ed., CRC Press, Boca Raton, FL, 1979.
21. Liley, P. E., private communication, School of Mechanical Engineering, Purdue University, West Lafayette, IN, May 1984.
22. Liley, P. E., Steam Tables in SI Units, private communication, School of Mechanical Engineering, Purdue University, West Lafayette, IN, March 1984.
23. *Liquid Materials Handbook,* 23rd ed., The Atomic Energy Commission, Department of the Navy, Washington, DC, 1952.
24. Perry, J. H., Ed., *Chemical Engineer's Handbook,* 4th ed., McGraw-Hill, New York, 1963.
25. Geankoplis, C. J., *Mass Transport Phenomena,* Holt, Rinehart & Winston, New York, 1972.
26. Barrer, R. M., *Diffusion in and Through Solids,* Macmillan, New York, 1941.
27. Spalding, D. B., *Convective Mass Transfer,* McGraw-Hill, New York, 1963.
28. Gubareff, G. G., J. E. Janssen, and R. H. Torborg, *Thermal Radiation Properties Survey,* Minneapolis-Honeywell Regulator Company, Minneapolis, MN, 1960.
29. Kreith, F., and J. F. Kreider, *Principles of Solar Energy,* Hemisphere Publishing, New York, 1978.

Patent Owner Manufacturing Resources International, Inc.
Exhibit 2017 - Page 961 of 999

APPENDIX B

Mathematical Relations and Functions

Section		*Page*
B.1	Hyperbolic Functions	960
B.2	Gaussian Error Function	961
B.3	The First Four Roots of the Transcendental Equation, $\xi_n \tan \xi_n = Bi$, for Transient Conduction in a Plane Wall	962
B.4	Bessel Functions of the First Kind	963
B.5	Modified Bessel Functions of the First and Second Kinds	964

Patent Owner Manufacturing Resources International, Inc.
Exhibit 2017 - Page 962 of 999

B.1 *Hyperbolic Functions*[1]

x	sinh x	cosh x	tanh x	x	sinh x	cosh x	tanh x
0.00	0.0000	1.0000	0.00000	2.00	3.6269	3.7622	0.96403
0.10	0.1002	1.0050	0.09967	2.10	4.0219	4.1443	0.97045
0.20	0.2013	1.0201	0.19738	2.20	4.4571	4.5679	0.97574
0.30	0.3045	1.0453	0.29131	2.30	4.9370	5.0372	0.98010
0.40	0.4108	1.0811	0.37995	2.40	5.4662	5.5569	0.98367
0.50	0.5211	1.1276	0.46212	2.50	6.0502	6.1323	0.98661
0.60	0.6367	1.1855	0.53705	2.60	6.6947	6.7690	0.98903
0.70	0.7586	1.2552	0.60437	2.70	7.4063	7.4735	0.99101
0.80	0.8881	1.3374	0.66404	2.80	8.1919	8.2527	0.99263
0.90	1.0265	1.4331	0.71630	2.90	9.0596	9.1146	0.99396
1.00	1.1752	1.5431	0.76159	3.00	10.018	10.068	0.99505
1.10	1.3356	1.6685	0.80050	3.50	16.543	16.573	0.99818
1.20	1.5095	1.8107	0.83365	4.00	27.290	27.308	0.99933
1.30	1.6984	1.9709	0.86172	4.50	45.003	45.014	0.99975
1.40	1.9043	2.1509	0.88535	5.00	74.203	74.210	0.99991
1.50	2.1293	2.3524	0.90515	6.00	201.71	201.72	0.99999
1.60	2.3756	2.5775	0.92167	7.00	548.32	548.32	1.0000
1.70	2.6456	2.8283	0.93541	8.00	1490.5	1490.5	1.0000
1.80	2.9422	3.1075	0.94681	9.00	4051.5	4051.5	1.0000
1.90	3.2682	3.4177	0.95624	10.000	11013	11013	1.0000

[1]The hyperbolic functions are defined as

$$\sinh x = \tfrac{1}{2}(e^x - e^{-x}) \qquad \cosh x = \tfrac{1}{2}(e^x + e^{-x}) \qquad \tanh x = \frac{e^x - e^{-x}}{e^x + e^{-x}} = \frac{\sinh x}{\cosh x}$$

The derivatives of the hyperbolic functions of the variable u are given as

$$\frac{d}{dx}(\sinh u) = (\cosh u)\frac{du}{dx} \qquad \frac{d}{dx}(\cosh u) = (\sinh u)\frac{du}{dx} \qquad \frac{d}{dx}(\tanh u) = \left(\frac{1}{\cosh^2 u}\right)\frac{du}{dx}$$

B.2 *Gaussi*

Patent Owner Manufacturing Resources International, Inc.
Exhibit 2017 - Page 963 of 999

	tanh x
22	0.96403
43	0.97045
79	0.97574
72	0.98010
69	0.98367
23	0.98661
90	0.98903
35	0.99101
27	0.99263
46	0.99396
68	0.99505
73	0.99818
08	0.99933
14	0.99975
10	0.99991
72	0.99999
32	1.0000
5	1.0000
5	1.0000
	1.0000

$$\frac{x}{x} = \frac{\sinh x}{\cosh x}$$

$$\left(\frac{1}{\cosh^2 u}\right)\frac{du}{dx}$$

B.2 *Gaussian Error Function*[1]

w	erf w	w	erf w	w	erf w
0.00	0.00000	0.36	0.38933	1.04	0.85865
0.02	0.02256	0.38	0.40901	1.08	0.87333
0.04	0.04511	0.40	0.42839	1.12	0.88679
0.06	0.06762	0.44	0.46622	1.16	0.89910
0.08	0.09008	0.48	0.50275	1.20	0.91031
0.10	0.11246	0.52	0.53790	1.30	0.93401
0.12	0.13476	0.56	0.57162	1.40	0.95228
0.14	0.15695	0.60	0.60386	1.50	0.96611
0.16	0.17901	0.64	0.63459	1.60	0.97635
0.18	0.20094	0.68	0.66378	1.70	0.98379
0.20	0.22270	0.72	0.69143	1.80	0.98909
0.22	0.24430	0.76	0.71754	1.90	0.99279
0.24	0.26570	0.80	0.74210	2.00	0.99532
0.26	0.28690	0.84	0.76514	2.20	0.99814
0.28	0.30788	0.88	0.78669	2.40	0.99931
0.30	0.32863	0.92	0.80677	2.60	0.99976
0.32	0.34913	0.96	0.82542	2.80	0.99992
0.34	0.36936	1.00	0.84270	3.00	0.99998

[1]The Gaussian error function is defined as

$$\text{erf } w = \frac{2}{\sqrt{\pi}}\int_0^w e^{-v^2}\,dv$$

The complementary error function is defined as

$$\text{erfc } w \equiv 1 - \text{erf } w$$

Patent Owner Manufacturing Resources International, Inc.
Exhibit 2017 - Page 964 of 999

B.3
The First Four Roots of the Transcendental Equation, $\xi_n \tan \xi_n = Bi$, for Transient Conduction in a Plane Wall

$Bi = \frac{hL}{k}$	ξ_1	ξ_2	ξ_3	ξ_4
0	0	3.1416	6.2832	9.4248
0.001	0.0316	3.1419	6.2833	9.4249
0.002	0.0447	3.1422	6.2835	9.4250
0.004	0.0632	3.1429	6.2838	9.4252
0.006	0.0774	3.1435	6.2841	9.4254
0.008	0.0893	3.1441	6.2845	9.4256
0.01	0.0998	3.1448	6.2848	9.4258
0.02	0.1410	3.1479	6.2864	9.4269
0.04	0.1987	3.1543	6.2895	9.4290
0.06	0.2425	3.1606	6.2927	9.4311
0.08	0.2791	3.1668	6.2959	9.4333
0.1	0.3111	3.1731	6.2991	9.4354
0.2	0.4328	3.2039	6.3148	9.4459
0.3	0.5218	3.2341	6.3305	9.4565
0.4	0.5932	3.2636	6.3461	9.4670
0.5	0.6533	3.2923	6.3616	9.4775
0.6	0.7051	3.3204	6.3770	9.4879
0.7	0.7506	3.3477	6.3923	9.4983
0.8	0.7910	3.3744	6.4074	9.5087
0.9	0.8274	3.4003	6.4224	9.5190
1.0	0.8603	3.4256	6.4373	9.5293
1.5	0.9882	3.5422	6.5097	9.5801
2.0	1.0769	3.6436	6.5783	9.6296
3.0	1.1925	3.8088	6.7040	9.7240
4.0	1.2646	3.9352	6.8140	9.8119
5.0	1.3138	4.0336	6.9096	9.8928
6.0	1.3496	4.1116	6.9924	9.9667
7.0	1.3766	4.1746	7.0640	10.0339
8.0	1.3978	4.2264	7.1263	10.0949
9.0	1.4149	4.2694	7.1806	10.1502
10.0	1.4289	4.3058	7.2281	10.2003
15.0	1.4729	4.4255	7.3959	10.3898
20.0	1.4961	4.4915	7.4954	10.5117
30.0	1.5202	4.5615	7.6057	10.6543
40.0	1.5325	4.5979	7.6647	10.7334
50.0	1.5400	4.6202	7.7012	10.7832
60.0	1.5451	4.6353	7.7259	10.8172
80.0	1.5514	4.6543	7.7573	10.8606
100.0	1.5552	4.6658	7.7764	10.8871
∞	1.5708	4.7124	7.8540	10.9956

B.4
Bessel

Patent Owner Manufacturing Resources International, Inc.
Exhibit 2017 - Page 965 of 999

B.4
Bessel Functions of the First Kind

x	$J_0(x)$	$J_1(x)$
0.0	1.0000	0.0000
0.1	0.9975	0.0499
0.2	0.9900	0.0995
0.3	0.9776	0.1483
0.4	0.9604	0.1960
0.5	0.9385	0.2423
0.6	0.9120	0.2867
0.7	0.8812	0.3290
0.8	0.8463	0.3688
0.9	0.8075	0.4059
1.0	0.7652	0.4400
1.1	0.7196	0.4709
1.2	0.6711	0.4983
1.3	0.6201	0.5220
1.4	0.5669	0.5419
1.5	0.5118	0.5579
1.6	0.4554	0.5699
1.7	0.3980	0.5778
1.8	0.3400	0.5815
1.9	0.2818	0.5812
2.0	0.2239	0.5767
2.1	0.1666	0.5683
2.2	0.1104	0.5560
2.3	0.0555	0.5399
2.4	0.0025	0.5202

Patent Owner Manufacturing Resources International, Inc.
Exhibit 2017 - Page 966 of 999

B.5
Modified Bessel Functions[1] of the First and Second Kinds

x	$e^{-x}I_0(x)$	$e^{-x}I_1(x)$	$e^{x}K_0(x)$	$e^{x}K_1(x)$
0.0	1.0000	0.0000	∞	∞
0.2	0.8269	0.0823	2.1407	5.8334
0.4	0.6974	0.1368	1.6627	3.2587
0.6	0.5993	0.1722	1.4167	2.3739
0.8	0.5241	0.1945	1.2582	1.9179
1.0	0.4657	0.2079	1.1445	1.6361
1.2	0.4198	0.2152	1.0575	1.4429
1.4	0.3831	0.2185	0.9881	1.3010
1.6	0.3533	0.2190	0.9309	1.1919
1.8	0.3289	0.2177	0.8828	1.1048
2.0	0.3085	0.2153	0.8416	1.0335
2.2	0.2913	0.2121	0.8056	0.9738
2.4	0.2766	0.2085	0.7740	0.9229
2.6	0.2639	0.2046	0.7459	0.8790
2.8	0.2528	0.2007	0.7206	0.8405
3.0	0.2430	0.1968	0.6978	0.8066
3.2	0.2343	0.1930	0.6770	0.7763
3.4	0.2264	0.1892	0.6579	0.7491
3.6	0.2193	0.1856	0.6404	0.7245
3.8	0.2129	0.1821	0.6243	0.7021
4.0	0.2070	0.1787	0.6093	0.6816
4.2	0.2016	0.1755	0.5953	0.6627
4.4	0.1966	0.1724	0.5823	0.6453
4.6	0.1919	0.1695	0.5701	0.6292
4.8	0.1876	0.1667	0.5586	0.6142
5.0	0.1835	0.1640	0.5478	0.6003
5.2	0.1797	0.1614	0.5376	0.5872
5.4	0.1762	0.1589	0.5279	0.5749
5.6	0.1728	0.1565	0.5188	0.5633
5.8	0.1696	0.1542	0.5101	0.5525
6.0	0.1666	0.1520	0.5019	0.5422
6.4	0.1611	0.1479	0.4865	0.5232
6.8	0.1561	0.1441	0.4724	0.5060
7.2	0.1515	0.1405	0.4595	0.4905
7.6	0.1473	0.1372	0.4476	0.4762
8.0	0.1434	0.1341	0.4366	0.4631
8.4	0.1398	0.1312	0.4264	0.4511
8.8	0.1365	0.1285	0.4168	0.4399
9.2	0.1334	0.1260	0.4079	0.4295
9.6	0.1305	0.1235	0.3995	0.4198
10.0	0.1278	0.1213	0.3916	0.4108

[1] $I_{n+1}(x) = I_{n-1}(x) - (2n/x)I_n(x)$

Patent Owner Manufacturing Resources International, Inc.
Exhibit 2017 - Page 967 of 999

APPENDIX C

Thermal Conditions Associated with Uniform Energy Generation in One-Dimensional, Steady-State Systems

Patent Owner Manufacturing Resources International, Inc.
Exhibit 2017 - Page 968 of 999

In Section 3.5 the problem of conduction with thermal energy generation is considered for one-dimensional, steady-state conditions. The form of the heat equation differs, according to whether the system is a plane wall, a cylindrical shell, or a spherical shell (Figure C.1). In each case, there are several options for the boundary condition at each surface, and hence a greater number of possibilities for specific forms of the temperature distribution and heat rate (or heat flux).

An alternative to solving the heat equation for each possible combination of boundary conditions involves obtaining a solution by prescribing *boundary conditions of the first kind,* Equation 2.24, at both surfaces and then applying an energy balance to each surface at which the temperature is unknown. For the geometries of Figure C.1, with uniform temperatures $T_{s,1}$ and $T_{s,2}$ prescribed at each surface, solutions to appropriate forms of the heat equation are readily obtained and are summarized in Table C.1. The temperature distributions may be used with Fourier's law to obtain corresponding distributions for the heat flux and heat rate. If $T_{s,1}$ and $T_{s,2}$ are both known for a particular problem, the expressions of Table C.1 provide all that is needed to completely determine related thermal conditions. If $T_{s,1}$ and/or $T_{s,2}$ are not known, the results may still be used with surface energy balances to determine the desired thermal conditions.

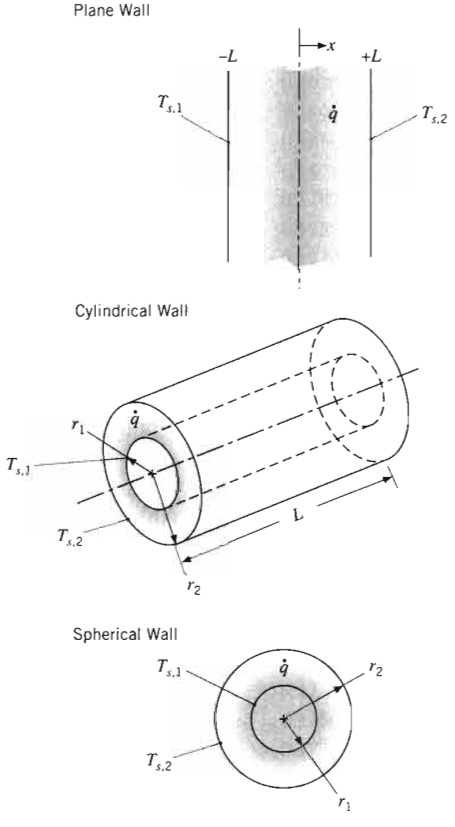


FIGURE C.1
One-dimensional conduction systems with uniform thermal energy generation: a plane wall with asymmetric surface conditions, a cylindrical shell, and a spherical shell.

TABLE C.
Heat
with

Plane Wall

Cylindrical

Spherical W

Plane Wall

Cylindrical

Spherical W

Plane Wall

Cylindrical W

Spherical Wa

Patent Owner Manufacturing Resources International, Inc.
Exhibit 2017 - Page 969 of 999

TABLE C.1 One-Dimensional, Steady-State Solutions to the Heat Equation for Plane, Cylindrical, and Spherical Walls with Uniform Generation and Asymmetrical Surface Conditions

Temperature Distribution

Plane Wall

$$T(x) = \frac{\dot{q}L^2}{2k}\left(1 - \frac{x^2}{L^2}\right) + \frac{T_{s,2} - T_{s,1}}{2}\frac{x}{L} + \frac{T_{s,1} + T_{s,2}}{2} \tag{C.1}$$

Cylindrical Wall

$$T(r) = T_{s,2} + \frac{\dot{q}r_2^2}{4k}\left(1 - \frac{r^2}{r_2^2}\right) - \left[\frac{\dot{q}r_2^2}{4k}\left(1 - \frac{r_1^2}{r_2^2}\right) + (T_{s,2} - T_{s,1})\right]\frac{\ln(r_2/r)}{\ln(r_2/r_1)} \tag{C.2}$$

Spherical Wall

$$T(r) = T_{s,2} + \frac{\dot{q}r_2^2}{6k}\left(1 - \frac{r^2}{r_2^2}\right) - \left[\frac{\dot{q}r_2^2}{6k}\left(1 - \frac{r_1^2}{r_2^2}\right) + (T_{s,2} - T_{s,1})\right]\frac{(1/r) - (1/r_2)}{(1/r_1) - (1/r_2)} \tag{C.3}$$

Heat Flux

Plane Wall

$$q''(x) = \dot{q}x - \frac{k}{2L}(T_{s,2} - T_{s,1}) \tag{C.4}$$

Cylindrical Wall

$$q''(r) = \frac{\dot{q}r}{2} - \frac{k\left[\frac{\dot{q}r_2^2}{4k}\left(1 - \frac{r_1^2}{r_2^2}\right) + (T_{s,2} - T_{s,1})\right]}{r\ln(r_2/r_1)} \tag{C.5}$$

Spherical Wall

$$q''(r) = \frac{\dot{q}r}{3} - \frac{k\left[\frac{\dot{q}r_2^2}{6k}\left(1 - \frac{r_1^2}{r_2^2}\right) + (T_{s,2} - T_{s,1})\right]}{r^2[(1/r_1) - (1/r_2)]} \tag{C.6}$$

Heat Rate

Plane Wall

$$q(x) = \left[\dot{q}x - \frac{k}{2L}(T_{s,2} - T_{s,1})\right]A_x \tag{C.7}$$

Cylindrical Wall

$$q(r) = \dot{q}\pi Lr^2 - \frac{2\pi Lk}{\ln(r_2/r_1)} \cdot \left[\frac{\dot{q}r_2^2}{4k}\left(1 - \frac{r_1^2}{r_2^2}\right) + (T_{s,2} - T_{s,1})\right] \tag{C.8}$$

Spherical Wall

$$q(r) = \frac{\dot{q}4\pi r^3}{3} - \frac{4\pi k\left[\frac{\dot{q}r_2^2}{6k}\left(1 - \frac{r_1^2}{r_2^2}\right) + (T_{s,2} - T_{s,1})\right]}{(1/r_1) - (1/r_2)} \tag{C.9}$$

Alternative surface conditions could involve specification of a uniform surface heat flux (*boundary condition of the second kind,* Equation 2.25 or 2.26) or a convection condition (*boundary condition of the third kind,* Equation 2.27). In each case, the surface temperature would not be known but could be determined by applying a surface energy balance. The forms that such balances may take are summarized in Table C.2. Note that, to accommodate situations for which a surface of interest may adjoin a composite wall in which there is no generation, the boundary condition of the third kind has been applied by using the overall heat transfer coefficient U in lieu of the convection coefficient h.

Patent Owner Manufacturing Resources International, Inc.
Exhibit 2017 - Page 970 of 999

TABLE C.2 Alternative Surface Conditions and Energy Balances for One-Dimensional, Steady-State Solutions to the Heat Equation for Plane, Cylindrical, and Spherical Walls with Uniform Generation

Plane Wall

Uniform Surface Heat Flux

$$x = -L: \quad q''_{s,1} = -\dot{q}L - \frac{k}{2L}(T_{s,2} - T_{s,1}) \tag{C.10}$$

$$x = +L: \quad q''_{s,2} = \dot{q}L - \frac{k}{2L}(T_{s,2} - T_{s,1}) \tag{C.11}$$

Prescribed Transport Coefficient and Ambient Temperature

$$x = -L: \quad U_1(T_{\infty,1} - T_{s,1}) = -\dot{q}L - \frac{k}{2L}(T_{s,2} - T_{s,1}) \tag{C.12}$$

$$x = +L: \quad U_2(T_{s,2} - T_{\infty,2}) = \dot{q}L - \frac{k}{2L}(T_{s,2} - T_{s,1}) \tag{C.13}$$

Cylindrical Wall

Uniform Surface Heat Flux

$$r = r_1: \quad q''_{s,1} = \frac{\dot{q}r_1}{2} - \frac{k\left[\frac{\dot{q}r_2^2}{4k}\left(1 - \frac{r_1^2}{r_2^2}\right) + (T_{s,2} - T_{s,1})\right]}{r_1 \ln(r_2/r_1)} \tag{C.14}$$

$$r = r_2: \quad q''_{s,2} = \frac{\dot{q}r_2}{2} - \frac{k\left[\frac{\dot{q}r_2^2}{4k}\left(1 - \frac{r_1^2}{r_2^2}\right) + (T_{s,2} - T_{s,1})\right]}{r_2 \ln(r_2/r_1)} \tag{C.15}$$

Prescribed Transport Coefficient and Ambient Temperature

$$r = r_1: \quad U_1(T_{\infty,1} - T_{s,1}) = \frac{\dot{q}r_1}{2} - \frac{k\left[\frac{\dot{q}r_2^2}{4k}\left(1 - \frac{r_1^2}{r_2^2}\right) + (T_{s,2} - T_{s,1})\right]}{r_1 \ln(r_2/r_1)} \tag{C.16}$$

$$r = r_2: \quad U_2(T_{s,2} - T_{\infty,2}) = \frac{\dot{q}r_2}{2} - \frac{k\left[\frac{\dot{q}r_2^2}{4k}\left(1 - \frac{r_1^2}{r_2^2}\right) + (T_{s,2} - T_{s,1})\right]}{r_2 \ln(r_2/r_1)} \tag{C.17}$$

Spherical Wall

Uniform Surface Heat Flux

$$r = r_1: \quad q''_{s,1} = \frac{\dot{q}r_1}{3} - \frac{k\left[\frac{\dot{q}r_2^2}{6k}\left(1 - \frac{r_1^2}{r_2^2}\right) + (T_{s,2} - T_{s,1})\right]}{r_1^2[(1/r_1) - (1/r_2)]} \tag{C.18}$$

$$r = r_2: \quad q''_{s,2} = \frac{\dot{q}r_2}{3} - \frac{k\left[\frac{\dot{q}r_2^2}{6k}\left(1 - \frac{r_1^2}{r_2^2}\right) + (T_{s,2} - T_{s,1})\right]}{r_2^2[(1/r_1) - (1/r_2)]} \tag{C.19}$$

Patent Owner Manufacturing Resources International, Inc.
Exhibit 2017 - Page 971 of 999

TABLE C.2 *Continued*

Prescribed Transport Coefficient and Ambient Temperature

$$r = r_1: \quad U_1(T_{\infty,1} - T_{s,1}) = \frac{\dot{q}r_1}{3} - \frac{k\left[\frac{\dot{q}r_2^2}{6k}\left(1 - \frac{r_1^2}{r_2^2}\right) + (T_{s,2} - T_{s,1})\right]}{r_1^2[(1/r_1) - (1/r_2)]} \tag{C.20}$$

$$r = r_2: \quad U_2(T_{s,2} - T_{\infty,2}) = \frac{\dot{q}r_2}{3} - \frac{k\left[\frac{\dot{q}r_2^2}{6k}\left(1 - \frac{r_1^2}{r_2^2}\right) + (T_{s,2} - T_{s,1})\right]}{r_2^2[(1/r_1) - (1/r_2)]} \tag{C.21}$$

As an example, consider a plane wall for which a uniform (known) surface temperature $T_{s,1}$ is prescribed at $x = -L$ and a uniform heat flux $q''_{s,2}$ is prescribed at $x = +L$. Equation C.11 may be used to evaluate $T_{s,2}$, and Equations C.1, C.4, and C.7 may then be used to determine the temperature, heat flux, and heat rate distributions, respectively.

Special cases of the foregoing configurations involve a plane wall with one adiabatic surface, a solid cylinder (a circular rod), and a sphere (Figure C.2). Subject to the requirements that $dT/dx|_{x=0} = 0$ and $dT/dr|_{r=0} = 0$, the corresponding forms of the heat equation may be solved to obtain Equations C.22 through C.24 of Table C.3.

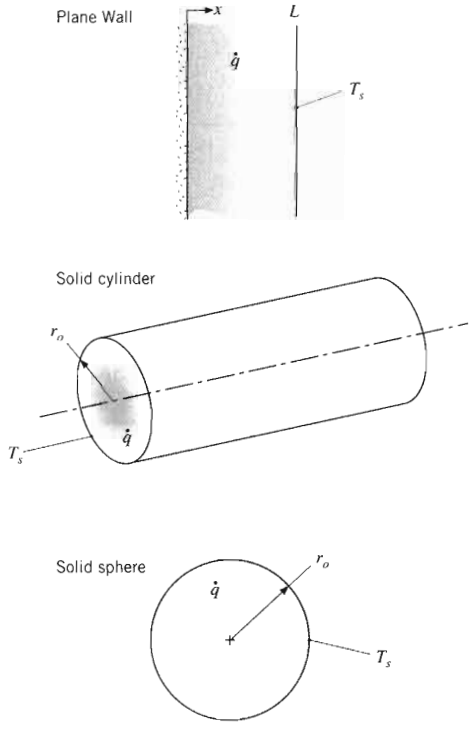


FIGURE C.2
One-dimensional conduction systems with uniform thermal energy generation: a plane wall with one adiabatic surface, a cylindrical rod, and a sphere.

Patent Owner Manufacturing Resources International, Inc.
Exhibit 2017 - Page 972 of 999

TABLE C.3 One-Dimensional, Steady-State Solutions to the Heat Equation for Uniform Generation in a Plane Wall with One Adiabatic Surface, a Solid Cylinder, and a Solid Sphere

	Temperature Distribution	
Plane Wall	$T(x) = \frac{\dot{q}L^2}{2k}\left(1 - \frac{x^2}{L^2}\right) + T_s$	(C.22)
Circular Rod	$T(r) = \frac{\dot{q}r_o^2}{4k}\left(1 - \frac{r^2}{r_o^2}\right) + T_s$	(C.23)
Sphere	$T(r) = \frac{\dot{q}r_o^2}{6k}\left(1 - \frac{r^2}{r_o^2}\right) + T_s$	(C.24)
	Heat Flux	
Plane Wall	$q''(x) = \dot{q}x$	(C.25)
Circular Rod	$q''(r) = \frac{\dot{q}r}{2}$	(C.26)
Sphere	$q''(r) = \frac{\dot{q}r}{3}$	(C.27)
	Heat Rate	
Plane Wall	$q(x) = \dot{q}xA_x$	(C.28)
Circular Rod	$q(r) = \dot{q}\pi Lr^2$	(C.29)
Sphere	$q(r) = \frac{\dot{q}4\pi r^3}{3}$	(C.30)

TABLE C.4 Alternative Surface Conditions and Energy Balances for One-Dimensional, Steady-State Solutions to the Heat Equation for Uniform Generation in a Plane Wall with One Adiabatic Surface, a Solid Cylinder, and a Solid Sphere

Prescribed Transport Coefficient and Ambient Temperature		
Plane Wall		
$x = L$:	$\dot{q}L = U(T_s - T_\infty)$	(C.31)
Circular Rod		
$r = r_o$:	$\frac{\dot{q}r_o}{2} = U(T_s - T_\infty)$	(C.32)
Sphere		
$r = r_o$:	$\frac{\dot{q}r_o}{3} = U(T_s - T_\infty)$	(C.33)

Patent Owner Manufacturing Resources International, Inc.
Exhibit 2017 - Page 973 of 999

The solutions are based on prescribing a uniform temperature T_s at $x = L$ and $r = r_o$. Using Fourier's law with the temperature distributions, the heat flux (Equations C.25 through C.27) and heat rate (Equations C.28 through C.30) distributions may also be obtained. If T_s is not known, it may be determined by applying a surface energy balance, appropriate forms of which are summarized in Table C.4.

Patent Owner Manufacturing Resources International, Inc.
Exhibit 2017 - Page 974 of 999

APPENDIX D

The Convection Transfer Equations

Patent Owner Manufacturing Resources International, Inc.
Exhibit 2017 - Page 975 of 999

In Chapter 2 we considered a stationary substance in which heat is transferred by conduction and developed means for determining the temperature distribution within the substance. We did so by applying *conservation of energy* to a differential control volume (Figure 2.11) and deriving a differential equation that was termed the *heat equation*. For a prescribed geometry and boundary conditions, the equation may be solved to determine the corresponding temperature distribution.

If the substance is not stationary, conditions become more complex. For example, if conservation of energy is applied to a differential control volume in a moving fluid, the effects of fluid motion (*advection*) on energy transfer across the surfaces of the control volume must be considered, along with those of conduction. The resulting differential equation, which provides the basis for predicting the temperature distribution, now requires knowledge of the velocity equations derived by applying *conservation of mass* and *Newton's second law of motion* to a differential control volume.

In this appendix we consider conditions involving flow of a *viscous fluid* in which there is concurrent *heat* and *mass transfer*. We restrict our attention to the *steady, two-dimensional flow* of an *incompressible fluid* with *constant properties* in the x and y directions of a Cartesian coordinate system, and present the differential equations that may be used to predict velocity, temperature, and species concentration fields within the fluid. These equations can be derived by applying Newton's second law of motion and conservation of mass, energy, and species to a differential control volume in the fluid.

⊗ *These equations are derived in Section 6S.1.*

D.1 Conservation of Mass

One conservation law that is pertinent to the flow of a viscous fluid is that matter can be neither created nor destroyed. For steady flow, this law requires that *the net rate at which mass enters a control volume* (inflow − outflow) *must equal zero.* Applying this law to a differential control volume in the flow yields

$$\frac{\partial u}{\partial x} + \frac{\partial v}{\partial y} = 0 \tag{D.1}$$

where u and v are the x and y components of the *mass average velocity*.

Equation D.1, the *continuity equation*, is a general expression of the *overall mass* conservation requirement, and it must be satisfied at every point in the fluid. The equation applies for a single species fluid, as well as for mixtures in which species diffusion and chemical reactions may be occurring, provided that the fluid can be approximated as *incompressible*, that is, constant density.

D.2 Newton's Second Law of Motion

The second fundamental law that is pertinent to the flow of a viscous fluid is *Newton's second law of motion*. For a differential control volume in the fluid, under steady conditions, this requirement states that *the sum of all forces acting on the*

Patent Owner Manufacturing Resources International, Inc.
Exhibit 2017 - Page 976 of 999

control volume must equal the net rate at which momentum leaves the control volume (outflow − inflow).

Two kinds of forces may act on the fluid: *body forces*, which are proportional to the volume, and *surface forces*, which are proportional to area. Gravitational, centrifugal, magnetic, and/or electric fields may contribute to the total body force, and we designate the x and y components of this force per unit volume of fluid as X and Y, respectively. The surface forces are due to the fluid static pressure as well as to *viscous stresses*.

Applying Newton's second law of motion (in the x- and y-directions) to a differential control volume in the fluid, accounting for body and surface forces, yields

$$\rho\left(u\frac{\partial u}{\partial x}+v\frac{\partial u}{\partial y}\right)=-\frac{\partial p}{\partial x}+\mu\left(\frac{\partial^2 u}{\partial x^2}+\frac{\partial^2 u}{\partial y^2}\right)+X \tag{D.2}$$

$$\rho\left(u\frac{\partial v}{\partial x}+v\frac{\partial v}{\partial y}\right)=-\frac{\partial p}{\partial y}+\mu\left(\frac{\partial^2 v}{\partial x^2}+\frac{\partial^2 v}{\partial y^2}\right)+Y \tag{D.3}$$

where p is the pressure and μ is the fluid viscosity.

We should not lose sight of the physics represented by Equations D.2 and D.3. The two terms on the left-hand side of each equation represent the *net* rate of momentum flow from the control volume. The terms on the right-hand side, taken in order, account for the net pressure force, the net viscous forces, and the body force. These equations must be satisfied at each point in the fluid, and with Equation D.1 they may be solved for the velocity field.

D.3 *Conservation of Energy*

As mentioned at the beginning of this Appendix, in Chapter 2 we considered a stationary substance in which heat is transferred by conduction and applied conservation of energy to a differential control volume (Figure 2.11) to derive the heat equation. When conservation of energy is applied to a differential control volume *in a moving fluid* under steady conditions, it expresses that the net rate at which energy enters the control volume, plus the rate at which heat is added, minus the rate at which work is done by the fluid in the control volume, is equal to zero. After much manipulation, the result can be rewritten as a *thermal energy equation*. For steady, two-dimensional flow of an incompressible fluid with constant properties, the resulting differential equation is

$$\rho c_p\left(u\frac{\partial T}{\partial x}+v\frac{\partial T}{\partial y}\right)=k\left(\frac{\partial^2 T}{\partial x^2}+\frac{\partial^2 T}{\partial y^2}\right)+\mu\Phi+\dot{q} \tag{D.4}$$

where T is the temperature, c_p is the specific heat at constant pressure, k is the thermal conductivity, $\dot{q}$ is the volumetric rate of thermal energy generation, and $\mu\Phi$, the *viscous dissipation*, is defined as

$$\mu\Phi\equiv\mu\left\{\left(\frac{\partial u}{\partial y}+\frac{\partial v}{\partial x}\right)^2+2\left[\left(\frac{\partial u}{\partial x}\right)^2+\left(\frac{\partial v}{\partial y}\right)^2\right]\right\} \tag{D.5}$$

Patent Owner Manufacturing Resources International, Inc.
Exhibit 2017 - Page 977 of 999

The same form of the thermal energy equation, Equation D.4, also applies to an ideal gas with negligible pressure variation.

In Equation D.4, the terms on the left-hand side account for the net rate at which thermal energy leaves the control volume due to bulk fluid motion (advection), while the terms on the right-hand side account for net inflow of energy due to conduction, viscous dissipation, and generation. Viscous dissipation represents the net rate at which mechanical work is irreversibly converted to thermal energy due to viscous effects in the fluid. The generation term characterizes conversion from other forms of energy (such as chemical, electrical, electromagnetic, or nuclear) to thermal energy.

D.4 *Conservation of Species*

If the viscous fluid consists of a binary mixture in which there are species concentration gradients, there will be *relative* transport of the species, and *species conservation* must be satisfied at each point in the fluid. For steady flow, this law requires that *the net rate at which species* A *enters a control volume* (inflow − outflow) *plus the rate at which species* A *is produced in the control volume (by chemical reactions) must equal zero.* Applying this law to a differential control volume in the flow yields the following differential equation, which has been expressed on a molar basis:

$$u\frac{\partial C_A}{\partial x} + v\frac{\partial C_A}{\partial y} = D_{AB}\left(\frac{\partial^2 C_A}{\partial x^2} + \frac{\partial^2 C_A}{\partial y^2}\right) + \dot{N}_A \tag{D.6}$$

An example problem involving the solution of the convection transfer equations is included in Section 6S.1.

where C_A is the molar concentration of species A, D_{AB} is the binary diffusion coefficient, and $\dot{N}_A$ is the molar rate of production of species A per unit volume. Again, this equation has been derived assuming an incompressible fluid with constant properties. Terms on the left-hand side account for net transport of species A due to bulk fluid motion (advection), while terms on the right-hand side account for net inflow due to diffusion and production due to chemical reactions.

Patent Owner Manufacturing Resources International, Inc.
Exhibit 2017 - Page 978 of 999

APPENDIX E

Boundary Layer Equations for Turbulent Flow

Patent Owner Manufacturing Resources International, Inc.
Exhibit 2017 - Page 979 of 999

It has been noted in Section 6.3 that turbulent flow is inherently *unsteady*. This behavior is shown in Figure E.1, where the variation of an arbitrary flow property P is plotted as a function of time at some location in a turbulent boundary layer. The property P could be a velocity component, the fluid temperature, or a species concentration, and at any instant it may be represented as the sum of a *time-mean* value $\overline{P}$ and a fluctuating component P'. The average is taken over a time that is large compared with the period of a typical fluctuation, and if $\overline{P}$ is independent of time, the time-mean flow is said to be *steady*.

Since engineers are typically concerned with the time-mean properties, $\overline{P}$, the difficulty of solving the time-dependent governing equations is often eliminated by averaging the equations over time. For steady (in the mean), incompressible, constant property, boundary layer flow with negligible viscous dissipation, using well-established time-averaging procedures [1], the following forms of the continuity, x-momentum, energy, and species conservation equations may be obtained:

$$\frac{\partial \overline{u}}{\partial x} + \frac{\partial \overline{v}}{\partial y} = 0 \tag{E.1}$$

$$\overline{u}\frac{\partial \overline{u}}{\partial x} + \overline{v}\frac{\partial \overline{u}}{\partial y} = -\frac{1}{\rho}\frac{d\overline{p}_\infty}{dx} + \frac{1}{\rho}\frac{\partial}{\partial y}\left(\mu\frac{\partial \overline{u}}{\partial y} - \rho\overline{u'v'}\right) \tag{E.2}$$

$$\overline{u}\frac{\partial \overline{T}}{\partial x} + \overline{v}\frac{\partial \overline{T}}{\partial y} = \frac{1}{\rho c_p}\frac{\partial}{\partial y}\left(k\frac{\partial \overline{T}}{\partial y} - \rho c_p\overline{v'T'}\right) \tag{E.3}$$

$$\overline{u}\frac{\partial \overline{C}_A}{\partial x} + \overline{v}\frac{\partial \overline{C}_A}{\partial y} = \frac{\partial}{\partial y}\left(D_{AB}\frac{\partial \overline{C}_A}{\partial y} - \overline{v'C'_A}\right) \tag{E.4}$$

The equations are like those for the laminar boundary layer, Equations 6.27 through 6.30 (after neglecting viscous dissipation), except for the presence of additional terms of the form $\overline{a'b'}$. These terms account for the effect of the turbulent fluctuations on momentum, energy, and species transport.

On the basis of the foregoing results, it is customary to speak of a *total* shear stress and *total* heat and species fluxes, which are defined as

$$\tau_{tot} = \left(\mu\frac{\partial \overline{u}}{\partial y} - \rho\overline{u'v'}\right) \tag{E.5}$$

$$q''_{tot} = -\left(k\frac{\partial \overline{T}}{\partial y} - \rho c_p\overline{v'T'}\right) \tag{E.6}$$

$$N''_{A,tot} = -\left(D_{AB}\frac{\partial \overline{C}_A}{\partial y} - \overline{v'C'_A}\right) \tag{E.7}$$

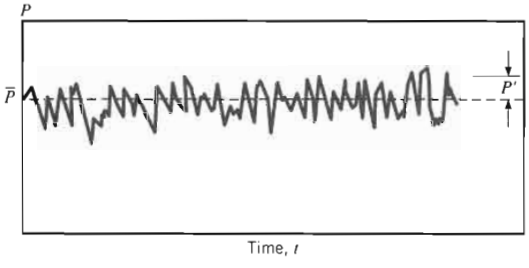


FIGURE E.1
Property variation with time at some point in a turbulent boundary layer.

Patent Owner Manufacturing Resources International, Inc.
Exhibit 2017 - Page 980 of 999

and consist of contributions due to molecular diffusion and turbulent mixing. From the form of these equations we see how momentum, energy, and species transfer rates are enhanced by the existence of turbulence. The term $-\rho\overline{u'v'}$ appearing in Equation E.5 represents the momentum flux due to the turbulent fluctuations, and it is often termed the *Reynolds stress*. The terms $\rho c_p\overline{v'T'}$ and $\overline{v'C'_A}$ in Equations E.6 and E.7, respectively, represent the heat and species fluxes due to the turbulent fluctuations. Unfortunately, these new terms introduced by the time-averaging process are additional unknowns, so that the number of unknowns exceeds the number of equations. Resolving this problem is the subject of the field of *turbulence modeling* [2].

References

1. Hinze, J. O. *Turbulence*, 2nd ed., McGraw-Hill, New York, 1975.

2. Wilcox, D. C., *Turbulence Modeling for CFD*, 2nd ed., DCW Industries, La Cañada, 1998.

Patent Owner Manufacturing Resources International, Inc.
Exhibit 2017 - Page 981 of 999

APPENDIX F

An Integral Laminar Boundary Layer Solution for Parallel Flow over a Flat Plate

Patent Owner Manufacturing Resources International, Inc.
Exhibit 2017 - Page 982 of 999

An alternative approach to solving the boundary layer equations involves the use of an approximate *integral* method. The approach was originally proposed by von Kárman [1] in 1921 and first applied by Pohlhausen [2]. It is without the mathematical complications inherent in the *exact* (*similarity*) method of Section 7.2.1; yet it can be used to obtain reasonably accurate results for the key boundary layer parameters (δ, δ_t, δ_c, C_f, h, and h_m). Although the method has been used with some success for a variety of flow conditions, we restrict our attention to parallel flow over a flat plate, subject to the same restrictions enumerated in Section 7.2.1, that is, *incompressible laminar flow* with *constant fluid properties* and *negligible viscous dissipation.*

To use the method, the boundary layer equations, Equations 7.4 through 7.7, must be cast in integral form. These forms are obtained by integrating the equations in the y direction across the boundary layer. For example, integrating Equation 7.4, we obtain

$$\int_0^\delta \frac{\partial u}{\partial x}\,dy + \int_0^\delta \frac{\partial v}{\partial y}\,dy = 0 \tag{F.1}$$

or, since $v = 0$ at $y = 0$,

$$v(y = \delta) = -\int_0^\delta \frac{\partial u}{\partial x}\,dy \tag{F.2}$$

Similarly, from Equation 7.5, we obtain

$$\int_0^\delta u\frac{\partial u}{\partial x}\,dy + \int_0^\delta v\frac{\partial u}{\partial y}\,dy = \nu\int_0^\delta \frac{\partial}{\partial y}\left(\frac{\partial u}{\partial y}\right)dy$$

or, integrating the second term on the left-hand side by parts,

$$\int_0^\delta u\frac{\partial u}{\partial x}\,dy + uv\Big|_0^\delta - \int_0^\delta u\frac{\partial v}{\partial y}\,dy = \nu\frac{\partial u}{\partial y}\Big|_0^\delta$$

Substituting from Equations 7.4 and F.2, we obtain

$$\int_0^\delta u\frac{\partial u}{\partial x}\,dy - u_\infty\int_0^\delta \frac{\partial u}{\partial x}\,dy + \int_0^\delta u\frac{\partial u}{\partial x}\,dy = -\nu\frac{\partial u}{\partial y}\Big|_{y=0}$$

or

$$u_\infty\int_0^\delta \frac{\partial u}{\partial x}\,dy - \int_0^\delta 2u\frac{\partial u}{\partial x}\,dy = \nu\frac{\partial u}{\partial y}\Big|_{y=0}$$

Therefore

$$\int_0^\delta \frac{\partial}{\partial x}(u_\infty \cdot u - u \cdot u)\,dy = \nu\frac{\partial u}{\partial y}\Big|_{y=0}$$

Rearranging, we then obtain

$$\frac{d}{dx}\left[\int_0^\delta (u_\infty - u)u\,dy\right] = \nu\frac{\partial u}{\partial y}\Big|_{y=0} \tag{F.3}$$

Equation F.3 is the integral form of the boundary layer momentum equation. In a similar fashion, the following integral forms of the boundary layer energy and species continuity equations may be obtained:

$$\frac{d}{dx}\left[\int_0^{\delta_t} (T_\infty - T)u\,dy\right] = \alpha\frac{\partial T}{\partial y}\Big|_{y=0} \tag{F.4}$$

Patent Owner Manufacturing Resources International, Inc.
Exhibit 2017 - Page 983 of 999

$$\frac{d}{dx}\left[\int_0^{\delta_c}(\rho_{A,\infty}-\rho_A)u\,dy\right]=D_{AB}\frac{\partial\rho_A}{\partial y}\bigg|_{y=0} \tag{F.5}$$

Equations F.3 through F.5 satisfy the x momentum, the energy, and the species conservation requirements in an *integral* (or *average*) fashion over the entire boundary layer. In contrast, the original conservation equations, (7.5) through (7.7), satisfy the conservation requirements *locally,* that is, at each point in the boundary layer.

The integral equations can be used to obtain *approximate* boundary layer solutions. The procedure involves first *assuming* reasonable functional forms for the unknowns u, T, and ρ_A in terms of the corresponding (*unknown*) boundary layer thicknesses. The assumed forms must satisfy appropriate boundary conditions. Substituting these forms into the integral equations, expressions for the boundary layer thicknesses may be determined and the assumed functional forms may then be completely specified. Although this method is approximate, it frequently leads to accurate results for the surface parameters.

Consider the hydrodynamic boundary layer, for which appropriate boundary conditions are

$$u(y=0)=\frac{\partial u}{\partial y}\bigg|_{y=\delta}=0 \qquad \text{and} \qquad u(y=\delta)=u_\infty$$

From Equation 7.5 it also follows that, since $u = v = 0$ at $y = 0$,

$$\frac{\partial^2 u}{\partial y^2}\bigg|_{y=0}=0$$

With the foregoing conditions, we could approximate the velocity profile as a third-degree polynomial of the form

$$\frac{u}{u_\infty}=a_1+a_2\left(\frac{y}{\delta}\right)+a_3\left(\frac{y}{\delta}\right)^2+a_4\left(\frac{y}{\delta}\right)^3$$

and apply the conditions to determine the coefficients a_1 to a_4. It is easily verified that $a_1 = a_3 = 0$, $a_2 = \frac{3}{2}$ and $a_4 = -\frac{1}{2}$, in which case

$$\frac{u}{u_\infty}=\frac{3}{2}\frac{y}{\delta}-\frac{1}{2}\left(\frac{y}{\delta}\right)^3 \tag{F.6}$$

The velocity profile is then specified in terms of the unknown boundary layer thickness δ. This unknown may be determined by substituting Equation F.6 into F.3 and integrating over y to obtain

$$\frac{d}{dx}\left(\frac{39}{280}u_\infty^2\,\delta\right)=\frac{3}{2}\frac{\nu u_\infty}{\delta}$$

Separating variables and integrating over x, we obtain

$$\frac{\delta^2}{2}=\frac{140}{13}\frac{\nu x}{u_\infty}+\text{constant}$$

Patent Owner Manufacturing Resources International, Inc.
Exhibit 2017 - Page 984 of 999

However, since $\delta = 0$ at the leading edge of the plate ($x = 0$), the integration constant must be zero and

$$\delta = 4.64\left(\frac{\nu x}{u_\infty}\right)^{1/2} = \frac{4.64x}{Re_x^{1/2}} \tag{F.7}$$

Substituting Equation F.7 into Equation F.6 and evaluating $\tau_s = \mu(\partial u/\partial y)_s$, we also obtain

$$C_{f,x} = \frac{\tau_s}{\rho u_\infty^2/2} = \frac{0.646}{Re_x^{1/2}} \tag{F.8}$$

Despite the approximate nature of the foregoing procedure, Equations F.7 and F.8 compare quite well with results obtained from the exact solution, Equations 7.19 and 7.20.

In a similar fashion one could assume a temperature profile of the form

$$T^* = \frac{T - T_s}{T_\infty - T_s} = b_1 + b_2\left(\frac{y}{\delta_t}\right) + b_3\left(\frac{y}{\delta_t}\right)^2 + b_4\left(\frac{y}{\delta_t}\right)^3$$

and determine the coefficients from the conditions

$$T^*(y = 0) = \left.\frac{\partial T^*}{\partial y}\right|_{y=\delta_t} = 0$$

$$T^*(y = \delta_t) = 1$$

as well as

$$\left.\frac{\partial^2 T^*}{\partial y^2}\right|_{y=0} = 0$$

which is inferred from the energy equation (7.6). We then obtain

$$T^* = \frac{3}{2}\frac{y}{\delta_t} - \frac{1}{2}\left(\frac{y}{\delta_t}\right)^3 \tag{F.9}$$

Substituting Equations F.6 and F.9 into Equation F.4, we obtain, after some manipulation and assuming $Pr \gtrsim 1$,

$$\frac{\delta_t}{\delta} = \frac{Pr^{-1/3}}{1.026} \tag{F.10}$$

This result is in good agreement with that obtained from the exact solution, Equation 7.24. Moreover, the heat transfer coefficient may be then computed from

$$h = \frac{-k\,\partial T/\partial y\big|_{y=0}}{T_s - T_\infty} = \frac{3}{2}\frac{k}{\delta_t}$$

Substituting from Equations F.7 and F.10, we obtain

$$Nu_x = \frac{hx}{k} = 0.332 Re_x^{1/2}\, Pr^{1/3} \tag{F.11}$$

This result agrees precisely with that obtained from the exact solution, Equation 7.23. Using the same procedures, analogous results may be obtained for the concentration boundary layer.

References

1. von Kárman, T., *Z. Angew. Math. Mech.*, **1,** 232, 1921.

2. Pohlhausen, K., *Z. Angew. Math. Mech.*, **1,** 252, 1921.

Patent Owner Manufacturing Resources International, Inc.
Exhibit 2017 - Page 985 of 999

egration con-

(F.7)

$\partial y)_s$, we also

(F.8)

ns F.7 and F.8
Equations 7.19

e form

(F.9)

ter some manip-

(F.10)

t solution, Equa-
uted from

(F.11)

n, Equation 7.23.
he concentration

, **1,** 252, 1921.

Index

NOTE: Page references preceded by a "W" refer to those pages that can be located on the Web site www.wiley.com/college/incropera.

A
Absolute species flux, 886, 893
Absolute temperature, 9
Absorption, 777
  gaseous, 843–847
  volumetric, 843
Absorptivity, 10, 754–755, 777
Adiabats, 202, W1
Adiabatic surfaces, 78
Advection, 6, 14, 886, 974, W26
American Society of Mechanical Engineers (ASME), 36
Analogy:
  conduction and diffusive mass transfer, 893
  heat and mass transfer, to boundary layers, 377–381
  Reynolds, 384–385
Anemometer, hot-wire, 43
Annular fins, 140, 150–151
ASME (American Society of Mechanical Engineers), 36
Azimuthal angle, 728

B
Band emission, 739–744
Base units, 35
Beds, external flow through packed, 452–453
Beer's law, 843
Bessel equations, modified, 151
Bessel functions:
  of the first kind (table), 963
  modified, of the first and second kinds (table), 964
Binary diffusion coefficients, 883
  for one atmosphere (table), 952
Bioheat equation, 162–166
Biot number, 260–261, 376
Blackbodies, 9, 10, 777
Blackbody radiation, 736–752
  and band emission, 739–752
  and emissivity, 744–752
  exchange, blackbody radiation, 830–831
  and Planck distribution, 737
  and Stefan–Boltzmann law, 738–739
  and Wien's displacement law, 737–738
Body forces, 975, W22
Boiling, 7, 8, 16, 620–640. *See also* Condensation
  definition of, 621
  dimensionless parameters in, 620–621
  forced convection, 636–640
    defined, 636
    external flow, 637
    in microchannels, 640
    two-phase flow, 637–640
  pool, 622–636
    and boiling curve, 622–626
    defined, 622
    film boiling, 626–626, 630–631
    free convection boiling, 624–625
    minimum heat flux for, 629–630
    nucleate boiling, 625, 627–629
    parametric effects on, 631–632
    transition boiling, 625, 629–630
  process of, 621
  subcooled vs. saturated, 622
Bond number, 376

Patent Owner Manufacturing Resources International, Inc.
Exhibit 2017 - Page 986 of 999

Boundary conditions, 77–78
discontinuous, 900
mass diffusion, 900–907
catalytic surface reactions, 905–907
evaporation, 901
solubility of gases in liquids, 901–905
solubility of gases in solids, 901–905
sublimation, 901
of the second kind, 134
of the third kind, 134
Boundary layer(s), 348–374
approximations, boundary layer, 365
concentration boundary layer, 350–352
dimensionless parameters, physical significance of, 374–377
equations, 364–367, 977–979
and evaporative cooling, 381–384
external flow
cylinder in cross flow, 423–425
mixed boundary layer conditions, 411–412
heat and mass transfer analogy to, 377–381
hydrodynamic, 6
laminar boundary layers, 359–364
mixed boundary layer conditions, external flow with, 411–412
normalized equations, 367–374
similarity parameters, boundary layer, 368–372
solutions, function form of, 368–372
and Reynolds number, 360–361
significance of, 352
thermal, 6, 349–350
transition, laminar–turbulent flow, 359–361
turbulence, effects of, 361–364, 978–979
turbulent boundary layers, 359
velocity boundary layer, 348–349
Boussinesq approximation, 564
British thermal unit (Btu), 36
Bubble diameter, 627
Bulk (macroscopic) motion, 3, 6
Bulk temperature, 492
Buoyancy forces, 8, 560–562
Buoyant jets, 561

C
Carbon nanotube, 109
Catalytic surface reactions, 905–907
Celsius, 37
Characteristic length, 208, 261, 290, 368
Chemical component of internal energy, 14
Chemical reactions, 905–910
heterogeneous, 905–907
homogeneous, 908–910
first order, 908
zero order, 908
Chilton–Colburn analogies, 385
Circular fins, 152
Circular tubes, *see* Tubes
Closed systems, 13
Coefficient matrix, 222
Coefficient of friction, 349, 376
Coherent structures, 360
Coiled tubes, 521–524
Colburn factor, 376, 385
Cold plates, 80
Column, evaporation in, 888–893
Column vectors, 223
Compact heat exchangers, 671–672, 683–686, 700–705
Complementary error function, 286
Composite walls, conduction with, 99–101
Concentration boundary layer, 350–352
Concentration gradient, 880
Concentric cylinders, free convection with, 590–591
Concentric spheres, free convection with, 591–592
Concentric tube annulus, 518–521
Concentric tube heat exchangers, 670
Condensation, 7, 8, 16, 642–655. *See also* Boiling
dimensionless parameters in, 620–621
dropwise, 641–642, 655
film
defined, 641
in horizontal tubes, 654
laminar, 643–646
on radial systems, 651–654
turbulent, 646–651
Conduction, 2–5, 58–82
and boundary/initial conditions, 77, 78
and Fourier's law, 58–60
with generation of thermal energy, *see* Thermal energy generation, conduction with
and heat diffusion equation, 70–77
microscale effects, 77
mechanisms of, 3–5
one-dimensional steady-state, *see* One-dimensional steady-state conduction

Patent Owner Manufacturing Resources International, Inc.
Exhibit 2017 - Page 987 of 999

shape factors, conduction, 207–212, W3–W5
and thermal properties of matter, 60–69
transient, *see* Transient conduction
two-dimensional steady-state, *see* Two-dimensional steady-state conduction
Conduction rate equation (Fourier's law), 58–60
Confinement number, 629, 640
Conservation of energy, 13–29, 975–976, W26–W28
for control volume, 13–25
internal flow, 497–504
general considerations related to, 497–498
surface heat flux, constant, 498–501
surface temperature, constant, 501–504
and methodology for application of conservation laws, 29
and surface energy balance, 25–28
Conservation of mass, 974, W21–W22
Conservation of species, 894–897, 976, W28–W29
for control volume, 894, W28
and mass diffusion equation, 895–897, W29
Contact resistance, thermal, 101–103
Continuity equation, W22
Control surface, 14
Control volumes:
conservation of energy for, 13–25
differential, 29, 70
Convection, 2, 6–9, 348–387. *See also* External flow; Internal flow boundary layers.
approximations, boundary layer, 365
concentration boundary layer, 350–352
dimensionless parameters, physical significance of, 374–377
equations, 364–367, 977–979
and evaporative cooling, 381–384
heat and mass transfer analogy to, 377–381
laminar boundary layers, 359–364
normalized equations, 367–374
and Reynolds number, 360–361
significance of, 352
thermal boundary layer, 349–350
turbulence, effects of, 361–364, 978–979
turbulent boundary layers, 359
velocity boundary layer, 348–349
coefficients, convection, 352–355, 385
forced, 7–8, 402
free, *see* Free convection
mass transfer by, 528–530
mechanisms of, 6–9
mixed, 7, 8, 593–594
problem of, 355
Reynolds analogy to, 384–385
Convection coefficients, 352–355, 385
Convection heat transfer coefficient, 8
Convection mass transfer coefficient, 353–354
Cooling:
evaporative, 381–384
Newton's law of, 8, 350
Cooling curve, 623
Counterflow heat exchangers, 679
Creeping flow, 433
Critical film thickness for conduction, 63
Critical heat flux, 625, 629
Cross-flow heat exchangers, 671, 680, 692, W38–W39
Curvilinear squares, W1–W2
Cylinder(s):
in cross flow, 423–433
flow considerations, 423–425
and heat and mass transfer, 425–433
free convection with
concentric cylinders, 590–591
long horizontal cylinder, 579–582
graphical representation of transient conduction in, W10–W11
one-dimensional steady-state conduction in, 116–121

D

Darcy friction factor, 490
Density gradients, 560
Derived units, 37–38
Differential control volumes, 29, 70
Diffuse emitters, 730
Diffusion:
of energy, 3, 4
mass, *see* Mass diffusion
Diffusion-limited processes, 907
Diffusive species flux, 886–888, 893
Dilute gas or liquid, 893
Dimensions, 35
Dimensionless conduction heat rate, 207–212

Patent Owner Manufacturing Resources International, Inc.
Exhibit 2017 - Page 988 of 999

Dimensionless parameters, 376–377
boiling, 620–621
boundary layers, 374–377
condensation, 620–621h
free convection, 565
Direct radiation, 772
Dirichlet conditions, 78
Discontinuous boundary conditions, 900
Discretization of heat equation:
explicit method of, 302–310
implicit method of, 310–317
Dittus–Boelter equation, 514
Double-pipe heat exchangers, 670
Drag coefficient, 425
Dropwise condensation, 641–642, 655

E
Eckert number, 376–377
Effectiveness–NTU method, 686–699
Electrical energy, conversion to thermal energy from, 126
Electromagnetic spectrum, 725, 726
Electromagnetic waves, 725
Elements (of coefficient matrix), 222
Emission:
band, 739–744
definition of, 777
gaseous, 843–847
and radiation intensity, 728–733
Emissive power, 9, 729, 777
Emissivity, 10, 744–752
of selected solids (table), 954–956
Empirical correlations, 404
Enclosed fluids, free convection with, 587–593
cylinders, concentric, 590–591
rectangular cavities, 587–590
spheres, concentric, 591–592
Energy, diffusion of, 3, 4
Energy balance method, 215–222
Energy carriers, 61
Energy changes, 14
Energy generation, 15
Energy sinks, 71
Energy sources, 71
Energy storage, 71
English system of units, 35–38
Enhancement surfaces, 632
Enhancement devices, 521–524
Entry region, 512–513
Environmental radiation, 770–776
Equilibrium states, 12–13
Error function, 961
Evaporation, 16
in column, 888–893
process of, 901
Excess temperature, 621
Extended surfaces, heat transfer from:
and fin effectiveness, 147–149
general conduction analysis for, 139–141
nonuniform cross-sectional area, fins of, 150–153
and overall surface efficiency, 153–158
uniform cross-sectional area, fins of, 141–147
External flow, 402–457
across banks of tubes, 436–447
cylinder in cross flow, 423–433
flow considerations, 423–425
and heat and mass transfer, 425–433
empirical approach to, 403–404, 415–420
flat plate in parallel flow, 405–414
laminar flow, 405–410
with mixed boundary layer conditions, 411–412
applied heat flux conditions, 413–414
unheated starting length, 412–413
turbulent flow, 410–411
forced convection boiling, 636–640
free convection, 571–584
cylinder, long horizontal, 579–582
inclined/horizontal plates, 574–579
spheres, 583–584
methodology for calculation of, 414–415
over a sphere, 433–436
parallel flow, flat plate in, *see* subhead: flat plate in parallel flow
through impinging jets, 447–452
considerations with, 447–449
and heat and mass transfer, 449–452
through packed beds, 452–453

F
Fanning friction factor, 490
Fiber-type insulations, 66
Fick's law, 882–883
Film boiling, 625–626, 630–631
Film condensation:
defined, 641
in horizontal tubes, 654
laminar, 643–646
on radial systems, 651–654
turbulent, 646–651

Patent Owner Manufacturing Resources International, Inc.
Exhibit 2017 - Page 989 of 999

Film temperature, 404
Finite control volumes, 29
Finite-difference methods:
  transient conduction, 302–317
    explicit method of discretization of heat equation, 302–310
    implicit method of discretization of heat equation, 310–317
  two-dimensional steady-state conduction, 212–234
    and energy balance method, 215–222
    and Gauss–Seidel iteration, 223–229
    heat equation, finite-difference form of, 214–215
    and matrix inversion method, 222–223
    nodal points, selection of, 214
    temperature distribution, determination of, 222
    verification of numerical solutions, 229–230
Fins, 137–139
  annular, 140, 150–151
  circular, 152
  evaluating performance of, 147–150
  of nonuniform cross-sectional area, 150–153
  overall surface efficiency of, 150–158
  parabolic, 152–153
  pin, 140, 152
  straight, 140, 152
  triangular, 140, 152
  of uniform cross-sectional area, 141–147
First law of thermodynamics, 13
First order chemical reaction, 908
Flake-type insulations, 66
Flat plate, parallel flow over, 405–414
  integral laminar boundary layer, solution for, 982–984
  laminar flow, 405–410
  with mixed boundary layer conditions, 411–412
  applied heat flux conditions, 413–414
  unheated starting length, 412–413
  turbulent flow, 410–411
Flow, *see* External flow; Internal flow
Flow work, 16
Fluids, thermal conductivity of, 64–65
Fluidized beds, 453
Flux plots, 203, W1–W2
Foamed systems, 66
Forced convection, 7–8, 402
  combined free and, 593–594
Forced convection boiling, 636–640
  defined, 636
  external flow, 637
  two-phase flow phenomena, 637–640
Form drag, 424
Fourier number, 376
Fourier's law, 4, 58–60
Free convection, 7–8, 560–597
  boiling, free convection, 624–625
  buoyancy forces in, 560–562
  combined forced and free, 593–594
  dimensionless parameters governing, 565
  with enclosed fluids, 587–593
    cylinders, concentric, 590–591
    rectangular cavities, 587–590
    spheres, concentric, 591–592
  equations governing, 563–564
  external flows, 571–584
    cylinder, long horizontal, 579–582
    inclined/horizontal plates, 574–579
    spheres, 583–584
  laminar free convection on vertical surface, 566–568
  and mass transfer, 594–595
  with parallel plate channels, 584–587
    inclined channels, 587
    vertical channels, 585–587
  physical considerations with, 560–562
  turbulence, effects of, 568–570
  vertical surface, laminar free convection on, 566–568
Free convection boiling, 624–625
Free jets, 448
Freezing, 16
Friction coefficient, 349, 376, 490
Friction drag, 424
Froude number, 639
Fully developed regions, 488–491

G
Gas(es):
  conduction in, 3–4
  solubility of (table), 953
  thermophysical properties of, at atmospheric pressure, 941–945
Gaseous radiation, 842–847
  emission and absorption, gaseous, 843–847
  volumetric absorption, 843
Gaussian error function (table), 961

Patent Owner Manufacturing Resources International, Inc.
Exhibit 2017 - Page 990 of 999

Gauss–Seidel iteration, 223–229
Generation of thermal energy, conduction with, *see* Thermal energy generation, conduction with
Graphical method (two-dimensional steady-state conduction), W1–W6
  and conduction shape factors, W3–W5
  flux plot, construction of, W1–W2
  heat transfer rate, determination of, W2–W3
Grashof number, 376, 565
Gray surfaces, 10
  radiation exchange between diffuse, in enclosure, 822–839
    black surfaces, 830–831
    reradiating surfaces, 835–839
    shields, radiation, 832–835
    at surface, net radiation exchange, 823–824
    between surfaces, net radiation exchange, 824–830
    two-surface enclosures, 831–832
  radiation from, 764–770

H

Heat capacity, volumetric, 67
Heat diffusion equation (heat equation), 70–77
  discretization of
    explicit method of, 302–310
    implicit method of, 310–317
  finite-difference form of, 214–215
  microscale effects, 77
Heat exchangers, 670–706
  compact, 671–672, 683–686, 700–705
  concentric tube, 670
  design problems, 694–695
  effectiveness–NTU method for analysis of, 680–699
  effectiveness of, 687
  log mean temperature difference for analysis of, 675–686
    counterflow heat exchangers, 679
    multipass and cross-flow heat exchangers, W37–W41
    parallel-flow heat exchangers, 676–678
    special conditions, operation under, 679–680
  overall heat transfer coefficient for, 673–675
  performance problems, 694–695
  shell-and-tube, 670–672
  types of, 670–672
Heat flow lines, 202
Heat flux, 4–5, 8, 59, 353
  critical, 625, 629
  pool boiling, 627–634
Heating curve, 622–623
Heat rate, 5, 59
Heat sinks, 33
Heat transfer:
  and convection heat transfer coefficient, 8
  definition of, 2
  determining rate of (two dimensional steady-state conduction), W2–W3
  enhancement of, with internal flows, 521–524
  from extended surfaces
    and fin effectiveness, 147–149
    general conduction analysis for, 139–141
    nonuniform cross-sectional area, fins of, 150–153
    and overall surface efficiency, 153–158
    uniform cross-sectional area, fins of, 141–147
  multimode, 839–841
  physical mechanisms of, 3–11
  practical relevance of, 32–35
  problems, methodology for analysis of, 29–30
  and radiation heat transfer coefficient, 10
  thermodynamics vs., 12–13
Hemispherical emissive power, 729
Henry's constant, 902
  for selected gases in water at moderate pressure (table), 953
Heterogeneous chemical reactions, 905–907
Homogeneous chemical reactions, 908–910
Host medium, 893
Hot-wire anemometer, 43
Hydraulic diameter, 518
Hydrodynamic boundary layer, 6
Hydrodynamic factors:
  with impinging jets, 447–449
  with internal flow, 486–491
  flow conditions, 486–487
  friction factor, 490–491
  in fully developed regions, 488–491

Patent Owner Manufacturing Resources International, Inc.
Exhibit 2017 - Page 991 of 999

mean velocity, 487–488
velocity profile, 488–490
Hyperbolic functions (table), 960

I
Ideal gas, 17
Impingement zone, 448
Impinging jets, 447–452
convection heat and mass transfer with, 449–452
hydrodynamic/geometric considerations with, 447–449
Incident radiation, 10
Incompressible liquids, 18
Initial conditions, 77–78
Insulation systems, thermal conductivity of, 66–67
Integral laminar boundary layer solution, 981–984
Intensity, 777
Internal energy, 14
Internal flow, 486–534
circular tubes
laminar flow in, 505–513
turbulent flow in, 514–518
coiled tubes, 521–524
energy balance in, 497–504
general considerations related to, 497–498
surface heat flux, constant, 498–501
surface temperature, constant, 501–504
heat transfer enhancement in, 521–524
hydrodynamic considerations with, 486–491
flow conditions, 486–487
friction factor, 490–491
in fully developed regions, 488–491
mean velocity, 487–488
velocity profile, 488–490
mass transfer by convection in, 528–530
microscale effects in, 524–528
hydrodynamic conditions, 524
thermal conditions, 525
thermal considerations in, 491–497
with fully developed conditions, 493–497
mean temperature, 492–493
Newton's law of cooling, 493
Irradiation, 10, 733–735, 752–753, 777
Isotherms, 59, 202
Isothermal surfaces, 59
Isotropic media, 60

J
Jakob number, 376
Jets:
buoyant, 561
impinging, *see* Impinging jets
Joule heating, 126

K
Kelvin, 37
Kilogram-mol, 37
Kirchhoff's law, 762–763, 777

L
Laminar boundary layers, 359–364
Laminar film condensation, 636–646
Laminar flow:
in circular tubes, 505–513
entry region, 511–513
fully developed region, 505–511
flat plate, parallel flow over, 405–410
Latent component of internal energy, 15
Latent heat, 620
Latent heat exchange, 8
Latent heat of fusion, 24
Lattice waves, 4
Leidenfrost point, 625
Length, 35
Lewis number, 375–376
Liquids:
conduction in, 4
incompressible, 18
Liquid metals, 410
thermophysical properties of, 951
LMTD method, *see* Log mean temperature difference method
Local heat flux, 350
Log mean temperature difference (LMTD) method, 675–686
counterflow heat exchangers, 679
multipass and cross-flow heat exchangers, W37–W41
parallel-flow heat exchangers, 676–678
special conditions, operation under, 679–680
Longitudinal pitch, 437
Lumped capacitance method, 256–270
assumption of, 256–257
and general lumped capacitance analysis, 263–270
theoretical basis of, 256–257
validity of, 259–263

Patent Owner Manufacturing Resources International, Inc.
Exhibit 2017 - Page 992 of 999

M
Macroscopic (bulk) motion, 3, 6
Mass, 35
Mass diffusion, 880–917
  boundary conditions and discontinuous concentrations, 900–907
    catalytic surface reactions, 905–907
    evaporation, 901
    solubility of gases in liquids, 901–905
    solubility of gases in solids, 901–905
    sublimation, 901
  homogenous chemical reactions, 908–910
  in nonstationary media, 885–893
    absolute species flux, 886
    diffusive species flux, 886
    evaporation in a column, 888–893
    mass-average velocity, 887
    molar-average velocity, 887
  in stationary media
    conservation of species, 894–897
      for control volume, 894
      mass diffusion equation, 894–897
    with specified surface concentrations, 897–900
  physical mechanisms of, 880–881
    Fick's law, 882–883
    mass diffusivity, 883
    mixture composition, 881–882
  stationary medium approximation, 893
  transient diffusion, 911–916
    analogy to heat transfer, 911
Mass diffusion equation, 894–897
Mass diffusivity, 883
Mass flow rate, 17
Mass transfer, 860. *See also* Mass diffusion
  and boundary layers, 350–352
  by convection, 528–530, 594–595
  with external flow
    cylinder in cross flow, 425–433
    through impinging jets, 449–452
Matrix inversion method, 222–223
Mean free path, 61
Mean temperature, 492–493
Mean velocity (internal flow), 487–488
Melting, 16
Metabolic heat generation, 162
Metals, thermophysical properties of liquid, 951
Metallic solids:
  emissivity of, 959
  thermophysical properties of, 929–932
Micro- and nanoscale effects in conduction, 62–67
  fluid state thermal conductivity, 65–66
  heat diffusion equation, 77
  insulation, 67
  solid state thermal conductivity, 62–64
Microscale effects in convection, 524–528
  hydrodynamic conditions, 524
  thermal conditions, 525
Mie scattering, 772
Mixed boundary layer conditions, external flow with, 411–412
Mixed convection, 7, 8, 593–594
Mixtures, composition of, 881–882
Mode(s) of heat transfer, 2
Modified Bessel equations, 151
Molar concentration, 881
Mole, 37
Molecular weight, 37
Moody diagrams, 491
Moody friction factor, 490
Multipass heat exchangers, 680, 689–691, W37–W38

N
Nano- and microscale effects in conduction, 62–67
  fluid state thermal conductivity, 65–66
  heat diffusion equation, 77
  insulation, 67
  solid state thermal conductivity, 62–64
Nanoshell, 293
Nanospring, 193
Nanostructured materials, 63
Nanotube, carbon, 109
Nanowire, 190
Natural convection, *see* Free convection
Neumann conditions, 78
Newton's law of cooling, 8, 493
Newton's second law of motion, 974, W22–W26
Nodal networks, 213–214
Nodal points (nodes), 213–214
Noncircular tubes, 518–519
Nonmetallic solids:
  emissivity of, 955–956
  thermophysical properties of, 933–934
Nonparticipating medium, 842
Nonstationary media, 885–893
  absolute species flux, 886
  diffusive species flux, 886
  evaporation in a column, 888–893

Patent Owner Manufacturing Resources International, Inc.
Exhibit 2017 - Page 993 of 999

mass-average velocity, 887
molar-average velocity, 887
Nuclear component of internal energy, 15
Nucleate boiling, 625, 627–629
Nusselt numbers, 371, 376

O
Ohmic heating, 126
One-dimensional steady-state conduction, 96–168
alternative approach, 112–116
bioheat equation, 162–168
extended surfaces, heat transfer from, 137–162
applicability, 137
and fin effectiveness, 147–149
general conduction analysis for, 139–141
nonuniform cross-sectional area, fins of, 150–153
and overall surface efficiency, 153–158
uniform cross-sectional area, fins of, 141–147
in plane wall systems, 96–116
composite walls, 99–101
and contact resistance, 101–103
standard approach, 96–112
temperature distribution, determination of, 96–99
thermal energy generation, conduction with, 126–132
thermal resistance, determination of, 98–99
in radial systems, 116–125
cylinder, 116–121
sphere, 121–125
thermal energy generation, conduction with, 132–137
thermal energy generation, conduction with, 126–137
plane wall systems, 126–132
in radial systems, 132–137
uniform energy generation, thermal conditions associated with, 966–971
Opaque surfaces, 10
Open systems, 14–18
Ordinary diffusion, 883

P
Packed beds, external flow through, 452–453
Parabolic fins, 152–153
Parallel-flow heat exchangers, 676–678
Parallel flow over flat plate, *see* Flat plate, parallel flow over
Parallel plate channels, free convection with, 584–587
inclined channels, 587
vertical channels, 585–587
Parameter sensitivity study, 28
Partition coefficient, 913
Peclet number, 237, 376
Penetration depth, thermal, 299
Pennes equation, 162
Perfusion, 162
Phase changes, 15–16
Phonons, 61
Photons, 725
Physical mechanisms of heat transfer, 3–12
Pin fins, 140–152
Pitch, 437, 523
Planck distribution, 737
Planck's law, 777
Plane wall systems:
one-dimensional steady-state conduction in, 96–116
composite walls, 99–101
and contact resistance, 101–103
standard approach, 96–112
temperature distribution, determination of, 96–99
thermal energy generation, conduction with, 126–132
thermal resistance, determination of, 98–99
transient conduction in, 272–275
approximate solution, 273–274
exact solution, 272–273
graphical representation of, W8–W9
roots of transcendental equation for (table), 962
and total energy transfer, 274–275
Plumes, 561
Pool boiling, 622–636
and boiling curve, 622–636
defined, 622
film boiling, 625–626, 630–631
free convection boiling, 624–625
minimum heat flux for, 629–630
nucleate boiling, 625, 627–629
parametric effects on, 631–632
transition boiling, 625, 629–630
Porosity, 453
Powder-type insulations, 66

Patent Owner Manufacturing Resources International, Inc.
Exhibit 2017 - Page 994 of 999

Power-controlled heating, 622
Prandtl number, 368, 369, 371, 376
Pressure drag, 424
Problems, methodology for analysis of, 29–30

Q
Quality of fluid, 638
Quanta, 61, 701
Quenching, 256
Quiescent fluid, 561

R
Radial systems:
  film condensation in, 651–654
  one-dimensional steady-state conduction in, 116–125
    cylinder, 116–121
    sphere, 121–125
    thermal energy generation, conduction with, 132–137
  transient conduction in, 276–283
    approximate solutions, 277–278
    exact solutions, 276
    and total energy transfer, 277–278
Radiation, 724–780. *See* also Radiation exchange
  and absorptivity, 754–755
  blackbody, 736–752
    and band emission, 739–744
    and emissivity, 744–752
    and Planck distribution, 737
    and Stefan–Boltzmann law, 738–739
    and Wien's displacement law, 737–738
  concepts related to, 724–726
  direct, 772
  environmental, 770–776
  gaseous, 842–847
    emission and absorption, gaseous, 843–847
    volumetric absorption, 843
  with gray surfaces, 764–770
  incident, 10
  intensity of, 727–735
    defined, 728–729
    and emission, 728–733
    and irradiation, 733–735
    and radiosity, 735
  and Kirchhoff's law, 762–763
  and reflectivity, 755–756
  surfaces, special consideration with, 757–758
  thermal, *see* Thermal radiation
  and transmissivity, 756–757
Radiation exchange, 812–849
  Beer's law, 843
  between diffuse gray surfaces in enclosure, 822–839
    blackbody, 830–831
    reradiating surfaces, 835–839
    shields, radiation, 832–835
    at surface, net radiation exchange, 823–824
    between surfaces, net radiation exchange, 824–830
    two-surface enclosures, 831–832
  gaseous radiation, 842–847
    emission and absorption, gaseous, 843–847
    volumetric absorption, 843
  and multimode heat transfer, 839–842
  and view factor, 812–822
    integral, view factor, 812–813
    relations, view factor, 813–822
Radiation heat transfer coefficient, 10
Radiosity, 735, 777
Random motion, 4
Raoult's law, 901
Rate basis, 13
Rate equations, 4
Rayleigh number, 569
Rayleigh scattering, 772
Reaction-limited processes, 907
Reciprocity relation, 813
Rectangular cavities, 587–590
Reflection, 10, 777
Reflective insulations, 66
Reflectivity, 755–756, 777
Relative species flux, 886
Reradiating surfaces, 832–835
Resistance:
  contact, 101–103
  thermal, 98–99
Resistance heating, 126
Reynolds analogy, 384–385
Reynolds number, 360–361, 368, 377
Reynolds stress, 979
Right-hand side vectors, 223

S
Saturated boiling, 622
Schmidt number, 368, 369, 372, 377
Semi-infinite solid, transient conduction in, 283–290, 292
Semitransparent media, 55

Patent Owner Manufacturing Resources International, Inc.
Exhibit 2017 - Page 995 of 999

Semitransparent surfaces, 10
Sensible energy, 8
Sensitivity study, parameter, 28
Separation of variables, method of, 203–207
Shape factors, conduction, 207–212, W3–W5
Shell-and-tube heat exchangers, 670–672, W37–W38
Sherwood number, 371–372, 377
Shields, radiation, 832–835
Similarity solutions, 406
Similarity variables, 406
Sinks, energy, 71
SI system, 36–37
Solar radiation, 812–814
Solar radiative properties of selected materials (table), 956
Solids:
  emissivity of selected, 954–955
  solubility of (table), 953
  thermal conductivity of, 60–64
  thermophysical properties of metallic, 929–932
  thermophysical properties of nonmetallic, 933–934
Solidification, 16
Solubility, 901–905
Solution vectors, 223
Sources, energy, 71
Species, 880
Species flux, absolute, 886, 893
Species flux, diffusive, 886
Species flux, relative, 886
Specific heat, 17
Spectral absorptivity, 754–755
Spectral distribution, 778
Spectral emissive power, 730
Spectral irradiation, 733, 752
Spectral radiosity, 735
Sphere(s):
  external flow over a
    forced convection, 433–436
    free convection, 583–584
  free convection with
    concentric spheres, 591–592
    external flows, 583–584
  graphical representation of transient conduction in, W11–W12
  one-dimensional steady-state conduction in, 121–125
Spines, 139
Stagnation point, 450
Stagnation zone, 448
Stanton number, 377, 384–385
Stationary media
  conservation of species, 894–897
    for control volume, 894
    mass diffusion equation, 894–897
    with specified surface concentrations, 897–900
Stationary medium approximation, 893
Steady-state conditions, 4, 15
Stefan–Boltzmann law, 9, 738–739, 778
Stefan–Boltzmann constant, 9
Straight fins, 140
Streaks, 360
Stress(es):
  Reynolds, 979
  tensile, W23
  viscous, W22
Subcooled boiling, 622
Sublimation, 901
Summation rule, 814
Surface(s):
  conservation of energy at, 25–26
  enhancement, 632
  net radiation exchange at, 823–824
  opaque, 10
  radiation exchange between, 824–830
  reradiating, 835–839
  semitransparent, 10
Surface forces, W22
Surface phenomena, 16
Surface tension, 620
Surroundings, 10

T

Temperature, 35, 37
  and conduction, 3–4
  excess, 621
  film, 404
  mean, 492–493
Temperature distribution, 70
  one-dimensional steady-state conduction, 96–98
  two-dimensional steady-state conduction, 207, 212
Temperature field, 70
Temperature gradient, 4, 59
Tensile stresses, W23
Thermal boundary layer, 6, 349–350
Thermal capacitance, 258
Thermal component of internal energy, 14–15

Patent Owner Manufacturing Resources International, Inc.
Exhibit 2017 - Page 996 of 999

Thermal conductivity, 4, 60–67
bulk, 62
definition of, 60
effective, 66
of fluids, 64–66
micro- and nanoscale effects, 65–66
of insulation systems, 66–67
of isotropic materials, 60
of solids, 60–64
micro- and nanoscale effects, 62–64
and state of matter, 60
Thermal contact resistance, 101–103
Thermal diffusivity, 68, 72
Thermal energy generation, conduction with, 126–137
plane wall systems, 126–132
in radial systems, 132–137
Thermal expansion (volumetric) coefficient, 563
Thermal penetration depth, 299
Thermal radiation, 3, 726, 778
mechanisms of, 9
Thermal resistance for conduction (plane wall), 98–99
Thermodynamics, 2
heat transfer vs., 12–13
Thermodynamic properties, 67
Thermophysical properties, 67
of common materials, 935–940
of gases at atmospheric pressure, 941–945
of liquid metals, 951
of metallic solids, 929–932
of nonmetallic solids, 933–934
of saturated fluids, 946–948
of saturated water, 949–950
Thermoregulation, 26
Thin film, 63
Time, 35
Time instant, 14
Time interval, 14
Total emissive power, 730
Total irradiation, 733, 752
Transient conduction, 256–319
finite-difference methods with, 302–317
explicit method of discretization of heat equation, 302–310
implicit method of discretization of heat equation, 310–314
graphical representation of one-dimensional, W8–W12
lumped capacitance method with, 256–270
assumption of, 256, 257
general lumped capacitance analysis, 263–270
theoretical basis of, 256–257
validity, method, 259–263
multidimensional effects with, W13–W18
plane wall approximation with, 272–275
approximate solution, 273–274
exact solution, 272–273
roots of transcendental equation for (table), 962
objects with constant surface heat flux, 292–294
approximate solutions, 293–294
exterior heat transfer, 293
interior heat transfer, 292–293
semi-infinite solid, 292
objects with constant surface temperature, 290–292, 293, 295
approximate solutions, 293, 295
exterior heat transfer, 291–292
interior heat transfer, 291
semi-infinite solid, 290–291
periodic heating, 299–301
and total energy transfer, 274–275
with radial systems, 276–283
approximate solutions, 277–278
exact solutions, 276
and total energy transfer, 277–278
with semi-infinite solid, 283–292
spatial effects with, W13–W18
Transient diffusion, 911–916
analogy to heat transfer, 911
Transition boiling, 625, 629–630
Transition, laminar–turbulent flow, 359–361
Transmission, 10, 778
Transmissivity, 756–757, 778
Transport properties, 67
Transverse pitch, 437
Triangular fins, 152–153
Tubes:
aligned vs. staggered arrangement of, 437
coiled, 522–524
concentric, 519–521
external flow across banks of, 436–447
film condensation in horizontal, 654
heat exchangers, shell-and-tube, 670–672, W37–W38
laminar flow in circular, 505–513

Patent Owner Manufacturing Resources International, Inc.
Exhibit 2017 - Page 997 of 999

entry region, 511–513
fully developed region, 505–511
noncircular, 518–519
turbulent flow in circular, 511–518
Turbulence:
effects of, on boundary layers, 359–364
and free convection, 568–570
modeling, 979
Turbulent boundary layers, 359
Turbulent film condensation, 646–651
Turbulent flow:
in circular tubes, 511–518
flat plate, parallel flow over, 410–411
Two-dimensional steady-state conduction, 202–235
alternative approaches with, 202–203
conduction shape factor, 207–212
dimensionless conduction heat rate, 207–212
finite-difference, method with, 212–235
and energy balance method, 215–222
and Gauss–Seidel iteration, 223–229
heat equation, finite-difference form of, 214–215
and matrix inversion method, 222–223
nodal points, selection of, 214
temperature distribution, determination of, 207, 212
verification of numerical solutions, 229–230
graphical method with, W1–W6
and conduction shape factors, W3–W5
flux plot, construction of, W1–W2
heat transfer rate, determination of, W2–W3
separation of variables method with, 203–207
Two-phase flow, 637–640
in microchannels, 640

U
Unheated starting length, 412–413
Units, 35–38
derived, 37, 38
English system of, 35–38
SI system, 35–38
Unit mass, 17

V
Vapor blanket, 625
Vaporization, 16
Velocity boundary layer, 348–349
Velocity profile (internal flow), 488–490
View factor (radiation exchange), 812–822
integral, view factor, 812–813
relations, view factor, 813–822
Viscous dissipation, 18
Viscous stresses, W22
Void fraction, 453
Volumetric absorption, 843
Volumetric flow rate, 18
Volumetric heat capacity, 67
Volumetric phenomena, 16
Volumetric thermal expansion coefficient, 563

W
Weber number, 377
Wien's displacement law, 737–738, 778

Z
Zenith angle, 728, 771
Zero order chemical reaction, 908

Patent Owner Manufacturing Resources International, Inc.
Exhibit 2017 - Page 998 of 999

0-470-05554-5
6809847

ANDARD FOR MASTERING
ND MASS TRANSFER

its readability, comprehensiveness, and relevance, Incropera and s the recognized standard for learning heat and mass transfer. This text combines detailed coverage with the resources students need to learn the concepts and apply them to solving realistic and relevant problems. Using a rigorous and systematic problem-solving methodology, the text is filled with examples and problems that reveal the richness and beauty of the discipline.

The 6th Edition introduces coauthors Ted Bergman and Adrienne Lavine, who bring their record of success in teaching and research in heat and mass transfer to the text.

NEW FEATURES

- Expanded coverage of areas of recent interest in heat transfer, including fuel cells and alternative energy devices, electronics cooling, micro-scale heat transfer, and biological as well as bioheat transfer. New examples and homework problems are included for each area.
- Introduction to the concepts of nano-scale transport and unified treatment of transient conduction.
- New material on two-phase heat transfer and enhanced internal forced convection.
- New and revised presentation of mass transfer including applications in materials science and biological engineering.
- New, revised, and updated problems and examples.

MODEL, SOLVE, AND EXPLORE HEAT TRANSFER PROBLEMS:

Interactive Heat Transfer and Finite Element Heat Transfer software with User's Guide CD and print booklet, ISBN: 0-471-76115-X

Completely updated with a modern graphical user interface and better graphing tools, ***Interactive Heat Transfer (IHT)*** software will help you learn how to build thermal models, solve specific conditions, and explore the effects of multiple parameter variations. IHT is now capable of solving 300+ equations. The ***Finite Element Heat Transfer*** software enhances capabilities for treating steady-state and transient one- and two-dimensional conduction problems.

SCJ
INCROPERA
USED
FUND.OF HEAT+MASS TRANS.-W/USER GDE.+CD
6TH 07 WILEY
978-0-470-05554-0
2 900470 055549
DM0007980410D
14 A
2

WILEY

www.wiley.com/college/incropera

Patent Owner Manufacturing Resources International, Inc.
Exhibit 2017 - Page 999 of 999